

**A
Revolution
in the
Physiology
of the
Living
Cell**



A REVOLUTION IN THE PHYSIOLOGY OF THE LIVING CELL

by

Gilbert N. Ling, Ph.D.

Damadian Foundation for Basic and Cancer Research

% Fonar Corporation, Melville, New York



KRIEGER PUBLISHING COMPANY
MALABAR, FLORIDA
1992

Original Edition 1992

Printed and Published by
KRIEGER PUBLISHING COMPANY
KRIEGER DRIVE
MALABAR, FLORIDA 32950

Copyright © 1991 by
KRIEGER PUBLISHING COMPANY

All rights reserved. No part of this book may be reproduced in any form or by any means electronic or mechanical, including information storage and retrieval systems without permission in writing from the publisher.

No liability is assumed with respect to the use of the information contained herein.

Printed in the United States of America

Library of Congress Cataloging in Publication Data

Ling, Gilbert N., 1919-

A revolution in the physiology of the living cell

Gilbert L. Ling.

p. cm.

Bibliography: p.

ISBN 0-89464-398-3 (alk. paper)

1. Cell physiology. 2. Biophysics. I. Title.

QH631.L562 1989

574.87—dc20

89-1100
CII

10 9 8 7 6 5 4 3 2

To
Raymond and Donna Damadian

CONTENTS

A Short History and Acknowledgments	xi
Introduction	xxi
Chapter 1. Early Theories of the Living Cell	1
1.1. Life and Death of a Living Cell	1
1.2. The Cell Theory and the Protoplasmic Doctrine	2
1.2.1. Gelatin as a Model of Protoplasm	3
1.2.2. Copper Ferrocyanide Gel as a Model of Plasma Membrane	3
1.3. The Membrane Theory	4
1.4. The Protoplasmic Theory and Colloid Chemistry	6
Chapter 2. The Membrane-Pump Theory	9
2.1. The Origin of the Membrane-Pump Hypothesis	9
2.2. The Excessive Energy Need of the Na Pump; A Decisive Disproof	10
2.2.1. The Effects of Metabolic Inhibition on Cell Na ⁺	10
2.2.2. The Original Calculations Comparing the Minimum Energy Need of the Postulated Na Pump with the Maximum Available Energy	12
2.2.3. Gross Underestimation of the Disparity Between Maximum Available and Minimum Needed Energy for the Na Pump	15
2.2.4. Remedial Postulations to Reduce the Energy Need of the Na Pump	16
2.2.5. Many More Pumps Required at the Plasma Membrane	17
2.2.6. Still More Pumps Required at the Membranes of Subcellular Particles	19
2.3. The Failure to Demonstrate Pumping of K ⁺ and Na ⁺ Against Concentration Gradients in an Ideal Cytoplasm-Free Membrane-Sac Preparation	20
2.4. Evidence Once Considered to Strongly Support the Membrane-Pump Hypothesis Shown to be Erroneous or Equivocal	20
2.4.1. Intracellular K ⁺ Mobility	20
2.4.2. Intracellular K ⁺ Activity	21
2.4.3. The Intracellular "Reference Phase" Studies	22
2.4.4. Active Transports in Hollow Membrane Sacs or Vesicles	22
2.5. Summary	28

Chapter 3. The Living State	31
3.1. The Story of the Living Cell: A System of Protein-Water-K ⁺ Interacting with an Environment of Water and Na ⁺	31
3.2. A Discrete High-(Negative)-Energy, Low-Entropy State Called the Living State	31
3.3 A Diagram of the Living Cell	33
Chapter 4. Cell Potassium	39
4.1. Enhanced Counterion Association with Charge-fixation	39
4.2. Stoichiometric Na ⁺ (and K ⁺) Adsorption on Protein β - and γ -Carboxyl Groups in Vitro	41
4.3. Demonstration of a Stoichiometric Relation Between Concentration of Cell K ⁺ and the Concentration of Cytoplasmic Proteins, Primarily Hemoglobin	44
4.4. Adsorption of Cell K ⁺ on β - and γ -Carboxyl Groups of Cytoplasmic Proteins	45
4.4.1. Localized Distribution of K ⁺ in Cell Regions rich in β - and γ -Carboxyl Groups	45
4.4.2. The Selectivity in Adsorption Among Tl ⁺ , Cs ⁺ and Other Ions Not Due to Functional Cell Membrane and Postulated Pumps	50
4.4.3. Demonstration of Specific Adsorption of Alkali-Metal Ions on the β - and γ -Carboxyl Groups Inside Living Cells	61
4.4.4. Evidence that in Living Muscle Cells β - and γ -Carboxyl Groups Carried by Myosin and Maintained at the Resting Living State Selectively Adsorb K ⁺ Over Na ⁺ .	62
4.4.5. Summary	65
Chapter 5. Cell Water	69
5.1. The Physics of Multilayer Adsorption of Water	69
5.2. The Polarized Multilayer Theory of Cell Water and Results of Experimental Testing	71
5.2.1. Background	71
5.2.2. The Polarized-Multilayer (PM) Theory of Cell Water	73
5.2.3. The Subsidiary Hypothesis of Solute Exclusion	77
5.2.4. Predictions of the Polarized-Multilayer (PM) Theory	80
5.2.5. Results of Experimental Testing of the Predictions of the PM Theory	81
5.3 Summary	106
Chapter 6. Induction	111
6.1. The Inductive Effect in the Properties and Behaviors of Small Organic Molecules	112
6.2. The Inductive Effect in the Properties and Behaviors of Proteins	116

6.2.1. Inductive Effect on Protein Conformation and Water Polarization	118
6.2.2. Inductive Effect on the Reactivity of Side-Chain SH Groups	121
6.2.3. Inductive Effect on the Fluorescence of Tyrosine and Tryptophane Residues	123
6.2.4 Inductive Effect on the Rank Order of Selective Ion Adsorption on β - and γ -Carboxyl Groups	125
6.3. Summary	130
Chapter 7. Coherent Behavior and Control Mechanisms	135
7.1. Theory of Cooperative Adsorption (the Yang-Ling Cooperative Adsorption Isotherm)	136
7.2. Experimental Findings in Harmony with the Theory of Spontaneous Autocooperative Transition	140
7.2.1. Cooperative Interaction Among Backbone NHCO Sites	140
7.2.2. Cooperative Interaction Among β - and γ - Carboxyl Groups	141
7.3. Theory of the Control of Transition Between Discrete Cooperative States by Cardinal Adsorbents	142
7.3.1. A Sketch of the Basic Concepts	142
7.3.2. The Definition and Classification of Cardinal Adsorbents	144
7.3.3. A Model Demonstrating How a Cardinal Adsorbent May Initiate and Maintain an All-or-None Change of a Protein System	145
7.4. Experimental Findings in Harmony with the Theory of Controlled Autocooperative Transition	149
7.4.1. Allosteric Control by Acid of the Shift Between Water Binding to Urea Binding on Bovine Serum Albumin	149
7.4.2. Zipper-Like Unmasking of Carboxyl Groups in Response to Acid Binding onto "Trigger Groups" on Ferri- and Carboxyhemoglobin	150
7.4.3. In Vitro Allosteric Control of Cooperative Binding of Oxygen on Hemoglobin by 2,3-DPG, IHP, and ATP	152
7.5. Summary	155
Chapter 8. Solute Distribution	159
8.1. Solute Distribution in Living Cells	160
8.1.1. Solute Primarily in Cell Water	162
8.1.2. Solute in Cell Water and on Adsorption Sites	162
8.1.3. Solute Primarily on Adsorption Sites	166
8.2 Cooperativity in Adsorption in Living Cells	169
8.3 Control of Cooperative Adsorption and Transition	171
8.3.1. Control by Ca^{++}	171
8.3.2. Control By Ouabain	172

8.3.3. The Indifference of the q -values of Large Solutes in Cell Water after Exposure to Insulin, Ouabain and Other Secondary Cardinal Adsorbents	177
8.4. The Role of ATP in Maintenance of the Living State and in Work Performance	178
8.4.1. ATP as a Reservoir of Utilizable Energy: the Attractive but Incorrect High Energy Phosphate Bond Concept	179
8.4.2. ATP as the Prime Living-State-Conserving Cardinal Adsorbent and its Role in Work Performance	179
8.4.3. Experimental Confirmation of Some Predictions of the Theory	187
8.4.4. In-Vitro Demonstration of the Maintenance of the Living State by ATP (and Its "Helpers")	197
8.5 Summary	198
Chapter 9. Permeability to Water, Ions, Nonelectrolytes, and Macromolecules	205
9.1. The Lipoidal Membrane Model in the Past and the Present	206
9.1.1. Overton's Original Model	206
9.1.2. Subsequent Modifications of the Overton Model	206
9.1.3. Overton's Lipid-Layer Model Once Again	208
9.2. The Cell Membrane as a Lipid-Protein-Polarized- Water System	212
9.2.1. Permeability to Water and Nonelectrolytes	213
9.2.2. Permeability to Ions and its Control	230
9.3. Summary	244
Chapter 10. Cell Volume and Shape	249
10.1. Cell Volume Maintenance and Regulation According to Traditional Hypothesis	249
10.2 Cell Volume Maintenance and Regulation According to the AI Hypothesis	253
10.2.1. A New Theory of Cell-Volume Maintenance	253
10.2.2. The Restraining Effect of Intracellular Salt Linkages in the Maintenance of Cell Volume, and Specific Swelling Effects of Some Electrolytes	259
10.2.3. Cytoplasmic Proteins and their Conformation in the Determination and control of Cell Shape	263
10.2.4. The Role of ATP in the Control of Cell Volume	265
10.2.5. The Role of ATP in the Control of Cell Shape	268
10.3 Summary	271
Chapter 11. Cellular Electrical Potentials	273
11.1. Bernsteins Membrane Theory of Resting and Action Potentials	273
11.2. The Ionic Theory of Resting and Action Potential of Hodgkin and Katz	275

11.2.1. Theory	27
11.2.2. Results of Experimental Testing	27
11.2.3. Modifications of Theory	27
11.2.4. Decisive Evidence Against Both the Original Ionic Theory and its Modifications	27
11.3. The Surface-Adsorption (SA) Theory of Cellular Resting and Action Potential	28
11.3.1. Theory	28
11.3.2. Results of Experimental Testing	28
11.4. Control of the Resting Potential According to SA Theory	28
11.4.1. Theory	28
11.4.2. Results of Experimental Testing of Theory and Other Related Observations	29
11.5. Action Potential According to Hodgkin-Huxley and According to AI Hypothesis	29
11.5.1. The Hodgkin-Huxley Analyses and Interpretation of the Action Potential	29
11.5.2. Action Potential According to the AI Hypothesis and Experimental Findings in Harmony with the Theory	30
11.6. Summary	31
Chapter 12. The Completion of a Scientific Revolution and Events Beyond	31
12.1. Definitions of "Scientific Revolution"	31
12.2. A Unique Feature of the Scientific Method as Applied to Cell Physiology	32
12.3. Outlines of Old and New Theory	32
12.3.1. The Membrane-Pump Theory	32
12.3.2. The Association-Induction (AI) Hypothesis	32
12.4. Results of Testing of Theoretical Postulates on Inanimate Models	32
12.5. The Fulfillment of All the Required Criteria for the Completion of a Scientific Revolution	32
12.6. Outstanding Features of a Valid New Theory	33
12.6.1. Expanding Coverage	33
12.6.2. Simplicity in Governing Rules	33
12.6.3. Predicting New Relations	33
12.7. The Future	33
References	34
Index	35

11.2.1. Theory	275
11.2.2. Results of Experimental Testing	276
11.2.3. Modifications of Theory	277
11.2.4. Decisive Evidence Against Both the Original Ionic Theory and its Modifications	279
11.3. The Surface-Adsorption (SA) Theory of Cellular Resting and Action Potential	280
11.3.1. Theory	280
11.3.2. Results of Experimental Testing	282
11.4. Control of the Resting Potential According to SA Theory	289
11.4.1. Theory	289
11.4.2. Results of Experimental Testing of Theory and Other Related Observations	290
11.5. Action Potential According to Hodgkin-Huxley and According to AI Hypothesis	299
11.5.1. The Hodgkin-Huxley Analyses and Interpretation of the Action Potential	299
11.5.2. Action Potential According to the AI Hypothesis and Experimental Findings in Harmony with the Theory	303
11.6. Summary	312
Chapter 12. The Completion of a Scientific Revolution and Events Beyond	319
12.1. Definitions of "Scientific Revolution"	319
12.2. A Unique Feature of the Scientific Method as Applied to Cell Physiology	320
12.3. Outlines of Old and New Theory	320
12.3.1. The Membrane-Pump Theory	320
12.3.2. The Association-Induction (AI) Hypothesis	321
12.4. Results of Testing of Theoretical Postulates on Inanimate Models	322
12.5. The Fulfillment of All the Required Criteria for the Completion of a Scientific Revolution	324
12.6. Outstanding Features of a Valid New Theory	335
12.6.1. Expanding Coverage	336
12.6.2. Simplicity in Governing Rules	336
12.6.3. Predicting New Relations	336
12.7. The Future	339
References	341
Index	357

A SHORT HISTORY OF THE REVOLUTION AND ACKNOWLEDGMENTS

The completion of the present volume gives me an opportunity to say thanks to America in general and to some special individuals. For without their support, I certainly would not be doing what I am doing now: reporting the completion of a major scientific revolution in cell physiology, the foundation science of biology and medicine. A revolution of this scope and in such a central field of knowledge happens only at long-time intervals. And of course each revolution can happen just once. To play a part in the development and completion of this revolution is an honor and privilege of the highest kind indeed.

To say thanks is not always an easy task. Because so many individuals and institutions have been involved in so many different ways and over such a long period of time; to recognize and thank each properly, a short history of the work is needed. This history began in China.

After my graduation from the National Central University in Chungking, I participated in a nationwide competitive examination and won the biology slot of what is known as the Boxer scholarships—a historically important gift of America to China in the wake of the Boxer rebellion (endnote 1). By the time the result of this examination was announced, I had enrolled in the graduate school of the National Tsing Hua University in Kunming. My roommate there, C. N. Yang—who, with T. D. Lee, was to be awarded the Nobel prize for physics in 1957—won the physics slot. Full of high hopes and wonderment, we flew over the Himalayan “hump,” and sailed from Calcutta. On a cold November afternoon in 1945, we first saw, through snow flurries, New York City’s looming majestic skyline.

With the encouragement of Prof. C. O-Yang, Head of the Department of Biology at the National Central University, I had taken many elective courses and read fairly extensively in order to prepare myself to study mechanistic biology (e.g., cell physiology). I came upon Ralph W. Gerard’s monograph: “The Unresting Cells” (Harper, 1940). I admired the “holistic” approach in his concept of the living cell. After the announcement of the result of the Boxer examination, I approached Dr. Gerard and was accepted as his graduate student in the world-famous Department of Physiology at the University of Chicago. From the time I knocked on the door of his third-floor office in Abbott Hall until his untimely death in 1974, Dr. Gerard had been unfailingly an inspiring and caring teacher as well as a scientist of lofty stature and broad vision.

Shortly after my arrival in Chicago, I met Dr. Steven W. Kuffler, who later offered me my first job in his laboratory at the Wilmer Institute of Ophthalmology, Johns Hopkins Medical School in Baltimore. In his kindly and generous way, he gave me full freedom to pursue my own direction of research.

It was in the Welch library—named after Dr. Henry Welch who had played an important historical role in bringing American medicine and medical research to the forefront of the world—where I spent much time browsing and just thinking. It was in this library I first conceived of a radically new mechanism for a major mystery of the living phenomenon: the ability of living cells to selectively accumulate potassium ion over the highly similar sodium ion (see Section 6.2.4.). In Baltimore I had another piece of great fortune, i.e., meeting and later marrying the beautiful and talented concert-pianist, Shirley Wong.

By this time Dr. Gerard had moved his staff from the University of Chicago to the Neuropsychiatric Institute (NPI) of the University of Illinois Medical School, also located in Chicago. He offered me an opportunity to continue my research in the well-equipped laboratory which he had designed.

At NPI, I wound up the experiments proving beyond any doubt in my mind that there is not enough energy for frog muscle (and other living cells) to operate the postulated sodium pump (as part of the so-called membrane-pump theory). The sodium pump was postulated to explain the same phenomenon mentioned above: the selective accumulation of potassium over sodium ion in living cells. It was at NPI I began to lay the foundation of the new general theory of the living cell that I was to launch later.

After Dr. Gerard had accepted a new job elsewhere, I too accepted in 1957 a position at the newly inaugurated Department of Basic Research at the Eastern Pennsylvania Psychiatric Institute (EPPI) in Philadelphia. The enthusiasm of Dr. George Eisenmann had influenced my relinquishing my Associate Professorship at the University of Illinois and in saying goodbye once more to Chicago and to my able assistants: Arlene Schmolinski, Mary Carol Williams and Margaret Samuels.

In the environment provided by EPPI, at once carefree and intellectually exciting, I continued to develop (and test the predictions of) the new theory of the living cell, which was to be named the association-induction (AI) hypothesis. My research work progressed well with the able help of Leo Kushnir, Margaret Ochsenfeld, Marilyn Welsh, Jeanne Chen, Kathryn Kalis and Kay Slemmer.

Soon after my arrival at EPPI, I began to put down in writing *A Physical Theory of the Living State*. Even though I had the efficient secretarial assistance of Betty Jane Bruecker and later Shirley Ripka (I am indebted to both), the volume took almost five years to complete. However, before the book appeared in print, the atmosphere at EPPI abruptly changed. Eventually, I and most of the Senior Research Scientists of the Basic Research Department left EPPI. After that, the Department survived for a number of years until it was shut down permanently.

Shortly afterward, I met Pennsylvania Hospital's Frank Elliott, M. D., a brilliant neurologist with a dry sense of humor, a sharp wit and an amazing range of knowledge. We hit off famously from the very first meeting—and have remained great friends ever since. Indeed, in recognition of his friendship and the key part he played in sheltering and helping the further development of the association-induction hypothesis, I dedicated my second book *In Search of the Physical Basis of Life* (Plenum, 1984) to him and to his always interesting, original, and charming wife, "Gee."

Through Frank Elliott's efforts, the John A Hartford Foundation (established by the A and P estate) provided the fund for constructing on the ground of the Pennsylvania Hospital, a new laboratory at the corner of 7th and Delancey streets in the Society Hill area of Philadelphia.

The Pennsylvania Hospital was the first hospital in this country, founded by Benjamin Franklin and Thomas Bond in 1751. Its amphitheater, still beautifully preserved, once witnessed routine operations without anesthesia and later, the eloquence of Joseph Lister advocating aseptic surgery.

When I joined the Pennsylvania Hospital it was just beginning a renaissance; outstanding research-minded scientist-physicians like Frank Elliott were enticed from all over the world. Led by the capable, and enterprising president, H. Robert Cathcart, the Pennsylvania Hospital saw rapid growth and modernization and in time became once again an outstanding hospital in the country. Illustrious and rich in history, prosperous and modern in its current fame, Pennsylvania Hospital was the home of the association-induction hypothesis for the next 27 years.

Soon after my arrival at the Pennsylvania Hospital, my first book, *The Physical Theory of the Living State* (Ling 1962) was published by the Blaisdell Publishing Company, a branch of Random House. The new theory was intended to replace the membrane-pump theory, but it offers much more. Though diverse in coverage, the new theory tells a "whole story," built upon a set of self-consistent basic postulates. In this aspect, the AI hypothesis is totally different from the ad hoc membrane-pump theory.

However, the introduction of a new theory was only the beginning. It was during the ensuing 27 years at the Pennsylvania Hospital, that the theory was put to extensive worldwide tests; and confirmed: the purely scientific part of the revolution—replacing the membrane-pump theory by the corresponding part of the AI hypothesis—had been accomplished.

In this period of time, the financial support of our research came from four sources: the National Science Foundation, the John A. Hartford Foundation, the Office of Naval Research (ONR), and the National Institute of Health (NIH), with the lion's share coming from the last two institutions. For this support, I say thanks. However, I would like to recognize two outstanding scientist-administrators in particular: Dr. Arthur B. Callahan, Program Director of the Medical and Dental Branch, ONR and Dr. Stephen Schiaffino, Associate Director of the Division of Research Grant, NIH.

In my view, both Dr. Callahan and Dr. Schiaffino are capable scientists and thoroughly familiar with the past history of scientific progress (endnote 2), the innovative, iconoclastic nature of my work, and its potential value to the future of biomedical sciences. They also know that it would be grossly unfair, indeed extremely naive to ask those scientific peers, whose fundamental beliefs I have already proved wrong, to judge the merit or lack of it of my work.

Continually monitoring progress made by both sides, Dr. Callahan gave support for my work, as he knew well that virtually all of the U.S. research funds allotted to this general area of research, had been supporting work based on the conventional view.

Drawing a similar conclusion from his first-hand knowledge, Dr. Schiaffino introduced the ad hoc “Special Study Sections” comprising knowledgeable but neutral scientists. From experience, he also seemed to realize that it was imperative not to include in these Special Study Sections, any scientists who had subscribed to the membrane-pump theory exclusively and are thus by definition, my scientific enemies.

Suffice it to mention here that without the support of Drs. Callahan and Schiaffino—often at the risk of their own job security and chance of future promotion—as well as the dedicated efforts of the many neutral and fair-minded scientists reviewing my research proposals over the years, the chance of continuing our work would have been nil.

As the AI hypothesis continued to develop, independent scientists began to test the predictions of the AI hypothesis on their own initiative, using among other methods, nuclear magnetic resonance (NMR) technology. Notable among those scientists, who on the basis of their own research came to confirm the AI hypothesis were Dr. Freeman Cope, Dr. Carlton Hazlewood and later Dr. Raymond Damadian. Damadian’s discovery of the difference in NMR signals from the water in normal and those from cancer cells set the stage for his invention of the new diagnostic tool now known as magnetic resonance imaging or MRI mentioned earlier (see endnote 1 of Introduction).

For their important contribution in accomplishing much of the work described in this volume, I also acknowledge the skill and dedication of my research associates, in particular Margaret Ochsenfeld, Mildred Gale, Dobrilla Gabrilovich, Marsha Hurok, Patricia Shannon, Grace Bohr, Ellen Ferguson, Cheryl Walton, (the late) Sandy Will, Ann Sobel, Sigrid Jaweed, Kim Peterson, T. Jennine Bersinger, Marianne Tucker, Andrea Ostroski, Christine Vetter, Joanne Bowes, Mary Brady, Chris Murray, Dianne Graham, Dee Zodda, Ya-tsen Fu, Ze-ling Niu, Randy Murphy, John Greenplate, Christopher Reid, Mark Sellers as well as Emmar-Lee Jackson, and Melissa Antley. Thanks are also due to my able secretaries over the years: Diane Weinstein, Nina Primakov, Nancy Hunt, Janice Malseed, Marilyn De Feo, and Jean Brogan.

I thank also my postdoctoral students, Drs. Ignacio Reisin (from Buenos Aires), William Negendank, Wei-hsiao Hu (from the Chejiang Institute of Technology), and Zheng-lian Zhang (from the Beijing Institute of Biophysics), all having contributed very substantially to the success of the revolution.

I am also indebted to my many summer students. With few exceptions they have demonstrated extraordinary capability in absorbing new knowledge quickly and in successfully carrying out demanding experimental studies all within the spell of a summer vacation. They include Edward Rossomando, Harriet Wells, Victor Smollen, E. Denise Campbell, Susan Sneider, Young Kwon, John Baxter, Mark Whalen, Kathlenn Boyce, Mark Ling, Tim Ling, Ken Weiss, Jim Butler, Marion Kelley, Laurie Tomkins, David Blackman, Michael Balter, Davida Kohler, Robert Houle, Jim Wood, Alain D’Andrea, Margaret Stienman, Curtis Cooke, Michael Leitman, Andrew Fischer, Bing Hong Cheak, Howard Dubner, Gerri Magavaro, Andrew Rosen, Sharon Horowitz, Thea Kolebic, Jill Wright, Karen

Holmes, Lisa DiSanto, Anna Marie Maguire, John O'Leary and others. Much of their work has either already been published or will be.

As mentioned above, under the protective wings of Drs. Callahan and Schiaffino our work was fairly judged periodically by neutral scientists who consistently recommended continued support. Unfortunately, Dr. Callahan and Schiaffino eventually left their posts. The new administrators held entirely different views in regard to my work. Thus the new Director of Division of Research Grants, Dr. Jerome Green and his subordinates believed strongly that no one applicant should be treated differently from all the others, and accordingly insisted that the new (in-name-only) Special Study Sections must include scientists from both sides. My repeated protests were to no avail. Strongly dominated by my scientific opponents in the panel—who have never openly defended their membrane-pump theory in public against my published refuting evidence, nor challenged in print the AI hypothesis and the confirmatory supportive evidence gathering in the literature for well over a quarter of a century—the panel “massacred” all three renewal proposals and NIH withdrew all its support. In consequence, my laboratory was forced to close on October 31, 1988 at the height of its productivity.

Since the Pennsylvania Hospital had no resources to support my research, the termination of all my research grants spelled the end of my salary and my research. There was no time left to complete the writing of this volume, no time to obtain a publisher, and no time to write up and publish the large amount of data essential in rounding up the logic of the revolution. It then dawned on me that the revolution so near completion might yet be buried alive forever.

Then from Long Island, my friend, Raymond Damadian came to my rescue. Seven large trucks came to Philadelphia and moved my entire laboratory to Melville, New York. Along with me also came my long-time associate, Margaret Ochsenfeld, and an associate of more recent times, Zhen-dong Chen. I completed the writing of the present volume and eventually signed a contract with Krieger Publishing Company of Melbourne, Florida. *The survival of the revolution was assured.* In our new environment, my little team soon rose up to a new challenge: to continue basic and cancer research in directions which enhance the chance of the long-term financial success of our host corporation.

The survival of the revolution was assured, because once published, the book will be in safe keeping in many libraries throughout the world, awaiting those scientists, young and old, who understand the nobility, purity and goodness in searching for the truth, in caring for the happiness and suffering of other human beings, and treasure both objectives far above money, power, prestige and public acclaim.

In closing this brief account of the history of this revolution, I want to say thanks to five categories of people not already acknowledged above: my scientific friends; colleagues at the Fonar corporation; Pennsylvania Hospital administrators; my publisher and his staff; and my family.

I have dedicated this volume to my friend, Raymond Damadian and his gracious wife, Donna. The fact that he had made it possible for me to publish this

volume and to survive as a working scientist adds yet another testimonial to his great friendship, his profound understanding of the role of correct basic knowledge to the development of beneficial practical applications, and his unshakable dedication to the common good of mankind.

The year 1973 not only saw the crisis in financial support for my laboratory, it also marked the beginning of increasing difficulties I encountered trying to publish my work in the scientific journals that had published my earlier work. It was Adam Lis and Diane Maclaughlin's introduction in 1969 of the journal *Physiological Chemistry and Physics* (PCP) that has made it possible to document the rapid progress we made in years following. Raymond Damadian (with Freeman Cope) acquired the journal in 1976 and again and again rescued it from bankruptcy before it was eventually on an even keel. This is an occasion for me to thank Adam Lis and Diane Mclaughlin for creating this journal and to point out how in yet another way Raymond Damadian contributed to the completion of this revolution and to the freedom of expression in biomedical sciences.

To the late Freeman Cope and to Carlton Hazlewood, I am deeply indebted for many reasons. As an example I may mention that without their introduction of NMR method to test my theory of cell water, Raymond Damadian might never have invented MRI. Without Raymond Damadian's invention of MRI, he might not have the necessary means to save my scientific life and the revolution.

How Carlton Hazlewood has maintained his scientific integrity and unswerving dedication to searching for truth in the trying environment he had to face from day to day commands respect from all who study the history of this scientific revolution.

To my long-time friend from our student days, physicist C. N. Yang and his profound knowledge about physics I owe much for the theoretical development of the cooperative aspect of the association-induction hypothesis. I also thank George Karreman, Bud Rorschach, Jim Clegg, Ivan Cameron, Charles Trombitas for their contribution to this volume; Walter Drost-Hanson, Herbert R. Catchpole, Milton B. Engel, for their friendship and support as well as constructive criticisms over the years. In particular, I want to thank Gerald Pollack for the time and efforts he spent in trying to rescue my laboratory from closing, and his many constructive criticisms and valuable suggestions that became a part of the present volume.

After losing so many of my one-time young comrades-in-arms, the continued friendship and unswerving loyalty (to the highest ideal shared) of Ludwig Edelmann of Homburg, Germany and Miklós Kellermayer of Pécs, Hungary are treasured and acknowledged with both gratitude and admiration. For maintaining his scientific honesty, Ludwig Edelmann had not only lost his job, but also the chance of continuing the career as a biophysicist for which he had been trained. Yet he had the resilience, resourcefulness and scientific originality to maintain his status as a first rate scientist, only switching to a different tool of investigation: electron microscopy. As an electron-microscopist, he has continued to introduce new methods leading to the capture of the *living state* in thin cell sections (see chapters 3 and 4) and to the vindication of the validity of his earlier conclusion concerning the true nature of the living cell.

Miklós Kellermayer's ability in carrying on first-rate research under difficult conditions and his special talent in inspiring a large group of young Hungarian scientists to examine and test the association-induction hypothesis are both important and timely. For these young scientist may very well become the vanguards of the new generation of scientists to lead the future world of biology and medicine. With this thought in mind, and with a very warm heart and many thanks, I welcome the succession of young Hungarian scientists from Miklós Kellermayer's group in Pécs, who have been writing me, communicating with me on science and best of all, coming to visit me at Melville. They include Attila Misetta, Peter Bogner, Szabolcs Somoskeöy, Tamas Henics and Eszter Nagy.

Once more I want to thank Margaret Ochsenfeld for her life-long dedication to her research work which has contributed so much to the completion of this revolution; and for her newly acquired responsibility in taking care of the publication of PCP, now bearing the name, *Physiological Chemistry Physics and Medial NMR*. For his vital help in moving my old laboratory and transporting it to a new location and for cheerfully carrying on research with our still limited facilities I thank also Zhen-dong Chen, the third member of my present laboratory staff.

Since our arrival at Melville, I have enjoyed the friendship and ever cordial hospitality of just about every member of our new host, the Fonar Corporation. Specifically, I thank Luciano Bonani, Kurt Reiman, Tim Damadian, Fred Peipman and their staff for many helps including the monumental task of moving my laboratory and equipment to its present location.

Of our friends at the Pennsylvania Hospital, I particularly want to acknowledge once more—as I did before with the publication of my second book, *In Search of the Physical Basis of Life* (Ling 1984)—the generous hospitality and efficient help from President H. Robert Cathcart, Vice President Harry Heston and all departments and their staff members. And with equal feeling, I acknowledge the occasional but as a rule timely financial assistance from the Hospital's General Research Support Fund.

I wish to express my appreciation to Robert Krieger of Krieger Publishing Company for publishing the present book. I say thanks to Marie Bowles, Krieger's production manager for her ever cheerful and efficient helpfulness; copy editor Miriam Champness for her meticulous, and thoughtful editing of the manuscript; Elaine Rudd for her constructive criticism and suggestions. This section will not be complete without my acknowledgement of J. Jarrett Engineering for the superb typesetting job it has done.

In my final acknowledgment, I want to remember with love, gratitude, (and infinite sadness), my ever-loving and scholarly father and mother (Mr. Yen-tze Ling and Mrs. Chi-lan Ho Ling) who gave me everything, but are no longer here to share with me this moment of triumph. I thank my brother (Morris Y. Ling) and his wife (Chuan-Yu Hua), for living by and passing on the family tradition of scholarship and excellence to their two children, my niece (Elizabeth) Ming-chu (Ling), and my nephew, (Robert) Ming-re, and for taking care of my ailing parents while I was far far away. I also want to thank my sister Nancy, Professor of microbiology at the University of California at Santa Barbara (and

her three attractive and accomplished children, James, Jennifer and Jackie) for a life-long close friendship from our earliest days.

With gladness I express my deep gratitude to my wife, Shirley for sharing my life. Her love of, and talent for classic music have enriched and added a new dimension to my life. Her teaching skill, and managerial ability combine to create a home at once cultured, purposeful, affectionate and well-run, making it possible for me to be engaged full time in my scientific pursuits, and for us both to raise three wonderful children, Mark, Tim and Eva. All have been nothing but constant sources of parental joy and pride since their arrival. They as well as their respective spouses Jenny, Kim and Neil have added to my life's journal, new frontiers of interest, abiding affection, and a great deal of happiness.

NOTES

1. In the year 1900, there was what has been known as the "Boxer Rebellion" in Beijing. In its aftermath, China paid indemnities to all eight nations involved. Japan used its indemnity money further to enhance its military power. America returned the money to found in Beijing the Tsing Hua University and an independent scholarship program. At two- or three-year intervals, some 20 "Boxer scholars" would be chosen in a nationwide, competitive examination open to all qualified college graduates. The winners, one in each field, would be given financial support to pursue graduate studies in the United States. Five groups of Boxer scholars had already successfully completed their much-coveted learning experience in America, when the Japanese invasion of China put an abrupt halt to the program.

Then in 1943 the program was activated once more—for the last time. For me, this resumption as well as its timing was a lucky break indeed: It was right after my graduation from the National Central University in Chungking, qualifying me for the competition. Good luck stayed with me and I won the biology slot.

2. Science progressed in the past not by a steady accumulation of knowledge, as had once erroneously been believed. Rather, steady accumulation of knowledge was interspersed by quantal jumps or revolutions. As result of each revolution, a set of long-held beliefs were replaced by a new constellation of ideas or what science historian Thomas Kuhn called "paradigm" (Kuhn 1962).

Kuhn separated scientists into two kinds: *normal scientists* whose scientific efforts follow conventional paradigms, and *revolutionary scientists* who introduce new ones. Pointing out that Kuhn's nomenclature is appropriate only for bygone scientists, I suggested the designations for *contemporary* scientists: Type 2 scientists (who follow accepted scientific practices and beliefs and are exemplified by Jonas Salk who developed the Salk vaccine) and Type 1 scientists (who go against conventional beliefs and practices and are exemplified by Louis Pasteur, who made the revolutionary discovery of bacterial and viral origin of diseases and vaccination) (Ling, *Physiol. Chem. Phys.* 10:95, 1978). *Only when Type 1 science has been proven to be correct does it become revolutionary.*

Both Type 1 and Type 2 scientists are necessary for the continued progress of science. Indeed, the discovery of Type 1 scientists provides the foundation for the Type 2 discovery of tomorrow. However, while Type 2 scientists strongly benefit from the Type 1 discovery of yesterday, *Type 2 scientists and their contemporary Type 1 scientists are at odds and natural enemies.*

At the end of the Second World War, the United States embarked on a new enterprise unknown before: large scale financial support of individual scientists for performing basic and practical research. This was an important and highly commendable undertaking. Unfortunately, the method chosen to award the money to some scientists while denying

it to others was not carefully thought through. As a result, the system hastily put together, and called the peer-review system, is strongly biased in favor of research that follows traditional ways of thinking (Type 2), while giving no consideration at all to Type 1 science. This system must be overhauled as soon as possible so that it will promote both Type 1 and Type 2 sciences.

INTRODUCTION

In this volume I present the essence of a major revolution in cell physiology, the first since the cell was recognized as the basic unit of life a century and a half ago.

In *A Physical Theory of the Living State* (Ling 1962), I presented decisive experimental evidence against the conventional membrane-pump theory of the living cell, and introduced a new and much broader theory called the *association-induction hypothesis*. Results of worldwide testing of my work in the twenty-one years following were cast in historic and contemporary perspective and published by Plenum in a monograph entitled *In Search of the Physical Basis of Life* (Ling 1984). Now, after several more years of intensive research, the revolution is finally completed and a new paradigm is launched.

Like many paradigms introduced in the past, this one holds great promise. In its brief history, it has already given rise to one life-enhancing diagnostic tool, magnetic resonance imaging (MRI).¹

Yet there has been strong resistance to the new concepts introduced. The extraordinary ferocity of this resistance may itself testify to the far-reaching importance of the present revolution. For, as pointed out by science historian I. B. Cohen, "Every . . . revolution in science has engendered an opposition among some scientists; the degree and extent of antagonism may even be taken as a measure of the profundity of the revolutionary changes . . ." (Cohen 1985, 18).

For reasons to be described, it is important that the revolution and the new opportunities it has created be made known to as many relevant persons as possible, and as soon as possible: To teachers, researchers, students, scientist-administrators, and science publishers, among others. This is because a correct basic theory of cell physiology, besides its great intrinsic value in mankind's search for knowledge about ourselves and the world we live in, will also play a crucial role in the ultimate conquest of cancer, AIDS, and other incurable diseases.

In the United States alone, a thousand men, women, and children die of cancer every day. AIDS is another killer, and as of now there is no cure. Nor is there assurance that AIDS will be the only deadly virus to confront mankind in the future. Drugs, our ultimate line of defense against fatal as well as nonfatal diseases, are still in a primitive state of development. So far, no drug has been created through understanding; most, if not all, were discovered by accident or by trial and error. But trial and error offers little hope in accomplishing complex objectives soon.

A nation that has achieved the proverbially impossible task of landing a human being on the moon has proven much less successful in conquering cancer and many other incurable diseases. To understand the cause of this disparity, let us consider the following thought experiment.

Suppose with the aid of a time machine we could send a transistor radio to Queen Victoria of England. Enthralled with this magic box, she breaks it by accident. The Queen vows to have it repaired at any cost. Yet we can advise her that no matter how much money she spends and how many scientific geniuses she enlists in her efforts, the radio cannot be fixed. That is, not until the basic knowledge of physics has matured; a transistor radio can then be repaired easily. War on cancer and war on AIDS cannot succeed yet for the same reason that Queen Victoria cannot repair her radio. There is not yet enough basic knowledge—in this case, cell physiology.

In its broad definition, cell physiology can be somewhat arbitrarily divided into two components. Genetics deals with what August Weisman (1834–1914) called “germ plasm.” Cell physiology proper deals primarily with what Weisman called “soma.” Before its recent spectacular development, genetics had already undergone two major revolutions, in which Charles Darwin and Gregor Mendel, respectively, played key roles. Large-scale federal research funding, beginning in the 1940s, then fueled dazzling progress. The deciphering of the genetic code testifies to the rapidity of progress guided by the correct theories. Yet the understanding of genetics alone is not enough; cell physiology proper must also be fully understood in order to provide the foundation for the conquest of cancers and other deadly diseases. **The ultimate aim of cell physiology includes the understanding of the most basic mechanisms underlying all living phenomena at the molecular and submolecular level.** Unfortunately, the version of cell physiology widely taught and subscribed to today has not reached the level of maturity genetics attained before the forties.

The hypothesis of the living cell widely taught as fact and explicitly serving as the foundation for most biomedical research, is called the *membrane-pump theory*. In this theory, interpretations of all the major physiological phenomena of the living cell are based on the assumption that the cell interior is in essence an aqueous solution of proteins, ions, and other small and large molecules. Postulated pumps in the cell membrane determine the chemical composition of the cell content at the expense of metabolic energy, *by molecular mechanisms still unknown*.

Theodor Schwann (1810–1882) founded the Cell Theory. Schwann argued then that all living cells and their nuclei are surrounded by a membrane, and that this membrane is prior in importance to its content. The content of the cellular cavity, i.e., of the interspace between the nuclear and cellular membranes was to Schwann typically a homogeneous, transparent liquid. In his view the cell membrane possessed “metabolic power” by which the membrane chemically altered the fluid substances adjacent to it—the *Zellenkeimstoff* outside and the cell content (*Inhalt*) within (see Hall 1969, 2:194). Comparing the current textbook version of the basic theory of cell physiology with what Theodor Schwann propounded in 1839, one is left with the almost incredible conclusion that little change has been made in this subject since Schwann’s time. Yet 148 years have gone by. To give us insight into just how long 148 years is, we need only recall that in 1900, physicists were not at all sure that atoms existed (Bronowski 1973, 351).

It is the purpose of this volume to document the full disproof of the membrane-pump theory and to document the verification of the association-induction hypothesis. It is only now that I can formally announce the completion of a revolution (in the area of cell physiology covered by the membrane-pump theory) because it is only now that all the requirements of a scientific revolution, listed in Chapter 12, have been met.

Why did it take 148 years to evolve a new paradigm? The purpose of cell physiology is not to discover new basic principles that govern the properties and behaviors of the entire universe. Rather, the purpose of cell physiology is to seek understanding of the unique set of natural phenomena we call “life” in terms of the principles of physics already understood from the study of the much simpler inanimate world. For this reason, the ideal time to study cell physiology would be after physics had solved all of the relevant problems. But as pointed out above, cell physiology was already old before physics had reached anywhere near its current state of maturity. As a result, correct early seminal ideas of cell physiology could not continue developing, and in time were checked and rejected, not because the ideas were wrong, but because the physics necessary for further development was not yet in existence.

The new theory of cell physiology, the association-induction hypothesis, traces its origin to the early perceptions of the gelatin-like properties of living matter, and of the unusual behaviors of water when associated with certain biomacromolecules, and referred to as *Schwellungswasser* or “imbibition water” (see Chapter 1).

Carl Ludwig (1816–1895) is often regarded as the father of modern physiology. With von Helmholtz, du Bois-Reymond, and Brücke, Ludwig overthrew the old vitalistic concept of life phenomena and inaugurated the physico-chemical approach familiar today. Ludwig discovered in 1849 that dried pig bladders, when soaked in a solution of sodium sulfate, took up much more water proportionately than they did sodium sulfate. He remarked that “the smallest components of the (bladder) membrane have a pronounced affinity for water—whether it is chemical or adhesive will one day be told us by chemistry when it lifts itself out of its present theoretical misery” (Ludwig 1849).

Seventy years later, J. R. Katz quoted this passage from Ludwig under the section title “Carl Ludwig’s Problem” in Katz’s paper entitled “The Role of Swelling” (Katz 1919). Katz then commented that chemistry had indeed lifted itself out of its theoretical misery, citing the work of van’t Hoff, Nernst, Ostwald, Arrhenius, Gibbs. Since Katz’s optimistic remarks, another seventy years have gone by.

Ironically, the theoretical work of the scientists Katz so proudly cited did little to promote the further understanding of either the observations of Ludwig or those of Katz. Instead, these scientists played key roles in the promotion and eventual acceptance of the membrane-pump theory. According to this theory, the cell interior is considered a dilute solution; the strong interaction of water with the bulk of the dry matter of living cells, observed by Ludwig and studied by Katz, is considered of minor or no significance. Nor was this outcome surprising. The work of most of these noted scientists dealt primarily with the

properties of *dilute solutions* and with physico-chemical manifestations associated with dilute solutions. Thus van't Hoff's law of osmosis, improperly applied, gave the initial impetus to the acceptance of the membrane theory (see Section 10.1); Arrhenius's theory of ionic dissociation, also improperly applied, became a major roadblock to the recognition of the role of ionic adsorption on proteins in cells (Section 4.2). The work of Ostwald and Nernst played key rôles in the development of the earlier membrane theory of cellular electrical potentials (Section 11.1). It is only in the much more recent past that physicists have moved rapidly forward into an area of knowledge that is of direct relevance to the focal interests of Ludwig, of Katz, and of myself.

A branch of modern physics of great importance, statistical mechanics, was pioneered by the great physicist Ludwig Boltzmann. Statistical mechanics has provided the broad conceptual framework on which the association-induction hypothesis is built (Ling 1952, 1962). The great theory of Boltzmann and the theories of physicists de Boer, Zwikker, and Bradley, as well as the association-induction hypothesis, have provided answers to Ludwig's questions and given new insights into the importance of the work of J. R. Katz. (See Section 5.2.5.3, including endnote 5 of Chapter 3.)

It has become increasingly clear that the fundamental laws of physics, even since the maturation of the science, are often too "remote" to be directly applicable to cell physiology. To explain complex living phenomena, cell physiologists must spend time developing and extending their specialized area of physics, and testing it out on inanimate models which are more complex than those physicists usually deal with—but far less complex, and thus more likely to provide unambiguous answers, than the living cells themselves.

History thus shows why a new paradigm of cell physiology could not have evolved earlier. History also shows us that, following a scientific revolution, only young and forward-looking scientists are able to fairly assess the value of and eventually inherit a new paradigm. Witness three of the world's greatest revolutionaries in their own words:

"I do not expect my ideas to be adopted all at once. The human mind gets creased into a way of seeing things. Those who have envisaged nature according to a certain point of view during much of their career, rise only with difficulty to new ideas. It is the passage of time, therefore, which must confirm or destroy the opinions I have presented. Meanwhile, I observe with great satisfaction that the young people are beginning to study the science without prejudice. . . ." (Lavoisier, *Reflections on Phlogiston*)

"Although I am fully convinced of the truth of the views given in this volume . . . , I by no means expect to convince experienced naturalists whose minds are stocked with a multitude of facts all viewed, during a long course of years, from a point of view directly opposite to mine . . . but I look with confidence to the future,—to young and rising naturalists, who will be able to view both sides of the question with impartiality." (Darwin, *Origin of Species*)

"A new scientific truth does not triumph by convincing its opponents and making them see the light, but rather because its opponents eventually die, and a new generation grows up that is familiar with it." (Planck, *Scientific Autobiography*)

To facilitate familiarity with this new theory and its broad implication, I have composed this volume in a certain way.

(1) It is concise, yet it contains extensive references to the more comprehensive foundational work *In Search of the Physical Basis of Life* (Ling 1984), offering its readers easy access to rich historical and contemporary background materials. Familiarity with these background materials will in turn provide the kind of firsthand, authoritative knowledge that inspires the self-confidence and the intellectual independence for studying science without prejudice, and for further developing and exploiting a new paradigm.

(2) It deals with all basic aspects of cell physiology as a harmonious and integral whole. Once this self-consistent, theoretical basis is mastered, a young researcher may discover new orders and perspectives in what may seem mere mountains and mountains of scientific “news” of bygone days.

(3) Most important of all, the volume reveals what may be startling to some and yet should be reassuring to all: At the most fundamental level, life phenomena are in fact not only coherent but simple. This simplicity forecasts great opportunities for rapid progress, both in terms of true understanding of living phenomena and in terms of practical application of knowledge obtained. Indeed, the time might not be too distant when we can cure cancer and eliminate other fatal diseases just as easily and routinely as we can repair Queen Victoria’s faulty transistor radio.

NOTES

1. MRI scanning, which allows continued quantitative investigation and monitoring of normal and diseased human body parts without surgery or x-ray irradiation, was invented by Dr. Raymond Damadian, holder of the patent (U.S. Patent 3,789,832), who wrote me on November 9, 1977: “On the morning of July 3, 1977, at 4:45 A. M. . . . we achieved with great jubilation the world’s first MRI image of the live human body. The achievement originated in the modern concepts of salt water biophysics [introduced by] your treatise, the association-induction hypothesis.” The homemade MRI scanner on which the first MRI image of a live human body was made, named “Indomitable” (see Damadian et al. 1977, Kleinfield 1985) is now on exhibit in the Smithsonian Institution, Washington D.C. (Hall of Medical Science, National Museum of American History). Dr. Damadian was awarded the National Technological Award by President Ronald Reagan on July 15, 1988. He was inducted into the National Inventors Hall of Fame on February 12, 1989.

EARLY THEORIES OF THE LIVING CELL

1.1. *Life and Death of a Living Cell*

The fact that a healthy human baby can develop from an embryo once frozen in liquid nitrogen throws doubt on criteria once widely believed to define life. Metabolism, excitability, locomotion, growth—these basic biological activities come to a halt at very low temperatures; life, if it were correctly defined by these activities, might be considered terminated. If ongoing activity does not correctly define life, what does?

In seeking a definition of life at a fundamental level, we must focus our attention on the living cell, the basic unit of all life. Our first question might be: “What is the difference between a living cell and a dead one? How can one tell them apart?”

A method using vital dyes can readily differentiate a dead cell from a live one. When one exposes a mixture of live and dead cells to a dye like trypan blue, erythrosine, or nigrosin, one can visually differentiate live cells from dead, because only dead cells stain deeply, while live ones do not.

The effectiveness of the dye method in differentiating between live and dead cells reflects the living cell’s ability to maintain, at once, both continuity with and discreteness from its environment. This dual ability is most conspicuously displayed toward the pair of alkali ions, K^+ and Na^+ , found in the cell’s natural environments. Though K^+ and Na^+ are chemically very similar, only K^+ is accumulated in most living cells to a level many times higher than in the surrounding medium. In contrast, the concentration of Na^+ in the cell is, as a rule, many times lower than that in the external medium (Figure 1.1). When a cell dies, the levels of these ions in the cell change sharply and abruptly in opposite directions: Na^+ rises and K^+ falls, to equal or approximate, respectively, the level of Na^+ and K^+ in the external milieu.

In trying to understand the mechanisms underlying the living cell’s ability to maintain discrete chemical composition as exemplified by K^+ and Na^+ , one asks a more general question: “What mechanisms are there that can maintain the level of a substance in one space at a different level from that in an immediately adjoining space?” In broad principle, there are three types of mechanisms.

Consider the case of a camper in a mosquito-infested camping site. To keep mosquitoes away, the camper might rely on one of three methods: he or she

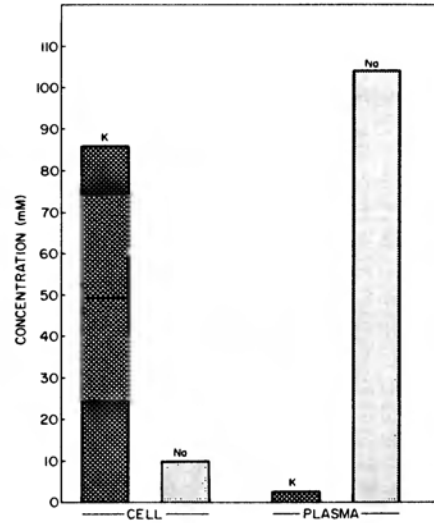


Figure 1.1. Equilibrium concentrations of K^+ and Na^+ in frog muscle cells and in frog plasma (Ling 1984, by permission of Plenum Publishing Co.)

could use a mosquito net, which acts as a *permanent barrier* (Type I); try to catch approaching mosquitoes and throw them away, or use any other more sophisticated *energy-consuming mechanisms*, unceasingly removing mosquitoes which steadily invade the defended space (Type II); or spray the site with an insect repellent, giving the site *attributes that repel mosquitoes* (Type III).

In this and the following two chapters, I will demonstrate how the equivalent of each of these three types of mechanisms has been invoked to explain the asymmetrical Na^+/K^+ distribution in living cells. To recount the full story, I begin with a brief history of early cell physiology.

1.2. *The Cell Theory and the Protoplasmic Doctrine*

Between 1835 and 1840, two major events occurred that were to set the course for the future development of cell physiology: Schwann's announcement of the *cell theory* (1839) and Dujardin's description of what was to be known as *protoplasm* (1835).

It is worthy of note that in Schwann's original theory of the cell¹ "the containing membrane—of cell or nucleus—was prior in importance to its contents" and control of cellular activities resided in the cell membrane—including the ability to (chemically) alter the fluid outside and inside the cell (see Hall 1969, 2:194). It is amazing how similar Schwann's original view of the living cell was to that taught in most textbooks today.

Felix Dujardin described a "pulpy, homogeneous, gelatinous substance," a substance which he recognized as a *living jelly* and to which he gave the name "*sarcodé*" (1835, 1838). Dujardin's sarcodé eventually became known as "*protoplasm*." In announcing the *protoplasmic doctrine*, Max Schultze (1825–1875), sometimes called the father of modern biology, regarded living cells as "mem-

braneless little lumps of protoplasm with a nucleus" (Schultze, 1861). Thus the divergent emphases on the cell membrane and on protoplasm were well established long before the introduction of the concept of colloids by Thomas Graham, to be described in the next section. The founding of the "membrane theory" by plant physiologist Wilhelm Pfeffer will be described in the section after that.

1.2.1 *Gelatin as Model of Protoplasm*

Felix Dujardin was not the first to describe protoplasm as *gelatinous*. In this, he only reiterated similar observations made during the entire century before, including those of Abraham Trembley, of C. F. Wolff, of Dane Otto Frederick Müller, and of Treviranus.

In 1861, Thomas Graham introduced the term *colloid* and the "*colloidal condition of matter*" in these words: "The comparatively 'fixed class' (of substances) . . . is represented by a different order of chemical substances . . . They are distinguished by the gelatinous characteristics of their hydrates . . . As *gelatine appears to be its type, it is proposed to designate substance of the class as colloids* (κωλλα, glue or gelatin) and to speak of their peculiar form of aggregation as the colloidal condition of matter" (Graham 1861, 183, italics mine). Thus, by coining the word colloid, Graham focussed attention on an often-observed, common set of attributes of living protoplasm which are also detected in gelatin. Among the various colloidal materials he studied was copper ferrocyanide gel (see Tinker 1916).

1.2.2 *Copper Ferrocyanide Gel as a Model of Plasma Membrane*

After Graham discovered that substances in a colloidal state cannot pass through dialysis membranes,² which were nevertheless quite permeable to water, Moritz Traube (1867) found a way to prepare an artificial semipermeable membrane. Such a membrane was formed when a solution of copper sulfate is brought into contact with a solution of potassium ferrocyanide. Once formed at the boundary, the copper-ferrocyanide gel membrane acts as a barrier to the further diffusion of both copper and ferrocyanide and hence to the further precipitation of more copper ferrocyanide.

To explain the permeability of the copper-ferrocyanide gel membrane to water, but not to various ions and sucrose, Traube proposed an "atomic sieve" theory. In this theory, copper-ferrocyanide gel has pores large enough to allow the passage of water, but not of copper or ferrocyanide ions. However, this theory was not supported by subsequent investigations, which revealed pore sizes of the membrane to be too large to act as a mechanical sieve when compared to the molecular sizes of the impermeant solutes (Findlay 1919, 95; Bigelow and Bartell 1909; Bartell 1911; Tinker 1916; Glasstone 1946).

Plant physiologist Wilhelm Pfeffer investigated osmotic phenomenon with the aid of a copper-ferrocyanide gel membrane made durable by being formed in the interstices of the wall of a porous pot. This model membrane is one of the best artificial semipermeable membranes ever known. The accurate experimental

data which Pfeffer obtained eventually led physico-chemist van't Hoff to the formulation of the law of osmosis and Pfeffer himself to the founding of the membrane theory (Pfeffer 1877).

1.3. *The Membrane Theory*

After Pfeffer's 1877 founding of the membrane theory, the cell membrane was considered permeable to water, but impermeable to both K^+ and Na^+ (Hamburger 1904). Later, the permeability of the cell membrane to K^+ was recognized (Mond and Amson 1928; Fenn and Cobb 1934; Hahn et al. 1939). In 1941 Boyle and Conway presented a comprehensive theory of the living cell which marked the peak of the development of the original (Type I) membrane theory.

The Boyle-Conway theory incorporated: (1) Netter's idea of the cell as representing a system following Donnan's theory of membrane equilibrium (Donnan 1924, Netter 1928; also endnote 6 of Chapter 2); (2) Mond and Amson's idea of cell membranes with rigid, sieve-like pores permeable to small hydrated K^+ but not to large hydrated Na^+ (Mond and Amson 1928); and (3) Boyle and Conway's own idea—contrary to prior belief—of the permeability of muscle cell membrane to Cl^- . Boyle and Conway's theory did not give due credit to Netter, and Mond and Amson, for the key ideas earlier published.

Boyle and Conway's theory explains selective membrane permeability of K^+ , selective accumulation of K^+ over Na^+ in terms of critical membrane pore sizes, cell-volume changes in solutions containing different concentrations of KCl as reflecting muscle cells behaving like osmometers (see Section 10.1), and the cellular resting potential (Ψ) as a *membrane potential*. This concept was first suggested by Ostwald (1890) and propounded by Bernstein (1902):

$$\Psi = \frac{RT}{F} \ln \frac{[K^+]_{in}}{[K^+]_{ex}}, \quad (1)$$

where R , F , and T are the gas constant, the Faraday constant, and the absolute temperature respectively. $[K^+]_{in}$ and $[K^+]_{ex}$ are the intracellular and extracellular concentration of K^+ .

The Boyle-Conway membrane theory rests upon the popular belief at that time that cell membranes were impermeable to Na^+ , a belief which in turn rests upon the observation that cells shrink and remain shrunken in solutions containing high concentrations of Na^+ . It was *assumed* that the cell membrane is impermeable to a solute which at a high concentration causes sustained cell shrinkage. (However, this assumption is wrong, see Section 10.2.1.2.)

Table 1.1, taken from Boyle and Conway, shows how in their theory a critical membrane-pore size permits passage of the smaller hydrated K^+ , H^+ , Cl^- but not that of the larger hydrated Na^+ , Li^+ , and Mg^{++} . Boyle and Conway's theory invoked a bona fide Type I mechanism in which the cell membrane acts like a mosquito net.

It is ironic that the Boyle-Conway Theory, the first theory capable of explaining coherently such a wide variety of cell physiological phenomena, should have

Table 1.1. Boyle-Conway Theory of the Segregation of Permeant and Impermeant Ions According to the Mobilities and Relative Diameters of Cations and Anions^a (Ling 1984)

	Velocities of ions under gradient of 1 V/cm or 0.5 V/cm for divalent ions				Relative ion diameters (diameter of K ⁺ = 1.00)			
	Cations		Anions		Cations		Anions	
Permeant ions	H ⁺	315.2	OH ⁻	173.8	H ⁺	0.20	OH ⁻	0.37
	Rb ⁺	67.5	Br ⁻	67.3	Rb ⁺	0.96	Br ⁻	0.96
	Cs ⁺	64.2	I ⁻	66.2	Cs ⁺	1.00	I ⁻	0.97
	NH ₄ ⁺	64.3	Cl ⁻	65.2	NH ₄ ⁺	1.00	Cl ⁻	0.98
	K ⁺	64.2	NO ₃ ⁻	61.6	K ⁺	1.00	NO ₃ ⁻	1.04
Impermeant ions	Na ⁺	43.2	CH ₃ COO ⁻	35.0	Na ⁺	1.49	CH ₃ COO ⁻	1.84
	Li ⁺	33.0	SO ₄ ²⁻	34.0	Li ⁺	1.95	SO ₄ ²⁻	1.89
	Ca ²⁺	25.5	HPO ₄ ²⁻	28	Ca ²⁺	2.51	HPO ₄ ²⁻	2.29
	Mg ²⁺	22.5			Mg ²⁺	2.84		

^aAfter Boyle and Conway (1941), by permission of *Journal of Physiology*.

enjoyed such a short life. Thus the cell membrane was postulated to be impermeable to hydrated Mg⁺⁺, because the ion is, according to the authors, 2.84 times bigger than hydrated K⁺ (Table 1.1). Yet four years before Boyle and Conway's masterful article of 1941 appeared in print, Mg⁺⁺ had already been shown to be permeant to muscle cell membrane. Even more startling, this finding was made in Conway's own laboratory (Conway and Cruess-Callaghan 1937, see also endnote [6] of Chapter 11).

From 1939 on, the availability of radioactive Na⁺ made possible the rapid establishment that the cell membrane is, contrary to traditional belief, quite permeable to Na⁺ (Cohn and Cohn 1939; Heppel 1939, 1940; Brooks 1940; Steinbach 1940). With these demonstrations, a great theory of the living cell built on the atomic sieve idea collapsed.

Disproof of the classic membrane theory, which explains K⁺ and Na⁺ segregation in terms of the membrane-barrier mechanism, left cell physiologists with only two alternatives: the protoplasmic theory, in which the cell interior has physiochemical properties different from the aqueous solution bathing the cells (a Type III mechanism); or a Type II mechanism, an "adenoid" or secretory mechanism—the forerunner of the membrane-pump concept to be described in the next chapter.

In the year 1940, participants in the Cold Springs Harbor Symposium on quantitative Biology witnessed a trend toward the protoplasmic theory. Thus B. Steinbach gave a paper of this kind (Steinbach 1940a). Eric Ponder argued against simple osmometer interpretation of the behaviors of red blood cells (Ponder 1940). S. C. Brooks (1940) also talked about ion permeability as an ion-exchange phenomenon seen in zeolites and soils. Shortly afterward, Brook's student, Lorin J. Mullins, even announced the demonstration of "Selective Ac-

cumulation of Potassium by Myosin" (Mullins 1942). However, these initial moves toward the protoplasmic theory proved short-lived. Mullin's preliminary report was not confirmed (see Steinbach 1940a, 251; Lewis and Saroff 1957). Momentum was beginning to gather against the protoplasmic theory, threatening to destroy it altogether. We can review the events that led to this state of affairs.

1.4. *The Protoplasmic Theory and Colloid Chemistry*

In 1908 Moore and Roaf had suggested that cell K^+ , the most abundant intracellular ion, is bound in the cell, like oxygen in erythrocytes. Martin Fischer and his coworkers believed protoplasm to be a hydrated colloidal system (Fischer and Moore 1907; Fischer 1921). In the 1920s, Ernst and Scheffer (1928) and Neuschloss (1926) suggested that the K^+ in cells exists in a bound and un-ionized form. In 1938, Fischer and Suer further suggested that protoplasm was "a union of protein, salt and water in a giant molecule" (Fischer and Suer 1938). Water in the protoplasm, in the view of Fischer and Suer, was not free but existed in a combined form.

In the early days of biology, the concept developed that water associated with living matter may exist in an altered form. Such altered water has often been referred to as "*Schwellungswasser*," "imbibition water," or simply "bound water" (Gortner 1938; Ling 1984, 44). In the 1920s and 1930s, bound water was often demonstrated and estimated by two methods. One method relied on the belief that bound water is "non-freezing" at temperatures well below the freezing point of normal water (i.e., $0^{\circ}C$) (Rubner 1922; Thoenes 1925; Robinson 1931; Jones and Gortner 1932). Another method relied on the belief that bound water is *nonsolvent* (i.e., it does not dissolve solutes), therefore, when sucrose is added to biological fluid containing bound water, the freezing point depression should be greater than if all the water is free. This method was used most extensively by Gortner and his coworkers in their studies of bound water (Newton and Gortner 1922; Gortner and Gortner 1934). Proponents of the protoplasmic concept were at least able to hold their own until two papers from Nobel Laureate A. V. Hill appeared in the *Proceedings of the Royal Society of London* in the year 1930.

In one paper, Hill showed that urea distributed equally between muscle cell water and the external medium (Hill 1930). Based on this finding, Hill announced that no nonsolvent bound water exists in frog muscle. In the second paper, Hill and Kupalov (1930) measured the vapor pressure of frog muscle and, not surprisingly, found it equal to that of an isotonic NaCl solution. Since no bound water exists in the muscle cells, so Hill argued, the major intracellular ions (mostly in the form of K^+ and organic phosphates) must also be free in order to balance the osmotic activity of indisputably free Na^+ and free Cl^- in the isotonic NaCl solution with which the cell is in osmotic equilibrium.

In support of Hill's conclusion that there is no nonsolvent water in living cells, McLeod and Ponder (1936) found that ethylene glycol also distributes equally between red blood cell water and the external medium. McLeod and Ponder's

finding was in turn confirmed by Hunter and Parpart (1938) who demonstrated equal distribution of ethylene glycol between water in frog abdominal muscle and the surrounding medium. In a comprehensive review on "Bound Water," Blanchard (1940) refuted the concept of non-freezing water by citing the observed non-freezing or supercooling of normal liquid water to as low as -20°C (Dorsey 1940). He contended further that it is not possible to meaningfully measure the freezing point of water in a protein solution or in cell protoplasm because the solid materials present would block ice crystal formation and propagation.

E. Ernst (1895–1981), whose work with Scheffer I have already mentioned, later recollected that it was primarily Hill's findings, just described, that dramatically altered the future course of cell physiology (Ernst 1963, 112).³ Overnight, the earlier concepts of bound K^+ and bound water were abandoned by the opinion-makers of the day, including R. Höber, W. O. Fenn, and F. Buchtal, in favor of a view of the living cell as a membrane-enclosed solution of free ions and free water much as Schwann had first suggested in his cell theory of 1834.

In the meantime, colloidal chemists relied more and more on the large molecular sizes as the distinguishing feature of colloids, and colloid chemistry soon lost its identity amidst the rising tide of macromolecular chemistry (Ferry 1948). The rejection of colloid chemistry was dramatically demonstrated by the merging of the *Journal of Colloid Chemistry* with the *Journal of Physical Chemistry*. These became for a while the *Journal of Physical and Colloid Chemistry*; the word colloid was dropped from the title a little later.

Thus the 1940s not only saw the end of the original Type I membrane theory, but also witnessed the demise of the original Type III (protoplasmic or colloidal) theory of the living cell. It was natural that the majority of cell physiologists turned to the only remaining mechanism, Type II, the pump.

NOTES

1. Reviewer Hall (1969, 2:208) pointed out that in later years "Schwann seemed to have been influenced by interim events not to change what he formerly said but to re-represent it in terms that conform more closely to discoveries made by others during the decades immediately following the presentation of the theory. . . ." Hall then continued, "The danger is constant in science that the parental concept will smother the new discoveries it spawns. . . ."

2. Although Graham spent his entire scientific life studying diffusion, and did not deal directly with living phenomena as such, his work provided a physico-chemical foundation for the future study of living phenomenon. Graham also invented "dialysis."

3. Ernst (alias Ernst Jenő in Hungarian) was a Jewish Hungarian scientist of originality, integrity, and perseverance who was able to survive the incredible hardships of World War II, and lived long enough to witness all of these developments.

THE MEMBRANE-PUMP THEORY

2.1. *The Origin of the Membrane-Pump Hypothesis*

Theodore Schwann, the founder of the cell theory, had believed that the cell membrane possessed “metabolic power” to control the chemical composition of the fluids adjacent to it—both the *Zellenkeimstoff* outside and the *Inhalt* (cell content) within (Hall 1969, 2:194).

Some sixty years later, E. Overton, a distant cousin of Charles Darwin, gained fame for his studies of cell physiology and his “lipoidal membrane theory.” In this theory, all living cells were covered by a continuous lipid membrane. Overton recognized that salt ions, though impermeant through a lipid membrane, nevertheless were accumulated inside plant cells. To explain the passage of lipid-insoluble substances into cells, he suggested what he called “adenoid” or “secretory activity” (Collander 1959, 9). However, he made no suggestion concerning the mechanism for this postulated adenoid activity.

Later yet, citing earlier failure to demonstrate significant binding of K^+ by isolated proteins (to be further discussed in Chapter 4), R. S. Lillie reasoned that K^+ accumulation in cells could not be due to binding. To explain the low level of Na^+ in cells, Lillie argued that “Either the (Na^+) salts do not diffuse across the membrane [a concept soon to be proven wrong (Section 1.3)] or some active physiological factor is at work which opposes or compensates for the effect of diffusion . . .” (Lillie 1923, 117).

Strangely, it is Robert Dean who has become widely quoted as the founder of the Na Pump Hypothesis. However, his advocacy was neither original nor enthusiastic, nor was it backed by extensive original work of his own on the subject. Rejecting the selective K^+ accumulation in, and Na^+ exclusion from cells as a result of different permeabilities of the cell membranes to K^+ and Na^+ in different directions—which Dean correctly pointed out was a “Maxwellian demon”¹ and not acceptable—Dean concluded his writing on “The Pump Theory” in these words: “It is safer to assume that there is a pump of unknown mechanism which is doing work at a constant rate excreting sodium as fast as it diffuses into the cell” (Dean 1941, 346).

We can note that, in stature, the sodium pump theory is by far a poorer theory than the membrane theory of Boyle and Conway, for the following reasons:

(1) The membrane theory was a general theory. It attempted to deal with the distribution of *all* solutes in living cells. The Na pump theory has never attempted to offer more than an *ad hoc*, patchwork theory dealing with *one* solute, Na^+ . Nearly half a century after the disproof of the atomic sieve theory of Boyle and Conway, no one has yet given even a rough estimate of just how many pumps are required to keep the cell “afloat.”

(2) Though proven wrong later, Boyle and Conway’s membrane theory offered a mechanism: the atomic sieve. In contrast, the sodium pump theory has ben without a mechanism since its inauguration. This lack of a mechanism was clearly stated by Dean in 1940 (see above). Thirty-five years later, the theory was still without a mechanism: in the first-of-its-kind review on the “Na Pump,” Glynn and Karlish (1975) apologized for not being able to compare “the great mass of work that has been done” with a “hypothesis accounting for the working of the pump,” because “no such hypothesis exists . . .” (p. 13).

2.2. *The Excessive Energy Need of the Na Pump: A Decisive Disproof*

The Na pump discussed here refers only to the pump postulated to account for the sustained low level of Na^+ in cells like muscle cells, nerve cells, and erythrocytes. These cells have a single type of cell membrane covering the whole cell and are referred to as “unifacial cells” (Ling 1984, 585). Epithelial cells of frog skin, intestinal mucosa, kidney tubules, etc., on the other had, have two different types of membranes and are referred to as “bifacial cells.” Active transport of Na^+ and other solutes *across* bifacial cells is not disputed and is in harmony with the AI hypothesis. For a molecular mechanism of active transport across bifacial cells according to the AI hypothesis, see Ling (1984, Chapter 17; 1990a).

2.2.1. *The Effects of Metabolic Inhibition on Cell Na^+*

In the membrane-pump theory, the level of Na^+ in living cells is maintained by membrane pumps expending metabolic energy. Inhibition of metabolism by the combined effects of anoxia (which stops respiration), iodoacetate (IAA, which arrests glycolysis), and cooling to 0°C (which slows down outward pumping more than inward leakage) should slow down pumping activity and cause an increase of cell Na^+ and a decrease of cell K^+ . This seemed to be a prediction of the membrane-pump theory that could easily be tested. I chose frog muscle because I was then most familiar with that tissue, but some of my more experienced friends advised that it would be unwise to use frog muscle. I proceeded anyway and found out in 1951 why my friends advised against it.

Neither the concentration of K^+ nor that of Na^+ showed any significant change after seven hours of combined cooling and poisoning (Table 2.1). This indifference to the combined action of anoxia and IAA (in addition to cooling) raised the question of whether there were some as-yet-undiscovered metabolic activities

Table 2.1. K^+ and Na^+ Contents of Frog Muscle after Prolonged Exposure to Nitrogen and Iodoacetate at $0^\circ C$ ^a (Ling 1984)

	K^+ (μ moles/g fresh tissue)	Na^+ (μ moles/g fresh tissue)
Control	74.9 ± 1.31	28.4 ± 1.21
Pairs after 7.74 hr ($0^\circ C$) in 5 mM IAA and pure nitrogen	76.3 ± 1.64	29.2 ± 1.72
<i>P</i>	> 0.5	> 0.7

^aData from Ling (1962).

that provided energy for the pump but were insensitive to those poisons. The question was soon answered in the negative; there were no undiscovered energy sources in frog muscle (see Ling 1952, 765; for a later more complete presentation of the same and newer data see Ling et al. 1973, 12). As my doubts about the pump concept increased, I realized that I must proceed to a more precise and quantitative approach to this question: "Does the cell have the energy to operate the postulated pump?" To proceed, I had to know how much energy the cell needed to operate the pumps. This in turn required a knowledge of the pumping rate.

Fewer Na^+ ions diffuse passively *outward* from living cells than Na^+ ions diffuse passively *inward* into the cells for two reasons: First, the intracellular concentration of Na^+ is some ten times lower than in the external medium. Second, outward traffic of positively-charged Na^+ is opposed by the *resting potential* (Chapter 11), which is negative inside and positive outside the cell. Therefore only a fraction of the would-be exiting Na^+ has kinetic energy high enough to jump over the resting-potential barrier. By taking both factors into account and at a resting potential of 90 mV, one calculates that only a minute fraction (ca. 0.2%) of the total outward Na^+ flux is due to passive diffusion. Therefore 99.8% of the Na^+ leaving the cell must be due to pumping (Ling 1965a, footnote on p. S105). Yet I soon found out that after suppression of respiration by anoxia and glycolysis by IAA, the rate of Na^+ efflux from frog muscle was not altered when compared with the control muscle (Ling 1952) (Figure 2.1A).

The demonstrated indifference of the Na^+ efflux rate of frog muscle to metabolic inhibitors was confirmed first by R. D. Keynes and G. W. Maisel (1954) (Figure 2.1B) (who studied the combined action of IAA and cyanide) and again by E. J. Conway et al. (1961) (who studied the action of IAA alone) (Figure 2.1C). For reasons not given, neither group mentioned similar conclusions concerning the lack of response of the Na^+ efflux rate in response to metabolic poison that I had reached earlier. *Their data (and my own) are reproduced here in Figure 2.1 to emphasize that as far as facts are concerned, there has been unanimity among all investigators on this crucial experimental observation.*

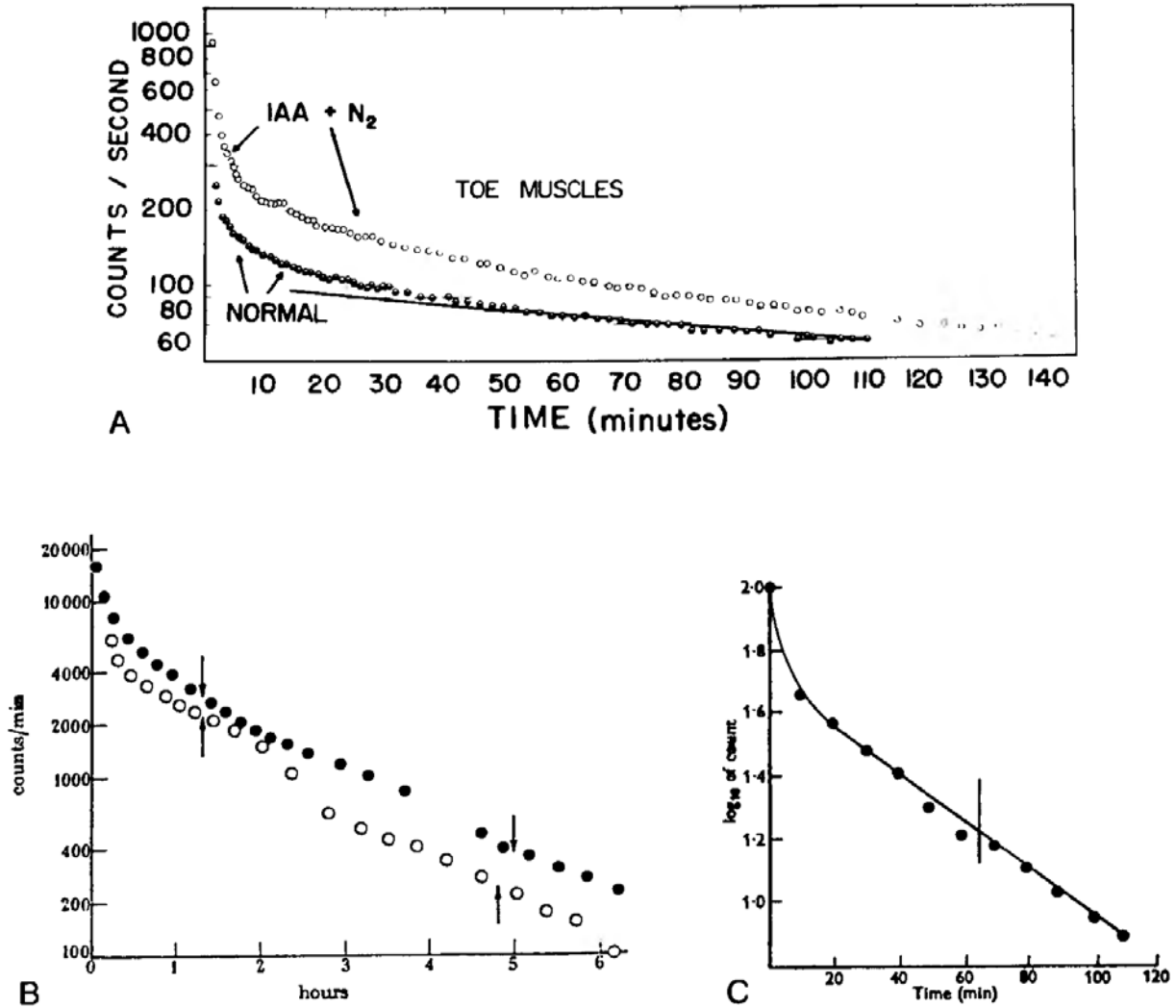


Figure 2.1.

- A. $^{22}\text{Na}^+$ efflux from frog toe muscle. Data indicate no significant change of Na^+ efflux rate after exposure to nitrogen and iodoacetate. Experiment was carried out at 0°C (from Ling 1962).
- B. Disappearance of $^{24}\text{Na}^+$ from sartorius muscles poisoned with metabolic inhibitors. ● treated with 0.2 mM 2,4-dinitrophenol for the period between the arrows, temperature 17°C ; ○ treated with 0.5 mM iodoacetate and 3 mM cyanide for the period between the arrows, temperature 21°C (from Keynes and Maisel 1954, by permission of *Proceedings of the Royal Society of London*)
- C. Effect of iodoacetate on loss of $^{24}\text{Na}^+$ from Na^+ -rich muscle. Inhibitor added at time indicated by vertical bar. (Conway et al. 1961, by permission of *Journal of Physiology*)

2.2.2 The Original Calculations Comparing the Minimum Energy Need of the Postulated Na Pump with the Maximum Available Energy

In the context of the popular beliefs at that time, a third and last possible energy source remained for operating the postulated Na pump: the store of

ATP and creatine phosphate (CrP) originally present in resting muscle. *The arrest of respiration by anoxia and glycolysis by IAA (as well as low temperature) had stopped new ATP and CrP synthesis.* Under these conditions, one could, by analyzing the ATP, ADP, and CrP contents of fully poisoned muscle tissues at the beginning and at the end of an incubation period, determine how much ATP, ADP, and CrP had been hydrolyzed during this period of time. From the energy contained in the high energy phosphate bonds hydrolyzed, one could determine the maximum energy the cells could have spent during this time period. One could then compare this maximum available energy with the minimum energy the pumping would require over the same time period, calculated from the measurements of (i) the electrical potential gradient (i.e., the resting potential), and (ii) the Na^+ -ion concentration gradient— Na^+ must be pumped against both gradients (i) and (ii)—and (iii) the rate of Na^+ pumping from the rate of labeled Na^+ efflux measured.²

The following experiment was carried out. To ensure the cessation of respiration and glycolysis, frog muscles were equilibrated first for 40 minutes at 0°C in a Ringer solution containing 1mM NaCN and 1 mM Na iodoacetate, bubbled extensively with a stream of pure nitrogen (i.e., 99.99% pure nitrogen further purified by passage first through heated copper turnings and then again through another “tower” of activated copper). The lactate contents of the muscle and bathing solution at the beginning and at the end of the incubation period were also analyzed to determine the minute glycolytic activity that had escaped the inhibition of IAA.

To eliminate unnecessary arguments, I chose from the literature the highest estimates of the utilizable free energy in the special “high energy phosphate bonds” of ATP, ADP, and CrP, equal respectively to -14.3 Kcal/mole ($\text{ATP} \rightarrow \text{ADP} + \text{P}$), -15.0 Kcal/mole ($\text{ADP} \rightarrow \text{AMP} + \text{P}$), -12.8 Kcal/mole ($\text{CrP} \rightarrow \text{Cr} + \text{P}$), and -28 Kcal/mole (glucose \rightarrow lactate) (see Ling 1962, 203).

All told, 28 sets of more or less complete experiments were carried out. Results of the last three sets of experiments performed in 1956 are shown in Table 2.2. In this table, the maximum available energy measured is compared with the minimum energy needs over a period of time ranging from 4 to 10 hours. Assuming further that the cell required energy only for the pumping of Na^+ , and that all energy utilization and transfer processes were 100% efficient, **the minimum energy needed by the Na pump at the plasma membrane alone was from 1542% to 3050% of the maximum available energy** (Ling 1962, Chapter 8).

However, it must be promptly pointed out that these estimates were in themselves a gross underestimation of the disparity between energy needed and energy available, because the calculations were made on the then widely accepted assumption that each ATP, ADP, and creatine phosphate (CrP) molecule contains, respectively, -29.3 , -15.0 , and -12.8 Kcal/mole of utilizable free energy in its phosphate bonds. Compelling evidence to be described in the next section indicates that in the phosphate bonds of ATP, ADP, or CrP there is no readily utilizable free energy.

Table 2.2. Energy Balance Sheet for the Na^+ Pump in Frog Sartorius Muscles (0°C)^{a,b}

Date	Duration (hr)	Rate of N^+ exchange integrated average (moles/kg per hr)	$\psi + E_{\text{Na}}/\mathcal{F}$ integrated average (mV)	Minimum rate of energy required for N^+ pump (cal/kg per hr)	Maximum rate of energy delivery (cal/kg per hr)	Minimum required energy	
						Maximum available energy	
9-12-56	10	0.138	111	353	11.57 (highest value, 22.19)	3060%	
9-20-56	4	0.121	123	343	22.25 (highest value, 33.71)	1542%	
9-26-56	4.5	0.131	122	368	20.47 (highest value, 26.10)	1800%	

^aThe minimum rate of energy delivery required to operate a Na^+ pump according to the membrane pump theory was calculated from integrated values of the measured rates of Na^+ exchange and the energy needed to pump each mole of Na^+ ion out against the measured electrical and concentration gradients. The maximum energy delivery rate was calculated from the measured hydrolysis of CrP, ATP, and ADP, (and the minute amounts of lactic acid formed) the only effective energy sources available to the muscles, which had been poisoned with IAA and nitrogen.

^bFrom Ling (1962).

2.2.3. Gross Underestimation of the Disparity Between Maximum Available and Minimum Needed Energy for the Na Pump

Podolsky and Kitzinger (1955) and Podolsky and Morales (1956), using highly refined and sophisticated instruments, redetermined the enthalpy³ of hydrolysis of ATP. The value obtained (-4.75 Kcal/mole) was far less than once believed (-12 Kcal/mole).

In a definitive review on the subject, "The High Energy Phosphate Bond Concept," George and Rutman (1960) described in detail why the measured *free energy of hydrolysis* of the "high energy phosphate bonds" does not (as was once widely believed) arise from utilizable energy or enthalpy stored in the phosphate bonds. It arises largely as an artifact from a Le Chatelier-principle-driven⁴ liberation of H^+ from ATP: the ATP hydrolysis reaction from which the "free energy" values were derived was carried out at neutral pH corresponding to a H^+ concentration of 10^{-7} M, rather than at the standard concentration of 1.0 M (pH = 0), as should be the case in any assay of the standard free-energy change of reaction where H^+ is a reactant (see Glasstone 1947, 283).

Table 2.3 is a partial reproduction of George and Rutman's original table. This table shows how most of the free-energy change measured for the hydrolysis of ATP, ADP, and CrP comes from the entropy term and another term $\phi RT \ln H^+$ (where ϕ is a number varying with the pH of the medium from 1.0 to 0). Neither term represents readily utilizable free energy. Indeed, the phosphate-bond enthalpy in ATP (in agreement with the findings of Podolsky and coworkers mentioned above) is actually not higher but lower than that in AMP, once considered to have a "low energy" phosphate bond (for more details, see Ling 1984, 311 to 313).

The maximum available energy presented in my calculation of the energy balance sheet of poisoned frog muscle given in Table 2.2 was almost entirely derived from the amounts of ATP, ADP, and CrP hydrolyzed (e.g., 98%, see Ling 1962, Table 8.5). Now that we know that their hydrolysis does not yield utilizable energy, the maximum available energy is drastically reduced to the

Table 2.3. Thermodynamic Data (in Kcal/mole) for Various Hydrolyses at pH 7.5^a [George and Rutman (1960), by permission of *Prog. in Biophys. and Biophys. Chemistry*]

Reaction	ΔF_{obs}	ΔF	ΔH	$-T\Delta S$	$\phi RT \ln H$
a. ATP + H ₂ O → AMP + pyrophosphate	~ -14.0	~ -4.2	-3.0	~ -1.2	-9.8
b. ATP + H ₂ O → ADP + orthophosphate	-8.3	-1.3	-4.8	+3.5	-7.0
c. Creatine phosphate + H ₂ O → creatine + orthophosphate	-10.6	-14.1	-4.8	-9.3	+3.5

$${}^a\Delta F_{\text{obs}} = \Delta F + \phi RT \ln H^+ = \Delta H - T\Delta S + \phi RT \ln H^+$$

minute free energy from the amount of lactate that has escaped the inhibition of iodoacetate. **A calculation based on this figure as the maximum available energy would make the 1500% to 3000% figure trivial by comparison.**

2.2.4. Remedial Postulations to Reduce the Energy Need of the Na Pump

Since publication in 1962, the validity and accuracy of this set of experimental findings, and my conclusion drawn from them, have never been challenged publicly in print. However, *three remedial postulations have been suggested in attempts to keep the energy requirement lower. In time, all have been disproved:*

- a. Ussing's exchange diffusion: postulated mandatory Na^+ -for- Na^+ "exchange diffusion" to minimize energy need for the Na pump⁵ was disproved by the demonstration of rapid Na^+ efflux from living cells in a Na^+ -free environment (Hodgkin and Keynes 1955; Buck and Goodford 1966; Hoffman and Kregenow 1966; Ling and Ferguson 1970).
- b. Sequestration of a large portion of cell Na^+ in the sarcoplasmic reticulum (SR) to reduce concentration of Na^+ in muscle cells (Zierler 1972; Rogus and Zierler 1970) was disproven by demonstration that most Na^+ is found inside the cytoplasm (Ling and Walton 1975a; Somlyo et al. 1977).
- c. Non-energy-consuming Na pump (Glynn 1977).

In this last remedial hypothesis, also intended to reduce the energy need of the hypothesized Na pump, it was postulated that the Na^+ diffusing into the cells also goes through the postulated Na^+ pump and in that process turns the "engine" backward, generating ATP. ATP is then used to pump the Na^+ out, maintaining its steady low level. It was argued⁵ that only *net* extrusion of Na^+ required metabolic energy. Since the resting cell does not gain or lose Na^+ , there is no net transport of Na^+ . The pumping of Na^+ in resting cells therefore requires no energy expenditure.

The foundation of this speculation (Glynn and Lew 1970) has long been shown to be wrong. After much effort intended to demonstrate the conversion of energy obtained by dissipating ion-concentration gradients into ATP, the decisive work of Kanazawa et al. (1970), Boyer et al. (1972), Masuda and deMeis (1973), Taniguchi and Post (1975), and Knowles and Racker (1975) unanimously established—within a short period of three years—that it was not the presence of an ion gradient that generates ATP which, as shown above, contains no utilizable energy in its phosphate bonds. (For details, see Ling 1984 514.) These new findings removed the experimental foundation on which Glynn's non-energy-consuming pump was based. However, to make certain that this remedial hypothesis is not slighted, let us consider some other relevant experimental facts. If a large share of inward Na^+ movement is via the Na pump, the exposure of the cell to the specific Na pump inhibitor, ouabain (that ouabain is a specific Na pump inhibitor is widely believed among proponents of the Na pump concept). In fact, ouabain has no influence on inward Na^+ -flux rate (Horowicz and Gerber 1965; Ling and Ochsenfeld, unpublished).

If outward Na^+ flux depends on inward Na^+ flux, then removal of the

outside-high–inside-low Na^+ gradient by replacing the external NaCl with isotonic sucrose or other non-sodium-chloride salts should have reduced the rate of Na^+ efflux. In fact, the reduction of external Na^+ concentration has no retarding effect on the rate of Na^+ efflux (Hodgkin and Keynes 1955; Buck and Goodford 1966; Ling and Ferguson 1970).

2.2.5. Many More Pumps Required at the Plasma Membrane

According to Boyle and Conway's membrane theory, all permeant ions should distribute themselves across the cell membrane in such a way as to exhibit a single Donnan ratio, r ,⁶ where r is defined as follows (Donnan 1924):

$$r = \left\{ \frac{[p_i^+]_{\text{in}}}{[p_i^+]_{\text{ex}}} \right\}^{1/n} = \left\{ \frac{[p_j^-]_{\text{ex}}}{[p_j^-]_{\text{in}}} \right\}^{1/m} \quad (2)$$

where $[p_i^+]_{\text{in}}$ and $[p_i^+]_{\text{ex}}$ are the equilibrium intracellular and extracellular concentration of the i th cations of valency n , and $[p_j^-]_{\text{in}}$ and $[p_j^-]_{\text{ex}}$ are the intracellular and extracellular concentration of the j th anion of valency m .

Table 2.4 shows the intra- and extracellular concentrations of eight major ions in frog muscle and in the external medium. The "Donnan ratios" were calculated on the basis of equation 2 and on the intra- and extracellular concentrations of the ions given in the first two columns, their respective valency and polarity. The data show that **no two ions exhibit the same "Donnan ratio."** Thus even if there were enough energy, the postulation of only one Na pump is, at best, a patchwork solution, leaving unsolved the larger problem concerning the distribution of all ions, as well as nonelectrolytes.

According to the membrane theory, the bulk of cell water is free,⁷ with the same solvency properties as the external medium. A permeant solute should be equally distributed between the cell water and the external medium. Experi-

Table 2.4. Ionic Distribution in Frog Muscle and External Medium^{a,b}

	Intracellular concentration (mEq/liter cell water)	Extracellular concentration (mEq/liter extra- cellular water)	Observed "Donnan ratio"
K^+	128.0	2.53	50.6
Na^+	16.9	105	0.16
Ca^{2+}	11.3	4.04	1.67
Mg^{2+}	31.6	2.46	3.61
Cl^-	1.04	76.8	73.8
HCO_3^-	9.2	26.4	2.86
Lactate	3.5	3.42	0.98
P_i	16.2	3.21	0.20

^aThe observed "Donnan" ratio is calculated according to equation 2 and the data given in the first two columns.

^bData from Ling (1962).

mental studies mentioned above have shown that this is true only for solutes like urea or ethylene glycol; larger solutes, like sugar and free amino acids, are found in lower concentration than in the external medium (see below and Ling 1984, 339 to 344).

As a specific example, consider L-glucose. It is the enantiomorph of the ubiquitous energy source of living cells, D-glucose. Unlike D-glucose, it is nonmetabolizable (Pigman, 1957). It is absent from the natural environment of most living cells, including frog muscle cells. Yet the equilibrium concentration of L-glucose in frog muscle is not unlike that of D-glucose, and is much lower than in the external medium (Figure 2.2). In terms of the membrane-pump theory, there must be a specific outward pump for L-glucose. There must also be pumps for other chemical compounds even less likely to have been experienced by and imprinted upon receptive genomes of surviving cells in evolution, including the bacteriocidal tetracycline and the arrow poison, curare. Indeed, a tetracycline pump for *E. coli* (Hutchings 1969) and a curare pump for mammalian muscle cells (Ehrenpries 1967) have both been proposed.

Then we have to consider the water-soluble, large, and complex organic compounds that came into being for the first time through the efforts of organic chemists. The number of these compounds already in existence is large; those yet to be synthesized, limitless. Thus far we have found that in terms of the membrane-pump theory, many a water-soluble, large, and complex organic compound requires a pump [see Section 5.2.5.1(4)]; we are thus forced to make the absurd forecast that there are already pumps in the cell membrane waiting for compounds already in existence (but not studied) or yet to be synthesized. Even if one completely disregards the energy problem—which in my view is an insurmountable difficulty—**cell membranes with finite dimensions cannot accommodate an endless number of pumps.**

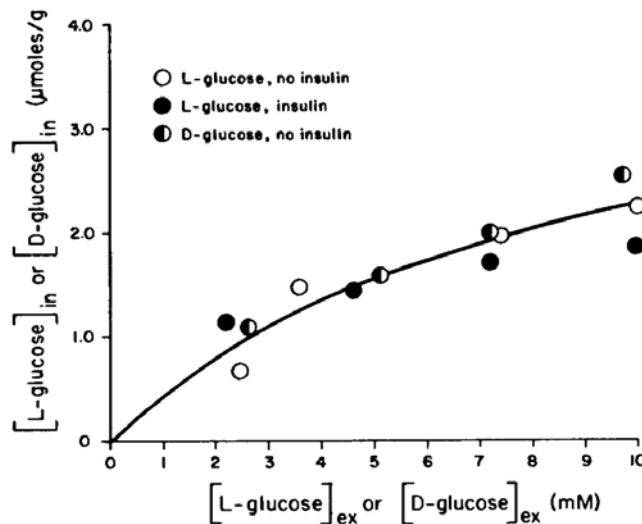


Figure 2.2. The equilibrium distribution of L- and D-glucose in frog sartorius muscle in the presence and absence of insulin at 0°C. At this temperature, even D-glucose is not appreciably metabolized. (Ling, unpublished).

One might ask: Is it possible that one pump could handle more than one solute? In principle, yes, but this would not be likely to change the picture materially. In the association-induction hypothesis, although a pump is not needed for solute distribution in resting *unifacial cells* (i.e., cells with a similar surface covering the entire cell), pumps are operative across active *bifacial cells* (i.e., cells covered with two different kinds of surfaces covering opposite sides of the cells like intestinal epithelium, toad bladder). Indeed, the extensive study of active transport of sugars and derivatives clearly points out how strongly specific are these real pumps. Thus only compounds highly similar to D-glucose and D-galactose are actively transported. Other modified D-glucose and D-galactose, other hexoses, all the pentoses, etc., diffuse through the intestine passively and are not pumped (see Wiseman 1964, 24–25). In agreement with the demonstrated high degree of specificity, a rather casual survey made in 1968 uncovered no less than 19 pumps, of which two are not single pumps but collections of different pumps (i.e., sugar pumps, free amino acid pumps) (Ling et al. 1973, 9). For additional reasons against the sharing of pumps see endnote [1] of Chapter 8.

2.2.6. *Still More Pumps Required at the Membranes of Subcellular Particles*

Thus far we have only considered pumps at the plasma membrane. There are also the membranes of subcellular particles to be considered. Pumps for natural and unnatural solutes discussed above are required here too. As examples, pumps have been suggested for liver mitochondria and muscle sarcoplasmic reticulum, because solute concentrations within subcellular particles are, as a rule, different from those in the cytoplasm. In liver cells, for example, the total surface area of the mitochondria has been estimated at 10 times that of the plasma membrane (Lehninger 1964); in muscle cells, the total surface area of the sarcoplasmic reticulum has been estimated at 50 times that of the plasma membrane (Peachey 1965). Since the energy needed by a pump is directly proportional to the surface area, the energy consumption for the diverse pumps at the plasma membrane may actually be exceeded by those of the subcellular particle membrane pumps by large factors.

In summary, under specified conditions, the Na pump at the plasma membrane of frog voluntary muscle would require a minimum of from 15 to 30 times as much energy as the cell commands when we assume that ATP, ADP, and creatine phosphate contain large quantities of utilizable energy—a concept long ago shown to be no longer tenable. Therefore, the actual factor by which the energy need exceeds the energy available must be vastly greater than the 1500%–3000% figures cited. *Since their publication in 1962, the experimental data and conclusions have remained unchallenged; their essence has been twice confirmed* (Jones 1965, Minkoff and Damadian 1973). Since the Na pump at the plasma membrane is only a very small part of the much greater energy needs of all the pumps needed to keep the cells “afloat,” **there is no alternative but to conclude that the membrane-pump theory has been disproven on energy grounds alone.**

Nevertheless, to put away a theory that has played such a dominant role in cell physiology for so long, one must examine critically all other evidence for and against the membrane-pump theory. The remaining pages of this chapter are given to this effort.

2.3. *The Failure to Demonstrate Pumping of K^+ and Na^+ Against Concentration Gradients in an Ideal Cytoplasm-Free–Membrane-Sac Preparation*

There are other grounds for rejecting the pump concept. By 1961, techniques for safely removing the axoplasm from isolated squid axons had been perfected (Baker et al. 1961, Oikawa et al. 1961). Axoplasm-free–squid-axon membranes can be filled with sea water and will then exhibit normal action potentials for hours. If ATP and CrP are also present in the sea water within the membrane, and the open ends of the membrane are tied, one obtains a membrane model ideally suited to test the membrane-pump theory. In the spring of 1963, Prof. Richard Keynes of the Physiological Laboratory of Cambridge University, England, announced at a lecture given at the Johnson Foundation, University of Pennsylvania, that all efforts to demonstrate active transport using this model had failed (see Ling 1965b, 95 footnote).

Similar failure to demonstrate net transport of Na^+ in “dialyzed squid axons” was reported by Brinley and Mullins in 1968, also Mullins and Brinley 1969; for more details, see Ling and Negendank 1980, 222.

To perceive their full significance, one must view these failures to demonstrate active K^+ or Na^+ transport in an ideal “pure” membrane preparation side by side with the successful demonstration in a later section (4.4.2.1.) of selective K^+ accumulation and Na^+ exclusion in a muscle-cell preparation without a functioning cell membrane and postulated pump.

2.4. *Evidence Once Considered to Strongly Support the Membrane-Pump Hypothesis Shown to be Erroneous or Equivocal*

Four sets of experimental findings were once widely interpreted as offering unequivocal evidence in favor of the membrane-pump hypothesis. In time, all of these findings proved to be either erroneous or equivocal.

2.4.1. *Intracellular K^+ Mobility*

In his monograph, *Nerve, Muscle, and Synapse*, Nobel laureate B. Katz wrote: “. . . Ernst (1958), Troshin (1958), and Ling (1962) . . . take the view that the potassium ions . . . possess selective affinity and are chemically bound⁸ to the proteinates.” “It seems, however, very difficult to support this view in face of the following pertinent observation by Hodgkin and Keynes, 1953. Their results are discussed here in detail because they are of crucial importance in the still persistent argument about the validity of the membrane concept” (Katz 1966, 42–43).

Katz then goes on to cite Hodgkin and Keynes's demonstration of K^+ mobility in squid axon close to the K^+ mobility in sea water. Somewhat similar observations were later reported by Kushmerick and Podolsky (1969) for K^+ diffusion in 3-mm-long frog muscle segments with both ends cut open.

Hodgkin and Keynes monitored the health of the axoplasm of the isolated cut squid axons by testing the ability of the axons to conduct electric impulses. However, as mentioned earlier, later work from Hodgkin's own laboratory (Baker et al. 1961) and elsewhere (Oikawa et al. 1961) showed that squid axons can conduct impulses in a perfectly normal fashion after the axoplasm has been removed and perhaps flushed down the drain—clearly demonstrating that the ability of the squid axons to conduct impulses normally does not guarantee the health of their axoplasm. Therefore, there is no assurance that the axoplasm of the squid axons Hodgkin and Keynes studied was healthy. In the case of frog muscle cells, there is clear-cut evidence that 3-mm-long cut frog muscle fibers immersed in Ringer solution deteriorate rapidly (see Figures 4.13, 8.22 and 8.23).

To reexamine the problem of K^+ mobility in healthy frog muscle cytoplasm, we developed a new method in which K^+ mobility was assessed in regions of the cell farthest from the cut (injured) end. From a total of 72 sets of experiments, Ling and Ochsenfeld (1973) showed that they could reproduce the essence of the earlier results of Hodgkin and Keynes (1953) and of Kushmerick and Podolsky (1969) if K^+ diffusion were measured in injured muscle near the cut ends, or in muscle deliberately killed with metabolic poisons. ***The diffusion coefficient of ^{42}K -labeled K^+ in normal intact muscle cytoplasm was only 1/8 that of ^{42}K diffusion in dilute salt solution.*** (A later query on our experimental design by Kushmerick was easily answered: Ling 1979c).

2.4.2. Intracellular K^+ Activity

Measurement with an intracellular K^+ -selective microelectrode also lead earlier investigators to conclude that the bulk of intracellular K^+ is free, as postulated in the membrane theory (Spanswick 1968). They reached their conclusion following a comparison of the measured K^+ activity (a_K) with the average total K^+ concentration (C_K) in squid axons (Hinke 1961), in giant crab muscle (Hinke 1959), and in barnacle muscle (Lev 1964). The K^+ activity coefficients determined ($\gamma_K = a_K/C_K$) were close to that of K^+ in simple salt solutions of similar ionic strengths.⁹ However, *ensuing extensive investigations revealed widely divergent activity coefficients*, no longer compatible with the prediction of the membrane theory, i.e., a *uniform* γ_K for all cells equal to that of K^+ in dilute salt solution. With different cell types and different experimental approaches, γ_K as low as 0.27 (White 1976) and as high as 1.2 (Lee and Armstrong 1972, Palmer et al. 1978) were reported (see Ling 1984, Table 8.2). ***This diversity of measured activity coefficients cannot be explained by the membrane-pump theory; but can readily be explained in terms of the extent of local injury created by the intruding electrode*** (Ling 1969a; for very recent experimental confirmation, see Edelmann 1989; also Figure 8.23) and the different proportions of K^+ and water released from adsorption in the immediate vicinity of the sensing surface of the meas-

uring electrode and throughout the cell (see Section 4.1 for the quantitative influence of adsorption on the activity coefficient of an ion). (For an explanation of the relevant concept concerning water and ion adsorption, see Section 5.2.2 and endnote 5 of Chapter 3.) Thus low γ_K may be measured in sturdy cytoplasm which releases a minimum of adsorbed K^+ to be “seen” by the electrode. Concomitant complete K^+ release and complete water depolarization throughout the cell, or at only the region immediately adjacent to the electrode, may yield (high) γ_K similar to that of Ringer solution. γ_K much higher than that in a Ringer solution may result from the combined effects of total depolarization of water in immediate contact with the sensing electrode surface, with proportionately more K^+ release from adsorption than water depolarization in regions away from the electrode (for details, see Ling 1984, 250 to 257).

2.4.3. *The Intracellular “Reference Phase” Studies*

Horowitz, Paine and their associates (Horowitz et al. 1979, Horowitz and Paine 1979) injected droplets of warm 10% gelatin solution into amphibian eggs, and analyzed the K^+ and Na^+ contents in these “reference phase” droplets after allowing the gelatin to cool and gel, and after enough time for equilibration. They demonstrated a maintained lower level of radioactively labeled Na^+ in the gelatin phase than in the external solution, long after equilibrium has been reached between Na^+ in these two places. Primarily on the basis of this finding, they argued that although some of the K^+ is bound, and some of the cell water has properties different from normal, the low level of Na^+ in the cell is due to the activity of a Na pump in the cell membrane.

Because it violates the law of conservation of energy in the same way, we must question this formulation, just as we questioned the original membrane-pump theory. In addition, this formulation violates the Law of Parsimony.¹⁰

There is a much simpler explanation for the key observations of Horowitz and his coworkers that does not violate the law of conservation of energy (Ling 1984a). Even though ^{22}Na in the gelatin phase reached equilibrium with external labeled Na^+ in a few hours, exchange of labeled K^+ in the gelatin phase with that in the external solution was much slower. Indeed, even after 7.9 hours, the exchange was only 33% complete (Horowitz and Paine 1979, 51). Thus, in this period of time, K^+ that had collected in the gelatin phase functioned as an *effectively impermeant* cation, its presence reducing the equilibrium concentration of the permeant Na^+ , for the same reasons that the presence of an impermeant anion keeps a permeant anion like Cl^- at a low level¹¹ in a Donnan equilibrium⁶ (for experimental evidence, see Donnan and Allmand 1914).

2.4.4. *Active Transport in Hollow Membrane Sacs or Vesicles*

2.4.4.1. *Synthetic Hollow Phospholipid Membrane Vesicles Containing K, Na-Activated ATPase*

Skou (1957) first suggested that a K, Na-activated ATPase isolated from membranes of crab nerves is either the whole or a major component of the Na pump.

In the 1970s, a number of papers appeared in which the authors claimed that active Na^+ transport had been demonstrated, using synthetic hollow membrane vesicles of pure phospholipids in which K, Na-activated ATPase was incorporated (Goldin and Tong 1974, Hilden et al. 1974).

The basic experimental procedures that were used are diagrammatically illustrated in Figure 2.3. After vesicles were prepared from cholate-solubilized lecithin and isolated Na, K-ATPase (postulated to be the Na pump) (Stage 1),

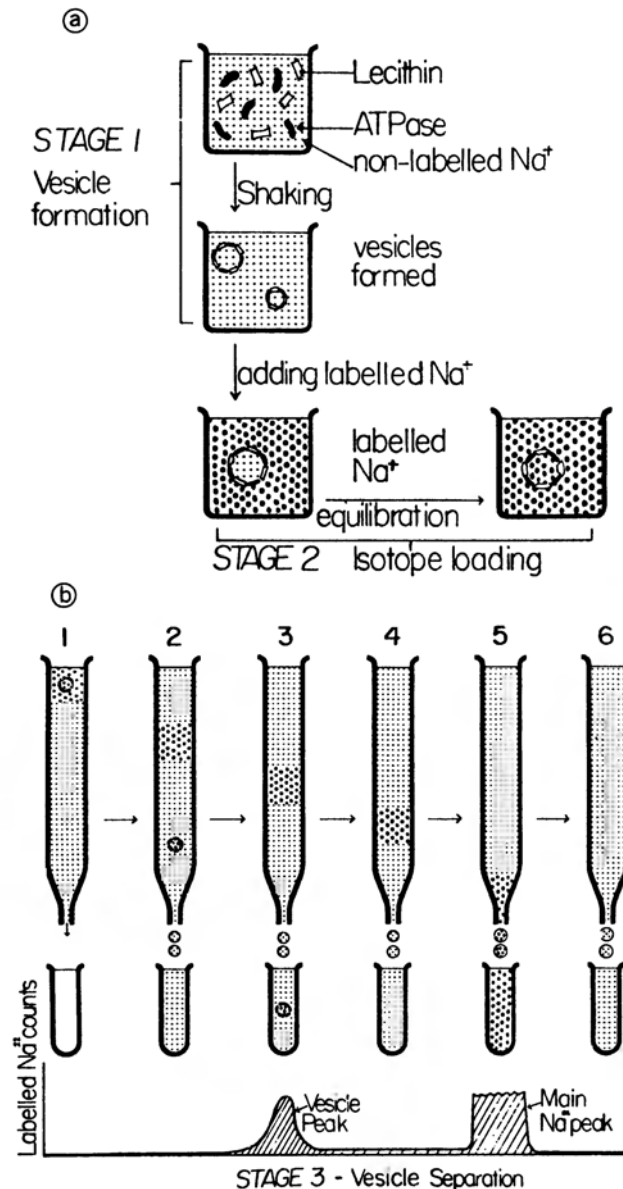


Figure 2.3. Schematic diagram of procedures used in attempted efforts to demonstrate ATP—energized pumping of Na^+ in synthetic phospholipid vesicles incorporating isolated K^+ , Na^+ -activated ATPase (Ling and Negendank 1980, by permission of Perspectives in Biology and Medicine).

- Preparation of reconstituted Na,K-ATPase vesicles. Phospholipid (e.g., lecithin) is solubilized in cholate, and vesicles are formed during prolonged dialysis
- Separation of vesicles through Sephadex column

they were exposed to and loaded with radioactively labeled Na^+ (Na^*) (Stage 2). The suspensions of Na^* -loaded vesicles, too fragile to be separated by conventional procedures (filtration or centrifugation), were loaded on top of a Sephadex column, eluted with a stream of a medium containing no Na^* , (Stage 3), collected in the earlier fractions, and thus separated from the free Na^* of the incubation solution collected in the later fractions. The main experimental finding from these studies was that a higher concentration of Na^* was found in vesicles exposed in Stage 2 to both Na^* and ATP than was found in vesicles exposed to Na^* alone. This finding was interpreted as demonstrating an ATP-energized pumping activity of inside-out Na pumps in the vesicular membrane.

Ling and Negendank, in a detailed analysis of the data published, concluded that *the observed difference was due to an artifact: varying Na^* -leakage rate in Stage 3* (Ling and Negendank 1980). In Goldin and Tong's original paper (1974), the "half time" of Na^* loading (i.e., the time needed for Na^* to reach 1/2 of its final equilibrium concentration in the vesicles) was 5–10 minutes, yet the elution of the loaded vesicles from the Sephadex column—a process in which the Na^* -loaded vesicles were exposed to a medium containing no Na^* —took 35 minutes. Clearly the final Na^* concentration in the vesicles collected could not have been that attained immediately at the end of the Stage 2 loading process, but was variously reduced by the "leakage" of the Na^* from the vesicles during the Stage 3 separation process. Indeed, the volumes of solution enclosed in the vesicles, called "trapped volumes", determined with labeled glucose or labeled inulin, were as a rule much larger than the trapped volumes determined by Na^+ , further confirming the suspicion of the leakage and loss of Na^* .

While the reader interested in more details should consult Ling and Negendank's review, let us look at a table (Table 2.5) constructed from the data presented by Hilden and Hokin (1976). In this table, the trapped volumes of the vesicles doubly labeled with ^{22}Na and ^{42}K are shown. If there had been no significant leakage of these labeled ions or even if both ions had leaked at the same rate, the trapped volumes determined with ^{42}K and with ^{22}Na should be equal. In fact, large discrepancies in trapped volumes determined on the basis of ^{42}K and ^{22}Na are found for the same vesicle in the absence of ATP, further refuting

Table 2.5. Trapped Volumes (% Isotope Content) of Double-Labeled Na,K-ATPase Vesicles^a (Ling and Negendank 1980 by permission of Perspectives in Biology and Medicine)

Probe	Ouabain	– ATP	+ ATP
^{22}Na	No	.22	1.35
^{42}K	No	1.29	.86
^{22}Na	Yes	.14	.15
^{42}K	Yes	.21	.20

^aHilden and Hokin (1976, Tables 2, 3).

the basic assumption of no or little leakage. Were it otherwise, it would be just as difficult to understand why the vesicles, in the presence of ATP (which is supposed to energize the pump) and in the absence of ouabain, pumped out only enough K^+ to reduce its content by a mere 33% (from 1.25% to 0.86%) while vesicles in the absence of ATP but in the presence of ouabain (which is supposed to inhibit the Na^+ pump) pumped out a great deal more K^+ , reducing its content by a hefty 80% to 85% (from 1.29% to 0.21%)!

2.4.4.2. *Supposedly Hollow But In Fact Solid Membrane "Vesicles" Prepared from Living Cells*

(1) *Red Cell Ghosts*

Exposure to a hypotonic solution (hypotonic shock) causes hemolysis of red blood cells. Addition of salt or sugar to the solution containing the hemolyzed cells leads to "resealing" of these red cell ghosts, which often have been indiscriminately referred to as resealed pure membrane vesicles. Thus Freedman (1976) demonstrated active transport of K^+ and Na^+ in the presence of ATP against concentration gradients in the ghosts he prepared (Figure 2.4). Subsequent electron microscopic and water content analyses revealed that several popular methods used to prepare these membrane "vesicles," including that used by Freedman, produce only solid ghosts (Ling and Balter 1975; Hazlewood et al. 1979; Ling 1984, 131) (Figure 2.5A). Other methods of ghost preparation, involving repeated washing in hypotonic solution of low ionic strength (Dodge et al. 1963, Marchesi and Palade 1967), do produce apparently hollow ghosts (Figure 2.5B). Though possessing normal ATPase activity, these hollow ghosts do not reaccumulate K^+ or extrude Na^+ (Figure 2.6) as solid ghosts do, as

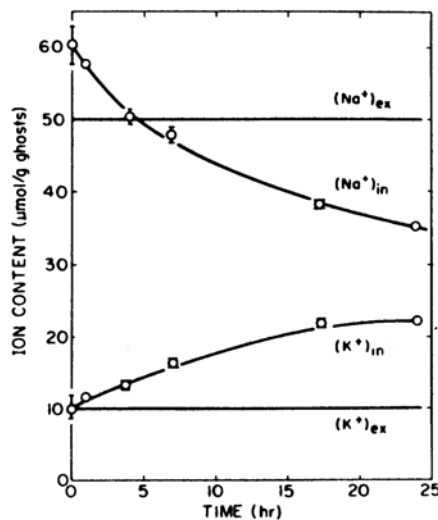


Figure 2.4. Time courses of rise in K^+ concentration, $(K^+)_{in}$ and fall of Na^+ concentration, $(Na^+)_{in}$ in human-erythrocyte ghosts. Concentration of K^+ and Na^+ in the bathing medium are shown by lines marked by $(K^+)_{ex}$ and $(Na^+)_{ex}$ respectively. Data indicate net accumulation of K^+ and extrusion of Na^+ against concentration gradients by human-erythrocyte ghosts. (Freedman 1976, by permission of Biochimica et Biophysica Acta)



Figure 2.5.A. Electron micrograph of human red cell ghosts prepared by the method of Freedman ("Freedman Ghosts") which was used in the study that gave rise to the data of Figure. 2.4. Magnification $18,000\times$ (Ling and Balter unpublished; see also Ling and Balter 1975)

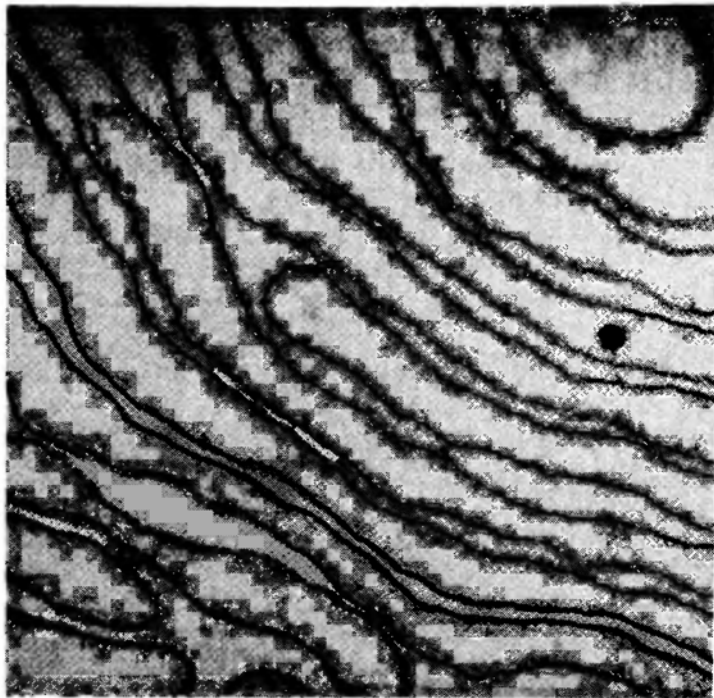


Figure 2.5.B. Electron micrograph of a representative area in a section through ghost membrane pelleted by high speed centrifugation ($100,000\text{ g}$, 30 min) and fixed in glutaraldehyde- OsO_4 . The ghosts appear as empty sacs bounded by continuous unit membranes. Fibrillar material is seen along the inner surfaces of the ghost membranes (magnification $90,000\times$). (Marchesi and Palade 1967, by permission of the *Journal Cell Biology*.)

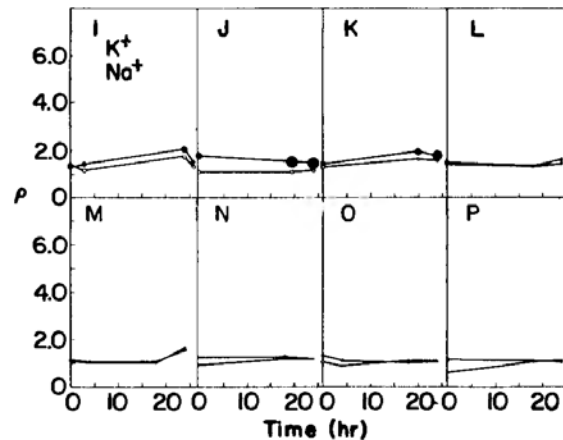


Figure 2.6. Demonstration of a lack of active transport of K^+ and Na^+ against concentration gradients in the “Marchesi-Parade ghosts” (see Figure 2.5B). Ordinate represents the ratio of the concentration of K^+ or Na^+ ion in the ghost water over the concentration of the same ion in the incubation medium. This ratio is called the ρ -value or ρ (see Section 5.2.3). Each point is the average of at least four determinations. The diameter of the solid circles (K^+) and hollow circles (Na^+) represents twice the standard error. (Ling and Tucker 1983, by permission of Physiological Chemistry Physics and Medical NMR)

demonstrated by Freedman (Figure 2.4) and later confirmed (Ling and Tucker 1983). In summary, hollow red cell ghosts do not transport K^+ and Na^+ against concentration gradients; only solid ones, retaining a good deal of the cytoplasmic protein hemoglobin, do. Indeed, these findings are a part of a larger truth. Later work (Ling et al. 1984) has shown that the level of K^+ reaccumulated and the amount of Na^+ extruded are quantitatively dependent on the amount of residual hemoglobin in the ghosts (see Section 4.3).

(2) Bacterial Vesicles

Many papers have been published on vesicles prepared from bacteria after removal of the cell wall or in response to hypotonic shock. These vesicles could serve as membrane models to demonstrate activities of membrane pumps if and only if they were freed of cytoplasm, i.e., with total solid content of 5% or less. Surprisingly, most of the published work gives no data on the solid contents of the vesicles studied. However, a few authors do provide these data. In these cases, the solid contents vary between 43% and 50% (Kaback 1976, Hirata et al. 1974, MacDonald and Lanyi 1975). This matches or exceeds the solid contents of most intact normal living cells from which the vesicles were prepared. Therefore, active transport demonstrable in these vesicles do not provide evidence in support of the membrane-pump theory because the data could just as well be explained by alternative hypotheses.

(3) Sarcoplasmic Reticulum Vesicles

Again, despite numerous publications on ion transport in sarcoplasmic reticulum (SR) vesicles, many authors do not give data on solid and water contents. However, McKinley and Meissner (1977) do. In this case, the water content was

below 75% and the solid content above 25%—higher than the total solid content of muscle cells (i.e., ca. 20%) from which the SR vesicles were isolated. SR preparations with high protein contents, like solid bacterial vesicles, cannot tell us whether ion transport is due to membrane pumps or to alternative adsorption mechanisms to be described below.

2.5. Summary

As of now, there is no longer any evidence known to me that can be considered to unequivocally favor the membrane-pump theory. Indeed, in the light of excessive energy needs (unchallenged for more than a quarter of a century and twice confirmed in essence) and the fact that cell membranes with finite dimensions cannot accommodate an infinite number of pumps, **the disproof of the membrane-pump theory can only be regarded as complete.**

In the chapters following, a new theory of the living cell called the *association-induction hypothesis* is presented, which was developed in an embryonic form in 1951–1952, and was for a while called (Ling's) fixed charge hypothesis (LFCH) (Ling 1951; 1952; 1984, 93). At approximately the same time, A. S. Troshin of the Soviet Union, a student of the original and important Russian cell physiologist D. N. Nasonov, presented his pioneering studies (Troshin 1951a, b, c, d, e) providing the foundation for his sorption theory¹² (Troshin 1956, 1958, 1966). In the following chapters, we will examine the association-induction or AI hypothesis as it stands today.

NOTES

1. By operating a frictionless shutter that opens or closes a hole in a partition separating two compartments of a box containing air, a being (later known as a "Maxwellian demon," after its creator, the great Scottish physicist James Clerk Maxwell (1831–1879)) is able to allow only faster-moving molecules to go from compartment A to B and only slower ones from B to A. The result is a rise of temperature in B and a fall of temperature in A without energy expenditure, in violation of the Second Law of Thermodynamics: heat cannot of itself, without the intervention of any external agency, pass from a colder to a hotter body.

In another version, the Maxwellian demon allows only nitrogen molecules to go from compartment A to B and only oxygen molecules to go from compartment B to A. As a result, pure nitrogen and oxygen have been prepared from their mixture, thereby creating free energy *de novo*, in violation of the First Law of Thermodynamics: although energy may be converted from one form to another, it cannot be created or destroyed.

It is both alarming and distressing to see that while Dean correctly rejected non-energy-consuming membranes behaving like Maxwellian demons, others have repeatedly reintroduced different versions of the same demon to explain selective distribution by pumps that require no energy expenditure in living cells (e.g., Glynn 1977, Deutsch 1981, Anner 1983; see also Greco 1982 for a lucid rebuttal).

2. The method used to calculate the minimum energy need of the sodium pump, is basically the same as that first used by Levi and Ussing (1948), and later used by Harris and Burn (1949), by Keynes and Maisel (1954), and given in detail in Ling 1962, 195–212 and in Ling 1984, 122–126.

3. The enthalpy (or heat content) change of a reaction, represented by ΔH , is equal

to the sum of energy change (ΔE) plus the product of $P\Delta V$ when P is the pressure and ΔV is the volume change of the system. For a gaseous reaction which involves large changes of volume, ΔH and ΔE may be quite different. However, for reactions occurring in solutions, as in biochemical reactions, the volume changes are small. ΔH and ΔE are then as a rule quite similar.

4. The Le Chatelier principle, also known as *principle of mobile equilibrium* was independently developed by H. Le Chatelier (1885) and F. Braun: if a change occurs in one of the factors, such as temperature or pressure, under which a system is in equilibrium, the system will tend to adjust itself so as to annul, as far as possible, the effect of that change.

5. According to the membrane-pump theory (and the laws of physics), virtually every Na^+ ion leaving a frog muscle cell requires considerable energy. To reduce the total energy need of the Na^+ pump, Ussing (1949) hypothesized that some Na^+ leaves the cell by a one-to-one exchange with incoming Na^+ . Such a Na^+ -for- Na^+ "exchange diffusion" is thermodynamically a non-event, since it leaves the chemical composition of the system unchanged and therefore would require no energy expenditure.

6. Frederick Donnan (1924) considered the rules governing the distribution of permeant ions between two contiguous phases separated by a semipermeable membrane when one phase contains an electrically charged impermeant ion, e.g., an impermeant anion, R^- . One set of rules is that described by equation 2, showing the constancy of the Donnan ratio, r . Another set of rules is that the equilibrium concentration of a permeant ion bearing the same charge as the impermeant ion is lower on the side containing the impermeant ion, while the concentration of permeant ion bearing the opposite charge as the impermeant ion is higher on the side containing the impermeant ion.

That the living cells may represent a system that follows Donnan's concept of membrane equilibrium was often advocated (see Netter, 1928). There was at one time also the belief that proteins provide the impermeant anions essential for the establishment of such a system. However, most isolated cell proteins have their isoelectric points not too far from the (neutral) pH of the cell interior. Therefore, from the conventional standpoint, they can provide not much more than a few mM of fixed anions (see Boyle and Conway, 1941, Table 2). For this reason Boyle and Conway made a new suggestion: instead of proteins, they designated as the impermeant anions, creatine phosphate, ATP, hexosephosphate, etc., which exist in high concentration in muscle cells. But this is also an ad hoc solution at best. The major intracellular anions of many cells are quite permeant (see Section 9.1.2). In red cells, the major anion is chloride, which is highly permeant (Dirkin and Mook 1931) and thus cannot serve as impermeant anion. Similarly, glutamate forms the major anion of certain nervous tissues; it too is quite permeant (see Ling 1984, 88). Thus the general applicability of Donnan's theory of membrane equilibrium is not tenable. [see also Ling 1977b, Ling et al 1979 and Section 8.1.2.(3)]

7. The membrane theory was a coherent theory of the living cell, a historic entity different and distinct from other versions resulting from attempts to tinker with it. The membrane theory, as it originated, included the concept that all, or virtually all, cell water is free. On this basic assumption the early theories of cell-volume regulation (see Section 10.1), of cellular electrical potential (Section 11.1 and 11.2), and of cellular ionic distribution (Section 1.3) were built. The membrane theory reached the zenith of its development in the self-consistent version of Boyle and Conway (Section 1.3), in which free cell water was assumed without qualification.

Recent years have witnessed repeated attempts to modify the original stand on the physical state of water by incorporating into the membrane theory the idea that a substantial part of the cell water is in fact not free.

To serve its (only) purpose in advancing knowledge, a scientific theory should be presented in the simplest and most unambiguous form possible; put to the most demanding test(s) one can devise; and, depending on the outcome of the testing, either accepted or rejected. It would create confusion, and, if widely practiced, defeat the purpose of science and desecrate its nobility and dignity, if, failing a crucial test, pieces of an opposing

theory—which the results of testing favors—are “appropriated” and grafted onto a popular but unpromising theory, so that it will now “pass the test.”

This is not to say one cannot produce a new theory that contains (compatible) components of old ones. Of course, one can and one must, when necessary. But to do so, one must carefully acknowledge and give credit to the true originator(s) of the concepts appropriated, describe how the new theory differs from the parent theories and produce evidence why the introduction of the hybrid new theory has genuine scientific merit of its own, not found in the parent theories. (For additional insight into the principle involved, see endnote 1 in Chapter 1, endnote 10 in Chapter 2 and endnote 11 in Chapter 11.)

8. This statement incorrectly represents my view. K^+ selectively adsorbed on β - and γ -carboxyl groups (see endnote 5 of Chapter 3) is a quite different case from its being “chemically bound”.

9. In contrast, the activity coefficient of Na^+ measured was, as a rule, below unity (Hinke 1961). In fact, this type of observation agrees with the notion that electrode insertion causes cytoplasmic injury, and in injured cytoplasm, there is an increase of Na^+ adsorption (see Section 9.2.2.3.2 and Section 10.2.4).

10. Recall William of Occam’s Razor: “Entia non sunt multiplicanda praeter necessitatem,” no more things should be presumed to exist than are absolutely necessary. Or even more appropriately, as stated by Sir William Hamilton in 1853 in his “Law of Parsimony”: “Neither more, nor more onerous causes are to be assigned than are necessary to account for the phenomenon.”

11. To maintain osmotic equilibrium:

$$[K^+]_{ref} + [Na^+]_{ref} + [Cl]_{ref} = [K^+]_{ex} + [Na^+]_{ex} + [Cl]_{ex} \quad (A)$$

To maintain macroscopic electric neutrality (See endnote 1 of Chapter 4):

$$[K^+]_{ref} + [Na^+]_{ref} = [Cl]_{ref}; [K^+]_{ex} + [Na^+]_{ex} = [Cl]_{ex} \quad (B)$$

From A and B

$$2\{[K^+]_{ref} + [Na^+]_{ref}\} = 2\{[K^+]_{ex} + [Na^+]_{ex}\}, \quad (C)$$

and

$$[K^+]_{ref} + [Na^+]_{ref} = [K^+]_{ex} + [Na^+]_{ex} \quad (D)$$

$$\text{Since } [K^+]_{ref} \gg [K^+]_{ex}, \quad (E)$$

$$\text{we conclude: } [Na^+]_{ref} \ll [Na^+]_{ex}. \quad (F)$$

12. For a brief outline of Troshin’s other work, see Ling (1984), in which both the LFCH and Troshin’s important contributions are presented in their historical perspectives. After the 1960s, Troshin did not pursue his research as vigorously as before; in December, 1985, this brilliant scientist died.

THE LIVING STATE

3.1. *The Story of the Living Cell: A System of Protein-Water-K⁺ Interacting with an Environment of Water and Na⁺*

The most abundant component of all living cells is water. By bulk, the next largest component is protein. By number, the next largest component is K⁺. The largest component of the external environment of most living cells is water; the next largest is Na⁺. Thus in the broad sense, cell physiology is a story of assemblies of water-protein-K⁺ in an environment of water and Na⁺.

Among the many physiological manifestations of the living cell, first and foremost in importance must be the mechanism that prevents the cell's dispersing and intermingling with the environment. The intuitively attractive idea that the preservation of cell contents is due to an enclosing membrane (with or without the help of membrane pumps) has not stood the test of time. A new and different mechanism is presented in the association-induction (AI) hypothesis.

If we visualize the characteristic aggregation of atoms in a living cell as being like a collection of fish in an ocean, then, in the membrane theory, the fish are, so to speak, held in by a net. In the AI hypothesis, the major forces holding most of the atoms and molecules together are more like those holding together a school of fish swimming in the ocean. **The cohesive forces are primarily interactions among individuals of the school.** Not only do these interactions keep the school together, they also enable the entire school to alter the direction of motion swiftly and coherently.

3.2. *A Discrete High-(Negative)-Energy, Low-Entropy State Called the Living State*

Having the correct components in the right proportion is a necessary but not a sufficient condition to produce a living cell. Each of the components must also occupy a specific position in relation to the other components. But even this is not sufficient to produce a living cell—a well-preserved dead cell may also satisfy these two criteria. In the AI hypothesis, this assembly of the right number and kind of atoms, molecules, and ions, each occupying the right relative spatial location, must also exist in a discrete *state*—in the sense the word is used to indicate, say, the liquid or solid state—called the **living state**, with high (negative)

energy¹ and low entropy². To clarify this important new concept of the living state I present a simple model.

Consider a collection of soft-iron nails tied end to end with bits of string. Scattered among them are iron filings (Figure 3.1A). A magnet is brought into contact with the end of one terminal nail (Figure 3.1B). The magnet magnetizes the first nail, which in turn magnetizes the next nail, and this goes on for a number of nails farther down the chain. As a result, not only are the nails locked into closer and tighter relation with one another, but the surrounding iron filings also become organized into definite patterns. Thus, depending on the strength of the magnet, interaction with the magnet causes the assembly as a whole to rise to a specific, discrete higher-(negative)-energy and less random, or lower-entropy state.

In living cells, according to the AI hypothesis, electrical polarization, or induction (hence the title association-induction hypothesis), takes the place of magnetic polarization in the model discussed. The polypeptide chains of proteins are the equivalent of the chains of nails; water molecules and K^+ are the equivalent of the iron filings. The equivalent of the magnet is a class of biologically potent substances of prime importance. They are called **cardinal adsorbents**. Cardinal adsorbents include drugs, hormones, transmitters, and Ca^{++} . One unique cardinal adsorbent of the greatest importance in maintaining the living cell in the specific and discrete high-(negative)-energy, low-entropy *living state* is the final product of cell metabolism: ATP.

In summary, and in answer to the question posed at the very beginning of this volume, one can state that for the cell, being alive does not mean continued functional activity of one sort or another. Rather, it means the cell exists in the specific, discrete high-(negative)-energy, low-entropy state called the *living state* (Figure 3.2).³ A functionally *active* (living) state and death represent two other *discrete* metastable equilibrium states of increasingly higher entropy and lower (negative) energy in the direction toward the ultimate random state.



Figure 3.1.

- A. A chain of soft-iron nails joined end to end with pieces of string is randomly arrayed and does not interact with the surrounding iron filings.
- B. The approach of a magnet causes propagated alignment of the nails and interactions with the iron filings. (Ling 1969, by permission of *International Review of Cytology*)

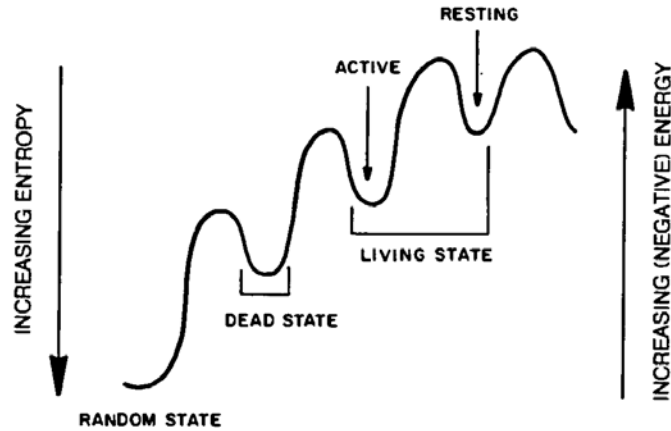


Figure 3.2. Diagrammatic illustration of the (negative) energy and entropy profile of the living (both resting and active), dead and random state.

3.3. A Diagram of the Living Cell

On two accounts I have already pointed out the importance of the asymmetric distribution of K^+ and Na^+ . First, K^+ and Na^+ are major components of the cell and its environment, respectively. Secondly, their characteristic distribution is at once the weathervane and the substance of the living state. **Therefore, the unique pattern of K^+ and Na^+ distribution will continue to be my focus for the presentation of the AI hypothesis as a general theory of the living cell.**

A theoretical diagram of the living cell is presented in Figure 3.3. Note that the cell membrane, mitochondria, and other subcellular structures are not represented. Rather, the illustration is to be seen as representative of the general makeup of all parts of the living cell. Unfortunately, static diagrams like this and others similar to it invariably mislead when intended to convey dynamic structures fluctuating in the four-dimensional time and space continuum (see Section 7.3.3.1). The reader must be alert to this problem.

According to the AI hypothesis, proteins in the cell do not all exist in the same steric and electronic conformation that they assume after isolation and purification (following conventional usage, referred to as *native proteins*⁴). Indeed special steric and electronic conformations are, as a rule, required for cell proteins to serve their roles in the asymmetrical distribution of K^+ and Na^+ ions.

Polypeptide chains (of the same proteins or a variety of proteins), which are found pervasively throughout the entire cell, exist in a **fully-extended** conformation. **By a fully-extended conformation, I do not mean that the proteins necessarily exist as perfectly straight chains, but rather that their backbone NHCO groups are not locked in α -helical, β -pleated sheets or in other intra- or intermacromolecular H bonds, and are therefore free to react with the bulk-phase water.**

The *fully-extended* conformation is different from what conventionally has been called the *extended conformation* denoting the β -pleated-sheet conformation. For reasons to be given in full in Chapter 5, the polypeptide chains in the fully-extended conformation polarize multiple layers of water molecules, and water

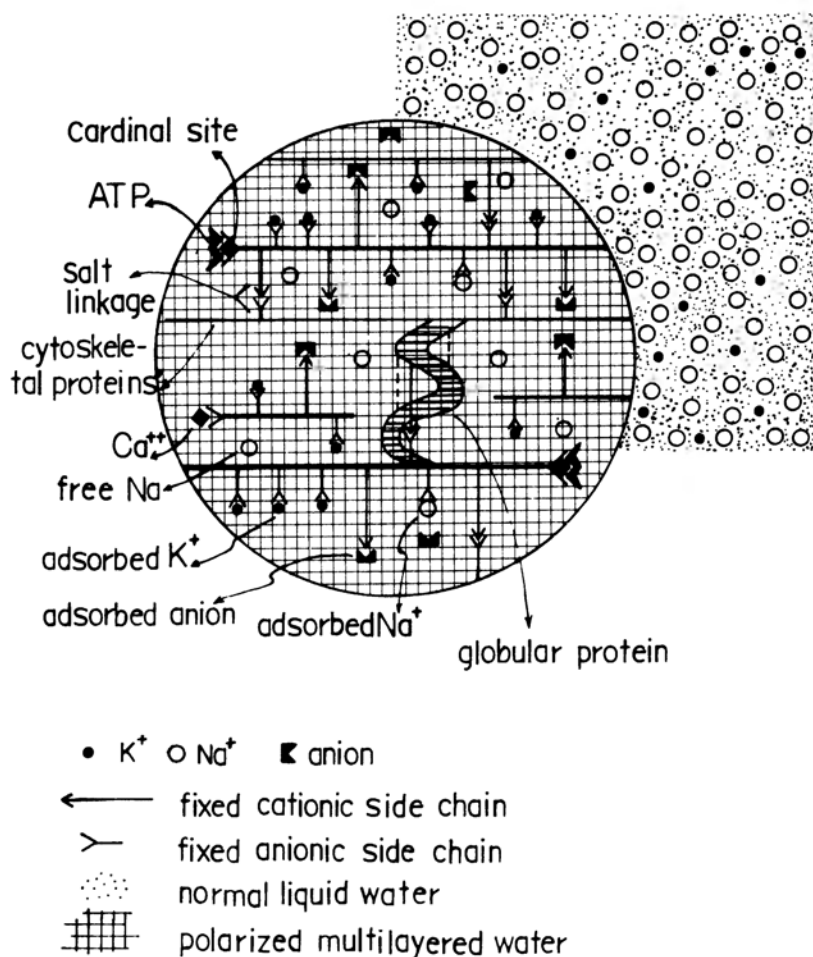


Figure 3.3. Schematic illustrations of a portion of a living cell. The picture presents the basic mechanisms of selective K⁺ accumulation (●) and Na⁺ (○) exclusion in living cells according to the AI Hypothesis. K⁺ accumulation results from preferential adsorption on fixed anionic β- and γ-carboxyl groups of cell proteins. Na⁺ exclusion results from failure to compete for β- and γ-carboxyl groups against K⁺ and partial exclusion from cell water existing in the state of polarized multilayers in consequence of interaction with the NH and CO groups of a matrix of fully-extended protein chains present throughout the cell.

existing in the state of polarized multilayers has reduced solvency for hydrated ions like Na⁺, as well as K⁺.

When amino acids are joined together to form a polypeptide or protein, their ionized and electrically charged α-amino groups and α-carboxyl groups react respectively with the α-carboxyl and α-amino groups of neighboring amino acids to form the (neutral) polypeptide chain. In the case of the trifunctional amino acids, aspartic and glutamic acids, their second (ionized) carboxyl groups, (i.e., β-carboxyl groups of the aspartic-acid residue and γ-carboxyl group of the glutamic-acid residue) remain as negatively charged functional groups shown as Y-shaped branches on the protein chains in Figure 3.3. Most of the Y's are occupied by a black circle representing a K⁺ ion. The mechanism that underlies the attachment of K⁺ to the β- and γ-carboxyl groups is (localized) **adsorption**.

Adsorption is of great importance to the living phenomena and will be referred to very frequently in pages following. For this reason, I have provided in an endnote⁵ a brief description of its history, and other relevant information on the phenomenon. Suffice to mention here that adsorption is, in general, electrostatic in nature. It represents an equilibrium phenomenon. The adsorbed ion or molecule, though constantly desorbing from and adsorbing onto this site or other sites, spends most of its time in close contact with the adsorbing site in a *one-adsorbent* (e.g., K^+), *one-site* (e.g., a β - or γ -carboxyl group) stoichiometry.

In a resting cell, the β - and γ -carboxyl groups preponderately prefer K^+ over Na^+ . As a result, almost all cell K^+ is adsorbed on these fixed β - and γ -carboxyl groups and few of these groups are available for the adsorption of Na^+ . However, they can become more available to Na^+ if, for example, K^+ is removed from the system.

In resting frog muscle cells, about half of the cell Na^+ is adsorbed on β - and γ -carboxyl groups and the other half exists as free Na^+ in the cell water (Figure 8.2A). The inability of Na^+ to compete successfully for the K^+ -preferring β - and γ -carboxyl groups and the low solubility of Na^+ in the cell water (virtually all existing in the state of polarized multilayers) explain the low concentration of Na^+ found in most resting living cells.

Since most cell proteins carry approximately an equal number of fixed cationic charges and fixed anionic charges, the concentration (in units of equivalents) of *adsorbed cations* and *adsorbed anions* should also be roughly equal as indicated in Figure 3.3.

In Chapter 4, K^+ adsorption is considered; Chapter 5 deals with water polarization and Na^+ exclusion; Chapter 6 discusses induction with emphasis on its operation in proteins; and Chapter 7 concerns itself with long-range coherent behaviors and control based on the short-range inductive effect. We will first examine results of studies on simple inanimate model systems, in order to test the validity of the basic mechanisms suggested in the AI hypothesis. After validity at this level is successfully established, the results of investigations of living cells will be discussed in these and still later chapters.

NOTES

1. I prefer the term "high energy," meaning "high negative energy" to the alternative "minimal energy."

2. Entropy is a measure of disorder or randomness. Direct definition of entropy in terms of thermodynamics is not easy, often avoided (Glasstone, 1946, 224; 1947, 143), or given in a way that I find not 100% satisfactory (Guggenheim, 1950, 11). Yet entropy is easily defined and more understandable in terms of *statistical mechanics*. For those not already familiar with the fundamental concepts of this branch of modern physics, the following analogy from Rushbrook (1949) may be helpful.

A pack of playing cards fresh from the store is perfectly ordered. There is one and only one way of arrangement corresponding to an entropy of zero. If one begins to shuffle the cards, there would be an increase in the degree of disorder, which can be expressed by the number ω_1 of a priori *equally probable arrangements* at the stage of shuffling we have reached. If we now introduce a second pack of cards and shuffle both packs simultaneously but independently, the number of equally probable arrangements of the

cards in both packs(ω) is then the *product* of ω_1 and ω_2 , corresponding to the first and second pack of cards.

$$\omega = \omega_1 \omega_2 . \quad (\text{A})$$

Thermodynamic studies have revealed that the entropy (S) of any assembly is equal to the *sum* of the entropies of its component parts (Guggenheim 1950, 11; Fowler and Guggenheim 1960, 57).

$$S = S_1 + S_2 . \quad (\text{B})$$

A comparison of the *multiplicative* property of ω and the *additive* property of S suggests the following relationship:

$$S = k \ln \omega , \quad (\text{C})$$

where k is a constant. When we are dealing not with cards but with assemblies of atoms and molecules, ω is replaced by Ω and

$$S = k \ln \Omega , \quad (\text{D})$$

where Ω represents the number of a priori equally probable micromolecular states of the assembly. k is the Boltzmann constant, equal to $(1.38047 \pm 0.00026)10^{-16}$ erg deg $^{-1}$.

(Equation D is, without doubt, one of the most important equations in physics and it was due to the great physicist, Ludwig Boltzmann (1834–1906). Nonetheless, during his life time, he was strongly opposed by his contemporary scientists. “Feeling isolated and defeated”, Boltzmann committed suicide at the age of 62 (Bronowski 1973, 351). Equation C was later carved on his tombstone as a memorial to his immortal achievements belatedly recognized.)

An idealized crystal of ice at the temperature of absolute zero may be compared with the deck of unshuffled card and as such has very low entropy. Warming and thus vaporizing the ice into water vapor, like card shuffling, leads to a large *gain of entropy* (dS), the magnitude of which can be assessed from the following thermodynamic equation:

$$TdS = dE + PdV - \mu dN , \quad (\text{E})$$

where dE is the change of total energy of the assembly, dV is the change of the volume, and dN is the change in the number of the systems the assembly contains. T , P and μ are the absolute temperature, the pressure, and the chemical potential respectively. Equation E shows that as a rule the change of entropy of the assembly is governed by the changes of the three independent quantities, E , V and N .

In warming up and sublimating the ice crystal, the gain of entropy is primarily due to the gain of total energy (both potential and kinetic) and the gain in volume. The gain in volume in turn affects the entropy gain in two ways: that due to the gain in available space or “sites” available to the vaporized water molecules (configurational entropy) and that due to the gain in rotational and other motional freedom of the vaporized water molecules, resulting in a narrowing of the “spaces” between, and hence number of quantum-mechanically allowed energy levels which, together with the configurational entropy determine Ω of equation D.

3. The concept of life as a high-(negative)-energy, low-entropy *living state* is different from all other ideas known; nonetheless, the concept of the living state contains in part what one finds in thoughts upon *what life is* from way back in history. The following are taken from Hall’s work on *Ideas of Life and Matter* (1969, vol. 1, 19–20). “Aristotle (384–322 B. C.) equated life-as-soul with *form*”. Although Renaissance theorists did not know about babies from frozen embryos—as I did and cited in Section 1.1—they did rely on other similar examples of (reversible) suspension of life, to argue that life is *organization*, rather than *activity* emerging therefrom (emergentist view). Lamarck (1744–1829) “equated life with *arrangement* and defined it as a special “state of affairs” (*état de choses*) existing in plant and animal bodies”.

Hall further pointed out that the emergentist view has won an immeasurably larger number of adherents than the organization view. Further developments of the emergentists' view led to the idea that life is locomotion, growth, excitability, metabolism etc. (mentioned in the opening paragraph of this volume), the concept of life as a flame (see Ling 1984, 57), and the sodium pump.

4. According to the dictionary, the word *native* means "found in nature esp. in an unadulterated form" (*Webster's New Collegiate Dictionary*, 1977, 765). Therefore, one may say that all proteins found inside a living cell *in vivo* are 'native' to the cell by definition. However, the term "native protein" as used in the literature has a different meaning—even though the earlier users of this term might have thought that their "native" proteins were in fact identical to the one defined above.

Studying isolated proteins *in vitro*, protein chemists soon discovered that these proteins could exist in more than one state (without changing their primary structure). Thus gentle heating may convert a water-soluble protein into a water-insoluble one. Wu (1931) offered the first definition of protein *denaturation*: "Denaturation is a change in the natural protein molecule whereby it becomes insoluble in solvents in which it was previously soluble." Wu's "natural protein" is the equivalent of the term "native protein" as used by the majority of workers in this field today, and it is in this context that I have used the term "native protein" throughout this volume.

If we could do it all over again, we might consider reserving the term native protein for the conformation in the living cell and introduce a new name for what it is now commonly used to designate.

Knowing how difficult it is to change convention, one might as well use the term "native" as it is being used today and introduce a new term for the state of protein existing in the living cell. Indeed, this is what I have done; it is called the *living state* (Ling 1962, xxii, 1984, 147).

5. The uptake of gases by liquids and solids was designated "absorption" more than a century and half ago (Gehler 1825). Later M. L. Frankenheim (1835, 158) introduced the term *adsorption* for uptake of gases in pores or upon surfaces. However, Frankenheim's term became forgotten; it was reintroduced by Kayser 46 years later at the suggestion of the noted physiologist, E. du Bois-Reymond (Kayser 1881).

Henceforth *adsorption* has been used exclusively to describe the occurrence of a higher concentration of any component at the surface of a solid or liquid, while the more or less uniform penetration into solids is called *absorption*.

In years following, one direction in ongoing investigation stresses adsorption as a macroscopic surface or interfacial phenomenon. Thus Gortner (1938, 211) stated "Those substances which decrease surface energy tend to concentrate at a liquid-vapor interface, and those substances that decrease interfacial energy tend to concentrate at a liquid-solid or liquid-liquid interface. This phenomenon of concentrating at the interface is called adsorption." Interfacial adsorption has become less "center-stage" as the precision of our knowledge of cell physiology increases and our approaches become more and more molecular in focus.

An important landmark in the progress of our broadening understanding of adsorption in general and what I shall refer to as "localized adsorption" in particular was the introduction of a theory on adsorption by Irving Langmuir (1881–1957). Langmuir visualized the adsorption of gases to occur not at a uniform, featureless solid surface but at a finite number of localized centers of attraction or "active spots" on the surface. The equation he introduced for the adsorption of gases at a fixed temperature bears his name, i.e., *Langmuir adsorption isotherm* (Langmuir 1918). Accordingly, the amount of gas adsorbed does not increase steadily with increasing concentration (or pressure) of the gas, but asymptotically approaches a limiting value corresponding to the density of "active spots" or adsorption sites on the surface.

As more and more knowledge was gained, it has become increasingly clear that adsorption of gases and other substances are not limited to the surfaces and interfaces of solids and liquids as once thought, but may occur on adsorption sites within what one

would recognize as a solid. A clear example is the adsorption of water vapor *within* crystalline and non-crystalline proteins. While inert gases like nitrogen, argon etc. do adsorb primarily on the exposed surfaces of these proteins, water adsorption, vastly larger in quantity, are on largely polar side chains and in particular the keto and imido groups of the polypeptide chains, in the interior of the proteins (Benson and Ellis 1950; Benson et al. 1950).

In an article entitled "Adsorption als Folge von Polarization. Die Adsorptionsisotherme" de Boer and Zwikker (1929) presented an adsorption isotherm describing adsorption of (polarized) *multilayers* of gas molecules on solid surfaces. In 1936, S. Bradley derived a formally similar polarized multilayer adsorption isotherm (equation 4 of this volume) with the main difference that gaseous molecules with large permanent dipole moments (e.g., H₂O, dipole moment 1.86 debyes) were considered. Later, theoretical considerations led Brunauer et al. (1938) to the conclusion that only molecules with permanent dipole moments can form deep polarized multilayers.

An implicit assumption in deriving the Langmuir adsorption isotherm was the absence of site-to-site interaction. In this model, each adsorption is independent of other adsorptions. In 1964, Ling and Yang, using one-dimensional Ising method, derived a cooperative adsorption isotherm for one(solute)-on-one(site) adsorption with *interaction between nearest neighboring adsorption sites* (equation 7 of this volume) (Ling 1964).

What then is localized adsorption? Localized adsorption involves the attraction of molecules (or ions) to, and momentary capture by, discrete sites on a much larger, and more or less immobilized macromolecule or polar solid surface. After a relatively long "residence time" on the site, each adsorbed molecule eventually returns to the surrounding medium without being chemically altered. Localized adsorption represents a reversible equilibrium phenomenon. Underlying the favorable free energy for the adsorption are attractive forces (between the adsorbed molecule and the site) which are fundamentally electrostatic in nature (e.g., Coulombic, ion-dipole, dipole-dipole, van der Waal).

The three adsorption isotherms (Langmuir, Bradley, Yang and Ling) offer part of the theoretical framework of the association-induction hypothesis.

CELL POTASSIUM

Historically, K^+ binding on cellular proteins has been suggested from time to time as the basis of K^+ accumulation in cells (Section 1.4); such suggestions have been vigorously and effectively resisted by majority opinion throughout the entire history of cell physiology. There have been reasons for the success of this resistance:

1. In the wake of the important findings of Arrhenius (1887), and of Debye and Hückel (1923), it had become widely accepted that the degree of association of K^+ and Na^+ with their counterions is sparse or nil.

2. Pure native proteins do not as a rule adsorb or adsorb very little K^+ and Na^+ (Lillie 1923; Höber 1929).

In Section 4.1 and 4.2, I will demonstrate why full ionic dissociation derived from the study of extremely dilute solutions does not apply to living cells or even models of the living cell; and why failure to demonstrate ionic adsorption on isolated *native proteins* in vitro tells us little or nothing about ionic adsorption in living cells where the key proteins involved do not exist in the same (native) conformations.

Section 4.3 is devoted to the experimental demonstration that in the presence of ATP, the amounts of K^+ reaccumulated in and Na^+ extruded from partially lysed human red blood cells are quantitatively related to the amount of the cytoplasmic proteins (e.g., hemoglobin remaining in the cells), which provides the β - and γ -carboxyl groups for selective K^+ adsorption and the fully extended polypeptide chains which reduce the solubility of the bulk-phase water in the cell for Na^+ (and other large hydrated ions and other solutes).

Finally, Section 4.4, by far the largest, provides experimental proofs that the bulk of intracellular K^+ is selectively adsorbed on the β - and γ -carboxyl groups respectively carried on the aspartic and glutamic acid residues, which, in the case of voluntary muscle, belong primarily to myosin in the A-bands.

4.1. *Enhanced Counterion Association with Charge Fixation*

In 1952 I pointed out that *full ionic dissociation occurs only in dilute solutions of K^+ and Na^+ salts of simple (monomeric) anions (e.g., Cl^-). In living cells, K^+ (or Na^+) associates with charge-bearing proteins, which are not monomeric anions, but polymeric, fixed-charge systems.* I offered the theory of profound enhancement of counterion association with charge fixation (Ling 1960, 1962, 1984; see also Manning 1969, 1978 for a later theory of ion association; most recently in answer

to question of von Zglinicki, Ling 1990). My theory can be briefly summarized as follows.

According to the association-induction hypothesis, enhanced counterion association with charge fixation is due to both enthalpic and entropic mechanisms. Overlap of electrostatic fields of neighboring fixed charges increases the energy (enthalpy) of association of the oppositely charged counterions like K^+ . The cumulative effect of the electrostatic attraction of the fixed charges is that the dissociated counterions cannot leave the volume occupied by the (macroscopic) fixed-charge system as an expression of the *law of macroscopic electro-neutrality*.¹ Since the volume of the fixed-charge system is as a rule smaller than the volume of the bathing solution, the space of "free volume" available to the dissociated ion is small, thereby reducing the entropy of dissociation in one way. Multilayer polarization of the water, which usually accompanies the charge fixation, further reduces the entropy of dissociation of the counterions (and hence enhances their association), because polarized water has reduced solubility for the dissociated counterions like K^+ as discussed in Section 5.2.3.

Kern's work shown in Table 4.1 provides unequivocal experimental proof that charge fixation with the joining together of singly charged isobutyric acid molecules into polyacrylic acid carrying many negative charges indeed profoundly enhances Na^+ association, and with this association comes a marked decrease of the activity coefficient of Na^+ . The essence of Kern's findings was confirmed by Ling and Zhang (1983). Additional confir-

Table 4.1. Electrometric Measurements of Na^+ Activity of Aqueous Solutions of Na^+ Isobutyrate and Na^+ Polyacrylate^a (Ling 1984, by permission of Plenum Publishing Co.)

Concentration of Na^+ (M)	Activity of Na^+ (M)	Activity coefficient
Isobutyric acid, $CH_3CHCOOHCH_3$		
0.2	0.186	0.93
0.1	0.090	0.90
0.05	0.049	0.98
0.025	0.025	1.00
0.0125	0.0122	0.98
Polyacrylic acid, $(-CH_2CHCOOHCH_2-)_n$		
0.2	0.060	0.30
0.1	0.0315	0.315
0.05	0.0146	0.292
0.025	0.0058	0.232
0.0125	0.0021	0.168

^aData from Kern (1948), by permission of *Makromolekulare Chemie*.

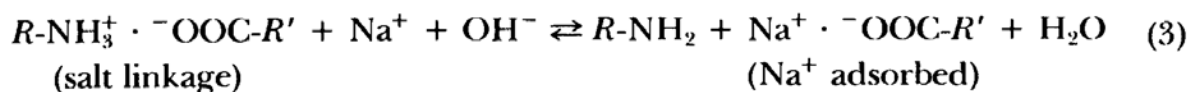
mation of the principle of enhanced counterion association is to be found in the study of K^+ and Na^+ adsorption on proteins, to be described next (see also endnote 8 of Chapter 11).

4.2. *Stoichiometric Na^+ (and K^+) Adsorption on Protein β - and γ -carboxyl Groups in Vitro*

If K^+ is adsorbed in red blood cells (and in all other living cells according to the AI hypothesis); in large measures, it is inevitable that hemoglobin provides many of the adsorption sites, because this protein constitutes 97% of the red blood cell's total proteins (Ponder 1948, 120). Yet consistently investigators have found no adsorption of K^+ or Na^+ on isolated hemoglobin in hemoglobin solutions (Beatley and Klotz 1951; Carr 1956) at the pH of cell interiors (i.e., neutral—see Aickin 1986). Similarly, if K^+ is adsorbed within muscle cells, myosin is likely to offer a significant part of its β - and γ -carboxyl groups for the adsorption (see Section 4.4). Yet despite Mullin's earlier report of success in demonstrating selective K^+ adsorption on isolated actomyosin (Section 1.3), subsequent thorough investigations also produced essentially negative results: only low level uptake was reported at neutral pH (Lewis and Saroff 1957).

*In 1952 I suggested that the failure to demonstrate adsorption of K^+ (Na^+ and other cations and anions) on "native proteins" (for definition, see endnote 4 of Chapter 3) in vitro might reflect the masking of the β - and γ -carboxyl groups when they form salt linkages with fixed cations (Ling 1952, 775, 779).² More recently, with the aid of Na^+ -selective glass electrodes, Ling and Zhang (1984) fully confirmed this **salt-linkage hypothesis**," and in so doing, removed both reasons for the early rejection of K^+ adsorption as the basis of selective K^+ accumulation in living cells—i.e., the lack of counterion association and the negligible adsorption of K^+ , Na^+ on proteins in vitro.*

Our experimental scheme to test the salt-linkage hypothesis is diagrammatically illustrated in Figure 4.1, and also in an equation form as follows:



This reaction scheme predicts that there is a one-to-one relationship between fixed cations ($R^-NH_3^+$) neutralized, and Na^+ adsorbed. This relationship is expected if one titrates a solution of hemoglobin, for example, with increasing amounts of NaOH. Allowing a suitable length of time for "unmasking" (Steinhardt and Zaiser 1955) and equilibration, one determines both the pH and the free Na^+ concentration (which the Na^+ -selective electrode registers). From these values and the known amount of Na^+ added as hydroxide, one obtains two sets of data: the OH^- bound, or the extent of neutralization of the cationic groups, and the moles of Na^+ adsorbed (which the Na^+ -selective electrode does not register).

The twofold theoretical predictions are: (1) that the experimental titration curve and the Na^+ -adsorption data should coincide with each other, and (2) that

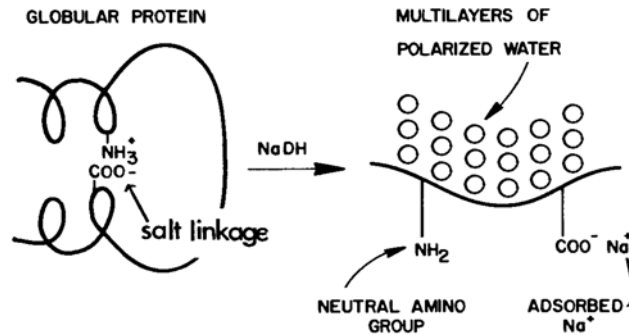


Figure 4.1. Diagrammatic illustration of the effect of NaOH on the neutralization of the fixed cationic NH_3^+ groups, the adsorption of Na^+ on the anionic β - and γ -carboxyl groups thus liberated from the salt linkages ($-\text{NH}_3^+ \cdot ^-\text{OOC}-$) in the native globular protein and the multilayer polarization of the bulk-phase water.

both sets of data should also coincide with the appropriate titration curve theoretically calculated from the known combinations of the fixed cationic groups of hemoglobin, and the known pK_a values of these groups. Figure 4.2 shows that the Na^+ -adsorption data does indeed coincide with the theoretically calculated titration curve. Figure 4.3 (D) shows that the experimental titration data also coincide with the theoretically calculated one. However, these two theoretical curves are not the same for the following reasons.

There are two theoretically calculated titration curves in Figure 4.3 (C and D). While Curve C fits the acid titration data, only Curve D fits the Na^+ -adsorption

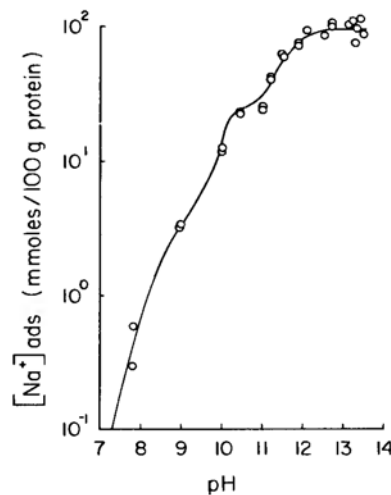


Figure 4.2. The quantitative relation between fixed cations neutralized by NaOH and Na^+ adsorbed. Points are the concentrations of Na^+ adsorbed in 10% bovine hemoglobin at different pHs experimentally measured. The solid line going through or near most of the experimental points represents the concentration of fixed cations neutralized (at the pH indicated on the abscissa) theoretically calculated from the titration curves of all the α -amino groups, ϵ -amino groups, and guanidyl groups of 100 g. of hemoglobin. (Ling and Zhang 1984, by permission of Physiological Chemistry Physics and Medical NMR)

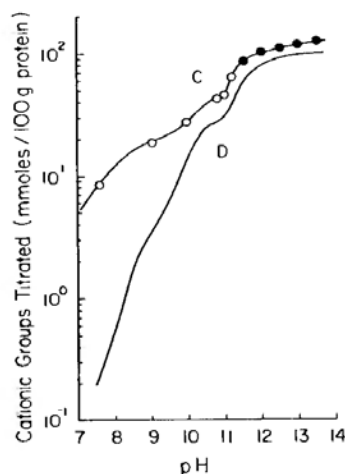


Figure 4.3. Comparison of theoretically calculated NaOH titration curve of hemoglobin (C) with experimental titration data shown as empty and solid circles. The theoretically calculated Curve C is a composite of five calculated curves corresponding to the titration of histidine groups, α -amino groups, ϵ -amino groups (2 types), and guanidyl groups. Curve D (which is the same as the solid curve of Figure 4.2) is the composite Curve C minus the histidine-group titration curve. (Ling and Zhang 1984, by permission of Physiological Chemistry Physics and Medical NMR)

data. The difference arises from the fact that while histidine groups are titrated in the pH range studied they are instantly titratable in near neutral pH range in the native hemoglobin, and are thus not masked (as all the other fixed anionic and fixed cationic groups have long been known to be, see Ling and Zhang 1984, 229; Edsal and Wyman 1958, 539). Not being masked means that histidyl groups do not participate in the reaction depicted in equation 3. Hence the correct theoretical titration curve to compare with the Na^+ -adsorption data is the one calculated from all basic groups except histidine, i.e., curve C of Figure 4.3.

The question may be asked "Since the salt-linkage hypothesis was offered in relation to the theory of selective K^+ accumulation in living cells, why are the studies here primarily on Na^+ ?" In answer I want to point out that the salt-linkage hypothesis was *not* suggested to explain K^+ accumulation *only*. It was suggested to explain why many free monovalent cations (including K^+ and Na^+) fail to adsorb on the β - and γ -carboxyl groups of native proteins. To verify the hypothesis, one may choose either K^+ or Na^+ or any other monovalent cation for study. However, for technical reasons, Na^+ was studied because the Na^+ -sensitive electrode available to us was far superior in specificity to the K^+ -selective electrode we could obtain. High specificity was essential in order to determine quantitatively the relative adsorption constants of different alkali-metal ions on the β - and γ -carboxyl groups, described by Ling and Zhang (1984).

It should also be mentioned that aside from their low capacity for K^+/Na^+ adsorption, isolated proteins per se do not as a rule have the preference for K^+ (over Na^+) detected in living cells (see Section 8.4.2.3 for possible reasons). Our study of alkali-denatured hemoglobin show that the cation adsorption demonstrated is specific, and that they all compete for the β - and γ -carboxyl groups.

The preference of these β - and γ -carboxyl groups follows the rank order: $\text{Na}^+ > \text{Li}^+ > \text{K}^+ > \text{Rb}^+, \text{Cs}^+$.

Just as significant was the finding that the adsorption of Na^+ is *autocooperative*, i.e., the binding of one Na^+ ion enhances the strength of binding of the next Na^+ ion, much as the binding of one oxygen molecule on hemoglobin enhances the affinity for a second oxygen molecule. The subject of *cooperativity* will be discussed in detail in Chapter 7.

Titration with alkali hydroxide has successfully verified the hypothesis that it is the formation of salt linkages between fixed anions and fixed cations that prevents native protein like hemoglobin from adsorbing K^+ , Na^+ and other alkali-metal ions. Nonetheless, the treatment with NaOH is drastic and unphysiological. To effectively eliminate similar competing fixed cations, the living cell must rely on a better method. Reserving a full discussion for a later section, I shall mention briefly here that “neutralization” of the fixed cationic charge in the living cell is achieved by the adsorption of a suitable anions on the fixed cations, under the guiding influence of an as yet unidentified protein and of the cardinal adsorbent, ATP (see Section 8.4.2.4 for details).

4.3. *Demonstration of a Stoichiometric Relation Between Concentration of Cell K^+ and the Concentration of Cytoplasmic Proteins, Primarily Hemoglobin*

The human red blood cell is unique among living cells in that 97% of its protein content comprises one single protein, hemoglobin. Thus if the β - and γ -carboxyl groups of the cytoplasmic protein selectively adsorb K^+ , and in the red blood cells, hemoglobin provides these β - and γ -carboxyl groups (a concept suggested by in vitro study of alkali-metal-ion adsorption on isolated hemoglobin discussed in the preceding section), then there should be a stoichiometric relationship between the concentration of K^+ and the concentration of hemoglobin in the cells.

As a rule it is very hard experimentally to vary protein concentrations in *living* cells over a wide range without cell destruction and death. Human red blood cells, however, offer yet another unique set of traits that allows just such a quantitative manipulation of the intracellular concentration of hemoglobin.

When human red blood cells are hemolyzed at 0°C in a hypotonic solution containing ATP, the cells swell and lose much of their intracellular hemoglobin. With these changes, the K^+ and Na^+ concentrations in the “red cell ghosts” become equal to those in the external medium. On return to an isotonic medium at 37°C containing ATP, the ghosts regain their original size and shape and also begin to reaccumulate K^+ and extrude Na^+ . However, under essentially the same experimental conditions, the levels of K^+ and Na^+ eventually attained vary widely with the blood donors.

Neither reaccumulation of K^+ nor extrusion of Na^+ occurs in ghosts retaining less than 2% proteins (and other solids) or in the absence of ATP. Above a protein (and other solids) concentration of 2% and in the presence of ATP, the protein concentration is linearly

correlated to the K^+ concentration reaccumulated, with a correlation coefficient of +0.78. (The corresponding correlation coefficient with Na^+ extruded is +0.81 see Figure 4.4.) (Ling et al. 1984). By extrapolation of the straight line obtained by the method of least squares, one obtains, at a concentration of cell proteins equal to that of normal human red blood cells (35%), the same concentration of K^+ as is found in normal cells (96 to 100 mmoles/liter of fresh cells). Since 97% of red cell protein is hemoglobin, the protein described in Figure 4.4 may be regarded as mostly hemoglobin (M. W. 67 kilodaltons). From the slope of the straight line obtained by the method of least squares, one calculates that about 23 moles of K^+ is bound to each mole of hemoglobin, as compared to its total content of 60 β - and γ -carboxyl groups per mole (Perutz 1969).

4.4. Adsorption of Cell K^+ on β - and γ -carboxyl Groups of Cytoplasmic Proteins

4.4.1. Localized Distribution of K^+ in Cell Regions Rich in β - and γ -carboxyl Groups

Frog muscles contain 20% dry matter, mostly proteins. Fifty-seven percent of muscle protein is myosin; 17.5% of the amino-acid residues of myosin carry

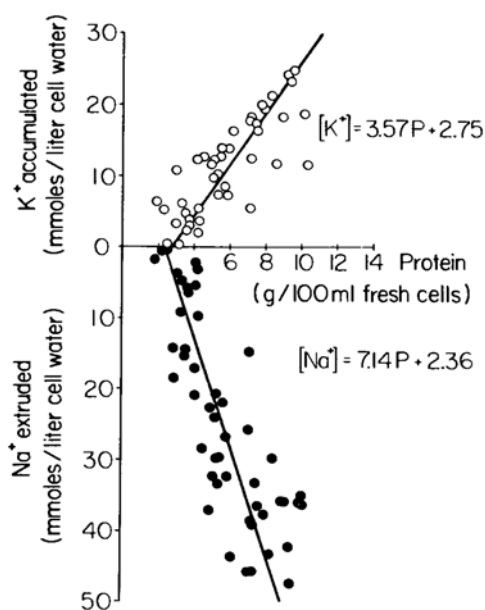


Figure 4.4. K^+ accumulation in and Na^+ extrusion from ghosts prepared by the procedure used in obtaining the data shown in Figure 2.4, see Section 4.3 in text. Blood of different donors and of the same donors (at times at least 6 weeks apart) was studied. Each data point represents the difference of K^+ or Na^+ concentration in the ghosts at the beginning of incubation and after 18 hours of incubation in the presence of ATP (37°C). Straight lines corresponding to the two equations shown in the graph were obtained by the method of least squares. Total protein content represented as P in the equations was obtained by subtracting weights of lipids, phospholipids, salt ions, and sucrose from the dry weights of the ghosts. (Ling, Zodda, and Sellers 1984, by permission of Physiological Chemistry Physics and Medical NMR)

anionic (free) β - or γ -carboxyl groups. Using an average amino acid residue weight of 112 (Ling 1962, 48), one estimates that myosin alone provides $(200/112) \times 0.57 \times 0.175 = 0.177$ M β - and γ -carboxyl groups per kilogram of fresh muscle cells, which amounts to from 62% to 69% (averaging 66%) of all the β - and γ -carboxyl groups in muscle cell proteins (Ling and Ochsenfeld 1966) (see endnote 3). *Thus if β - and γ -carboxyl groups are indeed the adsorption sites for K^+ , as postulated in the AI hypothesis, much of the cell K^+ must be adsorbed on myosin. Since myosin is found only in the A bands of skeletal muscle cells (Huxley 1853; Engelmann 1873; Huxley and Niedergerke 1958; see also Ling 1984, 228), much of the cell K^+ should be found in the A bands⁴.* Ludwig Edelmann, at Homburg, West Germany, and I began at the same time to test this prediction. I chose autoradiography. Ideally, one should use radioactive K^+ . Unfortunately, of the two radioactive K^+ isotopes, one (^{42}K) is too short-lived and the other (^{40}K) too expensive. Cs^+ offers itself as a suitable surrogate for K^+ for two reasons: Cs^+ is accumulated in the cell in the same manner as K^+ , and Cs^+ can replace K^+ stoichiometrically and reversibly; a long-lived and inexpensive radioactive isotope (^{134}Cs) is readily available.

Figure 4.5 shows an autoradiograph of an air-dried isolated single muscle fiber in which the bulk of cell K^+ was replaced by ^{134}Cs -labeled Cs^+ (Ling 1977). Since only part of the muscle fiber was covered by the photoemulsion, it is easy to see that *the silver granules which indicate the location of labeled Cs^+ are found primarily over the dark, or A bands, as predicted.*

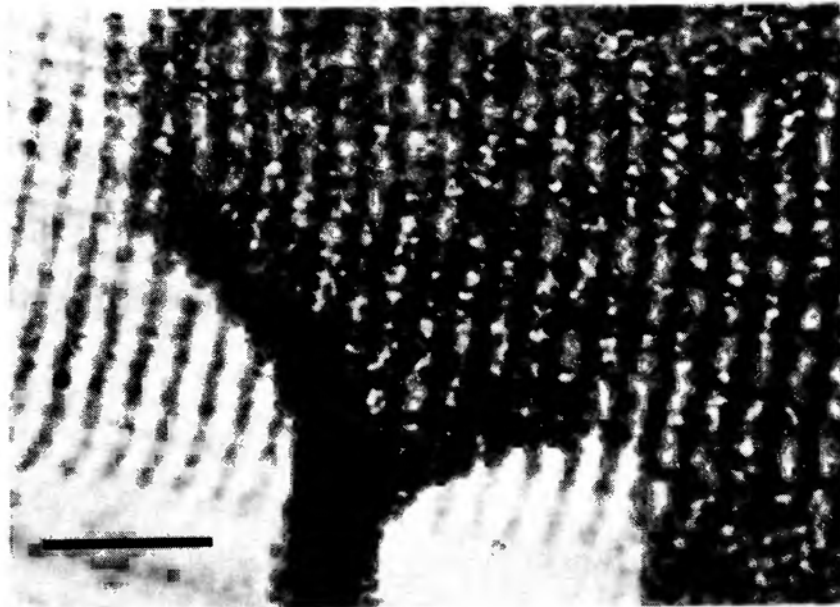


Figure 4.5. Autoradiograph of a portion of an air-dried single frog muscle fiber which had been loaded with ^{134}Cs -labeled Cs^+ while living and before drying. The part of the muscle fiber, not covered with photoemulsion, reveals directly the location of dark (A) bands and light (I) bands and indirectly the location of most of the silver-granules and hence that of labelled Cs^+ (in the A bands). (Ling 1977, by permission of Physiological Chemistry and Physics)

Edelmann used transmission electron microscopy. He examined the distribution of Cs^+ or thallium (Tl^+) in frog muscle cells in which the bulk of K^+ had been replaced by these ions. Here, Cs^+ (atomic weight, 133) and Tl^+ (atomic weight, 204) were chosen for their high *electron density*. Like electron-dense uranium, used to stain chemically fixed cell preparations, Cs^+ and Tl^+ can also effectively block the passage of an electron beam. As a result, cell structure adsorbing these ions under physiological conditions will appear dark in the electron microscopic (EM) plate, if the preparation of the EM plate does not disturb their normal physiological adsorption. Using a new method of freeze-drying which he developed to achieve this goal (see Edelmann, 1986a), Edelmann (1977) directly visualized Cs^+ or Tl^+ in the muscle sections that had not been chemically fixed or stained. From the darkened areas in his EM pictures, reproduced here in Figure 4.6B and C, one finds that the bulk of the K^+ -surrogates, Cs^+ and Tl^+ , are indeed located in the A bands (and much less, though at high density at the Z lines). That the darkened areas indicate the loci of adsorption of Cs^+ and Tl^+ is corroborated by the lack of similar dark areas in muscle which contain only the less electron-dense K^+ (Figure 4.6F) and by the disappearance of the dark materials by washing the section with water (Figure 4.6E). Furthermore, a comparison with an EM picture of a muscle fiber prepared by the conventional method of chemical fixation and uranium staining (Figure 4.6A) reveals a close similarity, suggesting

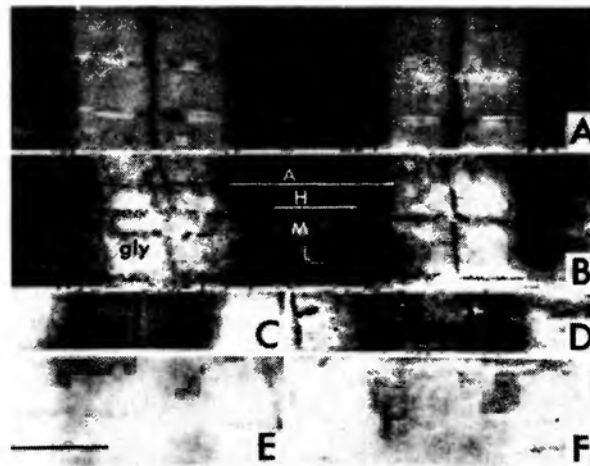


Figure 4.6. Electron micrographs (EM) of portions of single frog sartorius muscle fibers.

- (A) Muscle fixed in glutaraldehyde (only) and stained (only) with uranium by conventional procedure.
- (B) EM of section of freeze-dried Cs^+ -loaded muscle, prepared without chemical fixation or staining.
- (C) Tl^+ -loaded muscle prepared without chemical fixation or staining.
- (D) Same as (C) but following exposure of the section to moist air, which causes the hitherto evenly distributed Tl^+ in the A bands (and Z line) to transform into granular deposits.
- (E) Section of central portion of (B) after leaching in distilled water.
- (F) Normal " K^+ -loaded" muscle fiber. Scale bar: $1 \mu\text{m}$ [(A) from Edelmann, unpublished. (B–F) from Edelmann 1977, by permission of Physiological Chemistry and Physics]

that uranium also binds onto the same β - and γ -carboxyl groups in the muscle cells which, in the living state, selectively adsorb K^+ (see also Hodge and Schmidt 1960).

Since the data of Figures 4.5 and 4.6 were published, a great deal of work using a variety of independent methods has fully verified the earlier conclusions of Edelmann and of Ling, and has added new dimensions to the conclusion that the bulk of cell K^+ is located in the A bands. Since earlier findings have been repeatedly reviewed (Edelmann 1980–81, 1984; Ling 1984, 228), only a few important and new results will be briefly discussed.

(1) Conclusions from autoradiographic studies of air-dried muscle fiber loaded with Cs^+ (Figure 4.5) have been fully confirmed in frozen, *fully-hydrated* muscle fibers loaded with radioactively labeled Cs^+ and Rb^+ (Edelmann 1980) (Figure 4.7a, b, c). This confirmation has eliminated the possibility that the observed pattern of ion distribution shown in Figure 4.5 was an artifact arising from cell drying.

(2) Conclusions from the earlier transmission-electron-microscopic studies of freeze-dried specimens have been fully confirmed and verified in frozen, fully-hydrated cryosections of muscle physiologically loaded with thallium (Figure 4.8a) (Edelmann 1984a).

(3) Autoradiography of frozen-hydrated muscles previously loaded with ^{22}Na in a Ringer solution containing much ^{22}Na -labeled Na^+ but very little K^+ showed that the labeled Na^+ was also located primarily at the A bands (Figure 4.7d). This result confirms the hypothesis that the low level of Na^+ in cells is partly due to its inability to compete successfully against K^+ for the β - and γ -carboxyl groups (Section 3.3). When K^+ is removed from the bathing medium, Na^+ takes its place (primarily at the A bands.)

(4) While K^+ surrogates like Cs^+ and Tl^+ were used effectively in autoradiographic and transmission EM studies, dispersive-x-ray microanalyses reveal directly the distribution of K^+ itself, as shown in Figure 4.9 (Edelmann 1978, 1983; Trombitás and Tigy-Sebes 1979). Thus far investigations from my laboratory in the U.S., from Edelmann's laboratory in West Germany, and from Trombitás–Tigy-Sebes's laboratory in Hungary are in full agreement (see also von Zglinicki, 1988). However, from x-ray studies, Somlyo et al. (1981), using freeze-drying–cryosection techniques, reached an entirely different conclusion. These authors claim that the K^+ concentration is somewhat higher in the I band (which has a somewhat higher water content) than in the A band (which has a somewhat lower water content), in agreement with the membrane theory (see also Sjöström and Thornell 1975). This opposite conclusion was shown by Edelmann (1983), using similar freeze-drying–cryosection techniques, to be due to Somlyo et al.'s choice of the middle part of the I band (which includes the K^+ -rich Z line) to represent the I band, and the choice of the K^+ -poor middle portion of the A band to represent the A band. Edelmann showed that if x-ray beams are focused exclusively in the regions of the I band away from the Z line, then the K^+ abundance revealed is always lower than either that in the A bands or that in the Z line (Figure 4.10). The same relationships hold for Rb^+ , Cs^+ , or Tl^+ .

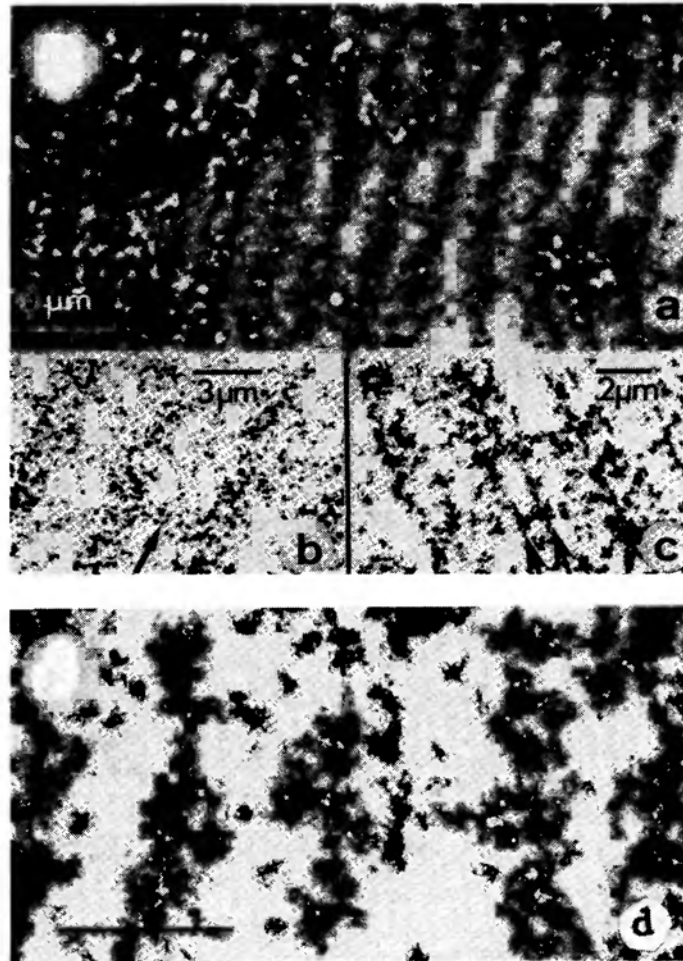


Figure 4.7. Autoradiographs of portions of single frozen fully hydrated frog muscle fibers.

- Light microscopic ^{134}Cs autoradiogram of a stretched Cs^+ -loaded fiber.
- Electron microscopic ^{134}Cs autoradiogram of a stretched Cs^+ -loaded fiber. The sarcomere length is about $4.4\ \mu\text{m}$. Between two dark bands (A bands) a line of silver grains indicates position of the Z line (arrow).
- Electron microscopic ^{86}Rb autoradiogram of a stretched Rb^+ -loaded fiber. The sarcomere length is about $3.3\ \mu\text{m}$. Arrows indicate dark lines at the outer edges of an A band. (Edelmann 1980a, by permission of Histochemistry)
- Electron microscopic ^{22}Na autoradiogram of a portion of a stretched K^+ -depleted frog sartorius muscle fiber which contained much Na^+ (labeled with ^{22}Na) and proportionately less K^+ . From the distance between neighboring rows of silver grains, sarcomere lengths of about $3\ \mu\text{m}$. are estimated. Bar = $3\ \mu\text{m}$. (Edelmann 1986, by permission of Scanning Electron Microscopy Inc.)

loaded muscles (Figure 4.10b, c, d). Edelmann was also able to reproduce Somlyo et al.'s results at will by following Somlyo et al.'s procedures.

In summary, there is now extensive and unanimous evidence demonstrating that intracellular K^+ in muscle cells is mainly located in the A bands and is least in the I band away from the Z line. These are highly important findings. However, localization cannot be equated to specific adsorption as predicted in the AI hypothesis. Thus it is conceivable that these ions only hover around fixed anions

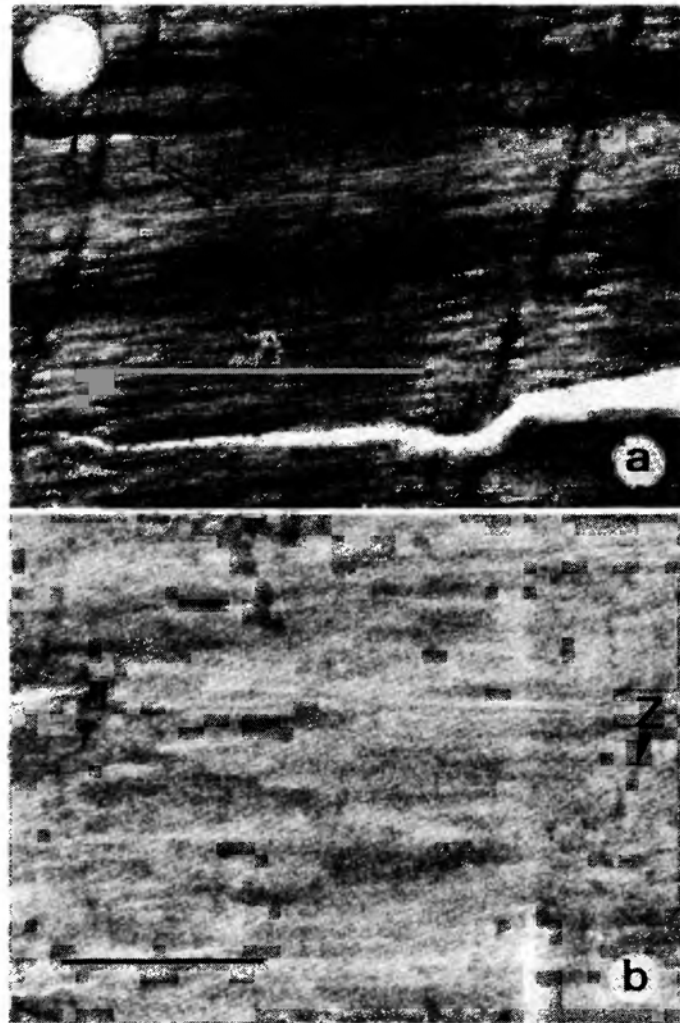


Figure 4.8. Frozen hydrated longitudinal cryosections of frog sartorius muscle.
 (a) Most of the cellular K^+ was displaced by Tl^+ . Dark Z lines (Z) and dark A bands (A) indicate sites of preferential Tl^+ accumulations.
 (b) Control: normal K^+ containing muscle. Only very faint Z lines (Z) of the slightly stretched muscle can be seen. Bar = $1\mu m$ (Edelmann 1984a, by permission of Physiological Chemistry Physics and Medical NMR)

in these loci,⁵ and that selectivity among the alkali-metal ions is achieved at the cell membranes. The following section will deal with this possibility.

4.4.2. *The Selectivity in Adsorption Among Tl^+ , Cs^+ , Na^+ and other Ions Not Due to the Cell Membranes and Postulated Pumps*

4.4.2.1. *Demonstration of Selective Ionic Accumulation in Cells Without a Functional Cell Membrane and Postulated Pumps*

The demonstration was done as follows. A frog sartorius muscle comprises about one thousand single muscle fibers, each running all the way from one end of the muscle to the other. After one end of the muscle was amputated, the cut

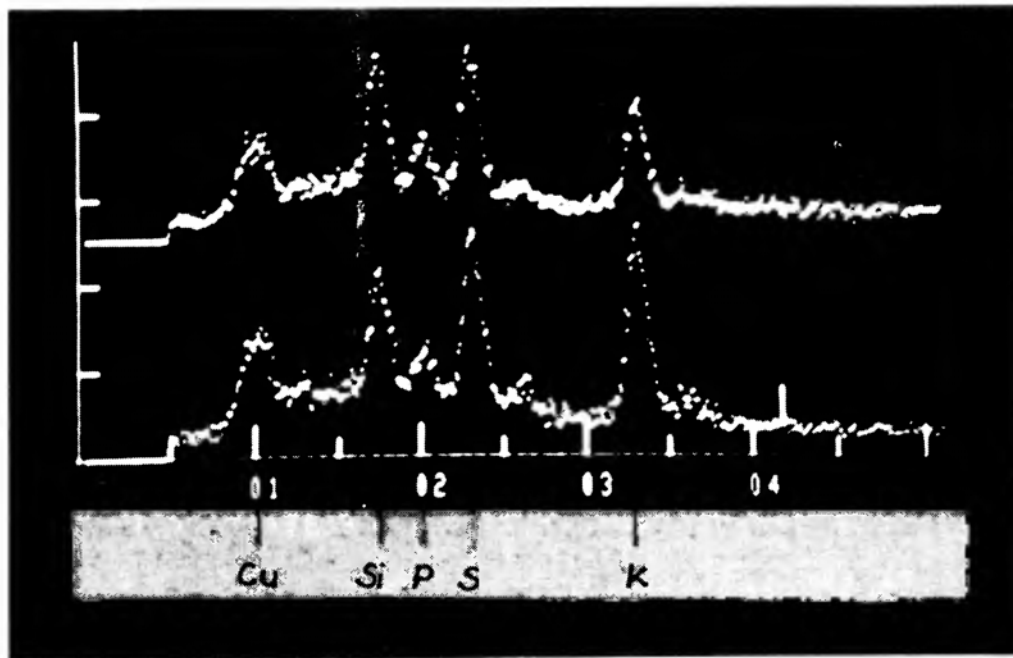


Figure 4.9. X-ray microanalytic curves of A bands (lower curve) and I bands (upper curve) of single isolated myofibril from honeybee thorax muscle. Greater abundance of K^+ in the A band is indicated by the larger peak (marked K) in the lower curve than in the upper curve. (Tigyi et al. 1981, by permission of Springer-Verlag)

ends of all the muscle fibers [which do not regenerate a new membrane (Figure 4.11 from Cameron 1988, see also Table 5.4 in Ling 1984, 136)] were exposed to a Ringer solution containing labeled ions, while the region of the muscle cells away from the cut was suspended in vaseline or air. In this preparation (Figure 4.12), the intact part of the cell membrane and its postulated pumps are made nonfunctional, because air (or vaseline) cannot serve as a “source” of K^+ for the postulated inward K^+ pump, nor as a “sink” for Na^+ for the postulated outward Na^+ pump. The tight-fitting gasket (Figure 4.12g) has effectively eliminated ion movement between fluids in the extracellular space on one side of the gasket and the Ringer solution on the other side of the gasket (for details, see Ling 1978). For these reasons, the preparation is referred to as an *effectively membrane-pump-less, open-ended cell (EMOC) preparation*. Figure 4.13 shows how, in the region of the muscle fibers remote from the gradually deteriorating cut end, accumulation of labeled K^+ reached higher levels than in the external medium, while the uptake of Na^+ stayed at levels consistently below that in the external medium—very much like normal muscle performance in a similar environment.

Figure 4.14 shows four more sets of labeled- K^+ and labeled- Na^+ distribution in EMOC preparations after 40 hours of incubation. These graphs also include the distribution profile of *total* K^+ concentration determined by atomic absorption spectrometry. Comparing the labelled-ion distribution with that of the total- K^+ distribution, one finds that the failing ability of the segments near the cut ends to accumulate labeled K^+ and to exclude labeled Na^+ follows the profile of the declining total- K^+ content of the muscle cells in a parallel and anti-parallel

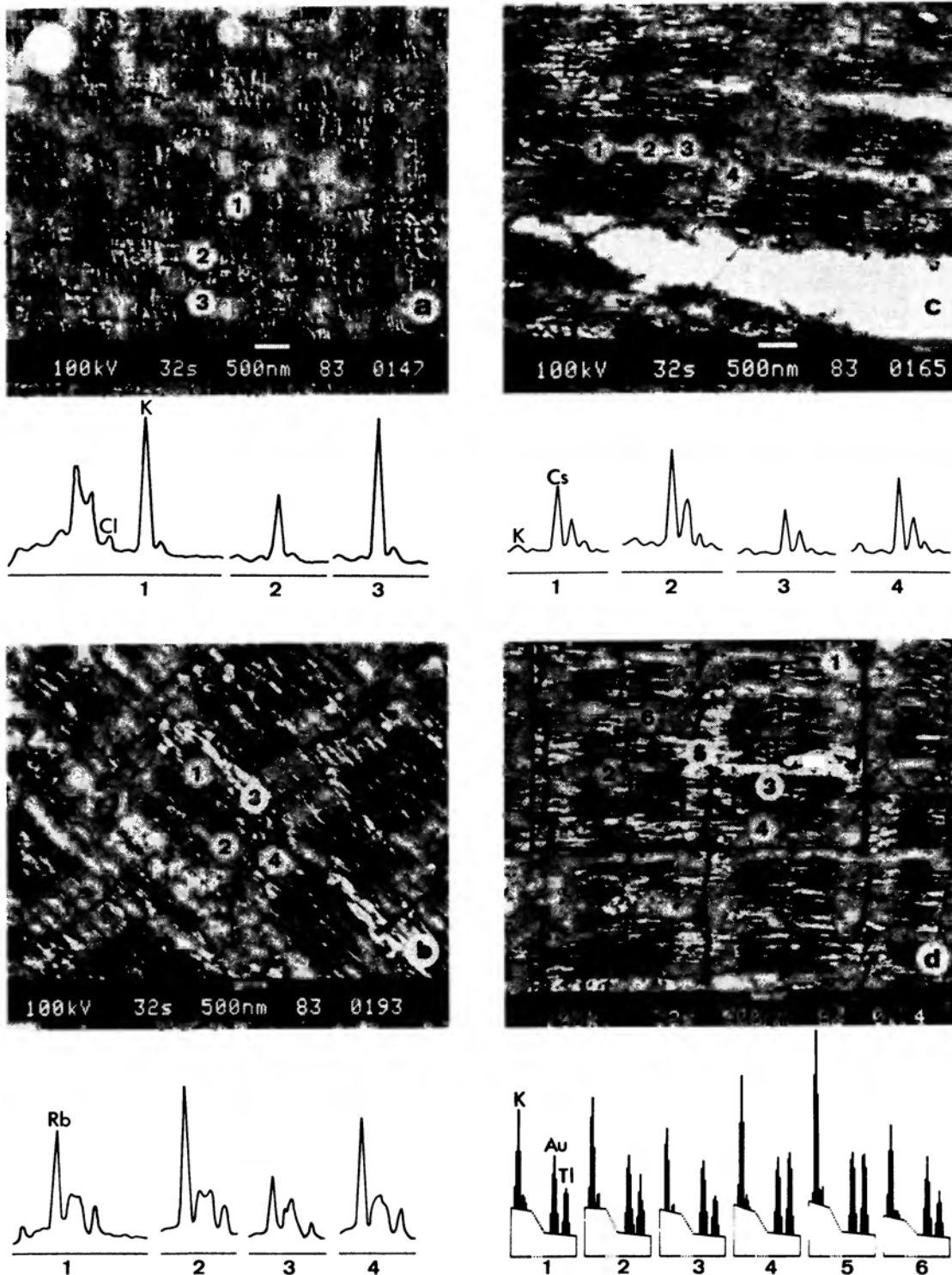


Figure 4.10. X-ray spectra from numbered areas of cryosections of frog sartorius muscle. (a) normal K^+ -containing muscle. (1) A band; (2) I band without Z line; (3) I band with Z line. (Energy of chlorine spectrum Cl : $K_{\alpha} = 2.621$ keV; energy of potassium spectrum K : $K_{\alpha} = 3.312$ keV. (b) Rb^+ -loaded muscle. (1) middle region of an A band; (2) marginal region of an A band; (3) I band without Z line; (4) I band with Z line. Rb : $L_{\alpha} = 1.694$ keV. (c) Cs^+ -loaded muscle. (1), (2) A band regions; (3), (4) I band regions. K : $K_{\alpha} = 3.312$ keV; Cs : $L_{\alpha} = 4.286$ keV. (d) Tl^+ -loaded muscle (1) 2 whole sarcomeres; (2) an entire A band; (5) edge of an A band; (6) center of an A band; (3) portion of an I band away from the Z line; (4) portion of an I band including the Z line. K : $K_{\alpha} = 3.312$ keV; Au : $L_{\alpha} = 9.712$ keV; Tl : $L_{\alpha} = 10.267$ keV. (Edelmann 1983, by permission of Physiological Chemistry Physics and Medical NMR)

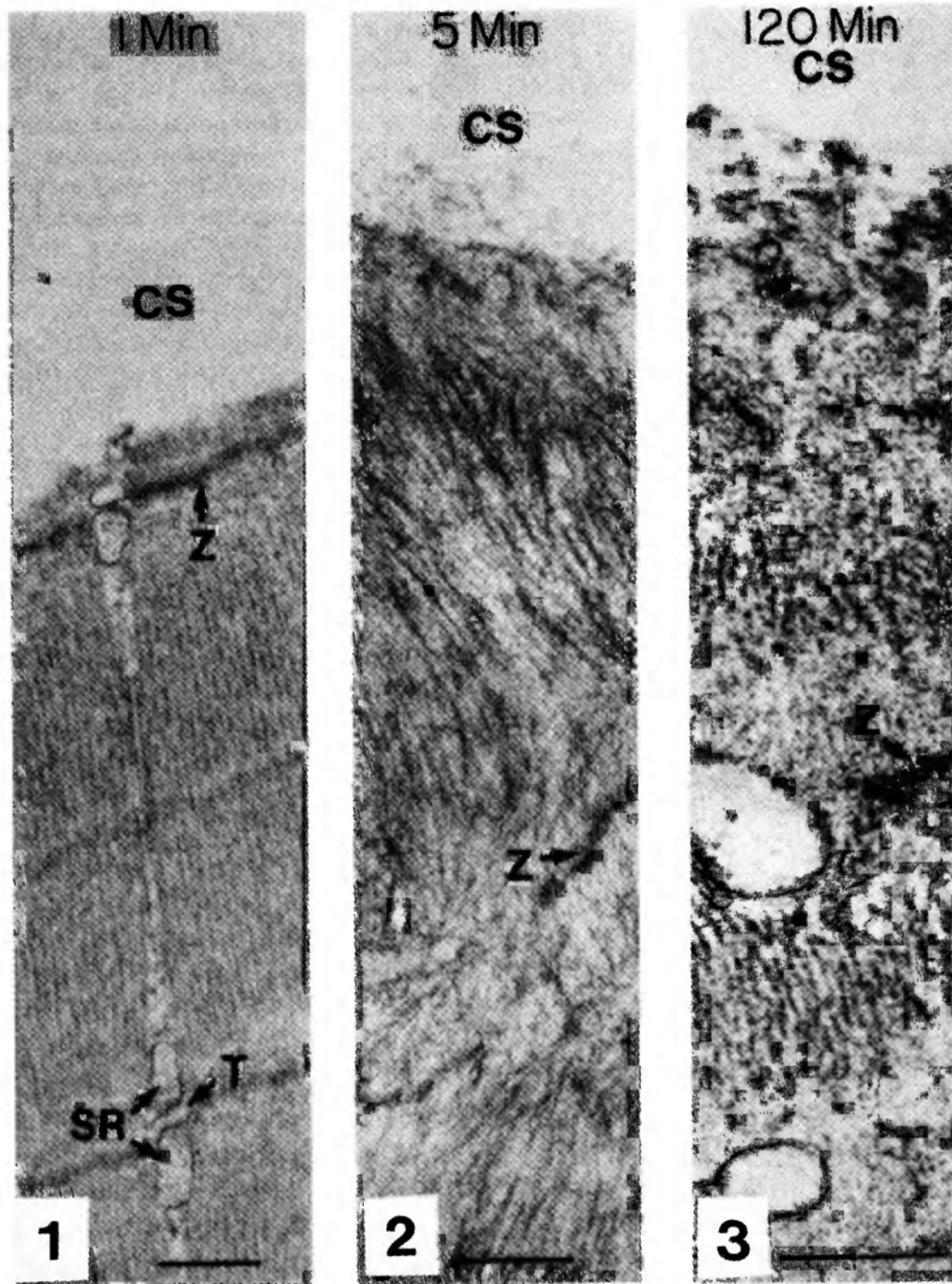


Figure 4.11. Electron-micrographs from the cut ends of longitudinally oriented one cm segments of muscle fibers fixed at 1 min. (Plate 1), 5 min. (Plate 2) and 120 min. (Plate 3) after transection of the muscle fiber. Plate 1 shows contraction of the sarcomere immediately next to the cut surface (CS). Plate 2 and 3 show progressive disorganization of the surface sarcomeres, and the failure of the cut surface to generate a plasma membrane. A one micron marker bar is present in each micrograph. Z, T and SR represent Z-line, T-tubule, and sarcoplasmic reticulum respectively (From Cameron, 1988, by permission of *Physiol. Chem. Phys. & Med. NMR*).

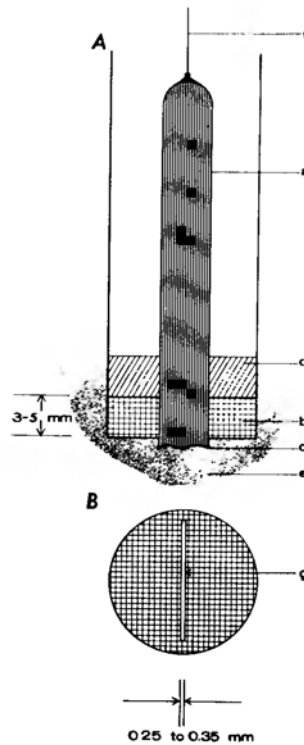


Figure 4.12. Diagram of the effectively membrane-pump-less open-ended cell (EMOC) preparation. (A) Side view; (B) bottom view. Only the cut end of the muscle (d) is in direct contact with the labeled Ringer solution (e); (a) sartorius muscle; (b) silicone rubber gasket; (c) vaseline; (f) anchoring string; (g) slit in silicone-rubber gasket. (from Ling 1978, by permission of Journal of Physiology)

fashion respectively. (For a “short-cut” to obtain the more relevant adsorbed labeled K^+ distribution rather than the total labeled K^+ distribution shown in Figure 4.14, see legend of the same figure).

The EMOC preparation of frog sartorius muscle was also used to investigate the mobility of K^+ in frog muscle cytoplasm (Section 2.4.1). Comparing the K^+ -mobility data with data shown in Figure 4.14, one finds that near the cut edge where the total K^+ has dropped to low levels, the K^+ mobility measured was three times faster than that measured in the region remote from the cut end and still retaining a normal concentration of K^+ . In the region far from the cut end the K^+ mobility is eight times slower than K^+ diffusion in 0.1 N potassium iodide solution.

Persistent selective K^+ accumulation and Na^+ exclusion in EMOC preparation of frog muscle show that intact and functional cell membrane are not necessary for the accumulation of K^+ and exclusion of Na^+ . These findings provide the counterpart of the failure to demonstrate active transport in axoplasm-free, squid-axon-membrane sacs (Section 2.3). Together, they offer convincing evidence against the membrane-pump hypothesis, and equally convincing evidence for the AI hypothesis.

Figure 4.15 shows that the rank order of frog muscle's preference for Tl^+ , Cs^+ , and Na^+ ($Tl^+ > Cs^+ > Na^+$) also persists in the EMOC preparation in which

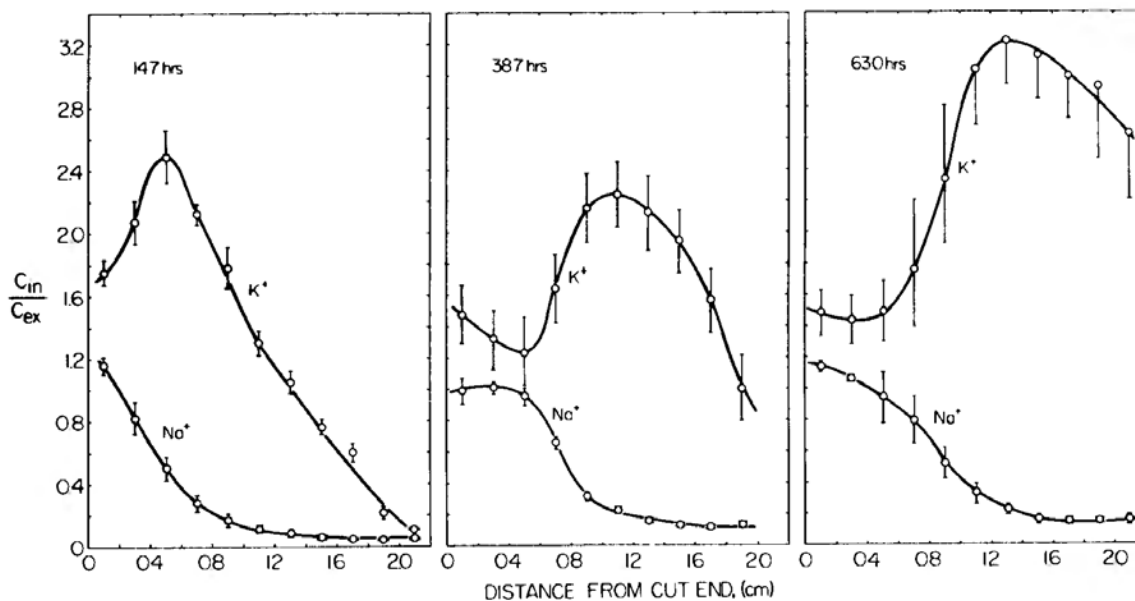


Figure 4.13. Simultaneous influx of labeled K^+ and labeled Na^+ into sartorius muscle EMOC preparations through their cut ends (see Figure 4.12 for experimental setup used). The three groups of frog sartorius EMOC preparations studied were exposed to normal Ringer solutions labeled with both ^{42}K and ^{22}Na for 14.7, 38.7, and 63.0 hr, respectively at 25°C. The abscissa represents the distance of the midpoint of each cut segment from the cut surface of the muscle fibers. The ordinate represents the ratio of the labeled K^+ or Na^+ concentration in the water of each muscle segment (C_{in}) to the concentration of the same labeled ion in the solution bathing the cut end of the muscle at the conclusion of the experiment (C_{ex}). (Ling 1978, by permission of Journal of Physiology.)

no pumps could operate. *These three ions, as well as other alkali-metal ions, share the same long-range attributes of all univalent cations, and differ only in their short-range attributes. In other words, the difference among the three ions could not be "perceived" without close-contact interaction with the fixed anions.* The preservation of the normal rank order in the EMOC preparation also shows that the discriminatory close-contact adsorption of these ions is not at the cell membrane, and must occur after the ions have entered into the cytoplasm, which is, in essence, water and proteins. Since water does not offer binding sites for ions, but proteins do, the required close-contact adsorption could only have occurred on cytoplasmic proteins. In the following section, further confirmation of this conclusion is provided by Edelmann using yet another new approach.

4.4.2.2. Selective adsorption of K^+ (and Cs^+) over Na^+ in freeze-dried and embedded thin muscle sections

According to the AI hypothesis, selective adsorption of K^+ over Na^+ on protein carboxyl groups occurs in cells maintained at their living state. The maintenance of the living state, in turn, depends on the adsorption of certain *cardinal adsorbents* on appropriate sites on the protein involved. Among the cardinal adsorbents, the most important is ATP (Section 3.2).

In theory, a most direct way of testing this hypothesis would be to isolate

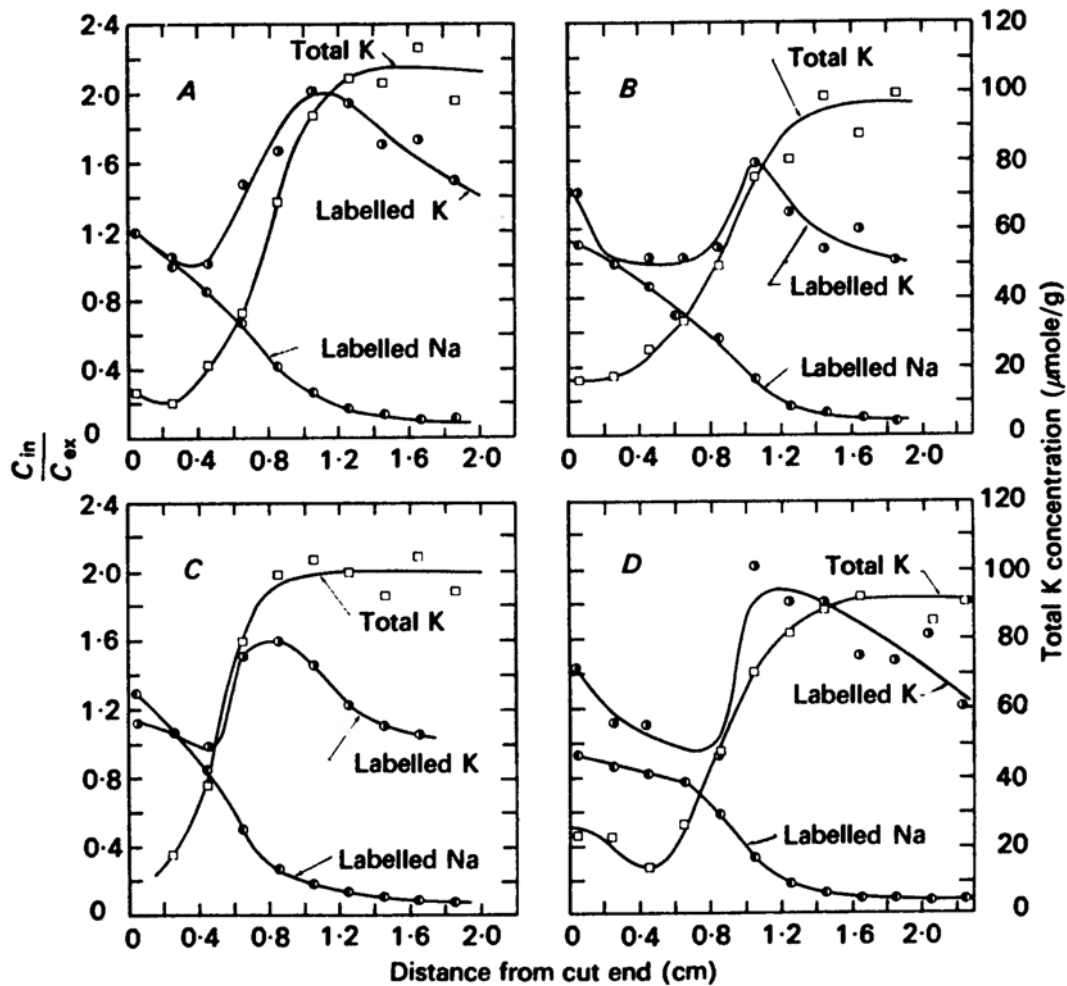


Figure 4.14. The distribution of total K^+ , labeled K^+ , and labeled Na^+ in cut frog sartorius muscles. The duration of the experiment was 40 hours at $25^\circ C$. Total K^+ of muscle segments was analyzed after a second counting of the radioactivity of the HNO_3 extract; otherwise similar to data given in Figure 4.13. To roughly assess the concentration profile of *adsorbed* labeled K^+ along the length of the muscle, one subtracts the value of (C_{in}/C_{ex}) of labeled Na^+ —as a substitute for the corresponding, but unmeasured value of labeled K^+ in the muscle water—from the (C_{in}/C_{ex}) of labeled K^+ of the corresponding section. A labeled K^+ profile so obtained will give a clearer insight into the closer true relationship between labeled K^+ adsorption and the total K^+ distribution profile. (Ling 1978, by permission of Journal of Physiology)

(physically) the cytoplasmic-protein complex in its living state and test its predicted ability of selectively adsorbing K^+ over Na^+ *in vitro*. In practice, this *direct* approach proves difficult, because the living state is metastable and topples easily. (Nonetheless, the EMOC preparation had *in effect* achieved a similar aim; see Section 4.4.3 for still another effort in this direction).

Some years ago, Ludwig Edelmann thought that rapid freeze-drying and embedding in plastic might be able to trap the (muscle) cell in its living state. If so, one might be able to demonstrate the highly selective type of adsorption of K^+ (and its surrogates, Cs^+ and Rb^+) over Na^+ —thus far seen only *in vivo*—in thin sections of freeze-dried, embedded muscle sections after exposure to an

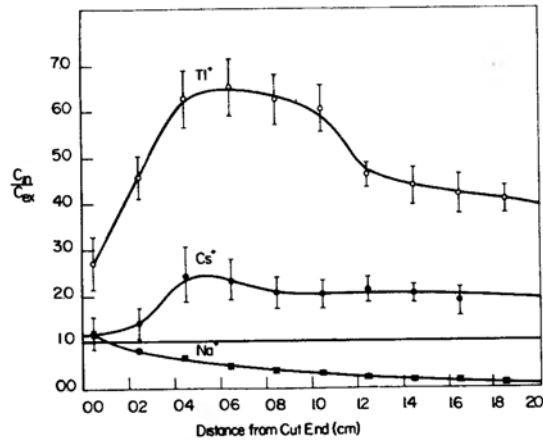


Figure 4.15. Accumulation of labeled Tl^+ , Cs^+ , and Na^+ in frog sartorius EMOC preparation (see Figure 4.12 for experimental setup used). Source solution bathing cut ends of the muscles contained 1 mM ^{204}Tl -labeled Tl , 1 mM ^{134}Cs -labeled Cs^+ , and 100 mM ^{24}Na -labeled Na^+ . Ordinate represents ionic concentration in cell water divided by the final concentration of the same ion in the source solution at the conclusion of the experiment. Incubation was for 3 days at 25°C. Each point is the average of 4 determinations; the distance between the two horizontal bars equals twice the standard error. (Ling 1977a, by permission of Physiological Chemistry and Physics)

aqueous solution containing a mixture of alkali-metal ions. He used two techniques to visualize and analyze the ions in his sections.

4.4.2.2.1. Transmission electron microscopy (TEM):

Figure 4.16(a) shows a TEM picture of a freeze-dried embedded muscle section after a 5 minute exposure to a solution containing 50 mM each of LiCl and NaCl; and 10 mM each of KCl, RbCl, and CsCl. These sections and those in (b) and (c) are only 0.2 μm thick and thus only 1/300 of the diameter of the muscle cells. Figure 4.16(b) shows another section following a similar 5-minute exposure to a solution containing 100 mM LiCl and 10 mM of CsCl. Figure 4.16(c) shows a section which had been exposed to the same mixture as (b) except that the section had been fixed in glutaraldehyde following conventional procedure rather than freeze-dried according to the method of Edelmann (1986a).

As mentioned earlier, the lighter ions like K^+ , Na^+ and Li^+ cannot be visualized clearly in the TEM pictures, while the electron-dense Cs^+ and Rb^+ can (Figure 4.6B; Ling 1984, 233). Clearly (a) and (b) bear strong resemblance to TEM pictures of muscles which were loaded with Cs^+ *physiologically* while they were still fully alive (Figure 4.6B). In both sets of pictures (Figure 4.6 and Figure 4.16), the electron-dense Cs^+ and Rb^+ [in (a)] are primarily located in the A bands (which contain the majority of the muscle cells' β - and γ -carboxyl groups); in both sets of pictures, enough Cs^+ (and Rb^+) were taken up to make visualization easily possible. This similarity in TEM visibility in turn suggests that the 5-minute exposure *in vitro* must have enabled the thin sections to adsorb a comparable level of Cs^+ in the section to that achieved *in vivo* after many hours of incubation of the intact muscles in a Ringer solution containing Cs^+ . Experimental confirmation of this belief will be presented in the section following.

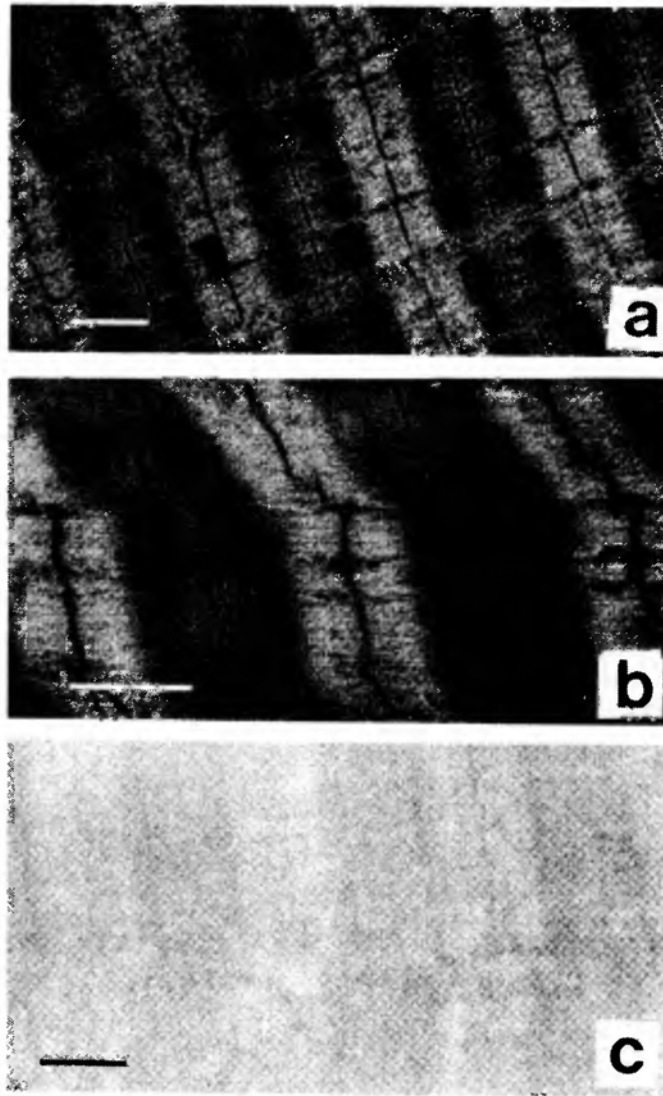


Figure 4.16. Sections of freeze-dried and embedded muscle sections exposed to alkali-metal-ion solutions:

- (a) was exposed to a solution containing 50 mM LiCl, 50 mM NaCl, 10 mM KCl, 10 mM RbCl, and 10 mM CsCl.
- (b) was exposed to a solution containing 100 mM LiCl and 10 mM CsCl.
- (c) was a glutaraldehyde-fixed-muscle section exposed to a solution similar to that for (b).

All sections were $0.2 \mu\text{m}$ thick and exposed to the salt solution for 5 minutes. Length of bars, $1 \mu\text{m}$. (Edelmann 1984, by permission of Scanning Electron Microscopy)

Since in muscle sections producing the pictures shown as (a) and (b) of Figure 4.16, *the cytoplasmic proteins came into contact with Cs^+ and Rb^+ only after the proteins had been freeze-dried, embedded, and cut into thin sections*, the presence and localized distribution of Cs^+ (and Rb^+) could not have in any way depended upon or otherwise involved the cell membranes and the postulated membrane-pumps which would have been destroyed. Instead, the Cs^+ and Rb^+ could only have been adsorbed onto these proteins in the A bands (and elsewhere), while the cut sections were briefly exposed to the Cs^+ - (and Rb^+ -) containing solutions. The

high degree of similarity of Figure 4.6(B) and Figure 4.16 (a and b) leaves no doubt that the selective accumulation of K^+ surrogates, Cs^+ and Rb^+ in living muscle cells is due to (close-contact) adsorption on cytoplasmic proteins, primarily located in the A bands.

That fixation with glutaraldehyde—unlike freeze-drying—cannot preserve the ability of the A-band and other proteins to adsorb Cs^+ in vitro lends insight into the difference between the mere **preservation of cell structure**—which glutaraldehyde can achieve—and the **preservation of the living state**—which only freeze-drying and other related procedures involving rapid freezing can accomplish, as the next section will show with greater clarity (see Section 3.2).

While transmission electron microscopy (TEM) permits the visualization of the localized adsorption of high concentration of electron-dense ions in the A bands and elsewhere, TEM (at least for now) cannot tell us if the adsorption in the freeze-dried embedded sections demonstrates the kind and degree of ion selectivity seen in living muscle cells (see Section 8.4.4 below). To achieve that goal, Edelmann used another method bearing the acronym LAMMA (Edelmann, 1980).

4.4.2.2. Laser-Microprobe-Mass Analysis (LAMMA)

As illustrated in Figure 1.1, living cells as a rule contain a much higher concentration of K^+ than Na^+ even though the cells spend their lives in an environment abundant in Na^+ and poor in K^+ . This high degree of asymmetry of K^+/Na^+ distribution has played a key role in formulating virtually all theories of the living cell. In preceding chapters, the disproof of the (Type I) sieve-membrane theory and (Type II) membrane-pump theory have been described. Yet past efforts to demonstrate selective adsorption of K^+ over Na^+ on isolated cell proteins as part of a Type-III mechanism (including the “false alarm” of Mullins mentioned in Section 1.3) had all proved futile. It is only in the light of this long history of past failures that one can correctly assess the importance of what Edelmann achieved with his freeze-dried embedded frog muscle sections and the TEM and LAMMA techniques.

For LAMMA studies, the procedures of freeze-drying, embedding in plastic, and preparing $0.2\ \mu\text{m}$ thin sections of frog muscle cells were the same as described above for TEM visualization. In contrast to the TEM studies, which visualize entire sarcomeres, the LAMMA studies are more “focused”. That is, only a small locus (1.5 to $2.0\ \mu\text{m}$ in diameter) of a $0.2\ \mu\text{m}$ -thick, thin muscle section (or a thin gelatin film containing ion standards) was chosen and ionized by a laser beam, and the vaporized ions were collected and analyzed quantitatively with a mass spectrometer. Since the section thickness of the muscle cell is accurately known the LAMMA technique permits quantitative measurement of the concentrations of different ions in different areas of the thin section.

Figure 4.17(a) shows the spectrum of a gelatin standard containing 50 mM LiCl, 50 mM NaCl, 50 mM KCl and 10 mM CsCl. Note that the intensity of the LAMMA spectrum varied (not only with the concentration of each ion but also) with the nature of the ions; the same concentration of K^+ gave a much higher peak reading than Na^+ and an even greater reading than Li^+ .

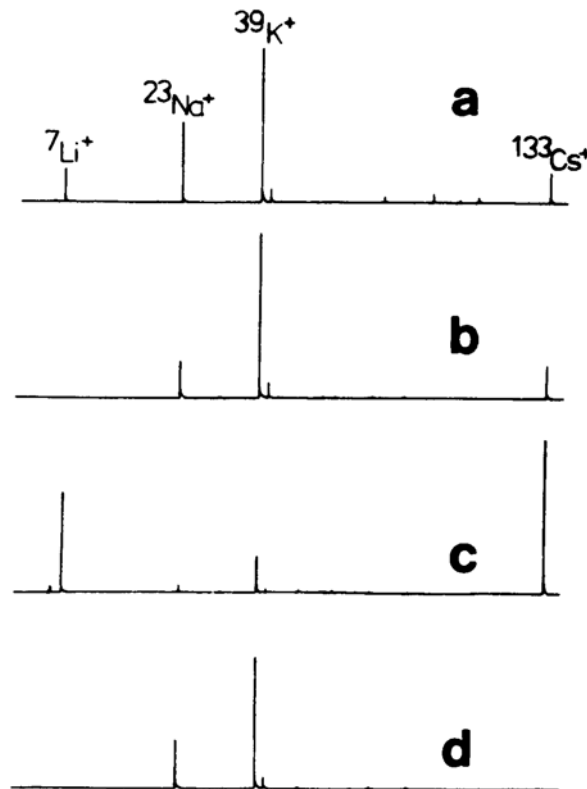


Figure 4.17. Laser Microprobe Mass-Spectrometer Analysis (LAMMA)-spectra (a) from a gelatin standard (gelatin keeps salt ions evenly distributed in samples) containing 50 mM LiCl, 50 mM NaCl, 50 mM KCl, 10 mM CsCl. Numbers over the ion symbols refer to their respective atomic numbers. LAMMA spectra, b, c, and d are from A-band regions of muscle sections following exposure of the sections respectively to (b) a solution containing 50 mM NaCl, 50 mM KCl, 10 mM CsCl; (c) a solution containing 50 mM NaCl, 50 mM KCl, 10 mM CsCl in addition to 50 mM LiCl, (d) a solution containing only 100 mM NaCl, 10 mM KCl. (Edelmann 1980, by permission of Physiological Chemistry and Physics)

Figure 4.17(b), (c), and (d) show spectra of vaporized loci of the *A bands* of muscle sections exposed to solutions containing respectively the following compositions: (b) 50 mM NaCl, 50 mM KCl, and 10 mM CsCl; (c) 50 mM NaCl, 50 mM KCl, and 10 mM CsCl in addition to 50 mM LiCl; (d) only 100 mM NaCl and 10 mM KCl. The rank order of ion selectivity in adsorption shown in Figure 4.17 is: $K^+ \gg Na^+$ in (d); $K^+ > Cs^+ > Na^+$ in (b); but $Cs^+ > Li^+ \gg K^+ > Na^+$ in (c). (Note that the inclusion of Li^+ strongly increased the relative affinity for Cs^+).

Thus preferential adsorption of K^+ over Na^+ was demonstrated in muscle sections that had been exposed to a salt solution containing Na^+ ten times higher in concentration than K^+ , Figure 4.17 (d). The concentration of K^+ thus selectively adsorbed was estimated to be about 40 mmoles per kilogram of fresh muscle-section weight. This finding, if fully confirmable in the future, will show that muscle proteins primarily located in the *A bands* (probably myosin) can indeed adsorb K^+ over Na^+ . Both in amount and in the degree of selectivity, this in-vitro adsorption is comparable to that seen in the living muscle cells

(Figure 1.1)—*directly* confirming the key prediction made in the earliest version of the association-induction hypothesis: **selective accumulation of K^+ over Na^+ in living cells is primarily in consequence of preferential adsorption of K^+ over Na^+ on the carboxyl groups of cytoplasmic proteins** (Ling 1951, 1952, 1962, 1984).

Similarly, Figure 4.17(c) demonstrates selective adsorption of alkali-metal ions in the rank order $K^+ > Cs^+ > Na^+$. This rank order too is in full accord with the rank order among these three ions observed in resting frog muscle cells (Figure 8.12, see also Figures 8.5 and 4.15).

Two tentative conclusions can be drawn from these findings of Edelmann: (1) **freeze-drying and embedding in plastic maintains (mostly intact) the living state**; (2) **intracellular proteins maintained in the living state preferentially adsorb K^+ (and Cs^+) over Na^+ in vitro which, in specificity and in the concentration of K^+ adsorbed, are comparable to those seen in living cells.**

4.4.3. *Demonstration of Specific Adsorption of Alkali-metal Ions on the β - and γ -carboxyl Groups Inside Living Cells*

When frog muscle cells are cut, deterioration soon sets in at the cut end and spreads slowly toward the intact end (see Figures 4.11, 4.13 and 4.14), with loss locally of the ability of selective K^+ accumulation and Na^+ exclusion. While freeze-drying and embedding in plastic provides a method of preserving the living state of very thin muscle sections, I discovered in 1985, a modified Ringer-solution formula containing 16.7% polyethylene glycol (PEG) (Mol. Wt. 80,000) that can also partially preserve the muscle cells' ability of accumulating K^+ in 2-millimeter long cut muscle segments for many hours (Ling, 1989)⁶. Since there is no membrane regeneration (Section 4.4.2.1), this preparation permitted us to carry out two independent tests of the basic prediction of the AI hypothesis—i.e., that ***it is primarily the β - and γ -carboxyl groups on proteins in the A bands that selectively adsorb K^+ over Na^+*** described next.

4.4.3.1 *Test Based on Acid Titration*

The prediction is that if we vary the pH of the medium, then the *adsorbed* alkali-metal ion (e.g., Na^+)⁷ in the muscle segment should be chased away by the H^+ at the higher H^+ concentrations (lower pHs). The pH at which half of the adsorbed Na^+ is replaced by H^+ should yield a pK_a typical of β - and γ -carboxyl groups. Figure 4.18 shows that this major prediction of the AI hypothesis was verified. The pK_a of 3.9⁸ observed shows that it is indeed the β - and γ -carboxyl groups that selectively adsorb K^+ , Na^+ and other monovalent cations. Equally important, the shape of the curve reveals a high degree of uniformity in the cation-adsorbing sites. In other words, all or virtually all the anionic sites in the muscle are β - and γ -carboxyl groups with similar pK_a values.

4.4.3.2 *Test based on the employment of carboxyl-specific reagents.*

Although biochemists have been using carboxyl-group-specific reagents to study proteins for a long time, only recently have reagents been developed that

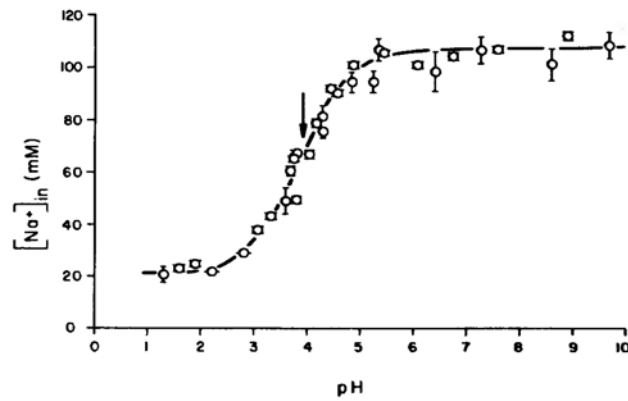


Figure 4.18. Effect of pH on the concentration of labeled Na^+ accumulated in 2 mm-long cut muscle-cell segments with both ends open. Bathing solution contained 16.3% (W/W) PE6-8000, 16.7 mM labeled Na^+ and 2.5 mM K^+ . Arrow indicates an inflection point of the curve at a pH of 3.9, which is within the pK_a range typical of β - and γ -carboxyl groups. (Ling and Ochsenfeld, 1991)

combine mildness of action with a high degree of specificity. Among these superior carboxyl-selective reagents are the water-soluble *carbodiimides*.

Since reaction with these reagents leads to the loss of the β - and γ -carboxyl groups and the negative charges they carry, the AI hypothesis predicts that interaction of the PEG-preserved, 2-mm-wide-open-ended frog muscle segments with these reagents should lead to loss of the alkali-metal ions accumulated at pH above the pK_a of the β - and γ -carboxyl groups as determined by the titration studies just described, i.e., 3.9, but little or no loss at pH considerably below 3.9. These predictions follow from the fact that at pH considerably below 3.9 the alkali-metal ions remaining in the cell segments exist as free ions in the cell water, and that these free ions are not affected by the carboxyl reagents. At pH above 3.9, however, most of the alkali-metal ions in the segments are adsorbed on the β - and γ -carboxyl groups and these adsorbed ions will be dislodged and lost to the external medium in response to the reagent.

Table 4.2 shows the results of exposure of frog-muscle segments to the water-soluble carbodiimide, EDC (1-ethyl-3-(3-dimethylamino-propyl)carbodiimide). The alkali-metal ion studied was Na^+ and it was labeled with ^{22}Na at a total Na^+ concentration of 18.9 mM. The data confirm the predictions of a substantial reduction of the accumulated labeled Na^+ at pH above 3.9 (8.0 and 11.0) but little or no reduction at pH below 3.9 (2.4).

4.4.4. Evidence that in Living Muscle Cells β - and γ -Carboxyl Groups Carried by Myosin and Maintained at the Resting Living State Selectively Adsorb K^+ Over Na^+ .

Thus far we have assembled a body of evidence which, taken as a whole, demonstrates that in frog voluntary muscle, protein carboxyl groups located at the A bands selectively adsorb the bulk of cell K^+ (and Rb^+ , Cs^+ and Tl^+) over Na^+ .

Table 4.2. The Effect of Treatment With Carboxyl Reagent EDC on the Labeled Na⁺ Uptake of Cut Muscle Segments

	PRETREATMENT			²² Na INCUBATION		
	Incub Time (hr)	pH	Incub Time (hr)	pH	Na* (μ moles/gm final wet weight)	H ₂ O (%)
Control	2	4.2	2.25	2.4	12.5 \pm 0.22 (n = 4)	52.5 \pm 0.56
			2.25	8.0	55.6 \pm 0.87 (n = 4)	58.8 \pm 1.43
			2.25	11.0	57.2 \pm 0.95 (n = 4)	63.4 \pm 0.79
EDC	2	3.8	2.25	2.4	10.7 \pm 0.14 (n = 4)	52.8 \pm 1.49
			2.25	10.5	29.0 \pm 0.58 (n = 4)	55.9 \pm 0.25
			2.25	11.0	37.0 \pm 0.90 (n = 4)	56.0 \pm 0.70

Note: Frog sartorius muscles were cut with a sharp razor blade into 2 mm long segments with both ends open. Joined together by fascia along the edges of the muscle segments, each cluster of 5 or 6 segments was handled as a unit. The control segments were first incubated for 2 hours at 4°C in a medium containing 16.7% PEG-8000 (Carbowax, Fischer), 2.5 mM KCl, 9.45 mM Na₂SO₄, while the experimental segments were incubated in a similar solution containing in addition 100 mM EDC. Both media were kept at approximately pH 4 by addition of H₂SO₄. Both control and experimental muscle segments were rinsed and transferred to another PEG-Ringer solution containing Na²². After 2¼ hours of incubation at 0°C, the segmented muscles were blotted dry, weighed and analyzed for the labeled Na content and water content. (Ling and Ochsenfeld 1992, by permission of Physiological Chemistry Physics and Medical NMR)

There is also suggestive evidence that at least a major share of these carboxyl groups belongs to myosin: (i) myosin, which contains 47% of all the β - and γ -carboxyl groups in the muscle cells is exclusively found in the A bands; and (ii) the K^+ -adsorbing sites, which in number are equal to one half of all the β - and γ -carboxyl groups in the muscle (see Section 8.1.3. below) are also primarily found in the A bands.

By the coordinated study of the effect of varying pH and of the carboxyl reagents on alkali-metal-ion accumulation in PEG-preserved-cut-muscle segments, we have established in the preceding section that β - and γ -carboxyl groups can be recognized by their high preference for H^+ over the alkali-metal ions, such that, at a concentration of approximately 0.1 mM (corresponding to a pH of 4.0), H^+ can chase away a major share of alkali-metal ions adsorbed on these carboxyl groups in a Ringer solution.

I will now make use of two additional sets of data—one to be presented later in this volume (but in a different context), and another one that has just been published by Edelmann (see Ling 1990 in answer to question raised by Edelmann)—to further strengthen the following conclusions:

- (1) the protein in muscle that carries most of the alkali-metal-ion—adsorbing carboxyl groups is myosin;
- (2) the alkali-metal-ion—adsorbing carboxyl groups are β - and γ -carboxyl groups; and
- (3) β - and γ -carboxyl groups carried by myosin in living muscle cells selectively adsorb K^+ (and Cs^+) over Na^+ , when the myosin-water-ion system is maintained at the resting living state.

Although myosin is the main protein in the A bands, A bands contain many other proteins besides myosin. To make sure that it is myosin that selectively adsorbs K^+ , Rb^+ , and Cs^+ ions, we studied (in vitro) the adsorption of Rb^+ on *isolated* pure actomyosin. Figure 8.2B shows that isolated actomyosin adsorbs a substantial amount of Rb^+ at near neutral pH. Yet lowering the pH to 4.3 eliminates all or virtually all the adsorbed Rb^+ . The only Rb^+ remaining in the dialysis bag at this pH is that dissolved in the water, recognizable by the rectilinear distribution characteristic of all solutes dissolved in solvents [Section 5.2.3.(1)]. This sensitivity to pH of 4.3 shows that it is the carboxyl groups of actomyosin that adsorbs the Rb^+ ion.

In resting muscle cells, actin is mostly located in the I bands. Proteins in the I bands (away from the Z lines) adsorbs little K^+ or its surrogates (Section 4.4.1). This fact suggests that of the two components of isolated actomyosin, actin and myosin, it is myosin that offers the Rb^+ -adsorbing sites in the form of β - and γ -carboxyl groups. The experimental data of Lewis and Saroff (1957) has confirmed these deductions. Lewis and Saroff found that isolated rabbit actin does not adsorb K^+ at all, and that actomyosin adsorbs only half as much K^+ as pure myosin. When actin is added to myosin (to form actomyosin), the K^+ adsorption of myosin is, as expected, reduced by one half, suggesting that fixed *cationic* groups on actin and fixed *anionic* β - and γ -carboxyl groups on myosin form salt linkages, thereby preventing these carboxyl groups from adsorbing K^+ . (For

additional evidence that the majority of muscle cell K^+ is adsorbed on myosin, see Ling and Ochrenfeld, 1991)

Myosin does not contain a significant number of α -carboxyl groups. Virtually all the free anionic groups of myosin are either the β -carboxyl groups of the aspartic acid residues or the γ -carboxyl groups of the glutamic acid residues (Bendall 1969, 28). This shortage of α -carboxyl groups establishes that the alkali-metal-ion-adsorbing carboxyl groups in the A bands are indeed β - and γ -carboxyl groups of myosin.

In Section 4.4.2.2, I presented the evidence of Edelmann's success in capturing the frog muscle in its resting living state with his new freeze-drying embedding technique: the preservation of the ability of thin sections of freeze-dried embedded frog muscle to selectively adsorb K^+ over Na^+ (and/or selectively adsorb Cs^+ over Li^+ of Na^+) has hitherto only been seen in living cells in a resting living state.

Very recently, Edelmann (1991) extended his earlier studies and investigated the effect of H^+ concentration on the *in vitro* selective adsorption of Cs^+ in thin sections of frog muscle maintained at the living state. He found that H^+ at a concentration (0.1 mM) corresponding to a pH of 3.0 greatly reduced the *in vitro* selective adsorption of Cs^+ , thereby establishing that the β - and γ -carboxyl groups of myosin in the A bands selectively adsorb Cs^+ and K^+ over Na^+ , when the muscle myosin and associated protoplasmic components are maintained at the living state.

4.4.5. Summary

There is extensive and unanimous evidence that K^+ (or its surrogates Cs^+ and Tl^+) in voluntary muscle cells are not distributed in the cell water as predicted by the membrane-pump theory. Rather, they are primarily localized in the A bands in agreement with the predictions of the AI hypothesis.

The selective accumulation of the four monovalent ions in the rank order: $Tl^+ > K^+ > Cs^+ > Na^+$ proves *close-contact adsorption* of these ions on cell sites because these ions differ from one another only in their short-range attributes which could not be "detected" by the cell without close-contact adsorption.

Studies utilizing the EMOC technique and the LAMMA technique show that the specificity in the ions accumulated does not originate from a functional cell membrane, but from the cytoplasmic protein(s).

Direct titration and sensitivity to specific carboxyl reagents of cut muscle segments prove that what causes the localization of alkali-metal ion accumulation at the A bands (and Z lines) is indeed selective close-contact adsorption on the protein carboxyl groups.

Studies of the adsorption of K^+ and of Na^+ on isolated actomyosin in the presence and absence of a low concentration of competing H^+ identified the carboxyl groups involved as the β - and γ -carboxyl groups and the protein in the A bands carrying these β - and γ -carboxyl groups as myosin.

Sensitivity in the adsorption of Cs^+ on thin sections of freeze-dried and embedded frog muscle section established that it is the β - and γ -carboxyl groups of

myosin maintained at the living state that provide the molecular mechanism for the selective accumulation of K^+ in living cells.

No less important was Edelmann's succession of successes climaxing with the capturing of the living state in ultra-thin frog muscle sections, which retained the elusive capability of selectively adsorbing K^+ over Na^+ as seen in intact living cells.

The question may be raised: "how far can one generalize the conclusion derived from the study of one kind of cells, the frog muscle cells? Is it justifiable to claim that since we have established K^+ adsorption on the β - and γ -carboxyl groups in this type of cells, therefore K^+ adsorption in *all* living cells must also be adsorbed on their β - and γ -carboxyl groups?" My answer to this important question would be twofold: a general affirmative; and a call for caution. We must not overlook the exceptions that prove the rule.

Gregor Mendel introduced the most basic laws of inheritance from the study of one plant, the garden pea. Subsequent successful investigations of the molecular biology of genetics was based overwhelmingly on the study of one microorganism, *E. coli*. In defending their belief that it is valid to apply knowledge from one organism to others, Jacques Monod and his coauthor François Jacob wrote: "... anything found to be true of *E. coli* must also be true of elephants" (Monod and Jacob 1961, 393).

While I feel equally strongly that the K^+ of most living cell types is selectively adsorbed on β - and γ -carboxyl groups, I also acknowledge that there are exceptions in the case of highly unusual cells living in highly unusual environments (see endnote 9).

The establishment of the adsorbed state of the bulk of K^+ in resting cells marks a decisive turning point in the historical controversy over the "free vs. bound" K^+ issue in living cells. Even more important, the recognition of the adsorbed state of this number-one intracellular cation on proteins affirms the broader theme of the association-induction hypothesis, i.e., that **it is the close association of all of its major components (proteins, K^+ and water) that underlies the maintenance of the living state.** In the next chapter, we will examine another predicted association, that between cell water and cell proteins.

NOTES

1. *Law of Macroscopic Electro-Neutrality*: in a large or macroscopic object, the total number of positive electric charges and the number of negative electric charges must be equal. To illustrate this law, Guggenheim (1950, 330) demonstrated that a departure corresponding to an excess of one kind of charge (in a sphere 1 cm. in radius) in an amount undetectable by chemical means (10^{-10} gram-ions) would generate an electric potential difference of a magnitude that one encounters only in high voltage laboratories (i.e., 9.5 million volts). (Whereas there is no clear line of demarcation separating a microscopic from a macroscopic object, one may safely regard a living cell, or even an isolated mitochondrion, as a macroscopic object.)

2. The *salt-linkage* concept was first introduced by Speakman and Hirst (1931). It became unpopular among protein chemists, apparently in response to the adverse criticism of Jacobson and Linderstrøm-Lang (1949), even though Linderstrøm-Lang changed his mind later (see Linderstrøm-Lang and Schellman 1959, 451). The existence of salt linkage

has now been established beyond any doubt from the elucidation of the exact structure of hemoglobin by Perutz and his group (Perutz et al. 1968, Perutz 1970) (see Figure 7.12). Hero worship, a human trait not always compatible with the search for truth, often creates what I call a "halo" effect, whereby all sentiments of a scientist with great past achievements may be given more weight than they deserve. The lengthy rejection of the salt-linkage concept offers an example.

3. Discoveries of new proteins (titin and nebulin) and refinement in the quantitative estimation of proteins in muscle cells led to new values of the percentage composition of muscle-cell proteins (Ohtsuki et al, 1986). Based on the new data, Ling and Ochsenfeld (1991) now estimate that myosin carries about 47% of the β - and γ -carboxyl groups of the muscle cells.

4. For the history of prior evidence in support of this prediction, especially from the laboratory of Ernst, Tigyí and their school, see Ling 1977, Ernst 1958, and Edelman 1984.

5. Although the concept of free counterions hovering around fixed ions is considered here, the theory of enhanced counterion association and experimental findings confirming the theory (Sections 4.1. and 4.2.) have made such consideration somewhat academic. They are included primarily for the completeness of the argument and for the additional safety of the conclusion to be drawn below.

6. This preservation of the living state is not as complete as in the freeze-dried embedded sections. Thus, although the ability to adsorb high concentrations of alkali-metal ions is preserved, the selectivity for K^+ in preference over Na^+ is quantitatively much reduced.

7. Na^+ , rather than K^+ , is studied because long-lived radioactive K^+ (K^{40}) is not available, while long-lived ^{22}Na is. Since Na^+ taken up is readily displaced by K^+ and since other studies with ^{86}Rb (which more closely resembles K^+) produced similar results, the study of Na^+ was found both necessary and sufficient to achieve the desired objective (see preceding endnote 6).

8. The β - and γ -carboxyl groups belonging respectively to the aspartic- and glutamic-acid residues of protein have a characteristic pK_a of around 4.0. However, it is also well known that there is considerable variation among different proteins. Edsall and Wyman cited pK_a values for β - and γ -carboxyl groups ranging from 3.95 to 4.7 (Edsall and Wyman 1958, Table VIII on 534).

9. Certain bacteria like *Halobacterium salinarium*, that live in very salty environments, selectively accumulate molar concentration of K^+ over Na^+ . Ginzburg et al. (1971) who studied K^+ distribution in *Halobacterium salinarium*, concluded that K^+ must be bound in the cells, but claimed that "the K^+ binding cannot even be accounted for by the cell proteins or other macromolecules" (p. 96). While agreeing fully with their conclusion that cell K^+ is bound—but preferring "adsorbed" over "bound"—I think the statement about the inability of proteins or other macromolecules to "bind" the K^+ in *Halobacterium* unnecessarily pessimistic.

Citing various evidence that the backbone carbonyl oxygen atoms offer adsorption sites for alkali-metal ions, I suggested in 1977 (Ling 1977c, 162) that similar backbone carbonyl groups may serve as K^+ -adsorbing sites (in addition to β - and γ -carboxyl groups) in *Halobacterium*.

Christian and Waltho (1962) showed that *Halobacterium salinarium* contains 50% water, and K^+ at a concentration of 4.57 molal. From the dry weight of the cells, and the weights of K^+ and all the other major ions and amino acids found in the cells, one estimates that there are approximately 600 grams of proteins per kilogram of cell water. Taking an average amino-acid-residue weight of 112 (Ling 1962, 48), the total number of amino-acid residues, and hence peptide carbonyl groups, is $600/112 = 5.36$ Molal in concentration. At least 10% of the amino acid residues carry free β - and γ -carboxyl groups (Ling 1962, 46–47), adding another $5.36 \times 0.1 = 0.54$ molal of potential K^+ adsorbing sites, to a total of $5.35 + 0.54 = 5.89$ Molal of potential K^+ adsorbing sites. This is more than adequate to adsorb all the 4.57 Molal of K^+ selectively accumulated in the *Halobacterium* cells.

CELL WATER

A lotus seed was once removed from an Indian tomb that was three thousand years old. Brought into contact with water, the seed sprang to life. It germinated, grew leaves, flowered, and in time bore new seeds.

How does water miraculously give life to the lifeless? Why should each type of living cell have a specific, essentially invariant water content? These are questions that cell physiology textbooks generally do not raise or answer. Ever since Hill, Blanchard, and others convinced the majority of their contemporary cell physiologists that cell water is just water (Section 1.4), many of their followers have been searching for the secret of life in membrane pumps—a direction that we now know to be without a future. However, from literature of the distant past, one finds interesting clues which may have bearing on the questions raised: an attraction of the dry matter of living cells for water.

It is on record that the dry seeds of the plant *Xanthium glubatum* can take up water from a saturated solution of lithium chloride, which has an osmotic pressure of 965 atmospheres (Shull 1913, 1924). Of these, salt ions in the seeds (even if assumed to be all free) could account for only a few atmospheres. ***The main purpose of this chapter is to present the theory and supportive evidence that water acted upon by proteins (assuming the fully-extended conformation) in vitro as well as in vivo could acquire a galaxy of new properties that we have long recognized as special to life—the ability to exclude Na^+ being but one example.***

5.1. *The Physics of Multilayer Adsorption of Water*

The water molecule, H_2O , is unusual. Its two H atoms are not symmetrically located along a straight line on either side of the oxygen atom. Instead they are placed on the two corners of a tetrahedron, with the oxygen atom occupying its center. This segregation of positive electric charges carried by the H atoms on one side of the molecule and the negative charges carried by oxygen on the other side endows the water molecule with a large *permanent dipole moment*, 1.86 debyes in magnitude. Water molecules are also readily polarizable, with a polarizability equal to $1.44 \times 10^{-24} \text{ cm}^3$.

Classic physics teaches us that when a polarizable molecule like water is placed near an electrically charged site, an *induced dipole* is created in the water molecule in addition to the permanent dipole moment the molecule already possesses.

With its combined permanent and induced dipole, the polarized water molecule is electrostatically attracted to and adsorbed on the charged site. Thus anchored, the adsorbed water molecule in turn polarizes and adsorbs another water molecule, creating an induced dipole in that water molecule, and the process repeats itself a number of steps beyond.

The effect of the electrically charged surface site on a chain of water molecules bears resemblance to that of a big magnet on chains of soft iron nails as shown in Figure 3.1. One propagates by magnetic polarization while the other does so by electrical polarization or *induction*. If the fixed charge site carries a positive electric charge and is flanked at a proper distance by another fixed charge bearing a negative electric charge, then the two rows of water molecules polarized by each of the fixed charges will be oriented in opposite directions. Since parallel dipoles oriented in opposite directions attract each other, the stability of the two chains of polarized water molecules is mutually enhanced and the chains lengthened. Now if instead of two fixed charges of opposite sign, we visualize a checkerboard of alternatingly positive and negative fixed charges over a solid surface, each fixed charge is surrounded, at suitable distances, by four fixed charges of the opposite polarity. In this way the stability and the reach of the polarized water molecules will be further enhanced. The water polarized will no longer be in chains or bundles, but will take the form of *polarized multilayers*.

Given the laws of physics and the properties of water molecules depicted above, it is inevitable that polarized multiple layers of water molecules will form on suitable solid surfaces. Indeed, this type of phenomenon was observed early in the history of physics (see McBain 1932). Nor is it surprising that physicists like de Boer, Zwicker, and Bradley long ago presented quantitative theories describing the multilayer adsorption of gaseous molecules on polar surfaces. Here only the equation of Bradley (1936) will be described.

This equation, in contrast to others, was derived specifically for the multilayer adsorption of gaseous molecules with a permanent dipole moment, like water. This type of equation is often referred to as an *adsorption isotherm*, because it describes the amount of gas adsorbed at one unchanging temperature as the concentration (or vapor pressure) of the gas in the environment varies. Representing the amount of gas adsorbed as “*a*,” and the partial vapor pressure as p/p_0 , where p is the existing vapor pressure and p_0 the corresponding vapor pressure at full saturation, the Bradley multilayer adsorption isotherm reads:

$$\log\left(\frac{p_0}{p}\right) = K_1 K_3^a + K_4, \quad (4)$$

where K_1 , K_3 , and K_4 are all constants under a defined set of physical conditions. Equation 4 can be written in a double-log form:

$$\log(\log\left(\frac{p_0}{p}\right) - K_4) = a \log K_3 + \log K_1, \quad (5)$$

which predicts a rectilinear relation between the value of a and the left hand term containing the reciprocal of the relative vapor pressure, p_0/p . Bradley dem-

onstrated how this equation described multilayer adsorption of various gaseous materials, including water vapor on copper oxide (Bradley 1936).

Twelve years after Bradley published his multilayer-adsorption isotherm, Brunauer, Emmett and Teller¹ reexamined the theoretical aspect of the problem, affirming that polarized multilayers will form on appropriate surfaces if the gas molecule, like water, possesses a *permanent dipole moment*, but not otherwise (Brunauer et al. 1936).

Later in this chapter the Bradley adsorption isotherm will be shown to offer a way of testing the theory of cell water according to the association-induction hypothesis. First let us review some experimental findings of William Harkins (1945). *Harkins gave a precise factual demonstration of how polarized multilayers of water form on a checkerboard of positively charged and negatively charged sites on the surface of titanium dioxide powder.* His data, shown as Table 5.1, present the measured “molar heat of desorption of water molecules minus the heat of vaporization” (i.e., the excess heat content (enthalpy) due to propagated polarization) for the successive layers of adsorbed water molecules. Harkins pointed out that “while the effect of the attraction of the solid dies off rapidly, it extends to somewhat more than five molecular layers.” These experimental data unequivocally demonstrate that polarized multilayers of water molecules do indeed form on suitable polar surfaces.

5.2 *The Polarized-Multilayer Theory of Cell Water and Results of Experimental Testing*

5.2.1. *Background*

I have already pointed out in Section 1.1 and elsewhere, that there are *only* three basic types of mechanisms to achieve a maintained low level of Na^+ in living cells, of which two (Na^+ -impermeable membrane and the Na pump) are no longer tenable. According to the AI hypothesis, it is the third mechanism that helps to keep the Na^+ concentration in cell water low, because the solvency

Table 5.1. Molar Heat of Desorption in Calories per Mole of Molecular Layers of Water From The Surface Of Titanium Dioxide (Anatase) Minus The Energy Of Vaporization Of Water ($E_a - E_1$). (Harkins 1945, by permission of Science)

Layer	Heat of Desorption	$E_a - E_1$
1	16,450	6,550
2	11,280	1,380
3	10,120	220
4	9,971	71
5	9,951	51
6	9,932	32

of cell water for Na^+ is lower than that of normal liquid water in tissue fluids or Ringer solution.

If the bulk of cell water is different from normal liquid water, this difference must arise from interaction with some other materials also present in the cell. The only other cell component large enough in quantity to bring about a more or less uniform change in the property of the abundant cell water is cell proteins. What kinds of interactions exist between water and proteins?

Benson and his coworkers tried to answer this question by studying sorption of water vapor and nonpolar gases on dry proteins (Benson and Ellis 1948, 1950; Benson, Ellis and Zwanzig 1950). They found that *in the case of nonpolar gases which have no permanent dipole moment (e.g., N_2 , O_2 , CH_4), the amount of gases sorbed depends only on the state of division of the proteins*: the finer the division, the more exposed surface; the more exposed surface, the more adsorption of nonpolar gases.

In sharp contrast, sorption of polar water molecules is quite different. First, the amount of water sorbed is several orders of magnitude higher than sorption of nonpolar gases. Secondly, the amount sorbed is indifferent to the state of division of the dry protein, and appears to depend only on the specific water-sorbing groups in the proteins, many of which are buried inside the protein. Our next question is: "What are these specific groups of proteins that sorb water?" There is an interesting story behind the answer.

Two categories of polar groups exist on a protein molecule. One is carried on side chains. Examples are: the OH groups carried on serine residue, β -carboxyl groups carried on aspartic residue, and ϵ -amino groups carried on lysine residue. The second category of polar groups, which in number far exceeds the number of side-chain polar groups, consists of the imido (NH) and carbonyl (CO) groups of the polypeptide chain.

In preparing to write a review on "Hydration of Macromolecules" (Ling 1972), I discovered that there were two divergent theories on the seats of protein hydration. In one theory, introduced by Pauling (1945), polar side chains are the only seats of hydration; in the other theory, introduced by Jordan-Lloyd (Jordan-Lloyd and Shore 1938), polar side chains as well as backbone NHCO groups are the seats of hydration.² Despite the fact that they seem mutually exclusive, both theories have been gaining more and more supportive evidence.

I then noticed that while the papers supporting Pauling's theory came almost entirely from scientists working in chemistry and biochemistry departments, usually using pure globular native proteins as objects of investigation, papers supporting Jordan-Lloyd's theory came largely from workers in industrial laboratories, using mostly fibrous proteins. With this clue, a possible solution of the apparent paradox came to mind: *In globular native proteins, hydration is limited to polar side chains.* Here, most, if not all, NHCO groups of the backbone are locked in α -helical and other intramacromolecular H bonds, and are thus unavailable for water sorption. *In fibrous proteins, some of the backbone NHCO groups are not locked in intramacromolecular H bonds, and are thus free to sorb water.* Hydration occurs both at polar side chains and at the backbone NHCO groups.

The polar side chains, as a rule, sorb relatively small amounts of water. In a

survey made in 1972 from in-vitro studies, I showed that most native proteins (for definition, see endnote 4 of Chapter 3) hydrate to the extent of 0.2 to 0.3 (averaging 0.25) grams of water per gram of dry protein (Ling 1972). Living cells like frog muscle contain 20% protein and 80% water. If all intracellular proteins in these cells exist in the native globular form, no more than $(0.25 \times 0.2) / (1 - 0.2) = 6.25\%$ of the cell water will be under the influence of cell proteins. This percentage of the total cell water is too small to account for the low level of Na^+ and other solutes strongly excluded from living cells. Thus, even if all the 6.25% of hydration water has zero solubility for Na^+ , the level of Na^+ in cell water alone will equal 73.7% of that in the external medium (100 mM), and thus circa 73.7 mM in concentration. 73.7 mM is a far cry from the Na^+ concentration in frog muscle observed (i.e., less than 20 mM—much of which is adsorbed—is freely dissolved in cell water; see Section 8.1.2).

Thus, to explain the low Na^+ concentration in living cells, one needs a theory of cell water in which the cell proteins must be able to exercise much greater influence on the cell water than that provided by their polar side chains. Since there is no other alternative, the theory must call upon the polypeptide NHCO groups to explain the more extensive interaction with the bulk of cell water. **The recognition of the central role of the polypeptide NHCO groups in multilayer polarization of water became the kingpin of the polarized-multilayer theory of cell water.**

5.2.2. *The Polarized-Multilayer Theory of Cell Water*

In 1965 I first suggested the *polarized-multilayer (PM) theory* of cell water as part of the association-induction hypothesis (Ling 1965). In this theory, all or virtually all cell water exists in the state of polarized multilayers, and it is this altered physical state of cell water that gives rise to the reduced solvency for Na^+ , sugars, and free amino acids usually found at low levels in living cells.

To simplify presentation of the theory, I will designate a negative fixed charge as an *N* site and a positive one as a *P* site. A checkerboard surface carrying alternating *N* and *P* sites at distances roughly equal to one water diameter between the nearest neighboring sites is called an *NP*-system. An example is the titanium-dioxide surface Harkins described. When two such *NP* systems are placed face to face at a reasonable distance apart, we speak of an *NP-NP* system. Examples of *NP-NP* systems include closely juxtaposed polished glass or quartz surfaces (see Figure 9.6 in Ling 1984) or polished AgCl plates (Figure 9.7 in Ling 1984). In each of these cases, profound changes in the freezing point and vaporization point of the water film have been observed, in agreement with the multilayer-polarization theory of cell water (see Section 5.2.5.5).

Figure 5.1 provides a diagrammatic illustration of these systems, including others where either *N* or *P* sites are replaced by a vacant (*O*) site and the systems are referred to as *NO-NO* or *PO-PO* systems, as the case may be. *However, it must be emphasized that this figure is only a static diagrammatic illustration of a dynamic structure.* A dynamic structure is by definition not static. It changes constantly with time, and is much less orderly than the impression a simple illustration of

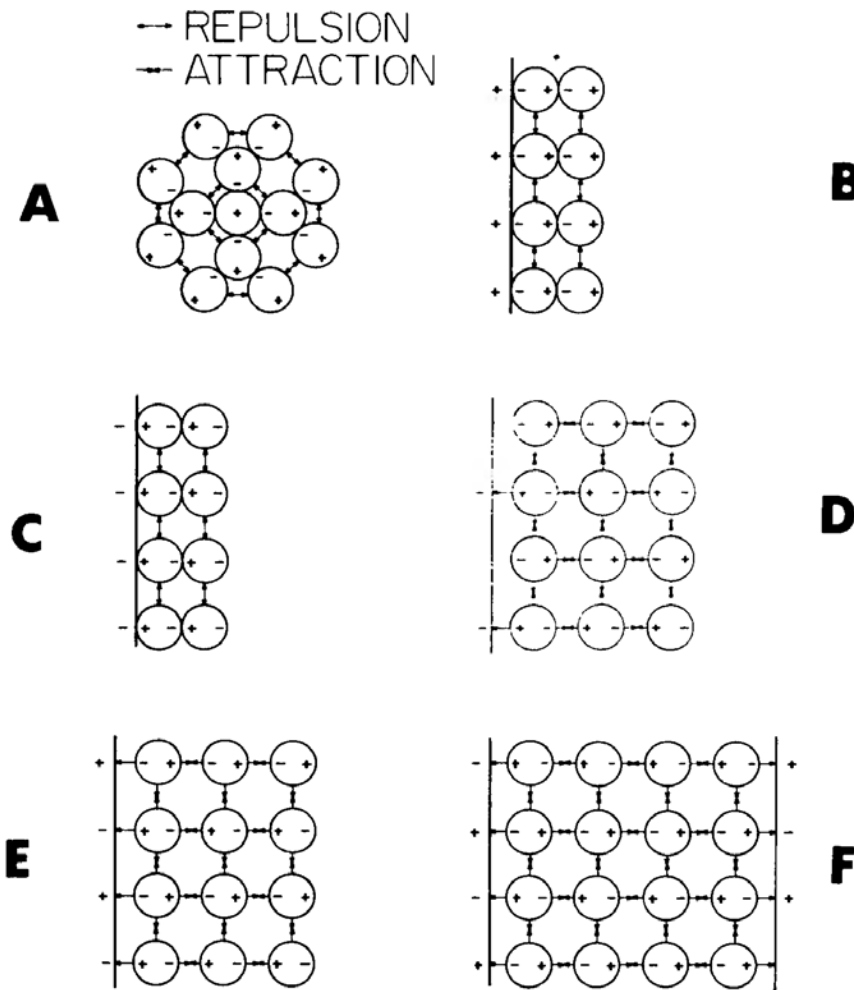


Figure 5.1. Effect of charged site distribution on the formation of dynamic structure of polarized multilayers of water molecules: (←→), repulsion; —> ← attraction. Unstable multilayers in A, B and C are produced at surfaces because of lateral repulsion between water molecules in the same layer: (A) P-type site, charged positive ion; (B) P-type site, uniformly positive sites separated by the distance of *one* water-molecule diameter; (C) N-type site, uniformly negative sites separated by the distance of *one* water-molecule diameter; (D) unipolar surface with charges separated by the distance of *two* water molecule diameters (NO type); (E) NP-type surface with alternating positive and negative sites separated by distance equal to the diameter of one water molecule; (F) two NP-type surfaces placed face to face (NP-NP type with greatest stability). (Ling 1972, by permission of Wiley-Interscience)

this sort tends to convey. However, what the diagram cannot directly convey, a little imagination can help with, as it does when one views a static picture of, say, a galloping stallion.

The volume of water polarized on an *NP-NP* system of polar solid surfaces is very small. To produce a maximum amount of polarized water within the limited space of a living cell, a more space-saving model is required. Such a model of the cell interior is suggested: a matrix of parallel linear chains carrying alternating *N* and *P* sites at proper distances apart, referred to as an *NP-NP-NP* system. In its effects on water polarization, such an array of parallel chains

of properly spaced N and P sites is not very different from juxtaposed NP - NP surfaces, but is a great deal more space-saving. Variants of an NP - NP - NP system are NO - NO - NO and PO - PO - PO systems when either the P or N sites are replaced by vacant sites.

According to the polarized multilayer theory of cell water, it is the NP - NP - NP system of fully-extended protein chains, with their exposed CO and NH groups acting as N and P sites, respectively, that are exposed to the bulk of cell water and polarize it in multilayers.

It has been shown that if as little as 5% of the cell weight exists in the form of fully-extended proteins, that is sufficient to polarize all of the cell water (Figure 5.2). The average number of layers of polarized water between the nearest neighboring chains would be about ten layers, twice the number of water layers Harkins has shown to be polarized by a *single* polar surface of titanium dioxide. But with the juxtaposition of two or more water polarizing chains, a synergistic effect takes place in polarizing and immobilizing especially the least intensely polarized water molecules farthest away from the polarizing chains. As a result, the degree of polarization and motional restriction of all ten layers

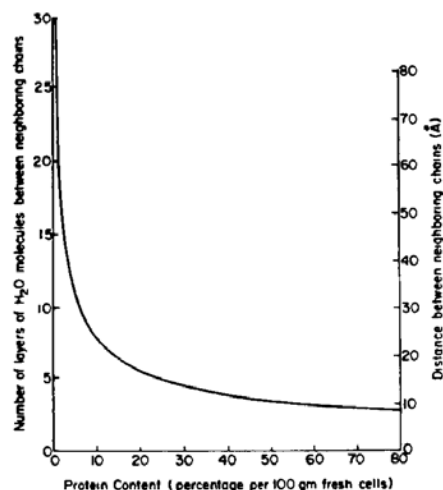


Figure 5.2. The average distance (right) and number of H₂O molecules (left) between evenly distributed proteins chains at varying protein contents (n grams/liter) of hypothetical cells. The data were calculated on the assumption that the average weight of each amino-acid residue in all the proteins is 112 (see Ling 1962, p. 48), the length of each peptide linkage is 3.5×10^{-8} cm and the Avogadro's number is 6.06×10^{23} . Further assuming that all the proteins exist in the fully extended form, the total length of the polypeptide chain joined end to end is then $(n/112) \times 6.06 \times 10^{23} \times 3.5 \times 10^{-8} = 1.89 \times 10^{13}n$ cm. Cut into 10-cm-long segments, the $1.89 \times 10^{13}n$ segments are uniformly distributed in a $10 \times 10 \times 10$ cube, the number of filaments on each side would be $\sqrt{1.89 \times 10^{13} \times n} = 4.35 \times 10^6 \sqrt{n}$. The distance, d , between each pair of nearest neighboring pairs of segments is then $10/(4.35 \times 10^6 \sqrt{n}) = (2.30 \times 10^{-6})/\sqrt{n}$. From this formula one calculates that for $n = 900$ (i.e., 90% protein), $d = 7.6$ Å. For $n = 50$ (i.e., 5% protein), $d = 32.5$ Å. Assuming the molecular diameter of each water molecule to be 3 Å, one finds, for example, 2.5 water molecules between the protein chains in cells containing 90% protein and 10.8 water molecules between the protein chains in cells containing 5% protein. (Ling 1983, by permission of Physiological Chemistry Physics and Medical NMR)

of water between the chains is more uniform, not tapering off rapidly from the *N* and *P* sites of the single surface as shown in Figure 5.3 (Ling and Ochsenfeld 1983). It is highly probable that a similar synergistic polarization causes the rather thick layer of water held between two juxtaposed glass or AgCl plates to be so resistant to freezing (see Ling 1984, 279–280). Since fully extended protein chains as well as globular proteins occupy space, the average number of water layers between adjacent chains is likely to be less than ten, considerably so in water-poor cells like red blood cells or brine-shrimp-cyst cells.

In summary, according to the PM theory, all or virtually all of the water in living cells exists in the state of polarized multilayers, in consequence of interaction primarily with the fully-extended polypeptide chains of some intracellular

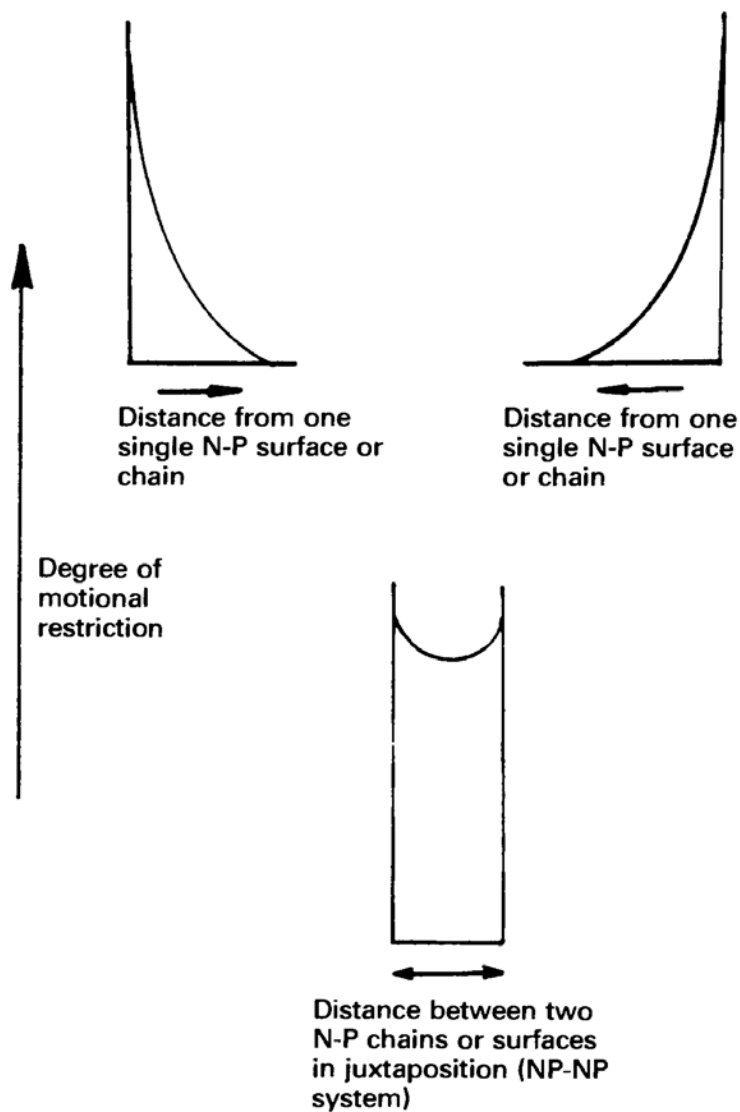


Figure 5.3. Diagrammatic illustration of the anticipated degree of motional restriction of water in the vicinity of isolated (top) and juxtaposed polar N-P surface(s) or matrix of NP-NP-NP chain(s) (bottom) demonstrating the synergistic effect of two closely juxtaposed NP surfaces in enhancing the degree and uniformity of the multilayer polarization of water molecules.

proteins, the NHCO groups of which are directly exposed to the bulk phase water. A corollary of this theory is that native proteins with most of their NHCO group locked in α -helical and other inter- or intramacromolecular H bonds have a much weaker or no effect on the properties of bulk-phase water *in vivo* as well as *in vitro*. In the next section, I will discuss an outstanding attribute of water existing in the state of polarized multilayers: its ability to exclude Na^+ and other solutes found at low concentrations in living cells.

5.2.3. *The Subsidiary Hypothesis of Solute Exclusion*

Let us begin the discussion of the subsidiary theory of solute exclusion with two definitions:

The *q-value* (true-equilibrium-distribution coefficient) is the ratio of the concentration of a solute in the water phase under investigation (Phase I) over that of the same solute in the external solutions containing normal liquid water (Phase II), after diffusion equilibration of the solute has been reached between the two phases and when the solute in both phases is entirely free and dissolved in the water. Phase I can be a living cell or a dialysis sac containing a protein or polymer solution. Phase II can be the Ringer solution bathing the living cell, or similar solutions bathing the dialysis sacs containing the protein or polymer solution.

The *ρ -value* (apparent-equilibrium-distribution coefficient) is also the ratio of the concentration of a solute in the phase under investigation over that of the same solute in the external solution containing normal liquid water when diffusion equilibrium of the solute has been reached between the two phases. The *ρ -values* differ from the *q-values* because the solute in Phase I is not necessarily all dissolved in water and may well include solute adsorbed on the macromolecular component of the phase. However, solute in Phase II is exclusively dissolved in the water. The *ρ -value* of a solute can be equal to but never lower than the *q-value* of a solute. With the *q-* and *ρ -values* defined, I now introduce two key predictions of the theory of solute exclusion derived from the basic concepts of the PM theory.

(1) ***The Linear Distribution Rule.*** In the PM theory, solute distribution between living cells (or model systems) and normal liquid water is a special case of solute distribution between two different solvents. As such, it follows the Berthelot-Nernst partition law (Berthelot and Jungfleisch 1872; Nernst 1891)³: a plot of the equilibration concentration of the *i*th solute in Phase I, $[p_i]_I$, against the concentration of the *i*th solute in Phase II, $[p_i]_{II}$, should yield a straight line with a constant slope equal to the *q-value*:

$$[p_i]_I = q[p_i]_{II} \quad (6)$$

(2) ***The Mechanism of Solute Exclusion, the Size Rule and an Important Exception.*** The *q-value* of a solute is an expression of an equilibrium phenomenon. As such, the *q-value* of the solute is determined by the standard-free-energy difference (ΔF°) of the solute in the two phases. The standard-free-energy difference in turn is composed of two terms: an enthalpy term (ΔH°) and an entropy term

($T\Delta S^\circ$), where ΔS° is the entropy change (for definition and concept of entropy, see endnote 2 of Chapter 3) and T is the absolute temperature. Since the enthalpy change differs from energy change (ΔE°) by a term equal to the product of pressure (P) and volume change, (ΔV), and since in the liquid system of interest ΔV is small, the enthalpy change is to all intents and purposes equal to the energy change.

The energy change in transferring a solute from the external normal aqueous medium to inside a living cell or a dialysis bag containing polarized water involves two components, a *volume component* and a *surface component*.

(i) Volume component: Since water molecules in the state of polarized multilayers are held together more strongly due to mutual polarization, the energy needed to excavate a hole in the polarized water is greater than the energy gained in filling the hole left behind in the external normal liquid water. Furthermore, the larger the probe molecule, the larger the size of the excavated hole; the larger the excavated hole, the greater the difference between the energy spent and gained. The greater the energy difference, the greater the degree of exclusion of the probe molecule from the polarized water ($q < 1$).

(ii) Surface component: If the probe molecules contain exposed polar groups of such a steric and electronic configuration that they can interact more strongly with water molecules and with more water molecules in the dynamic-polarized-water structure than in the external normal liquid water, this stronger interaction will create an energy difference in favor of the probe molecules being preferentially accumulated in the sac, resulting in a q -value equal to or above unity ($q \geq 1$). On the other hand, if the steric and electronic configurations of the exposed groups of the probe molecules do not fit or fit less well into the dynamic structure of polarized water in the sac than in the external medium, then the energy difference is unfavorable for the accumulation of the solute in Phase I, driving the q -value toward below unity.

The entropy change involved in moving a solute from the external normal liquid water to a phase containing polarized water reflects primarily the alteration in the degree of motional freedom of the solute, translational and rotational. Since water molecules in the state of polarized multilayers are more tightly held to immediately-neighboring water molecules and directly or indirectly immobilized through intervening polarized water molecules to the fixed N and P sites, the solute molecules are subject to greater translational and rotational motional restriction in polarized water than in normal liquid water (Figure 5.4A). Again, the larger the probe molecules, the more complex the structure, the greater is the loss of entropy, especially rotational entropy, for the same reason that a large butterfly becomes more easily snared and immobilized in a spider web than a tiny one does (Figure 5.4B).

Most probe molecules and hydrated ions find themselves at equilibrium at a lower concentration in polarized water than in external normal liquid water; the larger the probe molecule or hydrated ion, the lower the equilibrium-distribution coefficient, or q -value (the size rule). An important exception to the size rule relates to larger molecules that possess polar groups distributed in such a manner that they fit snugly into the dynamic water structure. The favorable surface component of the energy thus gained is enough or more than enough to offset the effects of

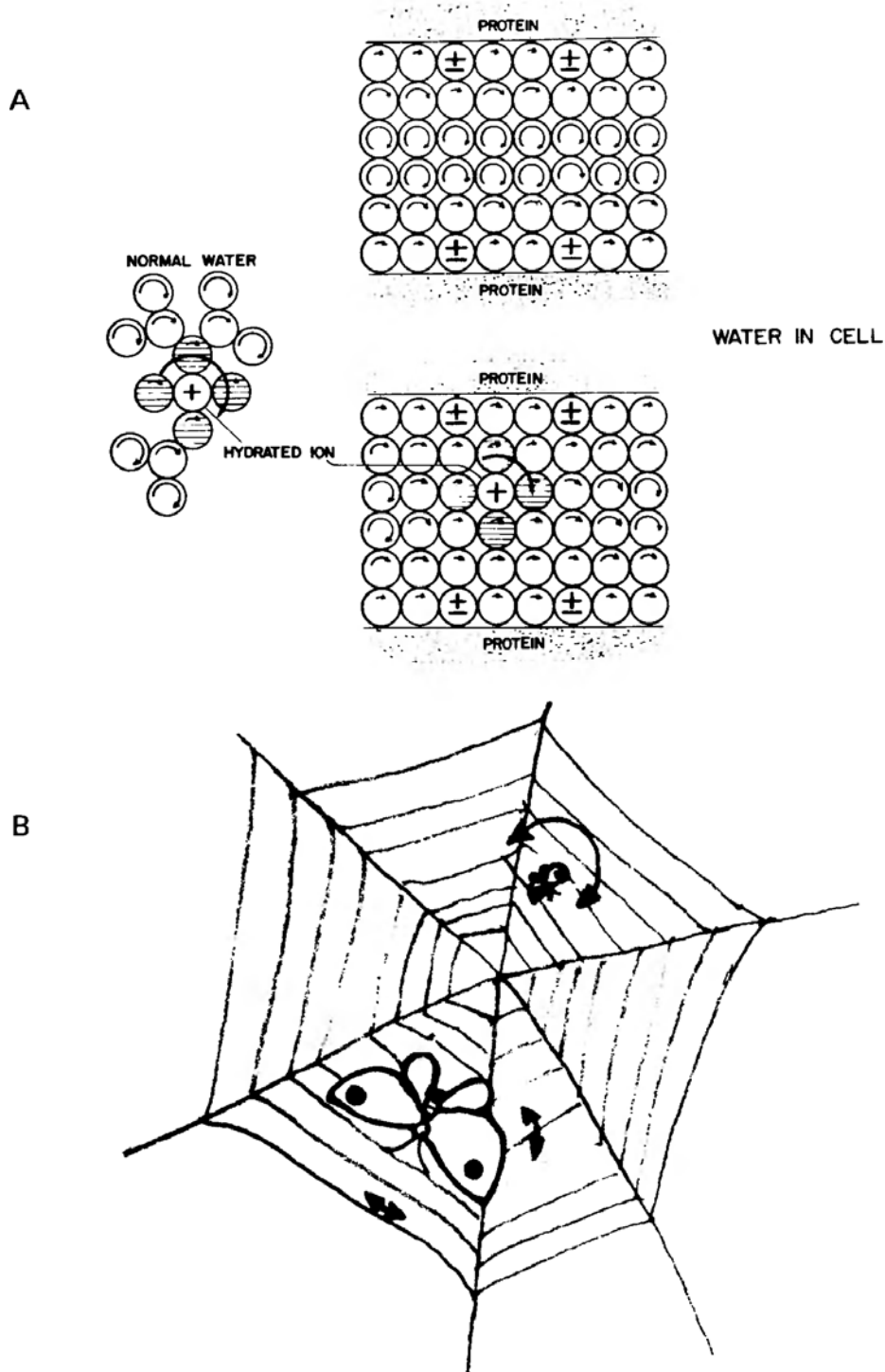


Figure 5.4.

- A. Diagrammatic illustration of the reduction of rotational (and translational) motional freedom of a hydrated Na^+ ion in water assuming the dynamic structure of polarized multilayers. Size of the curved arrows indicate motional freedom of both the water molecules (empty circles) and hydrated cations. Reduced motional freedom is indicated by the smaller sizes of the arrows. Taken from an early paper (Ling 1965) some aspects of this diagram are more applicable to models and less applicable to living cells, where the degrees of polarization among water layers near and away from the fully extended protein backbones tend to be much more uniform than indicated in the diagram, see Figure 5.3 for cause. (Ling 1965, by permission of Annals of New York Academy of Sciences)
- B. Illustration of the greater degree of motional restriction of larger butterflies snared in a spider web. (Larger) size of arrow represents (greater) degrees of motional freedom.

the unfavorable entropy and unfavorable volume component of energy. *Under this condition, a large probe molecule may enjoy a q -value equal to or exceeding unity.*

5.2.4. *Predictions of the Polarized-Multilayer (PM) Theory of Cell Water*

Prediction 1. Rotational-Motional Restriction of Bulk Phase Water. In the PM theory, all or virtually all of the water molecules in living cells (and in model systems containing fully-extended protein chains and their equivalent) are to varying degrees immobilized by interacting with neighboring water molecules and by indirectly interacting with the fixed-charged sites of an *NP-NP-NP* system. As a result, the motional freedom, especially the rotational-motional freedom, of all or virtually all the water molecules in the system is reduced.

Prediction 2. Size-Dependent Solute Exclusion. Interaction with neighboring water molecules and immobilization through direct and indirect interaction with fixed sites produce a size-dependent effect on the q -values of solutes in polarized water. Only fully-extended protein chains (and model systems) can polarize water in multilayers that are strong enough to exhibit the size-dependent solute exclusion seen in living cells. Native proteins (for definition see endnote 4 of Chapter 3) have no or much less effect.

Prediction 3. Multilayer Adsorption of Cell Water. Multilayer adsorption is the cause of the presence of water in living cells; it is also the cause of the essentially invariant water content of each specific cell type and of the different water contents of different cell types. The bulk of water in living cells and model systems should follow the Bradley multilayer-adsorption isotherm. Another prediction concerns the amount of water sorbed on proteins and polymers existing in the fully-extended conformation. At physiological vapor pressure ($p/p_0 = 0.9966$), water sorbed by proteins and polymers in the fully-extended state should, in quantity, match that of living cells, but exceed that of water sorbed by native proteins.

Prediction 4. Osmotic Activity Due to Multilayer Polarization of Water. Stronger electrical polarization (or induction) among neighboring, polarized water molecules reduces the activity of water beyond that of normal liquid water. For this reason, an aqueous solution of proteins and polymers existing in the fully-extended conformation should exhibit osmotic activity beyond that predicted by the molar concentration of the protein or polymer. Native proteins dissolved in water should show less osmotic activity than fully extended proteins.

Prediction 5. Freezing-Point Depression of Polarized Water. The stronger interaction among bulk-phase water molecules with fully-extended protein chains and polymer models enhances the overall stability of dynamic water structure, and hence greater resistance than normal liquid water to undergo cooperative transition to the ice state during cooling. Thus, polarized water should exhibit concentration-dependent freezing-point depression and a slower rate of freezing, while solutions of native proteins, which do not polarize water in multilayers or do so weakly, should exhibit little or no effect on the freezing of bulk-phase water.

5.2.5. Results of Experimental Testing of the Predictions of the PM Theory

The following is a brief summary of the results of experimental testing of the five predictions cited above. For convenience of presentation, Prediction 2 is given before Prediction 1.

5.2.5.1. Size-Dependent Solute Exclusion from Polarized Water

To test the hypothesis that fully extended proteins more effectively reduce the solvency of bulk-phase water for probe molecules and ions like hydrated Na^+ , we relied on the simple technique called “equilibrium dialysis” (Hughes and Klotz, 1956). A protein solution in a dialysis sac is incubated in a solution containing a high concentration of radioactively-labeled Na_2SO_4 . After diffusion equilibrium has been reached, the equilibrium concentration of Na^+ in the sac, and that in the external solution, were determined and their ratio or ρ -values calculated. The results are shown in Table 5.2 and discussed next.

(1) *New Insight into the Unusual Behaviors of Gelatin; New Definition of “Colloids.”* Table 5.2A shows the ρ -value of labeled Na^+ in solutions of native proteins (and one polysaccharide) initially at 20% concentration after equilibrium dialysis in 1.5 M ^{22}Na -labeled Na_2SO_4 solution at neutral pH. A high salt concentration was chosen to eliminate undesirable electrostatic effects. *Twelve native proteins and one polysaccharide (chondroitin sulfate) have minimal effects on the solvency of water; in all cases, the ρ -values of Na^+ (as sulfate) were close to unity. In sharp contrast, gelatin effectively reduces the solvency of water for Na sulfate and citrate (Table 5.2B).* This result confirms specifically the report of Na_2SO_4 exclusion from gelatin solution by Hollemann et al in 1934, and in a more general sense, the even earlier observation of Na_2SO_4 exclusion from the water in dried pig’s bladder by Carl Ludwig (1849) mentioned in the introduction of this volume.

Gelatin is denatured collagen and also the major solid component of “Jello.” Though 95% of Jello is water, it nevertheless stands up like a solid. It does not flow away like solutions of native proteins and it changes the solvency of water. What makes gelatin so unusual? The answer I suggested (1980) lies mostly in its unusual amino acid composition. Its amino acid residues contain 12% proline and 9% hydroxyproline (Piez et al. 1960). Neither of these residues carries a proton on its backbone N atoms, and hence cannot form the H-bonds required to hold together α -helical or β -pleated-sheet conformation. An even larger percentage of the amino-acid residues of gelatin (e.g., 33%) is glycine (Veis 1964). Glycine is one of the strongest “helix breakers”, i.e., from empirical rules, the NH and CO groups closest to a glycine residue in a protein have little tendency to form α -helical structures (see Section 6.2.1 and Table 6.2). In native collagen, some *interchain* H-bonds are formed among the three intertwining (α , β , and γ) collagen chains; after denaturation, these interchain H-bonds are broken. When dissolved in water, **gelatin, with 54% of its amino acid residues in the form of nonhelix formers and “helix breakers,” contains large segments of its polypeptide chains in the fully extended state.** According to the AI hypothesis, **it is the fully extended conformation of its polypeptide chain that gives gelatin the ability to**

Table 5.2. ρ -Values of Na^+ in Water Containing Native Globular Proteins, Gelatin, Polyvinylpyrrolidone, Polyethylene Oxide, and Methylcellulose^{a,b}

Group	Polymer	Concentration of medium (M)	Number of assays	Water content (%) (mean \pm SE)	ρ -Value (mean \pm SE)
A	Albumin	1.5 ^a	4	81.9 \pm 0.063	0.973 \pm 0.005
	Bovine serum Egg	1.5 ^a	4	82.1 \pm 0.058	1.000 \pm 0.016
	Chondroitin sulfate	1.5 ^a	4	84.2 \pm 0.061	1.009 \pm 0.003
	α -Chymotrypsinogen	1.5 ^a	4	82.7 \pm 0.089	1.004 \pm 0.009
	Fibrinogen	1.5 ^a	4	82.8 \pm 0.12	1.004 \pm 0.002
	γ -Globulin				
	Bovine	1.5 ^a	4	82.0 μm 0.16	1.004 \pm 0.004
	Human	1.5 ^a	4	83.5 \pm 0.16	1.016 \pm 0.005
	Hemoglobin	1.5 ^a	4	73.7 \pm 0.073	0.923 \pm 0.006
	β -Lactoglobulin	1.5 ^a	4	82.6 \pm 0.029	0.991 \pm 0.005
	Lysozyme	1.5 ^a	4	82.0 \pm 0.085	1.009 \pm 0.005
	Pepsin	1.5 ^a	4	83.4 \pm 0.11	1.031 \pm 0.006
	Protamine	1.5 ^a	4	83.9 \pm 0.10	0.990 \pm 0.020
	Ribonuclease	1.5 ^a	4	79.9 \pm 0.19	0.984 \pm 0.006
			4		
B	Gelatin	0.1 ^b	4	84.0 \pm 0.78 ^c	0.89 \pm 0.002
		1.5 ^a	37	57.0 \pm 1.1	0.537 \pm 0.013
C	Polyvinylpyrrolidone (PVP)	1.5 ^a	8	61.0 \pm 0.30	0.239 \pm 0.005

D	Polyethylene oxide (PEO)		0.75 ^a	5	81.1 ± 0.34	0.475 ± 0.009
			0.5 ^a	5	89.2 ± 0.06	0.623 ± 0.011
			0.1 ^a	5	91.1 ± 0.162	0.754 ± 0.015
E	Methylcellulose (MC)		0.1 ^b	4	89.3 ± 0.36	0.588 ± 0.006
			0.2 ^b	4	89.9 ± 0.06	0.955 ± 0.004
F	PVP	Q	0.2 ^b	4	87.2 ± 0.05	0.865 ± 0.004
		S*	0.5 ^b	3	83.3 ± 0.09	0.768 ± 0.012
		Q	0.5 ^b	3	81.8 ± 0.07	0.685 ± 0.007
		S	1.0 ^b	3	67.0 ± 0.26	0.448 ± 0.012
		Q	1.0 ^b	3	66.6 ± 0.006	0.294 ± 0.008
		S	1.5 ^b	3	56.3 ± 0.87	0.313 ± 0.025
			1.5 ^b	3	55.0 ± 1.00	0.220 ± 0.021

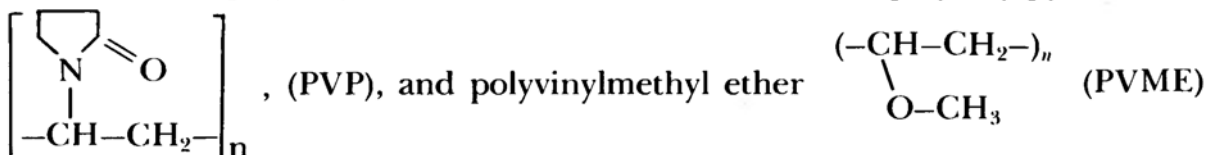
^aTemperature was 25 ± 1°C and test tubes were agitated, except in the experiments of (F), which were carried out at 0 ± 1°C and in which some test tubes, marked Q, were quiescent and unstirred. S represents sacs shaken in test tubes at 30 excursions/min (each excursion spans 1 in.), except the first set (S*), for which agitation was achieved by to and fro movement of silicone-rubber-coated lead shot within the sacs. The symbols *a* and *b* indicate that the media contained initially 1.5 M Na₂SO₄ and 0.5 M sodium citrate, respectively. In (D), PEO (molecular weight 600,000) was dissolved as a 10% (w/w) solution, and the viscous solution was vigorously stirred before being introduced into dialysis tubing. In (F), the quiescent samples contained more water. This higher water content accounts for only a minor part of the difference, as shown by comparison of the sixth and seventh sets of data: even with a larger water content, the *p*-value is lower in the stirred samples (sixth). Na⁺ was labeled with ²²Na⁺ and assayed with a gamma counter.

^bFrom Ling *et al.* (1980a) and Ling and Ochsenfeld (1983), by permission of *Physiological Chemistry and Physics*.

^cTemperature was 37°C.

polarize bulk-phase water in multilayers, with reduced solvency for Na^+ and other solutes.⁴ The data shown in Table 5.2B confirm this expectation.

Further support for this interpretation of gelatin behavior are the even stronger effects of polyethylene oxide ($-\text{CH}_2\text{OCH}_2-$)_n (PEO), polyvinylpyrrolidone



in reducing the solvency of water for Na sulfate and citrate (Table 5.2 C, D, F) (Figure 5.5). All of these *NO-NO-NO* polymers, like gelatin, also exist in the fully extended conformation (for evidence, see Stone and Stratta 1967, 113–4, 139) because they, too, lack an H on the N atom and they, too, cannot form α -helix or other intra- or intermacromolecular H bonds. The effectiveness of these polymers in reducing water solvency also demonstrates that CO sites are more important than NH sites in changing the solvency of water. Put differently, while both the NH and CO groups are essential for the formation of intramacro-

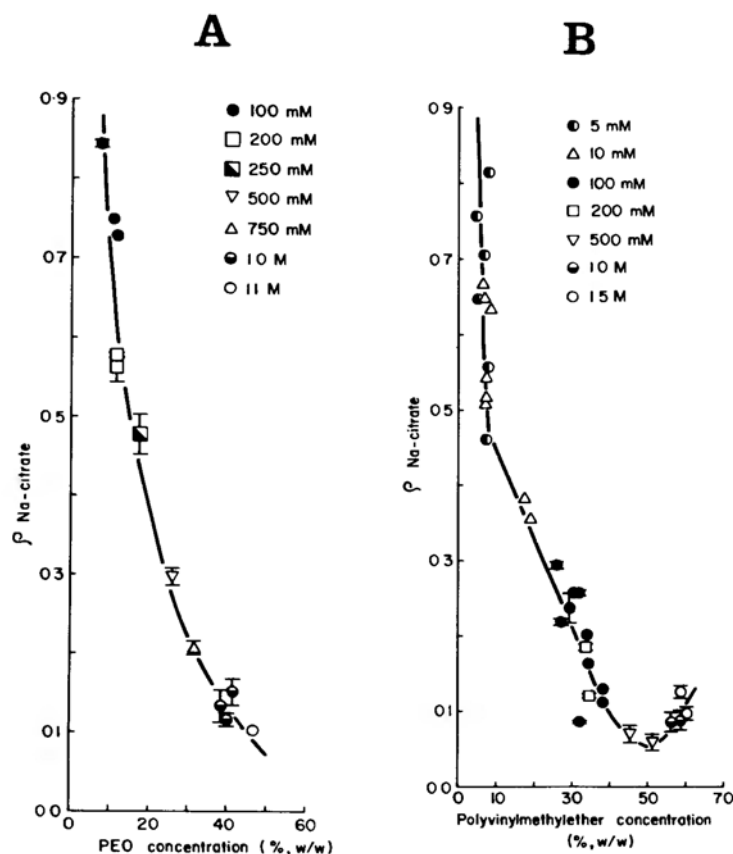


Figure 5.5. The apparent equilibrium distribution-coefficient (ρ) of Na citrate between water in solutions containing varying concentrations of poly(ethylene oxide) (A) and of poly(vinylmethylether) (B) in dialysis sacs and water in external bathing solutions. Different symbols denote different concentrations of Na citrate indicated in the figures. (Ling and Ochsenfeld 1983, by permission of *Physiological Chemistry Physics and Medical NMR*)

molecular H-bonds like the α -helical or β -pleated-sheet conformation, properly spaced CO groups by themselves are enough to polarize water though probably less efficiently than with NH groups in an *NP-NP-NP* system. Since solutions of these polymers are viscous liquids rather than gels, clearly, solute exclusion does not necessarily require the existence of the system in a gel or coacervate state (i.e., a liquid colloid-rich phase which separates out from the rest of the solution in a mixture of macromolecules) (Troshin 1966).

Thomas Graham defined colloids as gelatin-like (Section 1.2.1). With our recognition that gelatin is distinguished from native proteins because of its unique primary structure, *one can redefine colloids as chemical compounds that, dissolved in a polar solvent, polarize it in multilayers*. The most outstanding polar solvent is water. However, colloids do not reduce the solvency of water only; they reduce the solvency of other polar solvents as well e.g., formamide, DMSO (see Ling et al. 1980). The colloidal condition or state is therefore the state in which a polar solvent like water exists in the state of polarized multilayers. Of the accompanying characteristics, reduced solvency for Na^+ is an outstanding example. Other characteristic properties of polarized water will be referred to in following pages.

(2) *The Conversion of Non-Water-Polarizing Native Proteins by Denaturants, and Reversal of the Conclusion of A. V. Hill*. According to the AI hypothesis, native proteins do not intensely polarize water in multilayers for a similar reason that native proteins do not absorb large quantities of Na^+ (or K^+): the masking of the essential functional groups. For Na^+ adsorption, the essential functional groups are the β - and γ -carboxyl groups, which are masked by salt-linkage formation in native proteins (Figure 4.1). For water polarization, the essential functional groups are the backbone NH and CO groups, which are masked by formation of α -helical or other intramacromolecular H-bonds in native proteins. The masked β - and γ -carboxyl groups can be liberated by neutralizing the fixed cations. An unmasking of the CONH groups may be expected when the intermacromolecular and intramacromolecular H-bonds making up the secondary structure of the native proteins are broken by denaturants known to unravel secondary structures of proteins, e.g., urea, guanidine HCl (Tanford 1968) (Figure 5.6). With the backbone *N* (CO) and *P* (NH) sites thus unmasked by urea or guanidine HCl, one may expect the proteins to behave like gelatin. Reduction of the solvency of bulk-phase water may be expected for solutes that are partially excluded in living cells: sodium salts, sucrose, and glycine. On the other hand, denaturants like sodium dodecylsulfate (SDS) and n-propanol, known to break only tertiary structures (salt linkages and other structures involving protein side chains), while leaving α -helical and other secondary structures intact or even strengthened, are expected to have no or little effect on water solvency (Herskovits et al. 1970).

Figure 5.7 and Table 5.3 show that both expectations were confirmed. Significant reduction of ρ -value for sucrose occurred in urea- and guanidine-HCl-denatured proteins, but not in SDS and n-propanol-denatured proteins. Also shown in Figure 5.7 is the minimum "nonsolvent" water, an arbitrary parameter useful in illustrating the quantitative effects on water solvency observed. For a ρ -value of, say, 0.87 for sucrose, $(1 - 0.87)$ or 13% of the water is considered



Figure 5.6. Diagrammatic illustration of urea denaturation of a segment of a native protein backbone leading to the exposure of the backbone NHCO groups to bulk phase water (and urea) and the polarization in multilayers of water and urea.

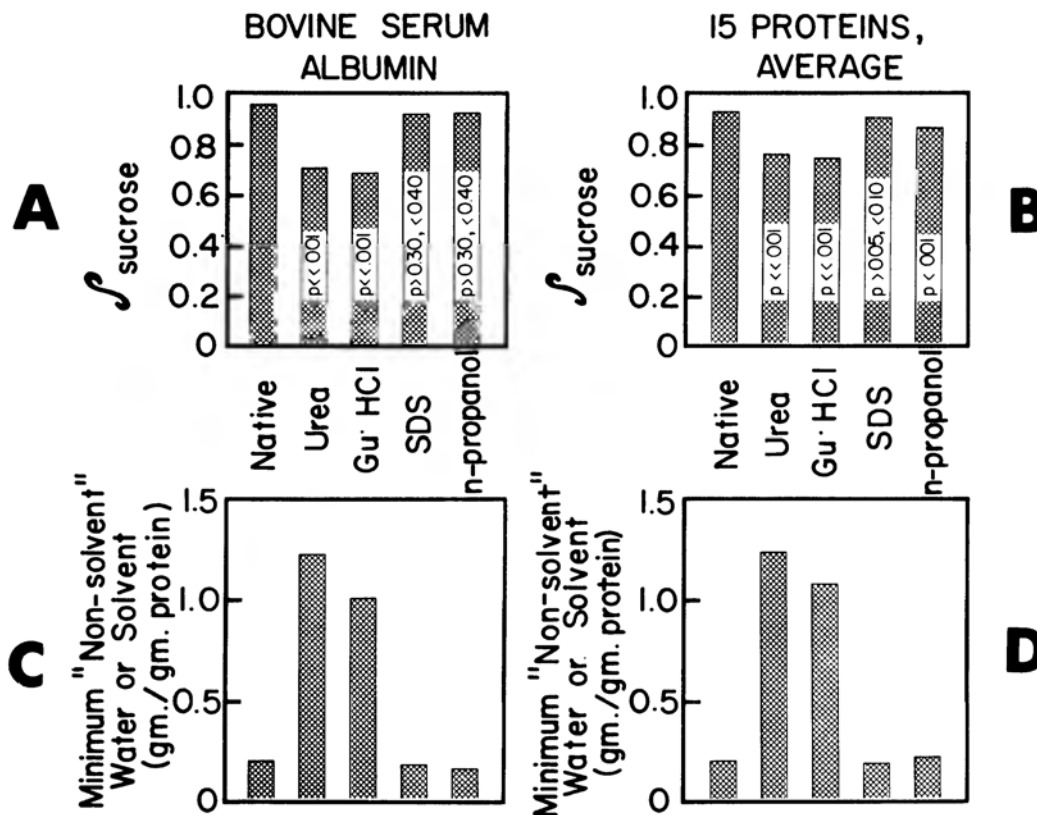


Figure 5.7. ρ -values of sucrose (A and B) and apparent minimum "nonsolvent" water for sucrose (C and D) of solutions of native and denatured proteins. ρ -values were determined by the method of equilibrium dialysis. (C) and (D) represent the averages of 14 proteins studied: actin, albumin (bovine), albumin (egg), α -chymotrypsinogen, edestin, fibrinogen, γ -globulin, hemoglobin, histone, β -lactoglobulin, lysozyme, myosin, trypsin, and trypsin inhibitor and one polysaccharide, chondroitin sulfate. Values for the native and urea-denatured states were determined from all 14 proteins and chondroitin sulfate; guanidine HCl values, from 12 proteins; and sodium dodecyl sulfate (SDS) and n-propanol values, from 10 proteins. Incubating solutions contained Na_2SO_4 (100 mM), glycine (10 mM), sucrose (10 mM), and MgCl_2 (10 mM). In addition, urea (9 M) and guanidine HCl (6 M), SDS (0.1 M), and n-propanol (2 M) were present as indicated. Incubation at $25 \pm 1^\circ\text{C}$ lasted from 28 to 96 hr, to reach diffusion equilibrium. (Ling et al. 1980a, by permission of Physiological Chemistry and Physics.)

as minimum “nonsolvent” water for the sucrose probe. Actually, the amount of water affected must be more than 13%, because the q -value is probably not zero for any (macroscopic) portion of the water. There is also no categorically “nonsolvent” water, only water with reduced solubility for large and complex solutes in a size-dependent manner.

In solutions of the 15 urea-denatured proteins, the ρ -value of ^{14}C -labeled urea was also determined. An average of ρ -value for urea of 0.991 ± 0.055 was observed, even though the ρ -values for sucrose in the same denatured protein solutions were much reduced (Ling et al. 1980a; Ling 1984, 177; for more complete data see Ling and Ochsenfeld 1989). This distinction of near-normal solvency for urea on the one hand and low solvency for sucrose on the other offers new insight into A. V. Hill’s conclusion of historic consequence mentioned earlier (see Section 1.4). Hill (1930) observed near unity ρ -value for urea in frog muscle cell water and used this finding as disproof that frog-muscle water is partly “nonsolvent” (in the outdated and incorrect sense that “nonsolvent” water is nonsolvent for all solutes). In fact, *Hill’s findings are in harmony with the polarized-multilayer theory of cell water, which predicts near normal q -value for solutes like urea and ethylene glycol (see below) that can fit into the dynamic, polarized-multilayered water structure, but predicts reduced q -value for large hydrated Na^+ , sucrose, and other solutes normally found at low levels in the cell water.* However, Hill’s data offered no evidence for the concept that all cell water is normal liquid water, a concept which, though proven wrong now, prevailed at one time and changed the course of history for the ensuing half century (Section 1.4).

(3) *Size-Dependent Solute Exclusion due to Fully Extended Proteins and Polymers but not Native Proteins.* Urea distribution in frog muscle offers a limited confirmation of the predicted **size rule**. However, it was ρ -values (and not q -values) that Hill (and coworkers) measured and reported on and as mentioned above, we confirmed. If a substantial part of urea in the cell is adsorbed, then the true equilibrium-distribution coefficient or q -value would be much lower. In that case, the data can no longer be considered to confirm the size rule. More rigorous proof of the size rule is required and has been achieved.

In the preceding chapter we demonstrated how titration with NaOH unmasked fixed anions (i.e., α -, β -, and γ -carboxyl groups) which then adsorb Na^+ , one mole for each mole of fixed cation eliminated. Figure 4.1 diagrammatically illustrates this change. In addition, the diagram also illustrates an important side event occurring in the alkali-induced denaturation, i.e., an apparent polarization of the bulk-phase water. Ling and Hu (1988) recently studied the equilibrium distribution of 14 compounds in solutions of native hemoglobin and alkali-denatured hemoglobin, and PEO (polyethylene oxide). The results show that all solutes studied uniformly demonstrated rectilinear distribution, indicating that in these solutions all or virtually all solutes studied are found only in the water (Figure 5.8A). The slopes of these straight lines are, of course, equal to the q -values.

In Figure 5.9A, the q -values of these solutes in solutions of NaOH-denatured

Table 5.3. The Effects of 3M Guanidine HCl, 9M urea, 0.1 M Sodium Dodecylsulfate (SDS) and 2M n-Propanol upon the ρ -Values of Sucrose in Solutions of Nine Proteins." (Ling and Ochsenfeld 1989, by permission of Physiological Chemistry Physics and Medical NMR)

		ρ_{sucrose}	H ₂ O Content* (%)	pH	P
Albumin (serum)	H ₂ O	0.946 ± 0.015	72.07 ± 0.012	5.2	< 0.001
	Gu. HCl	0.607 ± 0.030	38.01 ± 0.45	5.6	
Albumin (egg)	H ₂ O	0.877 ± 0.013	68.50 ± 0.38	5.8	<< 0.001
	Gu. HCl	0.569 ± 0.004	37.82 ± 0.086	6.1	
	SDS	0.943 ± 0.014	67.31 ± 0.26	6.4	
	n-propanol	0.813 ± 0.009	61.01 ± 0.24	6.4	
α -chymo-trypsinogen	H ₂ O	0.900 ± 0.013	59.46 ± 0.045	3.45	< 0.001
	Gu. HCl	0.718 ± 0.015	41.56 ± 0.660	4.55	
	SDS	0.847 ± 0.009	52.39 ± 0.605	3.90	
	n-propanol	0.878 ± 0.002	51.55 ± 0.154	4.25	
Edestin	H ₂ O	0.833 ± 0.030	50.58 ± 0.98	5.55	< 0.001
	Urea	0.641 ± 0.018	41.26 ± 0.23	7.2	
	Gu. HCl	0.641 ± 0.006	39.96 ± 0.044	6.2	
	SDS	0.823 ± 0.002	46.28 ± 0.390	6.3	
	n-propanol	0.820 ± 0.005	50.44 ± 0.610	6.0	
Fibrinogen	H ₂ O	0.856 ± 0.011	66.85 ± 0.080	7.3	<< 0.001
	Gu. HCl	0.650 ± 0.004	39.62 ± 0.010	5.3	
	SDS	0.893 ± 0.007	58.92 ± 0.270	5.4	
	n-propanol	0.874 ± 0.006	61.31 ± 0.075	5.2	

γ -globulin	H ₂ O	0.907 ± 0.009	65.66 ± 0.150	7.1	<< 0.001 0.02 > P > 0.01 0.1 > P > 0.05
	Gu. HCl	0.620 ± 0.011	38.88 ± 0.240	7.0	
	SDS	0.852 ± 0.008	59.94 ± 0.140	7.5	
	n-propanol	0.866 ± 0.008	58.91 ± 0.360	7.1	
Hemoglobin	H ₂ O	0.824 ± 0.018	68.47 ± 0.069	4.8	<< 0.001 0.5 > P > 0.4 0.005 > P > 0.001
	Gu. HCl	0.634 ± 0.002	41.58 ± 0.100	5.8	
	SDS	0.843 ± 0.012	63.56 ± 0.260	5.5	
	n-propanol	0.743 ± 0.005	51.74 ± 0.17	5.5	
β -lacto- globulin	H ₂ O	0.872 ± 0.008	68.80 ± 0.24	5.6	<< 0.001 0.02 > P > 0.01 0.5 > P > 0.4
	Gu. HCl	0.632 ± 0.014	39.11 ± 0.19	5.1	
	SDS	0.930 ± 0.020	66.27 ± 0.44	6.0	
	n-propanol	0.864 ± 0.015	63.05 ± 0.37	5.7	
Lysozyme	H ₂ O	0.992 ± 0.005	63.67 ± 0.015	5.0	<< 0.001 0.005 > P > 0.001 0.7 > P > 0.6
	Gu. HCl	0.635 ± 0.001	39.62 ± 0.010	5.3	
	SDS	0.929 ± 0.008	58.92 ± 0.270	5.6	
	n-propanol	1.004 ± 0.013	61.31 ± 0.075	5.2	

For the majority of experiments, the mean and standard errors (S. E.) were from four independent assays in one set of experiments. However, in other cases the values were based on more assays and sets of experiments. For all samples of proteins treated with n-propanol, the total H₂O content is not merely water but the entire solvent, i.e., water plus n-propanol. For all other samples H₂O contents refer to the contents of water only. The low water contents of guanidine HCl experiments, like those of urea experiments, are due to the large amount of GuHCl present. P represents the level of significance between the control (H₂O) and protein treated with denaturants. n is 4 in most cases.

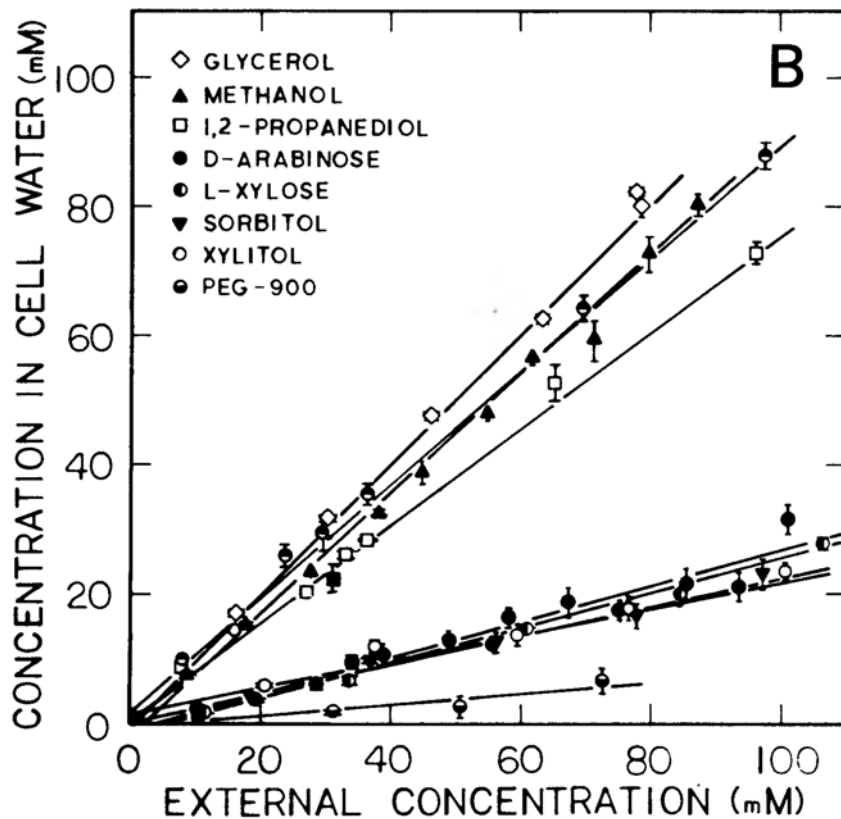
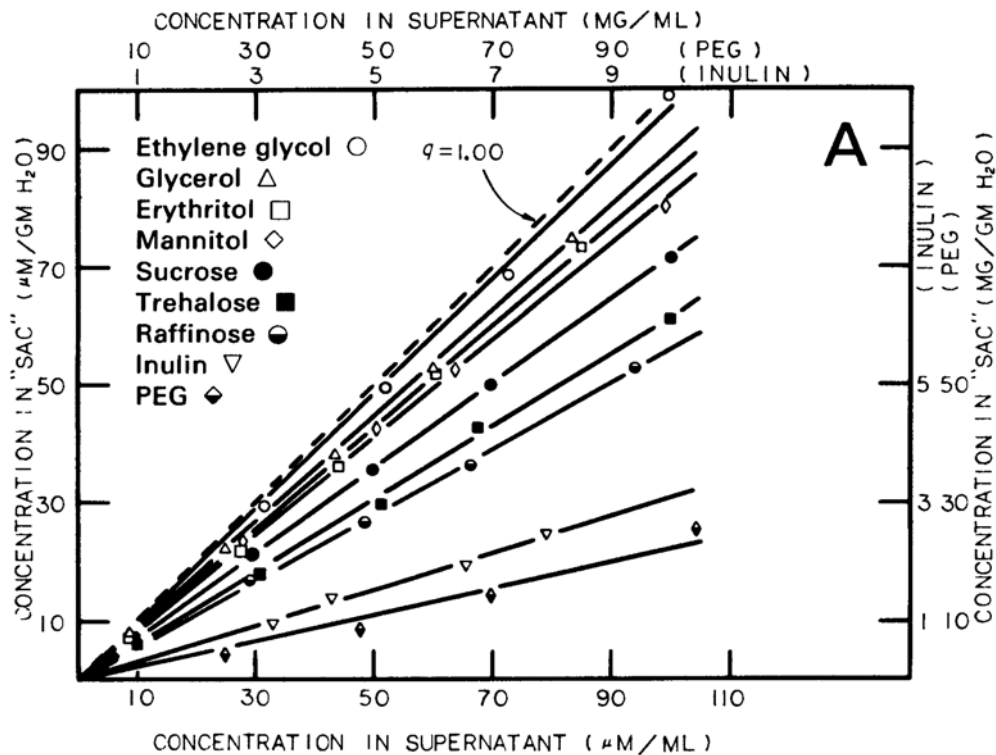


Figure 5.8. Equilibrium distribution of nonelectrolytes between solutions of (A) an 18% solution of NaOH-denatured bovine hemoglobin in dialysis sacs and external bathing solutions (Ling and Hu 1988, by permission of Physiological Chemistry and Physics and Medical NMR); and (B) between water in living frog muscle cells and their bathing Ringer solutions (Ling, Niu, and Ochsenfeld, to be published). Slopes of the rectilinear distribution curves, obtained by the method of least squares, are equal to the (true) equilibrium distribution coefficients (or q -values) of the respective nonelectrolytes between water in the muscle cells (or the NaOH-denatured hemoglobin solutions) and their respective external bathing solutions.

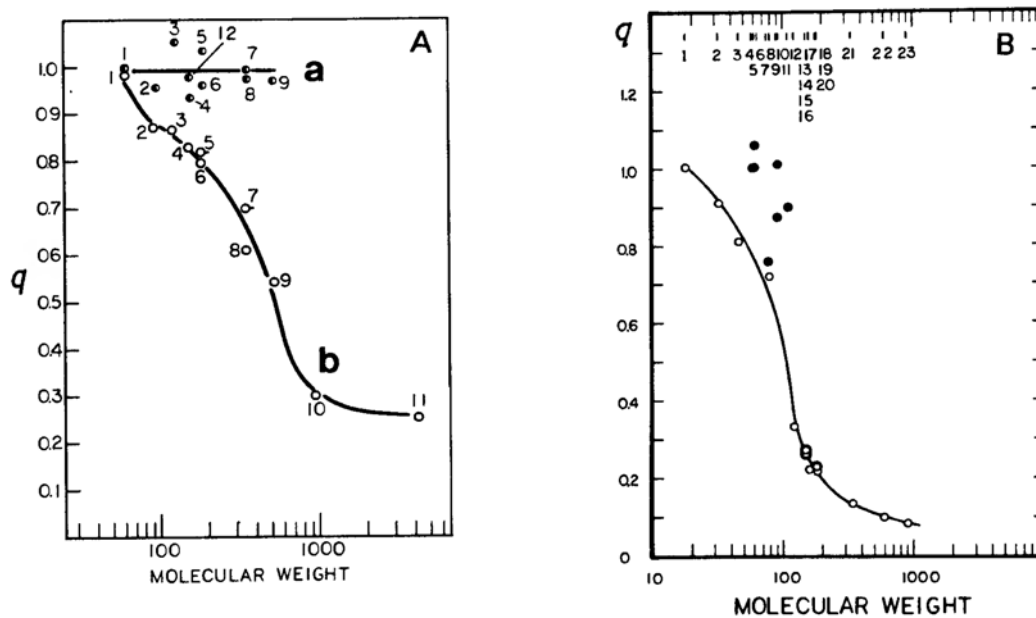


Figure 5.9

- A:** The equilibrium distribution coefficients (or q -values) of various nonelectrolytes in a 39% solution of native bovine hemoglobin (a) and in an 18% solution of NaOH-denatured hemoglobin (b) plotted against the molecular weights (MW) of the nonelectrolytes. The q -values were obtained by the method of least squares and are equal to the slopes of the rectilinear plots similar to, and including those shown in Figure 5.8A. Number designation of nonelectrolytes and their MW are as follows: [1] ethylene glycol (MW 62.1); [2] glycerol (92.1); [3] erythritol (122.1); [4] D-xylose (150.1); [5] D-mannitol (182.2); [6] sorbitol (182.2); [7] sucrose (342.3); [8] trehalose (342.3); [9] raffinose (504.4); [10] inulin (990); [11] polyethylene glycol, PEG 4000 (4000). (Ling and Hu 1988, by permission of Physiological Chemistry Physics and Medical NMR)
- B:** The equilibrium distribution coefficients (or q -values) of various nonelectrolytes and one polymer in the water in living frog muscle cells plotted against the molecular weights of the nonelectrolytes and polymers. Of the seven "aberrant" points represented as solid circles, four are established cryoprotectants (see Ling 1991); their high q -values indicate exceptional affinity of these compounds to stay in the polarized water. The q -values were obtained from the slopes of the rectilinear plots similar to and including those shown in Figure 5.8B. 1: water (MW. 18.02); 2: methanol (32.04); 3: ethanol (46.07); 4: acetamide (59.07); 5: urea (60.06); 6: ethylene glycol; 7: 1,2-propanediol (76.10); 8: dimethyl sulfoxide (78.14); 9: 1,2-butanediol (90.12); 10: glycerol; 11: 3-chloro-1, 2-propanediol (110.5); 12: erythritol; 13: D-arabinose (150.1); 14: L-arabinose (110.5); 15: L-xylose (150.1); 16: D-ribose (150.1); 17: xylitol (152.2); 18: D-glucose (180.2); 19: sorbitol (182.2); 20: D-mannitol; 21: sucrose; 22: raffinose; 23: PEG-900 (900). (From Ling, Niu and Ochsenfeld, 1991); by permission of Physiological Chemistry Physics & Medical NMR).

bovine hemoglobin and in solutions of native bovine hemoglobin are plotted against the respective molecular weights of the solutes. In native-hemoglobin solution at a concentration of 39% (w/v), the q -values of solutes ranging from ethylene glycol, with a molecule weight (mol wt) of 60, to raffinose with mol wt of 504, remained more or less constant, at or close to unity. On the other hand, in solutions of alkali-denatured hemoglobin at a concentration (18%), only half the strength of the native hemoglobin solution, the q -values decreased steadily

with increasing molecular weight. Similarly, a 19% solution of PEO and a 18% solution of gelatin gel (data of Gary-Bobo and Lindenberg 1969) exhibit molecular weight-dependent q -values (PEO) and ρ -values (gelatin) (Ling, and Hu 1988). These findings at once confirm two major predictions of the PM theory in model systems: size-dependent solute distribution in polarized water created by fully-extended protein and polymers and the inability or lesser ability to achieve the same of native hemoglobin, twice the strength of the fully-extended proteins and polymers.

(4) *Size-Dependent Solute Exclusion in Living Cells.* According to the AI hypothesis, the cell interior contains proteins existing in the fully-extended conformation with their NHCO groups directly exposed to and polarizing the bulk of cell water. If this hypothesis is correct, we must be able to demonstrate similar size-dependent solute exclusion in living cells, as has been successfully demonstrated for alkali-denatured hemoglobin, PEO, and gelatin. On the other hand, if all intracellular proteins exist in the native state, the q -value for all solutes with molecular weights ranging from 60 to 504 should also be close to unity, as already shown in a 39% solution of native hemoglobin. ***Our demonstration of rectilinear distribution and size-dependent q -values of 23 substances in frog voluntary muscle (Figure 5.8B) confirms the expected size-dependent solute exclusion (Figure 5.9B). These findings offer, in my view, the most direct and convincing evidence that cell water exists in the state of polarized multilayers in consequence of interaction with fully-extended intracellular proteins. And as such, the bulk of cell water exhibits size-dependent solute exclusion.*** Notice in particular that, like urea, ethylene glycol is also not excluded by either muscle-cell water or by a solution of NaOH-denatured hemoglobin, even though both muscle cell water (Figure 5.9B) and its model (Figure 5.9A) demonstrate size-dependent solute exclusion. One recalls that historically, the non-exclusion of urea and ethylene glycol had led to a wrong conclusion of lasting influence: that cell water is normal liquid water (Section 1.4).

5.2.5.2. *The Rotational (and Translational) Motional Restriction of Water in Living Cells: A Key Prediction and Its Verification*

In the PM theory, the bulk of water in resting cells exists in the state of polarized multilayers. That is, all the water molecules are held to their neighboring water molecules more tightly than are water molecules in normal liquid water. All the water molecules are directly or indirectly (through the intervening water molecules) anchored to the fully-extended, water-polarizing protein chains, which in turn, are attached to a matrix-protein network and thus partially immobilized. [The matrix-protein network may be in full or in part identical to cell proteins now known as "cytoskeletal proteins" (Schliwa 1986)]. Emerging from this set of fundamental concepts is another central prediction of the PM theory: **All or virtually all water molecules in the living cell are subject to translational and, especially, rotational restriction.**

It is easier to make such a prediction than to put the prediction to a rigorous test. The fact that we and other interested scientists have been, nevertheless, able to do so, is the direct result of new methods of testing that the genius, skill,

and effort of other scientists produced while they were pursuing their own unrelated subjects of study.

Three methods are available which can, under favorable conditions, determine the motional freedom of bulk-phase water. They are the nuclear magnetic resonance (NMR) method; the ultrahigh-frequency–dielectric-dispersion (UHFD) method; and the quasielastic neutron-scattering (QENS) method. Since the publication of the PM theory in 1965, and especially during the early 1980s, all these methods have been used to test the predicted rotational (and other) motional restriction of water in both living cells and in models of living cells (e.g., solutions of PEO). From these studies, a self-consistent picture has emerged confirming the central prediction of the theory.

(1) *Nuclear Magnetic Resonance (NMR) Method.* If water is placed in a strong (static) magnetic field and an oscillating electromagnetic field of a suitable frequency is applied at a direction perpendicular to the direction of the static magnetic field, the two hydrogen nuclei of the water molecules will be brought into an excited state. If the oscillating electromagnetic field is suddenly switched off, the hydrogen nuclei will dissipate their extra magnetic energy and return to the ground state by a process called *relaxation*. The rate of this relaxation process is expressed as the reciprocal of *relaxation times*, measured in milliseconds or seconds. The length of the relaxation times depends intimately upon the availability or unavailability of a magnetic-energy-accepting environment, much as a heated object dissipates its thermal energy slowly or rapidly depending upon the availability of a thermal-energy-accepting environment. Rapid thermal relaxation occurs if the heated object is placed on a metal conductor which accepts heat energy readily; slow thermal relaxation occurs if the object is placed in an insulator which accepts heat energy poorly. The most important dissipating mechanism of magnetic energy is via magnetic dipole-dipole interaction, i.e., interaction between the excited hydrogen nuclei (protons) in the water molecules and other hydrogen nuclei of the same and other surrounding water molecules. Motional restriction, especially rotational restriction of the water molecules, increases their efficiency in dissipating magnetic energy and shorten the NMR relaxation times.⁵ Therefore, by measuring the NMR relaxation times of water protons in the living cell, we can, theoretically at least, find out if all the molecules making up the bulk-phase water are motionally restricted as predicted by the AI hypothesis.

A parameter that determines the effectiveness of surrounding water in causing the NMR-relaxation processes is called the (NMR) *rotational correlation time*, represented as τ_r . τ_r is defined as the time required for the water proton to rotate from one position to another recognizably different position. NMR theory provides quantitative relationships between τ_r and the NMR relaxation times (Bloembergen, Purcell, and Pound 1948). Rotational motional restrictions lead to longer τ_r . Longer τ_r is accompanied by shorter relaxation times—over a limited lower range of τ_r ; at a higher range of τ_r values, this relation holds only for T_2 but does not hold for T_1 (see endnote 5 and Ling 1984, 299–300).

Pioneering work of Odeblad et al. (1956), Bratten et al. (1965), Cope, (1969), Hazlewood et al. (1969), (see also Hazlewood 1979 for review), and others led

to recognition that NMR relaxation times for water protons in living cells are indeed much shorter than those of normal liquid water—findings that are, at first sight, at least qualitatively in harmony with PM theory, which predicts rotational-motional restriction of bulk-phase water and hence longer τ_c and shorter relaxation times. However, a closer look reveals that the marked shortening of relaxation times, if entirely attributed to motion restriction of bulk-phase water protons, would lead to unreasonably severe reduction of the translational-diffusion coefficient of cell water far beyond the modest reduction actually observed (Reisin and Ling 1973; Seitz et al. 1980). As a result of this and other considerations, various workers expressed the opinion that the reduced NMR relaxation times were due entirely to extraneous causes and not to the motional restriction of bulk phase water (Cooke and Kuntz 1974, Kuntz and Zipp 1977). Others claimed that the observed variation of NMR relaxation times among different normal tissues and between normal and cancer tissues (Damadian 1971) was entirely due to the variation of water contents (Inch et al. 1974; Eggleston et al. 1978). However, the persuasiveness of this set of views did not last long.

A more careful study of the role of the water content of living cells, both normal and cancerous, led to the conclusion that variation of water contents among normal and cancer cells plays a significant but relatively small role in the observed difference in relaxation times (Ling and Tucker 1980). However, when a large variety of tissues were examined together, it became obvious that another potential source of NMR relaxation, hitherto underestimated, plays a much more important role than previously thought: paramagnetic ions (e.g., Mn, Fe) in cells. Differences in paramagnetic ion content are in part responsible for differences in the NMR relaxation times among normal tissues (Ling 1979, 1983a), but especially for differences between normal tissues and cancer cells. Lower manganese (and iron) contents were found in all highly malignant cancer cells than in all normal tissues examined (Ling 1983b; 1989a; Ling et al. 1990) (Table 5.4). The presence of paramagnetic ions and proteins themselves—which like paramagnetic ions also cause NMR relaxation of water protons—make it very difficult, if not downright impossible, to prove unequivocally that bulk-phase water in living cells does indeed have shorter rotational correlation time (τ_c) than that of normal liquid water, as predicted by the PM theory.

Fortunately, by this time we had already discovered that polymers like polyethylene oxide (PEO), polyvinylpyrrolidone (PVP), and polyvinylmethyl ether (PVME) have the same capacity as fully extended proteins to reduce the solvency of bulk phase water for Na^+ , sugars, and free amino acids, found, as a rule, in low concentration in living cells (Figures 5.5, 5.8; Table 5.2). But unlike proteins, these polymers themselves do not directly cause NMR relaxation of water protons. Studies of solutions of these polymers soon led to the conclusion that water, made nonsolvent for Na citrate and other large solutes by the polymer (Figure 5.5), does indeed suffer rotational restriction and a lengthening of τ_c by a factor of 3 to 19, increasing with increasing polymer concentration. Ling and Murphy (1983) then concluded that *the restricted motional freedom of bulk-phase water is indeed a significant contributing factor to the rapid NMR relaxation rates of water protons in*

Table 5.4. NMR Relaxation Times, T_1 and T_2 , of Pure Ovalbumin Solutions and Ovalbumin Solution Containing the Dissolved Ashes of Normal Mouse Tissues and Ascites Cancer Cells. (from Ling 1983b, by permission of Physiological Chemistry Physics and Medical NMR)

Sample	Tissue	T_1 (msec)	T_2 (msec)
A. P	ovalbumin (no ashes)	1325 \pm 10	470 \pm 7
B. A	muscle	550 \pm 4	266 \pm 4
B. B	liver	109 \pm 3	67 \pm 1
B. C	spleen	49.5 \pm 1.0	30 \pm 0.7
B. D	kidney	176 \pm 2	116 \pm 1
B. E	heart	93 \pm 3	65 \pm 1
B. F	lung	91 \pm 3	65 \pm 1
B. G	brain	441 \pm 7	245 \pm 4
C. H	LSA	710 \pm 17	354 \pm 3
C. I	Meth A	938 \pm 10	361 \pm 4
C. J	hepatoma 134	853 \pm 18	388 \pm 15
C. K	sarcoma 180	970 \pm 20	373 \pm 6
C. L	P815	950 \pm 10	405 \pm 7
C. M	Ehrlich	910 \pm 17	330 \pm 7

Note: T_1 and T_2 were measured at a resonance frequency of 17.1 MHz. T_1 was determined with $180^\circ\text{-}\tau\text{-}90^\circ$ pulse sequence; T_2 with Carr-Purcell spin echo method. Sample temperature was 25°C . T_1 and T_2 values are average of three determinations \pm S. E. Ovalbumin was from Nutritional Biochemical Co., Chagrin Falls, Ohio, and by ashing shown to contain no significant amount of paramagnetic impurities. All cancer cells were in the ascites form: LSA (lymphoma); Meth A (fibrosarcoma); sarcoma 180 (pleomorphic leukocyte sarcoma); P815 (mast cell leukemia); Ehrlich (mammary adenocarcinoma).

living cells. In frog muscle, it is estimated that between 30% to 40% of the observed NMR relaxation rate is due to this cause.

(2) *Ultrahigh Frequency Dielectric Dispersion (UHF) Method*. When water is placed between two condenser plates and a voltage applied across them, water dipoles will reorient themselves in such a way as to create an opposing voltage, which is high enough in magnitude to reduce the original applied voltage by a factor (called the *dielectric constant*) equal to 78.5 (25°C). If the polarity of the applied voltage is now reversed, the water dipoles will follow by again changing their orientation. With steady increase of the frequency of the back-and-forth flipping of the directions of applied voltage, a point will be reached at which the water molecules can no longer move fast enough to follow the change of the applied voltage. A decrease of the dielectric constant then follows further increase of

the frequency, until a new but much lower constant value (4.5–6.0, Eisenberg and Kauzmann 1969, 207) is reached—a phenomenon called *dielectric dispersion*. The frequency at the midpoint of the dispersion is called the *characteristic frequency*.

The dielectric dispersion of normal liquid water occurs at an extremely high frequency (i.e., 20 gigahertz (GHz) or 20×10^9 cycles/sec). In comparison, the dielectric dispersion of ice occurs at the much lower frequency of 10 kilohertz (KHz) or 10×10^3 cycles/sec. This large difference arises from the grossly reduced motional freedom of water molecules in solid ice as compared with those in liquid water.

The NMR rotational correlation times, τ_c , determine the NMR relaxation time. There is a similar parameter called Debye dielectric relaxation time or simply dielectric relaxation time (τ_D), which is the time constant for the dissipation of macroscopic electrical polarization when the applied electric field is turned off. In magnitude, τ_D equals the reciprocal of 2π times the characteristic frequency.

Due to the technical difficulties associated with the measurement of dielectric properties at extremely high frequency, only a very few laboratories in the world are equipped to study the dielectric dispersion of cell water and model systems. One laboratory so equipped is that of Kaatze at the University of Göttingen, West Germany. Kaatze and his coworkers extensively studied the dielectric dispersion of solutions of PEO, PVP, and PVME at frequencies up to 70 GHz (Kaatze 1975, Kaatze et al. 1978). Their data indicate that τ_D of water associated with the polymer is longer than the τ_D of normal liquid water by a factor of 2, rising to 5 at very high polymer concentration.

Since Debye dielectric relaxation τ_D is equal to three times the NMR rotational correlation time, τ_c (Bloembergen et al. 1948), the UHFD data of Kaatze et al are in general agreement with τ_c obtained from NMR studies of Ling and Murphy on solutions of the same kind of polymers.

Another laboratory equipped to study dielectric dispersion at ultrahigh frequencies is that of Grant at Queen Elizabeth College of London. Cooperating with other workers at Grant's laboratory, Clegg studied the dielectric dispersion of the living cells of brine shrimp cysts. From these studies Clegg reached two important conclusions: (1) ***no water in these living cells behaves like normal liquid water***; (2) *the characteristic frequency of water in brine shrimp cysts was 5.5 or 7.3 GHz, corresponding to a τ_D of either 2.9×10^{-11} or 2.18×10^{-11} sec. (depending on formulae used in computing the data), which is thus 3.6 or 2.7 times longer than that of normal liquid water* (Clegg et al. 1982; 1984). Other studies of water in rabbit tissues led to generally similar conclusions (Dawkins et al. 1981; Gabriel et al. 1983).

Ultrahigh frequency dielectric studies of cell water and polymer-dominated water have thus further confirmed that water molecules dominated by PEO, PVP, and PVME suffer rotational restriction, as do (all) the water molecules in the living cells of brine-shrimp cysts and other tissues. (However, the UHFD method does have some shortcomings, as addressed in the next section).

(3) *Quasielastic Neutron Scattering (QENS)*. Slow neutrons from neutron reactors travel at the speed of 10^5 cm/sec. When they impinge on water molecules, the

neutrons are scattered at all angles. The energy spectrum of the scattered neutron broadens as a result of the rotation and translational motion of the bombarded water molecules. Since the prediction of the PM theory is that the rotational and translational motion of the water molecules is restricted in living cells and model systems, QENS offers another powerful tool to test the prediction of this hypothesis. QENS method is also superior to both NMR and UHFD studies: as mentioned earlier, a small fraction of rapidly relaxing water (tightly bound to proteins or paramagnetic ions) has a disproportionately large influence on the NMR relaxation rates of water protons observed; a small fraction of free liquid water present in the system may exercise a disproportionately large influence on the τ_D measured in UHFD studies. ***QENS, in contrast, measures the unbiased average rotational and translational diffusion coefficients of all the water molecules present.***

Figure 5.10 represents plots of *line widths* of the scatter spectrum at different values of Q^2 , where Q , multiplied by the Plank constant, \hbar , is the momentum change of the scattered neutrons (Trantham et al 1984). The data provided in Figure 5.10A shows that ***in brine-shrimp cysts, the translational-diffusion coefficient (D_t) is reduced more than threefold from that in normal liquid water. The rotational-diffusion coefficient (D_r) is reduced by a factor of 13!*** The authors concluded: "This result supports hypotheses such as those of Berendson (1962) [on hydration of collagen] and Ling (1965, 1970, 1972, 1979, 1979a; Ling et al. 1980) [on the multilayer polarization of bulk water in living cells]." Just as interesting is Figure 5.10A, where a similar plot was made on ***QENS data from 35% PEO solution*** (Rorschach 1984). The results ***bear strong resemblance to those from Artemia cysts***, indicating strong rotational and translational motional restriction of bulk-phase water in this model system also.

Figure 5.10C shows a plot of the line width of isolated surviving frog muscle at 2°C against Q^2 , with a similar plot of line widths of a 0.15 M KCl solution at the same temperature (Heidorn 1985, Heidorn et al. 1986). The data show that ***the rotational-diffusion coefficient (D_r) for the bulk-phase water in frog muscle is 1.8 times longer than that of the 0.15 M KCl solution.*** The results agree with conclusions from NMR and dielectric studies regarding the effect of protein or polymer concentration on τ_c or τ_D . Thus cells like frog muscle, with a lower protein content (20%), have a rotational-diffusion coefficient (D_r) only two times slower than that of a 0.15 M KCl solution. Cells like Artemia cyst, with a much higher protein content (40%), have a rotational-diffusion coefficient 13 times slower than that of pure water.

In summary, QENS studies have fully confirmed the prediction that the bulk-phase water in living cells, as well as in model PEO solutions, suffers rotational-motional restriction. This confirmation is in full harmony with and is corroborated by the results of the NMR and UHFD studies just described.

5.2.5.3. *Multilayer Adsorption: the Cause of Invariant Cell-Water Content*

A great deal of effort has been spent in trying to explain the uniformly high K^+ and low Na^+ concentration in living cells. Yet, as mentioned in the opening

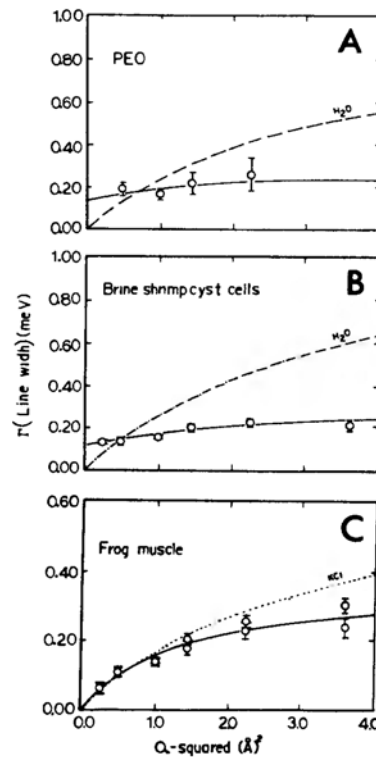


Figure 5.10. Quasielastic Neutron Scattering Studies of Water. In A, a 30% Solution of Polyethylene Oxide (PEO) at 21°C; in B, Brine Shrimp Cyst Cells at 21°C; and in C, frog muscle at 3°C.

Linewidth (MeV) vs. Q^2 (\AA^{-2}) plot for pure water is shown as dashed line in A, and as dash-dot line in B. A similar plot of water in dilute KCl solution is shown as dotted line in C. Similar plots of water in PEO solution, in brine shrimp cyst cells, and in frog muscle are given as means \pm standard error.

The “jump diffusion” model gives a Lorentzian line the width of which at half maximum is described by

$$\Gamma(Q) = 2A^2D_t/(1 + Q^2D_t\tau) + 4D_r \quad (\text{A})$$

where $\hbar Q$ is the momentum change of the scattered neutron. D_t is the translational diffusion coefficients and τ is the residence time between jumps. A second contribution to the line width comes from rotational motion of the water molecules equal to $4D_r$ where D_r is the rotational diffusion coefficient. The line width of water in brine shrimp cyst cells is described by eq. A with $D_t = 0.29D_0$, $\tau = 3.9\tau_0$, and $D_r = 6 \times 10^9$ sec. Thus the translational diffusion coefficient of water in the brine shrimp cysts is reduced to about 29% of the of free water (D_0); the rotational diffusion coefficient is reduced to 7.5% of that of free water. Water in PEO solution resembles brine shrimp cyst cells with large reduction of both D_t and D_r , indicating strong translational and rotational motional restriction of the bulk phase water. Rotational motional restriction of the bulk phase water by a factor of 1.8 was also indicated by the data of C.

(A from Rorschach 1984, by permission of Plenum Publishing Company; B from Trantham et al. 1984, by permission of Biophysical Journal; C from Heidorn 1986, by permission of Biophysical Journal)

paragraph of this chapter, thus far, little attention has been paid to the striking invariance of the most abundant component of all living cells, water. Since water and proteins make up virtually the total cell contents, the invariance of cell water means that there is an invariant ratio between cell proteins and cell water. Except for a shortlived effort to explain cell water distribution by postulating another pump (a water pump) by Robinson (1950; 1956), neither the membrane theory nor the membrane-pump theory offers any explanation why the amount of cell water should maintain an invariant ratio to the amount of cell proteins.

According to the PM theory, water exists in living cells as a result of multilayer adsorption on certain fully extended protein chains in the cells. Water is in the cell not because the cell is soaked in a liquid water environment and becomes accidentally water-logged, but rather, water is in the cell because polarization, adsorption, and accumulation of exactly that much water maximizes the total negative free energy. For a similar reason, water on the surface of the earth, flows from a high position to a low position.

If the PM theory is correct, firstly, the cell should retain the same water content whether it is soaked in a Ringer solution or suspended in an atmosphere with a vapor pressure equal to that of a Ringer solution. Secondly, one must be able to show that only proteins existing in the fully-extended conformation (or fully-extended polymers like PEO, PEG, etc.), sorb water enough at equilibrium to match the normal water content of living cells, while native proteins do not.

Confirmation of the first prediction was achieved when Ling and Negendank (1970) showed that *at a partial vapor pressure equal to that of a Ringer solution (0.9966), frog muscle cells retain their normal water content.* At lower vapor pressure, frog muscle retains less water. ***Over the entire range of partial vapor pressure from near zero to near saturation, 95% of the water content of muscle cells behaved in a way rigorously following the Bradley multilayer-adsorption isotherm, equation 4*** (see Figure 9.17 in Ling 1984).

Confirmation of the second prediction was achieved by Ling and Hu (1987) with the aid of a new method they developed for the study of equilibrium water sorption at vapor pressure at or near saturation⁶. The results shown in Figure 5.11 clearly demonstrate that *at physiological vapor pressure (partial vapor pressure equal to 0.9966), gelatin, PEO, and PEG adsorb water exceeding the water sorbed by living frog muscle; while, at the same vapor pressure, native proteins (hemoglobin, bovine serum albumin, and γ -globulin) adsorb not enough water to match that of frog muscle.*

Being a protein, gelatin is a more cogent model of the fully-extended protein chains postulated to exist in living cells. It is therefore significant that even though gelatin adsorbs less water than PEO and PEG, nevertheless, the amount of water gelatin adsorbs at physiological vapor pressure corresponds to 12.5 layers of water molecules between adjacent protein chains, thus confirming a basic postulate of the PM theory that a matrix of fully-extended protein chains can polarize and adsorb multiple layers of water molecules to account for the total water content of the living cell (see Section 5.2.2.; for calculation of water layers adsorbed by gelatin, see Ling and Ochsenfeld 1989, 40; see also Ling and

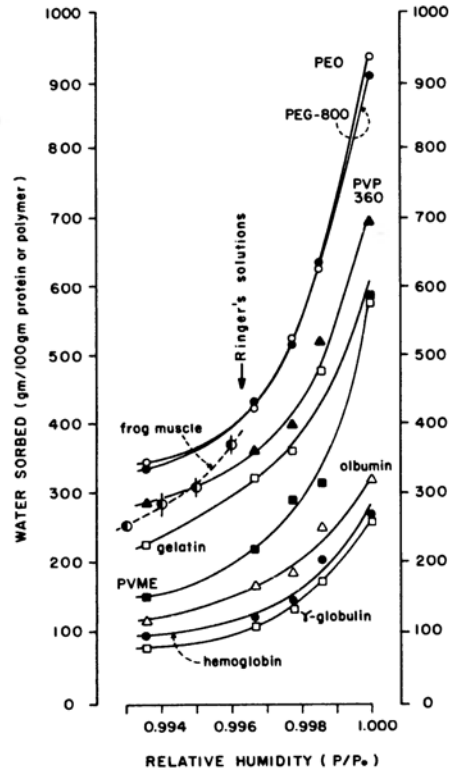


Figure 5.11. Equilibrium water vapor sorption obtained with the newly introduced Null-Point Method at extremely high relative vapor pressures (from 0.99354 to 0.99997) of polyethylene oxide (PEO), polyethylene glycol (PEG-8000), polyvinylpyrrolidone (PVP-360), polyvinylmethyl ether (PVME), gelatin, bovine serum albumin, bovine hemoglobin, and γ -globulin at 25°C. Data on water sorption of surviving frog muscle taken from Ling and Negendank (1970). Relative vapor pressure of frog Ringer's solution (0.9966) is indicated by arrow. (Ling and Hu 1987, by permission of Physiological Chemistry Physics and Medical NMR)

Ochsenfeld 1983, 132 for calculation of number of layers of "apparent minimal nonsolvent water" adsorbed on PEO).

While Ling and Hu's study did not cover water sorption of the proteins and polymers studied over the entire range of vapor pressures, J. R. Katz's data of water sorption of gelatin does (Katz 1919). As with frog muscle, water sorption on gelatin rigorously obeys the Bradley multilayer-adsorption isotherm (see Figure 9.15 in Ling 1984).

In conclusion, proteins that assume the fully-extended conformation (but not native proteins) adsorb water in the form of polarized multilayers. The quantity of the polarized water adsorbed exceeds or matches the water present in living cells on a gram of water per gram of dry-protein basis. **Both water sorption in fully-extended proteins and that in living cells follow Bradley's multilayer-adsorption isotherm.** Since one may reasonably expect that in a given type of living cell, a definite proportion of its protein content exists in the fully-extended conformation, multilayer adsorption also explains why each type of living cell under similar conditions has an essentially invariant water content (Ling and

Hu 1987, 262). This subject will be discussed again in Chapter 10 on cell volume and shape.

5.2.5.4. *Multilayer Polarization: A Major Source of the Cell's Osmotic Activity*

Since the founding of the cell theory, students of biology have been taught that living cells maintain their normal size because the total concentration of ions and other solutes inside the cell matches that of the external medium, which is primarily an isotonic NaCl solution. This view is no longer tenable because we now know that the major intracellular ion, K^+ , is not free but adsorbed, and thus osmotically inactive.

According to the AI hypothesis, only a small part of the osmotic activity of the cell can be attributed to intracellular ions, mostly NaCl, which occurs in cell water at about 1/5 of the external NaCl concentration due to the reduced solvency of cell water for NaCl (see Section 8.1.2(2), also legend of Figure 8.2A). *The major part of the osmotic activity of the cell comes from cell proteins especially those existing in the fully-extended conformation.*

To test the hypothesis that fully-extended proteins or polymers generate high osmotic activity, we measured the osmotic activity of solutions of various proteins and polymers at different concentrations (Ling 1983). Two sets of data are given in Figure 5.12. Note that gelatin, and PEO, known to exist fully or partially in the fully-extended conformation, exhibit much greater osmotic activity than solutions of native hemoglobin at similar strengths. Yet even solutions of native hemoglobin exhibit osmotic pressure higher than ideal, i.e., directly proportional

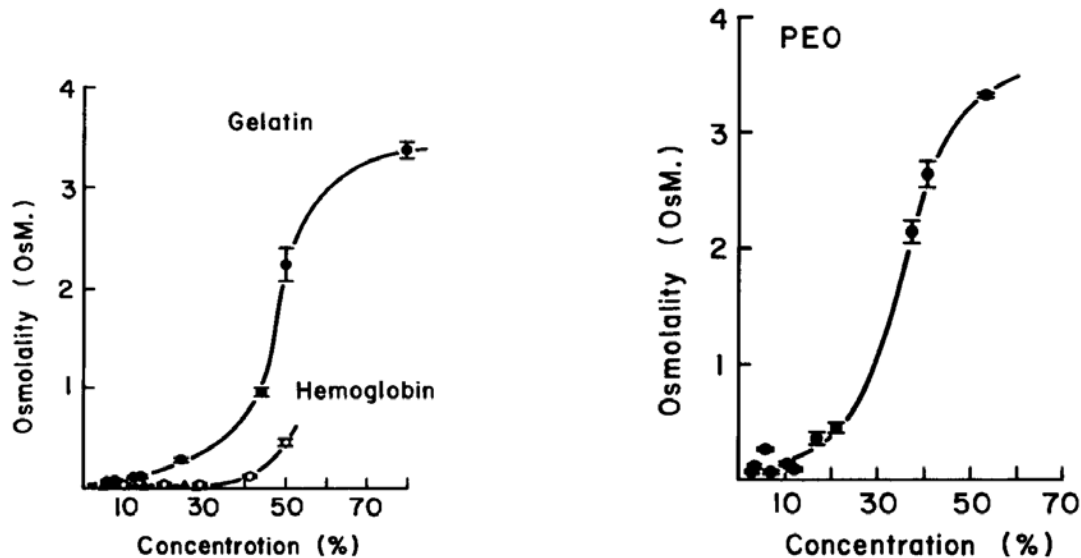


Figure 5.12. Osmolality of solutions of gelatin, native hemoglobin, and polyethylene oxide (PEO) of varying concentration. Note that due to the enormous molecular weight of the polymer (e.g., PEO, 600,000) the molar concentration of PEO is exceedingly small (e.g., 50% PEO solution, 0.83 mM). (Ling 1983, by permission of Physiological Chemistry Physics and Medical NMR)

to molar concentration. The activity of native proteins in reducing water activity indicates that even native proteins display interaction with bulk-phase water, though vastly less than fully-extended protein chains.

5.2.5.5. *Multilayer Polarization: The Cause of Freezing-Point Depression, Freezing Retardation, and Irregular Ice Crystal Formation in Living Cells*

When a frog muscle cell is gradually cooled to below freezing temperature, a point will be reached at which the Ringer solution *surrounding* the cell rapidly freezes. Ice crystals, which penetrate all nooks and crannies of the extracellular space, do not, however, penetrate *into* the muscle cells. But if a muscle cell is first amputated at one end, and a metal needle, chilled to very low temperature, is brought into contact with the cut cell surface, one or more ice “spikes” will form and grow rapidly along the length of the muscle fiber (Chambers and Hale 1932). The ice spikes formed are more or less straight if the muscle is held at its original natural orientation, Figure 5.13B. The spikes formed become twisted like pretzels if the muscle fiber is held twisted during freezing (Figure 5.13C). **The ice spikes in normal muscle cells never form branches, while ice formed in normal liquid water invariably does** (see Figure 5.13A). If by exposure to 5 mM caffeine the distal end of the muscle fiber is made to contract first, then the rapidly propagated ice spike growing toward the contracted region slows down on approaching the contracted region. Irregular-shaped ice grows, but no longer only in a fixed direction, Figure 5.13D, E (Miller and Ling 1970).

The nonbranching ice spikes formed in resting muscle cell and the irregularly shaped ice formed in the (chemically) contracted muscle cell are both profoundly different in shape from ice formed in normal liquid water. Are these aberrations caused by the nonwater cell components, primarily salt ions and proteins?

First, consider the salt ions. The ion that exists at the highest concentration in living cells is K^+ (0.1 M). Luyet and Rapatz (1956) showed that even in a concentrated NaCl solution, 2.57 M in strength, the ice formed is still hexagonal and normal. Therefore, salt ions could not be the answer. This exclusion leaves only cell proteins. The effect of proteins on ice formation was studied extensively by Luyet and Rapatz (1956). Again, in a concentrated solution of **native** bovine serum albumin (35%), ice formed is still essentially normal, hexagonal with six regular radiating arms (Figure 5.14a). However, ice formed in **gelatin** solution is totally different.

In a 65% gelatin solution, no ice forms at all. In a gelatin solution 50% or lower in concentration, ice does form. But in contrast to the hexagonal ice with six radiating arms, ice formed in gelatin appears as irregular “rosettes” (Figure 5.14b). Going back to Figure 5.13E, one finds that ice formed in the contracted region of frog muscle resembles a branch of the ice rosette formed in gelatin. However, this is not the only similarity between ice formed in gelatin and that formed in frog muscle cells. When a supercooled solution of gelatin is touched by a cold rod, the ice formed may assume the form of a long, unbranching rod, resembling the ice spike formed when the supercooled cut muscle is touched with a cold needle (Figure 5.13A).

The (35%) solution of bovine serum albumin studied by Rapatz and Luyet in

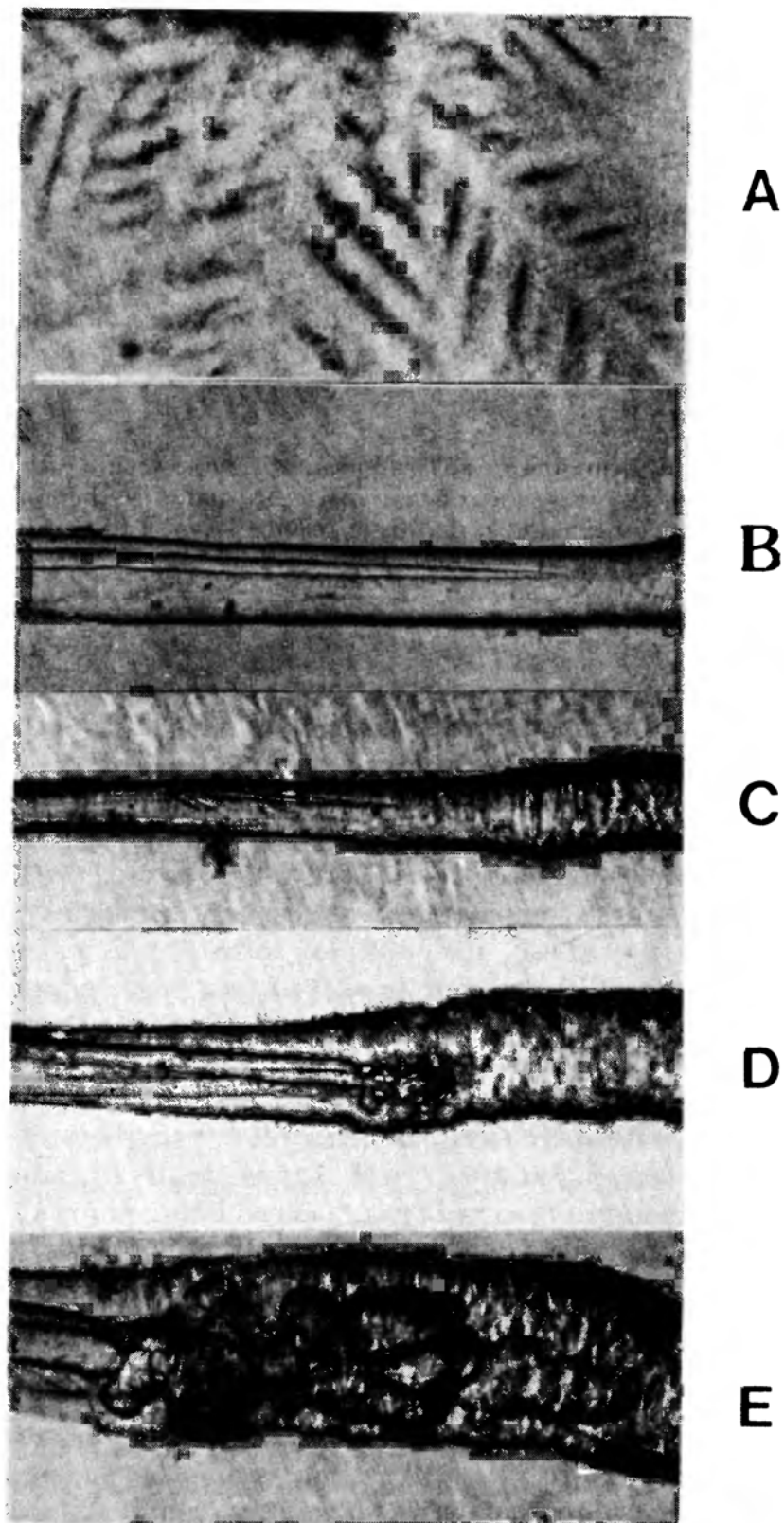


Figure 5.13. Patterns of ice formation in single isolated bullfrog muscle cells. All muscle fibers after isolation were blotted on wet filter paper and allowed to dry for 15 seconds in the air to minimize surface ice formation which obscures vision and to prevent simultaneous formation of too many spikes.

- A. Normal ice crystal in liquid water (Hallet 1965).
- B. Ice growth at -2.5°C in muscle fiber.
- C. Ice growth in twisted muscle fiber, -2°C .
- D. Same as C, after entering contracted region, 20 secs. after C.
- E. Final state of contracted region after growth had slowed to negligible rate, 10 min. after D.

(Miller and Ling, 1970, by permission of Physiological Chemistry and Physics)

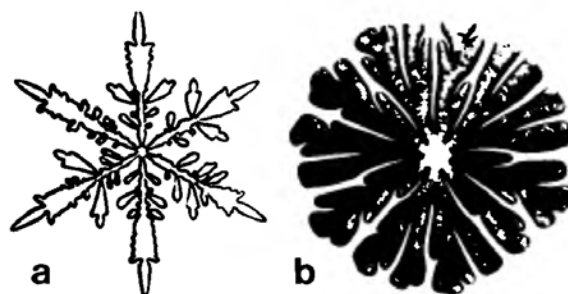


Figure 5.14. Ice crystal formation in 35% solution of bovine serum albumin (a) and in 50% solution of gelatin (b). Note regular hexagonal ice formation in the solution of (native) bovine serum albumin but irregular dendritic rosette formed in the gelatin solution. (Luyet and Rapatz 1956)

1956 was a solution of a *native* protein with most of its backbone NHCO locked in α -helical and other intramacromolecular H bonds. Gelatin, on the other hand, is at least partially *fully-extended* (Section 5.2.5.1.(1)); so is PVP, only more so. Indeed, *Luyet and Rapatz found that out of the 15 substances they studied: "All solutes, except gelatin, permitted the formation of hexagonal structure. . . None, except gelatin and PVP (polyvinylpyrrolidone), led to the growth of irregular rosette . . ."* (Luyet and Rapatz 1956, 31). From these comparisons, one reaches the conclusion that, in full accord with the AI hypothesis, **irregular ice formation is not common, but occurs in solutions of PVP and gelatin and in frog muscle and other living cells** (Chambers and Hale, 1932). Next we examine ice formation not by visual observation but by microcalorimetry.

Silver-iodide crystals have long been in use for inducing cloud formation. Their inclusion reduces supercooling of water. Yet even in the presence of silver-iodide crystals, the freezing points as well as the rates of freezing of solutions of bovine serum albumin measured in a differential scanning calorimeter remained essentially unchanged when the concentration of this native protein increased from 0% to 50% (Figure 5.15a) (Ling and Zhang 1983a). With 5% to 50% solutions of five other native proteins (egg albumin, bovine hemoglobin, γ -globulin, β -lactoglobulin, and protamine sulfate) similar results were obtained. These findings shows quite clearly that **mechanical blocking due to the presence of a high concentration of macromolecules alone does not alter either the freezing point of water or its rate of freezing**, as Blanchard suggested in 1940. They also confirm once more that native proteins have limited influence on bulk-phase water.

An altogether different behavior was seen in the case of solutions of gelatin, PVP, PEO, and urea-denatured proteins (Figure 5.15b). Here the freezing point as well as the rate of freezing became steadily lower with progressive increase of the protein or polymer concentration. At the highest concentration studied (50% to 60%), some of the solutions studied could no longer be frozen, confirming the reported failure to freeze concentrated gelatin by Moran (1926) and by Luyet and Rapatz (1956) just mentioned.

These data show that proteins or polymers existing in the fully-extended

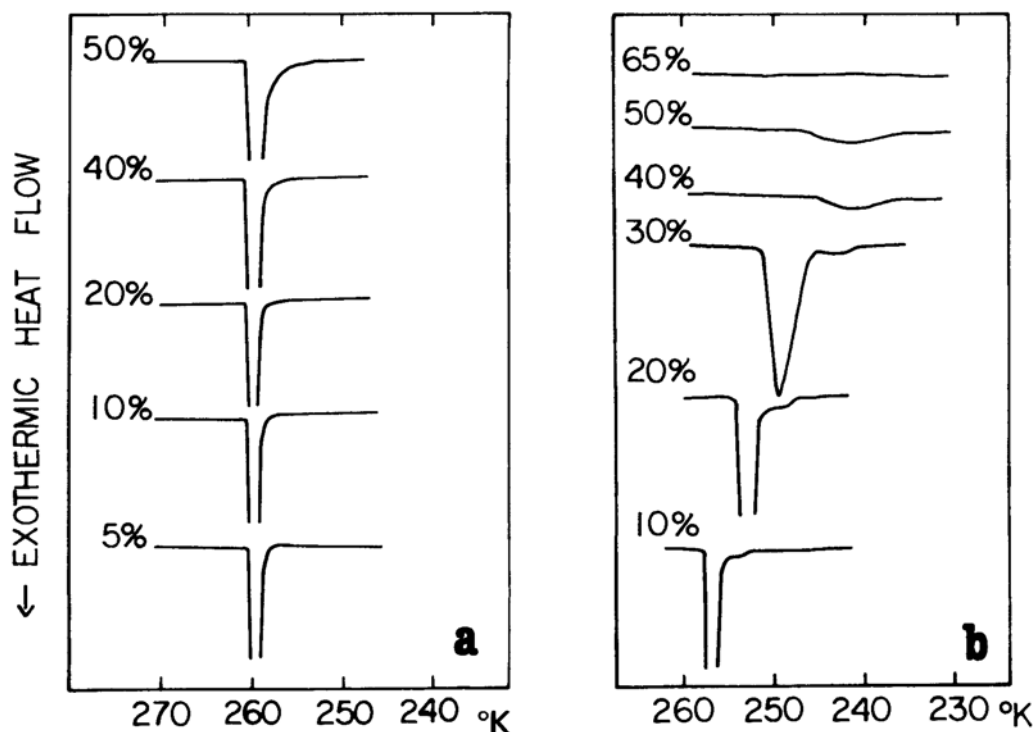


Figure 5.15.

- A. Cooling thermograms of increasing concentrations of native-bovine-hemoglobin solutions, indicating unchanging freezing temperature and rate of freezing.
- B. Cooling thermograms of increasing concentrations of polyvinylmethylether (PVME) solutions, indicating trend of lowering of freezing rate and temperature.

(Ling and Zhang 1983a, by permission of Physiological Chemistry Physics and Medical NMR)

conformation polarize water in multilayers; the intensity of polarization varies with the protein concentration. *Polarized water has a lower freezing point and freezing rate, both in proportion to the intensity of polarization. When the fully-extended protein or polymer reaches a high enough concentration, the intensity of polarization reaches a point where the polarized water can no longer be frozen.*

Freezing-point depression was a major criterion which Gortner and others in the twenties and thirties used to detect and measure “bound” water. Blanchard (1940), by citing supercooling of normal liquid water to -20°C , and by citing mechanical obstruction effects of proteins as the cause of lowering of freezing point, played a key role in abruptly bringing to an end the colloidal approach to cell physiology. The present findings show that, on this issue, Gortner and his scientific allies were fundamentally not wrong.

Increasing the concentration of native proteins to near saturation (50%) produces no observable freezing-point depression of bulk-phase water, while increasing the concentration of proteins and polymers existing in the fully-extended conformation invariably does. Since ice crystals formed inside the cell in the form of unbranching spikes or irregular rosette-like structures are seen only in gelatin and in solutions of PVP, which also cause freezing-point lowering and (at high enough concentration) prevent ice formation altogether, we are led once more

to the conclusion that some proteins in muscle cells, like gelatin and PVP, also exist in the fully-extended conformation, and as such they polarize cell water in multilayers.

5.3. Summary

This chapter began with a description of the unusual properties of the water molecule, including its large permanent dipole moment and polarizability, and pointed out that it is theoretically inevitable and experimentally established that given a dipolar solid surface with alternating positive and negative sites at proper distances apart, water will collect on such a surface and form polarized multilayers.

The polarized multilayer (PM) theory of cell water was then presented, in which the existence of all or virtually all water in a resting cell in the dynamic structure of polarized multilayers is due to direct and indirect interaction with the alternately positive NH and negative CO groups of fully extended polypeptide chains pervasively present in all living cells.

A number of predictions of this theory were then presented, of which the two most important are: (1) there is rotational (and translational) motional restriction of the water existing in the state of polarized multilayers in living cells and model systems; (2) there is rectilinear distribution of solutes in water existing in the state of polarized multilayers in living cells and model systems, with slopes which equal the equilibrium-distribution coefficient or q -value of that specific solute and which follow the *size rule*, i.e., the larger the solute molecule, the lower the q -values.

In the early days of testing the prediction of size-dependent solvency reduction of protein solutions, an important discovery was made which enabled me, on the one hand, to resolve a paradox concerning which protein groups function as the seats of protein interaction with water (polar side chains alone in native globular proteins; polypeptide NHCO groups in addition to polar side chains in fibrous protein) and, on the other hand, to explain why gelatin is profoundly different from native proteins. Due to its unique amino-acid composition, gelatin (which is denatured collagen) cannot form extensive α -helical and other secondary structures, and must therefore remain at least partially in the fully-extended conformation. This conclusion was confirmed when it was shown that dissolved gelatin reduces the solubility of bulk-phase water for Na^+ salts, while dissolved native proteins have no or much smaller effect—and that synthetic polymers like PVP, PEO, PVME, and PEG (which like the proline and hydroxyproline residues in gelatin also contain no proton-donating NH groups, but properly spaced oxygen atoms with their lone pair of electrons) are even more effective than gelatin in reducing solvency for large solutes like hydrated Na^+ .

Another significant finding further confirms the theory that it is intracellular proteins existing in the fully-extended conformation that polarize water in multilayers: secondary-structure-unravelling denaturants (e.g., urea, guanidine HCl) but not tertiary-structure-unravelling denaturants (e.g., SDS, n-propanol) reduce

the solvency of bulk-phase water in solutions of native proteins for large solutes excluded by living cells (e.g., Na^+ salts, sucrose, glycine).

Thus the study of solvency properties has permitted us to evolve two sets of models for the cellular proteins: (1) **extroverts**: (in which the NH group and/or oxygen atoms are exposed to bulk-phase water) gelatin, PVP, PEO, PEG, PVME, urea- and guanidine-HCl, as well as alkali-hydroxide denatured proteins—all capable of reducing the solvency of bulk-phase water for large solutes excluded by most living cells; and (2) **introverts**: (in which the CO and NH groups are locked in intermacromolecular H-bonds and thus unavailable to interact with external water): most native proteins, SDS and n-propanol denatured proteins. The development of these two sets of models has been of critical importance in the further testing and understanding of the behaviors of the living cell.

In my opinion, a most direct and convincing set of evidence for the polarized multilayer theory of cell water is the striking similarity observed in the solvency property of water in living cells (e.g., frog muscle) and in that of the extrovert models (e.g., solutions of gelatin, PEO and NaOH denatured hemoglobin). Each demonstrates a similar pattern of decreasing q -values for solutes with increasing molecular weights ranging from 18 to 4000 or even higher.

Quasielastic neutron scattering (QENS) studies have provided the most straightforward confirmation of the predicted rotational (and translational) motional restriction of bulk-phase water in a 30% PEO solution and in two kinds of living cells: water-rich frog muscle (80%) and water-poor brine-shrimp cyst cells (60%). The reduced rotational-motional freedom of the bulk-phase water in brine-shrimp-cyst cells and in solutions of fully-extended PEO, PVP, PVME and PEG models is fully confirmed by ultrahigh frequency dielectric (UHFD) studies and by NMR studies of solutions of PEO, PVP, and PVME.

Additional predictions of the PM theory of cell water—beyond the rotational and other motional restriction of the bulk phase water and size-dependent solute exclusion—include strong osmotic activity, vapor sorption, obedience to Bradley's multilayer adsorption isotherm, and freezing-point depression. **In all cases examined, each of these distinctive properties has been confirmed in both living cells and in the fully-extended extrovert models, but not at all or only weakly in the introvert models.** A brief summary of these data as portrayed in Table 5.5 provides an easier grasp of their comprehensive nature.

Since a solution or gel of gelatin (the first fully-extended model studied, after which colloid is named) duplicates such a wide variety of cell properties, ranging from partial exclusion of Na^+ to freezing-point depression and distortion of ice-crystal forms, clearly the description of living cells as basically colloidal in nature has general validity if one clearly recognizes that the colloidal state reflects not the properties of the proteins (or polymers) that create the multilayer polarization of the bulk-phase water—but primarily the properties and behavior of water existing in the dynamic state of polarized multilayers.

When viewed side by side with the conclusion of the preceding chapter—i.e., cell K^+ is adsorbed on β - and γ -carboxyl groups—the establishment of the adsorbed state of the bulk of cell water on fully extended polypeptide chains in

Table 5.5. Summary of the Comparative Studies of Eight Physico-chemical Properties of Living Cells and Model Systems.

	Living Cells	Fully Extended Protein Chains and <i>NO—NO—NO</i> Polymers	Native Proteins
Solute Exclusion	Partial of Na^+ salts (Fig.8.2) of sugars (Fig. 8.1; Ling, 1984, Fig. 11.17), and of free amino acids. (Ling, 1984, Fig. 11.19). None of urea (Hill, 1930).	Partial of Na^+ salt, of sugars, and of free amino acids. None of urea (Section 5.2.5.1).	Little or none of Na^+ salt, of sugars, or of free amino acids (Section 5.2.5.1).
Osmotic Activity	Far exceeds that due to <i>free</i> solutes in the cell. The major intracellular cation, K^+ is adsorbed and, hence, osmotically inactive (Sect. 5.2.5.4).	Far exceeds that estimated on the basis of the molar concentration of the polymers and proteins (Section 5.2.5.4)	Also in excess of ideal values but only weakly so. (Section 5.2.5.4).
Swelling and Shrinking	Sustained normal swelling and shrinkage cells without an intact membrane (Figures 10.2 and 10.8).	When enclosed in dialysis bags and incubated, (membraneless) sustained swelling in hypotonic solution and sustained shrinkage in hypertonic solution (Figure 10.3).	When enclosed in dialysis bags and incubated, little or no sustained shrinkage or swelling. (Ling and Ochsensfeld, 1987 Fig. 6).
Freezing Point Depression of Water	Unusual patterns of ice formed in muscle cells (Fig. 5.13). Occurs in <i>Artemia</i> cyst cells (at -28°C). (Ling, to be published).	Concentration dependent in gelatin and <i>NO—NO—NO</i> polymers. (Figure 5.15B).	None observed in solutions in concentrations as high as 50% (Figure 5.15A).

Vapor Sorption	Large quantity of water vapor sorbed at physiological vapor pressure (0.9966) (Ling and Nengdank, 1970). 95% of water in frog muscle obeys Bradley's multilayer adsorption isotherm (Section 5.2.5.3).	Large quantity of vapor sorbed at physiological vapor pressure. All water in gelatin gel obeys Bradley's multilayer adsorption isotherm (Section 5.2.5.3).	Low level of vapor sorbed at physiological vapor pressure (Section 5.2.5.3).
NMR Rotational Correlation Time (τ)	Reduction of τ , estimated for frog muscle (Ling & Murphy, 1983); not directly measurable due to the camouflaging (see) of diamagnetic proteins & paramagnetic ions (Section 5.2.5.2 (1)).	Reduction of τ , of bulk-phase water protons by a factor of 3 to 19 depending on polymer concentration. (Section 5.2.5.2(1)).	Studied but data difficult to interpret due to profound camouflaging effect on relaxation of bulk-phase water protons.
Debye Reorientation Time (τ_D)	Lengthening in Artemia cyst cells and mammalian cells in ultra high frequency (up to 75 GHz) dielectric studies. (Section 5.2.5.2(2)).	Lengthening of water molecules by a factor of 2 to 5, increasing with polymer concentration in ultra high frequency dielectric studies. Since $\tau_D = 3 \tau$, their data agree with NMR data described above (Section 5.2.5.2 (2)).	Not known
Quasi-elastic Neutron Scattering	Strongly reduce rotational diffusion coefficient of bulk-phase water in water-poor Artemia cells (13 times) (Trantham et al., 1984). More weakly reduced rotational diffusion coefficient in frog muscle (2 times) (Heidorn et al., 1986) (Section 5.2.5.2(3)).	Water in 35% PEO solution suffers strong reduction of both translational and rotational motional reduction (Rorschach, 1984) (Section 5.2.5.2(3)).	Not known

Note: Data illustrate close similarity between living cells and solutions of fully extended protein chains or *NO-NO* polymers, not seen in solutions of native proteins.

the cell completes the foundation for the *living-state concept*. In the two immediately following chapters, I will discuss molecular mechanisms that may endow the associated protein-K⁺-water systems of the living cell *discreteness* in the *resting living state* maintained and *coherence* in switching between that state and the *active living state*.

NOTES

1. Edward Teller is more popularly known for his role in the development of the H bomb.

2. For other theories of protein hydration, see Bull 1944; Hill 1946; Forslind 1952; Jacobsen 1955; Szent-Györgyi 1957; Klotz 1958; Berendson 1962; see also the review of Ling 1972; and of Kuntz and Kauzmann, 1974.

3. If to a system of two contiguous, immiscible or slightly miscible liquids is added a third substance, then the third substance will distribute itself between the two liquid phases in such a manner that the ratio of the concentration of the third substance in the two liquid phases is a constant, independent of the total amount of the substance added. This relationship is known as the *distribution law* or *partition law* (Berthelot and Jungfleisch 1872; Nernst 1891; see also Glasstone 1946, 735). Henry's law,—according to which the ratio of the concentration of a gas in a liquid phase over that in a gaseous phase is a constant at equilibrium—represents a special case of the more general distribution law.

4. Multilayer polarization is one of the factors responsible for the stand-up consistency of “jello”; another one is the presence of cross-links (e.g., salt linkages) formed between adjacent protein chains.

5. If water molecules tumble about rapidly as in a normal liquid water, the local magnetic fields they generate cancel out. As a result, liquid water is poor in dissipating magnetic energy; both T_1 and T_2 of normal liquid water are very long (about 2 to 3 seconds), corresponding to a short rotational correlation time (τ_r) of 10^{-11} second (Eisenberg and Kauzmann 1969, 215). (For a definition of τ_r , see text immediately following). In contrast, water molecules in ice are more rigidly fixed; the local magnetic fields of the water molecules in ice do not cancel out and function quite effectively in absorbing and dissipating the magnetic energy of activated water protons. The T_2 of water protons in ice (ice I) is only a minute fraction of a millisecond long; the corresponding τ_r is some 5 orders of magnitude longer than that of liquid water. (ca. 1.4×10^{-5} second) (Eisenberg and Kauzmann 1969, 112).

The extreme example of ice I is cited to demonstrate how rotational restriction in the motional freedom of water molecules—which is a prediction of the polarized multilayer theory of cell water but at a vastly more modest magnitude—leads to a lengthening of τ_r and a shortening of both T_1 and T_2 according to the PM theory of cell water.

It should be mentioned, however, that while T_2 decreases steadily with increase of τ_r , T_1 follows a similar course of change until τ_r reaches a certain value; from there on, instead of steadily decrease with increase of τ_r , T_1 now increases with further increase of τ_r . Fortunately for the degree of motional restriction that occurs in the bulk-phase water in living cells, the relevant range of τ_r changes is well below the T_1 minimum. In other words, for our special interests, we may regard that both T_1 and T_2 decrease with τ_r increase.

6. At near saturation, water vapor sorption equilibrium is extremely slow to attain. Thus, at a relative vapor pressure of 0.99858, water sorption on poly(vinylpyrrolidone) was nowhere near equilibrium after 319 days (25°C) (Ling and Hu 1987). This was undoubtedly the reason that, to the best of my knowledge, J. R. Katz was the only author who had published results of his studies of water sorption on proteins and other biological materials at saturation vapor pressure, until the work of Ling and Hu (1987), who introduced their new “null point” method, making water sorption at extremely near-saturation vapor pressure an easily achievable task.

INDUCTION

From the preceding two chapters we learned that proteins have the innate capability to adsorb K^+ and other alkali-metal ions and to polarize bulk-phase water in multilayers. In solutions of isolated *native* proteins, however, these capabilities of protein are held largely dormant due to *masking* of the adsorption sites (for a definition of native protein, see endnote 4 of Chapter 3). Thus the β - and γ -carboxyl groups capable of adsorbing alkali-metal ions cannot do so because they are locked in salt linkages; similarly, the backbone NHCO groups capable of polarizing and adsorbing water in multilayers cannot do so because they are locked in intra- or intermacromolecular H bonds. Yet exposure of native proteins to alkali hydroxides alters these submerged abilities dramatically (Figure 4.1): the β - and γ -carboxyl groups will now stoichiometrically adsorb alkali-metal ions; the backbone NHCO groups will polarize and adsorb water in multilayers.

That some proteins in the living cell selectively adsorb K^+ and polarize and adsorb bulk-phase water has been experimentally verified (Chapters 4, 5). Obviously, not all cell proteins exist in the ineffective *introverted* native state. A substantial portion of the proteins in the resting cell must be kept in the K^+ -adsorbing and water-polarizing state. The question is: how? The pH of the cell interior is near neutral and definitely not highly basic, as in the solutions of alkali-hydroxide treated proteins (Roos and Boron 1981; Aickin 1986). Therefore these proteins must be kept in their K^+ -binding and water-polarizing state by some other means than high pH. Indeed, in Section 3.2, I have already mentioned that, to maintain the living state, K^+ -binding–water-polarizing protein(s) must be attached to and interact with some other specific protein(s) and small molecules; they must also bind ATP at cardinal sites.

In the tethered-nail, iron-filing analogy, it is the big magnet that enables the randomly-distributed iron filings, near and far away from the nails, to assume an ordered, associated configuration. It is *magnetic polarization* along the tethered chain of soft iron nails that provides the basic mechanism for the far-reaching, one-on-many effects initiated at one end of the nail chain by the big magnet. According to the AI hypothesis, the adsorption of ATP (and other “helpers,” see Section 8.4.2.4. below) on key controlling sites that enables the β - and γ -carboxyl groups to adsorb K^+ selectively from the medium and enables the polypeptide chains to polarize the bulk of cell water in multilayers. Here, it is *electrical polarization* or *induction* propagating along partially resonating polypeptide chains that provides the basic mechanism for the far-reaching, one-on-many

effects produced at one or a few key cardinal sites of the protein by the binding of ATP.

To introduce the major topic of this chapter, **induction**, let us begin with a short sojourn into the past.

The development of quantum mechanics revolutionized physics and chemistry. In 1933, James and Coolidge, using elaborate wave mechanical methods, were able to produce properties of the hydrogen molecule with accuracy correct to the sixth decimal place. The feeling was not uncommon that it would be just a matter of time before physical theories could predict all organic chemistry. Yet 57 years after James and Coolidge's achievement, neither wave-mechanics nor other sophisticated physics have succeeded in explaining the striking differences in the acid dissociation constants (pK_a) of acetic acid (CH_3COOH) and trichloroacetic acid (CCl_3COOH). Indeed, one cannot be sure that waiting another 55 years would bring us any closer to this modest goal. The lesson is self-evident. Organic chemistry even at the simplest level is at this moment far too complex to be handled by even the most sophisticated theoretical physics. It is from this perspective that I look to G. N. Lewis's Induction Theory (Lewis 1923), which is less sophisticated than wave-mechanical approaches to organic chemistry and yet more powerful. With this theory, we will build a conceptual bridge toward the understanding of the quintessence of life: **control of the reversible interactions of water and ions with proteins in living cells, the basis of physiological activity.**

6.1 *The Inductive Effect in the Properties and Behaviors of Small Organic Molecules*

As a bridge toward further understanding of gigantic organic molecules, proteins, I choose a very small organic molecule, acetic acid (CH_3COOH). This weak acid, which makes vinegar pleasantly sour, has an acid dissociation constant (pK_a) of 4.76; the proton of its carboxyl group is held rather tightly. Substitution of one of the H atoms on the methyl group by a Cl atom reduces the affinity of the carboxyl group for the proton; its pK_a is then reduced to 2.8, and a much stronger acid is formed. Substitution of a second H by Cl makes the affinity of the carboxyl group for the proton still weaker; its pK_a is further reduced to 1.3. Substitution of a third H by Cl creates a very strong acid with very weak attraction for protons, and the pK_a is further reduced to less than 1. All of these changes of the pK_a are due to the fact that a chlorine atom is more *electronegative*¹ than the H atom for which it substitutes. As a result, the chlorine atoms have a greater power to draw electrons toward themselves than the protons they displace. The stepwise decrease of the pK_a , with increasing substitutions of H by Cl, illustrates one of the most basic mechanisms of organic chemistry. **It shows that electronic events occurring at the methyl carbon can be transmitted by the inductive mechanism over a distance to affect the properties of a distant negatively charged carboxyl oxygen atom in such a way that its affinity for H^+ is reduced.**

It was based on this and other similar observations that G. N. Lewis proposed the *induction theory* in 1923.

Lewis's induction theory has long been a major pillar of theoretical organic chemistry (Hammett 1940, Branch and Calvin 1941; Dewar 1949; Smith et al. 1951; Ingold 1953; Taft 1960; Chapman and Shorter 1972). However, the application of this theory has been limited to small organic molecules until I invoked it to explain protein behavior and cell physiology in 1960 and 1962 (Ling 1960, 1962). For most organic chemists, the theory provides a conceptual framework that enables the chemist to predict and to understand unknown quantitative behaviors of compounds. Thus, by using empirical **induction constants** for chlorine atoms, one can predict the pK_a value of chloroacetic acid from that of acetic acid (see below).

A shortcoming of using empirical induction constants (e.g., Hammett's inductive constants, Taft's inductive constants) is the restriction to substituents whose induction constants are already available. However, in 1963, Chiang and Tai profoundly altered the picture when they introduced a new method for *calculating*—on the basis of molecular structures, atomic electronegativity and bond lengths—what they call **inductive indices**. Inductive indices are equivalent to empirical induction constants. Chiang and Tai's new method has liberated us from the limitations imposed by the availability of empirical constants, and allows us to predict properties of molecules not predictable before.²

Figure 6.1 shows how, in small organic molecules, the inductive effect underlies the different acid dissociation constants (pK_a) of the amino groups of substituted methylamine and ethylamine and of the carboxyl groups of substituted n-propanoic acid and acetic acid. Each point in the graph represents the experimentally determined pK_a value of a substituted compound plotted against the empirically predetermined induction constant of that substituent group from Taft and Lewis (1958). The fact that these points follow a straight line shows that each substituent has a characteristic quantitative **electron-donating** or **electron-withdrawing effect** in agreement with the induction theory.

Figure 6.1 also shows that with the lengthening of the saturated hydrocarbon chain separating the substituent groups from the target carboxyl or amino groups (e.g., from one CH_2 group in acetic acid derivatives to two CH_2 groups in propionic acid derivatives), the transmitted inductive effect is uniformly reduced, as indicated by the unchanging slope of each rectilinear curve. According to Chiang and Tai, the **transmissivity factor** which measures this reduction is 0.33 through each additional intervening CH_2 group. Others gave a higher value (e.g., 0.48) (Ling 1964; Taft 1953).

Figure 6.2 shows that substituents that affect the pK_a s of distant carboxyl and amino groups produce parallel effects on the strength of distant H-bonding groups. Various substituents like CH_3O , CH_3 , H, (represented as X in the inset), when introduced at the para position³ of the acetophenone oximes molecule (inset of Figure 6.2), affect the **free energy of dimerization** (ΔF°) differently (Reiser 1959). Here two pairs of H bonds are formed between the N and OH groups of one interacting acetophenone oxime molecule with the OH and N

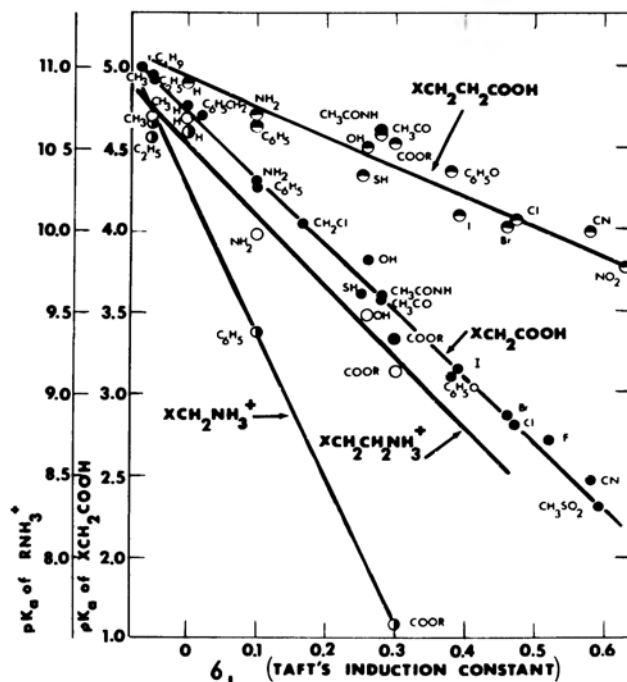


Figure 6.1. Relation between Taft's induction constant σ_1 and the acid dissociation constants (pK_a) of α -substituted acetic acid (XCH_2COOH), β -substituted propionic acid (XCH_2CH_2COOH), α -substituted methyl ammonium ion ($XCH_2NH_3^+$), and β -substituted ethylammonium ion ($XCH_2CH_2NH_3^+$). In the molecular formulas shown, X represents the substituents, which vary. The abscissa represents the σ_1 of each substituent indicated in the graph. The ordinate gives the acid dissociation constant of that particular substituted compound as it is indicated in the graph.

- XCH_2CH_2COOH
- XCH_2COOH
- $XCH_2CH_2NH_3^+$
- $XCH_2NH_3^+$

(Ling 1964a, by permission of Texas Reports on Biology and Medicine)

respectively of the other acetophenone oxime molecule. Although the inductive effect of each substituent affects both the proton-accepting strength of the N atom and the proton-donating strength of the OH groups of the same molecule, it is primarily the change of the electron density of the proton-accepting group (which in this case is the N atom) that determines the strength of the H-bond formed, and hence free energy of dimerization. This is why strongly electron-donating substituents like CH_3O enhance the dimerization, while electron-withdrawing substituents like NO_2 weaken dimerization. As in the case of substituted carboxylic acids and amines described in Figure 6.1, the relative effects of the different substituents are predetermined by their (Hammett's) empirically determined inductive constants.

In the examples of acetic acid and trichloroacetic acid cited above, the substitution involves the breakage of old **covalent bonds** and the formation of new ones. The question arises, "If a molecule is attached to the target molecules not

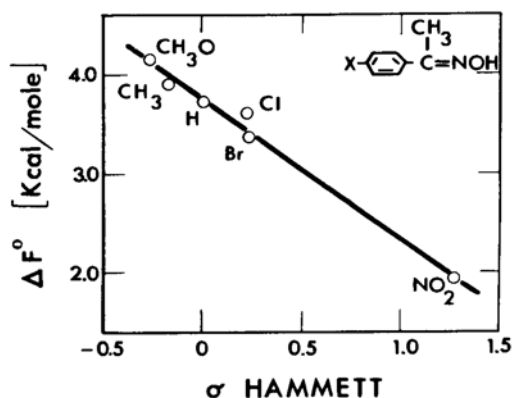


Figure 6.2. Linear relation between the calculated standard free energy of dimerization (ΔF°) of *p*-substituted acetophenone oximes (see inset formula) and Hammett's σ constants of the various substituents shown in the graph. Data recalculated from Reiser (1959), under the assumption that no higher polymer exists in significant amount than dimers. (Ling 1964, by permission of Biopolymers)

by covalent bonds but by other noncovalent bonds, can we still anticipate similar inductive effects?" The answer is a definite yes. In support, two specific examples are cited.

(1) The Hammett inductive constant, σ , for the metasubstituent NH_3^+ (i.e., when the NH_3^+ group is attached to the meta position of an aromatic benzene ring³) is +0.634, while that of the metasubstituent NH_2 is entirely different, i.e., -0.161. Similarly, the metasubstituent COOH is +0.355, while that of the metasubstituent COO^- is +0.104 (Hammett 1940). The difference between NH_3^+ and NH_2 , as well as that between COOH and COO^- , is the detachment or attachment of a proton which is linked to the NH_2 or COO^- group, not by covalent bonds but primarily by **electrostatic forces or ionic bonds** (see Kosciakoff and Harker 1938).

(2) Inductive effects exerted by H-bond formation were studied by Burawoy (1959, 259). He found that the formation of an H-bond of the phenolic hydroxyl group with ethanol produced an even greater inductive effect than the substitution of the same hydroxyl group by the far more electron-donating methyl group. Thus Taft's (empirical) induction constant, σ_7 , for a hydroxyl group is +0.25, and that of a methyl group is -0.05 (Taft and Lewis 1958). This example demonstrates how strong inductive effects may be produced by the formation or dissociation of H bonds on the properties of the target groups. Nor is this surprising since H bonds are also primarily electrostatic in nature (Coulson, 1959, p. 341; see also Feynman 1939).

In summary, *inductive effects produced by diverse substitutes affect both the acid dissociation constants of carboxyl and amino groups and the strength of H bonds formed on spatially separated sites. Substitutions may involve displacement of functional groups held by covalent bonds or displacement of ions and molecules held, respectively, by ionic or H-bonds.* (for additional experimental evidence see Section 8.4.2.3)

6.2. *The Inductive Effect in the Properties and Behaviors of Proteins*

The Induction Theory of G. N. Lewis has become a highly successful theory in explaining and quantitatively predicting the properties and behaviors of small organic chemicals. Since macromolecules, like proteins, are small organic chemicals joined together into linear chains, it seemed logical that the Induction Theory should also be able to explain and predict properties of proteins (and other macromolecules) which constitute the premier components of all living cells (Ling 1962).

In the AI hypothesis, the inductive effect operating over a relatively short distance provides the basic mechanism for the coherent behavior of the living cell. *This short-range inductive effect in protein also known as the **direct F-effect**⁴ is the main concern of this chapter.* How the short-range inductive effect serves as the foundation of propagated long-range effects will be the subject of the following chapter.

Most functional groups of a protein are carried on segments of saturated hydrocarbon side chains attached to polypeptide chains. The inductive effect is attenuated rapidly by passage through saturated hydrocarbon groups. As mentioned above, the transmissivity factor through each —CH₂—group has been estimated at 0.33 or 0.48. In contrast, the *transmissivity factor* through an entire

peptide linkage $\left(\begin{array}{c} | \\ \text{---N---C---C---} \\ | \quad | \quad || \\ \text{H} \quad \text{H} \quad \text{O} \end{array} \right)$ has been estimated *roughly* at 0.51 (range: 0.15 to 0.73) (Ling 1964, 103; 1984, 190).

The rapid loss of electrical polarization through saturated hydrocarbon chains suggests that only functional groups carried on short side chains are physiologically active. In this category, one finds functional groups belonging to serine, threonine, histidine, cysteine, tyrosine, tryptophan, aspartic, and glutamic residues. The functional groups that are closest to the *main stream* of inductive effect are, of course, the peptide CO, NH groups themselves. In the AI Hypothesis, the primary emphasis thus far is on the interaction of water with peptide NHCO groups and on the interaction of K⁺ with β- and γ-carboxyl groups carried respectively on the short side chains of aspartic- and glutamic-acid residues. This emphasis is in harmony with the molecular “anatomy” of the protein molecules and the limited transmission of inductive effects.

In contrast, the ε-amino group of lysine and guanidyl groups of arginine residues are separated from the polypeptide chain by four methylene groups. The electrical insulation thus provided may account for the relative constancy in the properties of these cationic functional groups. As an example, the relative affinities of proteins and cationic-amino-group-carrying models of proteins for anions consistently follow one specific unchanging rank order, often referred to as the Hofmeister, or lyotropic, series (Figure 6.3), while the affinities for cations and water vary widely both among different proteins and in the same protein in different environments.

Due to its partially resonating nature and hence high electrical polarizability,

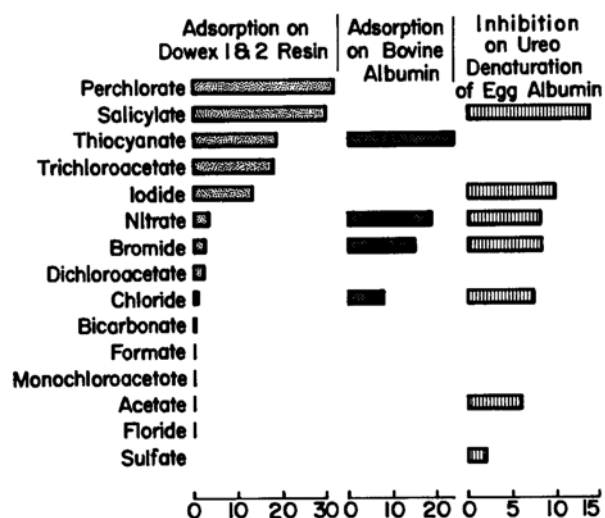


Figure 6.3. Relative affinity of various anions for the cationic fixed amino groups of the model ion exchange resins carrying fixed cationic amino groups (Dowex 1 and 2) and two proteins. Units of anion affinity given in the abscissa are arbitrary. For a more detailed description, see Ling 1962, Table 7.5. (from Ling 1984, by permission of Plenum Publishing Co.)

the polypeptide chain is eminently suited for transmitting the inductive effect. Table 6.1 shows that the pK_a values of the α -amino group of glycine continue to decrease as more and more glycine residues are introduced to form diglycine, triglycine, up to hexaglycine. These changes of the pK_a suggest that transmission of the inductive effect through polypeptide chains is usually efficient (see Ling 1984, 189–190).

In discussing the inductive effect in small organic molecules (Section 6:1), I have cited acetic acid and the changes of its pK_a values with increasing substi-

Table 6.1. Dissociation Constants of the Carboxyl and Amino Groups of Glycine Peptides (Ling 1962).

	Amino group		Carboxyl group		
	Water	1 M NaCl	Water	1 M NaCl	
NH_2CH_2COOH	9.70	9.60*	2.42	2.34*	3.02
$NH_2CH_2CONHCH_2COOH$	8.20	8.13	3.13	3.06	3.33
$NH_2(CH_2CONH)_2CH_2COOH$	8.00	7.91	3.00	3.26	3.39
$NH_2(CH_2CONH)_3CH_2COOH$	7.75	7.75	3.05	3.05	3.50
$NH_2(CH_2CONH)_4CH_2COOH$	7.70	7.70	3.05	3.05	
$NH_2(CH_2CONH)_5CH_2COOH$	7.60	7.60	3.05	3.05	

Note: The results of titration in water and in 1 M NaCl in aqueous solution are given. The data in water are from Stiasny and Scotti (1930), who give two sets of values. Those values indicated by an asterisk (*) are from Czarnetszky and Schmidt (1931). The results of titration in 1 M NaCl are from Ling (1962).

tution of the protons on the methyl group by the more electronegative chlorine atoms. In retrospect, one may analyze the operations of the inductive effect in the acetic-acid model into three components:

- (1) the effector: the chlorine-for-proton substitution
- (2) the transmission: through two saturated CH₂ groups
- (3) the target: the singly charged carboxyl oxygen, changing its pK_a.

In the following four subsections (6.2.1. to 6.2.4.), identification of these three components in the operation of the inductive effect in proteins will be a secondary objective, presented in such a way that it will not upstage the primary objective described under the title of each of the subsections.

6.2.1. *Inductive Effect on Protein Conformation and Water Polarization*

When a protein is exposed to a concentrated urea solution, it becomes denatured and assumes a new conformation, the denatured conformation (Figure 5.6). Anfinsen and others demonstrated that after extensive dialysis, which removes the urea, the denatured protein resumes its original native conformation (for definition of native protein and its conformation see endnote 4 of Chapter 3). From these renaturation experiments, it was concluded that the **conformation of a protein (secondary and tertiary structures) is a natural consequence of its specific amino-acid sequence (primary structure)** (Anfinsen 1962, 1967; Ling, 1962).

As a rule, a major portion of the amino-acid residues of protein exist in the form of α -helices in the native conformation. In 1962 and later, I suggested that the α -helical content of a protein may be related to the electron-donating strength of its side chains. In support of this view, I cited indirect evidence that it is primarily the electron-donating strength of the carbonyl oxygen of the polypeptide NHCO groups that determines the strength of the α -helical H-bond formed (Ling 1962, 1964, 1969, 1984). Proteins with many strong electron-donating side chains will tend to assume a more α -helical conformation than others with many electron-withdrawing side chains.

Since 1962, other investigators have carried out extensive comparisons of the amino-acid sequences of diverse proteins with the proteins' structures. From these studies, three types of interactions have been found: long-range, intermediate-range, and short-range. Of these, ***the short-range interaction between a side chain and its own backbone—CO—C—NH-group in the protein plays the dominant role in determining the overall secondary structure of the protein*** (Scheraga 1974; Finkelstein and Ptitsyn 1971). However, other than my earlier brief suggestion just mentioned, no other mechanism for the short-range interaction was proposed.

From the above studies, several tables of numerical values for the propensity of each amino-acid residue to form α -helix (sometimes referred to as the *α -helical potential*) and to form β -pleated sheets etc., have been published. The best-known tables are those of Chou and Fasman (1978), shown in Table 6.2.

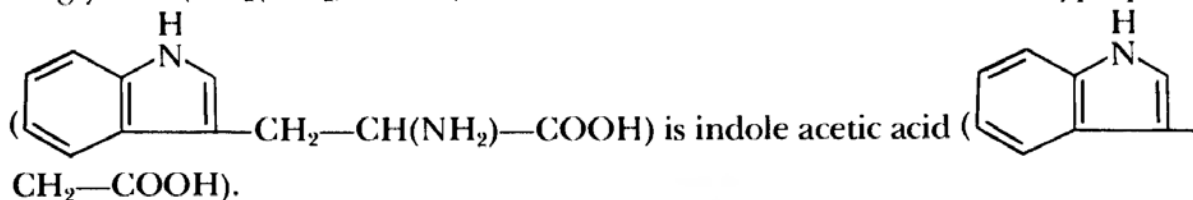
If the α -helical potential of a side chain is indeed an expression of the electron-

Table 6.2. The α -helical Potentials ($P_{\alpha}, \omega_{h,j}, j$) of Nineteen α -amino Acids and the (Corrected) Acid Dissociation Constants (pK_a) of their Analogous Carboxylic Acids. (Ling 1986a, by permission of Physiological Chemistry Physics and Medical NMR)

	Chou and Fasman (P_{α})	Tanaka and Sheraga ($\omega_{h,j}$)	Garnier et al. (j)	Corrected pK_a of Analogous Carboxylic Acids
Glu(-)	1.51	1.188	164	5.19
Ala	1.42	1.549	151	4.75
Leu	1.21	1.343	118	4.77
His(+)	1.00	0.535	98	3.63
Met	1.45	1.000	139	4.50
Gln	1.11	0.795	96	4.60
Trp	1.08	1.105	98	4.75
Val	1.06	1.028	100	4.82
Phe	1.13	0.727	102	4.25
Lys(+)	1.16	0.726	109	4.70
Ile	1.08	0.891	92	4.84
Asp(-)	1.01	0.481	91	4.56
Thr	0.83	0.488	60	3.86
Ser	0.77	0.336	47	3.80
Arg(+)	0.98	0.468	77	4.58
Cys	0.70	0.444	73	3.67
Asn	0.67	0.304	35	3.64
Tyr	0.69	0.262	41	4.28
Gly	0.57	0.226	0	3.75

Note: α -helical potential values from Chou and Fasman (1978), Tanaka and Sheraga (1976), and Garnier et al. (1978). Sources and corrections of pK_a of analogous carboxylic acids are given in Ling (1986a)

donating (or withdrawing) strength of the side chains, a positive correlation must exist between the α -helical potential of a specific amino-acid residue (see Table 6.2) and the pK_a of the corresponding α -carboxylic acid, which is also determined by the electron-donating (or withdrawing) strength of the same side chain. As examples, it may be pointed out that the α -carboxyl-acid equivalent of glycine ($\text{CH}_2(\text{NH}_2)\text{COOH}$) is formic acid (HCOOH); that of tryptophan



With this simple approach, I found that the helical potentials of the amino acid residues given by Chou and Fasman (1978), Tanaka and Scheraga (1976), and Garnier et al. (1978) are indeed all positively correlated with the pK_a s of the corresponding α -carboxylic acid, with linear correlation coefficients of +0.75, +0.77, and +0.72, respectively (Ling 1986a).

These demonstrated positive correlations between the electron-donating strength of a side chain and its “ α -helical potential” show that the secondary structure of a protein depends primarily upon the electron density of the carbonyl oxygen (Ling 1969, 41; 1984, 192). High electron density of the carbonyl oxygen enhances the α -helical conformation; low density weakens it. The AI hypothesis has thus provided a possible mechanism for the short-range interaction underlying Anfinsen’s finding (1962, 1967) that the secondary structure of a protein is determined by its primary structure.

Another significant finding from this piece of work was derived from the data of Garnier et al. (1978) just mentioned. Here, in addition to the linear correlation between the pK_a of the corresponding α -carboxylic acid and the α -helical potential of this amino-acid residue’s own peptide group, I also studied the correlation between the pK_a of the corresponding α -carboxylic acid and the α -helical potentials of the peptide groups of *neighboring* amino-acid residues. *The results revealed that the inductive effect on one side chain extends at least 3 peptide groups both “upstream” and “downstream” along the polypeptide chain* (Figure 6.4), confirming our earlier conclusion from the consideration of the acid dissociation constants of the glycine peptides.

The inductive interpretation of the secondary structure of protein also offers a solution to an apparent paradox: the structure of a protein is determined by its amino-acid sequence, which is finite and unchanging. Therefore, for each protein, there should be one and only one uniquely defined protein conformation. Yet there is an abundance of evidence that a protein can change its conformation in response to the binding of a drug or hormone molecule (Klotz 1973; Aizono et al. 1974; Imae et al. 1975; Changeux 1981). *The solution to the apparent paradox is as follows: A side chain exerts its effect on protein conformation*

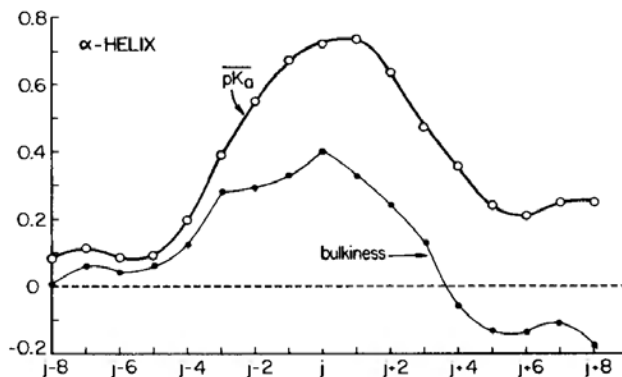


Figure 6.4. Linear correlation coefficients (r) between α -helical potentials of 19 α -amino acids on the one hand; and on the other hand, the *bulkiness* as well as the electron-donating power of their separate side chains expressed as the acid dissociation constants pK_a s of their α -carboxylic-acid analogues at residue position j and $j + m$ (m varied between -8 to $+8$). $j - m$ represents a residue on the N-terminal side of the j th residue; $j + m$ represents a residue on the C-terminal side of the j th residue. α -helical potentials are the directional information measure given by Garnier et al. (1978). (Ling 1986, by permission of Physiological Chemistry Physics and Medical NMR)

via the inductive effect; ligand binding changes the protein conformation by modifying the inductive effect of the side chains.

In summary, protein side chains control the secondary structure through the inductive effect they exert on the electron density of the backbone carbonyl oxygen of the side chains' own peptide groups, as well as those of the immediately neighboring peptides. Strong electron-donating side chains favor α -helical conformation; weak ones favor *random-coil* and other conformations. If the binding of a ligand onto a side chain reduces the electron-donating power of the side chain, the α -helical conformation may transform itself into a random coil, or what I call *fully-extended conformation*. Multilayer polarization of the bulk-phase water may then follow as a result. **Thus the primary structure of a protein and ligand binding can determine indirectly the physical state of the bulk-phase water.**

6.2.2. Inductive Effect on the Reactivity of Side-Chain SH Groups

Earlier I have mentioned why functional groups on short side chains are more likely to participate in physiological activities than long side chains. Among those functional groups with short side chains is the sulfhydryl group of cysteine residues ($-\text{CH}_2-\text{SH}$). The reactivity of the SH group toward nitroprusside reagent, like all other oxidative-reduction reactions, depends on the *oxidation-reduction potential* of the SH groups (see Ling 1962, 134; 1984, 193). The oxidation-reduction potential of the SH group in turn depends on the electron-donating strength of the chemical groups to which the SH is attached. Thus, SH reactivity has been shown to decrease in the rank order $\text{CH}_3\text{CH}_2\text{CH}_2\text{CH}_2\text{SH} > \text{CH}_1\text{CH}_2\text{CH}_2\text{SH} > \text{CH}_3\text{CH}_2\text{SH} > \text{CH}_3\text{CH}_2\text{SH} > \text{CH}_3\text{SH}$, since the electron-donating power increases with the number of the saturated hydrocarbon chains (Ling 1964).

Figure 6.5 shows the reactivity of the SH groups of several simple thiols. The observed SH reactivity follows the rank order thioglycolic acid ($\text{SHCH}_2\text{COO}^-$) $>$ homocysteine ($\text{SHCH}_2\text{CH}_2\text{CH}(\text{NH}_3^+)\text{COO}^-$) $>$ cysteine ($\text{SHCH}_2\text{CH}(\text{NH}_3^+)\text{COO}^-$) $>$ glutathione (γ -L-glutanyl-L-cysteinyl glycine). This rank order is reasonable in light of the following considerations: (1) The carboxylic equivalent of thioglycolic acid is malonic acid ($\text{COOHCH}_2\text{COO}^-$). The pK_a of the second dissociating carboxyl group of malonic acid is 5.69 (see Ling 1986a, Table 1). (2) The carboxylic equivalent of homocysteine is glutamic acid ($\text{COOHCH}_2\text{CH}_2\text{C}(\text{NH}_3^+)\text{COO}^-$). The pK_a of the γ -carboxylic group is 4.25 (Stecher 1968). (3) The carboxylic equivalent of cysteine is aspartic acid ($\text{COOHCH}_2\text{CCNH}_3^+\text{COO}^-$). The pK_a of the β -carboxyl group is 3.65 (Stecher 1968). From the rank order of the pK_a values of the carboxylic equivalents, one can reasonably deduce that thioglycolic acid is a better reductant than homocysteine, and homocysteine is a better reductant than cysteine. (4) We do not have an α -carboxyl equivalent of the SH group of glutathione. However, glutathione is a tripeptide. Since the peptide groups is a powerful electron-withdrawing entity—witness that the pK_a of the amino group of hexaglycine is 7.60,—the pK_a of its non-peptide-containing equivalent CH_3MH_3^+ is 10.62 (Ed-

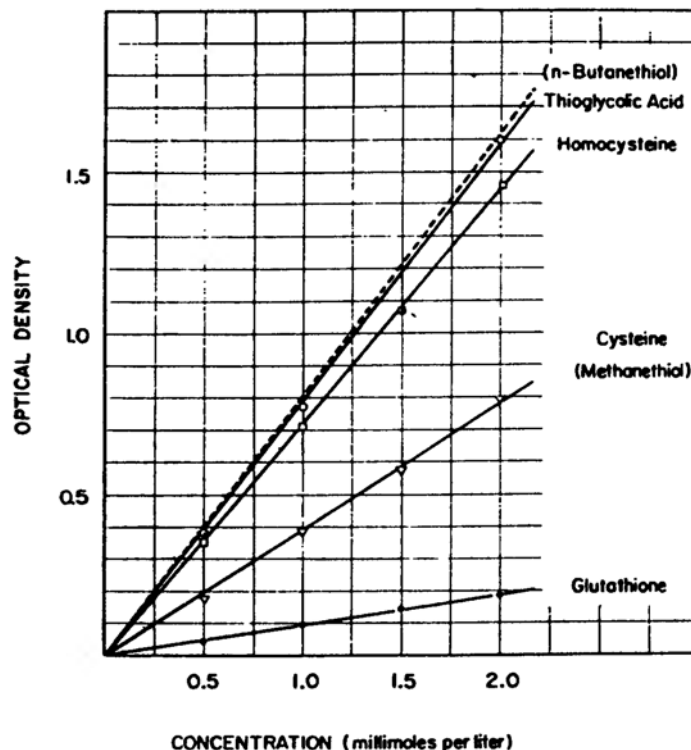


Figure 6.5. Reactivity of six simple thiols. Curve for cysteine coincides with that of methanethiol. (Ling 1964, by permission of Biopolymers)

sall and Wyman 1958, 452)—it is certainly understandable that glutathione should be the least effective reductant.

An amide like urea (NH_2CONH_2) is a *weaker* proton donator than a simple peptide ($\text{RNHCO} > \text{NH}_2\text{CONH}_2$); conversely, urea is a *stronger* proton acceptor than a simple peptide ($\text{NH}_2\text{CONH}_2 > \text{RNHCO}$) (Tsuboi 1951, 1952; see also Mizushima 1954). Thus, if urea reacts with the backbone NHCO groups, disrupting an α -helical bond, it will exercise an overall stronger effect as a proton acceptor. This is equivalent to saying that urea binding has an overall electron-donating effect.

Thus: if a native protein containing SH groups on cysteine residues is exposed to a high concentration of urea, displacement of peptide-peptide H bonds by urea should lead to an overall electron-donating effect which may inductively increase the oxidative-reduction potential of SH and its reactivity toward nitroprusside reagent. Such phenomena have long been recognized, but were often explained as due to some sort of unravelling effect, exposing a buried SH group normally unreactive due to steric hindrance. The data of Benesch et al. (1954), along with confirmatory work of Ling and Kalis (unpublished), showed that in simple SH containing peptides (where folding and burial of SH group is not possible), urea demonstrates a similar effect in enhancing the SH activity (Table 6.3). Furthermore, the urea effect increases with an increasing number of peptides and decreases with a decreasing number of side chain CH_2 groups separating the SH group from the polypeptide chain.⁵ Taken as a whole, these findings

Table 6.3. Effect of 7 M Urea on the Reactivity of Sulfhydryl Groups with Nitroprusside Reagents^a (from Ling 1964, by permission of Biopolymers).

	No. of peptide linkages	$\epsilon_{\text{urea}}/\epsilon_{\text{H}_2\text{O}}$	
		Benesch et al. ^b	Ling et al. ^c
Methanethiol	0		1.16
Ethanethiol	0	1.0	
Thioglycolic acid	0	1.0	
Homocysteine	0	1.14	1.35
Cysteine	0	1.43	1.73
L-Cysteinyl-D-valine	1	1.71	
L-Glutamyl-L-cysteine	1	1.78	
L-Cysteinyl-L-valine	1	1.71	
Glutathione	2	2.34	2.83
Phenacetylcysteinyl-D-valine	2	2.51	


^a $\epsilon_{\text{H}_2\text{O}}$ and ϵ_{urea} are, respectively, the molecular extinction coefficients of the thiols when the reaction occurs in water and in 7M aqueous solutions of urea. A close to unity value for the quotient $\epsilon_{\text{urea}}/\epsilon_{\text{H}_2\text{O}}$ for methanethiol, indicates that urea does not directly interfere with the nitroprusside reactions (by, for example, forming H-bonds with the sulfhydryl group). The quotient rises above unity for simple compounds with H-bonding groups; it then rather sharply increases with the number of peptide bonds in the molecule.

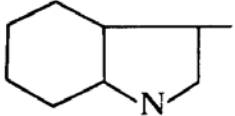
^bBenesch et al. (1954)

^cLing et al. unpublished

affirm our earlier conclusions that the inductive effect can be transmitted effectively through a short side chain and a stretch of peptide chains and that the electron-donating effects experienced at neighboring NHCO groups can produce an additive influence on the oxidative-reduction potential, and hence reactivity, of the cysteine SH group toward the nitroprusside reagent. For a similar effect of urea in enhancing the electron density of other functional groups (β - and γ -carboxyl groups) on short side chains, see Foster and Sterman 1956.

6.2.3. Inductive Effect on the Fluorescence of Tyrosine and Tryptophane Residues

The phenol group of tyrosine residue (HO ) and the indole group

of tryptophane residue () are carried on short side chains, like

the SH group of cysteine. Both adsorb light in the near-ultraviolet region and give off light (fluoresce). It has been known for some time that if these amino-acid residues are incorporated into peptides, there is a reduction of the fluorescence yield, or **quenching**. Further quenching of these peptides can be produced by the addition of a proton to the ionized α -carboxyl group ($-\text{COO}^-$),

or to an unionized α -amino group ($-\text{NH}_2$). These quenching effects have been explained respectively by: the electron-withdrawing tendency of the peptide bond; and by the greater electron-withdrawing effect of COOH than of COO^- and of NH_3^+ than of NH_2 (Cowgill 1963; Konev 1967; see Section 6.2.1. also).

Table 6.4 further shows how fluorescence of tyrosyl and tryptophyl residue decreases, as expected, with increase of the number of peptide bonds attached directly or indirectly to the tyrosyl or tryptophyl residue.

Tournon and El-Bayoumi (1971) prepared a series of phenylalkylcarboxylic

acids, $\text{Ph}-(\text{CH}_2)_n-\text{C} \begin{array}{l} \text{=O} \\ \text{OH} \end{array}$ (where n varied between 1 and 4) and studied the

effect of pH on the fluorescence intensity. They found that the fluorescence intensity dropped sharply as the pH of the medium was lowered to a value close to the pK_a of the carboxyl group, and that the extent of this quenching decreased with the number of methylene groups (n) separating the phenyl from the carboxyl group. However, even when four methylene groups separate the carboxyl and the phenyl group, the quenching effect, though weak, is still noticeable. Since the quenching was found to be indifferent to the concentration of the acid, the authors concluded that "*the quenching is essentially an intramolecular inductive effect.*"

Another very interesting series of model studies on fluorescence quenching was published by Edelhoch et al. (1967). The models they synthesized were (glycyl) $_n$ -L-tryptophane. Like Tournon and El-Bayoumi, they also studied the effect of pH on fluorescence intensity. The data reproduced here as Figure 6.6 show pronounced quenching at pH in the vicinity of the pK_a of the α -amino group of the glycyl residue in glycyl-L-tryptophane. However, even in the glycyl-glycyl-glycyl-L-tryptophane, the quenching effect is still noticeable, even though the α -amino group of the terminal glycyl residue is separated from the tryptophane group by three peptide linkages.

Table 6.4. Decrease in Fluorescence of Tyrosyl and Tryptophyl Residues with Increase in the Number of Peptide Bonds (Cowgill 1963, by permission of Arch. Biochem. Biophys.)

Compound	Number of peptide bonds	Per cent of the fluorescence of the free amino acid at neutral pH
Tyrosine	0	100
Gly-Tyr	1	35
Tyr-Gly	1	33
Gly-Tyr-glycinamide	3	17
Tryptophan	0	100
Gly-Try	1	28

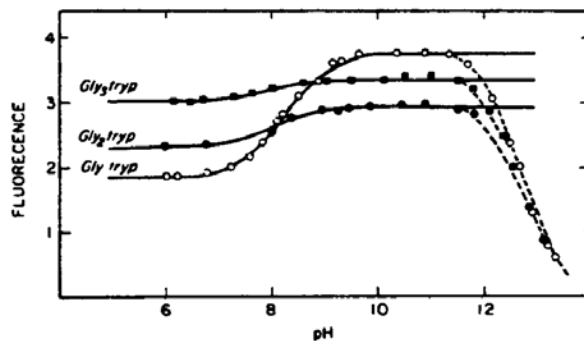


Figure 6.6. Relative fluorescence intensity of (glycyl) $_n$ -L-tryptophan compounds as a function of pH. The continuous lines are theoretical curves based on the following values of pK_a and degree of quenching by the charged amine group: Glycyl-L-tryptophan, 8.20, 50%; (glycyl) $_2$ -L-tryptophan, 8.00, 21%; (glycyl) $_3$ -L-tryptophan, 8.00, 10%. Points are experimental values. The fluorescence intensities are based on solutions of equal absorbance at 280 $m\mu$ (Edelhoc et al. 1967, by permission of Biochemistry)

If we accept inductive interpretations offered for the observed effects on fluorescence quenching by Cowgill (1963), Konev (1967), Tournon and El Bayoumi, and others, then *Edelhoc et al.'s data would be the third set of independent evidence that the inductive effect can be transmitted over three peptide linkages, to reach a functional group on the end of a short side chain.*

As mentioned in the preceding section, urea has no effect on the reactivity of simple alkyl thiols containing an —SH group but no H-bonding groups. However, urea has an increasing effect with an increasing number of peptide bonds attached to the SH group and a decreasing effect with an increasing number of methylene groups separating the SH group and the peptide bonds. If this is correctly interpreted as due to the greater electron-donating effect of urea-peptide bonds than of peptide-H $_2$ O or peptide-peptide bonds, then urea should also enhance fluorescence of these simple peptides containing a tyrosine residue, and of tyrosine-containing proteins. In fact, both of the expected effects have been observed (Fukunaga et al. 1982; Yao et al. 1984).

In concluding this section, I must point out that while the inductive effect plays an important role in fluorescence quenching of tyrosine- and tryptophane-containing proteins and models, it is not the only factor that determines quenching (for details, see Konev 1967).

6.2.4. Inductive Effect on the Rank Order of Selective Ion Adsorption on β - and γ -Carboxyl Groups

In Section 4.2 I demonstrated that the β - and γ -carboxyl groups, when unmasked, can stoichiometrically adsorb alkali-metal ions. The data discussed in the preceding section and illustrated in Tables 6.1 and 6.4 and Figures 6.4, 6.5, and 6.6 also suggest that the inductive effect can be mediated through short segments of saturated CH $_2$ chains and longer stretches of partially resonating polypeptide chains. With this background information, we shall next examine

what will happen to the ionic preference of β - and γ -carboxyl groups (which are also on short side chains) if their electron density changes as a result of the inductive effect as the work of Foster and Sterman (1956) mentioned above had already suggested. To answer, we need a new theoretical model (Ling 1960, 1962).

The first step in constructing the model involves *the introduction of a parameter called the c -value, a very important parameter to be used again and again in the following pages*. The c -value is a quantitative analogue of the *independent parameter* underlying differences in acid dissociation constants (pK_a). Very roughly, the c -value represents the *electron density* of a singly-charged carboxyl-oxygen atom. Thus the carboxyl-oxygen atom of the weak acetic acid has a high affinity for H^+ and a high pK_a value (4.76) due to its high c -value; the carboxyl-oxygen atom of the strong trichloroacetic acid has a much lower pK_a value (<1.0) due to its much lower c -value. The pK_a is not an independent parameter and therefore cannot be equated to the c -value.

More rigorously, the c -value⁶ is defined as the displacement in Ångstrom units of the unit negative charge carried by the singly-charged-carboxyl-oxygen atom. The displacement is from the center of the oxygen atom either away (negative c -value) or toward (positive c -value) the interacting cation (C) along a straight line joining the centers of the oxygen atom and the interacting cation. The displacement is such that quantitatively the interaction of the unity negative charge with the cation matches the cumulative inductive (I) effect and direct electric (D) effects exerted by the rest of the molecule carrying the singly charged carboxyl group (Figure 6.7).

The first theoretical model of selective K^+ absorption over Na^+ on β - and γ -carboxyl groups introduced in 1952 was based on the assumption that hydration for K^+ and Na^+ is specific to each ion and *unchanging* (Ling 1952; 1984, 94; see also Harris and Rice 1954; Joseph et al. 1961). In the later model, no such a priori assumption was made; the degree of hydration was determined by energy minimization.

A cylindrical cavity was carved out in the continuous dielectric of bulk water, and into the cavity were placed the single-charged-oxygen atom, the interacting cation, and a varying number of water molecules ranging from 0 to 3. These combinations were named, respectively, Configuration 0, I, II, and III (Figure 6.6 in Ling 1984). Altogether seven cations were considered: H^+ , Li^+ , Na^+ , K^+ , Rb^+ , Cs^+ , and NH_4^+ . The polarizability (α) of the carboxyl oxygen atom was given 3 values (0.876×10^{-24} , 1.25×10^{-24} , and $2.0 \times 10^{-24} \text{ cm}^3$). Instead of the simple Coulombic interaction considered in the 1952 model, seven other types of interaction were taken into account. For each cation at a specific c -value and α , the calculated total interaction energies determined the statistical weights of each configuration. The association energy (ΔE) of each ion at each c -value was then calculated, using a Born charging method. The result is shown in Figure 6.8. (for full details, see Ling 1962).

In comparing the association energy of a specific ion, called X^+ (ΔE_X), with that of K^+ (ΔE_K), the selectivity ratio of X^+ over K^+ (K_{X^+}/K_{K^+}) is calculated from the relationship $K_{X^+}/K_{K^+} = \exp - \{(\Delta E_{X^+} - \Delta E_{K^+})/RT\}$, where K_{X^+} and K_{K^+} are,

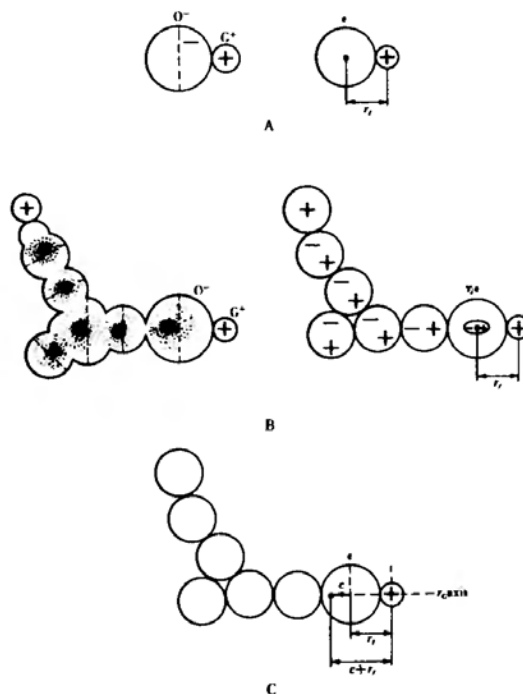


Figure 6.7. Definition of the c -value. The c -value is the displacement in Å units of the unit-negative charge carried by the oxygen atom of the oxyacid functional group from the center of the atom: either away (negative c -value) or toward (position c -value) the interacting cation (C) so that the net interaction with the cation matches the cumulative action of the inductive effects exerted by the rest of the molecule (B). (Ling 1962, by permission of Ling)

respectively, the association constants of ion X^+ and K^+ , and R and T are the gas constant and absolute temperature, respectively. The result is illustrated in Figure 6.9.

Only at low c -value is K^+ preferred over Na^+ : here the ratio of the association constant of Na^+ (represented by K_{X^+}) over that of K^+ (K_{X^+}/K_{K^+}) is less than one. As the c -value increases, however, the relative preference changes, until Na^+ is preferred over K^+ . This inversion is not limited to this pair of ions, but occurs between other pairs of ions as well. With these ions, the relative affinity for NH_4^+ is worth special attention.

The three major fixed cations of proteins are α -amino groups, ϵ -amino groups, and guanidyl groups. All are modifications of NH_4^+ . Therefore the theoretically calculated change of the affinity for NH_4^+ with c -value change may at least give us a hint as to how one may expect the fixed cations to behave. These fixed cations are, as was pointed out earlier, ever-present competitors for the β - and γ -carboxyl groups. When these fixed cations are adsorbed on β - and γ -carboxyl groups, salt linkages are formed. The theoretically calculated results (Figure 6.9) show that with increasing c -value, the changes of the affinity of fixed carboxyl groups for K^+ closely parallels the changes of the affinity of the fixed carboxyl groups for NH_4^+ . Therefore c -value changes that may increase for instance, K_{Na^+/K^+} , may also increase the relative affinity for Na^+ in comparison with that

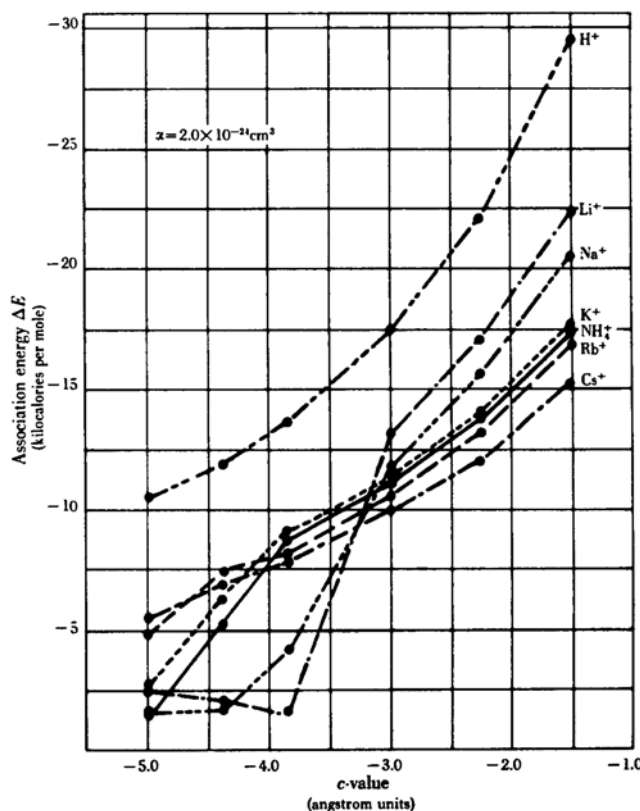


Figure 6.8. Relation between calculated association energy ΔE of various cations and c -value of the anionic group. Polarizability of anionic site, α , is $2.0 \times 10^{-24} \text{cm}^3$. (Ling 1962, by permission)

for the fixed cations. In that case, not only K^+ -for- Na^+ displacement but salt-linkage dissociation may occur concurrently. However, there are reasons why the fixed cations and NH_4^+ do *not* behave entirely in the same way.

The fixed cations are tied to the rest of the protein molecules and hence to the fixed-charge system of the cell. In contrast, the NH_4^+ is a free entity by itself. If the protein undergoes a major cooperative change of conformation, leading to a large increase of the c -value of its β - and γ -carboxyl groups, and the c -value-analogue of the backbone carbonyl groups, the bulk of water adsorbed on the protein backbone will be depolarized (see Section 7.3.3.2 below). Such a local or global depolarization of the cell water increases the entropy of dissociation of free cations like K^+ or NH_4^+ and reduces their free energy of adsorption. In the meanwhile, little gain of entropy of dissociation of the fixed cations accompanies this change, because the tethered fixed cations are not free to dissociate and diffuse away and thus unable to increase their entropy of dissociation and reduce their free energy of adsorption in the way the free cations do. As a result, *with the large increase of the c -value of β - and γ -carboxyl groups (and accompanying increase of the c -value-analogues of the backbone carbonyl groups) the relative adsorption energy of the fixed ϵ -amino and guanidyl groups increases and the probability of salt-linkage formation sharply increases.*

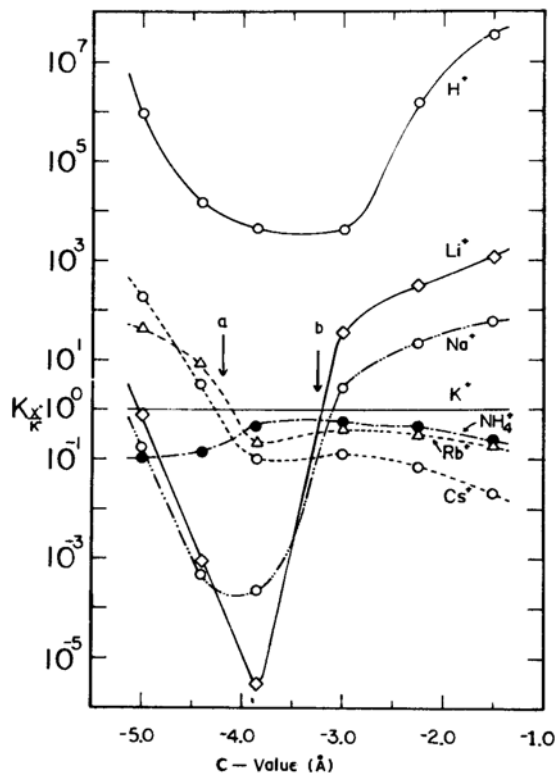


Figure 6.9. The relation between the selectivity ratios of various cations in comparison with K^+ and the c -value. Polarizability of anionic oxygen atom is $2.0 \times 10^{-24} \text{cm}^3$; a and b point to c -value of -4.20 and -3.25Å respectively. The selectivity ratios (K_{X^+/K^+}) are calculated from the theoretically calculated association energies in Figure 6.8. (Ling and Bohr 1971, by permission of *Physiological Chemistry and Physics*)

Before concluding this chapter, I would like to present some evidence that the theoretically calculated data shown in Figure 6.9 have already received experimental support. These supportive data were acquired before the theoretical calculations were made, and their special significance here was neither sought nor recognized by the original authors.

Table 6.5 from Bregman (1953) shows the selectivity ratios ($K_D = K_{Na^+}/K_{X^+}$) for the alkali-metal ions Li^+ , Na^+ , and K^+ in three types of ion-exchange resins with different acidic groups. In the strongly acidic sulfonic type, pK_a and hence

Table 6.5. Selectivities for Alkali Cations (Bregman 1953, by permission of Annals NY Academy Sciences)

Cation	K_D for Different Resin Types		
	Sulfonic	Carboxylic	Phosphonic
Li	1.97	0.72	0.65
Na	1.00	1.00	1.00
K	0.80	1.14	1.51

c -value are low. The preference is $K^+ > Na^+ > Li^+$, as expected theoretically. In the more weakly acidic carboxylic and phosphonic types, the pK_a s and hence c -values are high; the preference is reversed: $Li^+ > Na^+ > K^+$, also as expected theoretically.

Figure 6.10, also taken from Bregman (1953), shows how the experimentally measured selectivity coefficients (K_D s) for Li^+ , Na^+ , K^+ , NH_4^+ , and H^+ , in comparison with K^+ in sulfonate ion-exchange resin, change with varying percentages of the cross-linking agent, divinylbenzene (DVB). K_D is equal to the reciprocal of K_{X^+/K^+} of Figure 6.9. Other experimental evidence indicates that DVB not only joins the linear polyvinyl sulfonate into a three-dimensional network, it also increases the pK_a value of the acidic groups (see Ling 1984, 160). Therefore, increasing DVB percentage brings about a progressive increase of the c -value of the sulfonate groups. The experimental data of Figure 6.10 thus affirm in a general way the theoretical curves calculated with a polarizability of the fixed anion equal to $0.878 \times 10^{-24} \text{ cm}^3$ (see Ling 1962, Figure 4.12), since the essence of the two sets of curves is quite similar⁷. In contrast, the affinity for H^+ is much weaker in Figure 6.10 than in the theoretical curves calculated with a higher polarizability intended for carboxyl groups and shown in Figures 6.8 and 6.9.⁸

6.3. Summary

This chapter began by recalling the magnet-iron-filing analogy to illustrate that, for it to function coherently, an equivalent of propagated magnetic polarization must exist in living matter. In the AI hypothesis, the equivalent is *electric polarization* or *inductive effect*.

The inductive effect—best known in substitution of covalent-bonded atoms or groups of atoms—is also operative in substitutions of ions and molecules held by ionic and H-bonds, respectively. The limited reach of the inductive effect (or direct F -effect) confines the *unit distance* of operation in protein molecules to

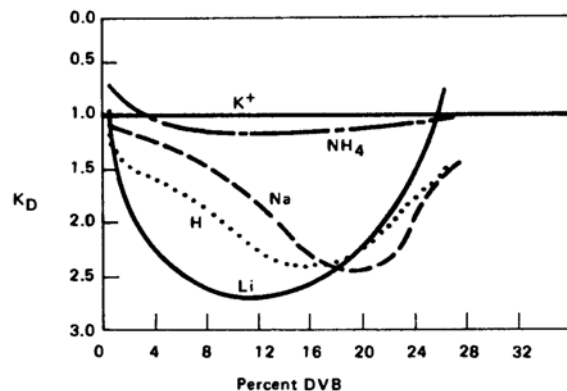
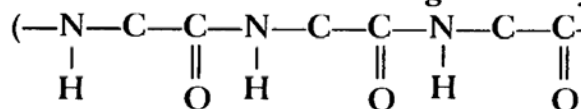


Figure 6.10. Relative selectivity coefficients of H^+ , NH_4^+ , and alkali metal ions compared to K^+ in sulfonate ion-exchange resin with varying percentage of the cross-linking agent, divinyl benzene (DVB). (Redrawn, from Bregman 1953, by permission of Plenum Publishing Co.)

that between a functional group on a short side chain (e.g., β - and γ -carboxyl group, SH group) and lengths of the polypeptide chain both upstream and downstream from the point of attachment of the short side chain to the polypeptide chain. Indeed, there are at least three sets of independent evidence which show, in a consistent and mutually supportive manner, that **the inductive effect can be detected after transmission through as many as three consecutive peptide linkages**



short segment of side chains.

These sets of evidence include (1) the continually changing pK_a of the α -amino groups of glycine, diglycine, etc.; (2) the effectiveness of a side chain's electron-donating strength in influencing the NHCO groups belonging to the third neighboring amino acid residue both "upstream" and "downstream"; and (3) the effectiveness of fluorescence quenching of the tryptophane functional group produced by the protonation of the glycylic α -amino group on the glycylic-glycyl-glycyl-L-tryptophane. In addition, the quenching effect on phenol fluorescence

due to the protonation of the carboxyl groups of $\text{Ph} \cdot (\text{CH}_2)_3 - \text{C} \begin{array}{l} \text{O} \\ // \\ \text{OH} \end{array}$ and the

electron-enriching effect of urea on functional groups on short side chains including SH, β -, γ -carboxyl, tyrosine and tryptophan groups, further support the notion that there is effective transmission of inductive effects between side chains and at least one (possibly more) polypeptide NHCO group(s) in both directions along the polypeptide chain. Figure 6.11 provides a diagram of these sets of evidence.

Besides demonstrating effective transmission of the inductive effect over distance, Figure 6.11 also illustrates the variety of *effectors* for the inductive effects on proteins, including: the substitution of a carboxyl OH group by a glycylic group (A); what one may call the substitution of an electron-withdrawing side chain by an electron-donating side chain or vice versa (B); the protonation of an α -carboxyl (or α -amino) group (C); and the substitution of a peptide carbonyl group by the carbonyl groups of the stronger electron-donating urea (D).

Figure 6.11 also illustrates the varieties of *target* groups on proteins for the inductive effect: the pK_a of the α -amino group (A); the H-bonding groups of the polypeptide chain (B); the fluorescence and its quenching of phenolic and tryptophane side chains (C); and the reactivity of the SH group of the cysteine residue (and β - and γ -carboxyl groups) (D). Taken as a whole, the data verify the prediction that the polypeptide NHCO groups and functional groups on short side chains respond effectively to the inductive effect and according to the AI hypothesis, it is these inductively mediated effects that underlie all physiological activity.

Of particular importance is the recognition that each side chain of a protein molecule plays a part in the determination of the secondary structure of the protein by the inductive effect it exerts. **Cardinal adsorbents** and other ligands adsorb onto the side chains and backbone sites, and by so doing alter the in-

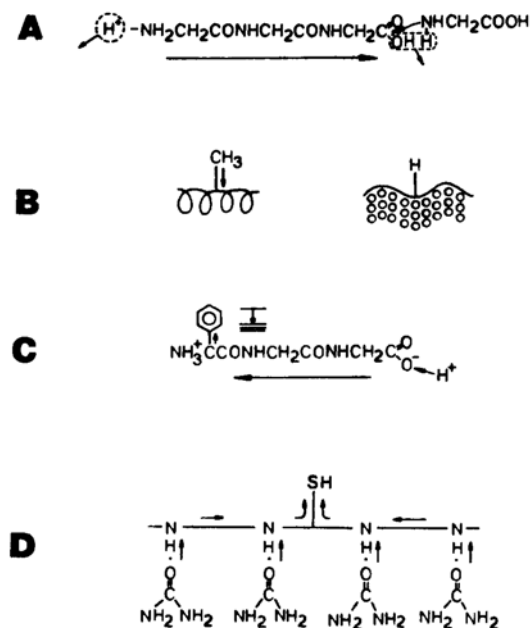


Figure 6.11. Diagrammatic illustration of four types of experimental evidence for the transmission of the inductive effect through a length of the polypeptide chain and short segments of saturated hydrocarbon side chains. (A) Decrease of the affinity of the terminal amino group as indicated by a decrease of $\text{p}K_a$ in response to distant substitution of the carboxyl OH group by an electron withdrawing glycol group. (B) Secondary structure of protein and multilayer polarization of the bulk-phase water determined by the electron-donating strength of side chains. Strongly electron-donating CH_3 group enhances the probability of α -helical structure; weakly electron-donating H favors the alternative fully-extended conformation with multilayer polarization of water. (C) Fluorescence quenching by protonation of distant carboxyl group. (D) Enhancement of SH groups reactivity by reaction of backbone with urea.

ductive effect exerted by the unadorned side chains (and backbones) so that an alternative secondary structure of the protein is determined. The existence of this alternative secondary structure makes possible the all-or-none transition of the protein conformation in response to interaction with a suitable cardinal adsorbent.

Also presented in this chapter are the theoretically calculated relationships between the electron density—or, more precisely, the c -value—of β - and γ -carboxyl groups and the relative affinity among the five alkali metals, H^+ , and NH_4^+ . NH_4^+ may be regarded, in a limited way, as the prototype of the fixed cations carried on proteins. However, when the c -value of the β - and γ -carboxyl groups reaches high values, the accompanying water depolarization promotes the formation of salt linkages between the fixed cations and the β - and γ -carboxyl groups.

The evidence presented in this chapter makes a clear case that the inductive effect not only dictates the properties and behaviors of *small* organic molecules, but dictates the (short-range) properties and behaviors of *large* protein molecules as well. In the next chapter I will discuss mechanisms which can translate the

short-range inductive effect discussed in this chapter into all-or-none coherent behaviors covering distances much longer than those depicted in Figure 6.11.

In Chapter 8 I will provide a *full* answer to the question raised at the beginning of this chapter, by demonstrating how such long-range effects—built on the basic element of short-range inductive effects—in turn, provide the mechanism which enables ATP (and its “helpers”) to keep the key intracellular proteins in the K^+ -adsorbing, water-polarizing conformation of the living state.

NOTES

1. Being more electronegative means that the electrons of the atom are more strongly attracted toward its nucleus, which possesses a higher number of positively charged protons. A chlorine atom is more electronegative than a hydrogen atom because chlorine has 17 protons in its nucleus, while hydrogen has only one (see Pauling 1960, 88).

2. Chiang and Tai's useful guidelines were originally available only in Chinese, but have been recently published in English, along with a description of the basic methods (Chiang 1987; see also Chiang and Tai 1963, 1985; and Ling 1984, 185).

3. A benzene ring has six carbon atoms. Substitution at or characterization by two positions in the benzene ring that are separated by one, two, or no carbon atom(s) are referred to respectively as *meta*, *para* and *ortho*.

4. Direct electrostatic effect transmitted through the intervening space is called D-effect; electrostatic effect transmitted through the connecting atoms is called the inductive or I-effect. Combined D- and I-effect is called F-effect (Ling 1962, 87).

5. It should be pointed out that Benesch et al., who first described the effect of urea on free cysteine and cysteine peptides, offered an altogether different interpretation: urea breaks an H-bond formed between ionized sulphydryl groups (S^-) and some proton-donating group. There are reasons to doubt this interpretation, described in full elsewhere (Ling 1964, 109, footnote).

6. Although in this presentation stress is placed on the c -value of anionic oxy-acid groups (e.g., β - and γ -carboxyl groups), a c' -value has also been introduced for the positive charge of cationic groups (Ling 1962, 57, 60), and alteration of selectivity for anions with charges of c' -values discussed (see Ling 1962, 407). See also Section 7.3.3.2. below for definitions of c -value- and c' -value-analogues.

7. There are other differences between the two sets of figures. The most prominent is that the K_{X^+/K^+} of Figures 6.9 here and Figure 4.12 in Ling (1962) is much larger than the reciprocal of K_D of Figure 6.10. The explanation for this disparity is as follows: The theoretical data of Figure 6.9 and in Figure 4.12 in Ling (1962) were derived without assuming any external forces limiting the number of water molecules allowed in the different configurations. In contrast, the presence of a rigid framework in the cross-linked ion-exchange resin limits the number of water molecules that can enter the system, thereby discouraging the higher configurations with more water molecules between the anion and the cation. This limitation, in turn, compresses the differences in the association energies, and lower K_{X^+/K^+} (or K_D) values follow as a result. Living cells are likely to fall between the two extreme cases of no limitation and severe limitation.

8. The importance of choosing the correct polarizability of the fixed anionic group in computing the adsorption energies of cations becomes obvious if one compares the relative affinities for the alkali-metal ions and for H^+ in two theoretical models: in the model (Model III) that produced the result shown in Figure 6.9 of this volume, α is given the values of $2.0 \times 10^{-24} \text{ cm}^3$; in another model (Model I) α is given the value of $0.876 \times 10^{-24} \text{ cm}^3$ (see Figure 6.7 in Ling 1984). In Model III, the affinity for H^+ computed is much greater than those for K^+ throughout the entire c -value range considered; in Model I, in contrast, the affinity for H^+ stays consistently below that for K^+ . It is also known that carboxyl groups have a high polarizability (see Ling and Bohr 1971, footnote on 580).

In physiological studies of ion adsorption, the anionic functional groups of prime importance are carboxyl groups (see Section 4.4.3., also Ling 1990, answers to questions); and carboxyl groups, as a rule, have much *stronger* affinity for H^+ than for the alkali-metal ions—a fact that has already been demonstrated for cytoplasmic carboxyl groups in the data shown in Figure 4.18 and discussed in Sections 4.4.3.2. and 4.4.4. Here in the PEG-preserved 2-mm-wide muscle segments, the adsorption of labeled Na^+ in the muscle cytoplasm in the presence of 16.8 mM of external Na^+ is reduced to half by H^+ at a concentration corresponding to a pH of 3.9, i.e., $10^{-3.9}$, or 0.126 mM. Thus the carboxyl groups in these partially-preserved cytoplasmic proteins have an affinity for H^+ more than ten times stronger than that for Na^+ . In Chapter 11, other data will be presented showing a still greater relative affinity for H^+ than for K^+ where the carboxyl groups are located on the cell surface and where the cells were in their fully normal physiological condition.

COHERENT BEHAVIOR AND CONTROL MECHANISMS

When one tosses a coin, it is not possible to predict whether it will land head up or head down. However, if one tosses a million coins, one can predict with high accuracy that half of the coins will land heads up and the other half heads down. Since each coin toss is independent from other tosses, there is no way to alter the result. As long as the coins are not “loaded,” the result will inevitably be 1:1.

Cells are composed of many millions of molecules and ions. Consider a single frog-muscle cell. Sixty micrometers in diameter and 3 cm long, it is barely visible to the naked eye. Yet, in it one find two million trillion water molecules, five thousand trillion K^+ ions, and eleven trillion myosin molecules. These numbers are so large that they are not within the usual human experience. Yet a single cell is very much a coherent entity: it responds quickly, decisively, and meaningfully to changes of the external environment. *By what mechanism can such large numbers of units be transformed from the “random inevitability” of a million coin tosses to such highly disciplined coherence? The answer is neighbor-to-neighbor interaction.*

The Great Wall of China is 4,000 miles long. Built largely across mountain terrain, it served as a major defense against northern invaders. It greatly predated the telegraph or telephone. The wall was effective because sentinels were stationed in watchtowers within sight of an immediate neighbor with whom each sentinel was in communication by light, or even by sound. With this near-neighbor communication, the entire wall functioned as one.

A second example of communication, mentioned earlier, occurs in a school of fish. Swimming in the ocean as a unit, a school can change its direction instantaneously and as a group. Again, the secret of this coherence in the multitude is near-neighbor interaction: each fish sees and responds to the activity of its immediately neighboring fish (Figure 7.1).

Comparing, on the one hand, the million tossed coins, and, on the other hand, the Great Wall defense and the school of swimming fish, one reaches the conclusion that for an assembly of a very large number of units, coherent behavior is possible because of neighbor-to-neighbor interaction.

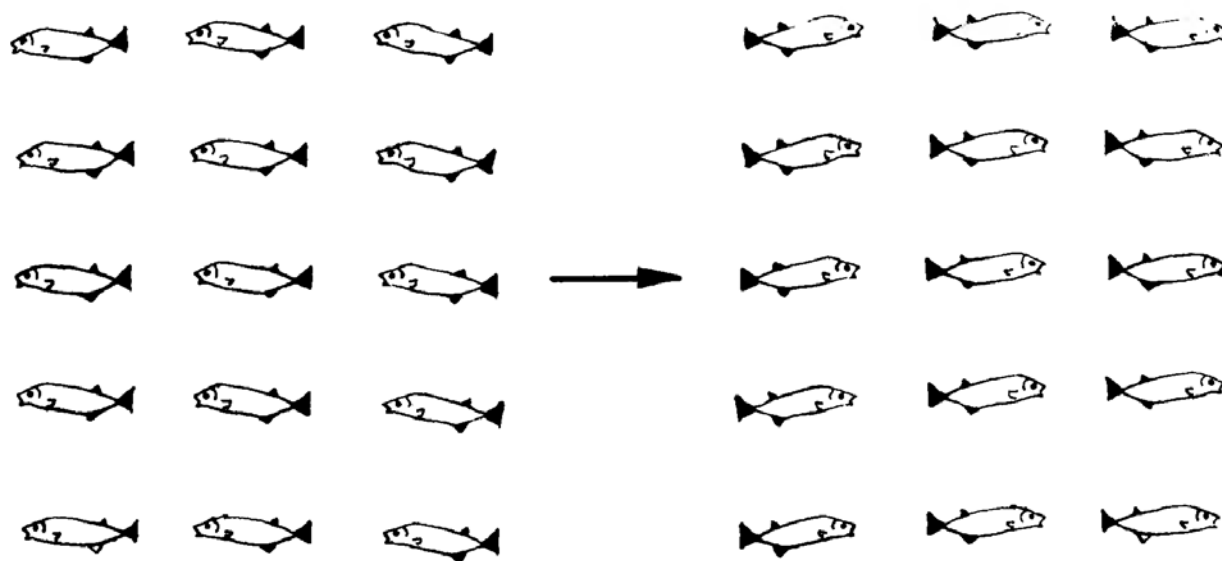


Figure 7.1. Synchronous directional change of a school of swimming fish.

7.1. *Theory of Cooperative Adsorption (the Yang-Ling Cooperative Adsorption Isotherm)*

Although physicists and chemists have long been aware of the enormous number of molecules in any macroscopic assembly, the exact science dealing with the physics of these large assemblies, called **statistical mechanism**, came into being late in the history of physics. This new branch of physics deals with large assemblies of atoms and molecules that exhibit near-neighbor interaction—known as **cooperative phenomena**. However, even though biological systems comprise large assemblies, the recognition that statistical mechanism finds major application in biology is very recent.

Early in the history of respiratory physiology, it was discovered that the ability of red blood cells to transport oxygen between the lungs and oxygen-consuming tissues resides in the major protein of the red blood cells, hemoglobin. This ability of hemoglobin to serve an oxygen-transport function was easily demonstrable in test tubes. In the presence of high oxygen tension, the hemoglobin solution takes up a large quantity of oxygen; in the presence of lower oxygen tension, the oxygen load is promptly released.

After exact methods to measure oxygen uptake were developed, it became obvious that the uptake of oxygen by hemoglobin is unusual. In the more familiar inanimate world, adsorption usually follows a simple rule (see endnote 5 of Chapter 3). If one plots as ordinate the amount adsorbed against the concentration of the adsorbate in the surrounding medium, one obtains a curve that is described as a *hyperbola*: strong uptake at the lowest concentration at a time when most of the adsorption sites are empty, followed by weaker and weaker uptake as the concentration of the adsorbate increases in the external medium and more and more adsorption sites are already occupied (for an example of hyperbola, see curve labeled $-\gamma/2 = 0.0$ Kcal/mole in Figure 7.2). This is, how-

ever, not the case for the uptake of oxygen by hemoglobin. Here, the uptake is weak at the low external oxygen concentration, when the sites are still mostly vacant; as the sites are occupied, the uptake becomes much stronger. In other words, the uptake curve is *S-shaped* or *sigmoid*.

To explain this odd behavior, the *crevice hypothesis* was suggested. In this hypothesis, the oxygen-binding sites, four per hemoglobin molecule, are postulated to have different affinities for oxygen. The sites with high affinity are considered buried inside “crevices,” while the sites with weak affinity for oxygen are on the outside at the entrance of the crevice. The high-affinity sites become accessible to oxygen only after oxygen molecules have become adsorbed to the weak-affinity sites and the crevice thereby pried open. The crevice hypothesis held sway for many years, before its eventual disproof by Perutz and his coworkers (Perutz and Mitchison 1950; Perutz et al. 1968). The exact study of crystalline hemoglobin revealed that all four oxygen-binding *heme* sites are on the surface of the hemoglobin molecules, and none are buried in crevices. Some other mechanism must therefore be the cause of the unusual S-shaped adsorption curve of oxygen. In 1962, I suggested that the underlying mechanism was cooperative, near-neighbor interaction among the four heme sites (Ling 1962, 104; 1964; 1969, 49).

Using the one-dimensional Ising method, Yang and Ling presented a *cooperative adsorption isotherm* for adsorption on proteins (Ling 1964, 1980a; see also Karreman 1980). In this derivation, it was assumed that a protein can be represented as linear arrays of similar sites, infinite in length or arrayed in a circle. Each site adsorbs either one of a pair of solute molecules or ions, i and j , and there may be interaction among nearest neighboring sites. In the Yang-Ling cooperative adsorption isotherm (i.e., an equation describing the cooperative adsorption at a constant temperature):

$$[p_i]_{\text{ad}} = \frac{[f]}{2} \left[1 + \frac{\xi - 1}{\sqrt{(\xi - 1)^2 + 4\xi \exp(\gamma/RT)}} \right], \quad (7)$$

where $[p_i]_{\text{ad}}$ is the concentrations of the i th solute (e.g., O_2) adsorbed on the protein and $[f]$ is the total concentration of the adsorption sites in the system. ξ is defined as follows:

$$\xi = \frac{[p_i]_{\text{ex}}}{[p_j]_{\text{ex}}} \cdot K_{j \rightarrow i}^{00}, \quad (8)$$

where $[p_i]_{\text{ex}}$ and $[p_j]_{\text{ex}}$ are the concentration of the i th and j th solute in the surrounding medium. $K_{j \rightarrow i}^{00}$ is the *intrinsic equilibrium constant* for the j th to i th adsorption exchange. $-\gamma/2$ stands for the important *nearest-neighbor interaction energy*, defined as the energy change each time a new ij pair is created on two neighboring sites (for further details, see Ling 1984, 208–209).

Figure 7.2 represents plots of equation 7 with different values of $-\gamma/2$. When $-\gamma/2$ is equal to zero, equation 7 reduces to (a simplified version of) the *Langmuir adsorption isotherm* (Langmuir 1916, 1918, see endnote 5 of Chapter 3 and equation 21):

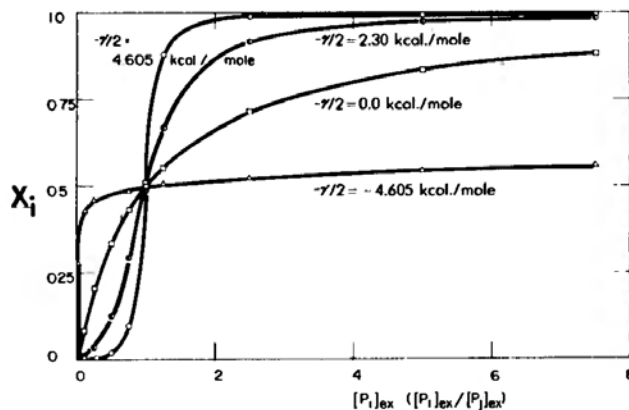


Figure 7.2. Theoretical plots of cooperative adsorption isotherms with different nearest-neighbor-interaction-energy ($-\gamma/2$). $[P_i]_{\text{ex}}$ and $[P_j]_{\text{ex}}$ are respectively the concentration of the i th and j th solute in the bathing medium. X_i is the mole fraction of adsorption sites occupied by the i th solute. (Ling 1984, by permission of Plenum Publishing Co.)

$$[p_i]_{\text{ad}} = \frac{[f]K_{j \rightarrow i}^{00}[p_i]_{\text{ex}}}{[p_j]_{\text{ex}} + K_{j \rightarrow i}^{00}[p_i]_{\text{ex}}} \quad (9)$$

In this case a plot of $[p_i]_{\text{ad}}$ against $[p_i]_{\text{ex}}$ is a hyperbola. When $-\gamma/2$ is negative, we have what is called a *heterocooperative adsorption isotherm*, and the plot is a flattened hyperbola. However, the most important of all is cooperative adsorption with a high positive $-\gamma/2$. In this case, the adsorption is “autocooperative.” The plot is S-shaped or sigmoid.

In autocooperative adsorption, the adsorption of an i th solute favors the adsorption of more i th solute; in a heterocooperative adsorption, the adsorption of an i th solute favors the adsorption of the alternative j th solute. Autocooperative behaviors, like those of a school of swimming fish and the sentinels guarding the Great Wall of China, tends to be all-or-none. In the AI hypothesis, autocooperative adsorption is the backbone of coherent behavior in living cells including the maintenance of the living state.

Having explained in some detail the Yang-Ling cooperative adsorption isotherm (equation 7), I now proceed to put the equation in a different form. Remembering that each site must adsorb either i or j , one can easily find the concentration of adsorbed j solute $[p_j]_{\text{ad}}$, by subtracting $[p_i]_{\text{ad}}$ from $[f]$. Introducing $[p_j]_{\text{ad}}$ and rearranging terms, we obtain the following different form of equation 7:

$$\frac{[p_i]_{\text{ad}}}{[p_j]_{\text{ad}}} = \frac{\sqrt{(\xi - 1)^2 + 4\xi \exp(\gamma/RT)} + \xi - 1}{\sqrt{(\xi - 1)^2 + 4\xi \exp(\gamma/RT)} - \xi + 1} \quad (10)$$

Figure 7.3 represents a log-log plot of the highly accurate data of oxygen binding on human hemoglobin (from Lyster); the solid line is theoretical according to equation 10, with $K_{\text{O}_2}^{00}$ equal to 5.88×10^{-6} M and $-\gamma/2 = +0.67$ Kcal/mole (Ling 1970a). The good accord between the theoretical curve and the experimental points supports the theory that it is the **cooperative near-neighbor**

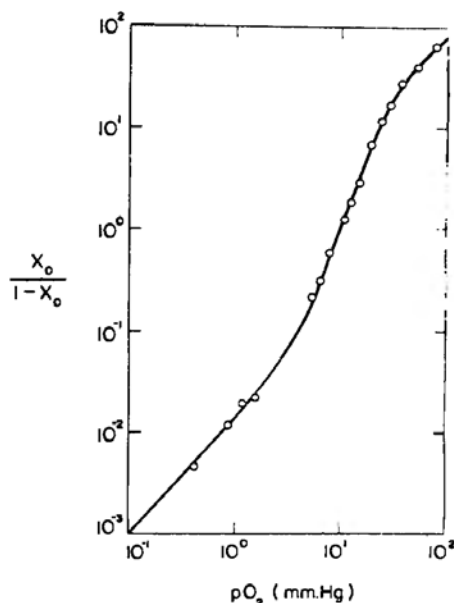


Figure 7.3. A log-log plot of oxygen uptake by human hemoglobin at pH 7.0 and 19°C. Points are experimental; the line is theoretical according to equation 10 with $K = 0.1 \text{ (mm Hg)}^{-1}$ and $-\gamma/2 = 0.67 \text{ Kcal/mole}$. X_o is the mole fraction of heme sites binding oxygen and $1 - X_o$ is the mole fraction not binding oxygen. Data of Lyster, cited in Rossi-Fanelli et al., 1964. (Ling 1969, by permission of International Review of Cytology)

interaction among the four heme sites that gives rise to the sigmoid oxygen uptake curve of hemoglobin—a trait that facilitates efficient transport of oxygen.

Many years ago A. V. Hill introduced an (empirical) equation describing oxygen binding on hemoglobin (Hill, 1910):

$$\log \frac{y}{1-y} = n \log [\text{O}_2]_{\text{ex}} + n \log K \quad (11)$$

where y is the mole fraction of the sites binding oxygen, $1 - y$ the sites not binding oxygen. The *Hill coefficient*, n , describes the “sigmoidity” of the oxygen-binding curve. It can be shown that Hill’s empirical equation is in form identical to the equation representing the *tangent* to the adsorption isotherm in the form of equation 10 at equal occupancy by i and j in a log-log plot:

$$\log \frac{[p_i]_{\text{ad}}}{[p_j]_{\text{ad}}} = n \log \frac{[p_j]_{\text{ex}}}{[p_i]_{\text{ex}}} + n \log K_{j \rightarrow i}^{00}, \quad (12)$$

K of Equation 11 is equal to $K_{j \rightarrow i}^{00}$. *The Hill coefficient, n , long suspected to be a parameter related to cooperativity, is now shown to be equal to $\exp(-\gamma/2RT)$* (Ling 1964, 1980a). A $-\gamma/2$ of $+0.67 \text{ Kcal/mole}$, for example, is equivalent to an n of 3.1. Another parameter used from time to time is θ , which equals $\exp(\gamma/RT)$ or $1/n^2$.

As mentioned above, the key to cooperative interaction is $-\gamma/2$, the nearest-neighbor interaction energy. **In the association-induction hypothesis, $-\gamma/2$, as a rule, contains a major induction component.**

In magnitude, $-\gamma/2$ is related to the absolute value of the intrinsic free energy of j th-to- i th adsorbent exchange, $|\Delta F_{j \rightarrow i}^{00}|$ by the following equation:

$$-\gamma/2 = +\tau|\Delta F_{j \rightarrow i}^{00}|, \quad (13)$$

where τ is the *nearest neighbor transmissivity factor*. Experimental confirmation of the relationship shown in equation 13 will be presented in Section 8.2 below.

7.2 *Experimental Findings in Harmony with the Theory of Spontaneous Autocooperative Transition*

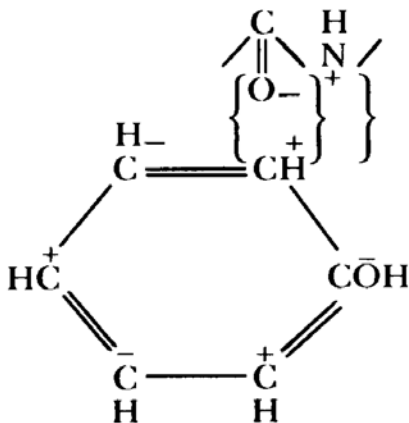
In Chapter 3, I pointed out that living cells are primarily systems of protein-water- K^+ in close association. In confirmation I have demonstrated in Chapter 4 that the bulk of cell K^+ in voluntary muscle cell is adsorbed on the β - and γ -carboxyl groups of cell proteins, and in Chapter 5, that the bulk of cell water is adsorbed on the fully-extended polypeptide chains of the same and/or other cell proteins.

I also pointed out in the opening section of this chapter that for the vast number of cell K^+ , water, and protein molecules to function coherently as a single unit—like a school of swimming fish—there must be *nearest-neighbor interactions* within the protein molecules themselves.

The Yang-Ling adsorption isotherm offers a quantitative method to test this major postulate of the AI hypothesis i.e., the hypothesis that proteins possess the inherent capability of behaving autocooperatively. That capability originates from large and positive nearest-neighbor-interaction energy ($-\gamma/2$) between nearest-neighboring-polypeptide CONH groups—which adsorb the bulk of cell water—and between nearest-neighboring β - and γ -carboxyl groups—which adsorb virtually all cell K^+ . Let us look at interaction between neighboring polypeptide CONH groups next.

7.2.1. *Cooperative Interaction Among Backbone NHCO Sites*

Figure 7.4 is a double log plot of the binding of phenol on collagen in the form of hide powder from Küntzel and Schwank (1940) where $-\gamma/2$ is equal to $+0.74$ Kcal/mole. There is convincing evidence that phenol binds onto backbone CONH groups, as suggested by Küntzel (1944):



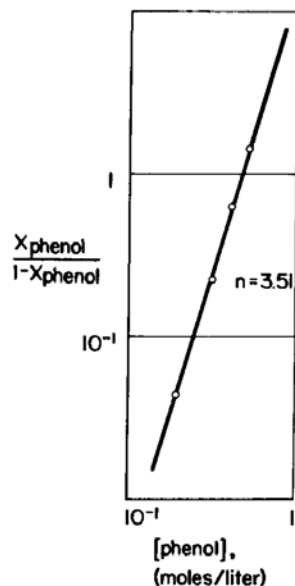


Figure 7.4. Phenol adsorption on collagen. Ordinate represents, on a logarithmic scale, the mole fraction of collagen sites adsorbing phenol (X_{phenol}) divided by the mole fraction of sites not adsorbing phenol ($1 - X_{\text{phenol}}$). Total number of binding sites used in calculating $1 - X_{\text{phenol}}$ is the total number of backbone NHCO groups in 1 kg of collagen. Slope of 3.51 corresponds to a nearest-neighbor interaction energy ($-\gamma/2$) of $+0.74$ kcal/mole. The collagen used was in the form of skin powder. Data of Küntzel and Schwank (1940). (Ling 1966, by permission of Federation Proceedings.)

Thus in a 5% phenol solution, collagen takes up 60% of its weight of phenol. The molecular weight of phenol is 94.11; the average amino acid residue weight may be estimated at about 110 (Ling 1962, 48). Since $110/94.1 \times 0.6 = 0.7$, 70% of the amino acid residues of the collagen bind phenol. Only the peptide NHCO groups are numerous enough to bind this much phenol (see also Gustavson 1956). ***The strongly positive $-\gamma/2$ in the binding of phenol to collagen demonstrates strong interaction between nearest-neighboring peptide CONH groups.***

7.2.2. Cooperative Interaction Among β - and γ -carboxyl Groups

Figure 7.5 shows a Scatchard plot of the adsorption of Na^+ on β - and γ -carboxyl groups of bovine hemoglobin after neutralization of the fixed cations with NaOH (discussed in Section 4.2). Note that the plot of $[\text{Na}^+]_{\text{ad}}/[\text{Na}^+]_{\text{free}}$ against $[\text{Na}]_{\text{ad}}$ concaves upward in agreement with the theoretical characteristic of autocoperative adsorption. ***The data indicates strong interaction between nearest neighboring β - and γ -carboxyl groups*** (Ling 1984, 215), with $-\gamma/2$ estimated at $+0.824$ Kcal/mole (Ling and Zhang 1984, 230).

In summary, the data presented immediately above and in Figure 7.3 have shown that autocoperative interaction exists among nearest-neighboring polypeptide CONH groups, among nearest-neighboring β - and γ -carboxyl groups carried on short side chains, and among nearest-neighboring heme groups carried on histidine groups which are also on short side chains. Together they affirm the notion that cooperative behavior is not limited to any specific functional

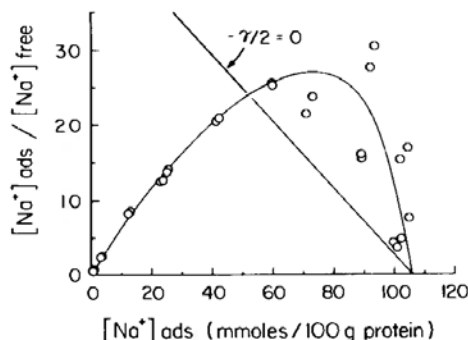


Figure 7.5. Scatchard plot (Scatchard 1949) of the adsorption of Na^+ on 10% solution of NaOH-denatured bovine hemoglobin. Curve shows upward convexity typical of *auto-cooperative* adsorption with $-\gamma/2 > 0$ Kcal/mole. Straight line shows a theoretical (Langmuir) adsorption isotherm with $-\gamma/2 = 0$ Kcal/mole. (Ling and Zhang 1984, by permission of Physiological Chemistry Physics and Medical NMR)

groups or types of proteins (e.g., those with symmetrical subunits), but is an inherent attribute of all proteins.

In the preceding chapter, I have shown that the inductive effect can be effectively transmitted through *at least* one short side chain and one peptide unit ($-\text{NHCCO}-$). Clearly that kind of direct short-range inductive effect (or the *direct F-effect*, endnote 4 in Chapter 6) is more than adequate to provide the needed mechanism for the nearest-neighbor interaction of the autocoperative adsorption of phenol on collagen i.e., between immediately neighboring peptide units. In contrast, each pair of immediately neighboring β - or γ -carboxyl groups in a hemoglobin molecule, for example, and each pair of immediately neighboring heme sites in the same protein, are, on the average, separated from one another by longer distances—or more correctly, by more peptide units. They are thus beyond the *unit distance* of operation of the direct *F-effect*. In these cases, another mechanism, known either as the *indirect F-effect* or *indirect F-process* (Ling 1962, 95; to be described in detail in Section 7.3.3.2.) answers the need. Incorporating the direct *F-effect*, the indirect *F-effect* or process entails a far-reaching, self-propagating partner exchange of the successive NH and CO groups along the length of the polypeptide chain.

7.3. Theory of the Control of Transition between Discrete Cooperative States by Cardinal Adsorbents

7.3.1. A Sketch of Basic Concepts

As mentioned earlier, for a population of adsorption sites that are physically isolated from one another, the adsorption of a solute designated as *i* has the shape of a **hyperbola** with increasing external concentration of this solute. However, when the individual adsorption sites are functionally linked, say by a polypeptide chain, and the nearest-neighbor interaction energy ($-\gamma/2$) is significantly greater than zero, the adsorption isotherm is **sigmoid** or S-shaped. In

the case where $-\gamma/2$ is large, a sharp transition occurs between a state in which only solute i is adsorbed to a state where only the alternative solute j is adsorbed. Such a dramatic change may follow only a small increment of the ratio of external i and j concentrations. This type of **spontaneous autocoooperative transition** between two discrete states is illustrated in Figure 7.6A; it is of importance in the coherent physiological functioning of erythrocytes, which rely on this sharp transition for full and efficient oxygen loading in the lung and for full and efficient unloading among oxygen-poor tissues.

However, few other living cells constantly shuttle back and forth between two different environments as do erythrocytes. The great majority of living cells are stationary in an unchanging environment. Nevertheless, the contraction of muscles and the conduction of nerves illustrate that to serve their diverse functions, these stationary cells must also undergo efficient, all-or-none autocoooperative transitions. But here these transitions are not triggered by a changing i and j concentration in the environment. Rather, the transition occurs in response to a class of physiologically potent molecules, collectively referred to as **cardinal adsorbents**.

To introduce a theoretical model for this type of controlled autocoooperative

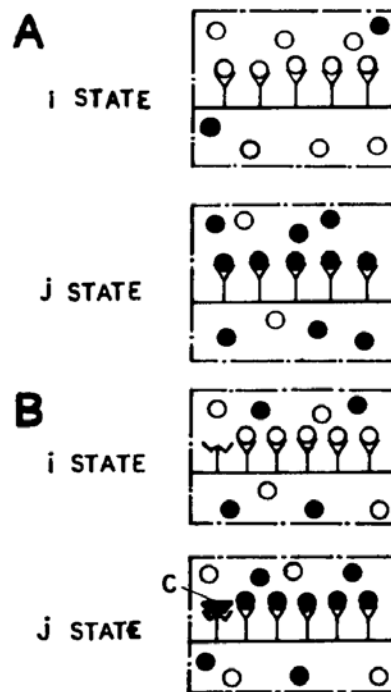


Figure 7.6

A. *Spontaneous autocoooperative transition*

Cooperative shifts between i and j states owing to a change in the relative concentration of the i and j solutes in the environment. (○, i th solute; ●, j th solute).

B. *Controlled autocoooperative transition*

Cooperative shift between i and j states owing to adsorption or desorption of cardinal adsorbent, c on the cardinal site in an environment with unchanging i and j concentrations. (Redrawn after Ling and Ochsenfeld 1973a, by permission of Annals of the New York Academy of Sciences.)

transition, once more I draw upon the model of magnetization of a chain of iron nails, shown in Figure 3.1.

Each iron atom possesses a magnetic dipole. In the absence of the external field, these individual magnetic dipoles are randomly oriented and their magnetic fields annul one another. When an external magnet is brought close to one end of the chain of iron nails, the hitherto randomly oriented magnet dipoles of iron atoms suddenly begin to orient themselves in a parallel manner. As a result, a strong magnetic field is created and iron filings in the vicinity are taken up in an ordered array. In the AI hypothesis, an analogous redistribution of electrons or reorientation of electric dipoles in a protein-water-ion system occurs in consequence of the adsorption of a *cardinal adsorbent*. A diagrammatic illustration of the cardinal adsorbent **controlled autocoperative transition** is shown in Figure 7.6B. Here the $i \rightarrow j$ transition in an environment containing unchanging concentrations of i and j is brought about by the adsorption of the cardinal adsorbent c .

The progress of the transition in both time and space is profoundly different in *spontaneous autocoperative transition* and in *controlled autocoperative transition*. In spontaneous autocoperative transition, there is no prescribed time or site where the transition begins and where it ends; in controlled autocoperative transition, the transition always begins in space at the controlling cardinal site, in time immediately following the adsorption or removal of the cardinal adsorbent, progressing centrifugally toward more and more remote sites. Clearly both **directionality** and **timing** are of vital importance for the kind of fine-tuned coordination we observe in physiological activity.

A third distinguishing feature of controlled autocoperative transition is its **one-on-many** relationship. By adsorbing onto a cardinal site, a single cardinal adsorbent brings about the adsorption or desorption of solute molecules on many cooperatively linked *regular sites*, called a *gang* of sites.

A fourth distinguishing feature of controlled autocoperative transition is its **here-to-there** capability, which provides the means to reach from a proximal (cardinal) site to distant (regular) sites.

A more detailed model of controlled autocoperative transition will be presented in Section 7.3.3., following the next section, in which the *cardinal adsorbents* will be the topic of discussion.

7.3.2. *The Definition and Classification of Cardinal Adsorbents*

*I introduced the term **cardinal adsorbent** in 1962, in response to the need for a generic name for a divergent group of biologically potent molecules and ions (e.g., drugs, hormones, transmitters, ATP, Ca^{++}) which occur at low concentrations and yet are capable of bringing about biological responses. These cardinal adsorbents achieve their physiological functions by first combining with key sites which I call **cardinal sites**. Cardinal sites include **receptor sites**, usually found on the cell surface to "receive" drug and other molecules administered from without, as well as other key controlling sites within the cell essential for the maintenance of the living state.*

Drugs have been likened to keys that fit certain lock-like receptor sites.¹ However, a key that fits a lock does not open a door; to open the door, the appropriate key must be **turned**. Until the AI hypothesis was introduced, there was no proposed molecular mechanism equivalent to this turning. *The AI hypothesis suggests that “turning” is electrical polarization (or induction) imposed on the protein-water-ion system by a cardinal adsorbent* which initiates its activity by binding strongly onto an appropriate, usually stereospecific, cardinal site and, in this process, creates strong electronic polarization with far-reaching consequences.

A cardinal adsorbent once adsorbed may draw electrons towards itself. This type of *electron-withdrawing cardinal adsorbent* is given the acronym **EWC**. Another type of cardinal adsorbent donates electrons and is called an *electron-donating cardinal adsorbent (EDC)*. Still a third conceivable type, although an ineffective one, does not draw electrons towards itself nor donate electrons. Nevertheless such an adsorbent does occupy a cardinal site like a fitting but non-turning key, and is called an *electron-indifferent cardinal adsorbent (EIC)* (Ling 1981).

I now present a (still tentative) molecular and electronic scheme whereby an autocoperative transition between two alternative states is triggered by the binding of a suitable cardinal adsorbent.

7.3.3. *A Model Demonstrating How a Cardinal Adsorbent May Initiate and Maintain an All-or-None Change of a Protein System*

7.3.3.1. *Background Concepts and Facts*

The idea that the binding of one *small* molecule on one protein site can produce significant changes on *many* sites *near* and *far* seems at first glance magical and perhaps even unreasonable. It is my intention to demonstrate that this first impression might be the consequence of not seeing the “whole elephant.” To illustrate, let us conduct a thought experiment.

A chain of perfectly balanced and frictionless seesaws are joined end to end with bits of string. Though made of heavy gauge steel, the entire seesaw chain will nevertheless promptly shift to a different configuration when a small mouse lights on one of the terminal tethered seats (Figure 7.7A). There is no magic involved.

However, if one’s view of the seesaw chain is partly blocked, say, by a long wall, as in Figure 7.7B, all one sees is a mouse, weighing not more than an ounce, lifting a steel plate 2,000 times its weight, from a distance of 30 yards away! The look of magic is created.

Like the magnet-controlled chain of tethered nails, the mouse-controlled seesaw chain is introduced to illustrate how an agent can control events, some of which may be far away. In addition, the seesaw model shows how, in these models, the propagated information and energy transfer over distance can be achieved with minimal energy expenditure when the gains and losses of energy in some components of the system are balanced by equal losses and gains of other linked components.

Another important point to be made here is that while, with the mouse sitting

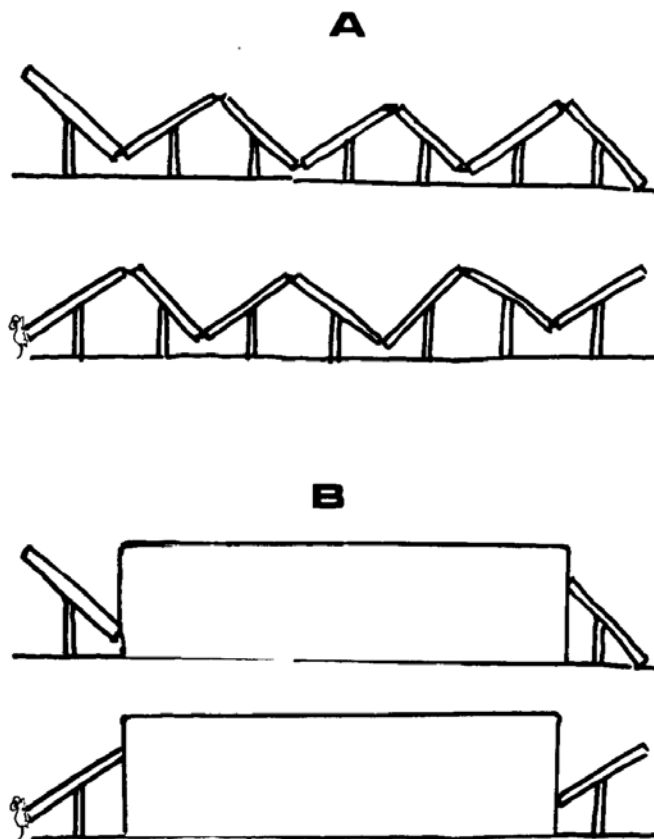


Figure 7.7. *Mouse and Seesaw Chain Model*. Model A demonstrates how extensive changes over long distances can be achieved in a delicately balanced system in response to a minute energy input applied at a suitable site. Partial perception of the system (B) may give the impression of a “magical” happening.

on one end, the seesaw chain assumes one stable configuration (Figure 7.7A), the seesaw does not necessarily revert to the alternative configuration instantly when the mouse jumps off. Instead, with the mouse gone, the perfectly balanced seesaw chain will most likely go back and forth between the alternative configurations in response to random perturbations of air, vibration of the ground, perhaps even loud noise. Indeed, it is precisely this delicately poised and fluctuating condition that makes the most exquisite response control possible.

A similar instability, in fact, is seen increasingly in systems containing isolated proteins and polypeptides, leading to the realization that the concept of proteins as rigid solids must be abandoned. Instead, gathering evidence indicates that **proteins are dynamic systems**. The exceedingly rapid helix/random-coil transition (at 10^{-8} sec. or faster) tells part of the story (Eigen and Hammes 1963; Schwarz and Seelig 1968; Ullman 1970; Wada et al. 1972). Other evidence of intramolecular movements in proteins has been observed (Gurd and Rothgeb 1979), including segmental motions, reversible unfolding, “breathing,” etc. (Careri et al. 1975; Englander and Rolfe 1973).

7.3.3.2. Models of Controlled Autocooperative Transitions via the Indirect F-Process

Before describing the model of *controlled cooperative transition* of protein systems illustrated in Figure 7.8, I need to introduce several new parameters: (These new parameters are referred to in the inset to Figure 7.8.)

(1) the c' -value in Figure 7.8 is analogous to the c -value of anionic sites described in Section 6.2.4, but refers to cationic sites;

(2) the c -value analog (Ling 1962, 57) is the equivalent of the c -value in cases where the negatively charged site, as with the peptide carbonyl group, does not carry a net negative electric charge;

(3) c' -value analog is the equivalent of the c' -value in cases where the positively charged site, as with the peptide amino group, does not carry a net positive electric charge.

Next we generalize the relationships theoretically demonstrated between the c -value and the adsorption energies of different cations, as shown in Figure 6.8, by extending them to c' -value, c -value analogs, and c' -value analogs; we assume

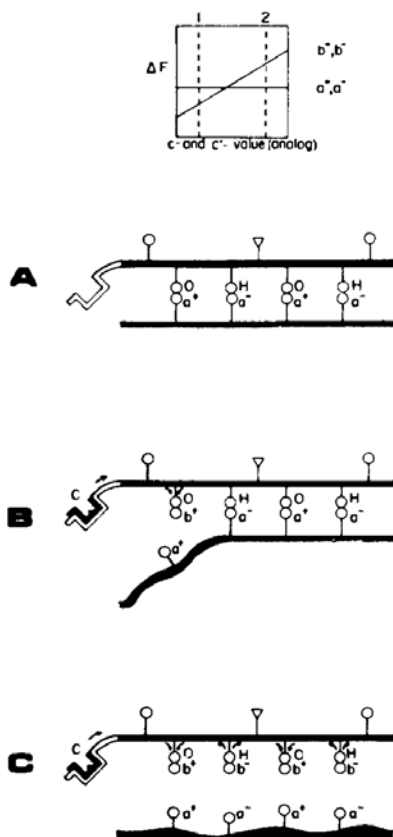


Figure 7.8. A model of controlled autocooperative transition emphasizing backbone sites.

Model of a small segment of a protein chain with backbone peptide groups (H and O) and a cardinal site (C). Adsorption of the *electron-donating cardinal adsorbent*, ω , leads to an all-or-none propagated displacement of the adsorbed a^+ by b^+ and the adsorbed a by b^- . (Modified after Ling 1969, by permission of International Review of Cytology)

that, as these parameters change, the free energies of adsorption of the alternative partners also change at different rates, as indicated by the different slopes of the lines in the inset of Figure 7.8.

Next we examine two specific models. In one model (to be referred to as Model 1), the c -value analog of the carbonyl oxygen and the c' -value analog of the peptide NH groups are initially at the low value of 1 (see inset). In this condition, the CO and NH groups prefer, respectively, the partners a^+ and a^- , as shown in the inset and Figure 7.8A. When W , an electron-donating cardinal adsorbent (or EDC), reacts with the cardinal site C , the inductive effect of W repels electrons, raising the c -value analog of the nearest neighboring CO group (represented as 0 in the figure) from 1 to 2. At this c -value-analog, the inset shows that b^+ is preferred over a^+ , and an exchange of a^+ for b^+ occurs, as shown in Figure 7.8B. Because b^+ is more electron-withdrawing than a^+ , this interchange, on the one hand, reinforces the electron-donating effect of the cardinal adsorbent W , and, on the other hand, withdraws electrons from the nearest-neighboring NH group (represented as H in the figure) "downstream." The result is an increase of the c' -value analog of this NH group from 1 to 2, leading to an analogous exchange of b^- for a^- . This process (known as the indirect F-process) then repeats itself until all the adsorbed a^+ s and a^- s are replaced by b^+ s and b^- s as shown in Figure 7.8C.

In another model (to be referred to as Model 2), the c - and c' -value analogs are initially at a value of 2, and the cardinal adsorbent is not an EDC, but an electron-withdrawing cardinal adsorbent (or EWC). The result of the binding of the EWC would be an all-or-none exchange of the more strongly bound b^+b^- for the more weakly bound a^+a^- .

It is important to note that in response to an EDC, all of the carbonyl groups in the gang of backbone sites have increased their c -value analog; and that in response to the adsorption of an EWC, all the carbonyl groups in the gang have decreased their c -value analog. Since it is primarily the carbonyl groups that determine the strength of the H-bonds the peptides form (see Section 6.2.1.), this uniformity in response is essential for the uniformity of protein behaviors.

Thus far we have focused our attention on the backbone NHCO groups. In fact, all-or-none change also involves functional groups carried on short side chains (see Section 6.2).

To explain the *one-on-many* control of functional groups on short side chains, we can look at the schematic diagram shown in Figure 7.8 from a somewhat different angle. Thus in Figure 7.9 each peptide NH-C-CO group is treated as a single unit. Binding of the EDC (W) causes cascading exchanges of a^-a^+ for b^-b^+ , as in Figure 7.8. However, since the CO group is much more polarizable than the NH group (see Ling 1984, 192), and since the b^- for a^- exchange creates a larger electron-donating effect than the electron-withdrawing effect of a b^+ -for- a^+ exchange, the net effect of exchanging the pair a^-a^+ for the pair b^-b^+ is a donation of electrons to the polypeptide chain along the entire length of the polypeptide chain. **As a result, all functional groups on short side chains will gain electrons in consequence of the EDC interaction with the cardinal site C.** The electron gains in turn would lead to more reactive sulfhydryl groups,

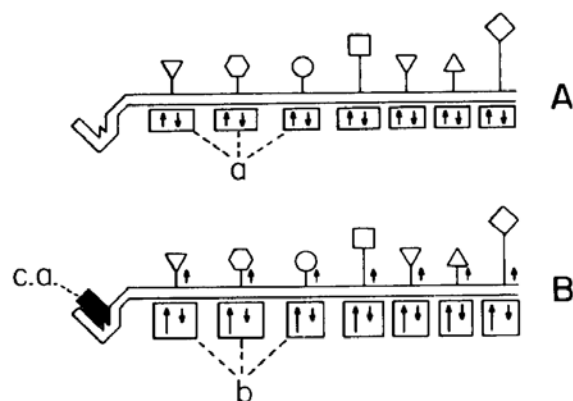


Figure 7.9. A different view of the model of controlled autocoooperative transition presented in Figure 7.8 emphasizing functional groups on short side chains.

Displacement of partners a 's of the backbone NHCO groups by more electron-donating b 's initiated by the adsorption of electron-donating cardinal adsorbent (c.a.) may lead to an increase of electron density of all side-chain functional groups with short side chains as indicated by the arrows. Length of upward arrow in the rectangular boxes indicates strength of electron-donating effect; length of downward arrow in the rectangular boxes indicates strength of electron-withdrawing effect.

quenching of tyrosine and tryptophane fluorescence, higher ϵ -values of β - and γ -carboxyl groups, and other parallel changes. The increase of the ϵ -value of the β - and γ -carboxyl groups leads to increased Na^+ -preference and increased salt-linkage formation. Concomitantly, of course, the higher ϵ -value analogs of the backbone carbonyl groups also bring about the formation of α -helical or other inter- and intramolecular H bonds and the liberation of adsorbed water.

7.4. *Experimental Findings in Harmony with the Theory of Controlled Autocoooperative Transition*

7.4.1. *Allosteric Control by Acid of the Shift between Water Binding to Urea Binding on Bovine Serum Albumin*

From light-scattering studies, Doty and Katz found that, at pH 8, serum albumin in 8 M urea preferentially binds 2000 molecules of urea. At pH 3, the protein preferentially binds 3000 molecules of water (Katz 1950; Doty and Katz 1951; Putnam 1953, 847). Now urea is more strongly bound than water. Note that most proteins are not "denatured" in the presence of 55 M water, but denature in urea at a concentration more than five times lower. Thus one may argue that due to its cationic charge, H^+ acts as an electron-withdrawing cardinal adsorbent or EWC. In the acidic medium (pH 3), H^+ binds onto some key cardinal sites, causing an all-or-none autocoooperative shift from urea to water binding. In general, these remarkable findings agree well with the theoretical Model 2 discussed above (Figure 7.8), where the NH_2 and CO groups of urea are equivalent to b^+ and b^- , and where the H and O and water molecules are

respectively equivalent to a^+ and a^- . The overall effect of the EWC, H^+ , is to produce an all-or-none shift from b^+b^- or urea binding to a^+a^- or water binding.

Bovine serum albumin contains 89 free β - and γ -carboxyl groups and 17 histidine groups (Hughes 1954, 687), the sum of which (106) offers the maximum number of H^+ ions taken up by the protein in consequence of lowering the pH from 8 to 3. As a result of the binding of these 106 (or less) H^+ , 3000 urea molecules are adsorbed by the serum albumin, affirming experimentally the one-on-many relationship of the controlled autocoooperative transition.

Looking back to Section 6.2.2. where I discussed how urea binding on the backbone could lead to greater reactivity of SH groups (carried on short side chains), one might anticipate that acidity would augment the effectiveness of urea in enhancing SH-group reactivity. In fact, this was found true in the case of egg albumin (see Burk 1943; Ling 1962, 176).

7.4.2. Zipper-Like Unmasking of Carboxyl Groups in Response to Acid Binding onto "Trigger Groups" on Ferri- and Carboxyhemoglobin

There is also evidence that acidity influences functional groups on short side chains, i.e., the carboxyl groups. Steinhardt and Zaiser titrated ferri- and carboxyhemoglobin with HCl (Steinhardt and Zaiser 1951, 1955; Ling 1984, 220). In the pH range of 3.1 and 3.5, the binding of two or three H^+ on what the authors referred to as *trigger groups* of the proteins elicited the explosive liberation of 36 carboxyl groups from an originally untitratable condition (Figure 7.10). Like the H^+ described in the study of serum albumin just mentioned, the H^+ here clearly also functions as an EWC.

These findings offer additional, striking experimental verification of the **one-**

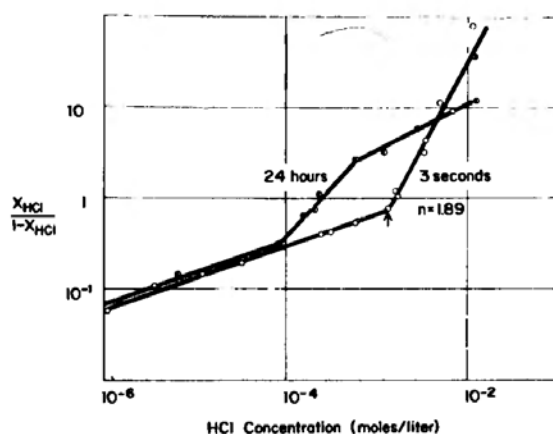


Figure 7.10. Acid binding by carboxyhemoglobin at 25°C. Ordinate represents, on a logarithmic scale, the ratio of the mole fraction of HCl bound over the mole fraction of sites not binding HCl. Abscissa represents, also on a logarithmic scale, the HCl concentration. Total number of acid-binding sites is that given by the authors (i.e., 1.6 moles/kg of protein). The curve labeled "3 seconds" was measured 3 sec. after mixing the protein and acid; the curve labeled "24 hours" was measured 24 hr. after mixing. Arrow indicates that acid concentration at which the protein becomes denatured. Data from Steinhardt and Zaiser (1951). (Ling 1966, by permission of Federation Proceedings)

on-many control of autocoooperative transition already demonstrated in the case of serum albumin. Only here, the target regular sites are not backbone NHCO groups (that adsorb urea), but β - and γ -carboxyl groups on short side chains (that adsorb H^+).

Steinhardt and Zaiser (1955) as well as Ling and Zhang (1984) found that titration with either HCl or NaOH dissociated salt linkages (Section 4.2). In addition, titration with NaOH not only unmasked the β - and γ -carboxyl groups, it also liberated the backbone NHCO groups concomitantly, apparently from an initial state in which they were locked in inter- and intramacromolecular H bonds. As a result, water became polarized and adsorbed in multilayers (see Figure 4.1). In work as yet unpublished, Ling and Hu further show that HCl titration of hemoglobin also liberates the backbone NHCO groups and leads to the polarization of bulk-phase water in multilayers.

When seen together, Steinhardt and Zaiser's findings and those of Ling and Hu showed that the unmasking of β - and γ -carboxyl groups of hemoglobin (previously locked in salt linkages, see Figure 4.1) in consequence of interaction with the EWC (H^+), go hand in hand with the unmasking of the backbone NHCO groups, in harmony with the theoretical model depicted in Figures 7.8 and 7.9.

In the study of serum albumin by Doty and Katz (Section 7.4.1.), the sites adsorbing urea and the (cardinal) sites adsorbing H^+ are distinctly different. In the context of the AI hypothesis, the phenomenon can only be described as *controlled autocoooperative transition*.

It is different in the ferri- and carboxy-hemoglobin titration data. Here, following Steinhardt and Zaiser's own description (1955), some of the H^+ binding sites were seen as "trigger groups". Binding of (the cardinal adsorbent) H^+ on these trigger groups causes the explosive liberation of many other H^+ -adsorbing groups. Yet judging from the pH range involved, the trigger groups as well as the unmasked acid-binding groups are all carboxyl groups—even though their locations in the primary structure, the nature of their neighboring functional groups, etc. may well set apart one or two of the carboxyl groups as the "trigger groups" or cardinal sites. It is in this light that I have used this set of observations to illustrate controlled autocoooperative transitions.

However, the same set of data of Steinhardt and Zaiser shown in Figure 7.10 may be viewed in a different way (as I did earlier, Ling 1962, 1966): then no recognition was given to one or two group(s) as triggering group(s); instead, all acid-binding groups were treated alike. In this case, a log-log plot of the 3-second titration data show two straight-line segments (Figure 7.10). The main portion of the plot shows autocoooperativity with an n value of 1.89, corresponding to a $-\gamma/2$ of +0.39 Kcal/mole. (These values would be higher if the carboxyl groups not linked cooperatively with the main group and shown as the flat segment of the titration curve of Figure 7.10 were excluded).

The positive $-\gamma/2$ represents interaction between the nearest neighboring β - and γ -carboxyl groups. In Section 7.2.2. I have raised the question: how can there be nearest-neighbor interaction between groups that are so far apart? The indirect F-process discussed above, involving both the peptide CONH groups and β - and γ -carboxyl groups on short side chains provides an answer.

7.4.3. *In Vitro* Allosteric Control of Cooperative Binding of Oxygen on Hemoglobin by 2,3-DPG, IHP, and ATP

7.4.3.1. *Quantitative Accord with Theory*

The affinity of hemoglobin for oxygen was dramatically reduced by the binding of inositol hexaphosphate (IHP) or of 2,3-diphosphoglycerate (2,3-DPG) (Chanutin and Curnish 1967). For illustration, *the experimental data points of Benesch and Benesch (1969) are plotted in Figure 7.11, showing how IHP promotes deoxygenation of hemoglobin in a highly quantitative manner. The solid lines going through or near most of the data points are theoretical (according to equation 7), with the assumption that binding of IHP to hemoglobin lowers the intrinsic equilibrium constant ($K_{O_2}^{(0)}$) for oxygen binding on the protein from 3.33 to $0.67 \text{ (mm Hg)}^{-1}$ (Ling 1970a). This agreement between experimental data and theory supports the AI hypothesis. However, it does not prove that this is the only theory that can explain the data.*

For example, one might assume that hemoglobin has the inherent ability to exist in two conformation states, the oxygenated state (*R* state) and the deoxygenated state (*T* state), and that it is the *T* state that has a greater affinity for 2,3-DPG or IHP. However, *it is not at all clear why hemoglobin should exist in two conformation states.* Indeed, as discussed in Section 6.2.1., the structure of a protein is *uniquely* defined by its amino-acid sequence. Since the amino-acid sequence of hemoglobin is finite and unchanging, *there should be only one conformation state.* Secondly, the binding of IHP actually brings about a change of the intrinsic equilibrium constant of the binding of *oxygen* on the heme groups. Such a change is not predicted by the simple two-state model. The explanation offered by the AI hypothesis, to be described, does not suffer these shortcomings.

According to the AI hypothesis, it is in consequence of the multiple binding of a suitable solute [e.g., oxygen on hemoglobin (Figure 7.3), Na^+ and OH^- onto

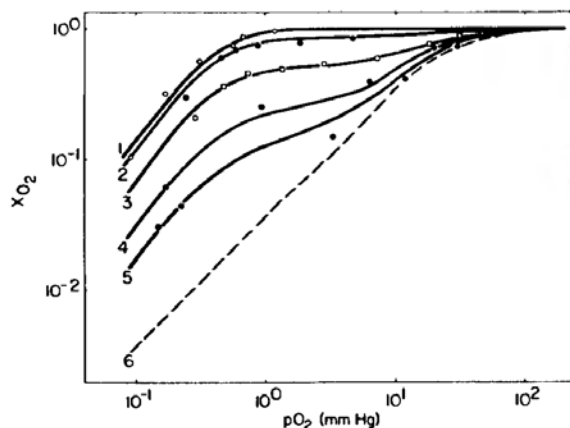


Figure 7.11. Oxygen uptake by hemoglobin in the presence and absence of inositol hexaphosphate (IHP). Hemoglobin solution was 0.3% at pH 7.0, and 10°C. (1) No IHP. (2) $1.2 \times 10^{-5} \text{ M}$ IHP. (3) $2.4 \times 10^{-5} \text{ M}$ IHP. (4) $3.6 \times 10^{-5} \text{ M}$ IHP. (5) $4.8 \times 10^{-5} \text{ M}$ IHP. Points are experimental from Benesch and Benesch (1969). Lines are theoretical, calculated according to theory. (Ling 1970a, by permission of National Academy of Sciences)

alkali-denatured hemoglobin (Figure 7.5), phenol on collagen (Figure 7.4)], **and the strong autocoperative interaction ($-\gamma/2 \gg 0$) each of the binding processes entails, that a second discrete conformation state is created**, comprising both the protein and the solutes it binds. This second conformation state is created because the binding of these solutes has effectively altered the inductive effects exerted by the protein's own unique amino-acid composition and sequence, which together create the one (and only one) native conformation. The cardinal adsorbent, like the mouse of Figure 7.7, then tips the delicate balance in favor of one of these conformation states.

From the theoretical model presented in Figures 7.8 and 7.9, one can expect to find more extensive changes in the hemoglobin molecules than merely alterations in the affinity of the heme sites for oxygen. Indeed, this was precisely what was observed by Max Perutz and his group in their monumental work on the study of hemoglobin. Illustrated in the schematic diagram (partially reproduced here as Figure 7.11) is what Perutz postulated as a possible initial (1) and final (2) conformation during the oxygenation of hemoglobin (Perutz 1970).

This diagram clearly shows that oxygenation and deoxygenation do not involve just the oxygen binding on the four heme sites. Rather, the entire hemoglobin molecule comprising two α -chains and two β -chains undergoes a global change with oxygenation or deoxygenation. Among the many changes, the dissociation and association of salt linkages between β - and γ -carboxyl groups and fixed cations play key roles.

As pointed out earlier, the binding of one molecule of 2,3-DPG or IHP on sites located on the β -chains may bring about a cooperative shift of all four chains from the relaxed, oxygenated R state to the salt-linkage-bound, tense, deoxygenated T state. Under these conditions, 2,3-DPG and IHP function as *cardinal adsorbents*. However, even the complex schematic diagram of Perutz (Figure 7.12) reveals but a fraction of the events that accompany the 2,3-DPG and IHP-induced cooperative transition. Known events that attend the $R \rightarrow T$ transition accompanying deoxygenation include:

- (1) formation of six pairs of interchain salt linkages and two pairs of intrachain salt linkages (Perutz 1970);
- (2) increase of the c -values (and hence pK_a 's) of some anionic groups (Bohr effect) (Bohr et al. 1904);
- (3) an increase of entropy (Manwell 1958);
- (4) a decrease of the reactivity of the sulfhydryl groups (Riggs 1961);
- (5) a decrease of the solubility of hemoglobin in water (Edsall 1958).

Thus *the* binding of a *single* 2,3-DPG or IHP molecule to a hemoglobin molecule brings about not merely a five-fold decrease of the oxygen affinity of *four* remote heme sites (see Figure 7.11), but a global change involving many of the functional groups of all four hemoglobin chains. If attention was exclusively focussed on the changes of the four remote heme sites brought about by the binding of 2,3-DPG or IHP, one might have experienced the same kind of wonderment as when watching a mouse lift a heavy steel plate from 30 yards away. Yet when one sees all of the other associated events, what appears magical

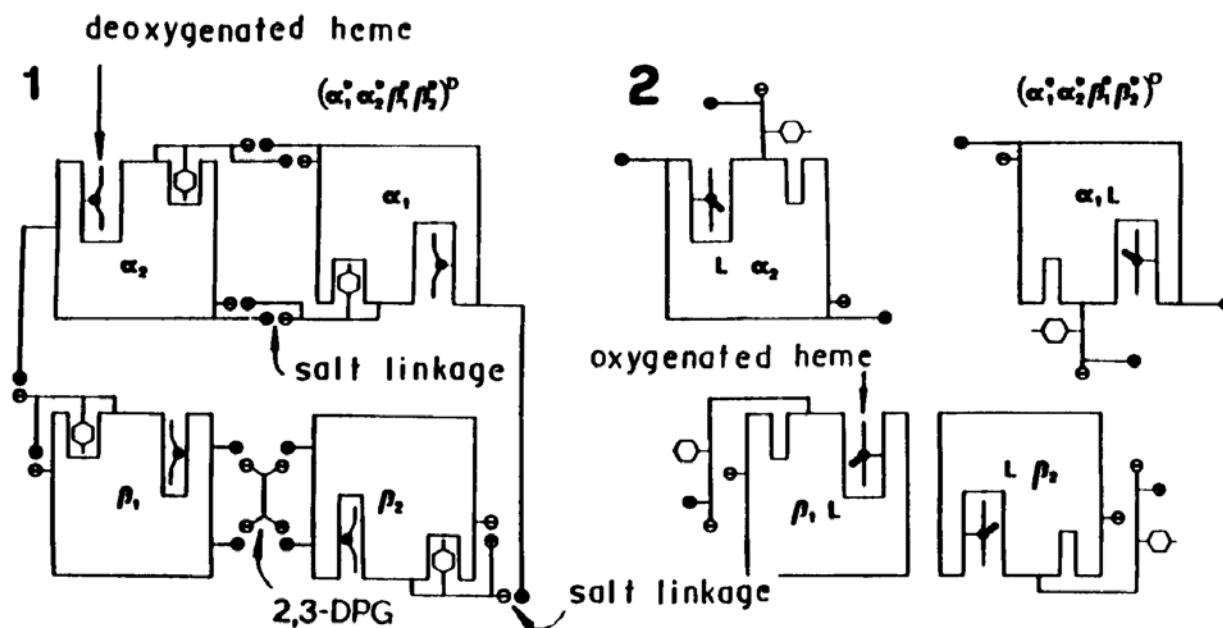


Figure 7.12. The initial (1) and final (2) conformation of hemoglobin during oxygenation according to Perutz (1970). (Perutz 1970, by permission of Nature)

and unreasonable becomes highly reasonable, because the apparent imbalances of energy and entropy are balanced by compensatory changes of energy and entropy.

7.4.3.2. *The Stereochemical vs. The Inductive Mechanism*

As mentioned above, Perutz offered the stereochemical or mechanical interpretation of the heme-heme interaction (see Perutz 1970), while I offered an inductive mechanism (Ling 1964, 1969). It is well known that both the steric and the inductive mechanism act together in the chemistry of small organic molecules. There is no good reason to exclude one or the other in analyzing the behavior of macromolecules like proteins, which are only small organic molecules linked together. I am happy to read a 1979 review by Perutz in which, while still defending his stereochemical view, he also expresses the opinion that the regulation of the oxygen affinity of the heme sites by the protein moiety could be in principle accomplished by inductive effects (Perutz 1979, 383).

Is there evidence in favor of a combined steric and inductive interpretation in the controlled cooperative transition of hemoglobin between the oxygenated and deoxygenated states? Let us examine this question.

Although oxygenation and deoxygenation are not the same as oxidation and reduction, it has nevertheless long been recognized that the two sets of phenomena are very similar (Taylor et al. 1963; Brunori et al. 1964). Thus, like oxidation, oxygenation also involves removal of electrons from hemoglobin; deoxygenation involves donation of electrons to protein. On this basis, one might explain:

- (i) the Bohr effect (i.e., withdrawal of H^+ during deoxygenation) as due to

an increase of the c -value of the acidic groups near and far (increase of pK_a values) as a result of electron donation at the heme site by deoxygenation. A change of c -value from low to high naturally leads to enhanced affinity for H^+ and its withdrawal from the medium as observed;

(ii) an increase in entropy would also follow deoxygenation, with the increase of the electron density of the carbonyl oxygen of the polypeptide chain leading to the increased formation of α -helical and other inter- or intramolecular H bonds with the liberation of adsorbed water and hence entropy gain (Sect. 6.2.1.) (see Lauffer 1975);

(iii) increased salt-linkage formation during deoxygenation as observed by Perutz and coworkers would also follow from the c -value increase of β - and γ -carboxyl groups (see Section 6.2.4);

(iv) loss of solubility of hemoglobin would also follow deoxygenation due to the masking of both hydrophilic NHCO groups of the backbone described in (ii) and the masking of hydrophilic, free ionic side chains described under (i);

(v) if induction alone determines all changes, then deoxygenation should lead to increased reactivity of SH groups (see Section 6.2.2). In fact, the opposite is the case (Riggs 1961)—an unexpected behavior that may become explicable by assuming the burial of the SH group in the T -conformation and its release following oxygenation.

In summary, the **global** change of hemoglobin which may be triggered by the binding of 2,3-DPG or IHP can be explained with combined inductive and stereochemical mechanisms, with induction playing a dominant role.

7.4.3.3. *The Role of ATP as a Cardinal Adsorbent of Vast Importance*

Of great importance is the fact that ATP, like 2,3-DPG and IHP, exercises similar allosteric control on the affinity for oxygen on remote heme sites (Chanutin and Curnish 1967; Chanutin and Hermann 1969; Klinger et al 1971). Since hemoglobin is not an ATPase, the allosteric effect of ATP observed has no relation to ATP hydrolysis, but is entirely due to binding. That is, ATP acts as a bona fide cardinal adsorbent in vitro. The critical role of ATP in the maintenance of the living state and in biological work performance will be extensively discussed in Chapter 8 following.

7.5 Summary

- (1) The chapter began with an analogy of a million tossed coins to illustrate the “random inevitability” where each coin-toss is totally independent of the other coin tosses; and proceeded to show how an assembly of a large number of similar units—like the sentinels guarding the Great Wall of China and the school of swimming fish—can behave coherently as a single entity if there is near-neighbor-interaction among the individual units.
- (2) In the AI hypothesis, coherent behavior of living cells arises primarily from the cell proteins due to the presence of nearest-neighbor interactions be-

tween adjacent NHCO groups on the polypeptide chain and between functional groups carried on short side chains.

- (3) Representing a protein as an infinitely long (or circular) chain with equally spaced sites each capable of adsorbing one i th or j th solute, Yang and Ling have developed an equation (the Yang-Ling adsorption isotherm) which describes the quantitative relationship between the concentration of the i th and j th solute in the surrounding medium, their intrinsic equilibrium exchange constant, $K_{j \rightarrow i}^{00}$, and the nearest-neighbor interaction energy, $-\gamma/2$. When $-\gamma/2$ is large and positive, the shift from i th-solute-adsorption to j th-solute-adsorption is *all-or-none*. This type of transition is called *autocooperative*.
- (4) It was shown that $-\gamma/2$ is a function of the absolute value of $K_{j \rightarrow i}^{00}$.
- (5) With the aid of the Yang-Ling adsorption isotherm, and based on available experimental data in the literature, it was shown that a large and positive value of $-\gamma/2$ exists in the interaction (i) between adjacent NHCO groups of collagen molecules adsorbing phenol, (ii) between heme groups of hemoglobin—carried on short histidine side chains—adsorbing oxygen, and (iii) between β - and γ -carboxyl groups of hemoglobin—also carried on short side chains—adsorbing Na^+ .
- (6) The three types of autocooperative adsorption under (5) represent what is called *spontaneous autocooperative transition* which occurs in response to a change in the relative concentration of the i th and j th solute in the environment. Another type of autocooperative transition occurs in an environment containing unchanging concentrations of i th and j th solute. In this type, called *controlled autocooperative transition*, the all-or-none change of adsorption occurs in response to the adsorption or removal of a *cardinal adsorbent* on a key protein site called a *cardinal site*. Unlike spontaneous autocooperative transition, controlled autocooperative transition exhibits four important characteristics: directionality; controlled timing; one-on-many relationship; and here-to-there capability. Each of these characteristics plays an important role in the coherent behavior of the living cell.
- (7) Cardinal adsorbents were shown to fall into three classes: electron donating cardinal adsorbent (EDC); electron-withdrawing cardinal adsorbent (EWC); and electron indifferent cardinal adsorbent (EIC). Cardinal adsorbents resemble keys in Ehrlich's lock-and-key analogy, but unlike Ehrlich's analogy, which failed to provide the critical "turning" mechanism for the fitting key to produce an opening of the door, the AI hypothesis provides just such a turning mechanism in the form of electrical polarization, or *induction*.
- (8) A mouse-see-saw-chain model was presented to explain how the activity of a delicately balanced system can appear magical (e.g., action at a distance), when the observer sees only a part of the system, as in the fable of the blind men and the elephant.
- (9) A theoretical model describing the step-by-step repeated sequence, called the indirect F -process (and the effect, indirect F -effect) initiated by the adsorption of a cardinal adsorbent: (i) polarization or depolarization of the

nearest-neighbor CO or NH group of the polypeptide chain and (ii) replacement of the partner of the CO and NH groups in consequence of an altered preference for the alternative partners. The net result is a total replacement of one set of partners by an alternative set of partners. Two specific models were examined: in Model 1, the cardinal adsorbent initiating the all-or-none changes is an EDC and in Model 2, it is an EWC. It was pointed out that an EDC tends to increase the electron density (*c*-value analogue) of all the carbonyl groups of the polypeptide chain and an EWC tends to decrease the electron density of all the carbonyl groups.

- (10) A different view of the theoretical model summarized under (9) provides important insight into why interaction with an EWC may also lead to an *across-the-board decrease* of the electron density of all the protein's functional groups on short side chains and why interaction with an EDC may also lead to an *across-the-board increase* of the electron density of all the protein's functional groups on short side chains.
- (11) Two set of important experimental data were cited in support of the theoretical models of *controlled autocoperative transition* summarized under (9). In one, H^+ acting as an EWC brings about a one-on-many adsorption of urea on serum albumin; in the other, H^+ , again acting as an EWC, brings about a one-on-many adsorption of more H^+ on the β - and γ -carboxyl groups carried on short side chains of ferri- and carboxyhemoglobin.

The acid titration of carboxyhemoglobin was also analyzed and treated as a spontaneous autocoperative transition. And with the aid of the Yang-Ling adsorption isotherm, the data provide insight how the *indirect F-process* provides the underlying mechanism for the positive nearest-neighbor interaction among β - and γ -carboxyl groups which are too far apart to depend on the short-range *direct F-effect* for effective operation.

- (12) A third set of experiments supporting the theoretical model is derived from the shift of hemoglobin from the oxygenated state to the deoxygenated state in response to the adsorption of 2,3-diphosphoglycerate, inositol hexaphosphate or ATP. The data are quantitatively described by the Yang-Ling adsorption isotherm.
- (13) Since the secondary structure of a protein is uniquely defined by its amino-acid sequence, it is unjustified to *assume* that a protein can exist in *two* alternative conformations. The AI hypothesis offers a self-consistent interpretation for the existence of two such conformations.
- (14) The theoretical model of controlled autocoperative transition described above implies a **global** change of the protein structure and functional groups even though in the past, attention has been often focused exclusively on one set of such changes, i.e., oxygenation-deoxygenation of hemoglobin. By collecting the available data on other changes involved in the process, and viewing them together, it becomes evident that deoxygenation initiated by, for example, the adsorption of 2,3-DPG, indeed involves a global change of the entire hemoglobin molecule. It was further shown that the results can be explained by inductive mechanisms with some help from a steric interpretation.

- (15) The chapter ends with an affirmation of the experimental proof that ATP can serve as a cardinal adsorbent.

NOTES

1. The lock-and-key analogy has been cited widely from the early days of biology and medicine in explaining the specificity in the interaction of living protoplasm or its constituent parts with drugs and other small molecules. Emil Fischer (1894) used this analogy to describe the specificity in enzyme-substrate interaction. Paul Ehrlich used this concept in his side chain theory where certain receptive side chains of protoplasm bind vital dyes and other molecules with a high degree of specificity. See also Bayliss (1927, 732–734) for discussion on this analogy and its applications.

SOLUTE DISTRIBUTION

Solute distribution is of central importance to cell physiology: the basic mechanism underlying solute distribution also underlies the cell's separateness from its environment and hence its very existence (see Chapter 1). It is therefore not surprising that all of the major theories of the living cell have been developed with a focus on this phenomenon. In preceding chapters I have shown how past theories of the living cell, in which solute distribution is explained in terms of Type I and Type II mechanisms, have failed: neither membranes with sieve-like pores nor metabolic pumps explain solute distribution in living cells.

The original Type III protoplasmic or colloidal theory of the living cell was also rejected, not because it was fundamentally wrong, but because (among other reasons) the foundation science, physics, on which cell physiologists must rely to evolve newer and more defensible theories, was itself immature (see Introduction). However, by the time the new Type III mechanism represented by the association-induction hypothesis was launched in the early sixties, the overall situation had become more favorable. Statistical mechanics, a new branch of physics, offers insights into the properties and behaviors of assemblies of enormous numbers of molecules, which are the building blocks of life. Also, to produce useful products, industry has created highly valuable model systems, including cation-exchange resins—oxygen-containing, water-polarizing polymers like PEO and PVME—which are especially useful to a cell physiologist who must first test new ideas of cell physiology on inanimate models in order to assure their general validity.

The four basic postulations of the AI hypothesis are: (i) reversible specific adsorption of solutes on protein sites in the cell (see endnote 5 of Chapter 3 for definition of adsorption); (ii) reversible multilayer polarization and adsorption of the bulk of cell water, with reduced solvency for large and complex hydrated ions and molecules; (iii) electrical polarization, or induction, which provides the near-neighbor interaction essential for the maintenance of the protein-water-ion system at a discrete resting high-(negative)-energy, low-entropy state (in which K^+ is adsorbed and water polarized), and for its all-or-none transient reversible shifts during cell activity to a discrete lower-(negative)-energy, high-entropy state (in which K^+ is desorbed, and water freed); and (iv) that the control of the autocoperative shifts lies with the adsorption and desorption of *cardinal adsorbent* on key protein sites called *cardinal sites*. An electron-donating cardinal adsorbent (EDC) may cause, by propagated induction, an across-the-board increase of electron density in the CO groups of the polypeptide chain, in the β -

and γ -carboxyl groups and in other functional groups on short side chains. Conversely, an electron-withdrawing cardinal adsorbent (EWC) may cause an across-the-board decrease of electron density of similar groups. Data to be presented below suggest that the magnitude of the electron density change is specific to each cardinal adsorbent, EDC or EWC (Section 9.2.2.3.).

The basic theory of these four individual components of the association-induction hypothesis, as well as the results of their experimental verification, has been presented in the preceding four chapters. Armed with this basic theory, I will deal with the four classic subjects of cell physiology in this and the following three chapters: solute distribution, solute permeability, cell volume and shape, and cellular electrical potentials, in that order. Thus, broadly speaking, we are leaving the area where the emphasis has been on inanimate model systems and on isolated components of the living cell and entering the area where the emphasis will be on the *intact* living cell—the understanding of which constitutes cell physiology proper.

There are two alternative approaches one can adopt to present the association-induction hypothesis and its supporting evidence on the four classic subject of cell physiology proper: to make no further reference to the membrane-pump theory at all; or to include discussions of the membrane-pump theory on each of these four specific subjects as well. It is the second approach I decided to take. However, since a thorough and detailed presentation of the membrane-pump theory on solute distribution has already been presented in Chapter 2, this chapter on solute distribution will be limited to the presentation and discussion of the association-induction hypothesis alone.

It is often said that if one has truly mastered a subject, one can describe it succinctly. The great Chinese artist, Mu-chi did so in his paintings; so did Wolfgang Amadeus Mozart in his music. Scientists are privileged in that they can cast their ideas in the most concise form of all expressions, the form of equations. In the systematic approach to cell physiology illustrated in this and the following three chapters, theory will be presented not only in textual form but also in equations. It is only when cast in this rigorous form that a theory cannot be unwittingly misrepresented and that the predictions of a theory can be put to the most stringent experimental testing, leading to unequivocal conclusions otherwise impossible to achieve.

8.1. *Solute Distribution in Living Cells*

At any moment in time, a solute molecule inside a living cell may exist either free in the cell water or adsorbed on a site which has affinity for this solute. At equilibrium, the number of free solute molecules occupying and leaving the adsorption sites are equal. Similarly, at equilibrium, the number of molecules leaving and entering the cell are equal. If, in a cell, all the adsorption sites for a solute referred to as the *i*th (represented by the symbol p_i) are of the same type, then the total concentration of this solute in the cell (represented as

$[p_i]_{in}$ in units of μ moles per gram of fresh cell) is, according to the AI hypothesis, described by the following equation (Ling 1965b; 1966):

$$[p_i]_{in} = \underbrace{\alpha q_i [p_i]_{ex}}_{\text{free}} + \frac{[f]}{2} \underbrace{\left(1 + \frac{\xi - 1}{\sqrt{(\xi - 1)^2 + 4\xi \exp(\gamma/RT)}}\right)}_{\text{adsorbed}}. \quad (14)$$

The first term on the right-hand side of equation 14 represents free i th solute in the cell water, and is with the exception of the additional term, α , identical to the right hand side of equation 6. $[p_i]_{ex}$ is the concentration of the i th solute in the external medium and is in units of millimolarity. α is the water content of the cell, and is a fractional number in milliliters of water per gram of fresh cells. q_i , a dimensionless number, is the average equilibrium-distribution coefficient of the i th solute between the cell water and the external medium (see Section 5.2.3.). The second term on the right hand side of equation 14 represents adsorbed i th solute, and is identical to the right hand side of equation 7 (the Yang-Ling adsorption isotherm). $[f]$ is the concentration of the adsorption sites and is in units of μ moles per gram of fresh cells. $-\gamma/2$ is the nearest-neighbor interaction energy. Both $-\gamma/2$ and ξ have the same significance as described in Section 7.1.

In cases where there is no near-neighbor interaction and where there are a significant number of vacant sites, the Yang-Ling isotherm term in equation 14 can be replaced by the full Langmuir adsorption isotherm (Langmuir 1916; 1918). Equation 14 then becomes the simpler equation 15:

$$[p_i]_{in} = \alpha q_i [p_i]_{ex} + \frac{[f][p_i]_{ex} K_i}{1 + K_i [p_i]_{ex} + K_j [p_j]_{ex}}. \quad (15)$$

K_i and K_j are the *adsorption constants* of the i th and j th solutes competing for the adsorption sites and are in units of $(M)^{-1}$. The ratio of the adsorption constant for the i th and j th solute is equal to the *intrinsic equilibrium constant* for the i to j exchange adsorption, i.e., $K_i/K_j = K_{j \rightarrow i}^{00}$.

It is conceivable that within the cell there is more than one type of adsorption site for the i th solute, say N types. In that case, the *general equation for the distribution of all solutes in living cells* will be required (Ling 1965; 1966; 1984):

$$[p_i]_{in} = \alpha q_i [p_i]_{ex} + \sum_{L=1}^N \frac{[f]_L}{2} \left(1 + \frac{\xi_L - 1}{\sqrt{(\xi_L - 1)^2 + 4\xi_L \exp(\gamma_L/RT)}}\right), \quad (16)$$

where the second term on the right hand side is the sum of a collection of adsorption isotherms. $[f]_L$ is the concentration of one of all the N types of sites, called the L th. ξ_L and γ_L all have the same meaning as described above, except that they refer to the L th type of sites.

Having presented the general equation 16, I want to point out that since its introduction in 1965, I have yet to encounter a case where this equation was

found necessary in order to describe solute distribution in a living cell. All solute distribution in living cells thus far encountered can be described by equation 14, or by one of its simplified versions discussed below. Paradoxically, it is in the case of adsorption in vitro of a *pure isolated native protein* (bovine serum albumin), that the need of the complex equation 16 was first indicated (Figures 3, 6 in Ling 1966). Thus it seems that nature knows better than a biochemist how to make proteins behave in a uniform manner.

8.1.1. *Solute Primarily in Cell Water*

The simplest version of equation 14 is one in which the *i*th solute is not adsorbed at all. In consequence, the term representing the adsorbed *i*th solute vanishes, and the entire content of the *i*th solute is found in the cell water. At equilibrium, the *i*th solute is then linearly related to its concentration in the external medium:

$$[p_i]_{in} = \alpha q_i [p_i]_{ex} . \quad (17)$$

The equilibrium distributions of all fourteen nonelectrolytes studied in frog muscle and partly shown in Figure 5.8B illustrate the predicted rectilinear distribution pattern of equation 17. Indeed, as I have mentioned repeatedly before, strict rectilinearity indicates that all or virtually all of the solute exists in the cell water (see also endnote 1 of this chapter and endnote 3 of Chapter 5).

In other cases, part of the solute may be adsorbed. However, the adsorbed fraction may be artificially "chased away" by the presence of a high enough concentration of a solute competing effectively for the same sites. When all the adsorbed *i*th solute is thus removed, the remaining *i*th solute in the cell water exhibits rectilinear distribution in agreement with equation 17. This subject will be further discussed below.

Although overwhelming evidence against the Na-pump theory has already been presented, I believe that for a theory so long taught and accepted, additional evidence should still be presented. The benefit of additional reassurance more than offsets the risk of "gilding the lily." In this light I want to point out that ***the simple rectilinear relationship between the solute concentration in the cell water at equilibrium (as ordinate) and that in the water in the external medium (as abscissa) with a slope (i.e. q-value) less than unity, as demonstrated extensively in Figure 5.8B (and in Figures 8.1 and 8.2A), is itself powerful evidence against the pump hypothesis***¹ (see also Ling 1988a).

8.1.2. *Solute in Cell Water and on Adsorption Sites*

The year the basic concept of the AI hypothesis was first presented in its embryonic form (Ling 1951), A. S. Troshin of the Institute of Cytology of Leningrad in the Soviet Union published five short papers (Troshin 1951a, b, c, d, e) in which he introduced an equation describing sugar distribution in living cells and model systems:

$$C_r = C_s K \left(1 + \frac{A}{C_s K + a} \right), \quad (18)$$

where C_r and C_s are the concentrations of the solute in the cell water and external medium respectively; K is the coefficient of proportionality, and equivalent to q_i ; A_∞ , which Troshin called the limit of adsorption, is equal to $[f]/\alpha$; a , which Troshin referred to as "a constant characterizing the curvature of the rise in the adsorption isotherm," is, in comparison with equation 15, equal to $q_i(1 + K_j)/K_i$, or simply q_i/K_i in case the i th solute is the only one present.²

(1) *D-glucose Distribution*

At 0°C, frog muscle does not metabolize D-glucose (Ling et al. 1969). Under this condition, the distribution pattern of this sugar in frog muscle depends on prior insulin treatment or its absence. In the total absence of insulin, D-glucose distribution is rectilinear according to equation 17 with a slope indicating a q -value well below one, i.e., 0.25 (see Figure 8.1 in agreement with its exclusive presence in the cell water). Inclusion of insulin in the preincubation medium adds a hyperbolic fraction to the D-glucose uptake (Figure 8.1). I conclude that insulin acts as a cardinal adsorbent which, by combining with cardinal sites of certain intracellular protein, allosterically makes available D-glucose adsorption sites (Ling and Will 1969, 267–268; see also Ling 1984, 367).

(2) *Na⁺ Distribution*

Figure 8.2A shows Na⁺ distribution in frog muscle cells at different external Na⁺ and K⁺ concentrations. In the presence of a normal concentration of K⁺

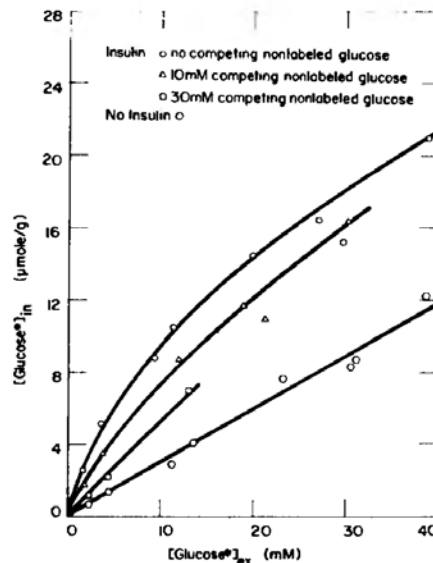


Figure 8.1. Steady level of D-glucose uptake at 0°C in insulin-treated (3 upper curves) and insulin-depleted (lowermost curve) muscles. Mixed muscles were preincubated in Ringer solution containing no D-glucose and no insulin (lowermost curve) or 24 mM D-glucose and 0.1 Unit insulin per ml. for 6 hours at 25°C. They were then incubated overnight at 0°C in Ringer solution containing varying concentrations of nonlabeled D-glucose and labeled D-glucose. (Ling and Will 1969, by permission of Physiological Chemistry and Physics)

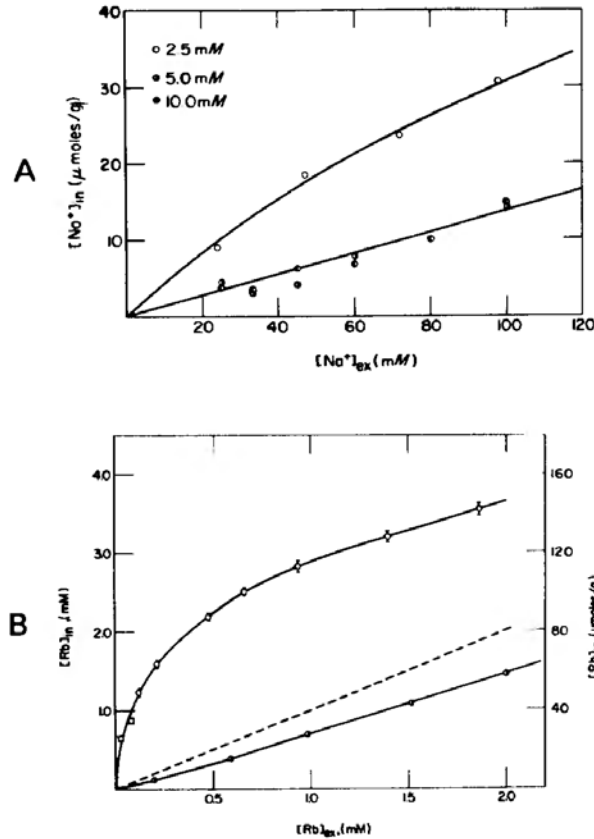


Figure 8.2.

- A. Equilibrium distribution of Na^+ ion in frog sartorius muscle in the presence of varying external K^+ ion concentrations (2.5 mM, 5.0 mM, and 10.0 mM). The data were calculated on the basis of a 10% extracellular space. The slope of the straight line going through the points at the higher K^+ concentrations is 0.14. The muscle cells contain 78% water. If all Na^+ in the cell at the higher K^+ concentrations is assumed to be in the cell water, the equilibrium distribution coefficient of Na^+ between the cell water and the external medium is 0.18.
- B. Equilibrium distribution of Rb^+ in solutions of isolated rabbit actomyosin (0.5% to 3%) at near neutral (6.7) (○) or acidic (4.3) (●) pH. Dotted line represents equipartition of Rb^+ between water in the actomyosin solution within the dialysis bag and external medium. The ordinate represents Rb^+ concentration in water and is applicable to the bottom curve (and the dotted line). Right ordinate represents Rb^+ concentration in $\mu\text{moles per gram of dry protein}$ and is applicable to the top curve. One can estimate the concentration of adsorbed Rb^+ by subtracting the bottom curve from the top curve. At the higher external Rb^+ concentration, the adsorbed Rb^+ concentration is approximately $90 \mu\text{mole/g}$ of actomyosin. (Ling 1969, by permission of International Review of Cytology)

(2.5 mM), the distribution curve can be roughly described by the Troshin equation (equation 18). Increasing concentrations of K^+ (to 5 and 10 mM) reduces the Na^+ concentration to a limiting, unchanging lower level, apparently by “chasing away” the Na^+ adsorbed. Now the distribution curve is rectilinear, in agreement with equation 17 and the conclusion of the presence, under that condition, of Na^+ only in the cell water. The slope of the straight line is well below unity, corresponding to q -value of 0.18 (Ling, 1969).

Figure 8.2B shows equilibrium Rb^+ distribution in isolated actomyosin—the main cytoplasmic protein of muscle cells—in the absence and presence of a significant concentration of competing H^+ . Note that the Rb^+ distribution curves also become a straight line (with a slope less than one) when most adsorbed Rb^+ is chased away by H^+ . Below unity q -value of Rb^+ indicates water polarization by actomyosin at pH of 4.3 (Ling 1969).

(3) Mg^{++} Distribution

The distribution of Mg^{++} in frog muscle can also be described by the Troshin equation (Figure 8.3) (Ling et al. 1979). Only here, the adsorption is very strong. Thus at an external Mg^{++} concentration below 1 mM, the adsorption sites are already fully saturated. With increasing Mg^{++} concentration, the additional Mg^{++} uptake is rectilinear with a slope less than 1, indicating exclusive existence of the additional Mg^{++} in the cell water. The slope of the straight line equals αq_{Mg} , indicating q -values well below one. By estimating the q -value at 5°C ($q = 0.281$) and at 25°C ($q = 0.264$), we were able to assess the underlying mechanism for the low q -value observed, and found it to be primarily entropic. Thus the ΔH determined is moderately favorable for Mg^{++} distribution in frog-muscle-cell water (-0.516 Kcal/mole). This advantage is, however, more than offset by the unfavorable entropy ($\Delta S = 4.37$ cal/degree/mole). Together they produce a positive free energy ($\Delta F = \Delta H + T\Delta S = +744$ cal/mole), and hence the below unity q -value in the cell water.

A remarkable finding also shown in Figure 8.3 is the total indifference of the equilibrium concentration of K^+ to that of Mg^{++} in the cells. Similarly, the

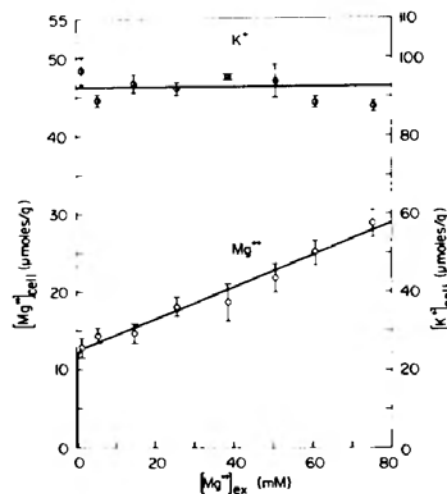


Figure 8.3. Equilibrium Mg^{++} and K^+ distribution in frog voluntary muscles at 25°C. Incubation lasted longer than needed to reach diffusion equilibrium (i.e., 17.5 hrs). Muscles were centrifuged to remove extracellular fluids by the method of Ling and Walton (1975) before extraction of and analysis for Mg^{++} . Each point is the average of four determinations; the distance between the horizontal bars is twice the SE (standard error of the mean). The solid line intersecting most of the Mg^{++} data points is theoretical according to equivalent of equation 15; the numerical values used are $\alpha = 0.78$, $q_{\text{Mg}} = 0.280$, $K_{\text{Mg}}^0 = 10^{-1}\text{M}$, $[f] = 12.3 \mu\text{moles/g}$ fresh muscle cells. (Ling et al. 1979, by permission of Journal of Cell Physiology)

Mg^{++} concentration in the cell was also found to be indifferent to the external K^+ concentration, which was 2.5 or 100 mM (Ling et al. 1979). In other words, while higher concentration of K^+ chased Na^+ away from its adsorption sites, higher K^+ concentration had *no* effect on adsorbed Mg^{++} . This mutual independence of K^+ and Mg^{++} concentrations in the cell is in direct contradiction to the Boyle-Conway theory of ion distribution in frog muscle, as representing a Donnan system of membrane equilibrium and thus being expected to exhibit strong mutual dependence (see equation 2 in Section 2.2.5). The observed mutual indifference is in full harmony with the AI hypothesis, according to which the bulk of K^+ is adsorbed on (isolated) β - and γ -carboxyl groups with no affinity for Mg^{++} . Conversely, sites binding Mg^{++} also have no affinity for K^+ .

8.1.3. Solute Primarily on Adsorption Sites

In the two preceding subsections, we examined Na^+ and Mg^{++} distribution in frog muscles. These differed, for example, from nonelectrolyte distribution in frog muscle cells (Figure 5.8B), in that Na^+ and Mg^{++} are not found exclusively in the cell water, but are also adsorbed. However, relatively speaking, the free fraction in the cell water and the fraction adsorbed on cell proteins are of comparable magnitude.

In this section, I will examine K^+ distribution in frog muscle. Note that the intracellular K^+ concentration (ca. 100 mM) exceeds the extracellular K^+ concentration (2.5 mM) by a factor of 40. Since the q -value of K^+ in muscle cell is well below unity (Ling 1977b), at least 39/40 or 98% of the cell K^+ must exist in the adsorbed state, with the free fraction making up the very small remainder. The question is: can we assume that there is only one type of adsorption site for K^+ , and in consequence, anticipate that K^+ distribution will follow an equation like equation 15? For the sake of simplicity of presentation, I will assume, a priori, that indeed the simpler equation 15 will suffice, and proceed to prove later that this a priori assumption is in fact correct.

Our experiment was to determine the equilibrium concentrations of K^+ in frog muscles which had been incubated in Ringer solutions containing different concentrations of K^+ . We can begin by neglecting the very small amount of free labeled K^+ in the cell water and by assuming further that there is no j th solute present; equation 15 then becomes a specific case of the simplified *Langmuir adsorption isotherm* shown as equation 9:

$$[K^*]_{in} = \frac{[f]K_K[K^*]_{ex}}{1 + K_K[K^*]_{ex}}, \quad (19)$$

where $[K^*]_{ex}$ and $[K^*]_{in}$ are the equilibrium extra- and intracellular concentrations of labeled K^+ respectively. $[f]$ is the concentration of the fixed anionic β - and γ -carboxyl groups in the cell which adsorb K^+ . K_K is the adsorption constant of labeled K^+ (K^*) on these fixed anionic sites. Equation 19 can be written in a reciprocal form:

$$\frac{1}{[K^*]_{in}} = \frac{K_K}{[f]} \cdot \frac{1}{[K^*]_{ex}} + \frac{1}{[f]}. \quad (20)$$

This equation predicts that a plot of $1/[K^*]_{in}$ as ordinate against $1/[K^*]_{ex}$ as abscissa at different $1/[K^*]_{ex}$ should yield a straight line. Experimental verification of this prediction would then confirm the a priori assumption that there is only one type of adsorption site. Experimental data indeed verified this prediction (see line marked 0 in Figure 8.4; see also the bottom line of Figure 8.5). However, we also studied labeled K^+ distribution in the presence of *different* concentrations of competing *nonlabeled* K^+ . For this, a modified equation 15 is needed and is shown below as equation 21:

$$[K^*]_{in} = \frac{[f]K_{K^*}[K^*]_{ex}}{1 + K_{K^*}[K^*]_{ex} + K_R[K^+]_{ex}} \quad (21)$$

where $[K^+]_{ex}$ is the concentration of external competing nonlabeled K^+ . Equation 21 can also be written in a double reciprocal form:

$$\frac{1}{[K^*]} = \frac{K_{K^*}}{[f]} \left(1 + \frac{[K^+]_{ex}}{K_R}\right) \frac{1}{[K^*]_{ex}} + \frac{1}{[f]} \quad (22)$$

Equation 22 predicts that a reciprocal plot of the equilibrium concentrations of labeled K^+ in frog muscle at different external K^+ concentrations, in the presence of different concentrations of competing nonlabeled K^+ concentrations, should yield a family of straight lines that converge on the same locus on the ordinate. The experimental data of Ling and Ochsenfeld (1966) shown in figure 8.4 fully confirm this prediction, and also confirm the underlying a priori assumptions that virtually all K^+ in the cells is adsorbed and that nonlabeled and labeled K^+ compete for the same binding sites of uniform properties. The ad-

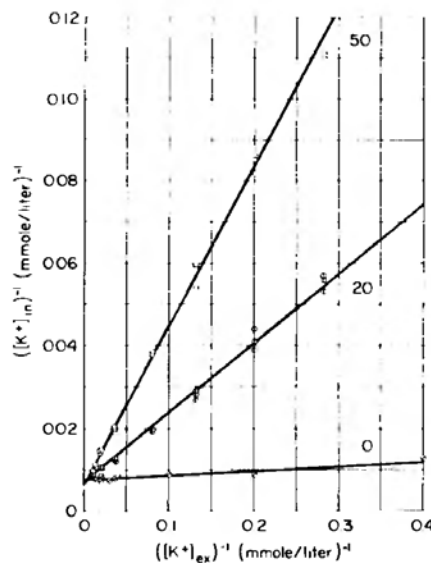


Figure 8.4. Intracellular labeled K^+ concentration plotted reciprocally against the external labeled K^+ concentration, with which it is in equilibrium, in the presence of 0, 20, and 50 μ moles/liter of nonlabeled potassium acetate. Labeled K^+ was in the form of acetate salt. Each point represents the labeled K^+ concentration in a single frog sartorius muscle; lines obtained by the method of least squares. (Ling and Ochsenfeld 1966, by permission of Journal of General Physiology)

sorption constant for both labeled and nonlabeled K^+ average $665 M^{-1}$, corresponding to a free energy of adsorption of -3.85 Kcal/mole. The intercept of the straight lines on the ordinate (equal to $1/[f]$) yields a concentration of K^+ adsorbing β - and γ -carboxyl groups or $[f]$ of 140 mmoles/Kg. This figure is about half the total concentration of β - and γ -carboxyl groups in frog muscle cells estimated from the amino acid composition of all muscle proteins: 260 to 288 mmoles/Kg (Ling and Ochsenfeld 1966). Thus there are more than enough anionic sites for the adsorption of K^+ . Nearly half of the β - and γ -carboxyl groups are not available for K^+ adsorption, presumably because they are locked in salt linkages.

Figure 8.5 shows a reciprocal plot of the effects of 20 and 50 mM external K^+ on the equilibrium concentration of labeled Cs^+ in muscle cells. Here the adsorption constant of Cs^+ estimated is lower than that of K^+ and equal to $488 M^{-1}$, corresponding to a free energy of adsorption of -3.66 Kcal/mole. Figure 8.5 also displays the data on the effects of 20 and 50 mM nonlabeled K^+ on the labeled K^+ distribution from Figure 8.4, to emphasize how much more effective K^+ is in displacing labeled Cs^+ than in displacing labeled K^+ . Since the

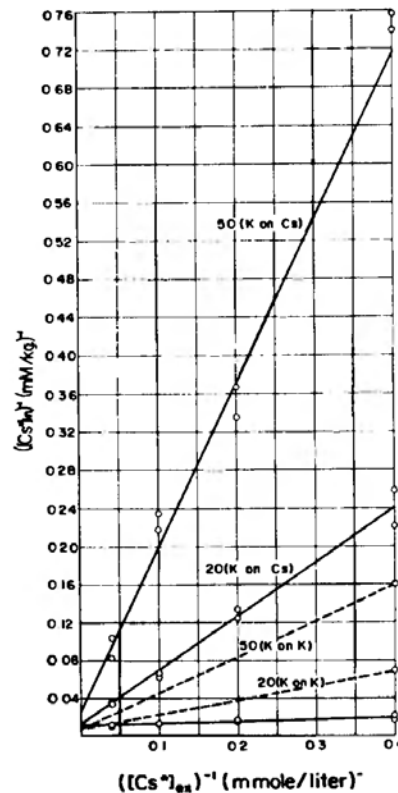


Figure 8.5. Equilibrium labeled Cs^+ concentration in muscle cells plotted reciprocally against the external labeled Cs^+ concentration, with which it is in equilibrium. Competing K^+ concentrations are 0, 20, 50 μ moles/liter, respectively. Both Cs^+ and K^+ were in the form of acetate ($24^\circ C$). Each point represents a single determination on one frog sartorius muscle; lines obtained by the method of least squares. The effect of K^+ ion on the accumulation of labeled K^+ ion (dashed lines) taken from Figure 8.4 for comparison. (Ling and Ochsenfeld 1966, by permission of Journal of General Physiology)

only differences between K^+ and Cs^+ are short-range attributes, this observed difference indicates close-contact adsorption of K^+ as well as Cs^+ , as we have already discussed in Sect. 4.4.2.1.

In summary, the distribution of K^+ and other alkali-metal ions in living cells follows the prediction of a single Langmuir adsorption isotherm, indicating a high degree of homogeneity in the different K^+ adsorbing sites. This is a remarkable phenomenon; it will be discussed again in the following section.

Other studies show that in normal frog muscle, thalium ion (Tl^+) is preferred by the adsorption sites over K^+ by a factor ($K_{K \rightarrow Tl}^{00}$) of about 2 (Ling 1977a; 1984 231 and 241) and that both Tl^+ and K^+ are preferred over Cs^+ . Tl^+ and Cs^+ both played key roles in establishing the localized distribution of K^+ and similar monovalent cations in frog muscle cells (Section 4.4.1).

8.2. Cooperativity in Adsorption in Living Cells

The oxygen uptake of hemoglobin solution in vitro is *autocooperative* and *sigmoid*; oxygen uptake in living red blood cells is also *autocooperative* and *sigmoid* (inset of Figure 8.6). The alkali-metal-ion uptake of alkaline hemoglobin is *autocooperative* and *sigmoid* (Figure 7.5; see also Ling and Zhang, 1984); the equilibrium concentration of K^+ in living frog muscle cells is also *autocooperative* and *sigmoid* (Figure 8.6). The similarity in the autocooperativity in the uptake of oxygen by red blood cells and of the uptake of K^+ by muscle cells gives a new dimension to the qualitative similarity between oxygen uptake and K^+ accumulation first pointed out by Moore and Roaf (1908); in both, adsorption on the principal cytoplasmic protein provides the physiological mechanism for selective accumulation in the cell.

Figure 8.7 shows a log-log plot of the uptake of K^+ (and Na^+) by frog muscle. The solid line is theoretical, according to equation 10, with $K_{Na \rightarrow K}^{00}$ equal to 100

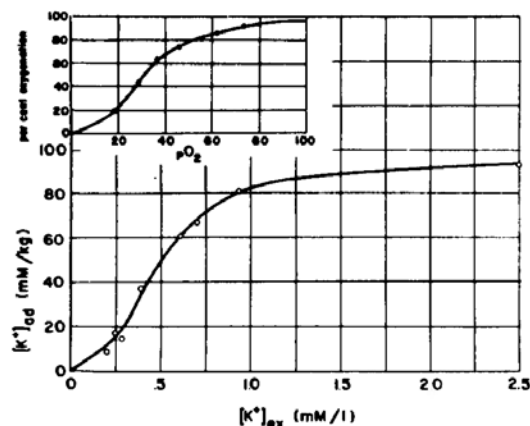


Figure 8.6. Equilibrium K^+ concentration in frog sartorius muscle in solutions with low K^+ concentrations but a high Na^+ concentration. Sterilely isolated sartorius muscles were shaken for 72 hr at 25°C in Ringer solutions containing a fixed concentration (100 mM) of Na^+ and varying low K^+ concentrations indicated on abscissa. Inset shows oxygen uptake by human erythrocytes. (from Ling 1966, by permission of Federation Proceedings)

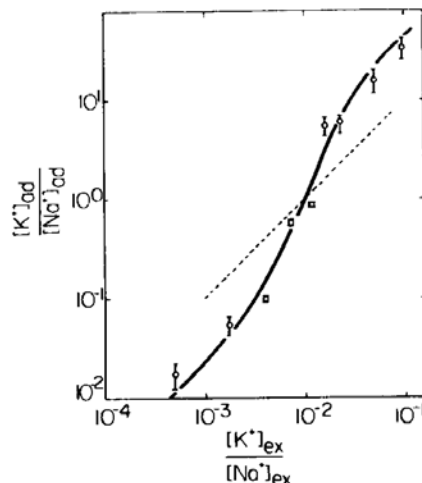


Figure 8.7. Log-log plot of the ratio of the equilibrium concentrations of adsorbed K^+ and adsorbed Na^+ in frog muscle against the ratio of external K^+ and Na^+ concentrations. The solid line is theoretically calculated according to equation 10, with $n = 3.0$ equivalent to a $-\gamma/2$ of $+0.62$ Kcal/mole. $K_{Na \rightarrow K}^{00}$ which is equal to $[K^+]_{ex}/[Na^+]_{ex}$ at equal adsorption of K^+ and Na^+ , is about 100. $\Delta F_{Na \rightarrow K}^{00} = -RT \ln K_{Na \rightarrow K}^{00} = -1.987 \times 298 \times \ln 100 = -2726$ cal/mole or about -2.73 Kcal/mole. Dashed line: $n = 1$, $-\gamma/2 = 0$. (Ling and Bohr 1970, by permission of Biophysical Journal).

and a $-\gamma/2$ equal to $+0.62$ Kcal/mole indicating strong autocoooperativity. The dotted line corresponds to a Langmuir isotherm ($n = 1$, $-\gamma/2 = 0$), which clearly cannot describe the experimental data. One may wonder why K^+ distribution in frog muscle as described in this section shows autocoooperativity with positive $-\gamma/2$, whereas K^+ distribution in the same tissue described in the preceding section demonstrates no autocoooperativity at all, but is perfectly described by a Langmuir isotherm, signifying $-\gamma/2 = 0$.

According to the AI hypothesis, the reason for this difference lies mainly in the different magnitudes of $|\Delta F_{j \rightarrow i}^{00}|$ involved and the relationship between $-\gamma/2$ and $|\Delta F_{j \rightarrow i}^{00}|$ described in equation 13. When the affinities of the adsorption sites for the competing ions i and j are widely different, as is the case where the strongly adsorbed K^+ competes against the weakly adsorbed Na^+ , the absolute value of $\Delta F_{Na \rightarrow K}^{00}$ is large (see legend of Figure 8.7) and equal to -2.73 Kcal/mole. Substituting this value into equation 13, a large and positive $-\gamma/2$ is obtained in agreement with experimental observation. Furthermore, since from the experimental data we already know $-\gamma/2$ to be $+0.62$ Kcal/mole, one can use this value and the value of 2.73 Kcal/mole to calculate from equation 13 a value of the nearest neighbor transmissivity factor, τ . Following this procedure, I obtained a τ value of 0.23 for the cooperative adsorption of K^+ and Na^+ in frog muscle.

It is quite a different story when the competing ions have roughly similar adsorption energies, as in the case where strongly adsorbed K^+ competes against strongly adsorbed labeled K^+ or Cs^+ .

Since the adsorption constant of *nonlabeled* K^+ and *labeled* K^+ may be assumed to be roughly equal, $K_{K \rightarrow K^*}^{00} = 1$ and $\Delta F_{K \rightarrow K^*}^{00} = -RT \ln K_{K \rightarrow K^*}^{00} = 0$ Kcal/mole.

Using the value of τ obtained above (0.23), one calculates from equation 13, $-\gamma/2 = +\tau \Delta F_{K^+ \rightarrow K^+}^{00} = +0.23 \times 0 = 0$ Kcal/mole as observed. Similarly in the case when K^+ competes against Cs^+ , the data shown in Figure 8.5 yield $K_K = 665 M^{-1}$ and $K_{Cs} = 488 M^{-1}$. $K_K/K_{Cs} = K_{Cs \rightarrow K}^{00} = 665/488 = 1.36$. $\Delta F_{Cs \rightarrow K}^{00} = -RT \ln 1.36 = -0.183$ Kcal/mole. $-\gamma/2 = +0.23 \times 0.183 = +0.04$ Kcal/mole, which is too small to be detected, again confirming equation 13.

Since the autocoperative uptake of K^+ and Na^+ was first reported (Ling 1966), there have been extensive reports of the study of K^+ and Na^+ distribution in a wide variety of tissues, including canine carotid arteries, rabbit myometrium, guinea pig smooth muscle, human lymphocytes, and Ehrlich carcinoma ascites cells. The K^+ and Na^+ distribution in these tissues also follows equation 14, with $K_{Na \rightarrow K}^{00}$ and $-\gamma/2$ quite close to the values from frog muscle (see Ling 1984, 347 for a more detailed review).

As mentioned earlier, the fact that the adsorption of K^+ and Na^+ in all of these tissues can be described by a single adsorption isotherm, rather than requiring a multitude of isotherms, is truly remarkable. Indeed this adherence to an equation containing a single adsorption isotherm seems to be the rule with all living cells thus far studied. Homogeneity produced by the assembly of vast numbers of highly similar units, like those in a large school of ocean fish, is of vital importance in functional coherence and effective control beside the presence of a positive energy of near-neighbor interaction, $-\gamma/2$.

8.3. Control of Cooperative Adsorption and Transition

In preceding sections of this and previous chapters, I have shown the obedience of experimental data to equation 14 for solute distribution in living cells or its simplified versions. Also shown were the size-dependent rectilinear distribution of *all* solutes in cell water studied (Figure 5.8B), and the existence of *some* solutes on specific adsorption sites which, under suitable conditions, exhibit positive nearest-neighbor interaction and autocoperativity. In discussing D-glucose distribution in nonmetabolizing frog muscle (0°C), I also pointed out how, with prior incubation in the presence of insulin and a *primer* (e.g., D-glucose, D-xylose), hidden D-glucose adsorbing sites are unmasked for the adsorption of this sugar and other structurally similar sugars at 0°C without altering the q -value for D-glucose (Ling et al. 1969b; Ling and Will 1969). Thus insulin is a cardinal adsorbent whose primary activity in this case is on the protein that provides D-glucose adsorbing sites; insulin apparently exercises little or no action on the water-polarizing proteins of the same muscle cells. In this section I analyze the control of solute distribution by two other cardinal adsorbents, Ca^{++} and ouabain. A third cardinal adsorbent, ATP, will be the subject of a new section, due to its crucial importance.

8.3.1. Control by Ca^{++}

Ca^{++} , like ATP, helps to conserve the cell in its normal, resting, living state; both ATP and Ca^{++} are referred to as *conservative cardinal adsorbents*, to be dis-

tinguished from many other cardinal adsorbents which often act to move a cell away from its resting, living state. However, this separation of conservative and nonconservative cardinal adsorbents is by no means absolute. Under differing conditions, a conservative cardinal adsorbent may act in a fashion opposite to its customary pattern.

Figure 8.8 shows the effect of varying Ca^{++} concentrations on the accumulation of K^+ in strips of smooth muscle, called taenia coli, found along the side of the intestine of guinea pigs. The points are experimental; the solid lines are theoretical according to equation 14 (Gulati 1973). Comparing the data with data in Figure 7.11, one finds that whereas inositol hexaphosphate (IHP) as well as 2,3-diphosphylglycerate and ATP *decreases* the affinity of hemoglobin for oxygen, Ca^{++} *increases* the affinity of K^+ (over Na^+). $K_{\text{Na} \rightarrow \text{K}}^{\text{O}}$ increases as a result of interaction with Ca^{++} .

8.3.2. Control by Ouabain

Since Schatzmann's demonstration in 1953 that cardiac glycoside inhibits the regain of K^+ and extrusion of Na^+ in K^+ -depleted red blood cells, it has been widely believed that cardiac glycoside in general and ouabain in particular are specific inhibitors of the Na pump. This belief was invalidated by the demonstration, with the aid of the effectively membrane-pump-less, open-ended cell (EMOC) preparation, that ouabain action on K-Na distribution does not require a functional cell membrane (and hence postulated Na pump) (Figure 8.9) (Ling 1973; 1978). Extensive evidence now demonstrates that ouabain acts as a cardinal adsorbent increasing the relative affinity of the cytoplasmic β - and γ -carboxyl groups for Na^+ . The following three subsections discuss this subject in more detail.

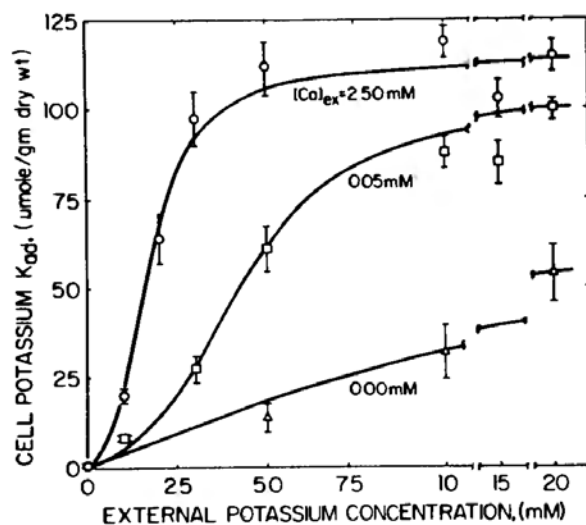


Figure 8.8. The effect of Ca^{++} concentration on the equilibrium concentrations of K^+ in guinea pig smooth muscle (taenia coli) at various K^+ concentrations. The solid lines are theoretical according to equation 14. The term $aq_{\text{K}}[\text{K}^+]_{\text{e}}$ is very small and ignored. (Gulati 1973, by permission of Annals of New York Academy of Science)

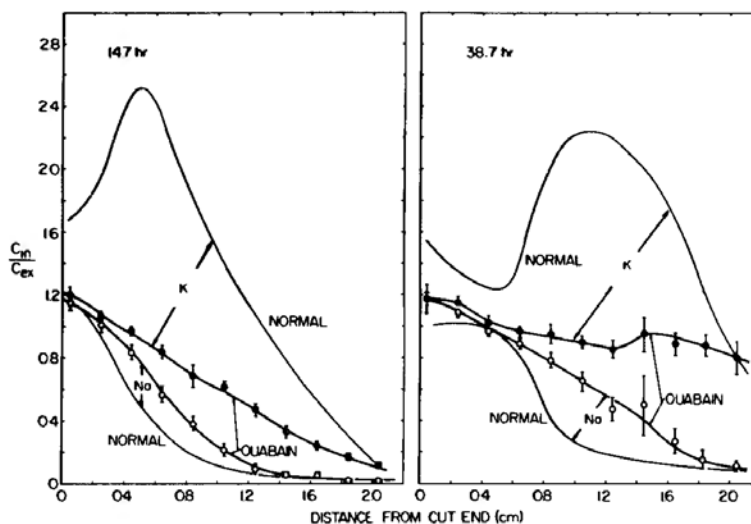


Figure 8.9. Effect of ouabain on the accumulation of labeled K^+ and Na^+ by EMOC preparations of frog sartorius muscles through their cut ends. Experimental procedures used were the same as those described in the caption of Figures 4.12 and 4.13 except that the Ringer solution bathing the cut end of the muscles contained initially 10^{-4} M ouabain. Continuous lines without experimental points were reproduced from the data of Figure 4.13 providing a basis for visualizing the effect of ouabain. (Ling 1978, by permission of Journal of Physiology)

(1) Effect on $K_{Na \rightarrow K}^{00}$

Different concentrations of ouabain alter quantitatively the equilibrium cell- K^+ levels in a manner similar to the effect of different concentrations of inositol hexaphosphate (IHP) on the oxygen uptake of hemoglobin (Figure 7.11), affirming that ouabain, like IHP, acts as a cardinal adsorbent (Figure 8.10).

In trying to drive home the similarity between the binding of one solute (oxygen) on one type of cytoplasmic protein (hemoglobin) and the binding of another solute (K^+) on another type of cytoplasm protein (myosin), I have deliberately refrained from mentioning Na^+ , which competes against K^+ for the same sites (Section 8.2). In oxygen binding, little attention is paid to what occupies the heme site when it does not bind oxygen. It may be vacant, or occupied by one or more water molecule(s). In K^+ binding in living cells, Na^+ is usually the alternative adsorbent. That is, in terms of equations 7 or 14, if K^+ is called p_i , then Na^+ is p_j . This is a one-for-one displacement, a relationship that is most clearly illustrated in Figure 8.11. Focusing on the X-shaped pair of curves to the left, one notices that the abscissa represents not just the K^+ concentration, but its ratio to Na^+ concentration in the external medium. As this ratio decreases from right to left, the equilibrium K^+ concentration in the cell drops in an *autocooperative* manner, and is paralleled by a mirror-image *autocooperative* uptake of Na^+ . The K^+/Na^+ concentration ratio on the abscissa corresponding to half-occupancy by K^+ and half-occupancy by Na^+ is equal to the reciprocal of the intrinsic equilibrium content, $K_{Na \rightarrow K}^{00}$, shown as $K_{j \rightarrow i}^{00}$ in equation 7 and in equation 14.

Next we turn to the second X-shaped pair of curves to the right in Figure

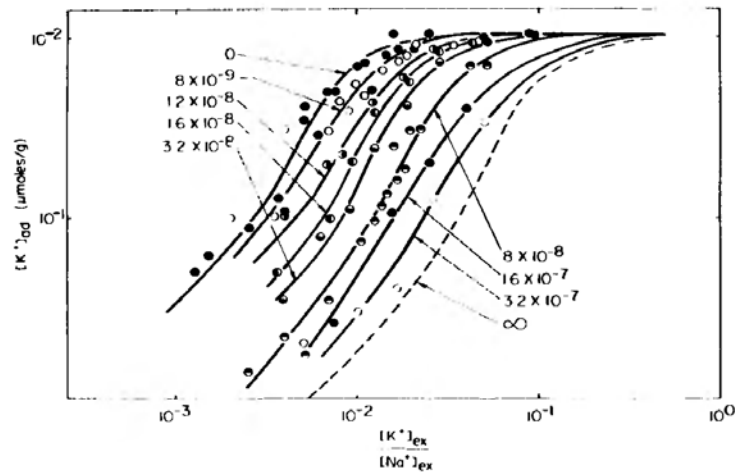


Figure 8.10. Effect of different concentrations of ouabain on the equilibrium concentrations of K^+ in frog muscle (25°C). Each point is the average of four determinations. Standard errors of the means, comparable in size as those shown in the following figure (Figure 8.11) are not shown to avoid confusion. Numbers in graph refer to the molar concentrations of ouabain in the external media. (Ling and Bohr 1971, by permission of Physiological Chemistry and Physics)

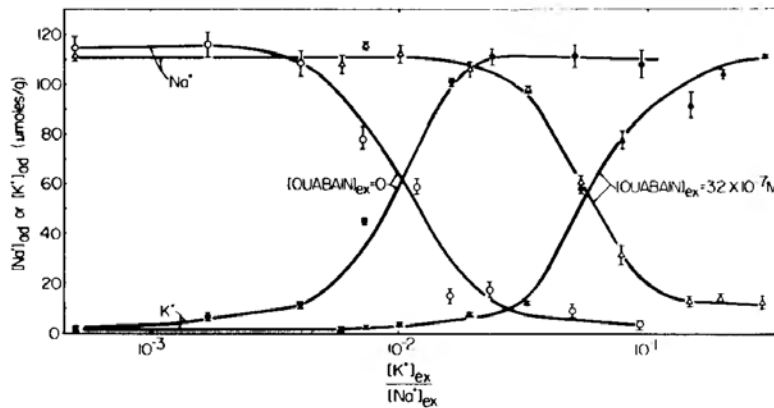


Figure 8.11. Effect of $3.2 \times 10^{-7}\text{M}$ ouabain on the equilibrium distribution of K^+ and Na^+ ion in frog muscle. Curves with open (Na^+) and filled (K^+) circles were equilibrium concentrations in control muscles not treated with ouabain. Curves with open (Na^+) and filled (K^+) triangles are equilibrium concentrations of ouabain-treated muscles. The point of intersection of the K^+ and Na^+ curves gives a $K_{\text{Na} \rightarrow \text{K}}^{00}$ of 100 in normal muscle. In muscles treated with ouabain, $K_{\text{Na} \rightarrow \text{K}}^{00}$ has shifted to 21.7. (Ling and Bohr 1971, by permission of Physiological Chemistry and Physics)

8.11. Here the muscles were equilibrated for about 72 hours at 25°C in the presence of different K^+ concentrations and a constant (100 mM) Na^+ concentration, in addition to $3.2 \times 10^{-7}\text{M}$ ouabain. As already shown in Figure 8.10, ouabain pushes both the K^+ and Na^+ adsorption curves to the right without major changes in the shape of the curves. $K_{\text{Na} \rightarrow \text{K}}^{00}$, however, has dramatically fallen from 100 to 21.7. Thus ouabain binding onto cardinal sites has produced a **uniform**

change in all the K^+ -adsorbing β - and γ -carboxyl groups in the muscle, decreasing their $K_{Na \rightarrow K}^{00}$, in agreement with theory (Figures 7.8 and 7.9).

(2) *The Adsorbed State of K^+ and of Na^+*

There is now conclusive evidence that the K^+ in frog muscle cells is adsorbed on the β - and γ -carboxyl groups of cytoplasmic proteins (Chapter 4). Seen in this light, the stoichiometric displacement of K^+ by Na^+ may simply represent an ion exchange: adsorbed Na^+ for adsorbed K^+ . However, a living cell is much more complex than a cation-exchange-resin bead in that there is always another type of competitor for the β - and γ -carboxyl groups, e.g., the fixed cations—as we have clearly demonstrated in the binding of Na^+ in vitro by hemoglobin (Figure 4.2). The Na^+ gained could therefore also be due to an increase in water solvency (Section 5.2.5.1). In the present case of frog muscle, however, there is independent evidence that the bulk of cell Na^+ that has replaced K^+ is also adsorbed.

One kind of evidence is from ^{23}Na -nuclear-magnetic-resonance (NMR) studies. They show that Na^+ that has replaced K^+ , in a low K^+ Ringer solution or in response to ouabain, is partly NMR-invisible and in an adsorbed state³ (Table 8.1). Similar NMR-invisible adsorbed Na^+ in liver tissues can be made visible when it is displaced from adsorption sites by adding high concentrations of competing cations (Monoi 1976; Ling 1984, 266).

A second type of evidence comes from the autoradiographic studies of Edelmann (1986). In frozen hydrated frog muscle previously loaded with ^{22}Na -labeled Na^+ the labeled ion is not evenly distributed, but is also primarily localized in the A-bands like ^{134}Cs or ^{86}Rb in Cs^+ - and Rb^+ -loaded muscles (Figure 4.7d) and K^+ in normal frog muscle (Figure 4.10).

The adsorbed state of the Na^+ , its apparent occurrence at the same loci normally occupied by K^+ , and the stoichiometry of the $K^+ - Na^+$ displacement, all considered together, offer compelling reasons that the Na^+ -for- K^+ exchange represents a displacement of one ion by another on the same adsorption sites.

Table 8.1. Concentration of Na^+ and K^+ in Frog Sartorius Muscle Preserved in a Medium with a Low K^+ Concentration (0.2–0.5 mM) and 118 mM Na^+ (Ling and Cope 1969, by permission of *Science*.)

Duration of <i>in vitro</i> incubation (days)	Total K^+ (μ mole/g)	Total Na^+ (μ mole/g)	NMR-visible Na^+ (μ mole/g)	NMR-invisible Na^+ (μ mole/g)	Sum of NMR-invisible Na^+ and total K^+ (μ mole/g)
0	89.9	23.3	9	14	104
2–5	34.5	81.3	28	54	89

Note: Total K^+ and Na^+ contents determined from hot HCl extracts by flame photometry. NMR-visible Na^+ determined with a wide-line spectrometer. NMR-invisible Na^+ determined as the difference between total Na^+ and NMR-visible Na^+ concentrations. Means of nine muscles incubated 2–5 days.

As illustrated in Figure 7.6A in more general terms, such a displacement takes place as a result of reduced external K^+ concentration in a Na^+ -rich environment. The highly similar $K^+ \rightarrow Na^+$ displacement brought about by exposure to ouabain in the presence of unchanging external K^+ (and Na^+) concentrations is less direct, but of even greater significance. As a special case of the control of autocooperative shift between the i th and j th state illustrated in Figure 7.6B, the ouabain control of the transition between the K^+ and the Na^+ state serves as an *in vivo* experimental demonstration that ouabain at very low concentrations can alter the relative preference for K^+ versus Na^+ of many far-removed protein carboxyl groups. In this, the ouabain action resembles that of IHP in altering the affinity for oxygen of hemoglobin sites (compare Figure 8.10 with Figure 7.11).

On the basis of the theoretical curves presented in Figure 6.9, one deduces that the effect of ouabain binding onto the cardinal sites, which control the K^+ binding sites, is to change the c -value of the K^+ -binding, β - and γ -carboxyl groups. Such a c -value change could lead to the observed decrease of the preference for K^+ over Na^+ . However, either an increase or a decrease in c -value could increase the relative preference for Na^+ (versus K^+). This ambiguity can be overcome by a new method, described next.

(3) *Ouabain Control of Autocooperative Transition between the K^+ and the Na^+ State by Increasing the c -value of β - and γ -carboxyl Groups: Ouabain as an EDC*

The new method that can diagnose whether an increase or a decrease in the relative preference for Na^+ is due to an increased or decreased c -value involves the determination of *five* alkali-metal ions in the cells before and after ouabain treatment: Li^+ , Na^+ , K^+ , Rb^+ , and Cs^+ . The method relies on the fact that a c -value *increase* will affect the relative preference of all five alkali ions in a way unequivocally different from the relative preference change produced by a c -value *decrease* (see Figure 6.9).

With this method, Ling and Bohr (1971) studied the equilibrium distribution of Cs^+ , Rb^+ , K^+ , Na^+ , and Li^+ in frog muscles in the presence of $3.2 \times 10^{-7} M$ ouabain (and in its absence). A new equilibrium was reached after incubation for three days at $25^\circ C$. The different steady levels of the five alkali-metal ions in the cells before and after ouabain (Figure 8.12) exhibit a rank order which, by and large, agrees with the theoretical rank order expected accompanying a c -value rise from -4.20 \AA to -3.25 \AA , but do not fit the pattern of distribution of c -value lower than -4.20 \AA (Figure 6.9). These findings demonstrate that ouabain is indeed an electron-donating cardinal adsorbent, or EDC.

Summarizing, one finds that insulin, Ca^{++} , and ouabain all can act as cardinal adsorbents controlling the adsorption of one or another type of solute on cell protein(s) without markedly disturbing the q -value of the solute in the cell water. Each of these cardinal adsorbents can only act on the cell, producing the changes observed if and only if the cell is maintained at its normal *resting living state*. The maintenance of the resting living state depends on the adsorption of other *conservative cardinal adsorbents*. The premiere conservative cardinal adsorbent is ATP (see Section 8.4 following). That is, if ATP is absent, the cell would be dead. On dead cells, insulin, Ca^{++} and ouabain cannot exercise their normal controlling functions. From this perspective, insulin, Ca^{++} and ouabain must be considered

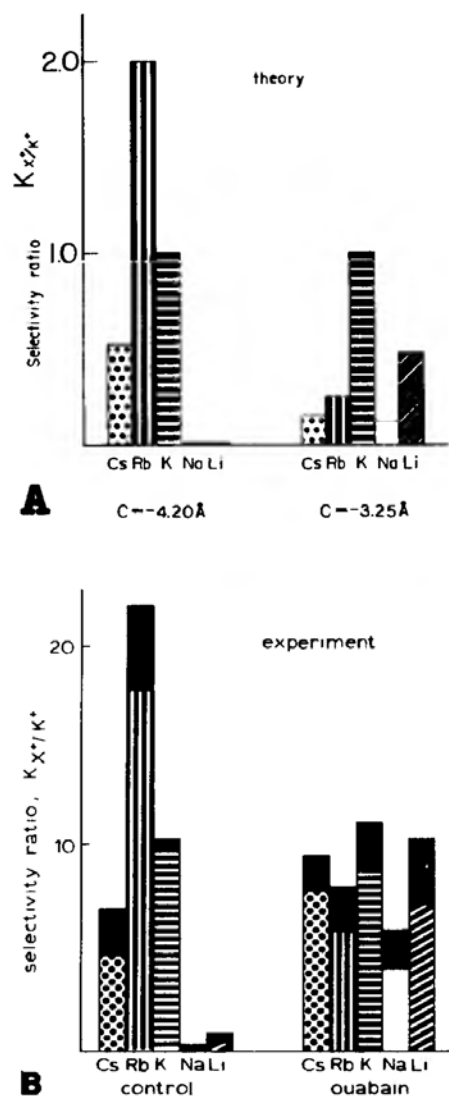


Figure 8.12.

- (A) Theoretical selectivity ratios obtained from Figure 6.9 at c -values of -4.20 and -3.25 Å, respectively.
- (B) Experimental selectivity ratios measured in normal control frog muscle and in muscle treated with 3.27×10^{-7} M ouabain. (Ling and Bohr 1971, by permission of Physiological Chemistry and Physics)

as *secondary cardinal adsorbents*. They modify the living state; they cannot maintain it.

8.3.3. *The Indifference of the q -Values of Large Solutes in Cell Water after Exposure of Cells to Insulin, Ouabain and other Secondary Cardinal Adsorbents*

As mentioned above, there is no pronounced change in the overall q -value of D-glucose, Na⁺ or other similar large solutes in the cell water in response respectively to insulin, Ca⁺⁺ or ouabain treatment—which dramatically brought about changes in the autocoooperative adsorption of D-glucose or K⁺/Na⁺ as the

case may be (Figures 8.1 and 8.8 to 8.10). Yet in the theoretical model of controlled autocoooperative transition (Section 7.3.3.), profound change in the relative affinity for K^+ and for Na^+ on β - and γ -carboxyl groups, for example, would not have been possible without the changing of the partners of the backbone NHCO groups. The most likely alternative partners of the backbone NHCO groups are: water and other backbone NHCO groups. If water is either adsorbed or desorbed, one would have expected to see changes of the q -value for Na^+ , contrary to observation.

While there are other possible alternative interpretations, the following one seems to me at this moment the most likely. Only future investigations can tell us if this is indeed the correct choice.

Teleologically speaking, the invariance of the water content of each type of living cell discussed in Section 5.2.5.3. suggests that gross and lasting depolarization of the cell water—which leads to water loss from the cell—is inimical to the cell's well-being. If this surmise is correct, then an apparent dilemma seems to have arisen from the need on the one hand of keeping the overall polarization of cell water unchanging and on the other hand the opposing need of permitting autocoooperative transitions that involve the polarization or depolarization of cell water.

In Section 5.2.2, I have shown that it would only take a fully-extended protein making up 5% of the weight of a cell to polarize all the cell's water. With this in mind, it seems that a logical solution to the dilemma would be to keep the entire water content polarized at all times by maintaining a small amount of more-or-less uniformly distributed cell protein in the fully extended state at all times. With this provision on hand, the effect on the overall dynamic water structure by the polarization or depolarization of a part of the cell's water would be, so to speak, buffered out. (For recent exciting new discoveries that are relevant to the present problem, see Endnote 5.)

That there is indeed a strong buffering capacity for added free water (by depolarization of previously polarized water) is shown by a lack of observable increase of the q -value of (non-adsorbed) pentoses in frog muscle cells which have been exposed to a hypotonic Ringer's solution and have in consequence gained much (free) water from the outside medium (Ling and Ochsenfeld, unpublished). Additional polarization of water already polarized, would produce, like "gilding the lily," a minimum effect.

In the following section on the control of ion adsorption and water polarization by the premier conservative cardinal adsorbent, ATP, I will point out some experimental observation that may have bearing on the existence of the postulated pervasive water-polarization-buffering protein(s).

8.4. *The Role of ATP in Maintenance of the Living State and in Work Performance*

In the opening section of Chapter 3, I used the nail-and-iron-filing model to illustrate how a magnet interacting with nails can increase the (negative) energy

and decrease the entropy of a system of nails and iron filings (Section 3.2). I also suggested that, in living cells, proteins may be compared with the nails, K^+ and water with the iron filings, and ATP with the magnet. But then how does one reconcile such an analogy with the concept taught in many textbooks that ATP contains a pair of “high energy phosphate bonds,” and that this energy trapped in the phosphate bonds is liberated to fuel biological work performance? The answer is that many textbooks tell only *part* of the story of ATP, which was initially widely hailed, with good justification, as the most important discovery of biochemistry; the part of the story often not told, however, has dramatically changed the picture of ATP function, as will be described next.

8.4.1. *ATP as a Reservoir of Utilizable Energy; the Attractive but Incorrect High Energy Phosphate Bond Concept*

Adenosine triphosphate (ATP) was discovered by K. Lohmann (1935). The initial calorimetric measurements of the heat of hydrolysis of ATP and other organic phosphates, by O. Meyerhof and his coworkers, yielded a heat of hydrolysis (ΔH) equal to -12 Kcal/mole of each phosphate bond, which was believed to be much higher than the ΔH of hydrolysis of ordinary, low energy phosphate bonds. Lipmann (1941) elaborated on the concept: that this excess high energy resides in high energy phosphate bonds (represented by the symbol $\sim P$), and that this energy can be harnessed to do all sorts of biological work. Thus actomyosin, the protein in muscles that provides the mechanism of contraction, was found also to possess specific enzymatic activity splitting ATP into ADP and inorganic phosphate. It was argued that energy stored in the $\sim P$ of ATP is thus liberated and utilized directly to perform mechanical work by the very same protein, actomyosin. It was certainly a most attractive idea.

Unfortunately, more precise calorimetric studies revealed that the ΔH of the phosphate bond of ATP is not different from other phosphate bonds (-4.7 Kcal/mole), and that the measured free energy of hydrolysis of ATP to AMP (equal to -14.0 Kcal/mol.) is largely an *artifact* due to the hydrogen-ion liberation (see Section 2.2.3., including Table 2.3).

While the high energy phosphate bond concept is no longer tenable, the central role of ATP in biological work performance is as crucial as ever. A new concept explaining the role of ATP in cell function was urgently needed. Such a new concept was introduced as part of the AI hypothesis in 1962 (Ling, 1962, 1977c).

8.4.2. *Theory of ATP as the Prime Living-State-Conserving Cardinal Adsorbent and its Role in Work Performance*

In Section 3.2, the hypothesis was briefly introduced that, like the magnet in the nail-iron-filing analogy, ATP is the cardinal adsorbent essential for the maintenance of the high-(negative)-energy, low-entropy living state. Here I examine this idea in the light of recently discovered facts. In addition, I discuss how the energy utilized in ATP resynthesis may in fact provide the key link in the en-

ergizing of biological work performance—in a way, however, entirely different from the high energy phosphate bond concept.

8.4.2.1. *ATP Acts as a Cardinal Adsorbent Producing an Allosteric Effect without Undergoing Hydrolysis*

In examining the effect of organic phosphates on the binding of oxygen on one cytoplasmic protein, hemoglobin, I have pointed out how ATP can allosterically control the binding affinity on remote heme sites, the formation of salt linkages between hemoglobin chains, and other activities that depend only on ATP binding onto the protein and involve no ATP hydrolysis (Section 7.4.3.3.). **Thus it has already been proven in vitro that ATP can and does act as a bona fide cardinal adsorbent.**

8.4.2.2. *Strong Binding Energy Which Enables ATP to Act as a Powerful Cardinal Adsorbent Producing Intense and Far-Reaching Influence on the Electronic Conformation of Proteins*

ATP is very strongly bound to the main muscle-cell protein, myosin, which, according to much of the experimental data presented in Chapter 4, offers the majority of β - and γ -carboxyl groups selectively adsorbing K^+ . The binding constant (K) of ATP on myosin is $10^{10} - 10^{11}$ (M^{-1}) (Goody et al. 1977; Cardon and Boyer 1978). The corresponding standard free energy of adsorption, ΔF° , can be calculated from the equation $\Delta F^\circ = -RT \ln K = -2.303 RT \log K$, where R , the gas constant, is equal to $1.987 \text{ cal deg}^{-1} \text{ mole}^{-1}$. T is the absolute temperature which at 25°C equals 298K . Substituting the binding constants of 10^{10} or 10^{11} , one finds a ΔF° of -13.6 and -15.0 Kcal/mole, averaging -14.3 Kcal/mole respectively. This ΔF° is as large as the observed free energy of hydrolysis of ATP to AMP (which, as mentioned above, is largely due to H^+ liberation and is not a true standard free energy, nor can it be utilized for biological work performance).

What is the cause and the significance of the unusually high ΔF° for ATP binding on myosin? ATP binding on myosin is an *adsorption* phenomenon. As in all adsorption phenomena, the basic mechanism is electrostatic in one form or another (see endnote 5 of Chapter 3). This strong electrostatic adsorption provides firm anchorage of ATP to the protein and causes polarization or electron redistribution at and in the nearby region of the ATP adsorption site.

8.4.2.3. *ATP Acts as an Electron-Withdrawing Cardinal Adsorbent (EWC)*

Earlier I have shown that isolated *hemoglobin*, the major protein of erythrocytes, and isolated *myosin*, the major protein of muscle, like other native proteins studied, do not selectively adsorb K^+ over Na^+ (Section 4.2), nor do they strongly polarize and adsorb water in multilayers (Section 5.2.5.1). Considered as a whole, the assembly of free water, free K^+ , and native proteins has high entropy and low (negative) energy because the native proteins are what one may call *introverted*. Their “eyes” as well as “hands” are turned inward. Thus their β - and γ -carboxyl groups are locked in salt linkages with the proteins’ own ϵ -amino and

guanidyl groups; their backbone NHCO groups are locked in α -helical and other intra- and intermacromolecular H-bonds.

We also have reason to believe that very high electron density or c -value of the β - and γ -carboxyl groups favors the formation of salt linkages (Section 6.2.4.) and that the high c -value-analog of the backbone carbonyl groups favors the formation of α -helical and other inter- and intramacromolecular H-bonds (Section 6.2.1.) The pervasive assumption of the introverted conformation suggests that native proteins in general and myosin and hemoglobin in particular have high c -value β - and γ -carboxyl groups and high c -value-analog backbone carbonyl groups.

Yet there is strong evidence that as part of living muscle cells, myosin offers its β - and γ -carboxyl groups for the selective adsorption of K^+ over Na^+ (see Chapter 4). Similarly, there is strong evidence that as part of living erythrocytes, hemoglobin provides its β - and γ -carboxyl groups for the selective adsorption of K^+ over Na^+ (see Section 4.3). In both, the β - and γ -carboxyl groups must have low c -value (see Figure 6.9).

Similarly, in both living muscle cells and living erythrocytes, the bulk of cell water exists in the state of polarized multilayers (see Chapter 5), indicating that the backbone carbonyl oxygen of a substantial portion of the cytoplasmic proteins must also exist in a low electron-density or low c -value-analog state.

Thus ATP (aided by its "helpers", see Section 8.4.2.4. below) must cause an autocoperative transition of myosin and hemoglobin (as well as other cytoplasmic proteins involved) from an initial introverted high c -value, high c -value-analog conformation into the low c -value, low c -value-analog conformation as diagrammatically illustrated in Figures 7.6B, 7.8 and 7.9. To bring about this pervasive reduction of electron density, ATP must be an electron-withdrawing cardinal adsorbent, or EWC.

To strengthen the result of this logical deduction, I present the following experimental evidence.

The antibiotic aurovertin shows weak fluorescence in an aqueous solution. When aurovertin is added to a soluble enzyme isolated from mitochondria, called F_1 -ATPase (Racker 1970), aurovertin binds stoichiometrically to the enzyme. This binding enhances the fluorescence of the antibiotic by as much as 100-fold (Lardy and Lin 1969; Bertina et al 1973).

Figure 8.13 shows that the fluorescence of the aurovertin- F_1 -ATPase complex was markedly reduced on exposure to Mg^{++} , and, even more important, on exposure to ATP. Exposure to ADP, on the other hand, enhances the fluorescence.

In Section 6.2.3 we have shown how by being incorporated into a polypeptide, the fluorescence of tyrosine and tryptophane decreases in response both to the electron-withdrawing effects of the polypeptide chain, and of the protonation of distant carboxyl or amino groups. The primary purpose of Section 6.2.3 was to demonstrate that the inductive effect could mediate interaction between effector groups and receptor groups which are connected to each other and thus separated by many intervening *covalently-linked* atoms.

The quenching of fluorescence of aurovertin- F_1 complex by Mg^{++} or ATP is different because the effector and receptor groups are not linked entirely by

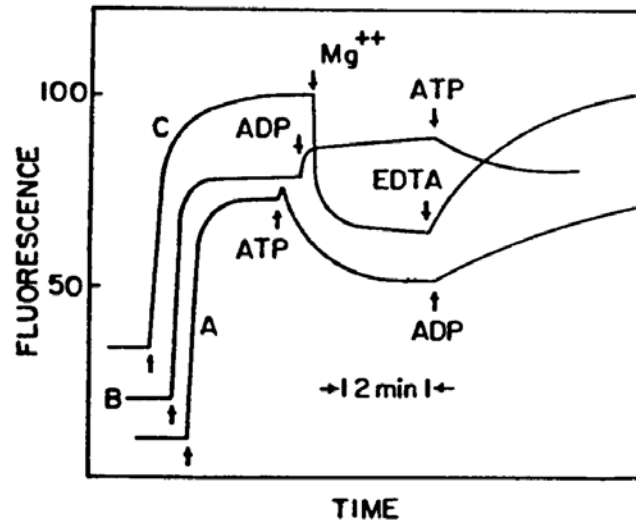


Figure 8.13. Effect of ATP, ADP and Mg^{++} on the fluorescence intensity of aurovertin- F_1 complex. Reaction mixture contains 3 ml. of buffer and either $1.15 \mu M$ (A,B) or $1.50 \mu M$ (C) of F_1 . At the first set of arrows, 3.3 (A,B) or 2.2 (C) nmoles of aurovertin were added. In all relevant cases, the final concentration of ATP was 1.6mM; ADP, 0.9 mM; and Mg^{++} 3 mM. (Chang and Penefsky 1973, by permission of Journal of Biological Chemistry)

covalent bonds. Rather they are in part linked by *adsorption*, first at the site of binding of aurovertin to the F_1 -ATPase, and again at the sites where Mg^{++} , or ATP is bound to the F_1 -ATPase (see Section 6.1).

Just as important, the data presented in Figure 8.13 show that Mg^{++} , a divalent cation, draws electrons toward itself and is an EWC. Of even broader significance is the demonstration that ATP also weakens aurovertin- F_1 complex fluorescence and is thus also an EWC, confirming the conclusion reached in the immediately preceding section.

The enhancement effect of ADP on the fluorescence of F_1 -ATPase-bound ADP marks it as an EDC (see Section 8.4.2.5).

8.4.2.4. *The Maintenance of the High (Negative) Energy Living State by ATP and Its "Helpers"*

The assembly of protein-water- K^+ in living protoplasm is at a state of lowered entropy due primarily to multilayer polarization and immobilization of water molecules (Figure 3.2). This low entropy of the living state is well demonstrated by the exquisite responsiveness of living cells to even a very moderate increase of temperature. Death, with the liberation of water as well as K^+ , is, according to the AI hypothesis, an entropy-driven process (see also Lauffer 1975).

The maintenance of the living state at ambient temperature, despite this unfavorable entropy, must be due to simultaneous compensatory (favorable) energy change. In the AI hypothesis, it is in this energy change that ATP plays a role similar to the big magnet in the nail-and-iron filing analogy.

Unfortunately, like many other analogies, this one also oversimplifies. While the big magnet by itself can polarize the nail chain and iron filings as illustrated in Figure 3.1, ATP by itself usually cannot bring about K^+ adsorption and mul-

tilayer water polarization. To accomplish these changes, ATP requires at least two “helpers,” one already known for some time, the other barely understood at all. These helpers are the subjects of our next two subsections.

8.4.2.4.1 Congruous Anions

According to the AI hypothesis, in death, certain cell proteins assume the introverted conformations seen in isolated “native” proteins and illustrated in the left-hand side picture of Figure 8.14: the backbone NHCO groups are locked in α -helical and β -pleated-sheet conformation; the β - and γ -carboxyl groups are locked in salt linkages.

In the AI hypothesis, the function of ATP and its helpers is to bring about an all-or-none autocoperative shift of the cell protein involved from the introvertively closed conformation to an open conformation illustrated on the right-hand side of Figure 8.14. More specifically, the function of ATP and its helpers is to pry loose the two sets of locked structures.

Since water molecules are at once proton donors and proton acceptors, the presence of an abundance of water in the cell makes it easier to pry loose the NH and OC groups engaged in α -helical and β -pleated-sheet conformations. As a result, the dislodged backbone NH group takes on a new partner in the form of the O end of an H₂O molecule, while the dislodged CO group takes on a new partner in the form of an H end of the same or another water molecule.

The prying loose of the salt linkages is, in contrast, more difficult, because K⁺, being a simple cation, can substitute only for the dislodged fixed cation. To substitute for the dislodged fixed anion, a congruous anion—an anion that sterically and electronically fits the cationic site—is needed, as illustrated in Figure 8.14.

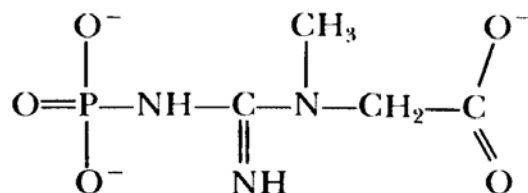
The facilitative effect of a congruous anion on the adsorption of the cation, H⁺ in sheep’s wool was long ago demonstrated by Steinhardt et al (1941). Thus, at a certain pH, no H⁺ was bound by the β - and γ -carboxyl groups, unless a strongly adsorbed, and thus, by definition, congruous anion was present (and adsorbed) (Ling 1962, 142).

For the selective accumulation of K⁺ in living cells the requirement of a congruous anion (besides ATP) is even more striking. Thus, for the accumulation of K⁺ in human erythrocytes, the congruous anion is a simple chloride. In muscle tissue, the congruous anions are mostly phosphates, in particular creatine phosphate (Ling 1952, 778).⁴ In squid axon, the congruous anion is primarily isethionate (Koechlin 1955). In guinea pig retina and brain the congruous anion is L-glutamate (Terner et al 1950, see Table 8.2).

The specific requirements of congruous anions like glutamate



and creatine phosphate



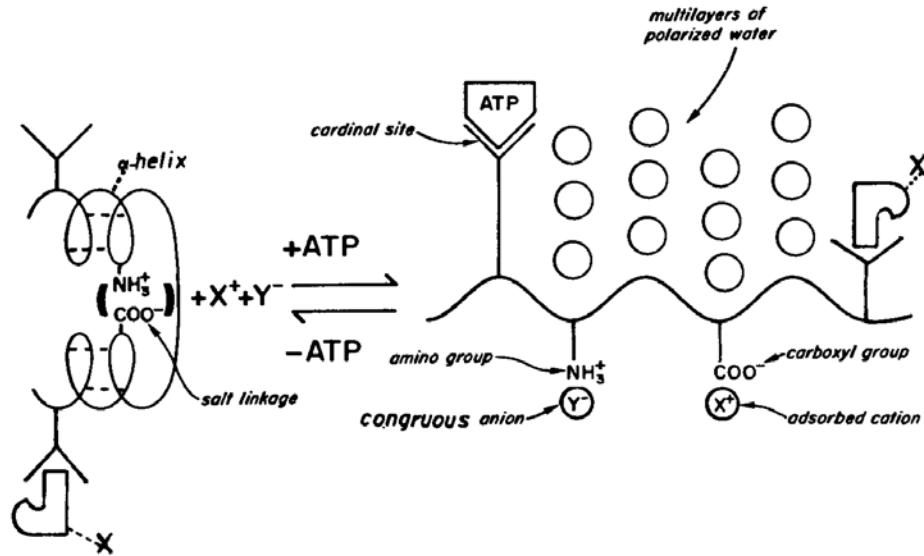


Figure 8.14. Diagrammatic illustration of how ATP adsorption on a key cardinal site might control the conformation of the cell protein and its ability to polarize water in multilayers and adsorb monovalent cation X^+ (e.g., K^+) on β - and γ -carboxyl groups and congruous anion (Y^-) on cationic amino groups. An unidentified auxiliary cardinal adsorbent essential for the effective ATP action is suspected to be a protein (or proteins) and is shown as $P-x$. For exciting new discovery that indicates the possible identity of $P-x(s)$, see Endnote 5.

indicate that the cationic sites in living cells adsorbing these anions might be more complex than a single cationic group (hence the high degree of steric specificity of the congruous anion), even though the cation being adsorbed, K^+ , is a simple monovalent cation [see also Section 9.2.2.3.2(3)].

8.4.2.4.2 An Unidentified Protein as an Essential Auxiliary Cardinal Adsorbent

In work yet to be published, I have shown that in the presence of ATP, the concentration of K^+ reaccumulated in and Na^+ extruded from resealed red cell ghosts depend on the *volume* of the lysing solution. K^+ reaccumulation and Na^+ extrusion occur when the lysing solution is ten times the volume of the washed cells lysed; neither K^+ reaccumulation nor Na^+ extrusion occurs if the lysing solution is thirty or more times the volume of the red cells lysed.

Since fresh lysing solution has the same chemical composition—including ATP—independent of the volume used, this striking volume effect suggests that it is the concentration(s) of other ingredient(s) in the lysing solution that came originally from the cells that is of critical importance.

The most conspicuous of the ingredients of the lysate coming from the cells is hemoglobin. Indeed in an earlier section (4.3), I have already shown that in the presence of ATP, the concentrations of K^+ reaccumulated in and Na^+ extruded from resealed ghosts do indeed vary with the concentration of residual hemoglobin left within the ghosts.

Further confirmation of the critical role of an adequate concentration of hemoglobin in the lysate came from our success in demonstrating reaccumulation of

Table 8.2. The effect of Glucose and Amino Acids on K⁺-Ion Loss or Gain by Retina or Brain Slices.

Experiment	Portion of tissue	Substrates added	Experimental condition	K ⁺ concentration in tissue, $\mu\text{M/g}$		
				Initial	Final	Change
A	1	—	—	90.04	—	—
	2	none	anaerobic	90.04	9.21	-80.83
	3	glucose	anaerobic	90.04	20.21	-69.83
	4	glucose; L-glutaminate	anaerobic	90.04	12.28	-77.76
	5	glucose; L-glutaminate; ATP	anaerobic	90.04	18.42	-71.62
	6	glucose; L-glutaminate	aerobic	90.04	94.65	+ 4.60
B	1	—	—	31.21	—	—
	2	glucose	aerobic	31.21	35.81	+ 4.60
	3	glucose; L-lysine	aerobic	31.21	30.70	- 0.51
	4	glucose; L-tyrosine	aerobic	31.21	27.63	- 3.58
	5	glucose; L-leucine	aerobic	31.21	36.83	- 5.63
	6	glucose; L-methionine	aerobic	31.21	40.42	- 9.21
	7	glucose; L-glutaminate	aerobic	31.21	60.62	+29.41

Note: A, guinea pig brain cortex slices or B, ox retina, were incubated in bicarbonate saline at 40°C for 60 minutes with various substances: glucose, 0.02M; ATP, 0.001M; and amino acids, 0.01M. Initial and final K⁺-ion contents were determined on portions of the same tissue and expressed as μM of K⁺ ion/g of fresh tissue. Tabulated values were corrected for weight changes and for the K⁺-ion content of the adhering medium. (Turner et al. 1950, by permission of the Biochemistry Journal.

K^+ and exclusion of Na^+ in resealed red cell ghosts which were lysed in 50 times its volume of lysing solution, to which was added—in addition to the usual component of the regular lysing solution and ATP—enough extraneous hemoglobin to match the hemoglobin concentration found in a $10\times$ lysate.

Yet if the ghosts are first exhaustively washed until entirely free of hemoglobin (and possibly something besides), reintroduction of extraneous hemoglobin and ATP do not lead to reaccumulation of K^+ and exclusion of Na^+ .

Since externally added ^{125}I -labelled hemoglobin was shown to fully exchange with hemoglobin originally present in the ghosts during the usual process of hemolysis, a key role of some tightly bound hemoglobin originally present in the ghosts in the reaccumulation of K^+ and extrusion of Na^+ seems unlikely. The failure of non-leaky *white ghosts* containing extraneous hemoglobin to reaccumulate K^+ suggests that there are some other nonhemoglobin protein(s) in the ghosts that the reintroduced hemoglobin depend on (in addition to ATP and the congruous anion, Cl^-) for the selective accumulation of K^+ and water polarization (leading to the exclusion of Na^+). The identity of this unknown protein (or proteins) remains elusive at this moment; nonetheless some guesses can be made.

The unknown protein, whatever it is, is obviously held very tightly within the (wide open) ghosts, or else it would have escaped during the usual procedure of lysing and would not have required exhaustive washing to remove it from the ghosts. The possibility that the unknown protein is profilamentous actin suggests itself (see Ling 1984, 568), since actin is usually one of the last proteins to be extracted from muscle and other cells (for exciting new findings on the possible role of actin on bulk-phase water, see endnote 5). If this speculation has validity, then hemoglobin, in order to serve its role, may have to be adsorbed onto the actin network as suggested in the diagram of Figure 3.3. Only then may actin function as an auxiliary cardinal adsorbent helping ATP in controlling the steric and electronic conformation of hemoglobin, for the selective adsorption of K^+ and multilayer polarization of water with the attribute of excluding Na^+ .

The unknown protein might also be related functionally and/or structurally to proteins that have the capability of keeping other proteins in the fully extended confirmation in the presence of ATP, including the unidentified protein present in reticulocyte lysate (Hurt 1987), 20S heat shock GroEL protein (Bochkareva et al. 1988) and what Rothman and Kornberg (1988) called “unfolding enzymes” (see also endnote 5 and Hazlewood and Kellermayer 1990 for additional relevant information). Only future investigations can enlighten us on this important question.

8.4.2.5. *The Source of Energy for Biological Work Performance*

According to the AI hypothesis, the physiologically active state of a living cell is a reversible step in the direction towards the death state (Figure 3.2). As such, one expects a similar sequela of water depolarization and c -value rise, leading to either salt-linkage formation or a shift of β - or γ -carboxyl groups from preferring K^+ strongly over Na^+ to a reduction of this preference or even its reversal.

Thus if work performance is coupled to this change (see Chapter 16 of Ling 1984), the energy needed is derived from the dissipation of the high potential energy of the resting, living state to the lower potential energy of the active, living state, distributed over the whole system.

If the adsorption of ATP on *key cardinal adsorbents* is responsible for the maintenance of the resting living state (Figure 8.14), clearly removal of ATP is the most convenient way of achieving work performance by driving the system to the active state. The most convenient way to remove ATP is by its enzymatic hydrolysis to ADP. This is a highly plausible model, supported by the fact that **the binding constant of ADP on myosin (i.e., 10^5) is 100,000 weaker than that of ATP (i.e., $10^{10} - 10^{11}$)** (Lowey and Luck 1969; Marsh et al. 1977). Therefore if the ATP-binding cardinal sites have potential ATPase activity and this activity is awakened by the initial event of physiological activation, ATP will be hydrolyzed to ADP, and the overall effect of the removal of a strong EWC (ATP) will be a shift of the protein-water-ion system to a higher-entropy, lower-(negative)-energy active state. In 1981 I was able to gather four kinds of experimental evidence, from analyses of data derived from mitochondrial studies, which support the view that whereas ATP is an EWC, ADP is actually an EDC (Ling 1981). The ability of ADP to enhance the fluorescence of aurovertin- F_1 -ATPase (Section 8.4.2.3) has added a fifth piece of evidence. If ADP is indeed an EDC, then dephosphorylation of ATP does not just remove an electron-withdrawing effect; it also replaces it with an electron-donating effect.

Interestingly enough, when the cell undergoes a sequence of work-performing, resting-state-active-state cycles (e.g., a muscle undergoing repeated contractions) ending with the cells at the initial resting state, the potential energy of the protein-water-K-cardinal-adsorbent system is unchanged at the end. Thus the energy source of such repeated work performance is in fact the energy needed to resynthesize the ATP hydrolyzed so many times. This energy is, of course, that provided by cell metabolism. Note that despite the profoundly different mechanism proposed here from that based on the high energy phosphate bond concept (now no longer tenable), the source of energy for the work performed is similar, i.e., energy to resynthesize the ATP hydrolyzed.

8.4.3. *Experimental Confirmation of Some Predictions of the Theory*

In Figures 7.6, 7.8, and 7.9, a quantitative relationship is indicated between the concentration of adsorbed cardinal adsorbent and that of the adsorbed solute which the cardinal adsorbent controls in an all-or-none manner. The group of “*regular sites*” under the control of each cardinal site is called a “*gang*” of sites (Section 7.3.1).

The demonstration that solute distribution in living cells can, as a rule, be described by a single adsorption isotherm rather than a multitude of isotherms (Section 8.1) indicates an extraordinarily high degree of uniformity of the adsorbing units. It was also pointed out that it would otherwise be impossible for the cell containing such a vast number of protein molecules (see opening paragraph of Chapter 7) to function as a coherent unit—as all cells do.

This high degree of uniformity among the adsorbing units demands that the number of regular sites in each gang under the control of one cardinal site described in the microscopic models of Figure 7.6, 7.8, and 7.9 should also hold for the whole cell containing trillions and trillions of highly similar adsorbing units. For this reason, one of the major predictions derived from the theoretical model of ATP as the prime conservative cardinal adsorbent in controlling the selective adsorption of K^+ in living cells is that there should be one (or a few) linear relationship(s) between the concentration of adsorbed ATP found in the cell and the concentration of adsorbed K^+ in the cell. Due to its high adsorption energy (Section 8.4.2.2.), practically all ATP in the cell is adsorbed; so is all the cell K^+ (Sections 8.1.3.; 8.3.2.). Therefore, the AI hypothesis predicts that if the cells is allowed to lose its ATP very slowly, so that equilibrium is always maintained between the ATP adsorbed and the K^+ adsorbed, then a plot of the concentration of ATP concentration and the concentration of K^+ should yield one (or at most a few) straight line(s), with the slope(s) equal to the number of regular sites in a gang of sites that each adsorbed ATP molecule controls.

Similarly, if the adsorption of ATP determines, in an all-or-none manner, the fully extended or the α -helical or other introverted conformation of the water-polarizing protein, and hence the polarized-multilayered or the free state of the water molecules in the domain controlled by the protein assembly, then there should also be a quantitative relationship between the concentration of ATP in the cell and the average q -value of normally extruded solutes like Na^+ . If the external Na^+ concentration is kept constant, then there should also be one (and no more than a few) linear relationship(s) between the Na^+ concentration in the cell water and the concentration of ATP in the cell.

Since there is a one-to-one relationship between the equivalent concentration of K^+ accumulated in the cell and that of congruous anion(s), the theory also predicts a positive one-to-one correlation between cell K^+ concentration and congruous anion concentration both in units of equivalents per unit weight of fresh cells.

8.4.3.1. *Relationships between ATP Concentration and the Intracellular Concentration of Selectively Accumulated Solutes*

(1) K^+

In theory, ATP adsorption onto a cardinal site transforms a *gang* of cooperatively linked β - and γ -carboxyl groups into a K^+ -preferring state (see Figure 7.6B). Therefore a quantitative relationship between the equilibrium level of ATP in the cell and the equilibrium level of K^+ in the cell should exist regardless of how one alters the level of ATP in the cell.

Gulati et al. (1971) studied the equilibrium concentration of ATP and of K^+ in frog muscles after exposure to 11 poisons of widely diverse toxicological effects. Their data reproduced here in Figure 8.15 clearly show that the predicted relationship between ATP concentration and K^+ concentration in the cells does indeed hold.

(2) *Soluble Proteins and Polypeptides*

In the AI hypothesis, soluble proteins and polypeptides, including many of the cells' important enzymes, are retained within the cell not by virtue of an

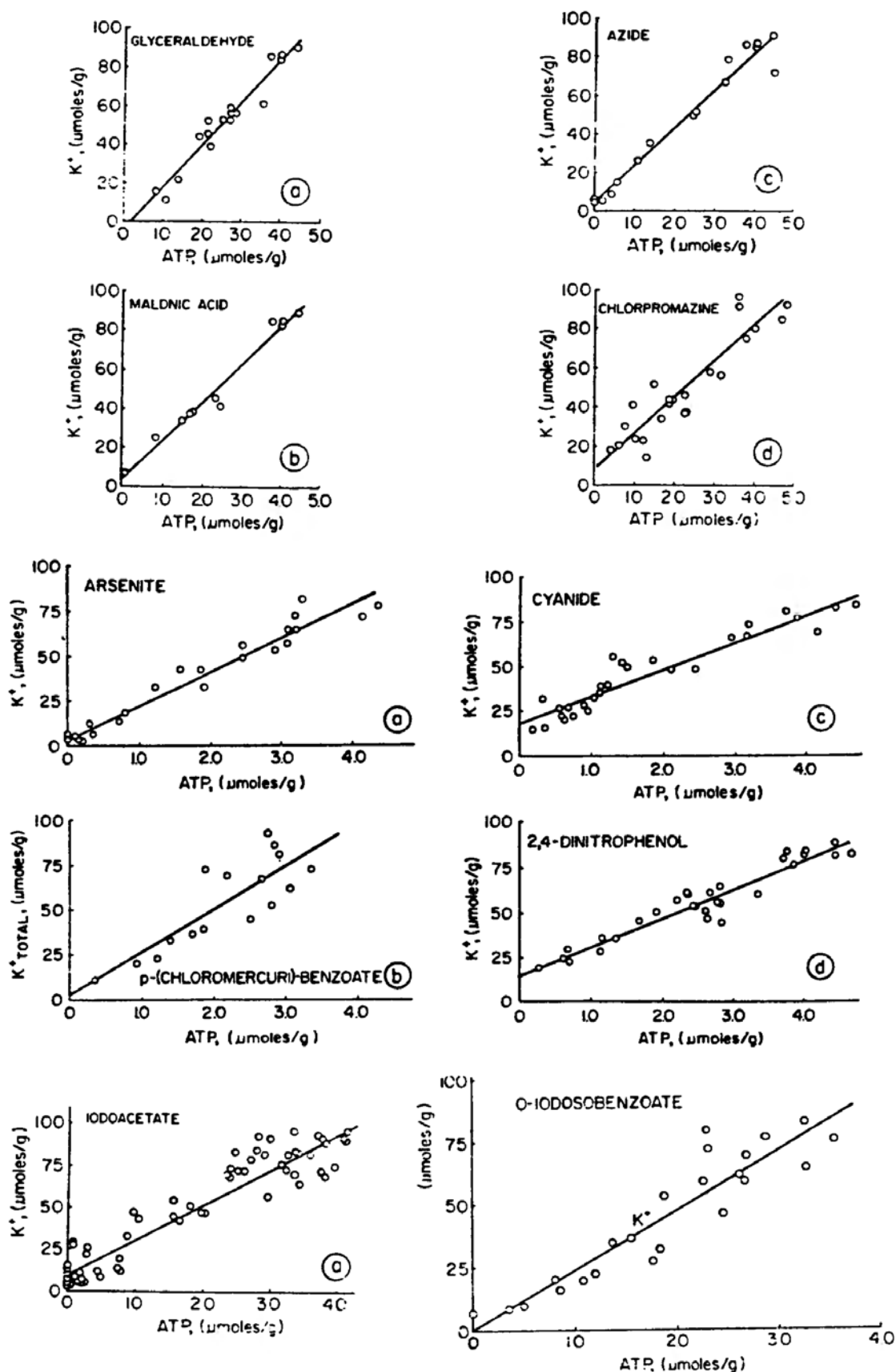


Figure 8.15. The relation between the equilibrium concentration of K^+ and the concentration of ATP in frog muscles exposed to 10 different poisons (as indicated) for different lengths of time at 25°C with shaking, followed by an equilibrium period of 2 to 4 hrs. at 1°C with shaking. (Gulati et al. 1971, by permission of Biophysical Journal)

absolute impermeability of a membrane barrier (see Section 9.1.2 for evidence against this old but incorrect concept), but by essentially the same mechanisms by which cells retain their K^+ , i.e., selective adsorption on cytoskeletal matrix proteins and/or protein(s) anchored onto the cytoskeletal proteins. While H-bonds, hydrophobic bonds, and S-S linkage may play varying roles in different proteins, it is hypothesized that the anchorage and retention are primarily due to *salt linkages* formed between the type of β - and γ -carboxyl groups selectively adsorbing K^+ (over Na^+) in resting cells and to fixed cations on the soluble proteins or polypeptides (see Ling 1982, 91–92). As with K^+ , the maintained accumulation and anchorage of the soluble protein requires the presence of ATP occupying key cardinal sites. Loss of ATP is thus expected to cause proportional release from binding on intracellular sites, and loss of the soluble protein to the bathing medium (see Kellermayer 1980–1981; Kellermayer et al 1986).

In the future, we expect to verify that soluble protein distribution should follow the same general equation for solute distribution (equation 16) or its variants, and be under the same kind of control as the more extensively studied small molecules and ions. As of this moment, research in this general direction has just begun. However, the few data already on hand are highly encouraging.

Piper et al. (1984) showed that the enzyme, malic dehydrogenase is released to the external medium from cultured heart-muscle cells or cardiocytes in response to oxygen deprivation. The amount of the enzyme released is linearly related to the concentration of ATP in the cells with a negative slope (Figure 8.16A). Similarly, Higgins et al. (1981) found that cell ATP concentration is linearly related, with a negative slope, to the concentration of lactate dehydrogenase released into the medium from myocytes in response to the presence of glucose metabolism-inhibiting, 2-deoxyglucose (Figure 8.16B).

Contrary to an old (but obsolete) belief, the living cell membrane is in various cell types studied permeable to ATP (for review of extensive evidence, see Section 9.1.2 below, also see Chaudry 1982). Is it then possible to prevent the leakage of soluble proteins from cells that, for various reasons, are unable to maintain their normal level of ATP? The answer to this question is yes. Wilkinson and Robinson (1974) showed that inclusion of ATP in the external medium in which isolated rat lymphocytes damaged by phospholipase A were incubated reduced the leakage of lactate dehydrogenase from the lymphocytes. As shown in Figure 8.17, there is a quantitative relation between the concentration of ATP added and the degree of reduction of lactate dehydrogenase (and other enzyme) leakage. On the other hand, neither ADP nor AMP nor adenosine had any effect even though they too can enter the cells. (Chaudry and Gould 1970; Chaudry and Baue 1980).

8.4.3.2. *Relationships between ATP Concentration and the Equilibrium Intracellular Concentration of Excluded Solutes*

(1) Na^+

Figure 8.18 shows the changes over time of the concentrations of K^+ , Na^+ , sucrose, and ATP in frog muscles exposed to a low concentration of the metabolic

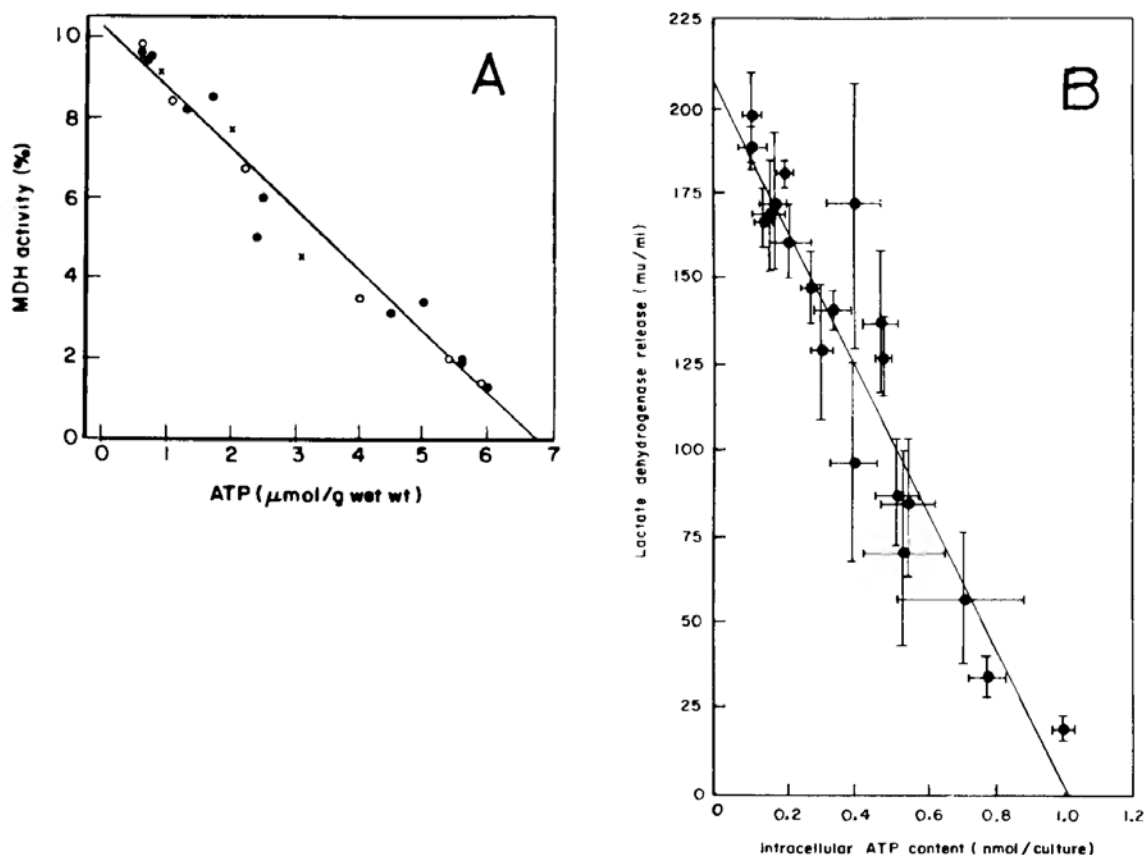


Figure 8.16.

- A. Relation of released malic dehydrogenase (MDH) activity (expressed as percent of total cellular activity) to ATP content of cardiocytes during anoxia. (Piper, et al. 1984, by permission of Journal Molecular and Cellular Cardiology)
- B. The relation between enzyme lactate dehydrogenase (LDH) release from, and ATP content of anoxic myocytes incubated in the presence of varied glucose and 2-deoxyglucose concentrations. Data are expressed as mean \pm S. E. M. for 5 cultures. (Higgins et al. 1981, by permission of Journal Molecular and Cellular Cardiology)

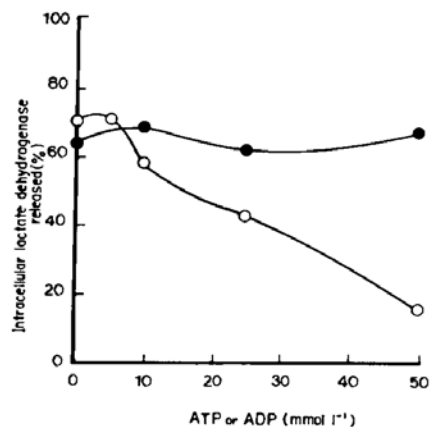


Figure 8.17. Effect of different concentrations of ATP (○) and of ADP (●) in the bathing solution on the leakage of lactate dehydrogenase from rat lymphocytes evoked by phospholipase A (50 mU ml⁻¹). (Wilkinson and Robinson 1974, by permission of *Nature*)

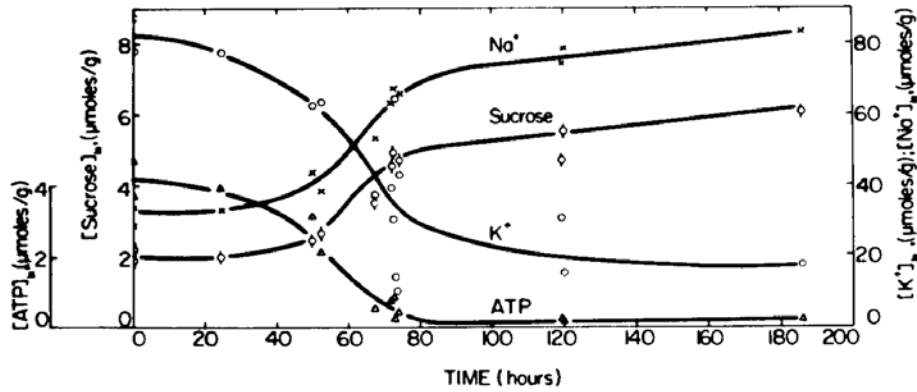


Figure 8.18. Time courses of changes in the concentrations of K^+ , Na^+ , ATP, and sucrose in frog muscles incubated in Ringer solution containing 0.1 mM Na iodoacetate and 10 mM labeled sucrose at $0^\circ C$. (Ling and Ochsenfeld, to be published)

poison, Na^+ iodoacetate (0.2 mM) at $0^\circ C$. In the course of the seven and half days following the introduction of the poisons to the bathing medium, the muscles lost ATP very slowly, allowing equilibration for K^+ distribution to be reached along the way. Note that the time course of ATP decline ran roughly parallel with the loss of K^+ . The time course of Na^+ concentration changes is roughly a mirror image of that of the cell K^+ concentration changes. Similar parallel changes between ATP concentration and K^+ concentration, and antiparallel changes between ATP concentration and Na^+ concentration were observed earlier in human erythrocytes and partially in rat uterine myometrium (Ling 1962, 253–254; 1984, 364–365).

There are two possible interpretations of these data. (i) The rise of Na^+ concentration, with decrease of the concentration of ATP, could be due to a stoichiometric displacement of the adsorbed K^+ by Na^+ —as already demonstrated for frog muscle in response to ouabain. (ii) An alternative is that as ATP concentration falls, the β - and γ -carboxyl groups, instead of picking up Na^+ , begin to form salt linkages with fixed cations. The parallel gain of Na^+ is then due to the progressive depolarization of the cell water (that often accompanies the salt-linkage formation, Section 5.2.5.1.) and the increase of q -value for Na^+ .

(2) Sucrose

A choice between these two alternatives could be made by including in the incubation medium a third solute that is noncharged, such as sucrose. A neutral probe like sucrose is not likely to be adsorbed on the β - and γ -carboxyl groups adsorbing positively charged K^+ or Na^+ , but is also excluded from the cell water as Na^+ is, following what is known as the *universality rule*, i.e., changes in the q -value for one solute are paralleled by similar changes in the q -values of other solutes normally excluded from the cell water. Sucrose distribution would remain unchanged if the extra Na^+ taken up is all adsorbed; sucrose concentration would also undergo changes paralleling Na^+ concentration change if the extra Na^+ taken up is all or mostly in the cell water. The explanation based on water depolarization was confirmed. Figure 8.19 represents a different way of presenting data like those shown in Figure 8.18. Here the equilibrium K^+ , Na^+ , and

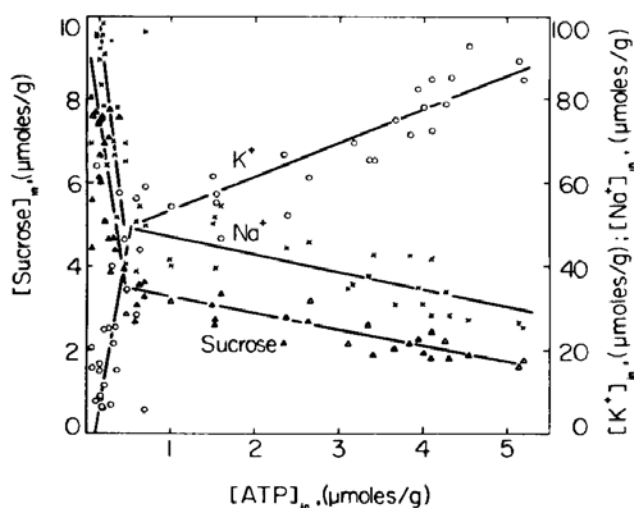


Figure 8.19. Equilibrium distribution of K^+ , Na^+ , and labeled sucrose in frog sartorius muscles containing different concentrations of ATP, having been exposed to 0.1 mM iodoacetate for up to 9 days ($0^\circ C$). Data include those shown in Figure 8.18. (Ling and Ochsenfeld, to be published).

sucrose concentration in the slowly dying muscle are plotted against the ATP concentration. Parallel changes of sucrose and Na^+ uptake are clearly evident in the data of both Figure 8.18 and Figure 8.19.

8.4.3.3. *The Relationships between the Concentration of Congruous Anions and the Concentration of Selectively Accumulated K^+*

As mentioned earlier, the major congruous anions in frog muscle cells are in the form of phosphates. Thus out of a total concentration of 170 mEq. of anions in a liter of cell water—not all of which is adsorbed—fully 3/4 or 129 mEq./l. are phosphates (Ling 1962, 217; 1955a, 90). Based on the concept of congruous anions presented earlier, one expects an essentially one-to-one milliequivalent relationship between muscle cell phosphates and K^+ selectively accumulated. The demonstration by Cameron et al. (1990) of a positive correlation between the concentration of cell K^+ and that of phosphorus in cultured muscle cells or myocytes are in harmony with the prediction.

Of the 129 mEq./l. of phosphates in frog muscle cell water, 71 mEq./l. (21.8 μ moles/g fresh muscle) belongs to creatine phosphate,⁶ another 27.4 mEq./l. (5.0 μ moles/g) belongs to ATP. The enzyme *creatine kinase* in the cell maintains an equilibrium between the concentration of ATP and creatine phosphate (CrP) in favor of the formation of more ATP at the expense of CrP.⁷ As a result, the concentration of CrP in the cell tends to fall before that of ATP. I will discuss next the possible role of CrP, inorganic phosphate (P_i), and hexose phosphates as congruous anions for the selective adsorption of K^+ in frog muscle exposed to pure nitrogen or the drug, fluorodinitrobenzene (FDNP).

(1) *Role of CrP and P_i under anoxia*

When frog muscles were exposed to pure nitrogen, and thus deprived of oxygen, a marked fall of the CrP concentration from 29 μ mole/g to a new steady

level at $11 \mu\text{mole/g.}$ occurred in 3 hours and maintained for at least another 4 hours (Figure 8.20). In parallel with this prominent change, the cell K^+ also fell from $86 \mu\text{moles/g.}$ to a new maintained level at $74 \mu\text{mole/g.}$ The ATP level, in contrast, remained at a near-normal $4.9 \mu\text{mole/g.}$ for the whole duration of the experiment after a slight initial fall from $5.2 \mu\text{mole/g.}$ (In squid axons, exposure to cyanide produces a similar fall of arginine phosphate—the invertebrate equivalent of CrP—without significantly diminishing the concentration of ATP (Caldwell, 1960), see Section 9.2.2.3.2.(2)).

Consideration of the quantitative relationship between ATP and K^+ concentration in Figure 8.19 shows clearly that a fall of ATP concentration from 5.2 to $4.8 \mu\text{mole/g.}$ would predict a change of K^+ concentration of no more than 1 or $2 \mu\text{mole/g.}$ Thus a fall of K^+ concentration accompanies a loss of CrP, in harmony with the view that CrP is the major congruous anion in muscle cells.

However, quantitatively, the parallel changes of the concentrations of CrP and K^+ are less impressive at first look. Thus, at the (neutral) pH of the cell interior, CrP has an effective valence of 2.18 (see Ling 1962, 217). If there is a one-to-one relationship between the equivalent concentration of lost congruous anion, CrP and lost K^+ , a drop of $18 \mu\text{moles/g.}$ of CrP should lead to a K^+ -concentration drop equal to $18 \times 2.18 = 39.2 \mu\text{mole/g.}$ In fact, only a drop of $12 \mu\text{mole/g.}$ occurred. An apparent disparity of $27 \mu\text{moles/g.}$ is found between the loss of K^+ and that of CrP. This disparity suggests that some other anion(s)

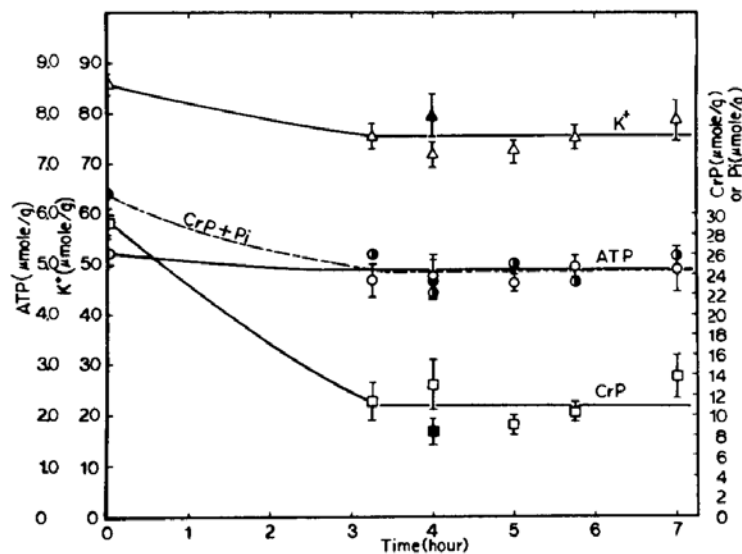


Figure 8.20. Effect of anoxia on the K^+ , CrP, Pi and ATP concentrations in frog sartorius muscles (25°C). Isolated frog sartorius muscles were incubated in Ringer solution bubbled with 95% nitrogen and 5% CO_2 . Each point represents the (average) value from 5 sartorius muscles analyzed together. Inorganic phosphate (Pi) contents were represented as the sums of Pi and CrP. Solid symbols represent results of analyses of a duplicate set of data of muscles that had been incubated first for 4 hours at 25°C before being transferred to and incubated in another similar solution kept at 0°C . $\text{K}(\Delta)$, CrP(\square), ATP(\circ), CrP + Pi(\bullet) (Ling and Ochsenfeld, to be published)

has emerged and partially replaced the lost CrP as congruous anion(s). Since there is no visible break in the level of K^+ concentration in the 7 hours under pure nitrogen, the substitute anion(s) must have become available as soon as CrP broke down. Only two known candidates can satisfy this criterion: both are the products of the CrP hydrolyzed; inorganic phosphate and hexosephosphates.

(i) *Inorganic Phosphate (Pi)* Evidence in favor of *Pi* serving the role of congruous anion came from the high level and time course of the concentration change of *Pi* in the muscle (Figure 8.20): *Pi* rose sharply from 3.4 $\mu\text{moles/g.}$ to a new steady level at 13 $\mu\text{mole/g.}$ for at least 4 more hours. (Note that in Figure 8.19, only the sums of CrP and *Pi* concentration were presented). At 13 $\mu\text{mole/g.}$, the intracellular concentration of *Pi* is more than three times that present in the bathing medium (3.2 mM) and must be mostly adsorbed (Section 8.1.3). At an effective valence of 1.57, the gain of (adsorbed) *Pi* would keep $(13 - 3.4) \times 1.57 = 15 \mu\text{Eq./g.}$ of β - and γ -carboxyl groups free for K^+ adsorption, leaving some 10 $\mu\text{moles/g.}$ of missing congruous anion yet to be accounted for.

(ii) *Hexosephosphates* Lundsgaard showed that when IAA-poisoned muscle lost all its CrP (and ATP) in response to stimulation, all the phosphate liberated was quantitatively converted into hexosemonophosphates and hexosediphosphate (Lundsgaard 1930, see also Ling 1952, 759). Both IAA and anoxia block further degradation "down-stream" of sugar phosphates formed during the early paths of normal metabolism. Thus it seems reasonable to expect some of the phosphate liberated from the hydrolyzed CrP to turn up in the form of sugar phosphates. The work of Kerly and Ronzoni (1933) showed that this is indeed the case. Hexosemonophosphate accumulated in frog muscle cells in a pH-dependent manner. In our own experiment illustrated in Figure 8.20, instead of a gas phase containing 3% CO_2 (which would have kept the pH at neutrality), a 95% $\text{N}_2 + 5\% \text{CO}_2$ mixture was used, producing a somewhat more acidic environment. Kerly and Ronzoni showed that the accumulation of hexosemonophosphate under anaerobic conditions at 25°C was most prominent in a somewhat acidic medium; the total hexosemonophosphate concentration reached as high as 8 $\mu\text{mole/g.}$ At an effective valence of 1.9, this is more than adequate to account for the 12 $\mu\text{Eq/g.}$ of missing congruous anion.

In summary, under anoxia, frog muscle loses K^+ and CrP but not ATP. It would seem that in the presence of the full amount of the premier conservative cardinal adsorbent, ATP; inorganic phosphate, and hexosemonophosphates could function as congruous anions in lieu of the lost CrP.

(2) *The Role of CrP in muscles treated with FDNP*

The reagent used extensively to determine the amino-acid sequence in proteins, fluorodinitrobenzene or FDNB, inhibits creatine kinase specifically (Infante and Davies 1962). FDNB therefore provides a way to insulate the CrP concentration in living cells from changes in the ATP concentration.⁷ With this in mind, Ling and Ochsenfeld (to be published) studied the combined effect of anoxia, 0.1 mM IAA and 0.4 mM FDNB on the concentration of CrP, ATP and K^+ in frog muscle cells at 0°C. Their results are reproduced here as Figure 8.21.

For about six hours, the concentration of CrP in the poisoned muscles re-

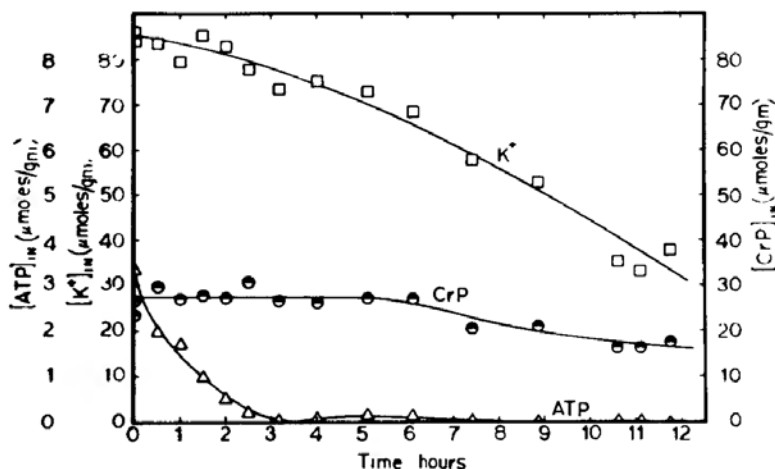


Figure 8.21. Effect of pure nitrogen, iodoacetate, and FDNB on the concentrations of K^+ , CrP, and ATP in frog sartorius muscles (0°C). Isolated frog sartorius muscles were first equilibrated in a Ringer solution (0°C) freed of oxygen (by bubbling with nitrogen which was purified by passage through a tower of heated "activated copper") for 20 minutes before their introduction to the Ringer solution similarly freed of oxygen but also containing IAA (0.1 mM), and FDNB (0.4 mM). Five muscles were taken out each time, frozen in liquid nitrogen, pulverized while frozen before extraction with 0.3M cold perchloric acid and analyzed for ATP, CrP, and K^+ . (Ling and Ochsenfeld, to be published)

mained essentially unchanged at $27 \mu\text{mole/g.}$ of fresh tissues, while the concentration of ATP had dropped to near zero after only three hours of exposure to the drugs. This isolation of CrP from ATP changes was expected. What was not expected was the profound alteration in the seemingly-unalterable relationship between the concentration of ATP and that of K^+ earlier described (Figures 8.15 and 8.18). Since Gulati et al. (1971) had shown that a 4-hour incubation at 0°C is long enough to establish diffusion equilibrium of K^+ in frog muscle, the level of ATP reached at the end of 3 hours of incubation (from 0 to $0.17 \mu\text{mole/g.}$) would predict a K^+ concentration of at most $10 \mu\text{moles/g.}$ at the end of 7 hours of incubation. What was observed was a K^+ concentration six times higher.

What FDNB has revealed is that CrP acts as a sort of a "deputy" *prime cardinal adsorbent*. As long as the cell contains a relatively high concentration of ATP, the inductive influence of the adsorbed CrP is eclipsed by that of ATP. Yet under the artificial condition provided by FDNB, CrP can apparently exercise an effect similar to ATP in maintaining the selective adsorption of K^+ on β - and γ -carboxyl groups. Surprising as it was to us when first observed, the phenomenon has become more understandable as we learn more about the mechanism underlying the control of autocoperative transitions. The boundary between the indirect F-effect exercised by the cardinal adsorbent and that exerted by the regular adsorbents in a gang of cooperatively linked sites begins to blur when the congruous anion also exercises a strong inductive effect, as apparently CrP does. Indeed, the two different ways of seeing Steinhardt and Zaiser's acid titration of ferri- and carboxyhemoglobin in Section 7.4.2. uncover a similar story.

8.4.4. *In-Vitro Demonstration of the Maintenance of the Living State by ATP (and its "Helpers")*

In the opening section of this volume, I pointed out that living cells selectively accumulate K^+ and exclude Na^+ while dead cells do not. The distribution of this pair of alkali-metal ions in a cell offers one of the most sensitive natural monitors of the preservation of the living state of a cell. Edelman made use of this set of natural monitors and the LAMMA technique when he demonstrated that by freeze-drying (according to a method he introduced) and embedding in plastic, he could preserve a muscle-cell section in its living state [Section 4.4.2.2.2.]. The key of his success lies in his ability to demonstrate selective K^+ adsorption over Na^+ *in vitro* after the muscle had been freeze-dried, embedded and cut into very thin sections.

In Figure 4.12, I illustrated the effectively membrane-pump-less open-ended cell (EMOC) preparation. In Figures 4.13 and 4.14, I demonstrated the ability of selectively accumulating labeled K^+ and the ability of excluding labeled Na^+ of the frog muscle EMOC preparation but only in the region of muscle cells away from the cut end. Deterioration, and with it the failing ability of selectively accumulating labeled K^+ and of excluding labeled Na^+ , spread slowly from the cut end toward the intact end of the muscle. In contour, the deteriorated region coincides with the region of the cell that has lost its total (nonlabeled) K^+ (Figure 4.14). Since, in the EMOC preparation, neither K^+ accumulation nor Na^+ exclusion could be due to the operation of membrane pumps (see Section 4.4.2.1.), the most straightforward explanation of this regional deterioration, in view of the evidence presented in the preceding sections (Sections 8.4.3.1. to 8.4.3.3.), is a loss of ATP in the deteriorated region and retention of ATP in the region away from the cut end. To test this idea, Ling and Blackman (to be published) analyzed the ATP concentration along the length of a frog sartorius muscle in an EMOC setup after four days of incubation at 25°C. The result shown in Figure 8.22 fully confirms what we expected.: the retention of ATP at its full normal concentration neatly confined to the region that retained its normal K^+ and Na^+ concentration. In the deteriorated region, which has lost its ability to selectively accumulate K^+ and excluding Na^+ , there is no ATP.

A proof, at once incisive and aesthetically appealing, of the cardinal role of ATP in the maintenance of the living state is now theoretically within reach. That is, if we could demonstrate with the LAMMA technique [Section 4.4.2.2.2.], selective adsorption of K^+ over Na^+ *in vitro* in thin sections prepared from the intact end of a transected frog sartorius muscle (like that in an EMOC preparation) but not in sections prepared from the same muscle near its cut end. As of now, this specific experiment has not yet been done. However, an experiment using an alternative method, has been successfully conducted, again by Ludwig Edelman.

Figure 4.17c demonstrates, with the LAMMA technique, *in vitro* selective adsorption of Cs^+ (over Li^+ , Na^+ , and K^+) in a similar freeze-dried embedded muscle section following a 5-minute exposure to a solution containing 10 mM Cs^+ , in addition to 50 mM each of Li^+ , Na^+ and K^+ . However, unlike the lighter

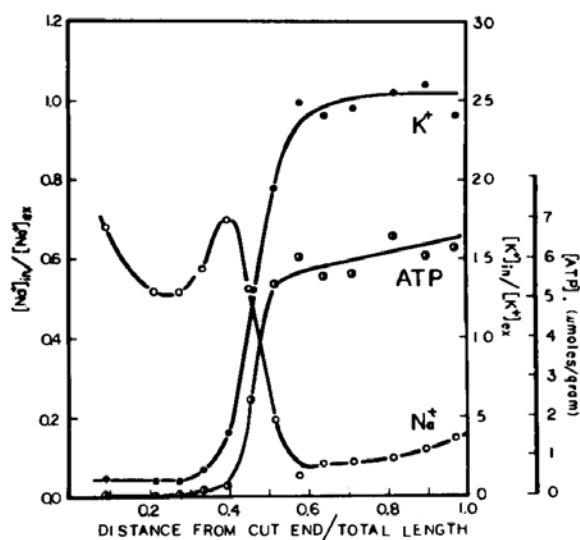


Figure 8.22. The concentration of ATP in segments of a frog sartorius muscle EMOC preparation at different distances from the cut end, which alone was immersed in Ringer solution. The muscle was in the EMOC setup for 3 days at 25°C. ATP concentration is given in $\mu\text{moles per gram}$ of fresh muscle sections. Distances from the cut end are given as a ratio of the distance from the cut surface to the center of the segment, divided by the total length of the cut muscle. ATP was analyzed using the fire-fly method, by a modification of that given by Stanley and Williams (1969). Also given are the K^+ and Na^+ concentrations measured with atomic absorption spectrophotometry on other aliquots of the same trichloroacetic-acid extracts of the muscle segments. Both K^+ and Na^+ concentrations are given as ratios to the final concentrations of the respective ions in the Ringer solution bathing the cut end of the muscle. (Ling and Blackman, unpublished)

elements K^+ and Na^+ , which can be detected and measured (only) by the LAMMA technique, the selectively adsorbed, *electron-dense* Cs^+ can also be detected by transmission electron microscopy, as shown by Edelman in Figure 4.16b.

Thus a full confirmation of the key role of ATP (and its *helpers*) in the selective adsorption of alkali-metal ions and in the maintenance of the living state can still be achieved without the use of LAMMA. That is, if one can successfully demonstrate (with electron microscopy) *in vitro* selective adsorption of Cs^+ in sections from a region of a transected muscle away from its cut end (now known to be replete with ATP) following a 5-minute exposure to 10 mM Cs^+ and 100 mM Li^+ , but not in sections from the muscle near its cut end (now known to be devoid of ATP). Figure 8.23 from a recent publication of Edelman (1989) fully confirms both expectations.

8.5 Summary

In this chapter (and Chapter 5) I have summarized the extensive studies of the equilibrium distribution of solutes in living cells, ranging from those that are the essential ingredients of the cell (e.g., K^+ , Na^+ , Mg^{++} , D-glucose), to the rare but extant solutes in the natural world (e.g., D-arabinose, L-xylose), to alien substances created for the first time by organic chemists (e.g., 3-chloro-1,2-propanediol; PEG 900). While frog muscle was the most extensively studied, in-

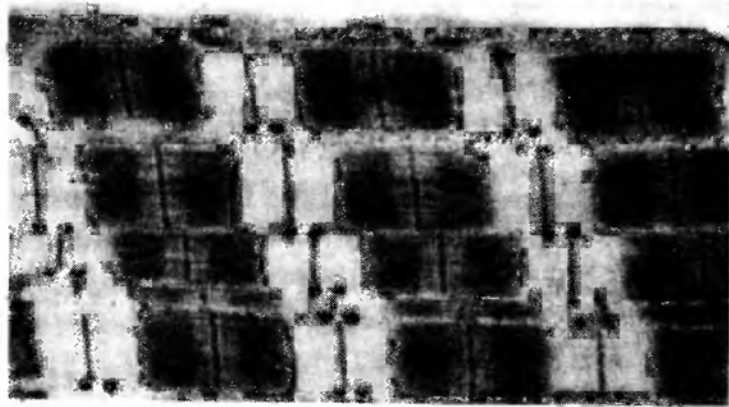
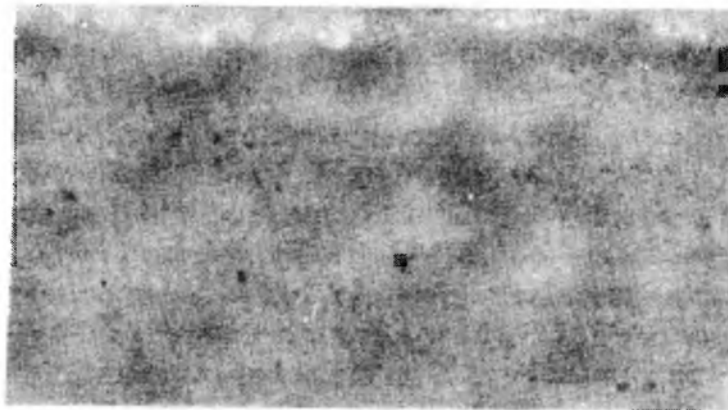
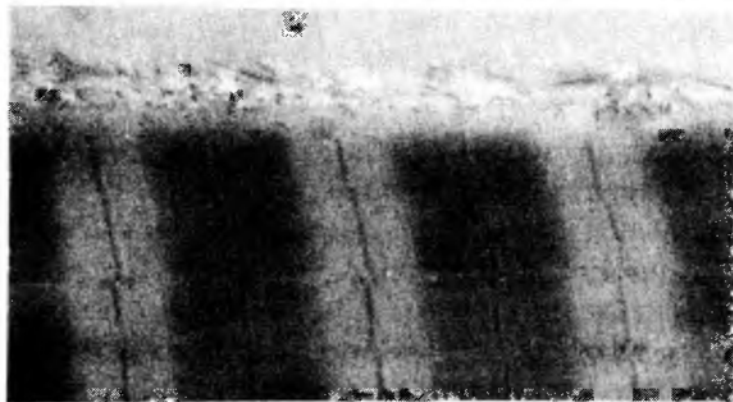
1**2****3****4**

Figure 8.23. Cut frog sartorius muscles after freeze-substitution and low temperature embedding. (1) Ultrathin section stained with uranyl acetate and lead citrate showing the cut end of a muscle fiber; (2) Similarly stained ultrathin section of the same cut fiber at a distance of about 0.4 mm from the cut end; (3), (4) unstained 0.2 μm thick wet-cut sections exposed to a solution containing 100 mM LiCl and 10 mM CsCl; (3) obtained from an area near the cut end, (4) obtained from the same place as (2). The section shown in (3) is almost unstained; (4) shows a staining pattern similar to that shown in (2). Magnification 16,000X. (Edelmann 1989, by permission of Scanning Microscopy International)

vestigations of a variety of other amphibian and mammalian tissues and cells yielded similar results.

The quantitative data collected from resting cells and from cells under the domination of various cardinal adsorbents all obey equation 14 (including, implicitly, its various simplified versions).

That the distribution of a wide variety of profoundly different solutes can be described by such a simple equation has laid to rest the pessimistic view that living phenomena are by nature too complex to be comprehended and mastered. The simplicity seen here pervades all aspects of basic cell physiology and it underlies my belief that complex as life is, its fundamental mechanisms are not at all beyond human understanding and control (see Introduction).

Obedience to equation 14 confirms the AI hypothesis (and Troshin's sorption theory) that solutes in living cells may exist in two forms, as *free solute* dissolved in the cell water and as *adsorbed solute* on cell proteins and other macromolecules.

Solutes in the cell water distribute themselves between the cell water and the external medium according to the partition law of Berthelot and Nernst. A plot of the equilibrium concentration of a solute in the cell water against that in the external medium yields a straight line, with a slope equal to the *equilibrium distribution coefficient* or *q-value* of that solute in the cell water.

The AI hypothesis predicted that solute distribution in cell water should follow the *size rule*: the larger the solute, the lower the *q-value*. Also predicted are exceptions to the size rule: i.e., *q-values* higher than their respective molecular volumes or weights predict for solute molecules that fit well into the dynamic structure of polarized water. The full confirmation of the size rule in both living cells and in inanimate model NP—NP—NP systems (or modifications) is a landmark in the understanding of this most basic phenomenon of cell physiology, solute distribution.

Free solutes in cell water as a rule exist at concentrations lower than in the external media. When a solute is found in the cell at a concentration much higher than that in the external medium, most of the cell solute is adsorbed. Adsorption occurs on specific adsorption sites carried primarily on cell proteins but sometimes also on other cell macromolecules. A high degree of specificity in adsorption usually exists, determined by both the steric and the electronic conformation of the adsorption sites (e.g., the *c-value*).

The adsorption of a solute in a living cell may follow a Langmuir adsorption isotherm (equations 19 and 21). Obedience to the Langmuir isotherm signifies that there is no significant interaction between neighboring adsorption sites. In living cells, this lack of cooperative interaction, as a rule, does not imply that the sites are separated by large distances or otherwise effectively isolated from neighboring sites, and thus inherently incapable of near-neighbor interaction. Rather, this apparent lack of interaction is the consequence of a very low absolute magnitude of the free energy of the *j*th-to-*i*th adsorbent exchange $|\Delta F_{j \rightarrow i}^{00}|$ in the specific cases being examined, and the fact that the nearest-neighbor interaction energy ($-\gamma/2$) is a function of $|\Delta F_{j \rightarrow i}^{00}|$. Only when $-\gamma/2$ is large and positive is autocoperative behavior observed.

A large and positive $-\gamma/2$ underlies autocoperative transition of the protoplasmic protein-water-ion system; it also underlies the control of cell behaviors

and properties by drugs, hormones, and other cardinal adsorbents. In agreement with this theory, the distribution of K^+ and Na^+ under the cardinal adsorbents ouabain and Ca^{++} follows the Yang-Ling cooperative adsorption isotherm (equation 7).

The consequence produced by the cardinal adsorbent is primarily a change of the intrinsic equilibrium constant $K_{j \rightarrow i}^{00}$, with or without a concomitant change of the value of $-\gamma/2$. Using NMR and electron microscopic methods we established that the change produced by ouabain involved primarily a reduction in the relative affinity of β - and γ -carboxyl groups for K^+ over Na^+ . The equilibrium distribution of the five 5 alkali-metal ions, Cs^+ , Rb^+ , K^+ , Na^+ and Li^+ , established that ouabain functions as an electron-donating cardinal adsorbent or EDC in frog muscle cytoplasm (a conclusion affirmed by studies of other protoplasmic systems in other cell types, to be described in Chapter 9).

Ouabain illustrates how a cardinal adsorbent can alter profoundly the K^+/Na^+ preference of β - and γ -carboxyl groups without changing the q -value of the solutes normally excluded by the cell water (e.g., Na^+). It was suggested that this was due to the masking effect of certain strongly water-polarizing protein(s), which maintain water polarization but do not themselves respond to ouabain.

By far the most important cardinal adsorbent is ATP. In this chapter we have described results of extensive experimental testing of the theory that ATP, acting as an electron withdrawing cardinal adsorbent (EWC), plays a key role in maintaining the living cell in its high-(negative)-energy, low-entropy living state.

When ATP and its "helpers" (congruous anions and the yet-to-be identified cytoplasmic protein X (or proteins Xs) occupy the appropriate regular sites, the cell proteins involved are maintained at such an electronic state (i.e., the resting living state) that β - and γ -carboxyl groups are held at a relatively low c -value state with high preference for K^+ and for certain fixed cationic groups of soluble proteins in the cell. Similarly, the backbone NHCO groups are kept at the fully-extended state, polarizing cell water in multilayers. Confirming the theory are (i) the recognition of quantitative relationships between ATP concentrations and the concentrations of K^+ and of Na^+ in poisoned frog muscles; and (ii) the demonstration of freeze-dried plastic-imbedded $0.2 - \mu m$ ultrathin muscle sections to selectively adsorb in vitro alkali-metal ions with a rank order usually seen only in healthy living cells (e.g., strong preference for K^+ over Na^+). (Apparently this is observed only if the section is prepared from a part of a frog sartorius muscle containing its normal ATP content, not from an injured region of the muscle containing no ATP.)

NOTES

1. To the best of my knowledge, no one has introduced a quantitative equation for Na^+ distribution in living cells in terms of the membrane-pump concept. Cohen and Monod (1957), however, did derive an equation for the distribution of lactose and other sugars in microbes. Using our symbols, their equation reads:

$$y \frac{[p_i]_{ex}}{[p_i]_{ex} + K} = c[p_i]_{in} \quad (A)$$

where y is the pumping rate (constant) and c is the exit constant. K is the dissociation constant of the sugar-pump complex. In fact, this equation is not complete. As such, it implies that the sugar can leak out but cannot leak in—a violation of the First Law of Thermodynamics (see endnote 1 of Chapter 2). A corrected version of the Cohen-Monod equation is

$$c[p_i]_{\text{ex}} + y \frac{[p_i]_{\text{ex}}}{[p_i]_{\text{ex}} + K} = c[p_i]_{\text{in}}. \quad (\text{B})$$

This equation describes an inward pump, the activity of which results in an accumulation of sugar in the cell at a concentration *higher* than in the external medium. In the rectilinear distribution of Na^+ (Figure 8.2A) and nonelectrolytes in frog muscle (Figure 5.8), the concentrations of Na^+ and nonelectrolytes in cell water are *lower* than in the external medium. Therefore one needs *outward* pumps, for which one writes an equivalent form of equation B:

$$c[p_i]_{\text{ex}} = c[p_i]_{\text{in}} + y' \frac{[p_i]_{\text{in}}}{[p_i]_{\text{in}} + K'}, \quad (\text{C})$$

where y' and K' have meanings similar to those in equation B, except that they refer to the outward pump actively transporting p_i from the cell to the external medium.

One can readily see that this equation, or anything similar to it, cannot produce a rectilinear distribution as experimentally observed. The pumping term is a hyperbola. When a hyperbola combines with the linear leak term, it cannot produce a straight line. One can put it another way: Let us arbitrarily assume that there *is* a rectilinear relation between $[p_i]_{\text{ex}}$ and $[p_i]_{\text{in}}$, then

$$[p_i]_{\text{in}} = k[p_i]_{\text{ex}}. \quad (\text{D})$$

Substituting equation D into equation C and rearranging terms, we obtain:

$$[p_i]_{\text{in}} = \frac{y'}{c(1 - k)} - K'. \quad (\text{E})$$

Since y' , c , k and K' are all constants, $[p_i]_{\text{in}}$ is a constant. This means that there is only a *uniquely defined* single intracellular i th solute concentration, $[p_i]_{\text{in}}$, that satisfies both equation C and D. That single value of $[p_i]_{\text{in}}$ and the value of k also uniquely define the value of $[p_i]_{\text{ex}}$. In other words, there are no other values of $[p_i]_{\text{in}}$ that correspond to other $[p_i]_{\text{ex}}$ with the same value of k . Hence no straight line is possible.

The observed, rectilinear distribution curves with slopes below unity also offer independent evidence against the concept of sharing of pumps as a way to reduce their total energy need. To understand this point, we need to examine some basic theoretical attributes of pumps.

Inherent in the concept of pumping is *specificity*. The pump, for example, must only pump out Na^+ but not closely similar ions like K^+ . Since K^+ and Na^+ differ from each other only in short-range attributes and the differences in these attributes cannot be told apart without close-contact association, the pump must begin its operation by making close-contact association with Na^+ . Or phrased differently, the pump must *adsorb* Na^+ in overwhelming preference over K^+ . A second essential attribute of pumping is *restrictiveness*, i.e., there can be only a limited number of pumping “sites.” Or else, both Na^+ and K^+ would be pumped—even though the sites strongly prefer Na^+ over K^+ . Both specificity and restrictiveness are implicit in the (modified) *Langmuir adsorption isotherm* (see endnote 5 of Chapter 3) which makes up the left hand side of equation A.

The restricted number of pumping sites leads to the manifestation of *saturation*. That is, as one increases the concentration of Na^+ in the external environment (and indirectly the intracellular Na^+ concentration), the number of available pump sites for additional adsorption of Na^+ decreases. Hence the rate of increase in pumping rate per unit increase

of external Na^+ concentration decreases. The limited number of pumping sites also gives rise to *competition*. That is, the rate of Na^+ pumping is reduced due to the presence of similar ions that compete for the pumping sites. Saturability and competition are fundamentally the same phenomenon, differing only in the nature of the additional ions involved.

The steady state established between nonsaturable inward leakage and saturable outward pumping generates a theoretical distribution curve—i.e., a plot of $[p_i]_{\text{in}}$ as ordinate against $[p_i]_{\text{ex}}$ as abscissa—that bends *upward* with increasing $[p_i]_{\text{ex}}$, its (below-unity) slope increasing asymptotically toward a slope of unity (see Ling 1988a). Indeed, for all solute that require outward pumping, this kind of upward-bending distribution curve is mandatory.

In reality, we have yet to observe a single case of solute distribution that follows this mandatory pattern. For large solutes, most clearly those that are not adsorbed inside the cell and found in concentration in the cell lower than in the external medium, the distribution curves are typically rectilinear, meaning that the maintenance of the low intracellular concentration does not depend on a *saturable* pumping mechanism. The ions (or other types of solutes) do not go through a step of combining with a restricted number of pump sites before exiting from the cell. Without such a step, there can be no outward pumping. Without pumping, it would be meaningless to contemplate sharing of pumping sites.

2. Troshin died of cancer in December, 1986. Equation 18, which is in essence the same as equation 15, has been amply confirmed by him, by us, and by others. I suggest that this equation be named the Troshin equation in his memory.

3. NMR spectra of ^{23}Na in frog muscle and sulfonate-ion-exchange resins are closely similar to each other (but different from the spectrum of a NaCl solution) in that only half of the ^{23}Na signal is “visible.” Berendsen and Edzes (1973) argue that this is evidence that ^{23}Na in cells is free because, following the conventional view of Gregor (1951), Na^+ and other counterions in ion-exchange resin are free. Cope (1967) and Ling and Cope (1969) postulated that the same evidence indicates the adsorbed state of Na^+ in living cells, because they believe Na^+ in sulfonate-ion-exchange resin is adsorbed. In 1983, Ling and Zhang, with the aid of a Na -selective electrode, established that Na^+ in sulfonate-ion-exchange resin is indeed adsorbed.

4. In the earliest version of the AI hypothesis (Ling 1951, 1952), selective adsorption of K^+ over Na^+ on anionic sites (rather than the membrane pump) was first introduced. While emphasizing the protein carboxyl groups as the main anionic sites for K^+ adsorption, I did, nonetheless, suggest that the residual negative charges of *adsorbed* multivalent ATP, phosphocreatine, etc., might also function as K^+ -adsorbing sites (see Ling 1952, Figure 8 on 778). This idea was mentioned again in 1966 (see Ling and Ochsenfeld 1966, 841). Yet in that same 1966 communication, one reason for rejecting (adsorbed) phosphates as K^+ -adsorbing sites was also presented, i.e., the high degree of *uniformity* in the adsorption of *all* the K^+ in muscle cells. K^+ adsorption on mixed carboxyl and phosphate sites would certainly not predict the observed uniformity.

A second reason for rejecting phosphates as K^+ -binding sites came from the recognition that K^+ adsorption in all types of living cells is basically alike, yet the major intracellular anions that are found in approximately the same concentration as K^+ are not always (multivalent) phosphates, as in muscle tissues. As mentioned in the text, major intracellular anions in other cell types may be monovalent (e.g., Cl^-), and as such cannot provide residual anionic charges for K^+ adsorption once they are adsorbed onto proteins. A third reason for rejecting phosphates as K^+ -binding sites is the gathering evidence that phosphates, Cl^- , isethionate, etc., are all *congruous* anions essential in dissociating intracellular salt linkages to liberate carboxyl groups which then provide the chemical basis for the *uniformity* in K^+ adsorption seen in all living cells.

5. Virtually all living cells partially exclude solutes like Na^+ , and sucrose. Phylogeny and ontogeny dictate that all living cells have a common origin. Considered together, these facts suggest (1) that an ubiquitous protein maintains the bulk of water in the state

of polarized multilayers in all living cells and (2) that this ubiquitous protein is actin (Ling 1979, p. 46–47)—not in the form of F actin but what I tentatively designated as “pro-filamentous” or G* (Ling 1984, p. 568).

While attending the Pfefferkorn conference in Santa Crus, Calif., in August 1990, I met Prof. Jacques Dubochet (from the University of Lausanne, Switzerland) who most kindly told me about the exciting work he and his colleagues had just completed: *the addition of 0.5% F-actin (or G-actin) and 0.1% α -actinin in an ATP-containing buffer, to an aqueous solution of 15% 1,2-propanediol and 8% glycerol prevents ice-crystal formation at liquid-nitrogen temperature* (Prulière and Douzou, 1989; Prulière et al, 1990).

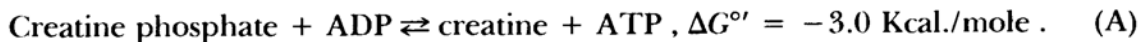
Since as a rule, freezing-point depression and inhibition of ice crystal formation result from multilayer polarization of the bulk-phase water (Section 5.2.5.5.), the new findings suggest that actin might indeed be the universal water-polarizing protein, and that α -actinin (and other similar actin-binding proteins) might indeed serve the role of protein X of Figure 8.14. Whether this interpretation is correct or not must await future investigations. (Size-dependent solute exclusion would offer one easy and unequivocal way proving or falsifying multilayer polarization of the bulk phase water containing actin, α -actinin, propanediol and glycerol in the proportion as described).

For possible additional implications of the new findings, see Section 5.2.2. on the subject of high efficiency in water polarization and Section 8.3.3. on the subject of “buffer protein” maintaining the bulk-phase water in living cells in the state of polarized multilayers at all times.

If the actin- α -actinin-ATP complex indeed functions as the universal water polarizing system, its relation to hemoglobin suggest even more complex interaction than that depicted in Figure 8.14. Does actin function as the protein X itself, while α -actinin functions as actin’s own protein X?

6. The CrP content of 21.8 μ mole/g. fresh muscle quoted from Ling (1962, 217) was obtained in the late 1940s from unfed, starving frogs. After ways of feeding and other better ways of caring for the captured frogs were found and instituted, the CrP contents of the frogs became considerably higher, often approaching 30 μ mole/g. (see Figures 8.20 and 8.21).

7. The enzyme, creatine kinase, catalyzes the following reaction:



The large negative value of ΔG° points out that the reaction tends to proceed to the right. That is, it will if all the reactants exist freely dissolved in water, as they have long been assumed to be in living cells—following the membrane-pump theory—and as they indubitably were in the test tubes where the value of ΔG° was determined (Lehninger 1975, 406).

However, there is strong evidence that contradicts the assumption that all biochemical intermediates in the living cells exist in the free state. For example, the adsorption constant of ATP on myosin—the most abundant protein in muscle cells—is $10^{10} - 10^{11}$ (Section 8.4.2.2). An adsorption constant of this magnitude assures us that in muscle cells virtually all ATP exists in the adsorbed state, and so are probably most of the other biochemical intermediates found predominantly within the cells—after all, the logic of the AI hypothesis dictates that all permeant solutes that exist at a concentration in excess of that found in the surrounding medium must be adsorbed. Therefore, the state of equilibrium between CrP and ATP in living cells may be quite different from predictions made on the basis of the assumption of free solutes in living cells.

Permeability to Water, Ions, Nonelectrolytes and Macromolecules

Membrane permeability has long been a *sine qua non* of the standard textbook version of cell physiology. The belief in an inseparable tie between cell functions and membrane functions began early. Theodor Schwann, the founder of the *cell theory*, held such a view (see Introduction). Serious challenges throughout history notwithstanding, the concept has dominated cell physiology ever since, becoming more enshrined with time. Thus, in recent years, classic cell physiology has been referred to with increasing frequency as “membrane physiology.” Incredible as it may seem, this continued belief in the cardinal role of plasma membranes in cell functions is not based solidly on experimental evidence, but is perhaps more a matter of tradition—or inertia.

The experimental findings documented in the preceding chapters have already shown that the living cell is not a liquid-filled pouch, nor can cell physiology be equated with membrane physiology. Thus out of the three classic subjects of cell physiology (besides permeability), two (solute distribution and volume regulation) have little or nothing to do with membrane function, nor does the generation of cellular resting potential, to be discussed below. The more limited role of membrane permeability in cell physiology is but one aspect of revolutionary changes in cell physiology that have occurred in the last half century. Other equally profound changes relate to such questions as these: What is a cell membrane? What is it made of?

The following pages will present an analysis of the conventional theory of cell membranes and of why the view of the cell membrane as a lipid bilayer punctured with a few pores has outlived its usefulness. I also present the theory of cell membrane(s) according to the AI hypothesis, which sees the major components of the cell membrane or membranes of subcellular particles as proteins and intensely polarized water, with lipids playing a secondary role. Not only is the new theory in harmony with the great majority of experimental facts, but it is also fully possessed of the key features that distinguish all valid scientific theories (features not possessed by the membrane theory): self-consistency and coherence.

9.1. *The Lipoidal Membrane Model in the Past and the Present*

9.1.1. *Overton's Original Model*

After the founding of the membrane theory (Pfeffer 1877), Overton hypothesized that all cells are covered by a continuous lipid membrane (Overton 1895). In his view, the widely different permeability of living cells to nonelectrolytes resulted from their widely different solubility in the membrane lipids. In support, Collander showed that the rates of permeation of 69 nonelectrolytes into the central vacuole of *Nitella* cells¹ correlated positively with their (olive) oil/water distribution coefficients (Collander 1959, Figure 9.1). Gorter and Grendell (1925) further demonstrated that red blood cells of diverse origins all possessed *just enough* lipids to form a continuous bilayer covering of the entire cell surface. For the permeation of lipid-insoluble electrolytes and other solutes that are insoluble in lipids, Overton postulated “adenoid” or secretory activities, but provided no mechanism for them (see Section 2.1.).

9.1.2. *Subsequent Modifications of the Overton Model*

Overton's lipoidal membrane theory predicts that the cell membrane should be more permeable to ethanol than to water, because ethanol is 75 times more soluble in oil than in water (Figure 9.1). This does not agree with one of the most outstanding features of cell membranes: their *semipermeability*. Thus in the first recorded demonstration of the semipermeability of biological membranes by Abbé Nollet, dried pig bladder was found to be much more permeable to water than to ethanol (see Glasstone 1946, 651). This and other inconsistencies between theory and fact led Collander and Bärland to postulate a *mosaic membrane*, in which the continuous lipid membrane covering the cell is punctured by pores just wide enough to allow the passage of water and other small molecules, but too narrow to permit passage of other larger solute molecules (Collander and Bärland 1933). The mosaic membrane theory incorporates both the lipid membrane concept of Overton and the atomic sieve idea of Traube; its authors were apparently unaware of, or at least did not discuss, the serious criticism of Traube's atomic-sieve hypothesis mentioned in Section 1.2.2. In the modified version of the lipoidal membrane theory, permeation by water (and other small molecules), nonelectrolytes, and electrolytes involved different routes: small pores for water, lipid layer for nonelectrolytes, and “adenoid” activity for electrolytes.

Soon afterwards, a much lower interfacial tension was measured at real cell surfaces (0.08 dyne/cm) than that measured at the interface between water and lipids (20–30 dyne/cm), (Cole 1932).² Harvey and Danielli (1939) then suggested that the lipid of the cell membrane is not directly exposed to the bulk phase water, but is sandwiched between layers of hydrophilic globular proteins, thereby reducing the surface tension of the living cells. They called this model of the cell membrane the *pauci-molecular membrane model* (Davson and Danielli 1943).

Five years before Collander and Bärland introduced their mosaic membrane model, Mond and Amson (1928) introduced another modified version of

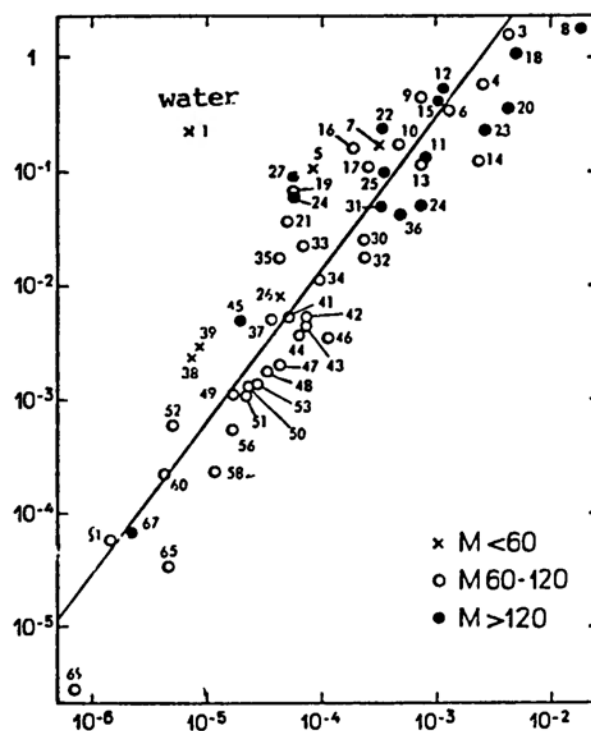


Figure 9.1. Correlation between the permeation power of several nonelectrolytes into *Nitella mucronata* cells on the one hand and their relative oil solubility and molecular weight on the other. Ordinate: $PM^{1.5}$, where M is the molecular weight of the nonelectrolyte; abscissa: distribution coefficient olive oil: water. The substances are: 1, HDO; 3, methyl acetate; 4, *sec*-butanol; 5, methanol; 6, *n*-propanol; 7, ethanol; 8, paraldehyde; 9, urethane; 10, isopropanol; 11, acetylacetone; 12, diethylene glycol monobutyl ether; 13, dimethyl cyanamide; 14, *tert*-butanol; 15, glycerol diethyl ether; 16, ethoxyethanol; 17, methyl carbamate; 18, triethyl citrate; 19, methoxyethanol; 20, triacetin; 21, dimethylformamide; 22, triethylene glycol diacetate; 23, pyramidon; 24, diethylene glycol monoethyl ether; 25, caffeine; 26, cyanamide; 27, tetraethylene glycol dimethyl ether; 30, methylpentanediol; 31, antipyrène; 32, isovaleramide; 33, 1,6-hexanediol; 34, *n*-butyramide; 35, diethylene glycol monomethyl ether; 36, trimethyl citrate; 37, propionamide; 38, formamide; 39, acetamide; 41, succinimide; 42, glycerol monoethyl ether; 43, *N,N*-diethylurea; 44, 1,5-pentanediol; 45, dipropylene glycol; 46, glycerol monochlorohydrin; 47, 1,3-butanediol; 48, 2,3-butanediol; 49, 1,2-propanediol; 50, *N,N*-dimethylurea; 51, 1,4-butanediol; 52, ethylene glycol; 53, glycerol monomethyl ether; 56, ethylurea; 58, thiourea; 60, methylurea; 61, urea; 65, dicyanodiamide; 67, hexamethylenetetramine; 69, glycerol. (Collander 1959, by permission of Academic Press)

Traube's atomic-sieve idea in which membrane pores are large enough to allow the passage of the smaller hydrated H^+ and K^+ but not large enough to permit the passage of the larger hydrated Na^+ , for example. As mentioned in Section 1.3, Boyle and Conway incorporated this idea in their broad theory of the living cell of 1941. However, soon afterwards, radioactive tracer and other types of studies showed that Na^+ (Cohn and Cohn 1939; Heppel 1939), Ca^{++} (Shanes and Bianchi 1959), and Mg^+ (Conway and Cruess-Callaghan 1937; Ling et al. 1979) are all able to cross the cell membranes. The Mond-Amson-Boyle-Conway sieve concept was thus disproven.

Further studies revealed the permeability of various cells to other solutes long

considered impermeant, including sucrose (Kolotilova and Engelhardt 1937; Levine and Goldstein 1955; Kipnis and Cori 1957; Norman et al. 1959; Ling et al. 1969a); free amino acids (Gale 1947; Christensen 1955); diamino acid, carnosine (Eggleton and Eggleton 1933); hexose monophosphate (Roberts and Wolffe 1951); ATP (Talaat et al. 1964; Boyd and Forrester 1968; Pratt and Marshall 1974; Hearse et al. 1976); and proteins (Zierler 1958; Ryser 1968; McLaren et al. 1960; Dawson 1966). In some microbial cells, the cell membrane has been shown to be permeable even to DNA (Avery et al. 1944) and RNA (Yamamoto et al. 1971). *Clearly, a theory postulating small pores in lipid membrane sandwiched between globular proteins for all living cells does not have the flexibility to cope with these findings* (see Section 9.2 below).

A theory postulating a larger pore could overcome some old difficulties, but would also create new ones. Thus, of the 69 organic compounds investigated by Collander and presented in his 1959 review (Figure 9.1), the compound with the *highest* oil/water distribution coefficient (paraldehyde)—and hence the most likely to enter the cell via the lipid phase—is not expected to do so because its oil/water distribution coefficient is 0.01. That is, the odds are 100 to 1 against paraldehyde entering the cell via the lipid route, and in favor of entrance via the aqueous route of equal area and depth. The probability of other compounds choosing the lipid route would be even more remote. Therefore, most non-electrolytes would shun the lipid phase, and would enter or leave the cells via the wide water-filled pores.

In travelling through these large pores filled with normal liquid water, the only variations in the rates of permeation of different solutes would be those due to their respective diffusion coefficients in (normal) water, and these differences are very limited indeed. As an example, the diffusion coefficient of tritiated water (THO) in water at 25°C is 2.44×10^{-5} cm²/sec (Wang et al. 1953), and thus only *4.67 times* faster than that of sucrose (5.226×10^{-6} cm²/sec, Hodgman et al. 1961). The actual permeability of inverted frog skin to water and sucrose is different by *5 orders of magnitude* (Figure 9.3). Clearly, a theory of transportation via large pores filled with normal liquid water is not the answer.

Other explanations have been proposed: one is the new model of the cell membrane derived from the AI hypothesis, which will be discussed in detail in Section 9.2 following; another one, surprising to scientists like myself, is a return to Overton's original continuous lipid-layer concept.

9.1.3. *Overton's Lipid-Layer Model Once Again*

The return to Overton's (1895) continuous lipid-membrane concept apparently began with a shift to a different concept of *lipids*. This time, a lipid is no longer regarded as a neutral fat exemplified by olive oil and used in Collander's studies, but is like the phospholipid bilayers employed in the Müller-Rudin-Tien-Wescott black-membrane technique (Müller et al. 1962), and illustrated by Singer and Nicolson (Figure 9.2, Singer and Nicolson 1972). One reason for this revision is the finding that phospholipid membranes have a relatively lower interfacial

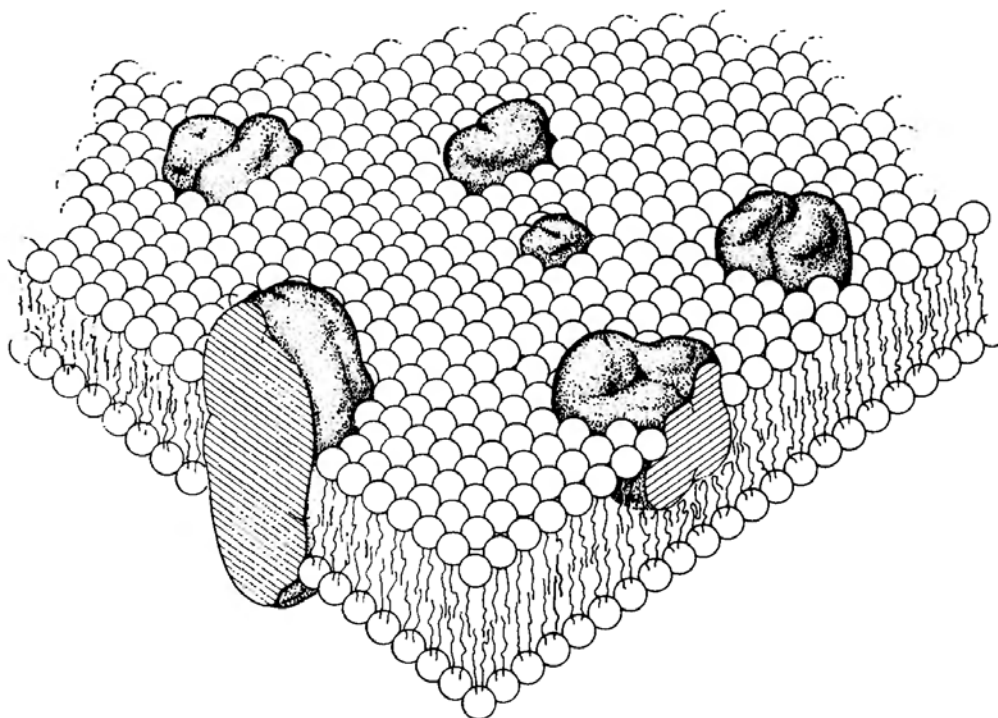


Figure 9.2. Lipid-globular protein mosaic model (fluid mosaic model): schematic three-dimensional view. The solid bodies with stippled surfaces represent the globular integral proteins, which at long range are randomly distributed in the plane of the membrane. At short range, some may form specific aggregates. (Singer and Nicolson 1972, by permission of Science)

tension (1.0 dyne/cm) than olive oil membranes (20–30 dynes/cm) (Jain 1972, Table 4–1). The need to cover the membrane with hydrophilic globular proteins in order to reduce the large interfacial tension seemed less pressing and the covering protein layers in the pauci-molecular-membrane model were removed quietly, thereby returning once again to Overton's lipid layer model.

Nevertheless, the interfacial tension at the phospholipid water interface is still ten times higher than that found at the cell surface, i.e., 0.08 dyne/cm (Cole 1932). Such a tenfold difference requires a better explanation for dismissal than the existence of an even larger difference between the surface tension of olive oil membrane and that of the living cell membrane. Yet no explanation was given.

A second reason for the return to the Overton model was the discovery that phospholipid bilayer membranes are much more permeable to water than olive oil layers. The water permeability of the phospholipid bilayer is in the range 10^{-4} to 10^{-3} cm/sec (Jain 1972, Table 4–1), and thus appears in keeping with water permeability measured in various types of living cells (Table 9.1, House 1974). Similarly, the permeability to various nonelectrolytes through the phospholipid bilayers also seems to lie in the same range of values as those measured in living cells (Redwood and Hayden 1969; Everett et al. 1969; Wood et al. 1968).

The apparent quantitative agreement between phospholipid membrane

Table 9.1. Apparent Water Permeability (P_d) of Various Cell Types (House 1974, by permission of Edward Arnold Publishers Ltd.)

Cell	$P_d \times 10^4$ (cm sec ⁻¹)
Dog erythrocyte	64
Human erythrocyte	53
Human erythrocyte	53
Cow erythrocyte	51
Human erythrocyte	48
Dog erythrocyte	44
Human (foetal) erythrocyte	32
Squid axon	4.0
Barnacle muscle	2.6
Squid axon	1.4
Frog (ovarian) egg	1.3
Crab muscle	1.2
<i>Xenopus</i> egg	0.90
Frog egg	0.75
Zebra fish (ovarian) egg	0.68
Zebra fish egg	0.36
Amoeba (<i>Chaos chaos</i>)	0.23
<i>Amoeba proteus</i>	0.21

permeability and cell permeability is limited to that of water and nonelectrolytes. It does not extend to ions like K^+ and Na^+ at all. **Living cells are, as a rule, quite permeable to K^+ , and Na^+ , and Cl^- ions.** Thus, in Ringer solutions containing K^+ , Na^+ and Cl^- as the major current-carrying ions, the membrane resistance of different cells measured are low (squid axon, 700 to 1000 ohm/cm²; frog muscle, 4000 ohm/cm²; human erythrocytes 7 ohm/cm²; see Ling 1984, 378 for a more complete set of data).

In contrast, phospholipid-bilayer membranes are highly impermeable to ions like K^+ , Na^+ and Cl^- (Miyamoto 1966; Miyamoto and Thompson 1967). Andreoli et al. (1967, 1967a) showed that *black membrane* prepared from phospholipids extracted from sheep erythrocytes have electrical resistance in the range of 1 to 3×10^8 ohm/cm², which is orders of magnitude higher than values for living cell membranes, especially erythrocyte membranes. This high resistance is also indifferent to the concentration of KCl solution on either side of the membrane. However, addition of certain macrocyclic compounds like valinomycin drastically increase the permeability to K^+ (but not to Na^+) across the membrane if the membrane is bathed in, say, 100mM KCl (Andreoli et al 1967a). Following this discovery, it was thought that similar K^+ -specific natural *ionophores* might exist in the (postulated) phospholipid bilayers of real cell membranes. In facilitating K^+ permeation in normal resting cells, the natural ionophores would perform the "adenoid" activity that Overton had long ago suggested.

Extensive efforts were made to isolate these postulated natural ionophores from living cell membranes and to introduce them into phospholipid bilayers in order to demonstrate an ion-specific ionophore effect. In 1975, Müller, who with Rudin introduced the black lipid membrane technique, ruefully remarked: "A lot of us have spent a wasted ten years or so trying to get these various materials into the bilayers . . ." (Müller 1975).

Failure to find a natural ionophore for K^+ (and for a host of other ions and electrolytes) left the continuous phospholipid membrane model with no mechanism at all to explain the relatively high permeability of resting cells to K^+ , Na^+ , Cl^- , and other electrolytes. We were therefore one full cycle back when Mond entered with his resurrected "atomic-sieve" idea from Traube. Sure enough, sieve-like rigid membrane pores called "Na channels" and "K channels" were once more postulated (Section 11.5.1.2(3)). However, there was one significant difference between the old and the new sieve models. While the Mond pores were *open at all times*, the newly postulated ion-specific Na^+ and K^+ channels are *closed in the resting cell*. Therefore, the phospholipid-bilayer membrane is without a mechanism for the busy traffic of K^+ , Na^+ , and other ions in their resting state (see Section 9.2.2.1.). However, incompetence in explaining electrolyte traffic in resting cells is not the only serious problem with the phospholipid-bilayer model. Other problems no less serious will be discussed next.

Electron microscopy has revealed the existence of the laminar cell-membrane structure. This finding was widely hailed as providing unequivocal evidence for the concept that the cell membrane represents primarily lipid bilayers (Robertson, 1960). This enthusiasm, however, did not last long. Soon afterwards it was found that ***removal of 95% of the lipids from the liver mitochondrial membranes*** (Fleischer et al. 1967) ***and from membranes of microbial cells*** (Morowitz and Terry 1969) ***did not destroy the trilaminar structure of the membranes at all.*** Yet in both the revived Overton model and the original paucimolecular-membrane model, the removal of 95% of the membrane lipids should have destroyed or at least severely altered the membrane structure (see Ling 1984, 382). In a section below, I demonstrate that there are also serious problems with the model as regards the agreement between water and nonelectrolyte permeability of lipid bilayers and of living cells. Once more, what was only recently regarded as providing strong evidence in favor of the phospholipid-bilayer model, turned out to be only a mistake—a big one to boot—in consequence of some seemingly harmless incorrect assumptions (Section 9.2.1.4).

It was in 1898 that Overton first presented, before the Naturforschende Gesellschaft of Zurich, his lipoidal membrane theory (Overton 1899). In the ensuing century, vast amounts of time and effort have been spent in developing and testing this theory. While there is no question that phospholipids are a component of many cell membranes, the evidence already cited and to be presented shows that the role of the phospholipid bilayer in determining permeability to water, nonelectrolytes, and ions is, at best, secondary, and perhaps limited to some unusual cells (e.g., erythrocytes). It is time to turn our attention to an altogether different model.

9.2. *The Cell Membrane as a Lipid-Protein-Polarized-Water System*

In 1951 and 1952, I introduced an electrostatic mechanism for the selective accumulation of K^+ over Na^+ , relying on close-contact adsorption of K^+ on β - and γ -carboxyl groups of cell proteins (Ling 1951; 1952; 1984, 93). I pointed out that, roughly speaking, the cell membrane could be visualized as a two-dimensional replica of the cytoplasm, containing water and proteins carrying β - and γ -carboxyl groups (Ling 1952, 782). Following the introduction in 1965 of the polarized-multilayer theory of cell water (Ling 1965), the concept of the cell membrane containing lipids, proteins, and domains of polarized water was introduced (Ling 1965a, S110). ***Such a wet membrane is in harmony with the very low surface tension of living cells measured and mentioned above.*** Such a wet membrane also stands in sharp contrast to the conventional view, in which the cell membrane is made of lipid and globular protein and is thus **dry** (see Figure 9.2).

Another major difference between the conventional concept and the new concept of the cell membrane introduced in the AI hypothesis originates from a profoundly different concept of the cytoplasm. In the membrane theory, the cell membrane is like the wall of a urinary or gall bladder; two more-or-less similar interfaces separate the membrane from free water within and outside the cell. In the AI hypothesis, the cell membrane and cell cytoplasm are both proteinaceous fixed-charge systems containing polarized water. Therefore, the cell membrane and the cytoplasm are not separated from each other by a discontinuity in their physical states, a discontinuity one finds only at the outer boundary of the cell membrane. The cell membrane is therefore more like the skin of, say, a carrot or a celery stalk, than a bladder.

The model of the cell membrane according to the AI Hypothesis has two additional features not found in the stereotyped lipoidal membrane models:

(1) *Variability*: The percentage of membrane area occupied by polarized water and the intensity of polarization of that water can both vary. So can the percentage of surface area occupied by membrane lipids; so can the percentage area occupied by proteins, their density and polarity, the c - or c' -values of the fixed ions and the c - and c' -value analogs of their backbone CO and NH groups (Section 7.3.3.2). The result is a model that can handle the high degree variability observed in different types of cells and of the same cells under different physiological conditions.

(2) *Coherence and Control*: The c -value of the β - and γ -carboxyl groups and the degree of polarization of water, for example, are under the control of the proteins. The proteins are in turn controlled by cardinal adsorbents. Thus, a second advantage of this membrane model is that it brings permeability to water, non-electrolytes, and ions under the coherent control of cardinal adsorbents.

The idea that the major nonaqueous component of the cell membrane is proteinaceous rather than lipoidal has been confirmed by chemical analyses—a fact, which of itself, offers serious challenge to the lipoidal membrane theory. Thus, in ten cell membranes analyzed, the average protein content was $66.7\% \pm 3.0\%$, while the average lipid content was only $30.1\% \pm 3.0\%$ (Dewey and Barr 1970). Among

the ten membranes analyzed, erythrocyte membranes contain 47% lipids. Since most living cell membranes analyzed contain a lower percentage of lipids than erythrocyte membranes (Ling 1984, 381), Gorter and Grendell's finding mentioned in Section 9.1.1. that erythrocytes have just enough lipids to form one continuous covering of the cell surface has offered evidence that *in most cell membranes, there is not enough lipid to form a continuous layer*. Indeed, other new evidence showing that the cell membrane contains large amounts of (polarized) water comes indirectly from the detailed analysis of the pattern of diffusion of water, into and out of living cells, to be described next.

9.2.1. *Permeability to Water and Nonelectrolytes*

9.2.1.1. *Domains of Polarized Water as a Major Component of the Semipermeable Membrane*

It was the semipermeable properties of the copper-ferrocyanide membrane that led to the formulation of van't Hoff's law of osmosis (1885) and the founding of the membrane theory (Ling 1984, 9 to 13). Copper ferrocyanide contains neither neutral fat nor phospholipids—nor do parchment paper, gelatin, metallic silicates, metallic tannate, and Prussian blue. Yet all of these materials in membrane form, demonstrate semipermeable properties like those of living cell membranes (see Graham 1861; Tinker 1916; Findlay 1919).

While these model semipermeable membranes do not contain lipids of any kind, they do, without exception, possess water and a solid matrix. *According to the AI hypothesis, the semipermeable properties of these models as well as those of phospholipid bilayers and of living cell membranes have a common origin: the water present therein, existing in the state of intensely polarized multilayers* in consequence of interaction with the solid matrix. To substantiate this view, we undertook a study comparing the permeability of a living cell membrane system with a model membrane containing polarized water. The results are described next.

Recall that cellulose is made up of glucoside chains that are rigidly interwoven and take up only a small amount of water. However, when substituents are introduced into the glucoside residues, they pry loose the cellulose chains. Enhanced water uptake follows as a consequence. Methylcellulose provides an example of this kind. Water in a solution of methylcellulose like gelatin and PEO excludes large and complex solutes (Table 5.2) in agreement with the notion that this water exists in the form of polarized multilayers (Ling et al. 1980, 1980a).

Another derivative of water-absorbing cellulose is cellulose acetate. It also takes up large amounts of water. Dissolved in acetone, cellulose acetate can be cast in the form of thin sheets. If heated (80°C, 15 min) after equilibration in water, the partially dried surface of these cellulose acetate membranes becomes "activated" (Loeb and Sourirajan 1960). This activation probably involves further loss of the water from the surface layer and *intensification of polarization* of the water remaining (Ling et al. 1980a; Ling and Ochsenfeld 1983). **According to the AI hypothesis, it is the intensely polarized water in the cell membrane that is responsible for size-dependent selective permeability to water and other**

nonelectrolytes. A comparative study of water and nonelectrolyte permeability through an activated cellulose acetate membrane and a living cell membrane provides an excellent opportunity to test this theory.

Figure 9.3 shows the results of such a comparative study (Ling 1973a). Here the permeability to 11 hydroxylic compounds at three different temperatures through heat-activated cellulose acetate sheet, on the one hand, and inverted frog skin, on the other, were cast as abscissa and ordinate respectively. A linear correlation coefficient of +0.961 was found. In both the living and model membranes, the permeability decreases sharply with the increasing size of the solute. Since the permeability constant (P_i) is equal to the product of the equilibrium-distribution coefficient (or q -value) of the solute and the diffusion coefficient (D) in the membrane substance (i.e., $P = qD$), the size dependence of the permeability observed is in harmony with the dependence of the q -value on solute size in polarized water discussed earlier (i.e., the size rule, Section 5.2.5.1(3)).

Actually, the data shown in Figure 9.3 demonstrate more than good correlation. Since the ordinate and abscissa are in the same units, there is an almost **1:1 correspondence**. By the method of least squares, one finds that the straight line that best fits the data points is described by the following relation:

$$\log (P_{\text{frog skin}}) = 0.990 (P_{\text{cellulose acetate}}) - 0.1659 ,$$

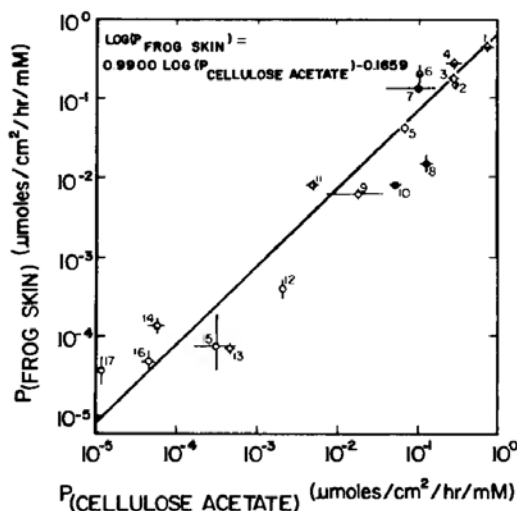


Figure 9.3. Plot of the permeability of reversed living frog skin against the permeability of heat-treated cellulose acetate membrane. Lengths of horizontal and vertical lines indicate $2 \times \text{SE}$ (twice the standard error of the mean) except in the few cases when no SEs are given since only two determinations were made. Straight line was obtained by the method of least squares. Numbers refer to different compounds: 1, THO, 25°C; 2, THO, 4°C; 3, THO, 0°C; 4, methanol, 25°C; 5, methanol, 0°C; 6, ethanol, 25°C; 7, n-propanol, 25°C; 8, ethylene glycol, 25°C; 9, ethylene glycol, 0°C; 10, glycerol, 25°C; 11, glycerol, 4°C; 12, glycerol, 0°C; 13, erythritol, 0°C; 14, xylitol, 0°C; 15, sorbitol, 0°C; 16, L-glucose, 0°C; 17, sucrose, 0°C. The empty circle (○) represents experiments of 0°C; circle with the right half filled (◐) 4°C; circle with the bottom half filled (◑) 25°C. (Ling 1973a, by permission of Biophysical Journal)

where $P_{\text{frog skin}}$ and $P_{\text{cellulose acetate}}$ are the permeability rates of frog skin and cellulose acetate respectively. Note that the solutes studied range from small molecules like water all the way to molecules as large as sucrose. Note also that unlike the olive oil/water distribution coefficient which predicts higher permeability to ethanol than to water, water has a higher permeability than ethanol, both in the model and in the living cell membrane. *Thus both the inverted frog skin and cellulose-acetate membranes behave like bona fide semipermeable membranes, and, as such, behave differently from the olive oil studied by Collander (1959), which demonstrates antisemipermeability.*

The almost 1:1 correspondence of the two sets of data at three different temperatures also indicates similar activation energies for the diffusion of different solutes in the model and in living membranes.

On the basis of theoretical reasoning and experimental observations, Schultz et al. (1969) estimated that the average diameter of the pores in the activated layer of the cellulose acetate membrane is about 44 Å, and thus 16 water-diameters wide (see also Schultz and Asunmaa 1969) and four times greater than the diameter of sucrose (8.8 Å, see Renkin 1954; House 1974, 131). Yet both the cellulose acetate sheet and the inverted frog skin have permeability to sucrose more than 10,000 times lower than to water! Schultz and Asunmaa also found that water in these wide pores of the activated cellulose acetate is highly structured, with a viscosity 37 times higher than that of ordinary liquid water.

Pores with limiting diameters sort solutes into two classes: permeable small ones and impermeable large ones. Within limits, a lipid layer offers a *continuous* range of decreasing permeability with increasing molecule size. A mosaic membrane combining sieve-like pores and lipid solubility should also demonstrate a *discontinuity* in the permeability of solutes of increasing size. No such discontinuity is seen in the results for inverted frog skin or for cellulose acetate membranes. Thus for more than one reason, intensely polarized water is a far better model of the living cell membrane than an atomic sieve, a lipid (or phospholipid) layer, or the two combined.

The results of our study comparing cellulose acetate membrane and inverted frog skin provide new insight for reviewing an earlier model of the cell membrane, the copper-ferrocyanide gel membrane. It was investigation of this artificial membrane that led Pfeffer to the founding of the membrane theory. Yet, as pointed out in Section 1.2.2., attempts of Traube to explain semipermeability in terms of an atomic sieve theory failed. The copper ferrocyanide "pores" are far too large to bar the permeation of solutes known to be virtually impermeant (e.g., sucrose). *Once one realizes that permeability to solutes through wide domains of water existing in the state of intensely polarized multilayers obeys the size rule, with high permeability to small molecules and low permeability to large ones; the permeability of some cells to proteins, DNA, and RNA (Section 9.1.2.) as well as the behaviors of copper-ferrocyanide gel membrane become readily understandable.* That the large pores of copper-ferrocyanide gel are also filled with multilayers of polarized and adsorbed water rather than normal liquid water is supported by the low solubility of sucrose in the water of this gel (McMahon et al. 1940).

9.2.1.2. *The Relative Areas of the Cell Membrane Occupied by Lipids and by Polarized Water*

So far I have suggested that cell membranes may have large pores or domains containing intensely polarized water, and that this multilayer polarization of membrane water is the consequence of interaction with certain cell-membrane proteins existing in the fully-extended conformation. Proteins lining these water domains may also offer fixed ions (e.g., β - and γ -carboxyl groups) whose presence offers selective mechanisms for ionic permeation (see Section 9.2.2.1.). As such, these earlier concepts offered no clue as to the proportion of the cell membrane area occupied by the fixed-ion-polarized-water domains and the area occupied by the lipid bilayer domains. However, new studies have provided information on this issue (Ling and Ochsenfeld 1986).

As mentioned earlier (Section 9.1.3), membranes of phospholipids isolated from sheep erythrocytes have a very high electrical resistance even when bathed in 0.1 M KCl solution ($1 - 3 \times 10^8$ ohms/cm²). Introduction of 10^{-7} M of the K⁺-specific ionophore valinomycin, or mixtures of monactin and dinactin, drastically reduces the bilayer membrane resistance by as much as 3 or 4 orders of magnitude, if the solutions bathing the membrane contain a high enough concentration of KCl (e.g., 10^{-1} M for valinomycin, 10^{-2} M for monactin-dinactin).

Figure 9.4 diagrammatically illustrates three hypothetical types of cell membranes bathed in KCl solution, and their anticipated responses to the introduction of ionophores like valinomycin. Type I is a pure lipid membrane; Type II, mixed (lipid, fixed-charge, polarized-water) membranes; and Type III, pure or effectively pure (fixed-charge, polarized-water) membranes. In the presence of suitable external K⁺ concentration, one would expect K⁺ ionophores to dra-

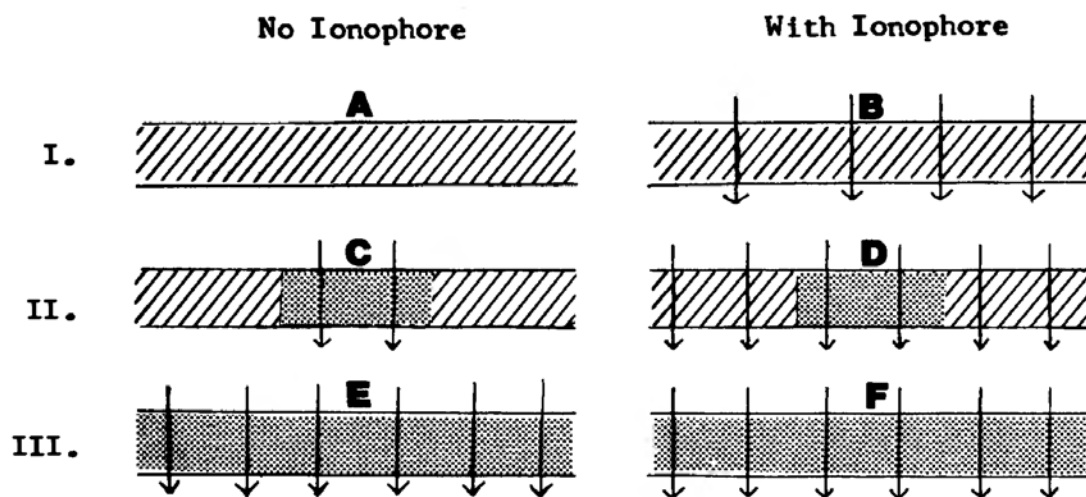


Figure 9.4. Diagrammatic illustration of three types of idealized cell membranes bathed in 0.1M KCl on both sides and the anticipated effects of added K⁺-specific ionophores on the rate of K⁺ permeation. Number of arrows roughly corresponds to relative rates of K⁺ permeation. Type I, pure lipid membrane; Type II, mixed (lipid, fixed-charge, polarized-water) membrane; Type III, pure or effectively pure (fixed-charge, polarized-water) membrane. (Ling and Ochsenfeld 1986, by permission of Physiological Chemistry Physics and Medical NMR)

matically increase the K^+ permeability of Type I pure lipid membranes, moderately increase that of Type II mixed membranes, but have no effect on that of Type III pure or effectively pure (fixed-charge, polarized-water) membranes. Thus valinomycin and similar K^+ -specific ionophores have provided a way to roughly assess the relative proportions of lipid-bilayer domains and polarized-water domains in different types of living cells.

We studied the effects of valinomycin, nonactin, and monactin (all at 10^{-7} M) on the K^+ permeability of frog ovarian eggs, frog voluntary muscle, and human erythrocytes (Ling and Ochsenfeld 1986). Figure 9.5 shows that the measured K^+ permeability is much higher in normal voluntary muscle and ovarian eggs than in normal erythrocytes. The erythrocytes showed a more or less consistent rise of K^+ permeability in response to all three antibiotics. However, this increase of K^+ permeability, ranging from 20% to 80%, is nowhere near the 1000-fold increase seen in phospholipid bilayers. No change whatsoever was observed in the K^+ permeability of frog muscles or frog ovarian eggs in response to any of the three antibiotics.

Comparing these results with other reports of failure to demonstrate K^+ -ionophore-mediated increase of K^+ permeability of squid axon (Stillman et al.

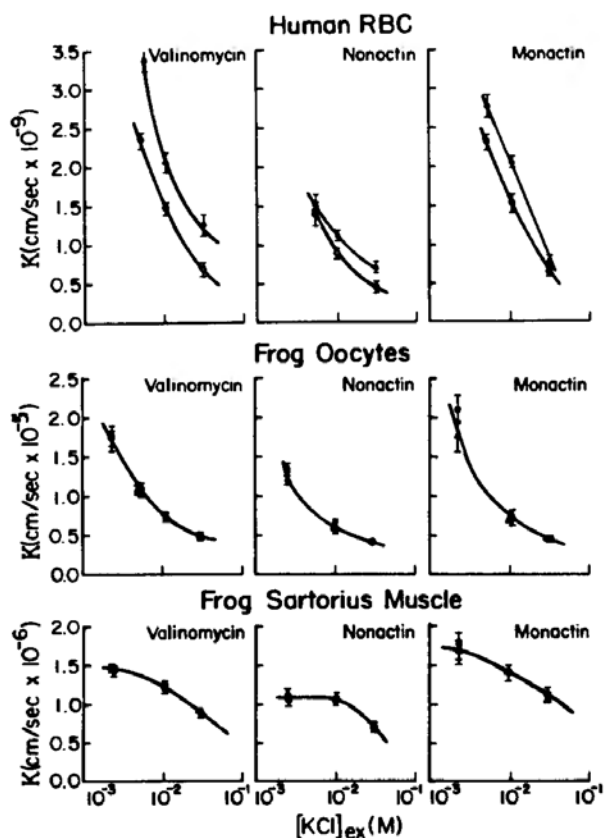


Figure 9.5. Effects of K^+ -specific ionophores valinomycin (10^{-7} M), nonactin (10^{-7} M) and monactin (10^{-7} M), on the inward K^+ permeability of human red blood cells, frog oocytes, and frog sartorius muscles at different external K^+ concentrations. K^+ permeability given in units of cm/sec. Δ , ionophore treated. \circ , control. (Ling and Ochsenfeld 1986, by permission of Physiological Chemistry Physics and Medical NMR)

1970) or of the inner membrane of the liver mitochondria (Maloff et al. 1978), we conclude that *among all the cells and cell organelles examined, only the lipid component of the red blood cell membrane acts as a significant barrier to the traffic of K^+ ion which can be partly overcome by the K^+ -ionophores. This conclusion agrees with the unusually high lipid content of the dried red cell membrane mentioned above (47%, Jain 1972), and with the presence of fixed cations in the aqueous domains of the red-cell membrane.* The presence of the fixed cations severely reduces the permeation of cations like K^+ through polarized water under the domination of the fixed cations. However as will be made clear in Section 9.2.2.1, fixed cations facilitate rapid anion traffic—hence the extremely low membrane electrical resistance mentioned earlier.

In the majority of membranes studied, including (1) the plasma membrane of frog eggs, (2) the plasma membrane of frog muscles, (3) the plasma membrane of squid axons, and (4) the inner membrane of liver mitochondria, the indifference of the K^+ permeability to the K^+ ionophores suggests that the primary, if not exclusive, route of K^+ traffic is via the polarized water-filled pores dominated by fixed anions. In other words, all of these membranes distinguished by their vigorous physiological activities belong to Type III, pure or effectively pure fixed-charge, polarized-water membranes. In the next section I present results of another assessment—using a different method—the relative proportions of the proteins, lipids, and polarized water in two types of cell membranes already familiar to us: those of eggs and of muscle cells.

9.2.1.3. *Evidence that Very Large Areas of the Egg and Muscle Surface Membrane are Occupied by Polarized Water: Bulk-Phase-Limited Diffusion of Labeled Water*

Thomas Graham, who introduced colloidal chemistry, spent most of his life studying diffusion. To him we owe Graham's law of diffusion, i.e., the diffusion rate of a gas is proportional to the square root of its density. Physiologist Adolf Fick (1829–1901) also studied diffusion; he introduced Fick's law. With a rich historical background, it is not surprising that the study of diffusion in living cells has continued to offer new insights.

Figure 9.6 presents a diagrammatic illustration of three types of diffusion into a living cell or a model. Together they serve as the basis for a method used to determine the rate-limiting step of diffusion into living cells (the *influx-profile-analysis method*) (Ling 1966a). In type A, called *surface- or membrane-limited diffusion*, the rate of inward diffusion of a substance is uniformly faster in the cytoplasm than is the rate of diffusion through the surface or membrane. Let M_t represent the amount of the labeled substance taken up at time t ; M_∞ , the level of the labeled substance taken up after immersion for an infinite length of time, and (M_t/M_∞) , the fractional uptake of the labeled substance t seconds after introduction of the cell into a solution containing the labeled substance. When M_t/M_∞ is plotted against the square root of the time of incubation, \sqrt{t} , an *S-shaped* diffusion profile is observed. In type B, called *bulk-phase-limited diffusion*, the rate of diffusion of the labeled substance is uniform throughout the entire cell. That is, the diffusion rate is not significantly slower through the cell

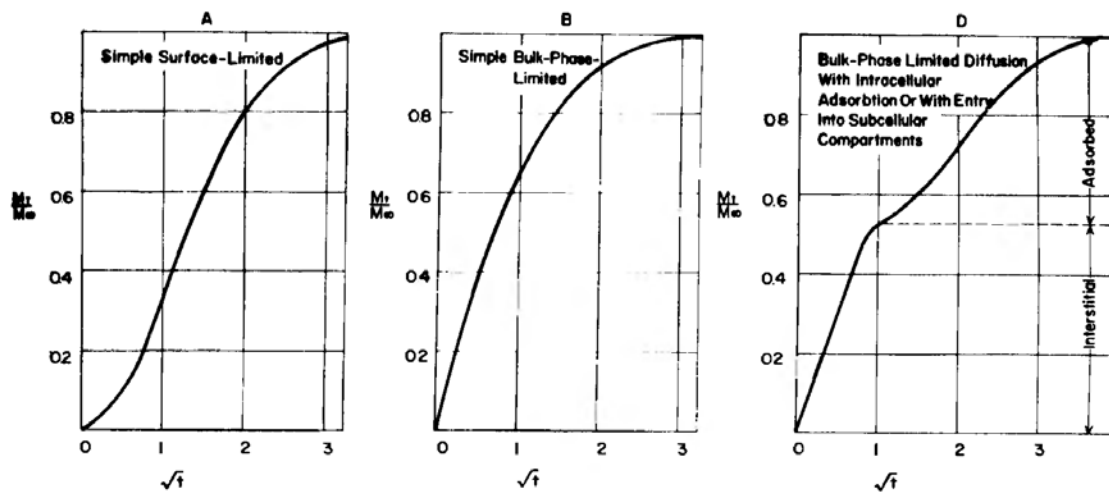


Figure 9.6. The time course of influx of a labeled substance into various systems with rate-limiting steps as indicated on each chart. The influx profiles are theoretically calculated. The ordinate represents the uptake M_t of the labeled material at time t as a fraction of the total amount of the material collected in the system at equilibrium (M_∞). The abscissa represents the square root of t . (Ling et al. 1967, by permission of Journal of General Physiology)

membrane than it is through the cytoplasm. In this case, the fractional uptake M_t/M_∞ , when plotted against \sqrt{t} , is initially a *straight line* before leveling off at a higher t .

Type C represents a *bulk-phase-limited diffusion with adsorption or entry into subcellular compartments*. In this case, the cell surface or membrane offers no greater barrier to diffusion than does that of the cytoplasm. However, once inside the cell, the substance becomes partly adsorbed or enters into subcellular compartments. Depending on the rate of adsorption and other factors, the profile may look different from that of simple bulk-phase-limited diffusion. Thus the break seen in Figure 9.6C may be conspicuous in some cases but inconspicuous in others. Since the underlying mathematics of diffusion of simple systems like these is well known, it is possible to use the analysis of the influx profile to accurately assess the relative diffusion rates of a labeled substance through the cell membrane or through the cytoplasm, as the case may be.

Besides the influx-profile-analysis method, there is a second method that can also differentiate between membrane-limited or bulk-phase-limited diffusion. Here one relies on the study of the outward movement or *efflux* of a labeled substance from a living cell or model which has previously been loaded with the labeled substance and is washed in nonlabeled Ringer solution. The logarithm of the amount of labeled substance remaining in the cell after t seconds of washing (M_t) is expressed as a fraction of the initial amount or concentration at $t = 0$, (M_0) and is plotted against the time of washing, t . Again, distinctly different efflux profiles are obtained, depending on whether or not the rate of diffusion of the labeled materials is slower through the cell membrane than through the cytoplasm.

In surface- or membrane-limited diffusion, diffusion through the cell membrane is slower than through the cytoplasm. The diffusion profile in the semi-logarithmic plot is a *straight line*, and the intercept of the straight line on the ordinate representing M_t/M_o is unity. In a bulk-phase-limited diffusion, the semi-logarithmic plot is curved in the beginning, but becomes a straight line after more washing. Extrapolation of the straight-line portion of the curve to zero time yields an intercept on the ordinate which is a constant, specific for each type of geometrical cell shape. Thus, for a long cylindrical cell, like muscle, the intercept is about 0.72.

Figure 9.7A shows the **efflux** of tritiated water (THO) from a thin cylindrical collodion-membrane-sac model which is 0.1 to 0.15 cm in diameter and contains labeled water. The straight line in a semilogarithmic plot and its extrapolation to a value of M_t/M_o equal to unity conform to typical membrane-limited diffusion. Figure 9.7C shows the **influx** profile of THO diffusion into such a microsac. The sigmoid solid line which fits most of the experimental data points is theoretically calculated also for membrane-limited diffusion.

Figure 9.7B shows the **efflux** of THO from another model, a thin filament of agar gel, 4% in dry weight and 0.104 cm in diameter. Great care was taken so that no surface drying occurred and that the gel remained homogeneous. From the straight-line part of the curve in the semilogarithmic plot, an ordinate intercept of 0.727 was obtained, in agreement with the theory of bulk-phase-limited diffusion. Figure 9.7D shows the **influx** of THO into a similar filament of agar gel, plotted against the square root of t . The solid line is a theoretical curve calculated for simple bulk-phase-limited diffusion.

Thus, as one would have expected, the diffusion of THO from and into the model of thin-collodion-membrane sacs filled with water follows the theory of a typically membrane-limited diffusion profile; diffusion of THO from and into the model of agar-gel filaments follows the theory of bulk-phase-limited diffusion.

Having verified in *inanimate models* the theoretically predicted diagnostic features of surface-(membrane)-limited and bulk-phase-limited diffusion in both influx and efflux studies, I now present results of our studies of two types of *living cells*, beginning with frog ovarian eggs.

Figure 9.8 shows the influx profile of THO for a single frog ovarian egg (D) or a cluster of a few eggs (A, B, C). The circles represent experimental data points. The data of A fit a theoretically calculated *simple bulk-phase-limited-diffusion profile* shown as the solid line (quite similar to that shown in Figure 9.6B). The data of B, C, and D best fit a bulk-phase-limited diffusion with intracellular adsorption or entry into subcellular compartments (quite similar to that shown in Figure 9.6C).

Figure 9.9 shows two sets of *efflux* curves of THO for single intact giant barnacle muscle fibers. The intercepts on the ordinate are 0.700 and 0.705 respectively, in harmony with the theoretical intercept for a bulk-phase-limited diffusion (i.e., 0.72). Figure 9.10 shows two sets of *influx* curves of THO for single barnacle muscle fibers. The circles are experimental data points; the solid curves are theoretically calculated for bulk-phase-limited diffusion with intra-

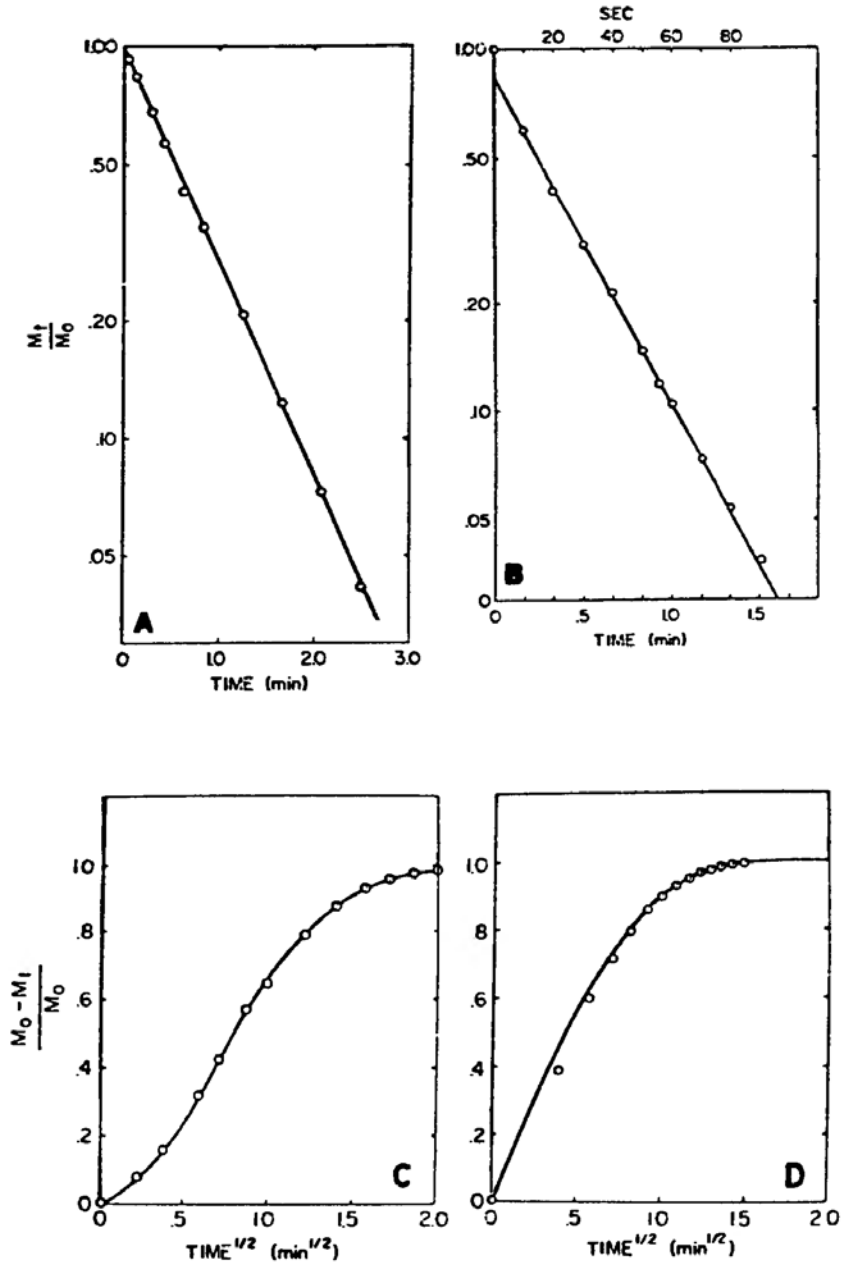


Figure 9.7. Efflux of labeled water from a collodion microsac (A), and from a cylindrical filament of agar gel (B). (A) Semilogarithmic plot of the amount of ³HHO remaining in the sac at time t (M_t) (as a fraction of the initial amount of M_0 in the sac) as a function of time t . The extrapolation of the straight line is 0.98 and the rate constant is 1.045 min^{-1} . (B) the filament of agar gel, 4% (w/v), is 0.520 cm in radius. The final straight line obtained by regression has an intercept of 0.727.

Influx of labeled water into collodion microsac (C), and into a cylindrical filament of agar gel (D). Data obtained from efflux studied by the inversion method (Ling et al. 1967). Points are experimental, solid lines are theoretical, for surface-limited (C), and bulk-phase-limited (D) diffusion. (Reisin and Ling 1973, by permission of Physiological Chemistry and Physics)

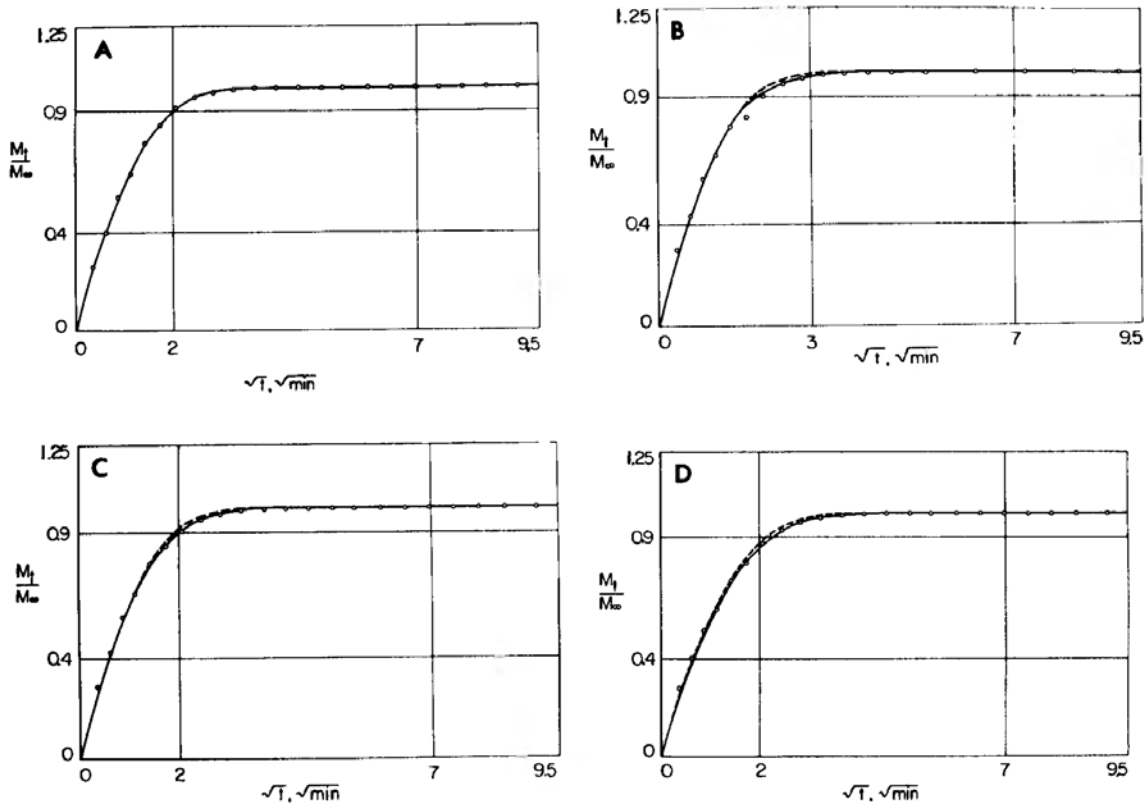


Figure 9.8. Influx profiles showing simple bulk-phase-limited diffusion and bulk-phase-limited diffusion with intracellular adsorption of THO-labeled water into a single (D) or a small cluster of a few frog ovarian eggs (A,B,C). Influx time course obtained by the *inversion method*. The solid curve A and the broken line curves in figures B through D show a theoretical plot for simple bulk-phase diffusion. All other lines are theoretical curves for bulk-phase-limited diffusion with intracellular adsorption. (Ling et al. 1967, by permission of Journal of General Physiology)

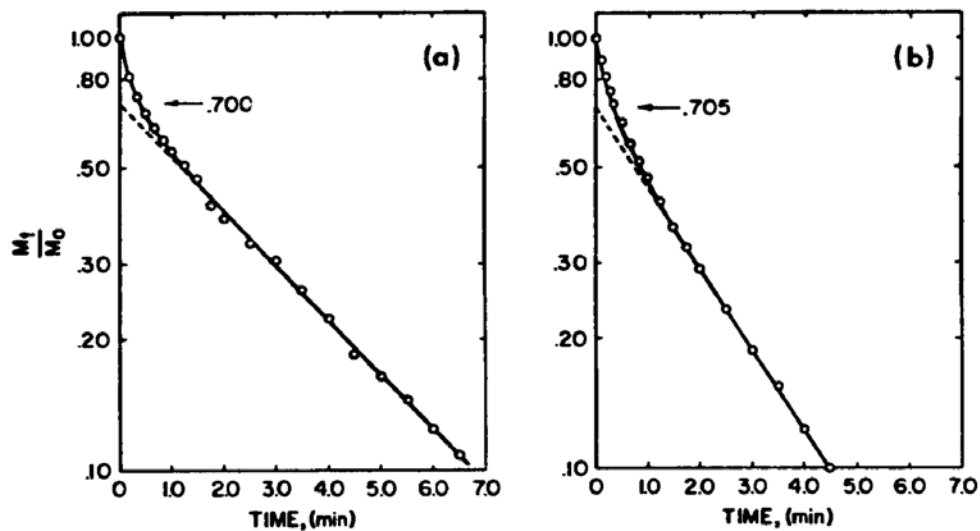


Figure 9.9. Efflux of labeled water (^3HHO) from intact single giant barnacle muscle cells. (a) cell radius, 0.075 cm; (b) cell radius, 0.067 cm. Intercepts of straight-line parts on the ordinates are 0.700 (a) and 0.705 (b) respectively. (Reisin and Ling 1973, by permission of Physiological Chemistry and Physics)

cellular adsorption or entry into subcellular compartments (quite similar to that shown in Figure 9.6C).

The experimental data of Figures 9.8 to 9.10 offer a revolutionary departure in the conceptualization of the manner of water diffusion in and out of living cells. Another view (i.e., that all traffic of water and solutes in and out of living cells is membrane-limited) has prevailed ever since the cell was recognized as the basic unit of life. However, at this juncture, I must also immediately point out that the conclusions just drawn do not imply that there is no cell membrane.³ Rather, they reflect one aspect of an unusual property of the cell membrane, recognized since the earlier days of biology, and referred to by van't Hoff as semipermeability meaning low in permeability to solutes but extremely high in permeability to water.

Nonetheless, *the conclusion that water diffusion in both frog ovarian eggs and giant barnacle muscle is bulk-phase-limited represents a finding of profound significance.* It is imperative that this conclusion be verified by other laboratories, preferably using other methods; and it has been (see below).

A unique byproduct of establishing the *bulk-phase-limited diffusion* of labeled water in frog egg and barnacle muscle cells is the intracellular diffusion coefficient of THO, D_{THO} through the cytoplasmic water in these two types of cells. For frog ovarian eggs, D_{THO} ranges from 0.721×10^{-5} to 1.47×10^{-5} cm²/sec, and is equal to from 30% to 60% of the THO diffusion coefficient in normal liquid water (2.44×10^{-5} cm²/sec, Wang et al., 1953). For barnacle muscle, D_{THO} is $(1.35 + 0.18) \times 10^{-5}$ cm²/sec, and thus equal to 55% of the diffusion coefficient of THO in water. If THO diffusion is membrane-limited (Type A) (Figure 9.6), the diffusion coefficient of THO in the cytoplasm would not have been obtainable from this type of study because the slower diffusion of labeled water through the cell surface (membrane) would have obscured from view its faster diffusion through the bulk-phase cytoplasmic water.

The diffusion coefficients (D_{THO}) thus determined from the experimental data of Figures 9.8 and 9.10 have also provided the means to check the validity of

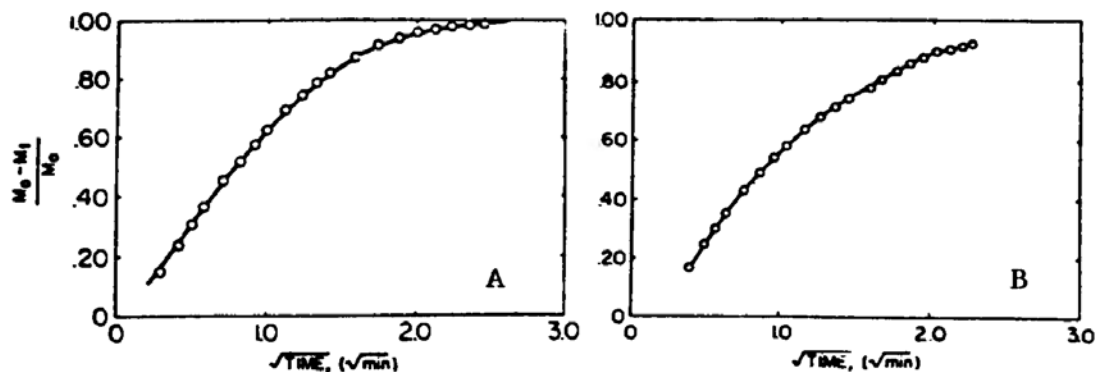


Figure 9.10. Influx of labeled water (³HHO) from intact isolated giant barnacle muscle cells. A and B represent two different muscle cells. Efflux data are inverted and represented as influxes as a function of the square root of the time of the washout. The continuous curves are theoretical for bulk-phase-limited diffusion with desorption. (Reisin and Ling 1973, by permission of Physiological Chemistry and Physics)

the conclusion drawn, that the diffusion of labeled water in the cells is bulk-phase limited, if we can quantitatively confirm the diffusion-coefficient data obtained by other, independent methods. Independent means to determine the diffusion coefficient of water in the same types of cells are in fact available: NMR study and tracer study of *longitudinal* diffusion of long cells with one open end. Both methods can measure water diffusion entirely within the cytoplasm without crossing the cell-surface membrane, and such measurements have been made. The results⁴ are in good agreement with ours, as shown in Table 9.2. If the diffusion of THO in frog ovarian eggs and barnacle muscle were in fact membrane-limited, the diffusion coefficient calculated from our measurements would have been much lower than that obtained by NMR and longitudinal diffusion studies. ***The similar D_{THO} confirms the earlier conclusion reached: diffusion of water in both frog ovarian eggs and barnacle muscle cells is bulk-phase limited.***

Bulk-phase-limited diffusion of tritiated water tells us that in moving from the center of the cell outward until they leave the cell, the THO molecules encounter a more or less uniform resistance throughout. Within the muscle cell, the barriers to water diffusion are primarily the contractile proteins, which in quantity amount to about 20% of the volume of the barnacle muscle cell. The barriers to water diffusion in frog ovarian eggs are more complex, including

Table 9.2. Diffusion Coefficients of Water in Ovarian Egg and Muscle Cells (Ling 1984, by permission of Plenum Publishing Co.)

	Organism	Method of study	(D^*) at 25°C ($\times 10^5$ cm ² /sec)	Reference
Egg	Frog	Radial diffusion	0.72–1.47	Ling <i>et al.</i> (1967)
		NMR	0.68	Hansson-Mild <i>et al.</i> (1972)
Muscle	Barnacle	Longitudinal diffusion	2.42	Bunch and Kallsen (1969) ^a
		Radial diffusion	1.35	Reisin and Ling (1973)
		Longitudinal diffusion	1.34	Caillé and Hinke (1974)
	Frog	NMR	1.56	Abetsedarskaya <i>et al.</i> (1968)
			1.20	Finch <i>et al.</i> (1971)
	Toad	NMR	1.35	Walter and Hope (1971)
Rat	NMR	1.43	Chang <i>et al.</i> (1972, 1973)	
Pure water			2.40	Mills (1973)
			2.44 (³ HHO)	Wang <i>et al.</i> (1953)
			2.43 (² HHO)	Wang <i>et al.</i> (1953)

^aThe exceptionally high value obtained by Bunch and Kallsen might be due to the use of muscle segments that were cut and short, which deteriorate rapidly (see Ling 1984, Section 5.2.6. and Section 8.4.1.4).

proteins, RNA and components of the yolk platelets (see Karasaki, 1963) totalling some 50% of the volume of the egg. The barriers to water diffusion in the cells' membranes include proteins and lipids; their total proportion of the cell membrane volume cannot be very much more than 20% or 50% in each case. Otherwise, water diffusion will be membrane-limited, contrary to fact.⁵

The experimental data presented above lends insight into the kind of cell membranes one finds in physiologically active types of living cells. Consider that, in insensitivity to valinomycin and other K^+ ionophores, four kinds of membranes resemble each other: liver mitochondrial membrane, squid axon membrane, frog muscle membrane, and frog ovarian egg membrane (Figure 9.5). From this insensitivity to K^+ ionophores, we reach the conclusion that these four types of membranes all belong to Type III—pure or effectively pure polarized-water, fixed-charge membranes (Figure 9.4).

I have now shown that in two of these four types of cells (ovarian eggs and voluntary muscle), diffusion of THO is bulk-phase limited. The liver mitochondrial inner membrane contains only 20% lipid in its total dry-solid content (Ernstter and Kuylenstierna 1970; Parsons et al. 1967); removal of 95% of the lipids in this membrane leaves the EM picture of the membrane essentially unchanged (Fleischer et al. 1967; Ling 1984, Figure 12.3). When all of these facts are considered together, they suggest that the plasma membranes of squid axon, frog muscle, frog eggs, and the inner membrane of liver mitochondria are similarly deficient in lipids. **Since these four types of cells are prominent examples of physiologically active cells, one is led to believe that the protein-fixed-ion-water domains represent the part of the cell membrane that plays key roles in the physiological activities of living cells.** Other considerations discussed in the remaining part of this section (9.2) lead to a similar conclusion.

9.2.1.4. *Critical Reassessment of the Apparent Accord Between Water and Nonelectrolyte Permeability Measured in Living Cells and in Phospholipid-Bilayer Membranes*

The tendency of charged groups on phospholipid molecules to assume orderly arrays suggests that phospholipid bilayers may transiently or permanently function as *NP-NP-NP* or *NO-NO-NO* systems in polarizing water (Section 5.2.2). This stipulation, referred to earlier, has been confirmed by the experimental findings of Katz and Diamond (1974), who showed partial sucrose exclusion from the water in liposomes made up of phospholipids and water. That the permeability of phospholipid membranes and cellulose acetate membranes should show general similarity is therefore not surprising: both provide polarized water as a diffusion medium.

Some proponents of the membrane theory have regarded the properties of living cell membranes and artificial phospholipid bilayers as so closely similar (both qualitatively and quantitatively) that they believe that the data have established that cell membranes are in fact phospholipid bilayers. It is the scientific foundation for this assertion (explicit or implicit), seen so often in today's vast literature on cell membranes, that will be carefully scrutinized next.

The demonstration of bulk-phase-limited diffusion of labeled water in frog

ovarian eggs and barnacle muscle is in severe conflict with the *alleged* quantitative accord between the permeability to water of many living cells and the permeability to water of phospholipid bilayers (Section 9.1.3). Thus, water is highly insoluble in the lipid phase of the phospholipid bilayers: The oil/water distribution coefficient of water is less than 10^{-5} (Figure 9.1). ***There is no way for a cell covered completely by a continuous phospholipid bilayer with such a low solubility for water to exhibit bulk-phase-limited diffusion to labeled water as observed*** (Section 9.2.1.3).

In the following section I analyze the experimental foundations of the assertion just mentioned: first, whether the conventional method of assessing the water permeability of living cells correctly represents the underlying phenomenon; and second, whether it is valid to compare the data on the water (and nonelectrolyte) permeability of living cells measured by conventional procedures with permeability data obtained from phospholipid-bilayer studies.

(1) *Serious Error in Past Estimation of Cell Membrane Permeability to Water*

In Figure 9.9 I have reproduced the THO efflux curve of two single giant-barnacle-muscle fibers. If, following conventional beliefs, we assume *a priori* that THO efflux, like the efflux of all other materials from living cells, is membrane-limited, one can estimate, from the slope of the straight-line part of the curve A, a half time exchange, $t_{1/2}$, of 89.0 seconds. The radius (r) of the muscle cell is 0.067 cm and its length is 1 cm, from which one calculates a volume (V) over surface (A) ratio (V/A): $(\pi r^2/2\pi r) = r/2 = 0.068/2 = 0.034 \text{ cm}^{-1}$. Since the permeability constant, κ , is equal to $(V/A \cdot \ln 2)/t_{1/2}$, one calculates a κ of $(0.034 \cdot 0.693)/89 = 2.65 \times 10^{-4} \text{ cm/sec}$. This value is very close to the value of $2.6 \times 10^{-4} \text{ cm/sec}$ reported by Bunch and Edwards from their studies of the THO permeability of similar giant barnacle muscle cells (Bunch and Edwards 1969).

It may be mentioned that, with very few exceptions, the method and its underlying assumption described above and used by Bunch and Edwards has been employed in many similar permeability studies of labeled water (Table 9.1). All were based on the fundamental tenet of the membrane theory, i.e., that the cell membrane acts as a *universal barrier* to all molecular traffic between cells and their environment, including that of water.

Let us next assume that the thickness (d) of the cell membrane is 60 Å, and that the membrane possesses pores containing normal liquid water. The equilibrium distribution coefficient (q) of THO in the membrane pore is therefore unity, and the diffusion coefficient (D) of THO is equal to that in normal water ($2.44 \times 10^{-5} \text{ cm}^2/\text{sec}$) (Wang et al. 1953). The percentage of membrane area covered by pores (ϕ) can then be calculated as follows:

$$\phi = \frac{d}{D} \cdot \frac{\kappa}{q} = \frac{60 \times 10^{-8}}{2.44 \times 10^{-5}} \cdot \frac{2.64 \times 10^{-4}}{1} = 6.49 \times 10^{-6}.$$

This number shows that only 0.00065% of the barnacle muscle surface is occupied by aqueous pores. If each pore is 5.0 Å in diameter, then out of $1 \mu\text{m}^2$ of the cell membrane there are only $6.49 \times 10^{-6}/(2.5 \times 10^{-8})^2 \times (10^{-4})^2 =$

33.1 pores, in apparent agreement with a postulated membrane model comprising mostly a water-impermeable lipid layer (Figure 9.2).

The THO-efflux curve of barnacle muscle (Figure 9.9) is quite similar to that of agar-gel filaments (Figure 9.7B). Both curves intercept the ordinate at a M_i/M_o of about 0.7, predicted by the well-known diffusion equation for bulk-phase-limited diffusion from a cylinder (Dünwald and Wagner 1934). However, following the conventional way of determining permeability constants, as Bunch and Edwards did, we may also ignore the initial 30% of the efflux for the agar-gel filament and estimate the permeability constant from the straight-line part of the curve in the semilogarithmic plot. Following similar steps described above for barnacle muscle, we calculate a pore area of 2.11×10^{-5} from the data shown in Figure 9.7B. That is, only 0.00211% of the agar gel surface is occupied by pores that allow passage of THO. This is obviously absurd. The agar gel surface has never been exposed to dry air; its surface layer must have roughly the same water content as the average water content of the agar gel, i.e., 96%. *An error of enormous magnitude has been committed*, since $0.96/0.0000211 = 4.54 \times 10^4$ (Ling 1987b). How did this happen?

There are two major errors made in both sets of calculations above. First, we have, by ignoring the earlier part of the efflux curves, artificially converted a bulk-phase-limited diffusion into a membrane-limited diffusion. This is a serious error, but an even more serious error is involved.

To measure accurately the permeability of a solute through a membrane structure, the standard and perhaps best-known method is to add the solute in a radioactively labeled form to the solution bathing one side of the membrane, while both solutions are being vigorously stirred. For sheetlike frog skin and other membranes like it, there is little difficulty in carrying out the permeability study properly (see Ling 1973a). Unfortunately, in the case of the plasma membrane of living cells, mostly in the form of minute globules filled with gel-like cytoplasm, the task of vigorously stirring cytoplasm facing the inside "surface" of the plasma membrane is difficult, to say the least. As a result most investigators **assume** that the labeled material, once inside the cell, is **instantly** mixed with its entire water content, as if the cell interior were being constantly stirred at infinite speed. *Since no such stirring has actually taken place, the time required for the labeled substance to reach diffusion equilibrium within the cell and the true time needed for the labeled substance to go through the cell surface are added together and attributed entirely to its passage through an assumed rate-limiting (membrane) permeability barrier. An extremely low κ is thus erroneously calculated.*

THO diffusion studies in agar gel demonstrate how very large errors can follow from seemingly reasonable assumptions. Unfortunately, the method based on the erroneous assumptions discussed was used not only by Bunch and Edwards in the study mentioned above, but by many others studying the water permeability of many types of living cells. Most of these data now needs careful reevaluation. One can say with assurance that the permeability of living cells to water is vastly higher than widely recognized. After all, there is no closer similarity between frog ovarian eggs and giant barnacle muscle than between any

two other types of living cells except that both of these cells are large. It is their large size that permits accurate analyses of the efflux and influx profiles, which in turn demonstrate the bulk-phase-limited nature of their water exchange. **Thus, bulk-phase-limited diffusion of water may well be the rule for all cells.**

The magnitude of the error from falsely attributing intracellular diffusion delay to the membrane barrier is related to the time for diffusion equilibrium to be reached within the cytoplasm. The time needed to reach diffusion equilibrium in turn varies with the square of the radius of spherical and cylindrical cells. Thus one would expect a dependency of the incorrectly determined "water permeability constant" (P_d) of the cell membranes of different types of cells on the size of the cells. The larger the cell, the greater the departure of the incorrectly measured values from the valid ones. This relationship is what I believe to be the main cause of the observed inverse relation between cell size and the so-called "water permeability constant" shown in Table 9.1.

(2) *Is It Appropriate to Compare the Water and Nonelectrolyte Permeability of Living Cells Obtained by Conventional Procedures with Similar Permeability Constants Measured Across Phospholipid Bilayers?*

It is the purpose of this section to examine another basic assumption that led to the belief that the cell membrane is in essence a phospholipid bilayer: that permeability data from studies of living cells and from studies of artificial phospholipid bilayers can be directly compared to yield valid conclusions.

Measurements have been made of the permeability of labeled water through artificial phospholipid bilayers containing amphotericin B, nystatin, etc. The permeability constants of water determined were 10^{-4} to 10^{-3} cm/sec [(Jain 1972, 91 (Table 4-1)], in apparent agreement with, for example, the data on barnacle muscle membrane by Bunch and Edwards mentioned above (2.6×10^{-4} cm/sec) and similar data from other cells measured by the same method (Table 9.1).

In determining the water and nonelectrolyte permeability of artificial lipid bilayers, labeled water was added to water in the compartment facing one side of the membrane and its rate of appearance in the other compartment monitored. The difficulty encountered in measuring permeability across living cell membranes in situ does not exist. Water on both sides of the membrane was vigorously stirred, therefore creating a nearly instant mixing after the passage of THO through the bilayer membrane, yielding the correct values of permeability constants (Andreoli et al. 1969; Andreoli and Troutman 1971).

As mentioned above, in determining the water and nonelectrolyte permeability of living cells, as a rule, only water on the outside of the cell was stirred, while water within the cell was not; as a result, an astronomically large error in the calculated permeability constant was made. ***The numerical agreement between the permeability constants of the lipid bilayers and those measured in living cells mentioned earlier in Section 9.1.3 are therefore not real, because correctly measured permeability through the phospholipid-bilayer membranes cannot be judiciously compared with incorrectly measured permeability through the living cell membranes.*** Mistaking bulk-phase-limited diffusion for membrane-limited diffusion,

as in the case of THO diffusion in barnacle muscle cells, further exacerbates the error.

Using data from phospholipid-bilayer membranes containing amphotericin B, with both sides being stirred, Andreoli et al. (1969) calculated that 0.0076% to 0.0103% of the membrane surface is occupied by pores with radii of 7 Å or 10.5 Å respectively. *These figures show how truly impermeable the phospholipid membrane is to water*, even after additional aqueous channels were artificially introduced by amphotericin B. And how curious it is that a combination of a preconception concerning membrane-limited diffusion and a faulty but widely used experimental procedure for determining membrane permeability have created the illusion that the (model) phospholipid-bilayer membranes and the membranes of living cells like frog ovarian eggs and barnacle muscle (see Table 9.2) have similar water permeability!

Does water alone demonstrate bulk-phase-limited diffusion in living cells? That is a question yet to be answered. But since the nonelectrolyte permeability of living cells was determined by the same method described, with the inside of the cell unstirred, permeability constants of the nonelectrolytes are faulted for the same reason that permeability constants of water are. Therefore, the agreement of the nonelectrolyte permeability data with those obtained from phospholipid bilayers discussed in Section 9.1.3 is equally fictitious.

In summary, phospholipid-bilayer membranes are somewhat closer approximations of living cell membranes than are olive oil layers discussed earlier (Section 9.1.1), especially in the presence of amphotericin B, nystatin, etc., presumably because the charged groups of phospholipid molecules can promote the formation of rather wide (but transient) pores of polarized water. As a result, unlike olive oil membrane, phospholipid membrane is semipermeable rather than antisemipermeable, and shows more or less size-dependent permeability to nonelectrolytes. Nevertheless, quantitatively speaking, the total area of the phospholipid membrane covered by such transient aqueous pores must be *vastly smaller* than in living cells. The demonstrated bulk-phase-limited diffusion of water in studies of frog ovarian eggs and giant barnacle muscle cells, and the establishment that these two types of cells share similar insensitivity to K⁺-ionophores with other physiologically active cell membranes (of squid axons and inner membranes of liver mitochondria), suggest that bulk-phase-limited diffusion of water is widespread, if not universal.

The remaining pages of this chapter will be devoted to a description of the molecular mechanism of permeation of *ions* into and out of living cells according to the AI hypothesis. One recalls that a neutral-lipid layer as exemplified by olive oil or phospholipid bilayers is virtually impermeable to ions (Section 9.1.3). Artificial ionophores hasten ion permeability through phospholipid membranes, but an intense search for their equivalents in natural cell membranes for well over twenty years has not produced positive results. The postulated "K⁺ channels," "Na⁺ channels," and "Ca⁺⁺ channels" are, according to their authors, closed in the resting cell membrane and open only momentarily during activity (see Section 11.5.1.2(3)). Therefore these channels cannot explain the by-now

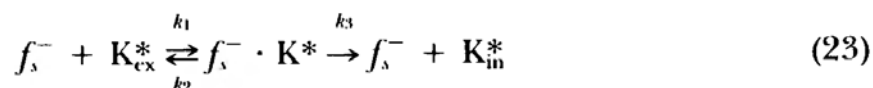
well-established fact that resting cell membranes are permeable to virtually all ions, some very rapidly so. For example, 15 seconds after immersion in a solution containing 5 mM radioactively labeled Na^+ , the level of the labeled Na^+ in a sample of *Spyrogyra* cells had already reached ten times the concentration in the external medium (Brooks 1940; see also Ling 1984, 53).

9.2.2. *Permeability to Ions and its Control*

9.2.2.1. *Different K^+ and Na^+ Permeability Due to Selective Adsorption on and Desorption from β - and γ -carboxyl Groups*

The methods of influx-profile analysis and of efflux-profile analysis described in Section 9.2.1.3 provided the means for establishing that ***the traffic of labeled water in and out of the cells of frog ovarian eggs and giant-barnacle-muscle fiber is bulk-phase limited. Similar studies of K^+ traffic across muscle and other cells led to just the opposite conclusion: K^+ traffic between most cells and their environments is surface limited*** (Ling et al. 1973, 13 and Figure 1; see also Ling 1984, 406). I earlier pointed out that K^+ traffic across the cell surface cannot be via the continuous lipid barrier postulated in the lipoidal-membrane theory, because K^+ permeability through a phospholipid layer is negligible, and apparently no natural K^+ ionophores exist in cell membranes. These facts led one one hand, to the “dead end” of the conventional phospholipid-bilayer theory and on the other hand, to the conclusion that K^+ traffic for resting muscle and egg cells may be primarily via the wide polarized-water domains of the cell membrane according to the AI Hypothesis. If so, the critical question becomes: by what mechanism can such passage of cations be made ion-specific in favor of K^+ over Na^+ ?

In 1953, I presented experimental evidence that the β - and γ -carboxyl groups—which were postulated to selectively adsorb K^+ over Na^+ in the cytoplasm—may also mediate the selective permeation of K^+ over Na^+ into living cells (Ling 1953; 1955a; 1960). The same mechanism that promotes full association of K^+ with β - and γ -carboxyl groups in the cytoplasm (Section 4.1.) also promotes transient association of K^+ with β - and γ -carboxyl groups found in the aqueous phase of the cell membrane; dissociation and entry into or exit out of the cell then follow (Ling 1953; 1955a). This mechanism—illustrated diagrammatically in Figure 9.11 as the *adsorption-desorption route*—can be written in the following form:



where f_s^- represents the fixed β - and γ -carboxyl groups at the cell surface. $f_s^- \cdot \text{K}^*$ is the transient complex between labeled K^+ (K^*) and the surface fixed anion. K_{ex}^* and K_{in}^* are the extracellular and intracellular labeled K^+ , respectively. k_1 , k_2 , and k_3 are the rate constants. Assuming that the adsorption of K^+ or other alkali-metal ions on β - and γ -carboxyl groups follows a Langmuir adsorption isotherm (as already established for K^+ adsorption on cytoplasm β - and γ -car-

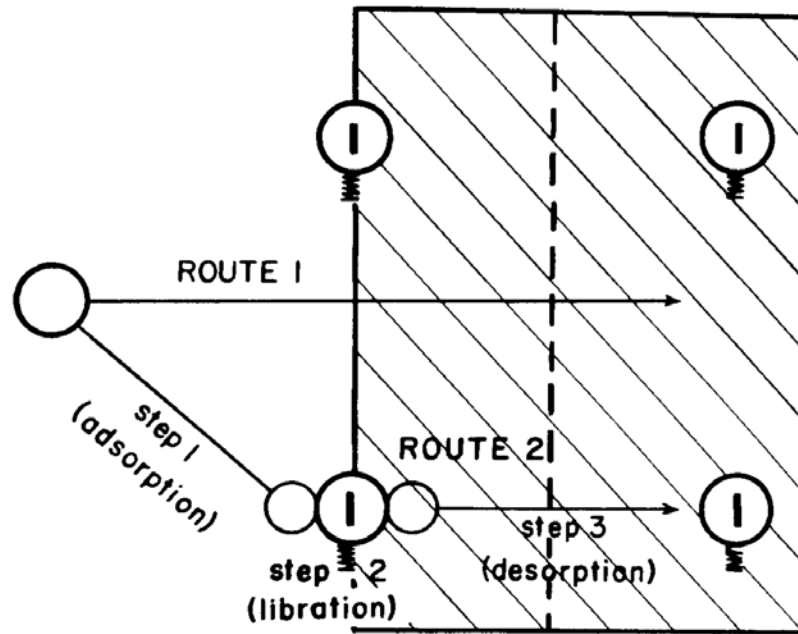


Figure 9.11. Diagrammatic illustration of the two suggested routes of entry of a monovalent cation into an anionic fixed-charge system (e.g., a living cell or a cation exchange resin sheet). Shaded area represents a microscopic portion of the surface of a fixed-charge system in which four fixed anions are represented. Route 1 is the *saltatory route* for cation entry via polarized water. Route 2, the *adsorption-desorption route*, involves a sequence of three steps: adsorption, libration around the fixed anion (e.g., a β - or γ -carboxyl group), desorption and entry into the cell. (Ling and Ochsenfeld 1965, by permission of Biophysical Journal)

boxyl groups, Figure 8.4 and 8.5), and that the external medium also contains competing nonlabeled Rb^+ , then the initial rate of entry of labeled K^+ (v_{K}^{in}) may be described by an equation as follows:

$$v_{\text{K}}^{\text{in}} = \frac{v_{\text{K}}^{\text{in(max)}} \tilde{K}_{\text{K}} [\text{K}^*]_{\text{ex}}}{1 + \tilde{K}_{\text{K}} [\text{K}^*]_{\text{ex}} + \tilde{K}_{\text{Rb}} [\text{Rb}^+]_{\text{ex}}}, \quad (24)$$

where $v_{\text{K}}^{\text{in(max)}}$ is the maximum rate of labeled K^+ entry. $[\text{K}^*]_{\text{ex}}$ and $[\text{Rb}^+]_{\text{ex}}$ are the external concentrations of labeled K^+ and nonlabeled Rb^+ . \tilde{K}_{K} and \tilde{K}_{Rb} are the adsorption constants on the *surface* β - and γ -carboxyl groups of (labeled) K^+ and (nonlabeled) Rb^+ respectively. Equation 24 can be written in the reciprocal form:

$$\frac{1}{v_{\text{K}}^{\text{in}}} = \frac{1}{v_{\text{K}}^{\text{in(max)}}} \left[\tilde{K}_{\text{K}} + \frac{\tilde{K}_{\text{K}} [\text{Rb}^+]_{\text{ex}}}{\tilde{K}_{\text{Rb}}} \right] \frac{1}{[\text{K}^*]_{\text{ex}}} + \frac{1}{v_{\text{K}}^{\text{in(max)}}}. \quad (25)$$

A plot of the reciprocal of the initial rate of entry of labeled K^+ ($1/v_{\text{K}}^{\text{in}}$) in the presence of different concentrations of Rb^+ against the reciprocal of the concentration of labeled K^+ ($1/[\text{K}^*]_{\text{ex}}$) should yield a family of straight lines converging on the same locus on the ordinate, equal to $1/v_{\text{K}}^{\text{in(max)}}$. The slope of the straight line varies with the concentration of the competing Rb^+ , $[\text{Rb}^+]_{\text{ex}}$. From these data, v_{K}^{in} , $v_{\text{K}}^{\text{in(max)}}$, \tilde{K}_{K} and \tilde{K}_{Rb} can all be calculated.

Figure 9.12A shows that expected results were confirmed in the case of labeled- K^+ entry into frog sartorius muscle. Epstein and Hagen (1952), a year prior to the presentation of my experimental evidence (Ling, 1953), made the first observation of this kind concerning the rate of Rb^+ entry into barley roots. In years following, equation 25 has been repeatedly demonstrated to correctly de-

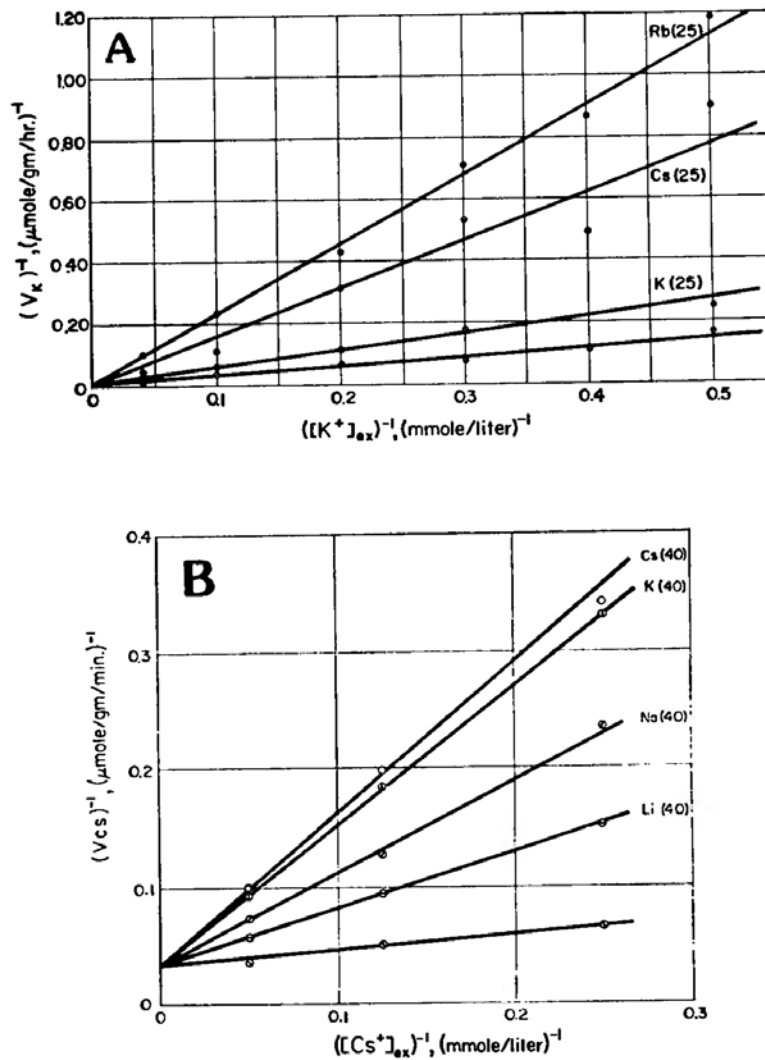


Figure 9.12.

- A. Inhibitory effect of 25 mM of Rb^+ , Cs^+ , or nonlabeled K^+ ion on the initial rate of entry of labeled K^+ ion into frog sartorius muscles. Lowest, unlabeled curve represents the rate of K^+ -ion entry with no added competing ion. Muscles soaked in solutions containing labeled ion for 30 minutes at 24°C , followed by 10 minutes of washing at 0°C . Each point represents a single determination on two sartorius muscles.
- B. Effects of 40 mM $CsCl$, KCl , $NaCl$, or $LiCl$ on the initial rate of entry of labeled Cs^+ ion into ion-exchange resin sheets. Nalfilm-1 strips soaked for 2 minutes at 5°C in an experimental solution containing (approximately) 2.5 mM Tris buffer at pH 7.0. The labeled entrant ion and non-labeled ion are indicated in the figure. Strips washed for 10 seconds in cold distilled water (0°C) before counting. (Ling and Ochsenfeld 1965, by permission of Biophysical Journal)

scribe the permeation of a number of alkali-metal ions into a wide variety of living cells (for review, see Ling 1984, 396).

In the study cited above, Epstein and Hagen interpreted their data in terms of ionic carriers. Their equation of ion permeation is in a form analogous to equation 24. However, most cell membranes do not have enough membrane lipids to form a continuous layer (Section 9.2; Ling 1984, 380), nor did an extensive search lead to the recovery of carriers or ionophores from natural cell membrane. These and other reasons mentioned above (Section 9.1.2), and to be discussed below, make the ion-carrier model highly unlikely (Ling et al. 1973, 40). On the other hand, *ion entry into various inanimate systems carrying fixed anions, including cation-exchange resin, sheeps' wool, oxidized-collodion membranes* (Figure 9.12B), *and even an actomyosin gel, all follow equation 25. Thus the presence of fixed anions at the cell or model surface is all that is required to provide a mechanism for selective-cation permeability into living cells following equation 25* (Ling 1953; 1960; 1962; 1984). From 1965 on, Passow, Schnell and their coworkers have proposed a similar role for *fixed cations* (e.g., ϵ -amino groups) in the cell membrane of red blood cells to mediate anion permeation (Passow 1965; Passow and Schnell 1969).

In 1965, Ling and Ochsenfeld demonstrated that a plot of K^+ -permeation rates into frog sartorius muscle, against pH, showed an inflection point at pH 4.75 (Figure 9.13). Since this is the pK_a value characteristic of β - and γ -carboxyl groups, *the data suggest that the fixed-anionic groups at the surface of muscle cells that mediate K^+ permeation—like their counterparts in bulk-phase cytoplasm* (Section 4.4.3)—*are indeed the β - and γ -carboxyl groups.*⁶

Figure 9.14 shows the K^+ and Na^+ permeability of normal frog sartorius muscles at various concentrations of these ions, in the absence (A, B) and presence (C, D) of high concentrations of strongly competing ions (i.e., Rb^+ against K^+ entry; K^+ against Na^+ entry) which strongly reduces K^+ (or Na^+) entry by the

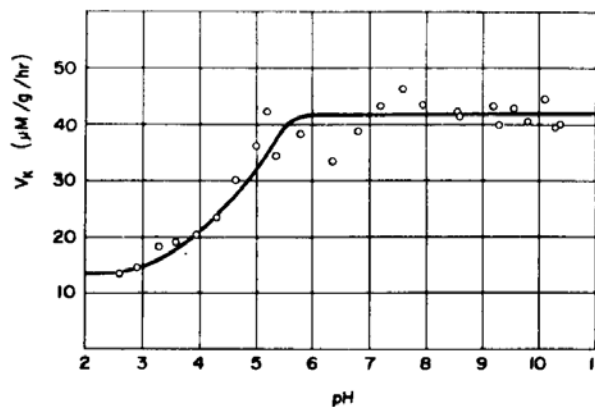


Figure 9.13. Effect of pH on the initial rate of entry of labeled K^+ into frog sartorius muscles. Concentration of labeled K^+ was 20 mM; of phosphate buffer, 10.8 mM; of the glycine, succinate, and veronal buffers, 5.4 mM. Fifteen minutes of soaking at 25°C were followed by 10 minutes of washing at 0°C. pHs of experimental solutions were measured after the experiment. Each point represents the average of three individual determinations. (Ling and Ochsenfeld 1965, by permission of Biophysical Journal)

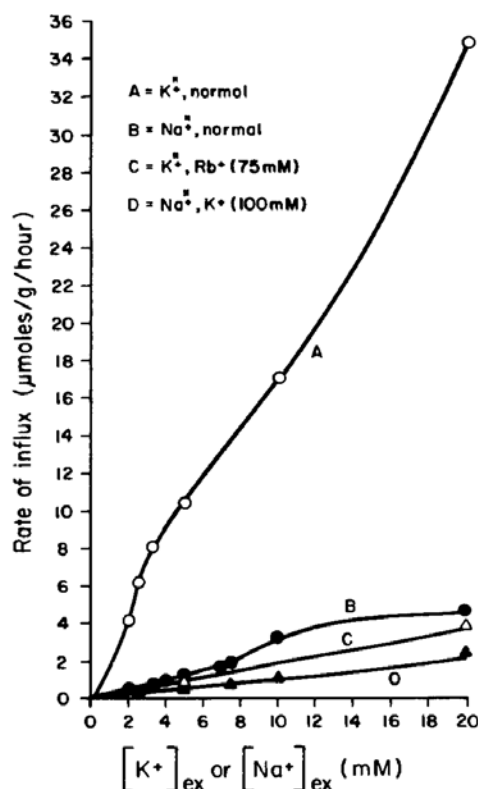


Figure 9.14. Rate of influx of labeled K^+ (K^{*+}) and labeled Na^+ (Na^{*+}) into frog sartorius muscle in the presence of 2.5 mM external nonlabeled K^+ (normal) (A,B), or higher concentrations of external nonlabeled K^+ (100mM) or nonlabeled Rb^+ (75 mM) (C,D). High concentrations of nonlabeled ions effectively competed for and thus “chased away” would-be entrant labeled K^+ or Na^+ from association with fixed anions on the cell surface, leaving only the saltatory route (Route 1 of Figure 9.11) for the entry of labeled ions. Ratios of (A-C)/A or (B-D)/B yield estimates of percentage of labeled ion entry by the adsorption-desorption route (Route 2 of Figure 9.11). (Ling, unpublished)

adsorption-desorption route. Comparing the rate of K^+ entry in A with that in C, one finds that at least 90% of the K^+ that enters the resting muscle cell does so by the adsorption-desorption route via the β - and γ -carboxyl groups. Comparing B with D one estimates that at least half of the entrant Na^+ competes for the same or similar routes. In the specific model shown in Figure 9.11, residual K^+ and Na^+ entry could be via the *saltatory route*, through the same large, intensely polarized, water-filled domains (containing the fixed β - and γ -carboxyl groups). In other cell types, like human erythrocytes, there may be intensely-polarized-water domains containing fixed-cationic groups. In both primarily fixed-anion-dominated and fixed-cation-dominated cell membranes, there may be other water domains containing stereospecific H-bonding sites that offer selective adsorption-desorption routes for the entry of sugars and other organic molecules and ions. We have already discussed the evidence that the polarized water domains of the cell membrane offer a pathway for the traffic of water and nonelectrolytes and, quite likely, also for the traffic of electrolytes bearing charges of the same polarity as that of the fixed ions. The data shown in Figure

9.14 suggest that in frog muscle cells, at least, 90% or more of the polarized water domains must be dominated by β - and γ -carboxyl groups.

9.2.2.2. *Cooperative Interaction Among Surface β - and γ -carboxyl Groups Mediating the Permeation of Ions into Living Cells*

In the AI hypothesis, the fundamental behaviors of β - and γ -carboxyl groups at the cell surface towards alkali-metal ions are similar to their counterparts in the cell cytoplasm. If a pair of ions with highly different adsorption energies compete for the β - and γ -carboxyl groups in the cytoplasm, cooperative interaction is expected and observed (see Section 8.2). One would, therefore, expect the same type of cooperative interaction among cell surface β - and γ -carboxyl groups mediating alkali-metal ion entry into cells. In that case, for cells containing N types of surface adsorption sites, the rate of permeation (v_i) would be described by the following general equation:

$$v_i = A_i [p_i]_{\text{ex}} + \sum_{l=1}^n \frac{v_i^{\text{max}(l)}}{2} \left[1 + \frac{\xi_l - 1}{\sqrt{(\xi_l - 1)^2 + 4\xi_l \exp(\gamma_l/RT)}} \right], \quad (26)$$

where A_i is a constant. $v_i^{\text{max}(l)}$ is the maximum rate of permeation of the i th solute via the l th type of sites by the adsorption-desorption route. ξ_l and γ_l have the usual meaning described in Section 7.1, except that here they refer to the l th type of cell surface sites.

A simpler version of this equation deals with cell surfaces containing only one type of surface adsorption sites:

$$v_i = A_i [p_i]_{\text{ex}} + \frac{v_i^{\text{max}}}{2} \left[1 + \frac{\xi' - 1}{\sqrt{(\xi' - 1)^2 + 4\xi' \exp(\gamma'/RT)}} \right]. \quad (27)$$

For experimental data that confirm equation 27, see Ling 1986b.

9.2.2.3. *Control of Ion Permeability by Cardinal Adsorbent*

9.2.2.3.1 Ouabain

Drugs like ouabain can control cell permeability to ions by essentially the same basic mechanism that controls the bulk-phase-equilibrium distribution of these ions.

I showed in Figure 8.11 how exposure to ouabain caused changes in the alkali-metal-ion-equilibrium distribution in agreement with the postulate that ouabain binding increased the c -value of the β - and γ -carboxyl groups of the cytoplasmic proteins from -4.20 \AA to -3.25 \AA [Section 8.3.2(3)]. This c -value increase, in turn, gives rise to a change of the rank order of selectivity for the five alkali-metal ions, in agreement with theory. Again, extending what we have learned about the EDC effect of ouabain on cytoplasmic β - and γ -carboxyl groups, one expects that ouabain may induce similar changes in the relative affinities for the five alkali-metal ions of the surface β - and γ -carboxyl groups.

To test this hypothesis, we studied the rate of entry of ^{134}Cs -labeled Cs^+ (2mM) into frog ovarian eggs. Isolated eggs were exposed for 13 minutes to labeled Cs^+ in the presence of 20 mM of nonlabeled Li^+ , Na^+ , K^+ , or Rb^+ with or without

ouabain (10^{-6} M). After blotting, the egg clusters were washed in aliquots of nonradioactive Ringer solution. The radioactivity of the washing solution and that remaining in the eggs at the conclusion of the efflux studies permitted us to reconstruct the efflux curves of the labeled Cs^+ .

In a plot of the logarithm of the remaining radioactivity against the duration of washing, three fractions, each represented by a straight line, could be sorted out, and they are referred to as Fraction 1, 2, and 3 respectively, the slowest being Fraction 1, etc. The intercepts on the ordinate of each of these straight lines extrapolated to zero time yield the amount of labeled Cs^+ belonging to each of the three fractions that had entered the cell during the 13-minute incubation. Each of these fractions responded to the ouabain treatment in an essentially similar manner. The inhibiting effects of 20 mM Li^+ or Na^+ on Cs^+ entry were enhanced by ouabain, resulting in lesser uptake of Cs^+ . The inhibiting effect of 20 mM Rb^+ on Cs^+ entry, on the other hand, was reduced, resulting in more uptake of Cs^+ . The effect of 20 mM K^+ on Cs^+ entry was enhanced in most cases, but reduced in others (see Figure 9.15).

One expects that the observed effect of ouabain can also be explained in terms of a rise of the c -values of the cell surface β - and γ -carboxyl groups. There is, however, a problem. This problem did not exist when we compared theory and experimental data from the equilibrium distribution of the five alkali-metal ions in frog muscle, because there, both theory and experimental data dealt with the

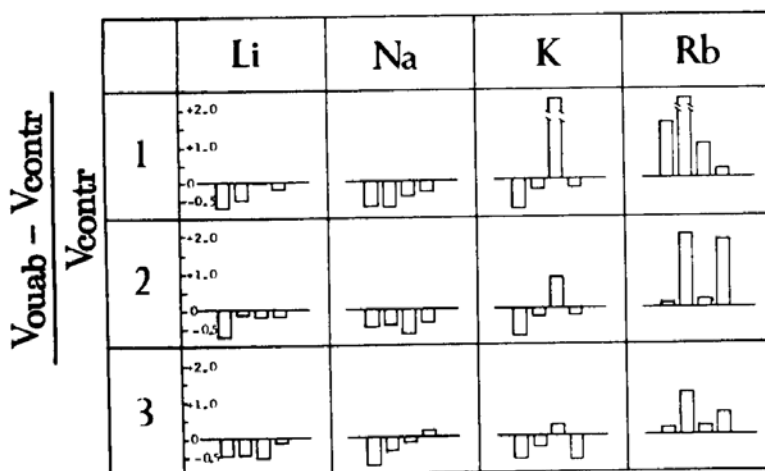


Figure 9.15. The effect of ouabain (10^{-6} M) on the rate of entry of labeled Cs^+ (2 mM) into frog ovarian eggs in the presence of 20 mM of competing Li^+ , Na^+ , K^+ , or Rb^+ . The influx rate during a 13 minute incubation of the egg clusters was determined from the zero time intercepts of the efflux curves which were resolved into three separate fractions 1, 2, and 3.

V_{contr} and V_{ouab} represent the rates of Cs^+ entry in the absence and presence of ouabain. Four complete sets of experiments were performed. In all four, exposure to ouabain *reduced* the zero-time intercepts of all three fractions (1, 2 & 3) of labeled Cs^+ entry in the presence of 20 mM competing Li^+ or Na^+ . In contrast, in all four sets of experiments, exposure to ouabain *increased* the zero-time intercepts of all three fractions of labeled Cs^+ in the presence of 20 mM Rb^+ . The effect of 20 mM K^+ was mixed. (Ling and Fu 1988, by permission of Physiological Chemistry Physics and Medical NMR)

relative affinity of *adsorption* for the alkali-metal ions. In contrast, the experimental data obtained here are in the form of relative *rates of permeation*. In order to make a comparison of permeability-rate data obtained here with both theory and earlier data cast in the form of relative adsorption constants, a theoretical “bridge” must be found between the two sets of parameters. With certain simplifying assumptions, I have derived such a theoretical bridge (see Ling and Fu 1988 for derivation):

$$\frac{V'_{Cs(Rb)} - V_{Cs(Rb)}}{V_{Cs(Rb)}} = \frac{\rho_{Rb(Cs)} - \rho'_{Rb(Cs)}}{\rho'_{Rb(Cs)}}, \tag{28}$$

where $V'_{Cs(Rb)}$ and $V_{Cs(Rb)}$ are the rates of Cs^+ entry in the presence of (a higher concentration of) Rb^+ with or without ouabain, respectively. \bar{K}_{Cs} and \bar{K}_X represent the adsorption constant of Cs^+ and of X^+ (representing Rb^+ , K^+ , Na^+ , or Li^+) on the cell surface β - and γ -carboxyl groups in the absence of ouabain. \bar{K}'_{Cs} and \bar{K}'_X represent their counterparts in the presence of ouabain. One then defines $\rho_X = (\bar{K}_X/\bar{K}_{Cs})$ and $\rho'_X = (\bar{K}'_X/\bar{K}'_{Cs})$.

Table 9.3 shows that the effects of ouabain on the influence of the four alkali-metal ions (Rb^+ , K^+ , Na^+ , and Li^+) on the rates of Cs^+ entry into frog eggs are in agreement with the prediction that the c -value of the surface β - and γ -carboxyl groups mediating Cs^+ entry into frog ovarian eggs was increased by ouabain, just as ouabain similarly increased the c -value of the β - and γ -carboxyl groups on the A bands and Z lines of frog muscle (Figure 8.12). *Indeed, both sets of data show rough agreement with each other, and both illustrate the theoretically predicted changes of ion preference accompanying a c -value rise from -4.20 \AA to -3.25 \AA (see Figure 6.9).*

Table 9.3. Observed Relative Adsorption Constants of the Alkali-Metal Ions on Cytoplasmic Anionic Sites and on Egg Surface Sites in Comparison with Theoretical Values. (Ling and Fu 1988, by permission of Physiological Chemistry, Physics and Medical NMR; refined theoretical values from Ling, work in progress)

	Theoretical	Experimental			
	$\frac{\rho_X - \rho'_X}{\rho_X}$	Muscle Cytoplasmic Sites	Egg Surface Sites		
		$\frac{\rho_X - \rho'_X}{\rho_X}$	$\frac{V'_{Cs} - V_{Cs}}{V_{Cs}} = \frac{\rho_X - \rho'_X}{\rho_X}$		
			Fraction I	Fraction II	Fraction III
Rb^+	+0.88	+3.34	$+2.78 \pm 1.8$	$+1.04 \pm 0.51$	$+0.56 \pm 0.23$
K^+	-0.76	+0.52	$+0.52 \pm 0.95$	-0.098 ± 0.34	-0.32 ± 0.22
Na^+	-1.0	-0.97	-0.52 ± 0.11	-0.49 ± 0.07	-0.28 ± 0.20
Li^+	-1.0	-0.89	-0.36 ± 0.15	-0.31 ± 0.15	-0.40 ± 0.09

Note: Measured in frog muscle and on surface anionic sites of frog ovarian eggs, in the presence and absence of ouabain; compared with their theoretical predicted values.

9.2.2.3.2. ATP, ADP and Arginine Phosphate (ArP)

The model of cell membrane according to the AI hypothesis is essentially similar to the model of cytoplasm: a fixed-charge system of closely associated protein-water. However, there can be great differences between real cell membranes and real cytoplasm, because, among other reasons, the cell-membrane structure and composition are far more variable than the cytoplasm (see Section 9.2). Nonetheless, there is remarkable similarity in the behavior of the two. Indeed, what could better illustrate this similarity than the effect of ouabain on the ϵ -value of the β - and γ -carboxyl groups in the cytoplasm and on the cell membranes just discussed? And what could offer a better reason to seek understanding of the properties and behaviors of the microscopically thin (and correspondingly difficult-to-approach) cell membrane by starting out with its abundant and accessible counterpart, the cytoplasm?—as I will do next.

(1) **Frog Muscle** Figure 8.11 suggests two ways to replace the cytoplasmic K^+ in frog muscle by Na^+ : (i) lowering the external K^+ concentration and (ii) exposing the cell to the EDC, ouabain. Conversely one can replace adsorbed Na^+ by K^+ on cytoplasmic β - and γ -carboxyl groups (i) by raising the external K^+ concentration or (ii) by removing ouabain from the medium.

Figure 9.11 shows how a monovalent cation like K^+ that becomes selectively adsorbed on the cell surface β - and γ -carboxyl groups will as a rule enter the cell via the **adsorption-desorption route** (Route 2). This route is by and large a slow one, since the adsorbed K^+ has to wait until it has gained sufficient kinetic energy to overcome the electrostatic attraction of the negatively charged fixed carboxyl group. In contrast, an approaching cation less preferred by the fixed carboxyl group, say Na^+ , usually cannot succeed in occupying a surface β - or γ -carboxyl group and will in most cases simply bounce back to where it came from. However, a few Na^+ ions will be so positioned and energized that they will sail through the cell membrane via the polarized-water domain (the **saltatory route**, Route 1).

The same basic principle applies to cations **exiting** from the cell. Only not all cations within the cell are at the same energy state. Most K^+ ions are adsorbed on β - and γ -carboxyl groups and are thus held at a high (negative) energy state. In contrast, rejected by most β - and γ -carboxyl groups, Na^+ ions remain free much of the time and bounce around at a state of high kinetic energy. For these reasons, efflux of K^+ from normal cells like frog muscle, is very slow, their exit being rate-limited by desorption from the surface carboxyl groups. The half time of exchange ($t_{1/2}$) for K^+ at 25°C is around 3 hours (Ling 1980, 229). Under the same condition, the efflux of Na^+ is much faster and can be resolved into two fractions. The $t_{1/2}$ for the fast fraction of Na^+ is 3 minutes; even $t_{1/2}$ of the slow fraction is no longer than 25 minutes (Ling 1980, 226). The fast fraction of exiting Na^+ is rate-limited by passage through the cell surface membrane; the slow fraction is rate-limited by desorption from cytoplasmic adsorption sites (Ling and Walton 1975a; Ling and Ochsenfeld 1977; Ling et al 1981; Negendank and Shaller 1979; Ling 1984, 411).

As pointed out above, one can replace adsorbed K^+ at the cell surface (and elsewhere in the cell) with Na^+ by either removing K^+ from the external medium

or by applying the EDC, ouabain. Therefore it is not surprising that in response to both treatments, the two fractions of the Na^+ efflux take on the appearance of a single fraction and that the $t_{1/2}$ lengthens to 2 hours in response to low K^+ (Ling 1978b, 358) and 5 hours in response to 10^{-6} M ouabain (Ling and Palmer 1972, 521).

Ouabain, an EDC, causes a rise of the c -value of the β - and γ -carboxyl groups and as a result K^+ is displaced by Na^+ on these anionic sites. ATP, on the other hand, is an EWC (Section 8.4.2.3). The question arises: "Does *withdrawal* of an EWC like ATP have an effect on the K^+/Na^+ adsorption similar to the *addition* of an EDC like ouabain?" It does, according to the AI hypothesis.

In muscle cytoplasm, apparently the decline of ATP concentration in response to metabolic poisons does indeed create, at 25°C, a transient increase of Na^+ adsorption at the expense of adsorbed K^+ (Ling et al 1981). However, *decline of ATP concentration in frog muscle cells does not produce a corresponding slowdown of Na^+ efflux* like that seen in response to lowering external K^+ concentration or to ouabain. I shall explain this departure from the theoretical expectation (that addition of an EDC should produce a similar effect as the withdrawal of an EWC), after reviewing some relevant work of Caldwell and his coworkers on giant squid axons, to be described next.

(2) **Squid Axon** *In contrast to frog muscle, metabolic poisons like 2 mM sodium cyanide does produce a marked slowdown of the Na^+ -efflux rate from squid axons*, see Figure 9.16 (Caldwell et al., 1960). This slowdown of Na^+ efflux rate occurs in parallel with a sharp reduction of the concentrations of both ATP and arginine phosphate (ArP) in the axons (Caldwell 1960). Note that ArP is the invertebrate counterpart of CrP in vertebrates.

Caldwell et al. then showed that the slowed-down Na^+ -efflux from cyanide-poisoned squid axons could be partially restored to its normal high rate by the injection into the axons of a concentrated solution of ATP (Figure 9.16A), or high concentration of ArP (Figure 9.16B); but not by injection of the hydrolytic products of ATP (largely adenosine-monophosphate and inorganic phosphate, P_i) or of ArP (largely arginine and P_i) also shown in Figure 9.16A and B.

Hodgkin and Keynes (1955a) had observed earlier what they called the *K-sensitivity* of the Na^+ efflux, i.e., acceleration of the rate of Na^+ efflux from squid axon in a K^+ -free medium by the reintroduction of a normal concentration of K^+ found in sea water (10 mM). The injection of high concentration of ATP or low concentration of ArP increased the rate of Na^+ efflux of the cyanide-poisoned squid axon but it did not restore its *K-sensitivity* (see Figure 9.17A). In contrast, injection of a high concentration of ArP (or of phosphoenolpyruvate, PEP) not only increased the Na^+ -efflux rate, it also restored the *K-sensitivity* (see Figure 9.17B).

Cyanide (2 mM) also reduced the rate of K^+ influx into squid axons to about 25–50% of its normal value. Injection of ATP into the axons did not produce a statistically significant increase of the K^+ influx rate. In contrast, injection of a high concentration of ArP produced a threefold increase of the rate of K^+ influx.

Just as intriguing was the observation that injection of ADP reduced the *K-*

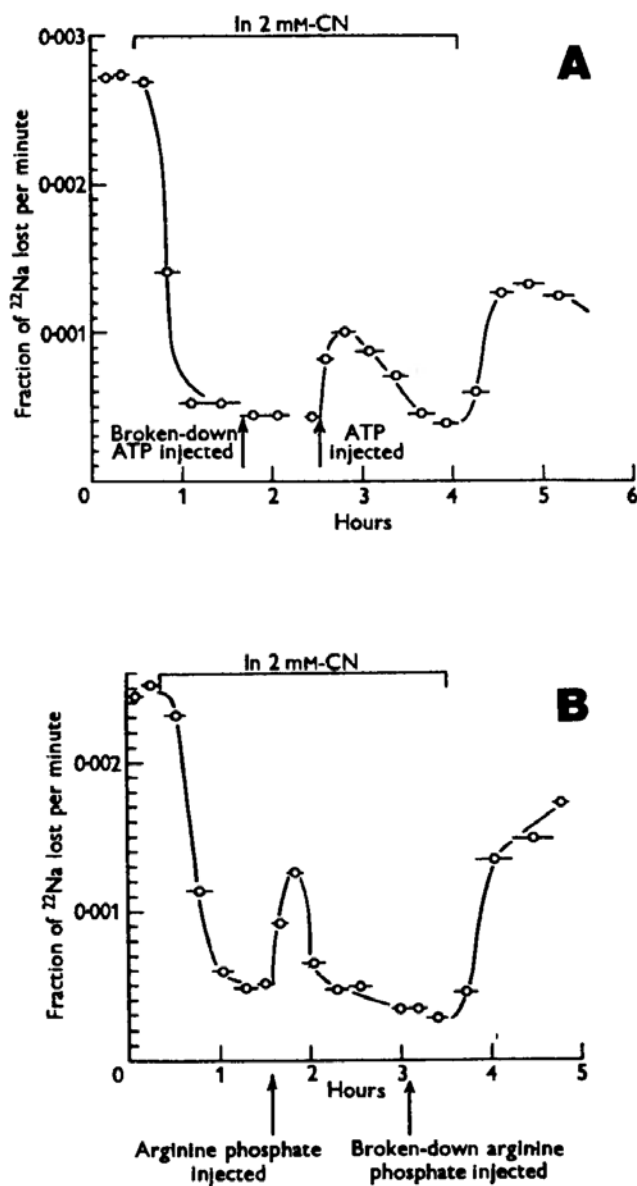


Figure 9.16. Effect of injection of ATP (A) and arginine phosphate (B) or their respective hydrolytic products on the Na^+ efflux of cyanide-poisoned squid axons.

- A. 780 μ squid axon loaded with ^{22}Na over 12 mm. At second arrow, 16.4 nmole ATP was injected over the same 12 mm, giving a mean internal concentration of 2.9 mM (5.8 mM \sim P). At the first arrow an equal volume of the same ATP solution which had been hydrolysed by boiling was injected. At the end of the experiment the action potential was 99 mV, and the resting potential 56 mV. Fibre reference, 19D6 (19 December 1956). 1 nmole = 10^{-9} mole.
- B. 800 μ squid axon loaded with ^{22}Na over 12 mm. At first arrow 32.4 nmole arginine phosphate was injected over same 12 mm, making mean internal concentration 5.4 mM. At second arrow an equal volume of the same solution, hydrolysed by heating, was injected. Temperature 20°C. At end of experiment resting potential was 58 mV, action potential 99 mV. Fibre reference, 406. [Caldwell et al. 1960, by permission of Journal of Physiology (London)]

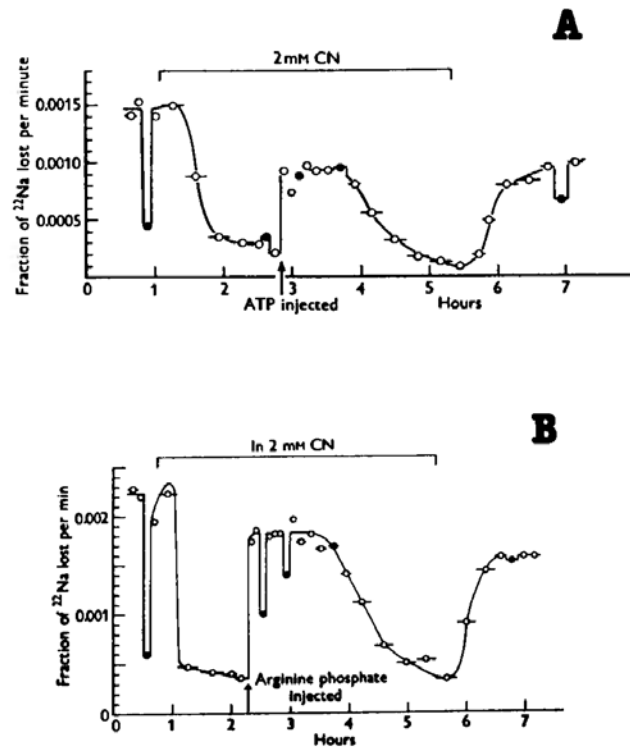


Figure 9.17. Effect of injection of ATP (A) and arginine phosphate (B) on the Na^+ efflux of cyanide-poisoned squid axons.

- A. Failure of ATP to restore a K-sensitive sodium efflux: ● K-free external solution; ○ 10 mM-K. The injection raised the concentration of ATP in the axon by 4.8 mM.
- B. Effect of injecting arginine phosphate in restoring a potassium-sensitive sodium efflux to a squid axon poisoned with cyanide. The injection raised the concentration of arginine phosphate in the axon by 33 mM.

[Caldwell et al. 1960, by permission of Journal of Physiology (London)]

sensitivity of the Na^+ efflux (Caldwell et al. 1960, 580). I will return to this observation below.

(3) ***Divergent Na^+ -efflux Patterns of Frog Muscle and Squid Axon Explained in terms of the AI Hypothesis*** Caldwell et al. interpreted their observations in terms of the membrane-pump theory. For reasons given in detail in Chapter 2, this line of thinking will not be pursued further here.

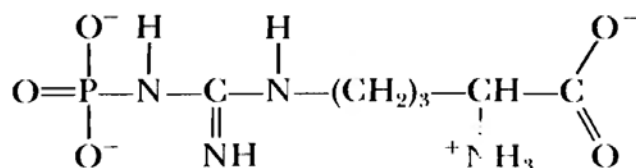
Poisoning with 2 mM cyanide of squid axons produced a slowdown of the Na^+ -efflux rate in parallel with a marked decrease in the concentration of the prime EWC of the cell, ATP. This Na^+ -efflux slowdown with ATP depletion resembles that brought on by the withdrawal of K^+ from the external medium (Keynes 1954) or by the application of the EDC, ouabain (Baker et al. 1971). This resemblance is in harmony with the theoretically predicted similarity in the behaviors of Na^+ following the withdrawal of its strong competitor (K^+); exposure to an EDC (ouabain); or withdrawal of an EWC (ATP).

Conversely, the same predictions in reverse were confirmed by the demonstration that injection of ATP accelerated the Na^+ -efflux rate of cyanide-poi-

soned axons. That injection of ArP also accelerated the Na^+ -efflux rate is reasonable as well. Through the activity of the enzyme arginine kinase (the counterpart of creatine kinase in vertebrates, see endnote 6 of Chapter 8), ATP was apparently regenerated from the injected ArP. Hence, from one standpoint, injecting ArP produced an effect similar to injecting ATP, as observed. Yet injecting high concentration of ArP, but not that of ATP, restored *K-sensitivity*. Clearly *ArP does more than merely functioning as a source of additional ATP*; but what?

The experiment on FDNB-treated frog muscle (Figure 8.21) offers a possible clue to the answer. With creatine kinase inactivated by FDNB, CrP was preserved at its high normal level even as nitrogen and IAA reduced the concentration of ATP to zero or near-zero. And despite the disappearing ATP, K^+ also remained selectively accumulated at its near-normal high level.

This isolation of CrP level in muscle cells from that of ATP offers a unique opportunity to witness and recognize CrP's full activity—whereas in the presence of uninhibited creatine kinase, the effect created by CrP may be eclipsed by that of ATP. The ability of CrP to preserve selective K^+ accumulation (without the help of ATP) emphasizes that *CrP exercises strong inductive or indirect F-effect on neighboring sites at the same time as it functions as the major congruous anion*. Indeed the molecular structure of CrP given in Section 8.4.2.4.1 and of ArP given below



suggest that besides attaching its anionic phosphate group onto fixed cationic groups on the protein (thereby keeping the β - and γ -carboxyl groups from forming salt linkages and making them available for the adsorption of K^+), the remaining portion of the molecules of CrP and ArP may well interact with the backbone CO and NH groups of the protein, thereby serving the role of a^+ and a^- of Model 2 (Figure 7.8) and of "a" in Figure 7.9.

The maintenance of a high concentration of K^+ over Na^+ (Figure 8.21) in the presence of no or minimal ATP, may explain why injection of high concentration of ArP into squid axon (e.g., 33 mM in comparison with 3.3 mM in normal squid axon, Caldwell et al. 1960, 551) may restore the *K-sensitivity* of the cyanide-poisoned squid axon. Remembering that cyanide does not inhibit arginine kinase, the activity of this enzyme could regenerate ATP at the expense of part of the abundant ArP injected. The combined activity of the restored ATP and the high concentration of ArP in the axon might have produced a more effective positioning of the c -value of the β - and γ -carboxyl groups so that the preference for K^+ over Na^+ of these surface anionic sites was further enhanced. As a result, (i) a modest concentration of K^+ (10 mM) added to the external medium significantly increased the rate of the Na^+ efflux in the cyanide-poisoned squid axon (*K-sensitivity*); and (ii) the K^+ -influx rate also increased as observed.

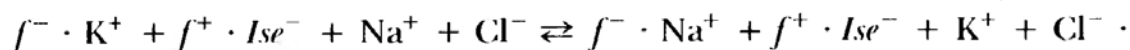
The observation that ADP *reduces* *K-sensitivity* is equally intriguing. In Section

8.4.2.5, I pointed out that there were no less than five sets of independent experimental observations which suggest that—in contrast to the EWC function of ATP—ADP acts as an EDC. Injecting ADP therefore would *decrease* the relative affinity for K^+ (over Na^+) of surface carboxyl groups and, as a result, further reduce the *K-sensitivity* as observed.

Finally I would like to answer the important question: “*Why do metabolic poisons sharply reduce the Na^+ -efflux rate in squid axons (Figure 9.16) but not that in frog muscle (Figure 2.1)?*”

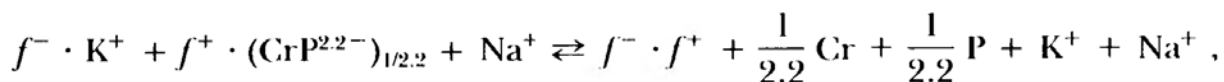
I suggest that this difference in response to metabolic poisons originates from the different nature of the major *congruous anions* in the surface of squid axons and that in frog muscle. In frog muscle, CrP is the major anion in the cell (cell concentration may be as high as 30 μ moles per gram of fresh muscle, see Figure 8.20), presumably including the cell surface. In contrast, the major anion in squid axon is isethionate ($HOCH_2CH_2SO_3^-$) at 250 μ moles/g. of axon water (Hodgkin 1971, 28), making up more than half of the total concentration of intra-axonal anions. The concentration of ArP in squid axons is quite low (3.3 μ moles/g.); therefore, ArP is only a minor congruous anion here.

When metabolic poisons arrest metabolism, the ATP concentration in squid axons decreases; through the activity of arginine kinase, the minor congruous anion, ArP also breaks down into arginine and inorganic phosphate which cannot function as congruous anion (see Figure 9.16B). In contrast, the major congruous anion, isethionate (Ise^-) remains unchanged. With the ϵ -value increase due to the loss of the major EWC (ATP), the persistent presence of a high concentration of this major congruous anion discourages salt-linkage formation in favor of an exchange of adsorbed K^+ for Na^+ on the β - and γ -carboxyl groups (f^-), while the isethionate ion remains adsorbed on the surface fixed cations (f^+):



The occupancy of a large part of the cell surface β - and γ -carboxyl groups by Na^+ signifies that most exiting Na^+ would follow the slow adsorption-desorption route. As a result, the Na^+ efflux slows down.

When metabolic poisons are applied to frog muscle, its ATP concentration also declines and with this change, the ϵ -value of the β - and γ -carboxyl groups rises. Through the activity of creatine kinase, its CrP also decomposes into ineffective creatine and inorganic phosphate (Figure 8.20). Since CrP is the major anion here, its loss leaves the cell surface without its major congruous anion. The reaction accompanying the ϵ -value rise of the β - and γ -carboxyl groups may take a different direction, as follows:



where 2.2 is the effective valence of CrP at neutral intracellular pH [see Section 8.4.3.3.(1)]. The fixed surface β - and γ -carboxyl groups normally adsorbing K^+ become engaged in salt linkages, f^-f^+ , rather than adsorbing Na^+ as in the case of squid axons. Failure of adsorption of Na^+ at the cell-surface carboxyl

groups signifies that most exiting Na^+ ions leave the cell via the fast saltatory route. As a result, no slowdown of the Na^+ efflux occurs in response to metabolic poisons, as observed (Figure 2.1).⁷

As mentioned above, there are gathering evidence that ADP is an EDC. Most of the ATP hydrolyzed in cell turns into ADP; the adsorption of this EDC may further increase the *c*-value of the fixed carboxyl groups and increase the tendency to form salt-linkages.

In summary, the **stability** of the major congruous anion (isethionate) of squid-axon surface enables the surface β - and γ -carboxyl groups to remain as free fixed anions, adsorbing Na^+ rather than K^+ when ATP concentration falls and the *c*-value of the fixed carboxyl groups rises. Transient occupancy of the surface anionic sites by Na^+ leads to the slowdown of the Na^+ -efflux rate. In contrast, the **lability** of the major congruous anion, CrP, in frog muscle cells leads to a loss of the major congruous anion when ATP synthesis has been arrested by metabolic poisons. This loss of the major congruous anion and the concomitant rise of *c*-value of the fixed β - and γ -carboxyl groups lead to the formation of salt linkages at the expense of ion-adsorbing free surface carboxyl groups. As a result, the efflux of Na^+ in the ATP-depleted muscle remain rate-limited partly by passage through the cell surface water domains (the saltatory route) and partly by desorption from the vanishing number of intracellular fixed anions, which too become increasingly engaged in salt linkages. As a result, no significant slowing down occurs in the Na^+ efflux of poisoned frog muscles.

9.3 Summary

The membrane-pump theory has dominated the world of life sciences for fully a century. In this theory, membrane permeability is the all-encompassing parameter of cell physiology. Selective membrane permeability is believed to underlie the three classic subjects of cell physiology: solute distribution and volume maintenance as well as cellular resting potentials. As shown at the beginning of this chapter, this belief is incorrect.

While permeability is not the parameter underlying the specific major cell physiological phenomena mentioned above, it is, nonetheless, a subject that deserves careful study, because permeability is itself a physiological manifestation of importance and because permeability underlies *other* important physiological manifestations including the *action potential* to be discussed in Chapter 11, and *active transport* across bifacial cells (Chapter 17 in Ling 1984; 1990a).

This chapter is devoted to explaining why the conventional concept of cell membrane structure and function is in need of profound revision and why the new model of structure and function of cell membranes presented as an integral part of the association-induction hypothesis agrees with more facts.

(1) ***Why is the lipoidal membrane theory as such, as well as its resurrected modern version, no longer tenable?***

- (i) To serve its segregating function, the cell membrane must contain enough lipids (or phospholipid) to cover the entire cell surface. Yet most cell mem-

- branes analyzed possess only enough lipids to cover *a part* of the cell surface (Sections 9.1.1 and 9.2).
- (ii) Electron microscopy reveals trilaminar structure covering the entire cell surface. If this “unit membrane” represents or contains the postulated continuous lipid layer as claimed, severe distortion of the structure must follow removal of the bulk of membrane lipids, contrary to fact (Section 9.1.3).
 - (iii) The surface tension of both neutral fat membranes as exemplified by olive oil, and phospholipid bilayers, are too high to match that of living cells (Section 9.1.3).
 - (iv) The living cell membrane is vastly more permeable to water than either neutral fat membranes (Section 9.1.2) or phospholipid membranes (Section 9.2.1.4). Attempts to increase water permeability by resurrecting Traube’s “atomic sieve” (Section 1.2.2) were foiled by the recognition that solutes of all sizes can enter and leave the cells (Section 9.1.2).
 - (v) Neutral fat or phospholipid membranes are virtually impermeable to ions, while living cell membranes are, as a rule, permeable to ions in a highly specific manner. Failed attempts to find natural ion-specific ionophores (Section 9.1.3) have left the lipoidal membrane theory unable to explain one of the most important discoveries in cell physiology of this century: cell membranes are permeable to ions, big and small (Section 1.3).

(2) *Why is the AI model (of the cell membrane as a fixed-charge system maintained at the resting living state, and containing domains of intensely polarized water dominated by fixed β - and γ -carboxyl and other groups) a better approximation of the living cell membrane?*

- (i) Cellulose acetate membrane containing large pores filled with intensely polarized water demonstrates size-dependent permeability to nonelectrolytes ranging from (small) water molecules to (large) sucrose at three different temperatures. *Quantitatively*, this model behavior closely approximates the permeability of inverted living frog skin to the same nonelectrolytes at the same temperatures (Section 9.2.1.1).
- (ii) Failure of K^+ -specific ionophores like valinomycin to increase the K^+ permeability of most living cells studied (plasma membranes of frog ovarian egg, frog muscle, and squid axon; inner membrane of rat liver mitochondria) (Section 9.2.1.2) affirms the conclusion that—with large portions of the cell membrane occupied by intensely polarized water—the percentage of phospholipids in the cell membrane is too low to serve as an effective barrier to ion traffic in most living cells.
- (iii) Demonstration of bulk-phase-limited diffusion of water in frog ovarian egg and in giant barnacle muscle fiber (Section 9.2.1.3) suggests that the domains of intensely polarized water in the cell membranes may be quite extensive, reaffirming the basic notion that it is the polarization of water (rather than the diameters of the pores containing the water) that gives rise to the size dependency in the rate of permeation.
- (iv) A membrane of fixed-charge-dominated, intensely polarized water is a *wet*

membrane. As such, it is expected to have very low surface tension, in agreement with observations (Section 9.1.2).

- (v) The demonstration of similar kinetics, involving “saturability” and “competition” in the permeation of ions into living cells and into inanimate model fixed-charge-systems (e.g., ion-exchange-resin sheet, sheep’s wool) confirms the basic mechanism (the adsorption-desorption route) proposed for species-specific permeation of ions and nonelectrolytes into living cells and other fixed-charge systems. The demonstrated existence of an alternative route of ion entry (the saltatory route) resistant to competing ions (Figure 9.14) affirms the theory of the saltatory route of ion entry and exit through the polarized water (Section 9.2.2.1).
- (vi) Studies of the effect of pH on the rate of K^+ entry into frog muscle reveal that the fixed anions mediating K^+ entry have a pK_a characteristic of the β - and γ -carboxyl groups, as predicted by the AI hypothesis of ion permeation (Section 9.2.2.1).
- (vii) Ouabain changes the relative effectiveness of alkali-metal ions (Li^+ , Na^+ , K^+ and Rb^+) in inhibiting the rate of entry of labeled Cs^+ into frog ovarian eggs. The data can be explained by an ouabain-induced c -value increase in the β - and γ -carboxyl groups mediating Cs^+ entry into the egg cells. *Quantitatively*, the magnitude and direction of the c -value change are similar to the those produced by ouabain on the equilibrium distribution of the five alkali-metal ions in frog muscle (Section 9.2.2.3.1). As a whole, the data affirms the theoretical model of solute distribution, of ion permeation as well as that of control of cell functions by cardinal adsorbents.
- (viii) A key finding that eventually led to my rejection of the membrane-pump theory and the introduction of the AI hypothesis is the indifference of the Na^+ efflux rate of frog muscle to the application of metabolic poisons (Section 2.2.1). Yet in squid axons, not only is the Na^+ efflux rate reduced by the application of poisons like cyanide, injection of ATP or ArP can partially restore the normal faster rate. However, the iconoclastic discovery that ATP and ArP do not carry a package of utilizable energy in their phosphate bonds (Section 2.2.3) left the original interpretation in favor of the membrane-pump theory untenable. Even before this discovery, the membrane-pump theory could not readily explain why injection of concentrated ArP restores *K-sensitivity* while injection of concentrated ATP does not. Nor why injected ADP decreases *K-sensitivity* of Na^+ efflux, while injected ArP increases K^+ influx.

In contrast, the AI hypothesis can explain these observations without difficulty: the rate of Na^+ efflux critically depends on whether or not the majority of exiting Na^+ can occupy the β - and γ -carboxyl groups at the cell surface and in consequence leave the cell via the (slower) adsorption-desorption route (rather than the faster saltatory route). In agreement with theory, the Na^+ efflux of both frog muscle and squid axon slows down following removal of external K^+ , which in normal cells occupies most of the cell surface carboxyl groups because, in the presence of ATP and its “helpers,” these carboxyl groups are kept at a K^+ -preferring (low) c -value.

In theory, exposure to the EDC ouabain raises the c -value of the surface β - and γ -carboxyl groups and hence increases the preference for Na^+ . In agreement, ouabain reduces the Na^+ -efflux rate in both frog muscle and squid axon (Baker et al. 1971).

Reduction of the major EWC ATP should in theory also raise the c -value of the surface carboxyl groups, increase occupancy of surface carboxyl groups by Na^+ , and reduce Na^+ efflux rate. In fact, as mentioned above, this occurs in squid axon but not in frog muscle. These divergent behaviors can also be explained now on the basis of the *lability* of frog muscle's major congruous anion CrP, and the *stability* of squid axon's major congruous anion, isethionate. In the presence of metabolic poisons, CrP in frog muscle readily decomposes. Without the protection of a strong congruous anion, the surface carboxyl groups become locked in salt linkages and Na^+ continues to exist via the faster saltatory route. In contrast, isethionate continues to function as the major congruous anion in the presence of metabolic poisons, preventing salt-linkage formation and allowing K^+ -to- Na^+ adsorption exchange at the cell-surface carboxyl groups, hence the observed slowdown of Na^+ efflux in squid axons.

The critical role of CrP and ArP as major congruous anions with their own strong inductive effects in preserving the K^+ -preferring state of the surface β - and γ -carboxyl groups is cited to explain the ability of injected ArP to restore the K -sensitivity of Na^+ efflux, and to accelerate K^+ influx. The role of ADP as an EDC is cited to explain why injection of ADP reduces K -sensitivity.

- (ix) The model of cell membrane proposed in the AI hypothesis provides a fundamental versatility, essential for explaining the diverse physiological properties of cell membranes of various cell types and for explaining different permeability properties of the same cells at rest and during activity as we will see in Chapter 11.

NOTES

1. The belief that the rate-limiting step in the permeation of nonelectrolytes into the central vacuoles of *Nitella* cells is at the plasma membrane has become questionable; evidence now exists suggesting that the rate-limiting step may be located at the more rigorously semipermeable vacuolar membrane or tonoplast (see Section 10.1).

2. Earlier, Harvey gave a surface tension of 0.2 dyne/cm, but only as a *maximum* estimate (Harvey 1931).

3. On more than one occasion, I have been described as "not believing in the existence of cell membranes" (e.g., Dick 1984). This is simply not true.

4. The exceptionally high value of Bunch and Kallsen (1969) shown in Table 9.2 may be at least partly due to their use of short cut muscle segments, which deteriorate very rapidly (Ling 1973, 1978, 1989, see also Sections 2.4.1.).

5. It is theoretically conceivable that what may appear as bulk-phase-limited diffusion may arise from the presence of a series of diffusion barriers in the form of concentric cylindrical or spherical shells one inside another, like a "Chinese box," with higher solid content in each barrier than the average solid content of the cell. However, electron microscopy of barnacle muscle cells and frog ovarian eggs reveals no such concentric structures. Furthermore, if such concentric barriers with higher solid content did exist,

it would make the radial diffusion coefficient in muscle cells a great deal lower than the longitudinal diffusion coefficient. In fact, they are essentially the same. (However, for the demonstration of a small, but significant, anisotropy in rat muscle, see Cleveland et al. 1976.)

6. The data shown in Figure 9.13 also offer significant insight into the relative affinities of the surface β - and γ -carboxyl groups for H^+ and for K^+ . The inflection point of the titration curve at a pH of 4.75 means that at this pH, one half of the carboxyl groups are occupied by K^+ and the other half by H^+ . A pH of 4.75 is equivalent to the H^+ concentration of 1.78×10^{-5} M. The external K^+ concentration was 2.5 mM or 2.5×10^{-3} M. The relative affinity of the cell surface β - and γ -carboxyl groups for H^+ over K^+ is therefore $(2.5 \times 10^{-3}) / (1.78 \times 10^{-5}) = 140$.

The high affinity for H^+ over K^+ at the normal muscle cell surface agrees, on the one hand, with a similar but less striking higher affinity for H^+ than for Na^+ demonstrated earlier in the β - and γ -carboxyl groups in muscle cytoplasm of PEG-(partially)-preserved 2mm cut muscle sections (see endnote 8 of Chapter 6); and on the other hand, with the theoretical model in which the high polarizability of the carboxyl groups is taken into consideration as it was in the model presented in Figure 6.8. It does not agree with models in which a lower polarizability is used or the polarizability is ignored in my 1952 model (Ling 1952) and as in the model proposed by Eisenmann (1961, 1967) (see endnote 8 of Chapter 6).

7. The question may be raised: "Why should P_i (and hexose phosphate) effectively substitute for the congruous anion, CrP for K^+ adsorption in the cytoplasm of metabolically inhibited frog muscle (Section 8.4.3.3.), while P_i is unable to serve a similar role at the cell surface of metabolically inhibited frog muscle?" The answer is: Only when the ATP concentration is or close to normal, can P_i (and hexose phosphate) partially substitute for CrP as congruous anions. When ATP is depleted, P_i can no longer serve the same role. The data presented in Section 8.4.3.3. was obtained in response to anoxia, which does not significantly reduce the ATP concentration of frog muscle (Figure 8.20). In contrast, the ATP concentration of cyanide treated squid axons (Caldwell 1960), as well as frog muscles exposed to IAA, or 2,4-dinitrophenol—alone or in conjunction with cyanide or anoxia—fell slowly or rapidly according to temperature (Ling 1962, Figure 15.24). The data of Figure 2.1.B and C resulted from the use of these metabolic poisons at room temperature, causing rapid ATP depletion.

CELL VOLUME AND SHAPE

If living cells were all spherical—a shape one could easily have anticipated if cells were all phospholipid-bilayer-enclosed globules of aqueous solutions containing free water, free ions, and native proteins—the shape of living cells would then be a nonproblem. In fact, different cells as a rule have different shapes. Even free-floating cells like erythrocytes are not spherical, but are biconcave discs. Nevertheless, the dominance of the membrane-pump theory has consciously or unconsciously directed and thus delegated the study of cell shapes to cytologists and anatomists, leaving cell volume divorced from cell shape as an independent physical trait of the living cell, up to the present.

The partial vindication of the early protoplasmic theory of the living cell described in this and preceding volumes (Ling 1962; 1984) as well as the emergence of cytoskeletal protein concepts (Schliwa 1986) have clearly indicated that **cell volume and cell shape are intimately associated manifestations of the same basic properties of living cells.** It is for this reason that the title of this chapter includes both subjects.

10.1. *Cell-Volume Maintenance and Regulation According to Traditional Hypotheses*

Moritz Traube's discovery in the middle 1860s of the copper-ferrocyanide gel membrane was a historic landmark. By precipitating copper ferrocyanide in the wall of a porous pot, Wilhelm Pfeffer (1877) added strength and durability to the nearly ideal semipermeable membrane.

Pfeffer connected the impregnated porous pot, which he filled with a sucrose solution, to a manometer. He measured the pressure (called *osmotic pressure*) that had to be applied to the content of the porous pot to bring to a halt the inflow of water from the dilute external solution bathing the porous pot. From these measurements, he demonstrated the proportionality of the osmotic pressure (π) to the concentration of the sucrose solution in the impregnated porous pot (C):

$$\frac{\pi}{C} = \text{constant} . \quad (29)$$

He also demonstrated the proportionality between π and the absolute temperature (T):

$$\frac{\pi}{T} = \text{constant} . \quad (30)$$

Together, these findings led van't Hoff (1885) to derive what has been known as the van't Hoff law:

$$\pi V = RT , \quad (31)$$

where R is the gas constant and V is the volume of the solution enclosed in the semipermeable membrane. Combining equations 29 and 31, one finds that at constant temperature,

$$V = \frac{\text{constant}}{C} . \quad (32)$$

Thus a plot of cell volume (V) against the reciprocal of the solute concentration ($1/C$) should yield a straight line. In subsequent research, when living cells were found to swell and shrink according to this prediction, they were described as behaving like *perfect osmometers* (Lucké and McCutcheon 1932).

The response of plant cells to concentration changes in their bathing solutions have been subjects of interest and research since the earliest days of biology (Hales 1732; Nasse 1869; de Vries 1884; Pfeffer 1877). The types of plant cells studied have been, as a rule, mature cells containing a large central vacuole which is separated from the surrounding layer of cytoplasm by a membrane called a *tonoplast* or vacuolar membrane (Figure 10.1A). On its outside surface, the cytoplasm layer is covered by the plasma membrane, and beyond that, the cell wall. When such a plant cell is placed in a concentrated solution of, say, NaCl or sucrose, the entire protoplasm, including the central vacuole it encloses (the

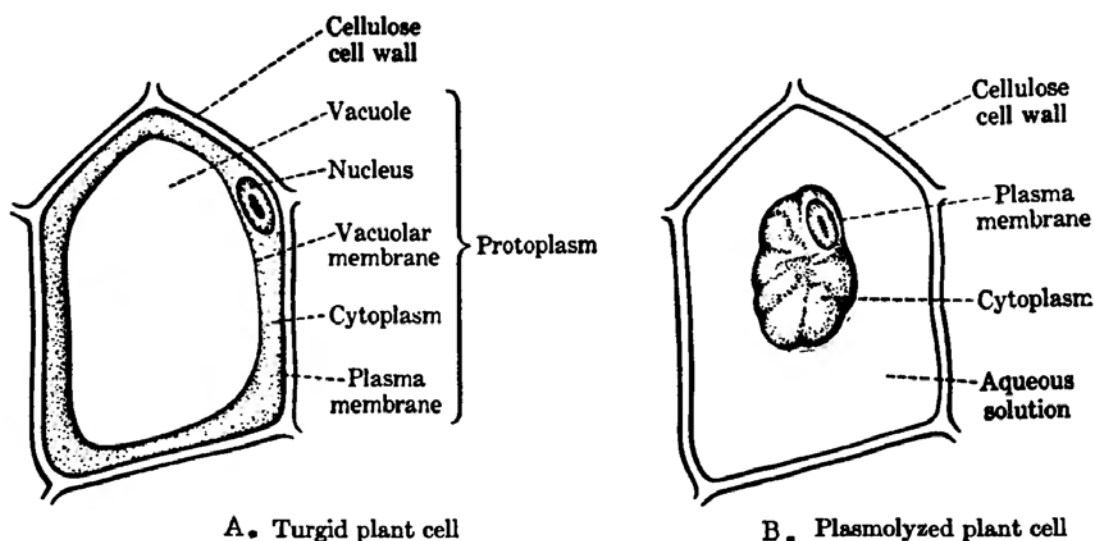


Figure 10.1. Diagrammatic illustration of plasmolysis of a plant cell. (Glasstone 1946, by permission of D. van Nostrand and Co.)

protoplasmic sac), shrinks away from the rigid cell wall (Figure 10.1B). The degree of shrinkage varies in proportion to the concentration of NaCl or sucrose in the surrounding medium.

A simple but accurate method for measuring the volume of the protoplasmic sac at equilibrium with an external bathing solution of a specific concentration was introduced by Höfler (1918). Using this method, Höfler showed that the volume (V) of the (shrunken) parenchyma cells of the plant *Tradescantia elongata* is inversely proportional to the concentration (C) of the sucrose in the bathing medium. In other words, $CV = \text{constant}$ (Table 10.1). Höfler's data offered support for Schwann's original cell theory (Section 1.2) and Pfeffer's membrane theory, according to which cells behave like perfect osmometers.

Continued studies of the volume changes in plant cells by Höfler and his coworkers led to unexpected results: *it was the tonoplast-enclosed central vacuole that behaved like a perfect osmometer; the cytoplasmic part of the cells did not*. In concentrated solutions of electrolytes, for example, the central vacuole shrank as expected, but at the same time, the cytoplasm actually expanded (Plowe 1931; Strugger 1932; Ullrich 1939). Using a microdissection technique, Chambers and Höfler (in 1931) isolated the tonoplast-enclosed central vacuoles. In various hypertonic solutions, these isolated vacuoles did indeed behave like osmometers. Since in its natural state the vacuole is filled with a dilute salt solution, true osmometer-like behavior is not surprising.

Reviewing the subject, Rubinshtein wrote in 1939: "... we are compelled to disregard completely in our calculations all results obtained by the osmotic method in the study of plant cells, results which historically, as is well known, were the basis of all contemporary teaching on the semipermeable plasma envelope" (English translation in Troshin 1966, 32). Rubinshtein then urged the study of animal cells, which do not contain large liquid-filled central vacuoles.

"Animal cells also do not behave like osmometers" (Troshin 1966, 32). Thus Overton (1902) found that the volume of frog muscles was not inversely proportional to the concentration of the solution in which they were incubated. For example, in a solution containing NaCl at half the strength of an isotonic NaCl, muscle cells swelled to a final volume only 30% larger than initial volume, rather

Table 10.1. Relation between the Volume of Plasmolysed Parenchyma Cells of *Tradescantia elongata* and the Concentrations of Sucrose in the Incubating Solution (Höfler, quoted in Lucké and McCutcheon 1932, by permission of *Physiol. Rev.*)

Concentration of Sucrose Mols C	Relative Volume of Plasmolyzed Cell V	Isotonic Concentration Calculated from $C \cdot V$
0.30	0.585	0.175
0.35	0.494	0.173
0.45	0.382	0.172
0.60	0.287	0.172

than twice the initial volume predicted by equation 32. *Overton concluded that the muscle cell cannot be simple aqueous solution, and that at least a part of the muscle cell water is in the form of "Quellungswasser" (imbibition water).*¹

Similar departures in volume changes in red blood cells from those predicted by equation 32 led to the postulation that a substantial fraction of the cell water is "osmotically inactive" (Ponder 1936). From a plot of the experimentally determined cell volume (V) as ordinate against the reciprocal of the external solute concentration, $1/C$, as abscissa, the "osmotically inactive volume" is obtained from the ordinate intercept at $1/C = 0$, corresponding to a solution of infinite concentration and zero water activity.

Ling and Negendank (1970) studied osmotically induced volume changes in frog muscle in a different way. Instead of immersing the muscles directly in solutions of different osmotic activities, they suspended small bundles of muscle cells in an enclosed vapor phase in equilibration with NaCl or H₂SO₄ solutions of different strengths. Since the cells and the solutions providing the specified vapor pressures were not in direct contact, concentrated H₂SO₄ could be used to provide very low vapor pressures for studies. The results showed that the V vs. ($1/C$) plot is rectilinear (according to equation 32) only over a *limited range* of NaCl concentrations, corresponding to relatively high vapor pressures. In the case of much lower vapor pressures, produced by concentrated sulfuric acid, the V vs. $1/C$ plot is no longer rectilinear, but curves downward to converge on the origin of zero volume at zero vapor pressure. *As a whole, the data clearly show that the cells definitely do not behave like perfect osmometers. Ling and Negendank's work also laid to rest the concept that a substantial part of the water in frog muscle is "osmotically inactive."* All water evaporates when vapor pressure is low enough.

In the view of A. V. Hill (1886–1977), an influential physiologist during his lifetime (see Section 1.4.; also Ling 1984, 57), the deviation of frog muscles from ideal osmotic behavior reported by Overton (1902) and confirmed by Hill himself was due to the loss of semipermeability of some 25% of the cells of the isolated muscle studied. This explanation is not acceptable now, for the simple reason that the swelling in a hypotonic solution of carefully dissected frog muscles is fully reversible and reproducible; other muscles dissected the same way can be kept in vitro at 25°C for up to eight days without significant impairment of its K⁺ content, resting potential or contractility (Ling and Bohr 1969). The persistence of a normal K⁺ content and other traits in isolated frog muscle rules out the existence of a significant fraction of damaged or dead cells. However, using well-preserved frog muscle cells, the deviation from ideal behaviors noted by Overton and confirmed by Hill can be regularly reproduced.

To explain the sustained shrinkage of living cells in concentrated NaCl solutions, Tosteson, Hoffman, and others proposed a "pump-leak hypothesis" (Tosteson and Hoffman 1960; for review see MacKnight and Leaf 1977). In this hypothesis, the cell membrane, though actually permeable to Na⁺, is made "effectively impermeable" by the operation of the Na pump (Wilson 1954; Leaf 1956). The evidence against the Na-pump hypothesis presented in Chapter 2 has rendered the "pump-leak hypothesis" not defensible.

In summary, neither plant nor animal cells behave like perfect osmometers, as predicted by the membrane theory. Remedial postulations of “osmotically inactive” water, of damaged cells, and of a “pump-leak hypothesis” have been shown to be untenable.

10.2. *Cell-Volume Maintenance and Regulation According to the AI Hypothesis*

As mentioned earlier, proteins and water make up virtually the entire volume of the cell. Cell volume is therefore, to all intents and purposes, the sum of the volume of the cell proteins and of cell water. Since, under most physiological conditions, the protein content of a cell does not change materially, cell volume maintenance and regulation are primarily the maintenance and regulation of cell water content.

According to the AI hypothesis, the size as well as shape of a living cell are determined primarily by the nature, amount, conformation, mutual interaction, and spatial orientation of cell proteins. Multilayer adsorption and polarization on the extended polypeptide chains of cell proteins then determine the total amount, as well as regional distribution, of water in the cell (see Section 5.2.5.3.).

In the following sections I discuss theory and supporting experimental evidence for the process by which cell-water content is also determined by the concentration of external solutes: nonelectrolytes and electrolytes. I also discuss how the cell-water content as well as cell shape are determined by other agents, including the ubiquitous conservative-cardinal-adsorbent, ATP.

10.2.1. *A New Theory of Cell-Volume Maintenance*

10.2.1.1. *Qualitative Theory and Evidence*

The osmotic activity of an aqueous solution measures the reduction of the *activity* (or “wateriness”) of the water in the solution. Concentrated solutions of sucrose or NaCl have high osmotic pressure because these solutes, at high strengths, reduce water activity strongly. Since the living cell is primarily a system of water, proteins, and K^+ , the only two cell components that can influence the activity of cell water are K^+ and proteins. However, K^+ exists in an adsorbed and hence osmotically inactive state. This exclusion leaves only proteins.

In their native state, proteins as a rule exercise only a moderate effect on water activity. However, when proteins, for one reason or another, exist in the fully-extended conformation, they influence the osmotic activity of the water profoundly, as shown earlier, through multilayer polarization (see Figure 5.12, Section 5.2.5.4). Fundamental observations on model systems and the fact that cell-volume maintenance does not require an intact plasma membrane (Figures 10.2 and 10.8) led to the AI hypothesis concerning cell volume maintenance and control. A qualitative presentation of this theory will now be offered, with a more rigorous quantitative expression to follow.

Water Content (% of final fresh weight)

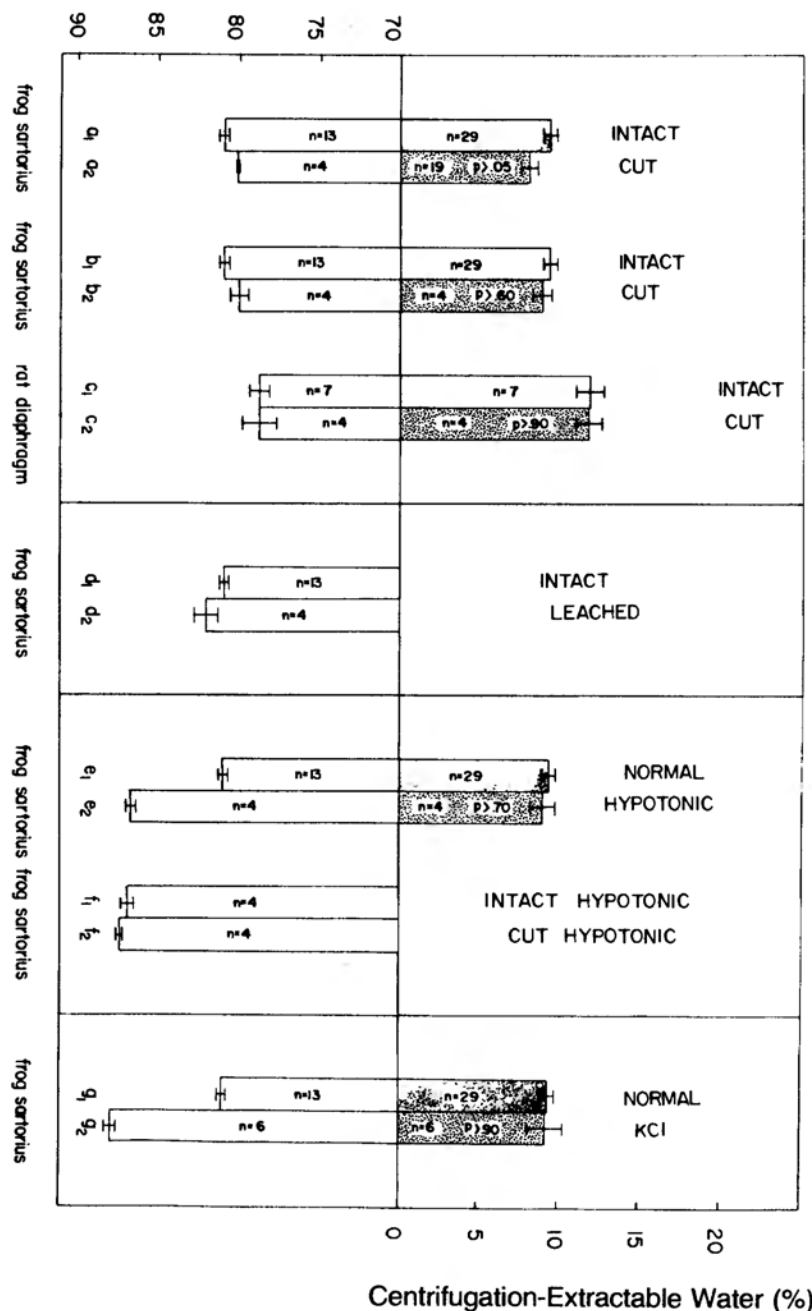


Figure 10.2. Water content and centrifugation-extractable fluid of intact voluntary muscle cells and muscle cells cut into 2 mm- and 4 mm-long segments (see Figure 10.7) with both cut ends open.

a -c, intact and cut muscle without prior treatments. Muscles in b₂ first exposed to a low Ca⁺⁺ Ringer solution. Centrifugation following the procedure of Ling and Walton (1975) (4 min. at 1000 g) removed the same percentage of water from intact and cut muscles.

d, leaching of muscle which removed most intracellular solutes does not significantly change the water content after centrifugation.

e, swelling following exposure to a hypotonic solution (osmolarity equal to 20% of normal Ringer solution) does not significantly change the percentage of centrifugation-extractable water.

f, after exposure to hypotonic solution, intact and cut muscle retain the same water content. These muscles were blotted but not centrifuged.

g, exposure to a high KCl (93 mM) Ringer solution, increased the total water contents but produces no significant change in the percentage of centrifugation-extractable water. (Ling and Walton 1976, by permission of Science)

Let us construct the following model: introduce a solution of a fully extended protein or model polymer into a dialysis bag permeable to water and small solute molecules or ions, but impermeable to the protein or polymer. We now close the open ends and immerse the sac in a solution of large nonelectrolyte or hydrated ions. The ability of the solution in the enclosed dialysis sac to assume and maintain a particular volume while immersed in a solution of specified type and concentration depends on the balancing of two opposing tendencies:

- (1) ***A tendency to draw more water into the sac*** by building up *additional* multiple layers of water upon those already adsorbed on the protein or polymer in the sac;
- (2) ***A tendency to lose water from the sac to the external medium*** in consequence of the lower concentrations of solutes in the sac—especially those solutes of large molecular size—than in the external medium. The lower solute concentration in the sac arises from the presence of polarized water in the sac and the size-dependent reduced solubility for solutes in polarized water.

For verification of the theory on an inanimate model, we chose a 30% aqueous solution of polyethylene oxide (PEO). An *NO-NO-NO* system, PEO exhibits high osmotic activity (Section 5.2.5.4) and (partially) excludes Na citrate ($\rho < 1$) (Section 5.2.5.1). ***When PEO is introduced into dialysis sacs immersed in solutions containing different concentrations of Na citrate (or sorbitol), concentration-dependent volume variation is indeed observed*** (Figure 10.3), ***even though the dialysis-sac membrane is freely permeable to both water and Na citrate (or a nonelectrolyte like sorbitol)***. The distinctive volume at each concentration is maintained indefinitely if the polymer does not leak out. Solutions of other water-polarizing polymers and of urea- or NaOH-denatured proteins, all of which partially exclude Na citrate, behave similarly. In contrast, solutions of native proteins, which do not or only weakly exclude Na citrate, do not maintain different volumes in solutions of Na citrate of different strengths. Taken together, the data indicate that ***the ability of a solute to cause the cell model to shrink and maintain the concentration-dependent volume depends on a low q -value of the solute in the cell model's water*** (Ling and Ochsenfeld 1987).

It should be emphasized that PEO, PEG, PVME, and PVP are all electrically neutral; they do not carry net electric charges. Solutions of these polymers do not retain water due to the establishment of Donnan equilibrium (Proctor and Wilson 1916; Ling 1984, 29), and their responses to electrically charged electrolytes (e.g., Na citrate) and neutral nonelectrolytes (e.g., sorbitol) are basically alike. Similarity in response to electrolytes and nonelectrolytes, however, does not extend to solutions of fully extended proteins, because proteins are (unlike PEO, PEG, etc.) themselves electrolytes, and may in consequence adsorb or undergo specific changes in response to high concentrations of electrolytes in ways not shared by most nonelectrolytes. A further discussion of this point follows in Section 10.2.2.

10.2.1.2. *Quantitative Theory and Evidence*

I now proceed to put the concept of cell volume regulation by external solutes into a quantitative form. I begin by writing down the relationship between the

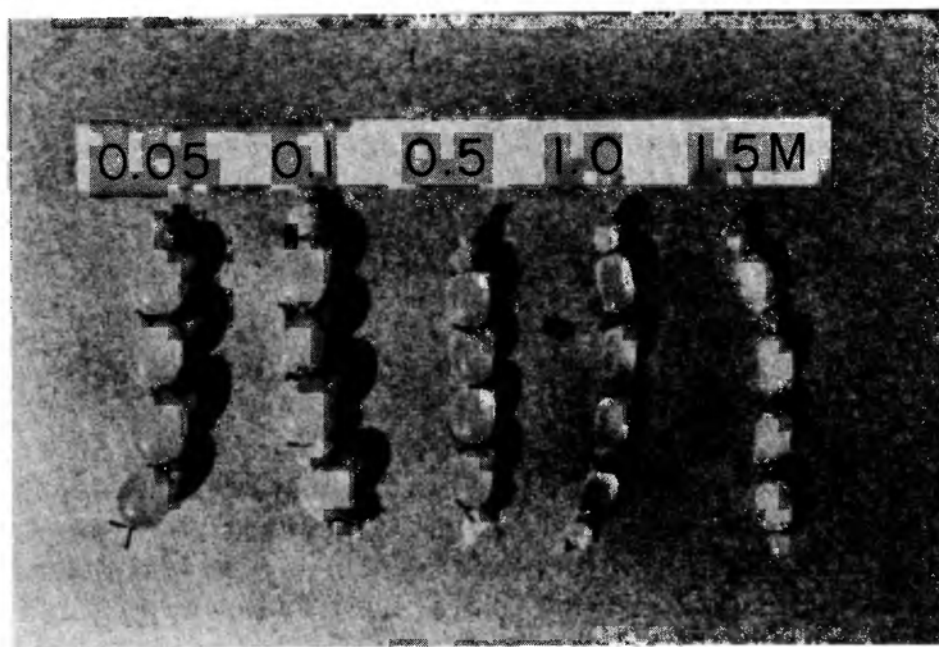


Figure 10.3. Swelling and shrinkage of dialysis bags filled (initially) with a 30% solution of polyethylene oxide (PEO) and equilibrated in solutions of sodium citrate at the molar concentrations indicated. PEO is a neutral polymer; swelling is not due to electrostatic (Donnan) effect (see text). (Ling 1984, by permission of Plenum Publishing Co.)

volume of a cell (V) to the weights of its water, proteins and other non-water, non-protein materials in the cell:

$$V = a \cdot (w_p/100) \cdot v_{\text{H}_2\text{O}} + w_p \cdot v_p + w_o \cdot v_o, \quad (33)$$

where w_p and w_o are respectively the weight of (all) proteins and the weight of (all) other non-water, non-protein materials in the cell. a is the weight of water in the cell in units of grams of water per 100 grams of protein. $v_{\text{H}_2\text{O}}$, v_p and v_o are respectively the partial specific volume of cell water, cell proteins, and non-water, non-protein materials. $v_{\text{H}_2\text{O}}$ is one. v_p is about 0.73 (Edsall 1953). v_o is unknown until we have an exact analysis of all the cell's constituents. Fortunately, for most cells not heavily loaded with fats, mucopolysaccharides etc., the term $w_o v_o$ is less than 1% of the cell volume and can usually be ignored. As mentioned above, the protein content of a cell is, over a short period of time, usually not changing; volume maintenance and regulation of a cell is therefore, to all intent and purposes centered on the water content of the cell, a or a -value.

With the basic relation between cell volume and cell water content clarified, my next objective is to derive an equation for the water content of living cells when they have been immersed in aqueous solutions containing different concentrations of a permeant or impermeant solute long enough to reach diffusion equilibrium. For the purpose of simplicity, we first consider only noncharged solutes, i.e., nonelectrolytes. (For a discussion of the control of cell volume by electrolytes, see Ling and Peterson 1977).

Three postulates used in deriving the new equations are:

- (1) water in the cell exists in the state of polarized multilayers and, as such, follows Bradley's multilayer-adsorption isotherm (equation 4);
- (2) the partial vapor pressure (p/p_o) of the solutions follows Raoult's law,

$$\frac{p}{p_o} = \frac{n_1}{n_1 + n_2},$$

where p and p_o are, respectively, the vapor pressure under study and the vapor pressure at full saturation under the same condition, and where n_1 and n_2 are the number of moles of solute and solvent (water), respectively, in the solution; and

- (3) *water uptake in multilayers depends upon the difference in the activity of water (measured as the relative vapor pressure, p/p_o) in the cell and in the external medium.*

The following equation describes the relationships between the water content, represented by the symbol a , the concentration of the (main) solute that is in the external bathing solution, and the equilibrium distribution coefficient (q -value) of this solute in the cell water (Ling, 1986; 1987):

$$\log \left[1 + \frac{(1 - q)n_2}{n_1} \right] = K_1 K_3^q + K_4, \quad (34)$$

or

$$a = \frac{1}{\log K_3} \left[\log \left[\log + \frac{(1 - q)n_2}{n_1} - K_4 \right] - \log K_1 \right] \quad (35)$$

where n_2 is the molal concentration of the solute, and n_1 is 55.51, the number of moles of water in which n_2 moles of the solute is dissolved.

Figure 10.4 is a theoretical plot of the water content of living cells according to equation 35. The cell water content (a or a -value) is expressed in grams of water per 100 grams of cell proteins, which is in essence equal to 100 grams of total (dry) cell solids. The concentration of nonelectrolyte solutions is expressed in molality. The equilibrium distribution coefficients or q -values of the nonelectrolytes vary from 0 to 0.98, as indicated in the graph.

Based on theory, one can make the following predictions:

Prediction 1. Solutes of larger sizes and higher molecular weights will tend to have lower q -values (as per the size rule) and lower a -values. Conversely, solutes with smaller sizes and lower molecular weights will tend to have higher q - and higher a -values.

Prediction 2. Solutes of the same size and molecular weight will tend to have the same q - and a -values.

Prediction 3. A positive correlation should exist between the q -values and the a -values when cells have been equilibrated in equimolar solutions of solutes of diverse sizes and molecular weights.

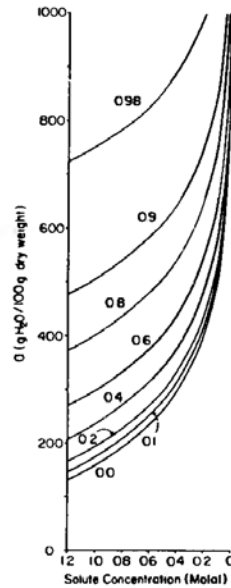


Figure 10.4. Theoretical curves of the water contents (a) of living cells or model systems equilibrated in solutions of different concentrations of solutes which distribute between the cell water and the external medium with different equilibrium distribution ratios, or q -values, as indicated, ranging from 0 to 0.98. Theoretical curves were calculated according to equation 35 with $\log K_3$ equal to 350, $K_1 = 0$, and $\log K_1 = 580$. a is given in grams of water per 100 grams of dry cell weight. Concentration of solutes is in molality. (Ling 1987, by permission of Physiological Chemistry Physics and Medical NMR)

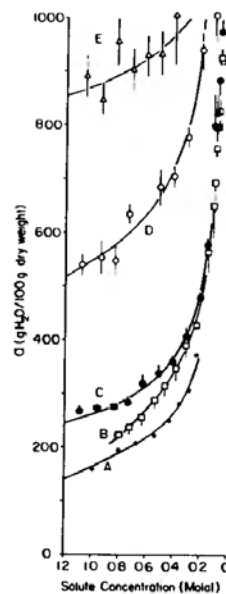


Figure 10.5. Water contents (a) of frog muscles equilibrated at 25°C in solutions of various sugars with the exception of Curve A. Curve A (taken from Ling and Negendank 1970) was from vapor-equilibrium studies. The equilibrium water uptake at different partial vapor pressure (p/p_0) of Curve A is plotted here against different sucrose concentrations giving the same p/p_0 studied and produced by NaCl and H₂SO₄ solutions of varying concentrations. Curve B, mannitol; Curve C, erythritol; Curve D, glycerol; Curve E, ethylene glycol. (Ling 1987, by permission of Physiological Chemistry Physics and Medical NMR)

Prediction 4. The cell water contents and hence volumes should vary with the concentrations and the q -values of the major solutes of the external solution in accordance with the general contours of the theoretical curves shown in Figure 10.4.

Prediction 5. Sustained cell or model shrinkage (lowered a value) is caused by exposure to a concentrated solution of solutes with low q -values. The solutes' impermeability to the cell or model membrane is of special interest only because impermeability represents a q -value of zero.

To test these predictions, I studied the equilibrium water content of isolated frog muscle in solutions of different concentrations of 7 pentoses, 7 hexoses, 7 disaccharides, 2 trisaccharides and 6 sugar alcohols. Figure 10.5 shows that the equilibrium water contents of frog muscles in sugar and sugar alcohol solutions do indeed follow the general shapes of the curves shown in Figure 10.4, in agreement with Predictions 1, 4, and 5. Data points of the bottom curve were taken from Ling and Negendank (1970), where the water contents were obtained not by direct immersion (as with the other data shown in Figure 10.5), but by the method of vapor equilibrium. Since the vapor phase served as a perfect semipermeable barrier to the solutes used, this data corresponds to a q -value of zero. In the actual experiments of Ling and Negendank, the solutes providing the different vapor pressures were NaCl at high p/p_o and H₂SO₄ at low p/p_o , respectively; the molal concentrations indicated on the abscissa of Figure 10.5 are those of sucrose solutions giving the same partial vapor pressures provided by the different NaCl and H₂SO₄ solutions.

The data presented in Table 10.2 confirm Prediction 2 as well as Prediction 1. Thus, similar a -values were obtained by sugars of the same molecular weights. The a -value is largely independent of the steric conformation, which differs from one pentose to another and from one hexose to another.² A linear correlation coefficient of +0.973 was found between the q -values and a -values for sugars and sugar alcohols, confirming Prediction 3. Finally, Figure 10.6 illustrates the linear relationship between molecular weights and average a -values, a relationship that further affirms Prediction 1.

In conclusion, the equilibrium volume of frog muscles in solutions of sugars and sugar alcohols follows equations 34 and 35. *The data not only affirm quantitatively the theory of the basic mechanism of volume maintenance, but also indirectly affirm, once more, the size rule*, as regards the distribution of sugars and sugar alcohols in cell water.

10.2.2. *The Restraining Effect of Intracellular Salt Linkages in the Maintenance of Cell Volume, and Specific Swelling Effects of Some Electrolytes*

In a 0.118 M solution of NaCl, frog muscle tissues maintain their normal weights just as they do in a 0.236 M solution of sucrose. Since 0.118 M NaCl and 0.236 M sucrose have essentially the same osmotic activity (or partial vapor pressure) (Frazer 1927), the maintenance of normal cell volume in 0.118 M

Table 10.2. Water Contents of Frog Muscles Equilibrated in 0.1 M and 0.4 M Pentoses, Hexoses, Disaccharides, and Tri-saccharides. (Ling 1987, by permission of *Physiol. Chem. Phys. and Med. NMR.*)

	0.1M	0.4M
D-arabinose	735 ± 31 [2, 8]	324 ± 9 [2, 8]
L-arabinose	894 ± 42 [2, 8]	355 ± 35 [2, 8]
D-xylose	836 ± 56 [1, 4]	340 ± 9 [1, 4]
L-xylose	861 ± 28 [2, 8]	340 ± 7 [2, 8]
D-lyxose	927 ± 26 [1, 4]	336 ± 10 [1, 4]
L-lyxose	709 ± 34 [1, 4]	347 ± 5 [1, 4]
D-ribose		368 ± 12 [1, 4]
D-glucose	691 ± 22 [1, 4]	326 ± 5 [1, 4]
fructose	639 ± 10 [1, 4]	339 ± 5 [1, 4]
L-glucose	713 ± 41 [2, 8]	318 ± 13 [2, 8]
galactose	705 ± 39 [1, 4]	336 ± 8 [1, 4]
fucose	728 ± 24 [1, 4]	367 ± 4 [1, 4]
mannose	648 ± 21 [2, 8]	342 ± 7 [2, 8]
tagatose	659 ± 30 [1, 4]	311 ± 4 [1, 4]
turanose	552 ± 12 [1, 4]	254 ± 23 [1, 4]
cellobiose	553 ± 11 [2, 8]	267 ± 4 [2, 8]
melibiose	578 ± 7 [1, 4]	268 ± 8 [2, 8]
sucrose	566 ± 16 [1, 4]	255 ± 5 [1, 4]
trehalose	580 ± 9 [1, 4]	262 ± 6 [1, 4]
maltose	599 ± 4 [2, 8]	265 ± 6 [1, 4]
lactose	588 ± 8 [2, 8]	267 ± 3 [1, 4]
melezitose	545 ± 10 [1, 4]	234 ± 5 [1, 4]
raffinose	539 ± 12 [1, 4]	

Note: Incubation time was 4 hours at 25°C. The first number in brackets indicates the number of sets of experiments, the second number represents number of individual assays.

NaCl indicates that, at least in this concentration range, a solution of NaCl is no different from other nonelectrolytes with similar low q -values.

However, an altogether different response is observed when frog muscle tissues are introduced into a 0.118 M solution of KCl. Even though 0.118 M KCl has the same osmotic activity as 0.118 M NaCl or 0.236 sucrose, in a 0.118 M KCl solution the muscles undergo intense swelling (Overton 1904; von Korösy 1914–1915; Ling and Peterson 1977; Ling 1984, 443). For some time, this divergence in the effects of KCl and NaCl solution on cell swelling was attributed to the permeability of the cell to KCl but not to NaCl. K^+ and Cl^- were believed to be permeant (Boyle and Conway, 1941) and to enter the cell together and cause swelling, while the impermeability of the cell membrane to Na^+ prevented

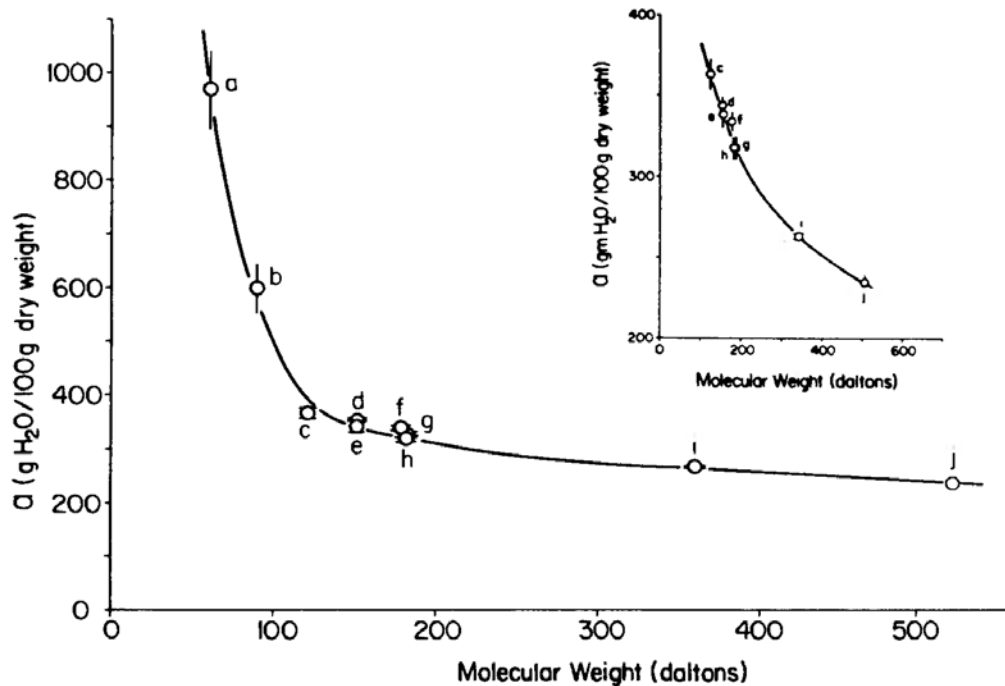


Figure 10.6. Water content of frog muscles after 4 hours incubation (25°C) in 0.4 M sugar and sugar alcohols solutions. Ordinate is *a*-value in grams of water per hundred grams dry weight. Abscissa represents the *molecular weights* of the sugars and sugar alcohols. a, ethylene glycol; b, glycerol; c, erythritol; d, 7 pentoses (average); e, xylitol; f, 7 hexoses (average); g, sorbitol; h, mannitol; i, 7 disaccharides (average); j, melezitose. In the inset, a and b are not shown. (Ling 1987, by permission of Physiological Chemistry Physics and Medical NMR)

both the entry of Na^+ (and Cl^-) and swelling. With the establishment that the cell membrane is permeable to Na^+ , this explanation was replaced by one based on the Na-pump concept: the operation of the Na pump makes the cell membrane “effectively impermeable” to Na^+ (Wilson 1954; Leaf 1956). But aside from the decisive evidence against the Na-pump concept in general (Chapter 2), there is additional, more specific evidence against this view.

In the pump-leak hypothesis (Tosteson and Hoffman 1960; Mac-Knight and Leaf 1977), the swelling and shrinkage of living cells intimately depend upon the presence of an intact plasma membrane, much as the swelling and shrinkage of a balloon depend on its intact membrane. Thus if frog muscle cells are cut into 2-mm- to 4-mm-long segments, as shown in Figure 10.7, the intactness of the membrane is destroyed, there is no membrane regeneration (see Figure 4.11), and the ionic contents rapidly reach equilibrium with the outside solution (see Ling 1989). Under this condition, neither isotonic KCl nor isotonic NaCl should cause swelling. Yet four hours after immersion, the 2–4 mm frog muscle cell segments in isotonic KCl were fully swollen, like their intact controls, while in isotonic NaCl, the cut segments remained unswollen (Figure 10.2). Clearly the pump-leak model cannot explain these observations.

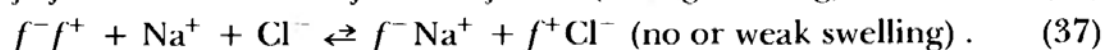
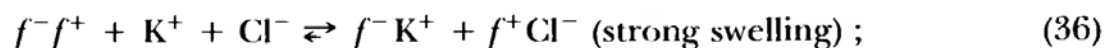
Centrifugation at 1000 g. for 4 minutes which quantitatively removes all extracellular space fluid (Ling and Walton 1975) did not remove any detectible



Figure 10.7. Cut frog sartorius muscle before (A) and after (B) stretching. The proportion of 2-mm-long segments tends to be less than that of the 4-mm-long segments unless special efforts are made to increase the length of the 2-mm segments by making the razor cuts still deeper.

amount of cell water even after the muscle had been cut into 2- and 4-mm wide segments with open ends (Figure 10.2). If only a significant part of the cell water exists as free water, that portion would certainly have been extracted. But that did not happen.

In the AI hypothesis, salt linkages formed between fixed anions (f^-) and fixed cations (f^+) of adjacent protein chains play a restraining role in the maintenance of normal cell volume as well as cell shape (Ling and Peterson 1977). KCl and NaCl produce divergent effects on cell volume because K^+ (and Cl^-) are more effective than Na^+ (and Cl^-) in competing against fixed cations for fixed anions, mostly β - and γ -carboxyl groups. Thus many more of the volume-restraining salt linkages (f^-f^+) are broken by KCl than by NaCl, and the cells swell as a result:



The much greater effectiveness of K^+ over Na^+ in competing for the β - and γ -carboxyl groups, in turn, results from the fact that normal cells and freshly cut segments retain enough ATP (and “helpers”) to keep the c -value of the β - and γ -carboxyl groups at a relatively low level (ca. -4.20\AA , see Section 8.4.2.4.). At such a low c -value, K^+ is overwhelmingly preferred by these fixed anions, while Na^+ is not (see Figure 6.9).

The time courses for swelling and shrinkage of 2–4 mm segments of frog muscles in eight isotonic salt solutions were observed at 0°C (Figure 10.8). Note that K_2SO_4 is far less effective than KCl in causing swelling, in agreement with the fact that SO_4^- is one of the anions least preferred by fixed cations, while Cl^- is, relatively speaking, more strongly adsorbed (Figure 6.3). Both isotonic $MgCl_2$ and $MgSO_4$ cause only shrinkage, in agreement with the fact that divalent Mg^{++} is very weakly, if at all, adsorbed on (isolated) β - and γ -carboxyl groups (see Section 8.1.2(3)). Note also that even though much less swelling occurred in isotonic NaCl or LiCl solutions than in isotonic KCl, some swelling did occur in both isotonic solutions of NaCl and LiCl. At first look, this swelling seems to contradict the lack of swelling of cut muscle described in Figure 10.2. An explanation for this disagreement may be found in the ways the cut muscle segments were treated in the two different studies: muscle segments used in the

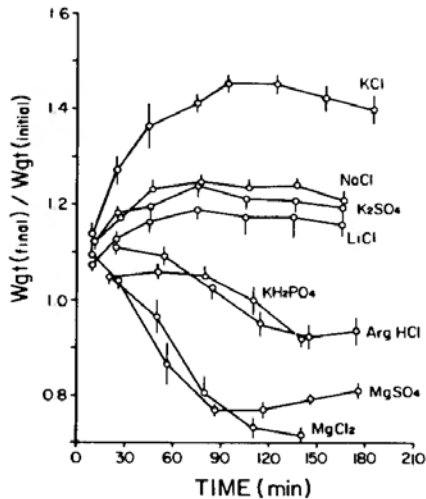


Figure 10.8. Swelling and shrinkage in isotonic salt solution (0.118 M or equivalent) of frog sartorius muscle cut into 2 mm and 4 mm segments with open ends and incubated at 0°C with bubbling air. Arg HCl stands for arginine hydrochloride. (Ling and Wright, unpublished)

experiments described in Figure 10.2 were left alone without any disturbance except a very gentle shaking. Muscle segments used in experiments described in Figure 10.8 had to be repeatedly fished out of solutions, blotted dry, and weighted at frequent intervals. These handlings apparently hastened the deterioration of the cut segments. It should be mentioned that for reasons soon to be made clear, the apparent discrepancy between the two sets of data is in itself an *affirmation* of the theory of injury-induced cell swelling, described below.

It is both interesting and enlightening to recall that almost exactly 100 years ago, Kunkel (1889) made the important observation that when a muscle cell swells or shrinks, the volume changes occur only in the lateral dimension and not in length. This observation strongly suggests that the shape of a living cell, like its volume, is less dependent on a macroscopically thin cell membrane than on the nature, conformation, and orientation of the intracellular proteins. Were it otherwise, the longitudinal dimension of the cell should not be exempt from swelling or shrinkage.

10.2.3. *Cytoplasmic Proteins and their Conformation in the Determination and Control of Cell Shape*

One of the most striking phenomena in the pathophysiology of living cells is seen in the red blood cells of patients suffering from *sickle-cell anemia*. While oxygenation or deoxygenation produces no change in the biconcave-disc shape of normal red blood cells, sickle cells assume a biconcave-disc shape only when in the oxygenated state. When the sickle cell is exposed to pure nitrogen, the biconcave-disc-shaped cell takes on either a curved, elongated sickle shape or a holly-leaf shape. Accompanying the shape change is a loss of cell water (Glader and Nathan 1978) and a fall of osmotic activity (Hargens et al. 1980).

Two kinds of explanations have been offered for the pathological shape change of sickle cells in nitrogen: in one, the shape change reflects a defect in the cell membrane; in the other, it reflects a defect of the cytoplasmic protein(s).

With the long dominance of the membrane theory as background, and its underlying assumption of the cell content as a dilute aqueous solution, workers in the past have frequently attributed the normal biconcave shape of mature human erythrocytes to the properties of the red-cell membrane. In more recent times, special emphasis has been placed on the specific role of the actin and spectrin components of the red-cell membrane (Elgssaeter et al. 1986). Following this line of thinking, some scientists have considered the phenomenon of sickling to be the result of membrane defect. In agreement, it has been observed that oxygenated ghosts made from irreversibly sickled cells remain sickled (Jenson et al. 1969; Lux et al. 1976), and that hemoglobin-free membranes from irreversibly sickled cells also retain a sickled configuration (Lux et al., 1976).³

However, there is also evidence in favor of the theory that cytoplasmic defect is the cause of the pathology of sickling. Thus it is well known that 97% of the cytoplasmic protein of the red blood cell is hemoglobin, and that it is in the hemoglobin from sickle cells that the result of a clear-cut genetic defect has been discovered. A single faulty gene leads to the substitution of a valine residue for a glutamic acid residue on each of the two β -chains of hemoglobin S (Hunt and Ingram 1959). Hemoglobin S has other physico-chemical properties distinctly different from (normal) hemoglobin A (see Murayama 1964). In this regard, an observation of J. W. Harris (1950) is worth noting. A 20% solution of hemoglobin S in an oxygenated state resembles a similar solution of normal hemoglobin A. Neither demonstrate birefringence; both exhibit a low viscosity. Yet, when the hemoglobin S solution is exposed to nitrogen, there is a marked increase of viscosity and the formation of spindle-shaped bodies (tactoids) which in appearance and size resemble intact sickle cells under nitrogen.

The dispute over the seat of the pathophysiology of sickling (membrane vs. cytoplasm) has been resolved in elegant hybridization experiments in which the hemoglobin and "cell membrane"⁴ of normal red blood cells are exchanged respectively with the hemoglobin and "cell membrane" of sickle cells (Clark and Shohet 1976, 1980–81). By removing homozygous normal hemoglobin (AA) from normal red cells and loading the ghosts thus formed with homozygous abnormal hemoglobin SS, hybrid cells of one kind were prepared ($M_{AA} Hb_{SS}$); the converse exchange produced a second kind of hybrid with sickle cell membrane and normal hemoglobin ($M_{SS} Hb_{AA}$).

Now, if it is the cell-membrane abnormality that leads to sickling, exposure to nitrogen should have no effect on the hybrid cells $M_{AA} Hb_{SS}$, but should cause sickling in hybrid cells $M_{SS} Hb_{AA}$. If it is the hemoglobin abnormality that leads to sickling, $M_{AA} Hb_{SS}$ should sickle in nitrogen, $M_{SS} Hb_{AA}$ should not. **Clark and Shohet showed clearly that it is the $M_{AA} Hb_{SS}$ hybrid that sickles; $M_{SS} Hb_{AA}$ does not** (Figure 10.9).

These findings, already confirmed by Sartiano and Hayes (1977), demonstrate that the cell shape is primarily determined, in red cells at least (but more likely in most, if not all, cells), by the major intracellular proteins, their conformation,

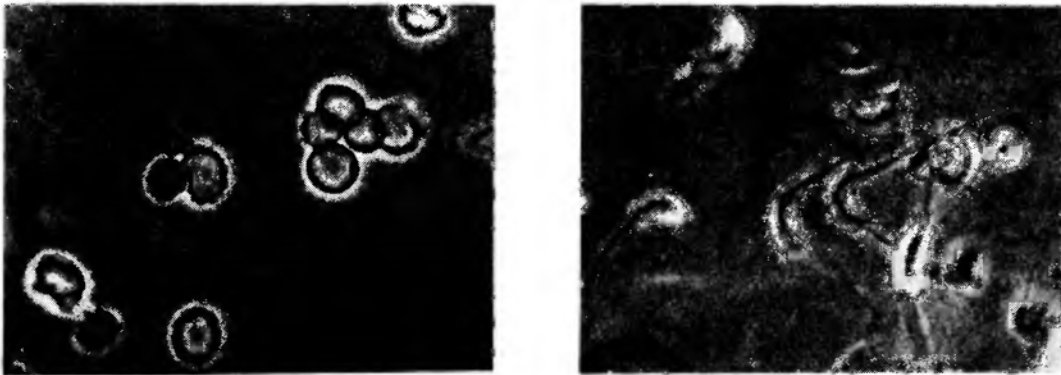


Figure 10.9. Effect of anoxia on the shape of hybrid red cell ghosts, reconstituted from “membranes” of normal red blood cell (containing Hb–A and sickle-cell hemoglobin (Hb–S)). Formation of sickle-shaped and holly-leaf-shaped cells in nitrogen is typical of sickle cells. (Clark and Shohet 1976, by permission of *Blood*)

their orientation, and their intermolecular bonds especially salt linkages (see Section 10.2.5).

Furthermore, the pronounced loss of water and osmotic activity of sickle cells with deoxygenation, mentioned above, takes on additional significance following the recognition of the source of sickling pathology. On the one hand, the large water loss produced during deoxygenation and sickling suggests an exaggerated expression of the water depolarization and loss revealed by the entropy gain during deoxygenation of the normal red cell mentioned earlier (Manwell 1958) (see Section 7.4.3.2.(2)). On the other hand, the loss of osmotic activity and water content (and hence cell size) offers additional evidence in support of the AI hypothesis: **that cytoplasmic proteins and their conformation states determine cell-water content and hence cell volume.**

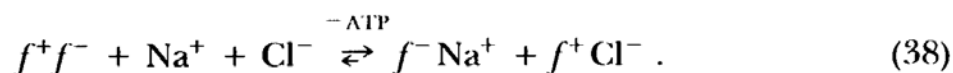
10.2.4. *The Role of ATP in the Control of Cell Volume*

Native proteins, as a rule, adsorb relatively little K^+ or Na^+ , because the β - and γ -carboxyl groups, potentially able to absorb K^+ and Na^+ , prefer fixed cations in the form of α -amino groups, ϵ -amino groups, and guanidyl groups, as discussed in Section 4.2 and studied by Ling and Zhang (1984). However, after the elimination of the positive electric charges on these fixed cationic groups, the β - and γ -carboxyl groups are unmasked and are able to stoichiometrically bind Na^+ or K^+ .

Earlier I discussed, in terms of the AI hypothesis, the key role of ATP in the preferential adsorption of K^+ in living cells (Sections 8.4.2; 8.4.3). Because it is an electron-withdrawing cardinal adsorbent (EWC), adsorption of ATP lowers the c -value of β - and γ -carboxyl groups; preferential K^+ adsorption (over both Na^+ and fixed cations) follows in consequence (Figures 6.9 and 8.14). With depletion of ATP, the β - and γ -carboxyl groups assume a higher c -value; the pref-

erence for Na^+ and/or fixed cations then increases. With total ATP depletion, even Na^+ adsorption is diminished. Most of the β - and γ -carboxyl groups then become locked in salt linkages (Section 6.2.4.). Simultaneously, the backbone NHCO groups also enter into α -helical or β -pleated conformation, releasing bulk-phase water from the state of polarized multilayers.

Working from these theoretical concepts, I have suggested that *the reason injured or poisoned tissues often swell in volume is as a consequence of ATP depletion*, but with at least part of the congruous anions in one form or another preserved (see Section 8.4.3.3. and end of Section 9.2.2.3.2). *The c-value rise in consequence of the loss of this EWC enhances the relative binding affinity of the β - and γ -carboxyl groups for Na^+* (see Figure 6.9). *As a result, 100 mM of Na^+ (Cl^-) present in plasma or a Ringer solution, and normally unable to cause cell swelling due to the low affinity of the fixed anion for Na^+* (equation 37), *can now effectively compete for the β - and γ -carboxyl groups against fixed cations and unravel the volume-restraining salt linkages*. Cell swelling occurs as a result, much as healthy cells expand in a 100 mM KCl solution (equation 36). In summary, depletion of the EWC, ATP increases the c -values of the fixed β - and γ -carboxyl groups (f^-), and drives the following equation to the right:



Swelling occurs with reduction of the restraining force of the salt linkages.

As in the case of cut frog muscle, one would anticipate that the degree of swelling of the ATP-depleted tissues in isotonic Na^+ solution would depend on the nature of both the cations and the anions. Both anticipations have been verified by the different degree of swelling of cold- and anoxia-injured mouse tissues in various isotonic solutions of Na and other salts (Figure 10.10).

Note that in a LiCl solution, the swelling of injured mouse kidneys was even more intense than in a NaCl solution of equal strength, suggesting that a very high c -value, far beyond the c -value range of normal resting cells, had been reached (Figure 6.9). Yet in a Li_2SO_4 solution, swelling was minimal, in agreement with the fact that sulfate is one of the anions least preferred by fixed cations (Figure 6.3). Divalent Mg^{++} is not adsorbed on isolated fixed β - and γ -carboxyl groups of either high or low c -value (see Figure 8.3). That isotonic MgSO_4 , which causes shrinkage rather than swelling of both intact (Ling et al. 1979) and cut muscle (Figure 10.8) should have a similar effect on injured mouse kidneys is to be expected and was observed.

The concept of ATP as a cardinal adsorbent controlling cell volume predicts that *in the presence of the same concentration of NaCl in the environment, the degree of swelling of injured tissues should be a function of the (residual) ATP concentration: the lower the ATP concentration, the greater the swelling*. That this is true is shown in the data of both Ling and Kwon (1983) on mouse brain tissue (Figure 10.11), and of Okamoto and Quastel (1970) on poisoned rat brain slices in Ringer solution containing 128 mM NaCl (Figure 10.12). Okamoto and Quastel also noted that the substitution of Cl^- by SO_4^- suppressed water uptake, in full

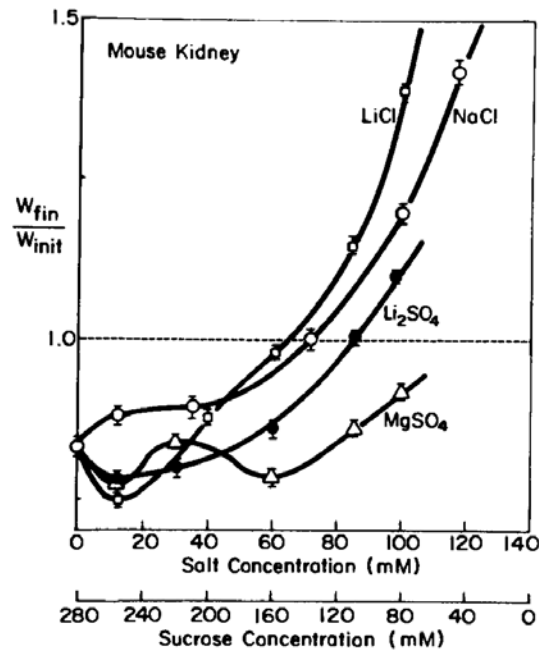


Figure 10.10. Weight changes of isolated mouse kidneys in response to cold (4°C) and anoxia in solutions containing different concentrations of NaCl, LiCl, Li_2SO_4 or $MgSO_4$. Incubation solutions were prepared by mixing in different proportions two stock solutions. One stock solution contained as its main ingredient sucrose; the other stock solution contained as its main ingredient NaCl, LiCl, Li_2SO_4 or $MgSO_4$. Weight changes are expressed as the ratio of final wet tissue weight (W_{fin}) over the initial wet tissue weight (W_{init}). (Ling and Kwon 1983, by permission of Physiological Chemistry Physics and Medical NMR)

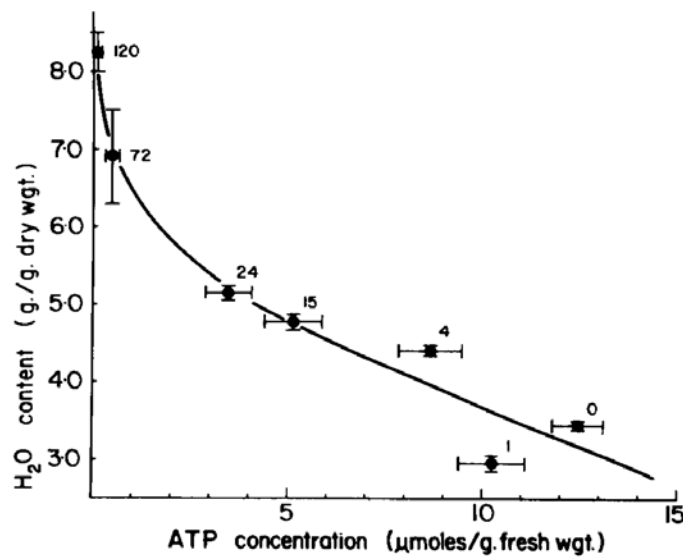


Figure 10.11. The relationship between the water contents of mouse brains and their ATP contents after the isolated half brains were incubated in a cold (4°C) and anoxic solution for various lengths of time (indicated by numbers of hours near each point). Each point represents an average of 3 or 4 determinations. (Ling and Kwon 1983, by permission of Physiological Chemistry Physics and Medical NMR)

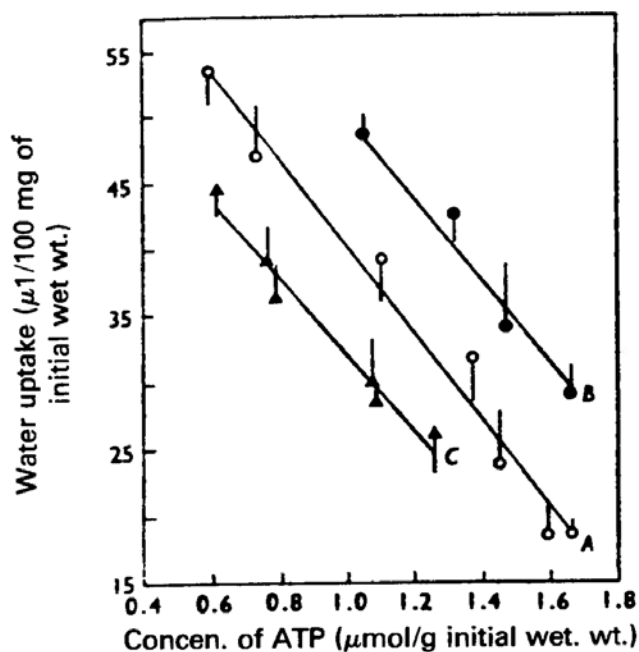


Figure 10.12. Relationship between tissue ATP concentrations and water contents in incubated rat-brain cortex slices. Line A, in the presence of various concentrations of glucose (○); line B, in the presence of 10 mM glucose and various concentrations of L-glutamate (●); line C, in the presence of 10 mM glucose and various concentrations of 2,4-dinitrophenol (▲). (Okamoto and Quastel 1970, by permission of Biochemical Journal)

agreement with both the AI hypothesis just described and the experimental data of Ling and Kwon (1983) shown in Figure 10.10.

10.2.5. *The Role of ATP in the Control of Cell Shape*

By exchanging “membranes” or hemoglobin from red blood cells of normal subjects with those from sickle-cell-anemia patients, Clark and Shohet demonstrated that it was the intracellular protein(s) rather than the cell “membrane” that determine the shape of red blood cells. To which I added that *cytoplasmic proteins may determine cell shape by the salt linkages they form with other similar and different cytoplasmic proteins.*

In earlier discussion of salt linkages in the maintenance of *cell volume*, I assumed that the salt linkages were more or less randomly distributed—which may be true for cells that are spherical. As a result, salt-linkage formation and dissociation affect these cells equally in all dimensions, producing homogeneous expansion or shrinkage.

However, as pointed out in the opening section of this chapter, many cells have shapes quite distinct from spheres. In hypotonic solutions, long and cylindrical muscle cells, for example, swell radially but not longitudinally.

Following this line of thinking, I suggest that the biconcave-disc shape of human red blood cells may reflect an asymmetrical and uneven distribution and orientation of salt linkages. For example, most salt linkages may be oriented in the shorter dimension of the cell (and in an uneven manner). It is the distribution

of these salt linkages that I suggest plays a key role in creating the normal biconcave-disc shape.

Figure 10.13 shows how with progressive decline of ATP concentration in human red blood cells—in response to the metabolic poison, sodium fluoride—the shape of the red cells changed from the normal smooth biconcave disc to crenated flat disc, to crenated spheres and finally to smooth spheres (Nakao et al. 1961).

These changes may arise from the uneven distribution of salt linkages maintaining the cell's short dimension, in combination with the ATP- and NaCl-dependent salt-linkage dissociation described in equation 38.

With the decline of the concentration of ATP—a strong EWC—the electron density or c -value of the carboxyl groups engaged in the salt linkages rises (see Figure 7.9 for a suggested mechanism). As a result, the relative affinity of these carboxyl groups for Na^+ rises—in comparison with that for the fixed cations (see Figures 6.8 and 6.9). The salt linkages maintaining the short dimension of the cell—normally resistant to the high concentration of Na^+ and Cl^- ions present in the surrounding medium—are no longer resistant; as a result, they are broken, as indicated in equation 38. Expansion in the short dimension of the red cell occurs, beginning with those isolated areas containing the fewest salt linkages. A flattening of the disc and crenation are the results. With further fall of ATP concentration, more and more salt linkages are broken by Na^+ and Cl^- until eventually the cell assumes the shape of crenated and then smooth spheres.

The fact that the ATP-dependent shape changes are reversible as convincingly

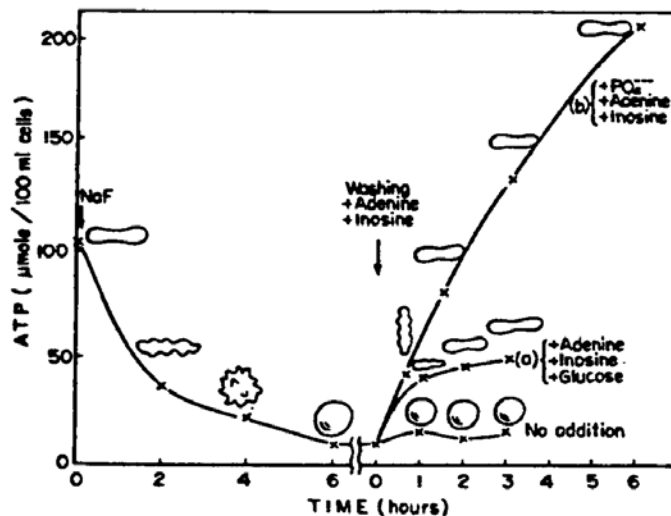


Figure 10.13. Effect of NaF addition (first arrow) and its subsequent removal (second arrow) on the shape of washed human red blood cells and the accompanying changes in their ATP contents. Washed human red blood cells were incubated with NaF at 37°C for 6 hours. After washing out fluoride, reincubation was carried out with addition of inosine, adenine, and glucose (a) and with addition of adenine, inosine, and inorganic phosphate (b). [Nakao et al. 1961, by permission of Journal of Biochemistry (Tokyo)]

shown in Figure 10.13 affirms that the reaction in equation 38 is indeed reversible as represented.

Figure 10.14 reproduced from Saladino et al. (1969) demonstrates the shape- (and size-) change of toad bladder cells following exposure to the antifungal antibiotic, amphotericin B. As the cells deteriorate and (presumably) their ATP content declines, the normally flat cells became thicker and thicker until—like the ATP depleted red blood cells—they too turned into spheres. The suggested mechanism for the conversion of the disc-shaped red blood cells to the final spherical shape can apply here as well.

Besides demonstrating another type of flat cells undergoing asymmetrical swelling in response to ATP depletion, Figure 10.14 offers additional significant data: *swelling of the bladder cells does not occur if the NaCl present in the Ringer solution is replaced by an isosmotic concentration of sucrose.* This finding further confirms equation 38, according to which Na^+ and Cl^- ions are essential for the swelling in consequence of ATP depletion.

The reader may also notice in Figure 10.14 that not only did the poisoned cells in sucrose Ringer solution fail to thicken and swell; in fact, they did just the opposite: they became thinner.

Shrinkage of ATP-depleted mouse kidney (Figure 10.10), liver and spleen in sucrose Ringer solution was also observed (Ling and Kwon, 1983), even though—

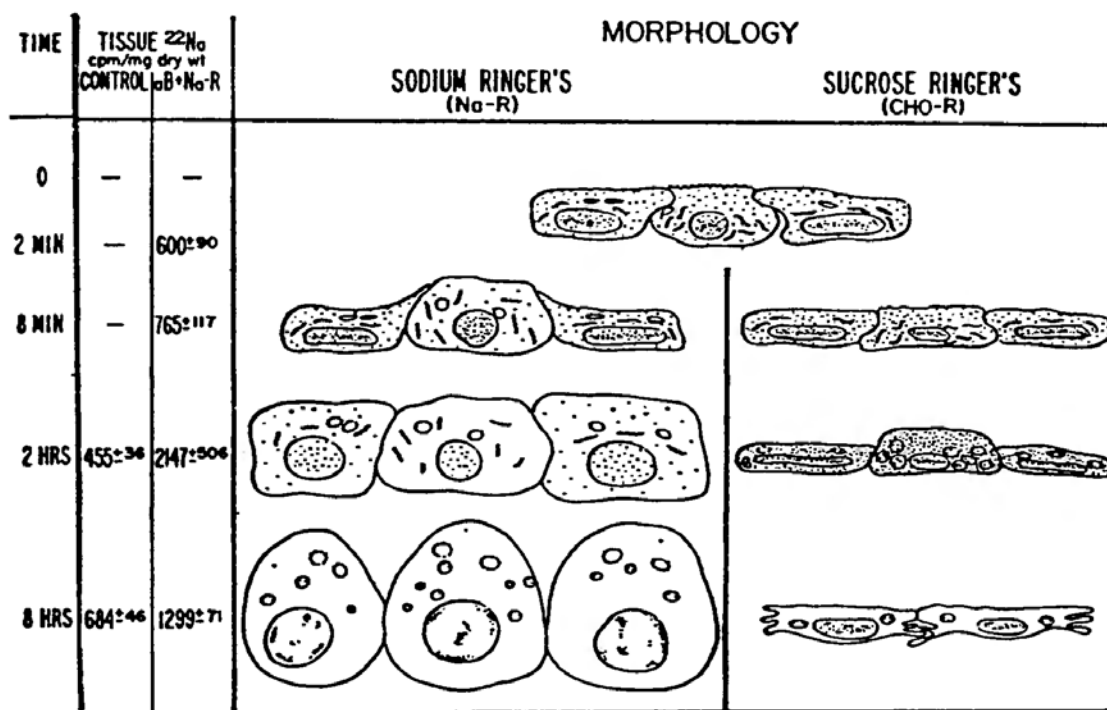


Figure 10.14. Sequential changes with time in morphology of toad bladder cells after addition of amphotericin B (aB) to mucosal sodium Ringer solution (Na-R) or sucrose Ringer solution (CHO-R). Changes in tissue-exchangeable Na^+ content are also shown. Each value is reported as the mean \pm SD of four separate experiments. (Saladino et al. 1969, by permission of American Journal of Pathology)

studying whole tissues rather than single cells—we were not able to tell if with the shrinkage there was shape-change or not. To explain this shrinkage of normal cells in NaCl-free Ringer solution, Ling and Kwon suggested that even in normal cells replete with ATP, a small number of the β - and γ -carboxyl groups with the potential of forming salt linkages and causing shrinkage are kept apart by the Na^+ and Cl^- in the normal plasma or Ringer solution. Removal of Na^+ and Cl^- from the medium brings about the shrinkage seen in Figure 10.10 and Figure 10.14. That removal of NaCl rather than the inclusion of sucrose brought about the observed shrinkage is supported by similar shrinkage observed in cut frog muscle segments suspended in a Ringer solution with all its NaCl replaced by isosmotic MgCl_2 or MgSO_4 as shown in Figure 10.8.

10.3 Summary

The early evidence of living cells behaving like osmometers was faulted when it was shown that the near-perfect osmometer-like behavior of mature plant cells reflects the property of the tonoplast-enclosed large central vacuole, rather than the cytoplasm. Animal cells—without such central vacuoles—do not behave like osmometers. The postulation of “osmotically inactive” water, the suggested loss of semipermeability of a substantial number of cells, and the pump-leak hypothesis have all been shown to be untenable in the light of newer knowledge.

The AI hypothesis concerning cell volume and its regulation rests upon the assumption that it is largely the multilayer polarization of the bulk of cell water (rather than free intracellular K^+) that gives rise to the osmotic activity of the cell. The equilibrium volume of a living cell reflects the balance between this osmotic activity found (only) within the cell and that due to the excess of sucrose or NaCl in the external medium (resulting from the reduced solubility of these solutes in the cell water). Based on this concept, an equation for cell water content (and hence cell volume) was introduced, tested experimentally, and confirmed.

The second part of the AI hypothesis concerning cell volume deals with the mechanism of volume control and the determination of cell shape. Citing the “sickling” phenomenon of red cells from sickle-cell anemia patients, and the experiment of Clark and Shohet (1976) in which they unequivocally established that the seat of the sickling phenomenon is the cytoplasmic proteins, I concluded that it is not the cell membrane, but the cytoplasmic proteins—their intra- and intermolecular structures and bonds—that control cell volume and mold cell shape. The most important intermolecular bonds in the regulation of cell volume are the salt linkages.

Salt linkages formed between different intracellular protein chains and within the same protein chain act as restraining forces. In agreement, it was shown that, at equal strength, salt solutions cause cell swelling or shrinkage, dependent on the affinity of the free cation and free anion for the fixed anions (i.e., β - and γ -carboxyl groups) and fixed cations (i.e., ϵ -amino groups, guanidyl groups) respectively. Free ions of greater affinity for the fixed ions of opposite polarity tend to dissociate more salt linkages and cause more swelling. Free ions of lesser

affinity for the fixed ions dissociate fewer salt linkages and cause less or no swelling.

In the presence of a normal concentration of ATP in healthy resting cells, K^+ (Cl^-) is overwhelmingly more effective than Na^+ (Cl^-) in causing cell swelling; with decreasing concentration of (the EWC) ATP concentration, Na^+ (Cl^-) becomes increasingly more effective in causing cell swelling. Since NaCl is present in high concentration in the cells' normal environment, cell swelling following injury or metabolic interference can be explained in terms of ATP depletion and consequent rise of the c -value of the β - and γ -carboxyl groups. The enhanced affinity for Na^+ then causes cell swelling in much the same way that an isotonic KCl solution causes swelling of normal tissue cells. With total ATP depletion, the cell dies.

Asymmetric and uneven distribution of salt linkages were offered to explain nonspherical cell shapes. In conjunction with the ATP- and NaCl-dependent dissociation of the dimension-maintaining salt linkages, the progressive shape changes of poisoned human red blood cells and of poisoned toad bladder cells—in the presence and absence of NaCl in the cells' surrounding medium—were explained.

NOTES

1. “. . . Da die elastische Spannung des Sarkolemmas und des Perimysiums nur eine geringe ist, beweist diese relativ geringe Gewichtszunahme, dass der Inhalt der Muskelfasern sich nicht wie eine einfache wässrige Lösung verhält, und dass nicht das gesammte in den Muskelfasern enthaltene Wasser sich in Form einer wässrigen Lösung befinden kann, sondern *wenigstens* zum Theil in Gestalt von Quellungswasser enthalten sein muss . . .” (italics mine) (Overton 1902, 273).

2. To the best of my knowledge, no theory has been proposed to explain the sustained shrinkage of living cells in concentrated solutions of *permeant* nonelectrolytes on the basis of the membrane-pump theory. A hypothesis could be derived from an extension of the pump-leak model explaining sustained shrinkage in concentrated Na^+ solutions (Tosteson and Hoffman 1960; Post and Jolly 1975). However, the same arguments cited against the pump-leak model apply here also. In addition, the insensitivity of the observed values to the steric conformation of the solutes makes it virtually impossible to conceive of a way that the same a -values (and q -values) could be obtained for sugars of the same molecular weights but different steric conformations. All told, I believe a pump-leak model for nonelectrolytes is not worthy of any more consideration than the Na pump itself.

3. There is indirect evidence that led me to suspect that the feltlike layer of actin and spectrin seen in EM plates of red cell ghosts is the collapsed remnant of an original cytoskeletal network present throughout the entire cell interior, known in many other cell types (Schliwa 1986). If this suspicion proves correct, the final sickle-shaped structure of the actin-spectrin network of the irreversibly sickled cell (with total ATP depletion) may be the consequence of fixation of a once more-flexible network, while being moulded by the shape determined by the stacking of Hb_{ss} molecules (see Murayama 1964).

4. There is evidence that the red-cell ghosts, even after exhaustive washing, may not be just the cell membranes, but retain remnants of cytoskeletal actin network (see Tilney and Detmar 1975; also endnote 3 of this chapter).

CELLULAR ELECTRICAL POTENTIALS

In moving from the outside to the interior of a resting nerve or muscle cell, one observes, as a rule, an electrical-potential difference of some 50 to 100 millivolts in magnitude across the cell-surface boundary, with the interior of the cell being negative. This steady electrical-potential difference is called the *resting potential*. In response to a suitable stimulus, a transient local depolarization or fall of the resting potential is initiated, which propagates itself along the length of the muscle or nerve. This “negative Schwankung” or “negative variation” is the electrical manifestation of the *nerve or muscle impulse*, and is now known as an *action potential* (du Bois-Reymond 1843, 1848–49).

To understand the molecular mechanism of resting and action potentials is another major task of a cell physiologist. It is the purpose of this chapter to present the different theories of these cellular electric potentials in their historic order, and to compare the predictions of each one with the results of extensive experimental testing carried out in the past century. We shall see that, as with the subjects of the preceding three chapters, the AI hypothesis is the only existing theory that agrees with most, if not all, key experimental observations.

11.1. *Bernstein’s Membrane Theory of Resting and Action Potentials*

From a brief suggestion of Wilhelm Ostwald’s (1890), Julius Bernstein (1902) propounded his *membrane theory of cellular electrical potential*. In this theory, the cellular resting electrical potential was seen as a modified form of ionic diffusion potential. “Garden variety” diffusion potential is a manifestation of unequal velocities of the positively and negatively charged ions of a dissolved electrolyte spreading from a region of high ionic concentration to a region of low ionic concentration. If, in the path of these moving ions, a *membrane* partition is inserted, and this membrane is selectively permeable to one or more ions of one electrical sign but not to the oppositely charged ion(s), the transient diffusion potential will be converted to a lasting one. *This arrested diffusion potential, due to the presence of a selective membrane barrier, is called a membrane potential. The generation of a membrane potential depends critically upon the permeability of the membrane to some ions and impermeability to other oppositely charged ions present in the cell and in its environment.*

Bernstein's membrane theory rests upon the fundamental assumption that the major cation in the cell, K^+ , is able to diffuse freely within the cell and traverse the cell membrane. He also assumed that the cell membrane is impermeable to all anions and to the major cation of the external medium, Na^+ . The resting potential, ψ , across an intact resting cell membrane is described by an equation known as the Nernst equation and referred to earlier as equation 1 in Section 1.3 (Nernst 1889, 1892):

$$\psi = \frac{RT}{F} \ln \frac{[K^+]_{in}}{[K^+]_{ex}}. \quad (1)$$

As was pointed out in the Introduction, the first steps in testing a new theory in cell physiology must be with inanimate models, in order to ensure that the theory has general validity and to forestall a return to vitalistic quagmires. Indeed, attempts have been made to verify the membrane-potential theory on a variety of inanimate model membranes. They include glass membranes, colloidion membranes, oil membranes, and phospholipid-bilayer membranes. The result has been a succession of failures (to be described in Section 11.3.2.1). **In no test has it been established that the measured ion-sensitive potential difference across the model membrane depends on the relative permeability of the ions through the model membranes.**

Although demonstrated in model studies, these failures were apparently known only to a few and soon forgotten; the findings and the serious warning they posed were not given deserved attention. As a result, experimental testing of equation 1 on *living cells* continued as if it were still on solid footing. At the outset, at least, these tests on living cells were successful. Thus the predicted logarithmic relationship between ψ and $[K^+]_{ex}$ has been repeatedly confirmed (MacDonald 1900; Curtis and Cole 1942; Ling and Gerard 1950; see also Ling 1984); so has the predicted rectilinear relationship between ψ and the absolute temperature, T (Ling and Woodbury 1949; Hodgkin and Katz 1949a; Draper and Weidmann 1951). Other studies, however, led to relevant but less reassuring results.

The demonstration that the cell membrane is permeable to Na^+ as well as to K^+ (see Section 1.3) seriously undermined Bernstein's membrane theory. If the membrane is permeable to both K^+ and Na^+ , the resting potential should depend on the ratio of the *sum* of both K^+ and Na^+ concentrations in the cell over the *sum* of both K^+ and Na^+ concentrations outside the cell, rather than on the ratio of the intra- and extracellular K^+ concentrations alone (equation 1). However, these sums are approximately equal; their ratio is close to unity. Since the logarithm of one is zero, no measurable potential difference would be expected, contrary to fact.

Bernstein also evolved a theory of the *action potential* in which he attributed the generation of the action potential to a transient, propagated increase in membrane permeability (Bernstein 1912). The predicted decrease of electrical resistance (or impedance) during an action potential was later verified by Cole

and Curtis (1938–1939). However, Bernstein's theory of action potential also proves to be only partly right. An increase of membrane permeability to all ions (as in Bernstein's theory) can at most reduce the resting potential to zero; yet it had long been known, and Cole and Curtis's studies further confirmed, that the action potential represents more than just an annulment of the inside-negative resting potential. The polarity of the electrical potential at the active region of the nerve or muscle surface actually reverses itself, creating a momentary inside-positive "overshoot" beyond the zero potential baseline (for details see Ling 1984, 71–73).

The shortcomings of Bernstein's membrane theory of resting and action potentials were, of course, a specific instance of the inability of the membrane theory to explain various aspects of cell physiology in terms of membrane permeability and absolute impermeability to specific ions. The most notable response was the adoption of the Na-pump hypothesis (Section 2.1). In parallel with and dependent upon this hypothesis, the *ionic theory* of cellular electrical potential was proposed (Hodgkin 1951). Shortly after that, a profoundly different theory of the cellular resting potential was also introduced, called the *surface-adsorption theory* (a part of the association-induction hypothesis). The ionic theory will be described next, and the surface-adsorption theory will follow.

11.2. *The Ionic Theory of Resting and Action Potential of Hodgkin and Katz*

11.2.1. *Theory*

In the year 1949, Hodgkin and Katz published a very important paper. They showed that during an action potential, the transient increase of membrane permeability is not general (as in Bernstein's membrane theory), but is specific to Na^+ ,¹ and the magnitude of the inside-positive "overshoot" varies with the logarithm of the external concentration of this cation (Hodgkin and Katz 1949). Eliminating Na^+ from the external medium suppresses the action potential. As a result the cell becomes inexcitable, as Overton first reported in 1902. In the same paper, Hodgkin and Katz (1949) presented a quantitative version of their ionic theory in the form of a new equation, known as the Hodgkin-Katz equation or Hodgkin-Katz-Goldman equation (because the derivation used was that given earlier by Goldman (1943) as the constant-field equation):

$$\psi = \frac{RT}{F} \ln \frac{P_K[\text{K}^+]_m + P_{\text{Na}}[\text{Na}^+]_m + P_{\text{Cl}}[\text{Cl}^-]_{\text{ex}}}{P_K[\text{K}^+]_{\text{ex}} + P_{\text{Na}}[\text{Na}^+]_{\text{ex}} + P_{\text{Cl}}[\text{Cl}^-]_m}, \quad (39)$$

where P_K , P_{Na} , and P_{Cl} are the permeability constants of K^+ , Na^+ , and Cl^- respectively. Though in form equation 39 bears resemblance to equation 1, in essence equation 39 is profoundly different from equation 1. Thus, the resting potential is no longer regarded as an *equilibrium phenomenon*, as in Bernstein's membrane theory, but as a *steady state phenomenon*. An equilibrium phenomenon

does not require a steady expenditure of energy. As a steady state phenomenon, the existence of the resting potential now intimately depends upon the continual operation of postulated energy-consuming Na^+ (and other) pumps.

According to Hodgkin and Katz's theory, the divergent sensitivity of the electrical potential ψ to K^+ and Na^+ reflects wide differences in the membrane permeability constants for these ions. At rest, the permeability constants, P_{K} , P_{Na} , and P_{Cl} , are, for some excitable tissues, in the approximate ratios of 1:0.04:0.45. During an action potential, they change to 1:20:0.45. Thus a postulated 500-fold increase of membrane permeability to Na^+ could convert the cell membrane from one behaving like a K^+ -sensitive electrode (i.e., a system that changes its electric potential with the logarithm of the external K^+ concentration as a K^+ -electrode does) to one behaving like a Na^+ -sensitive electrode. In the following section, I will briefly summarize the results of experimental testing.

11.2.2. Results of Experimental Testings

11.2.2.1. Model Systems

The inanimate model of cell membranes that corresponds to the Hodgkin and Katz version of membrane potential is fundamentally the same as the inanimate model sought (unsuccessfully) for Bernstein's theory (see Section 11.3.2.1. below). To the best of my knowledge, Hodgkin, Katz, and coworkers did not carry out further work on inanimate models to verify the membrane theory (and its variant, the ionic theory). However, a great deal of effort has been spent testing the theory on living cells directly.

11.2.2.2. Earlier Testing on Living Cells of Predictions of the Hodgkin-Katz Equation

The results of experimental testing described below (and earlier) refer to those directed at the predicted relationship between the cellular electric potential, ψ , and the variables in equation 39, including the absolute temperature, T , and the concentrations of K^+ , Na^+ , and Cl^- .

Confirmations: A relation between ψ and T has been verified for frog voluntary muscle (Ling and Woodbury 1949), frog cardiac muscle (Draper and Weidemann 1951), squid axon (Hodgkin and Katz 1949a), and (partially) calf and sheep cardiac muscle (Coraboeuf and Weidemann 1954). A relation between ψ and $\ln [\text{K}^+]_{\text{ex}}$ and between ψ and $\ln [\text{Na}^+]_{\text{ex}}$ have been verified *consistently* (Ling 1962, Figure 10.1; 1984, Figure 3.7).

Confirmation and Contradictions: A relation between ψ and $\ln [\text{K}^+]_{\text{in}}$ was (partially) verified by four laboratories (Baker et al. 1961; Adrian 1956; Hagiwara et al. 1964; Sato et al. 1967), but falsified by more (Tobias 1950; Falk and Gerard 1954; Kao 1956; Shaw and Simon 1955; Shaw et al. 1956; Koketsu and Kimura 1960; Tasaki and Takenaka 1963, 1964; Tasaki et al. 1965; Hazlewood and Nichols 1969; Thomas 1972; see Ling 1984, 466 for details).

Contradictions: A relation between ψ and $\ln [\text{Cl}^-]_{\text{ex}}$ could not be demonstrated (Adrian 1956; Hodgkin and Horowicz 1959). Other contradictions will be presented below.

In summary, **the results of world-wide testing over a period of more than 30 years have failed to verify the membrane theory of cellular potential and its variant, the ionic theory, on inanimate models. Only a part of the Hodgkin-Katz equation has been experimentally verified on living cells. This is the part enclosed in the dotted line in the equation shown below; the remaining parts were either refuted or are in doubt:**

$$\psi^+ = \frac{RT}{F} \ln \left[\frac{P_{\text{K}}[\text{K}^+]_{\text{in}} + P_{\text{Na}}[\text{Na}^+]_{\text{in}} + P_{\text{Cl}}[\text{Cl}^-]_{\text{ex}}}{P_{\text{K}}[\text{K}^+]_{\text{ex}} + P_{\text{Na}}[\text{Na}^+]_{\text{ex}} + P_{\text{Cl}}[\text{Cl}^-]_{\text{in}}} \right]. \quad (40)$$

11.2.3. Modifications of Theory

The responses to some of the contradictory findings above led to two new developments: a modification of the Hodgkin-Katz equation and the introduction of the electrogenic-pump theory as a supplemental modification for the generation of resting potential. These developments are described next.

11.2.3.1 Modification of the Hodgkin-Katz Equation:

In response to the failure to demonstrate the relation between ψ and $[\text{Cl}^-]_{\text{ex}}$, Hodgkin (1958) and Katz (1966) modified equation 39 to read

$$\psi = \frac{RT}{F} \ln \left(\frac{P_{\text{K}}[\text{K}^+]_{\text{in}} + P_{\text{Na}}[\text{Na}^+]_{\text{in}}}{P_{\text{K}}[\text{K}^+]_{\text{ex}} + P_{\text{Na}}[\text{Na}^+]_{\text{ex}}} \right), \quad (41)$$

or

$$\psi = \frac{RT}{F} \ln \left(\frac{[\text{K}^+]_{\text{in}} + b[\text{Na}^+]_{\text{in}}}{[\text{K}^+]_{\text{ex}} + b[\text{Na}^+]_{\text{ex}}} \right), \quad (42)$$

where $b = P_{\text{Na}}/P_{\text{K}}$. However, I have expressed the view that it is inappropriate to delete an integral part of a rigorously derived equation (Ling 1978a, 416, 1984, 465). To the best of my knowledge, no attention to or defense against my criticism of the deletion has been published.

11.2.3.2. Introduction of the Electrogenic Pump

Discrepancies were repeatedly observed between the resting potentials measured in a variety of living cells and those calculated on the basis of the measured intracellular K^+ contents of the cells according to equation 39 or 41 (for details, see Ling 1984, 468; Thomas 1972; Koketsu 1971). These and other discrepancies led to the postulation of another membrane pump called an *electrogenic pump*, which differed from the ordinary Na pump, now retroactively referred to as an *electroneutral pump*. Kernan described the new pump in these words: "The elec-

trogenic pumping of ions may be recognized by a change of the membrane potential which cannot be accounted for in terms of the passive ion movement and which has some of the characteristics of a metabolic process . . .” (Kernan 1970, 399). Thomas further explained. “If more sodium is extruded faster than potassium absorbed then the pump would be electrogenic, directly contributing to the membrane potential by generating a current across the cell membrane” (Thomas 1972, 564).

Earlier Mullins and Noda (1963) further modified the already-modified Hodgkin-Katz equation (equation 42):

$$\psi = \frac{RT}{F} \ln \frac{r[K^+]_{in} + b[Na^+]_{in}}{r[K^+]_{ex} + b[Na^+]_{ex}}, \quad (43)$$

where r , the new factor introduced, is the *coupling ratio* of the electrogenic pump, i.e., the number of Na^+ ions pumped out for each K^+ ion pumped in.

Evidence in support of a *dual mechanism* for the cellular resting potential was presented by Gorman and Marmor (1970), from studies of the resting potential of molluscan neurones (Figure 11.1). They observed that at the temperature of the mollusc's natural habitat ($17^\circ C$), the ψ vs. $\ln [K^+]_{ex}$ plot *cannot* be described by the Hodgkin-Katz equation or any of its modifications. However, when the temperature is reduced to $4^\circ C$, the ψ vs. $\ln [K^+]_{ex}$ plot *can* be accurately described by a modified Hodgkin-Katz equation (equation 41 or 42). From these data, the authors concluded that the resting potential of the molluscan neurones has a

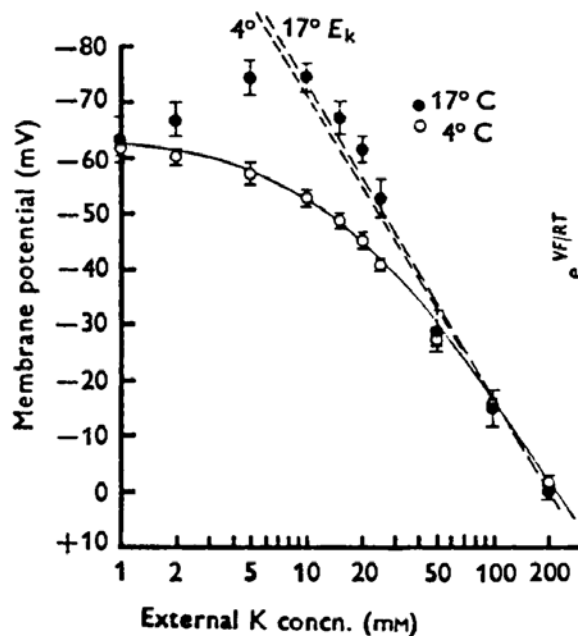


Figure 11.1. Effects of temperature on the relationship between resting potential of molluscan neurones and external K^+ concentration, $[K]_o$. Plot of resting potential vs. $\log [K]_o$ at 4° and $17^\circ C$ as indicated. Each point represents an average from five experiments with standard error of the mean shown. The dashed lines, E_K , have the slopes predicted by the Nernst equation for K electrodes at the temperatures indicated. The smooth curve through the experimental points at $4^\circ C$ was drawn from the constant field equation (equation 39). (Gorman and Marmor 1970, by permission of Journal of Physiology)

dual origin: cooling to 4° C, by suppressing the electrogenic pump, reveals the ionic component (which follows the ionic theory of Hodgkin and Katz); at 17° C, however, the second component, due to the electrogenic pumping of Na⁺, is also operative. Working with Na⁺-loaded rat muscles, Akaïke (1975) made similar observations (Figure 11.2) and accepted Gorman and Marmor's explanations. In addition, Gorman and Marmor as well as Akaïke found that ouabain exercised a similar effect on ψ of both rat muscle and molluscan neurones as cooling did on molluscan neurones: it changed a resting potential from one that is generally higher and does not obey the modified Hodgkin-Katz equation (equation 41) to one that does. Since ouabain, like low temperature, has often been regarded as an inhibitor of the activity of the Na pump, Gorman-Marmor-Akaïke's interpretation of the ouabain effects appeared reasonable. However, *neither the Mullins-Noda equation nor any other modification of the Hodgkin-Katz equation can describe the observed ψ vs. $\ln [K^+]_{ex}$ relationships at ambient temperature and before exposure to ouabain.* Additionally, there are other serious problems facing the ionic theory, with or without the electrogenic-pump addition, as will be made clear.

11.2.4. Decisive Evidence Against Both the Original Ionic Theory and its Modifications

The ionic theory and the early version of the electrogenic-pump addition were introduced in the late forties and early fifties. Both theories rely on the validity

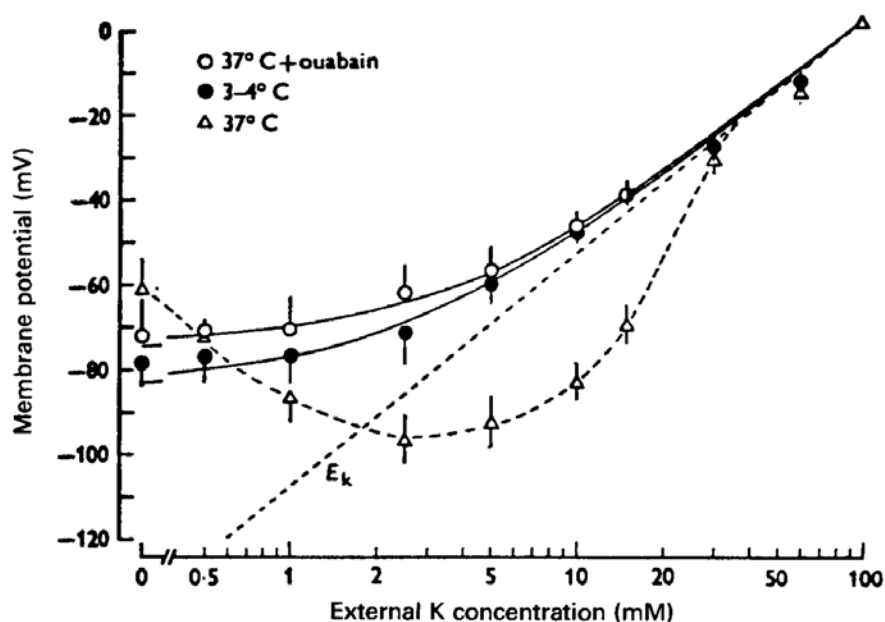


Figure 11.2. Effects of cooling and ouabain on the relationship between the “membrane potential” (quotation mark mine, see end of Section 11.3.2.1) and $\log [K]_o$ of “Na-rich” muscles in rats which had been fed a K-free diet for 40–49 days. Each point is the average value of 55 to 60 muscle fibers in six to eight muscles. Each vertical bar is the \pm S. D. of the mean. Two smooth curves through the experimental points were drawn by the modified constant-field equation (equation 42). Both the cooling and ouabain abolished the “hyper-polarizing” curve (Δ) at 37°C, which was quoted as a reference curve. (Akaïke 1975, by permission of Journal of Physiology)

of the assumption that the living cell has enough energy to operate all of the necessary membrane pumps of which the electroneutral and the electrogenic Na^+ pumps at the plasma membrane are examples. Both theories also rely on the validity of the assumption that the bulk of cell K^+ is free, as in a dilute KCl solution. Are these two assumptions valid? A brief review of the evidence is given below.

(1) *Insufficient Energy*

Decisive evidence that there is not enough energy to operate the (electroneutral) Na pump (alone) has been in the literature for 25 years (Section 2.2.) and has remained unchallenged. Without the Na pump, the cell cannot maintain the ionic concentration gradients on which both the resting potential and the action potential rely.

(2) *Adsorbed State of Cell K^+*

Extensive and essentially unanimous evidence now confirms that the K^+ in living cells exists in an adsorbed state in localized areas of the cells (see Chapter 4 above, and Chapter 8 in Ling 1984). Being adsorbed means that the bulk of cell K^+ is not free to diffuse. Yet in Bernstein's original membrane theory and in the Hodgkin-Katz ionic theory of resting potential, as well as the electrogenic-pump theory, the key underlying assumption on which the validity of the theories relies is the existence of the bulk of cell K^+ in a free state, free to diffuse.

In summary, *insufficient energy* to operate the Na^+ and other pumps and the *adsorbed state of the bulk of cell K^+* have left some major aspects of Bernstein's membrane theory of resting potential, and Hodgkin and Katz's ionic theory of resting potential, as well as their various modifications, in need of fundamental revision. The *surface-adsorption theory* of resting potential, a subsidiary hypothesis of the AI hypothesis, answers this need.

11.3. *The Surface-Adsorption (SA) Theory of Cellular Resting and Action Potential*

11.3.1. *Theory*

In 1955 I briefly suggested that resting potential is a surface-adsorption (SA) potential (Ling 1955). This theory is as valid today as when it was first introduced; only it has grown in depth, as will be made clear below. Like Bernstein's original membrane theory and unlike the ionic theory, the SA theory describes the resting potential as an equilibrium phenomenon, requiring no continual energy expenditure. A familiar example of surface-adsorption potential is the electrical potential of glass electrodes, with which one measures H^+ concentrations—albeit for some time in history the underlying mechanism for the glass electrodes was also widely believed to be a membrane potential. This belief has been proven wrong (see Section 11.3.2.1(1) below).

The basic mechanism of surface-adsorption potential bears resemblance to the mechanism that gives rise to the layer of dust particles surrounding the earth. Though each dust particle is drawn towards the earth by the earth's gravitational field, and most are kept down on earth as a result, a sufficient

number of particles gain enough kinetic energy to escape into, and stay for some time in, the air. At any one time there will be roughly equal numbers of particles settling down and flying off. In the SA theory, cellular resting potential (and the electrostatic attraction of the β - and γ -carboxyl groups on the cell surface) holds K^+ to the adsorption sites. Nevertheless, numbers of K^+ ions leave the cell surface, enter into the surrounding medium, and stay there for varying lengths of time. While one may visualize that the "first" departing positively-charged K^+ ions leaving behind negative charges in the form of unoccupied fixed anionic sites, at any time afterwards, the K^+ ions leaving the cell surface equal those returning to it. In number, the vacant negatively charged fixed sites are numerous enough to create an electrostatic potential difference between the cell and its surrounding medium—negative inside the cell and positive outside the cell. This potential difference is, according to the SA theory, the cell's *resting potential*, and its transient variation, the *action potential*.

On the basis of this concept, an equation² for the resting potential was published in 1959 and in 1960 (Ling 1959; 1960):

$$\psi = \text{Constant} - \frac{RT}{F} \ln \left[\bar{K}_K [K^+]_{\text{ex}} + \bar{K}_{\text{Na}} [\text{Na}^+]_{\text{ex}} \right], \quad (44)$$

where \bar{K}_K and \bar{K}_{Na} are the adsorption constants of K^+ and Na^+ on the surface β - and γ -carboxyl groups respectively. $[K^+]_{\text{ex}}$ and $[\text{Na}^+]_{\text{ex}}$ are, of course, respectively the extracellular K^+ and Na^+ concentration. R , F , and T have the usual meanings.³

Equation 45 represents an improved version of equation 44 (for derivation, see endnote 4):

$$\psi = \text{Constant}_1 - \frac{RT}{F} \ln \left[1 + \bar{K}_K [K^+]_{\text{ex}} + \bar{K}_{\text{Na}} [\text{Na}^+]_{\text{ex}} \right]. \quad (45)$$

Removing the constraint on the number and nature of competing monovalent cations (to Na^+), one obtains a general version of equation 45:

$$\psi = \text{Constant}_1 - \frac{RT}{F} \ln \left[1 + \bar{K}_K [K^+]_{\text{ex}} + \sum_{i=1}^n \bar{K}_i [p_i^+]_{\text{ex}} \right], \quad (46)$$

where $[p_i^+]$ is the concentration of the i th monovalent cation among n types. \bar{K}_i is the adsorption constant of the i th ion on the surface anionic sites in units of $(\text{M})^{-1}$, and

$$\text{Constant}_1 = \frac{RT}{F} \ln [f^-]. \quad (47)$$

The inclusion of vacant sites on the cell surface (represented by the first term, 1, in the parentheses of equation 45 and 46) improves the equation's ability to predict experimentally observed ψ , most noteworthy when the total *external* concentration of external cations or/and their respective adsorption constants is very low.

Like the β - and γ -carboxyl groups at the A bands and Z lines inside the muscle

cells, the β - and γ -carboxyl groups at the surfaces of healthy resting cells are also maintained at a relatively low c -value. As a result, these surface β - and γ -carboxyl groups also strongly prefer K^+ over Na^+ (see Figure 6.9), i.e., $\bar{K}_K \gg \bar{K}_{Na}$. The resting cell surface acts essentially like a K^+ electrode, responsive to changes of external K^+ concentration much more than to changes of external Na^+ concentration.

Equation 44, like the Hodgkin-Katz equation, is capable of explaining not only resting potential but the key component of action potential as well (see equation 55 for a more complete formulation).

The AI hypothesis has also provided a molecular mechanism for the abrupt switching from a K^+ -electrode-like behavior by the resting cell surface to a Na^+ -electrode-like behavior by an active cell surface: an autocoperative transition of the cell surface β - and γ -carboxyl groups from a low c -value state where K^+ is preferred over Na^+ (i.e., $\bar{K}_K \gg \bar{K}_{Na}$) to a high c -value when Na^+ is preferred over K^+ (i.e., $\bar{K}_{Na} > \bar{K}_K$). This subject will be discussed in greater detail in (Section 11.5.2.). In the next section, I discuss the experimental verification of the SA theory on inanimate models. Verification of the SA theory was not the objective most of the investigators initially set out to achieve nor did they recognize it afterwards, either because their work preceded the SA theory's introduction or because of an apparent lack of awareness of the SA theory. Nonetheless, their findings clearly affirmed the SA theory.

11.3.2. Results of Experimental Testing

11.3.2.1. Model Systems (Membrane Potential vs. Surface-Adsorption Potentials)

Over time, at least four types of artificial membranes have been extensively investigated: glass membranes, collodion membranes, neutral lipid membranes, and phospholipid membranes. Results of the investigations of more than 60 years are summarized next.

(1) *Glass Membrane Electrodes*: In the early days of cell physiology, glass electrodes were seen as models of cell membranes. However, Horovitz (1923; Lark-Horovitz 1931) discovered that *the response of glass-electrode potential to a specific ion is not due to the selective permeability of the glass membrane to that particular ion, but to the **specific adsorption** of that ion on the glass surface*. Horovitz's concept was experimentally confirmed by Nicolsky (1937), by Haugaard (1941), and by Ling (1960, 164; 1967). Horovitz's discovery offered strong but indirect evidence against the membrane-potential theory; it also played a key role in my introduction of the SA theory of cellular electrical potentials (Ling 1955, 1959, 1960).

(2) *Oil Potentials*: Ehrensvard and Sillen (1938) showed that the "*oil potentials*" measured across an oil layer (separating two aqueous solutions) are not due to the different permeation rates of positively and negatively charged ions through the oil layer as in membrane potentials, but to **adsorption** of ions at the **two oil surfaces**.

In an even more striking manner, Colacicco (1965) demonstrated the same truth (Figure 11.3). He showed, first, that the mere presence of an oil layer between two KCl solutions of different concentrations did *not* generate a potential

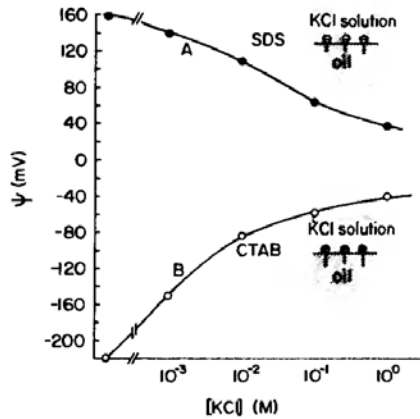


Figure 11.3. Electrical potential difference measured across an oil layer after introduction of sodium dodecyl sulfate (SDS) or cetyltrimethylammonium bromide (CTAB) at one of the oil-solution interfaces as indicated in the insets. An oil layer separates KCl solutions of the same concentration which varied as indicated on the abscissa. (Colacicco 1965, by permission of *Nature*)

difference. He then demonstrated that if one introduces the *anionic detergent*, Na^+ dodecylsulfate (SDS) at one of the oil-water interfaces, the anionic sulfate groups of the detergent molecules with their aliphatic “tails” anchored in the oil surface convert that specific oil surface to one functioning as a K^+ electrode. The electric-potential difference across the oil layer now responds to changes of the K^+ concentration in the solution bathing the oil surface enriched by SDS, but will not respond to changes of the K^+ concentration in the solution bathing the other oil surface, not treated with SDS. On the other hand, if one introduces the *cationic detergent*, cetyltrimethylammonium bromide (CTAB) at one of the oil-water interfaces, the fixed cationic surface thus created functions as a chloride electrode; it then responds to the Cl^- in a similar KCl solution bathing this CTAB-enriched oil surface (see Ling 1984, 472 for further details).

Colacicco’s experiments firmly established that the seat of the generation of an electrical-potential difference is the individual surface of the oil layer, and not the entire oil layer as a selective ion-diffusion barrier. The oil-potential studies of Ehrensvar and Sillen and of Colacicco offer strong evidence, once more, against the membrane theory, and equally strong evidence for the SA theory.

(3) *Collodion Membrane Electrode*: Collodion (i.e., nitrocellulose) membrane was extensively studied in the twenties and thirties by Leonor Michaelis as a model of the cell membrane (Michaelis 1926; Michaelis and Fujita 1925). He believed that it was selective ionic permeability through the membrane that determined ψ . Horovitz’s idea just mentioned was rejected by Michaelis and his coworkers because they believed that collodion or nitrocellulose was electrically *neutral* (Michaelis and Perlzweig 1927). Later investigations by Michaelis’s own students Sollner, Abrams and Carr, however, revealed that *pure, and hence electrically neutral, nitrocellulose membrane* (like Colacicco’s pure oil layer) **does not generate electric potential differences, and that the electric potential sometimes observed depends critically**

on the negatively charged **carboxyl groups** inadvertently present in the impure collodion originally used, or deliberately introduced by oxidizing the collodion membrane surface (Ling 1984, 108; Sollner, et al. 1941, 1941a).

Ling (1960, 1967) further showed that if one coats a Corning 015 soft glass electrode with a thin layer of oxidized collodion, the coated electrode now behaves like a collodion electrode, with sensitivity to K^+ which is not present in simple soft-glass electrodes. When fixed *cationic* ϵ -amino groups carried by polylysine were incorporated onto the collodion-coated glass electrode, the electrode became an *anion* electrode at an acid pH which suppressed the dissociation of the anionic carboxyl groups (Figure 11.4). These findings suggest once more that it is the dissociated carboxyl groups or dissociated ϵ -amino groups at the electrode surface that respectively determine the electrical potential sensitivity to monovalent cations like K^+ and Na^+ , or to monovalent anions like Cl^- .

(4) *Phospholipid Membranes*: Studies of electric potential across phospholipid bilayer membranes led to a conclusion similar to results from the three other types of studies of model membranes just described: *the potential difference across the phospholipid membrane is not a membrane potential; instead, it is the algebraic sum of two surface potentials, one at each phospholipid-water interface*. The surface potential is cation-sensitive when the phospholipid carries net negative charges (e.g., phosphatidic acid, phosphatidyl serine); it is anion-sensitive when the phospholipid carries net positive charges (e.g., lysyl phosphatidyl glycerol); it shows no (or only weak) ion selectivity when the phospholipid carries no net charge [e.g., phosphatidyl choline (Colacicco, 1965); diglycosyldiglyceride (Hopfer et al. 1970; Ohki 1972; MacDonald and Bangham 1972)].

Thus from the investigation of the ion-sensitive electric potentials of all four models of the cell membrane, one finds no evidence whatsoever that any potential originates from differences in ion permeability through the model membrane (see Ling 1984). Instead, across all four types of model membranes, the potential differences observed represent the algebraic sums of two independent surface poten-

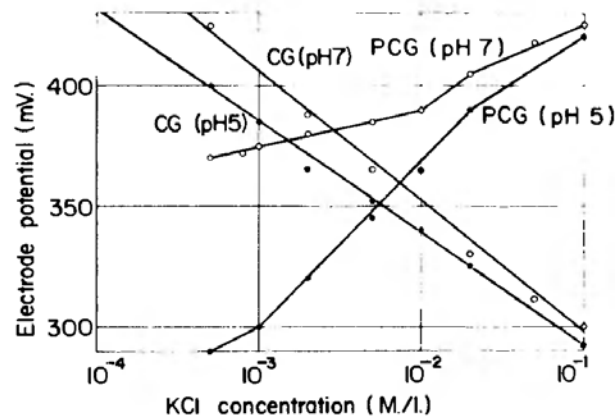


Figure 11.4. Anion and cation sensitivity of a collodion-coated glass electrode (CG) and of a polylysine-treated, collodion-coated glass electrode (PCG) exposed to solutions containing different concentrations of KCl at pH 5 or 7. (Ling 1967, by permission of Marcel Dekker)

tials, each arising from the presence of fixed ions of one polarity or another on one or both surface(s) of the membrane.

When considered as a whole, **the clear and unanimous conclusion of these four sets of studies offer a solid foundation for the surface-adsorption theory of cellular potential as part of the association-induction hypothesis.**

11.3.2.2. *Agreement of the SA Theory with Experimental Evidence from the Studies of Living Cells that Supports the Ionic Theory as well as with Evidence that Contradicts the Ionic Theory*

In form, equation 44 in its entirety is identical to that part of the Hodgkin-Katz equation that had been verified experimentally and encircled by the dotted line of equation 40. This formal identity of the encircled and verified part of equation 40 with equation 44 is of importance. It means that ***all of the relationships between the ψ and the variables in equation 44 based on the surface-adsorption model have already been verified***, including the relationship between ψ and the absolute temperature T ; the relationship between ψ and the logarithm of external K^+ concentration; and the relationship between ψ and the external Na^+ concentrations.

In addition, ***all of the experimental findings that contradict or are incompatible with the ionic theory (with or without the electrogenic pump) are also in harmony with the SA theory:***

- (1) The limited energy resource of the living cell is fully compatible with the surface-adsorption model, because the maintenance of the surface-adsorption potential is a (metastable) equilibrium phenomenon. As such, it requires no continual energy expenditure.
- (2) In the SA theory, it is the presence of surface *fixed anions* that gives rise to the sensitivity of that surface to external monovalent cations (e.g., K^+ and Na^+). On the other hand, the presence of surface *fixed cations* gives rise to the sensitivity to external anions (e.g., Cl^-) (see Section 11.3.2.1.(3)). The indifference of the ψ of living cells like frog muscle to external Cl^- is thus readily explained as due to an absence of fixed cations (e.g., ϵ -amino groups) at normal resting muscle cell surfaces.
- (3) The adsorbed state of the bulk of cell K^+ is also in harmony with the SA theory for two reasons: First, it is similar specific adsorption of K^+ on the surface β - and γ -carboxyl groups that has created the resting potential (see Section 11.3.1). Secondly, the adsorbed state of the bulk phase K^+ , in contradiction to the ionic theory, is irrelevant. **According to the SA theory, ψ depends on adsorbed K^+ on a submicroscopic surface layer of living cells.** No relation is expected between the concentration of bulk-phase K^+ and ψ , and none has been found.

Finally, I want to point out that three of the four sets of experimental evidence cited in favor of the membrane and ionic theory, i.e., confirmation of the predicted relationship between intracellular K^+ concentration and the resting potential cited in Section 11.2.2.2., are fully compatible with the SA theory (for

interested readers, see Ling 1982, 58; 1984, 476). The explanation of Sato and coworkers' findings, hitherto not discussed, is given in endnote 5 of this chapter.

11.3.2.3. *The Key Role of Surface Anionic Sites (β - and γ -Carboxyl Groups) in Creating the Resting Potential*

Although equation 44 (based on the SA theory) and the boxed-in part of equation 40 (based on the ionic theory) look formally alike, they differ profoundly in the meanings of the two sets of coefficients for the external ionic concentrations. In equation 44, the coefficients (\bar{K}_K , \bar{K}_{Na}) are the adsorption constants of K^+ and Na^+ respectively, on the surface β - and γ -carboxyl groups; in equation 40, they are the permeability constants (P_K , P_{Na}).

Cognizant of this fundamental difference, Ludwig Edelmann (1973) designed an experiment to test which assignment is closer to the truth. He chose to study the rates of alkali-metal-ion permeation into guinea pig heart muscle. With the aid of equation 25, he was able to determine both the permeability constants (given as v_K^{max}) and the surface-adsorption constants (e.g., \bar{K}_K). As often observed in other tissues, he found that the permeability constants for K^+ , Rb^+ , and Cs^+ follow the rank order $v_K^{max} > v_{Rb}^{max} > v_{Cs}^{max}$, whereas a different rank order was observed among their adsorption constants, i.e., $\bar{K}_{Rb} > \bar{K}_K > \bar{K}_{Cs}$. By trying each of these two different sets of experimental data in the equation and comparing the theoretically calculated ψ with those experimentally measured, he concluded that ***the resting potential is not related to the permeability constants of the alkali-metal ions through the cell membrane, but is quantitatively dependent upon the surface adsorption constants of these ions on the cell surface anionic sites***, according to an improved equation 44 described in Section 11.3.1. and called equation 46 (Figure 11.5). Having established that adsorption on surface anionic sites determines ψ , we can proceed to find out if these surface anionic sites are in fact β - and γ -carboxyl groups as predicted by the SA theory.

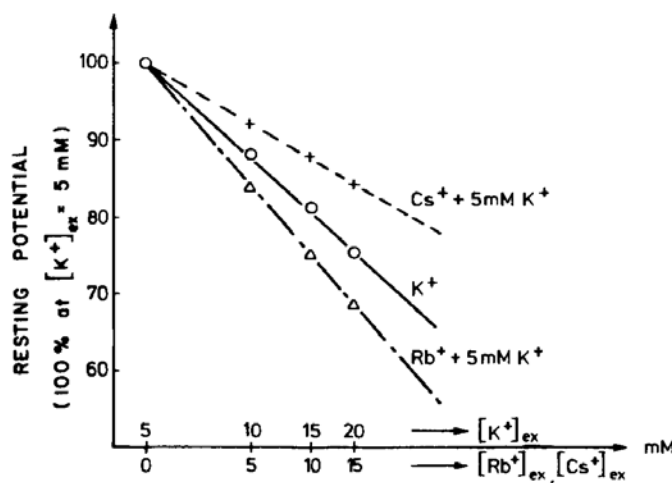


Figure 11.5. Effect of Cs^+ , K^+ , and Rb^+ on the resting potential of guinea pig heart muscle. Points are experimental; dashed lines are theoretical based on the experimentally determined adsorption constants of the 3 ions and equation 46. (Edelmann 1973, by permission of Plenum Publishing Co.)

Figure 9.13 shows that the anionic group mediating K^+ traffic through the resting frog muscle cell surface has a pK_a (4.75) characteristic of β - and γ -carboxyl groups. Edelman demonstrated that it is the specific adsorption constants of the K^+ and other ions on frog muscle surface groups that determine ψ (Figure 11.5). Taken together, these two sets of findings offer indirect evidence that surface β - and γ -carboxyl groups generate ψ (see also Section 9.2.2.1.; see also Engel et al 1960). However, there is other evidence to the same effect.

(1) Rank order of alkali-metal-ion selectivity: Figure 11.6 shows that selectivity of the fixed *carboxyl group* carrying collodion-coated glass electrodes towards the five alkali-metal ions (as revealed by the different depolarizing effects of these alkali-metal ions) follows the rank order: $Rb^+ > K^+$, $Cs^+ > Na^+ > Li^+$. This rank order is similar, for example, to those shown by Ling and Ochsenfeld (1965) for adsorption of the five ions on the surface anionic groups mediating alkali-metal ion entry into frog muscle, and by Edelman for the effect of these ions on the ψ of guinea pig heart muscle (Figure 11.5).

(2) Indifference to alkaline-earth ions: Similarly, the lack of sensitivity of the same carboxyl groups on the surface of collodion-coated glass electrode to alkaline-earth ion, Mg^{++} (Figure 11.7A) parallels a similar lack of sensitivity of the resting potential of frog muscle cells to Mg^{++} (Figure 11.7B)⁶.

(3) Strong preference for H^+ : Last, but not least, is the strikingly high sensitivity to H^+ (say, in comparison with K^+) of the carboxyl groups on the surface of a collodion-coated glass electrode. From the data of Figure 11.6 one estimates that it would require 3.2×10^{-3} M external K^+ to reduce the electrode potential to -100 mV, while it would take only 2.5×10^{-5} M external H^+ to do the same. Therefore the selectivity ratio of carboxyl groups for H^+ over K^+ is $(3.2 \times 10^{-3}) / (2.5 \times 10^{-5}) = 130$.^{7,8}

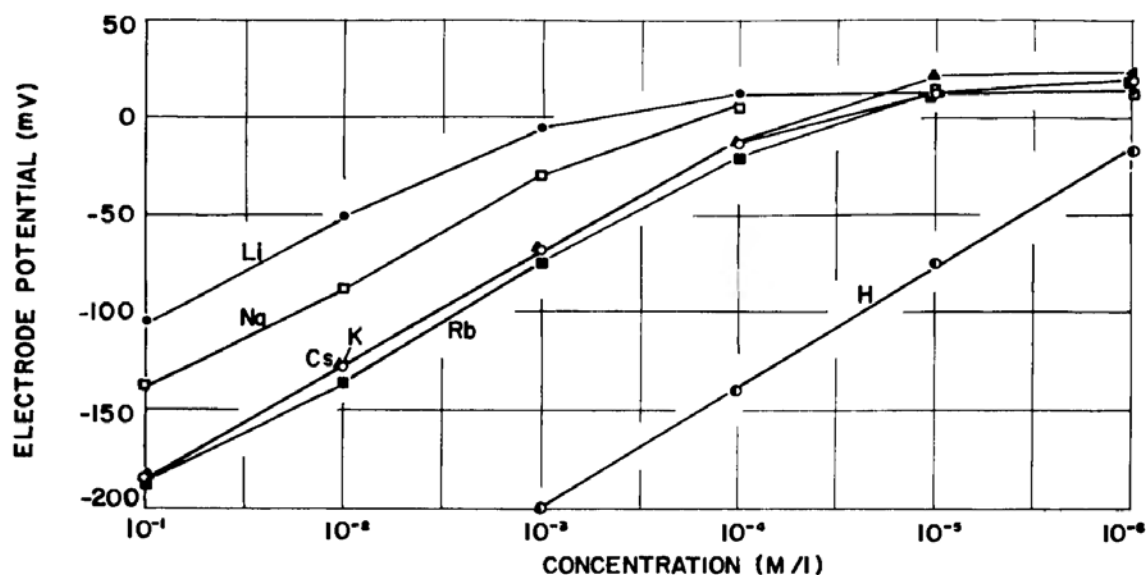


Figure 11.6. Monovalent cation sensitivity of a collodion-coated glass electrode. The potential is considered positive if the outside solution is positive with respect to the collodion-glass phase. (Ling 1967, by permission of Marcel Dekker)

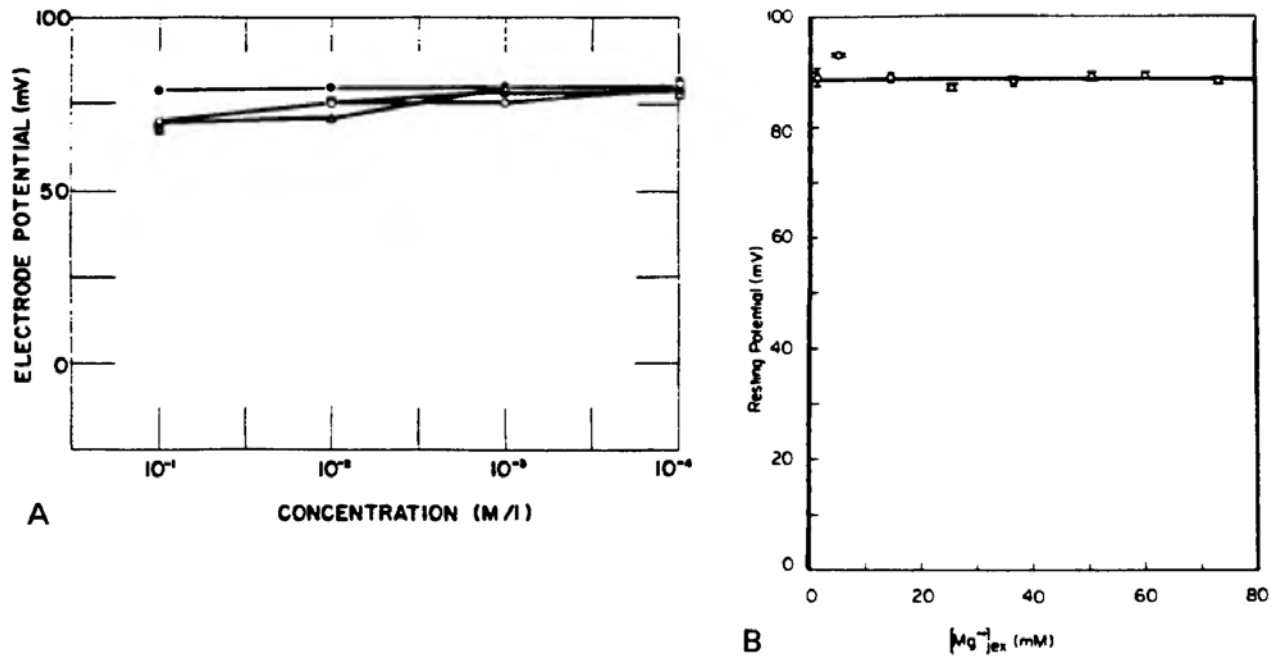


Figure 11.7.

- A. Low divalent cation sensitivity of a collodion-coated glass electrode that has been oxidized for 10 min. The abscissa gives the concentration of the chloride salt of the ion indicated. Note in particular the insensitivity to Mg²⁺. \bullet , Mg²⁺; \circ , Ba²⁺; Δ , Ca²⁺; \blacksquare , Sr²⁺. (Ling 1967, by permission of Marcel Dekker)
- B. The effect of external Mg²⁺ concentration upon resting potential of isolated frog sartorius muscles. The muscles were exposed to Ringer's solution with varying concentrations of Mg²⁺ for 18 hours at 4°C followed by warming to 25°C before measurements of resting potential were made. The 4°C incubation permitted Mg²⁺ to fully equilibrate between cell and external medium. (Ling et al. 1983, by permission of Physiological Chemistry and Physics and Medical NMR)

This high preference of H⁺ over K⁺ is in harmony with the known high polarizability of carboxyl groups (see endnote 8 of Chapter 6) and the theoretical higher preference for H⁺ (over K⁺ and other ions) computed on the basis of such a higher polarizability (Figure 6.8).

This high preference for H⁺ over K⁺ is specific to anionic groups with high polarizability like the β - and γ -carboxyl groups; sulfonate groups, for example, do the opposite, preferring K⁺ over H⁺ (Figure 6.10). If the anionic groups generating the cellular resting potential are indeed β - and γ -carboxyl groups, as the AI hypothesis contends, then the resting potential should demonstrate a similar high preference for H⁺ over K⁺.

Although the sensitivity of the resting potential of frog muscle to K⁺ is accurately known (Ling and Gerard 1950), we have only fragmentary data on the sensitivity of frog muscle resting potential to H⁺. Nonetheless, an estimate can be made from the data available. Ling and Gerard (1949, 389–390) showed that the resting potential was fully normal at a pH of 5, but became totally depolarized at the pH of 3. Based on these observations, I estimate that the external H⁺ concentration required to reduce the resting potential to one half of its normal

value is about 10^{-4} M, (equivalent to a pH of 4.0), adding further evidence that β - and γ -carboxyl groups at the cell surface generate the resting potential, (see endnote 8 of Chapter 4); the concentration of external K^+ required to do the same is 1.7×10^{-2} M. Therefore, *the surface anionic groups of frog muscle cells prefer H^+ over K^+ by a factor equal to $(1.7 \times 10^{-2})/(10^{-4}) = 170$. Considering the very limited data on which the estimate is based, it is notable that a figure of 170 is remarkably close to that of 130 for the (clearly identified) carboxyl groups on the surface of the collodion-coated glass electrode. This figure is also remarkably close to the H^+ over K^+ preference of the frog muscle surface anionic groups mediating K^+ entry, i.e., 140 (endnote 6 of Chapter 9),⁹ further strengthening the theory that **similar β - and γ -carboxyl groups on the muscle cell surface that mediate K^+ traffic also give rise to the resting potential.***

11.4 Control of the Resting Potential According to the SA Theory

According to the AI hypothesis the control of the resting potential, like the control of solute accumulation (Section 8.3), of ion permeability (Section 9.2.2.), and of cell volume and shape (Section 10.2.4; 10.2.5) follows the same basic mechanism introduced in Section 7.3, involving the control of transition between discrete autocoperative states.

11.4.1. Theory

In presenting the original equation (equation 44) for cellular electrical potential, I pointed out that the equation can explain *resting potential* as well as *action potential*. Following a transient and reversible cooperative transition, the c -value of the cell surface β - and γ -carboxyl groups switches abruptly and in an all-or-none autocoperative manner from a low c -value, K^+ -preferring state to a high c -value, Na^+ -preferring state. However, neither the original equation 44, nor its modified version, equation 45, incorporates *cooperative interaction* in their derivation. To remedy this deficiency, I introduced, in 1979 (Ling 1979b), an improved version of equation 44, in which nearest-neighbor interaction among surface fixed ionic groups is taken into consideration:

$$\psi = \text{constant} + \frac{RT}{F} \ln \frac{1}{[K^+]_{\text{ex}}} \left[1 + \frac{\xi^s - 1}{\sqrt{(\xi^s - 1)^2 + 4\xi^s \exp(\gamma/RT)}} \right], \quad (48)$$

where

$$\xi^s = \frac{[K^+]_{\text{ex}}}{[Na^+]_{\text{ex}}} \cdot K_{Na \rightarrow K}^{00(s)}, \quad (49)$$

and ξ^s , $K_{Na \rightarrow K}^{00(s)}$, and $-\gamma/2$ have the same meanings defined earlier (Section 7.1.), except that they refer only to the surface fixed ionic sites, rather than bulk-phase sites (as shown in equation 14). (For theoretical plots of equation 48, see Ling 1984, 478 and 482.)

Equation 48 can also be written in the following more explicit form:

$$\psi = \frac{RT}{F} \ln [f^-] + \frac{RT}{F} \ln \frac{1}{2[K^+]_{\text{ex}} \bar{K}_K} \left[1 + \frac{\xi^s - 1}{\sqrt{(\xi^s - 1)^2 + 4\xi \exp(\gamma^s/RT)}} \right], \quad (50)$$

where \bar{K}_K , as discussed before, is the adsorption constant of K^+ on the surface anionic sites. In the special case when the nearest-neighbor interaction energy is zero, equation 50 reduces to

$$\psi = \frac{RT}{F} \ln [f^-] + \frac{RT}{F} \ln \left[\bar{K}_K [K^+]_{\text{ex}} + \bar{K}_{\text{Na}} [Na^+]_{\text{ex}} \right], \quad (51)$$

which is in essence equation 45, minus vacant sites represented by the term 1 in the parentheses of equation 45. The loss of the vacant site term follows naturally from the original assumption used in the derivation of the Yang-Ling isotherm: all sites are occupied by either the i th (e.g., K^+) or the j th solute (e.g., Na^+); vacant sites are considered negligible and ignored.

The fundamental difference between the old equation of cell potentials (equation 44) and the new ones (equation 48 or 50) is the presence of the nearest-neighbor interaction energy ($-\gamma/2$). The introduction of $-\gamma/2$ opens the door to coherent behavior and control by cardinal adsorbents.

The original intention of introducing the concept of cooperativity and control was to explain the all-or-none transition of the K^+ -sensitive resting potential to the Na^+ -sensitive action potential. It soon became obvious, however, that the resting potential/action potential transition is only a specific example of cooperative control in cell function in general. **Thus the presence of positive nearest-neighbor interaction also offers explanations for a wide spectrum of experimental data demonstrating the regulation and control of the resting potential by drugs and hormones.** Some of these agents act as electron-donating cardinal adsorbents (EDC), others act as electron-withdrawing cardinal adsorbents (EWC). Examples will be described next.

11.4.2. *Results of Experimental Testing of Theory and Other Related Observations*

11.4.2.1. *Control of Resting Potential by Ouabain and Adrenalin*

Neither the data of Gorman and Marmor (1970) on the resting potential of molluscan neurones at 17° C, nor Akaike's data (1975) on the resting potential of Na^+ -loaded rat muscle (before exposure to ouabain), could be quantitatively explained by the ionic theory or its modifications (Section 11.2.3.). Nor could these data be explained by the original surface-adsorption theory shown as equation 44. The introduction of equations 48 and 50 with nearest-neighbor interaction energy changed the picture.

In Figure 11.8, I replotted the data points of Akaike (1975), presented in original form in Figure 11.2. These data show the dependence of the resting

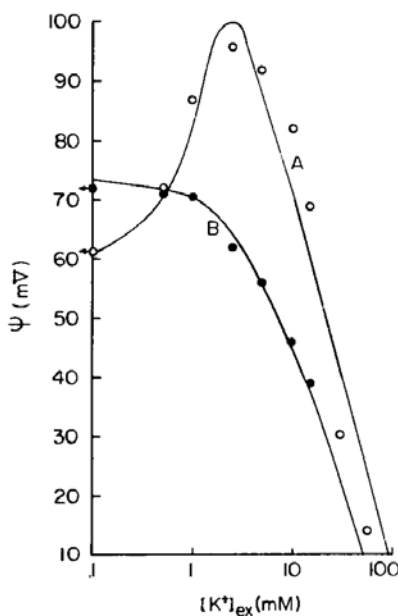


Figure 11.8. Effect of ouabain (10^{-4} M) on the resting potential of rat soleus muscles. A, untreated Na^+ -loaded soleus muscle and B, Na^+ -loaded muscles exposed to ouabain (10^{-4} M). (Experimental data of Akaike (1975), see Figure 11.2). Na^+ -loaded muscles, isolated from rats fed on a low- K^+ diet for 40 to 49 days, were exposed to solutions containing different concentrations of K^+ for 1.5 min or longer. Lines are theoretically calculated according to equation 48 and $-\gamma/2 = 0.67$ Kcal/mole ($\theta = 0.1$), $K_{\text{Na}^+ \rightarrow \text{K}^+}^{\text{eq}} = 96.3$, constant₁ = 116 mV in A, and $-\gamma/2 = 0$ Kcal/mole ($\theta = 1$), $K_{\text{Na}^+ \rightarrow \text{K}^+}^{\text{eq}} = 35$, constant = 76.4 mV in B (Ling, Baxter and Leitmann 1984a, by permission of Physiological Chemistry Physics and Medical NMR)

potential on the external K^+ concentration in the absence (empty circles) and presence (solid circles) of ouabain (10^{-4} M). Here in Figure 11.8, going through or near most of the data points, are theoretical curves calculated according to equation 48. Unlike the modified Hodgkin-Katz equation, which can only fit the ψ data of the ouabain-treated cells, **equation 48 fits the data both before and after ouabain treatment**. The presence of the hump at $[\text{K}^+]_{\text{ex}} = 1$ mM in curve A of Figure 11.8 marks the autocoperative transition of the surface β - and γ -carboxyl groups from a state in which K^+ is highly preferred over Na^+ to a state in which the preference of K^+ over Na^+ is reduced. The $-\gamma/2$ used in the calculation of curve A is $+0.67$ Kcal/mole, indicating autocoperativity. After ouabain treatment, $K_{\text{Na}^+ \rightarrow \text{K}^+}^{\text{eq}}$ dropped from 96.3 to 35, and $-\gamma/2$ dropped to zero. It is this annulment of $-\gamma/2$ that makes the ψ vs. $\ln [\text{K}^+]_{\text{ex}}$ curve fit equation 41 (and equation 42). Along with these changes, there was also a decline in the density of the surface free β - and γ -carboxyl groups (which give rise to the resting potential) presumably due to salt-linkage formation accompanying the ouabain-induced c -value rise (see equations 47, 50 and 51).

It should be noted that ouabain reduces $-\gamma/2$ to zero probably only at the high concentration used by Akaike: 10^{-4} M. A very modest reduction of $-\gamma/2$ occurred in the bulk phase K^+/Na^+ distribution in frog muscle in response to a much lower, though still effective, ouabain concentration (3.27×10^{-7} M).

These data and their new interpretation are in harmony with the view that *ouabain is an electron-donating cardinal adsorbent, or EDC, a conclusion we reached earlier from ouabain-induced changes in the equilibrium distribution of the five alkali-metal ions in frog muscle* (Section 8.3.2(3)), *and in the ouabain-induced changes in Cs^+ permeation into frog muscle and ovarian eggs in the presence of competing Li^+ , Na^+ , K^+ , and Rb^+* (Section 9.2.2.3). While some drugs like ouabain, acting as EDCs, increase the c -value of β - and γ -carboxyl groups, others have just the opposite effect.

Unlike ouabain, which causes *depolarization*, adrenaline produces a *hyperpolarization* of frog muscle cells (Figure 11.9). That is, in response to adrenaline, the inside negative resting potential becomes larger and the cell surface more strongly polarized. This observation suggests that *adrenaline is an EWC, which withdraws electrons from the cell surface β - and γ -carboxyl groups. The results are a decrease of the groups' c -value, an increase of $\text{K}_{\text{Na}^+ \rightarrow \text{K}}^{00(s)}$ from 40.0 to 66.7, no change of $-\gamma^s/2$, and a modest increase of the density of the surface free β - and γ -carboxyl groups, presumably due to dissociation of salt linkages accompanying the c -value decrease induced by adrenaline.*

Having demonstrated that the new equation 48 can describe resting potential before and after exposure to an EDC (ouabain), as well as before and after exposure to an EWC (adrenaline), let us now turn our attention to the effect of temperature change on resting potential, which we discussed earlier under Section 11.2.3.2.

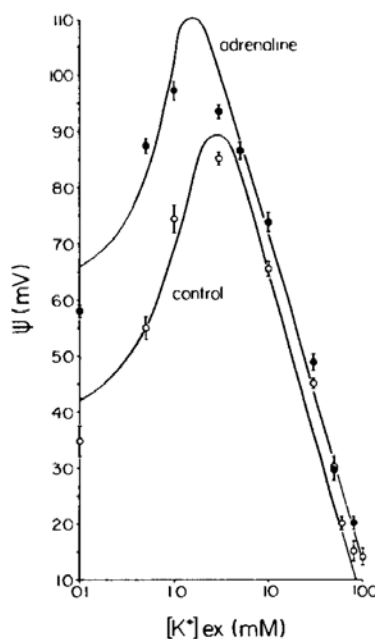


Figure 11.9. Resting potentials of frog sartorius muscles exposed to adrenaline (2.73×10^{-5} M) (25°C) and their controls. Solid lines were theoretical calculated according to equation 48. For the adrenaline-treated muscle, $-\gamma^s/2$ used is 0.75 Kcal/mole ($\theta = 0.0736$), $\text{K}_{\text{Na}^+ \rightarrow \text{K}}^{00(s)} = 40$, and constant = 105 mV. (Ling, Baxter, and Leitmann 1984a, by permission of Physiological Chemistry Physics and Medical NMR)

11.4.2.2. Control of Resting Potential by Temperature

To initiate a discussion of the effect of temperature on resting potential, I return to the subject of bulk-phase accumulation of K^+ and Na^+ in mammalian tissues. The data of Reisin and Gulati (1973) in Figure 11.10 show the effect of temperature changes on K^+ distribution in guinea pig smooth muscle, taenia coli. Comparing these data with Figure 8.8 in Section 8.3.1, one notices that cooling produces the same effect on K^+/Na^+ distribution as Ca^{++} deprivation. Both decrease $K_{Na \rightarrow K}^{00}$ and $-\gamma/2$. The quantitative parameters underlying these changes are shown in Table 11.1. Note that, like high concentrations of ouabain, very low temperatures also reduce $-\gamma/2$ to zero (i.e. $n = 1$). What we witness here is the *phenomenon of cooperative temperature transition¹⁰ in bulk phase cytoplasmic adsorption of K^+ and Na^+ . Apparently a similar temperature transition also occurs among the β - and γ -carboxyl groups on the cell surface of molluscan neurones during cooling* (Gorman and Marmor 1970).

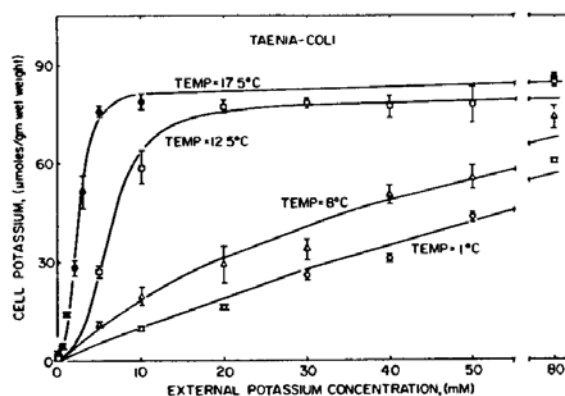


Figure 11.10. Effect of temperature on cell K^+ content of guinea pig taenia coli at various external K^+ concentrations. Solid line calculated according to equation 14. The term representing free intracellular K^+ (i.e., $\alpha q_K [K^+]_{c_i}$) was very small and ignored. (Reisin and Gulati 1973, by permission Annals of New York Academy of Sciences)

Table 11.1. Effect of Temperature on the Accumulation of Potassium and Sodium in *Taenia Coli*—Parameters of the Adsorption Isotherms (Reisin and Gulati 1973, by permission of Annals of New York Academy of Science.)

Temperature ($^{\circ}C$)	F_T^a ($\mu\text{mole/g}$)	$K_{Na \rightarrow K}^{00}$	n^b
36.	85	135	3
17.5	85	58.9	3
12.5	80	22.8	3
8	92	4	1.0
1	90	1.8	1.0

^a F_T is the total concentration of fixed anionic sites adsorbing K^+ .

^b n , the Hill coefficient, is equal to $\exp(-\gamma/2RT)$ (see end of Section 7.1).

The experimental points from Gorman and Marmor's data (1970) were presented in original form as Figure 11.1 (Section 11.2.3.2.). They are presented here once more in Figure 11.11. In contrast to Figure 11.1, where only one set of data points can be fitted by the theoretical constant-field equation (equation 42) while the other set of data was not explained, here both solid lines going through or near the data points fit the theoretical calculations from equation 48. The effect of cooling from 17°C to 4°C, like that on the K^+/Na^+ distribution in guinea pig taenis coli shown in Figure 11.10 and Table 11.1, lowered $K_{Na \rightarrow K}^{00(0)}$ (from 74 to 37.6) and $-\gamma/2$ (from 0.45 Kcal/mole to 0 Kcal/mole). There was also a decrease in the density of surface anionic sites at the lower temperature.

Concluding Sections 11.4.2.1 and 11.4.2.2, one may state that *the SA theory of cellular resting potential with cooperative interaction energy can explain the key relevant data in support of, as well as against, the ionic theory of resting potential and its various modifications.*

11.4.2.3. Control of Resting Potential by Creatine Phosphate (CrP) and ATP

In theory, the capability of ATP and CrP in maintaining (i) selective accumulation of K^+ in the bulk-phase cytoplasm (Section 8.4.3.1.), (ii) a fast rate of

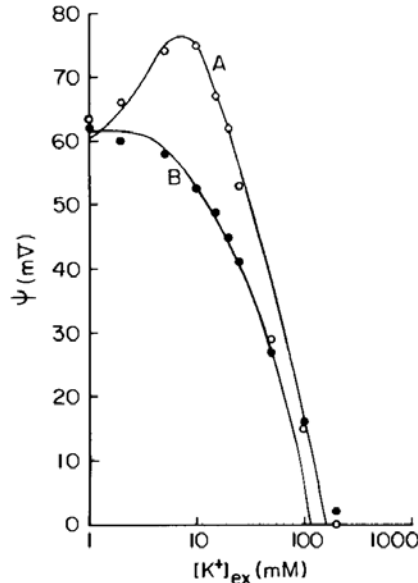


Figure 11.11. Effect of temperature on the resting potential of molluscan neurones at varying external K^+ concentrations. Each point represents the average of 5 experiments. Experimental data points from Gorman and Marmor (1970) reproduced above in Figure 11.1. Standard error of the means, usually less than 5 mV, are not represented. Empty circles (17°C); solid circles (3–4°C). Solid lines going through or near the data points are theoretical according to equation 48: Curve A calculated with $K_{Na \rightarrow K}^{00} = 64$, $-\gamma/2 = 0.45$ Kcal/mole ($\theta = 0.213$) and constant = 93.2 mV; Curve B with $K_{Na \rightarrow K}^{00} = 37.6$, $-\gamma/2 = 0$ Kcal/mole ($\theta = 1$) and constant = 66.4 mV (Ling, Baxter & Leitmann 1984, by permission of Physiological Chemistry Physics and Medical NMR)

Na^+ efflux (Section 9.2.2.3.2.(2)), as well as (iii) the resting potential, can all be traced to the ability of ATP and CrP in keeping the β - and γ -carboxyl groups in an unmasked, low c -value, K^+ -preferring state (Figure 8.14). Testing the predicted quantitative relationship between cell K^+ and cell ATP (and CrP) in the bulk-phase cytoplasm is relatively easy. Large quantities of pure cytoplasm are readily available and a high degree of uniformity pervades in the properties and behaviors of the protein-ion-water systems in the cytoplasm (Sections 8.1 and 8.2). As a result, quantitative data were within reach, and obtained (Figures 8.15 to 8.21).

In contrast, the β - and γ -carboxyl groups at the cell surfaces which determine K^+ and Na^+ flux rates and the magnitude of the resting potential are much smaller in number and proportionately difficult to isolate from the vastly more abundant cytoplasmic carboxyl groups. Here *direct* quantitative confirmation of the predicted relationships between say, ATP and K^+ , like those demonstrated for the bulk-phase cytoplasm, is difficult. However, *indirect* methods, like the injection of ATP and ArP into isolated squid axons, offer a promising alternative to a more direct approach (Figures 9.16; 9.17).

There is another approach to overcoming the difficulty posed by the small number of surface carboxyl groups, i.e., by making certain simplifying assumptions to bridge that which can be determined and that which cannot. Thus, if we assume that there is a state of equilibrium between ATP and CrP at the submicroscopic cell surface and their counterparts in the bulk-phase cytoplasm, then the concentration of ATP and CrP needed to maintain a certain number of carboxyl groups in the K^+ -preferring, low- c -value state at any one time after certain treatment would be similar throughout the entire cell. One can then indirectly assess the concentration of ATP and of CrP involved in the control of the β - and γ -carboxyl groups at the microscopic cell surface by assessing the ATP and CrP concentration of the similarly treated whole cells.

Clearly if the assumption is wrong, one would not find any reproducible positive correlation between K^+ (and Na^+) adsorption on the cell surface (and hence the magnitude of the resting potential, see equations 44 and 48) and the concentration of ATP and CrP of whole cells. On the other hand, if good correlation can be demonstrated, this success can be taken as indication that both the bridging assumption and the predicted relationship may be correct. It is with this approach that the following conclusions were derived:

(1) Anoxia: Figure 8.20 demonstrates that exposure of frog muscles to pure nitrogen produced no significant change in the concentration of ATP, but a marked drop in the concentration of CrP from 29 $\mu\text{moles/g}$. fresh tissue to a new steady level of 11 $\mu\text{mole/g}$. Figure 11.12 shows that in response to pure nitrogen, there is a drop of the resting potential to a new and lower steady level (Ling and Gerard 1949a). The close parallelism between the data of Figure 8.20 and those of Figure 11.12 is in harmony with the theory that CrP functions as a congruous anion facilitating K^+ adsorption on the cell surface proteins (just as it does in bulk-phase cytoplasm). By adsorbing onto fixed cations, the congruous anion CrP liberates β - and γ -carboxyl groups for the adsorption of K^+ .

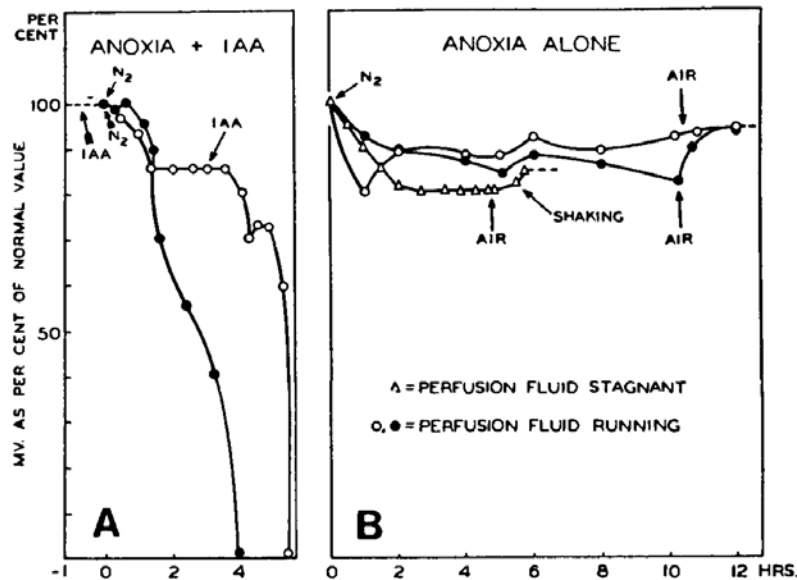


Figure 11.12. Effect of anoxia alone (B) and with IAA (A) on the resting potential of frog sartorius muscle. Resting potential expressed as percentage of initial value measured (before treatment began) on the same muscles. (Ling and Gerard 1949, by permission of Journal of Cellular and Comparative Physiology)

The selective adsorption of K^+ , in turn, leads to the creation of the resting potential.

(2) Tetanic stimulation: A rapid burst of electrical stimuli (tetanization)—directly applied to frog sartorius muscle, or indirectly applied to the sciatic nerve innervating the muscle—caused a rapid drop of the resting potential followed by recovery apparently in two stages (Figure 11.13). Long before these observations were made and reported (Ling and Gerard 1949a), it had been known that tetanization of frog muscle led to the loss of CrP (but not of ATP), followed by recovery of the lost CrP in two stages (Meyerhof and Schultz 1931; Goroditsky 1928; von Muralt 1934). This close parallelism in the change of the resting potential on the one hand, and the change in the concentration of CrP on the other hand, again affirms the predicted relationship between CrP as a congruous anion at the cell surface and the resting potential.

(3) Intermittent stimulation of IAA-poisoned muscle: Sacks showed that if iodoacetate (IAA)-poisoned frog muscles were stimulated by short bursts of electric stimuli, their CrP content fell, in step with each burst. The ATP level, on the other hand, remained largely unchanged until nearly all the CrP was hydrolyzed and the muscle had gone into full rigor (Sacks 1939).

Figure 11.14 diagrammatically illustrates the change of the resting potential of IAA-poisoned frog muscle in response to one prolonged burst of stimuli (left) and in response to intermittent short bursts of stimuli (right) (Ling 1952). For convenience of designation, Ling and Gerard (1949a) referred to the part of the resting potential that could be removed by a prolonged burst of stimuli as A potential; the remaining part as the B potential. Figure 11.15 shows a plot of

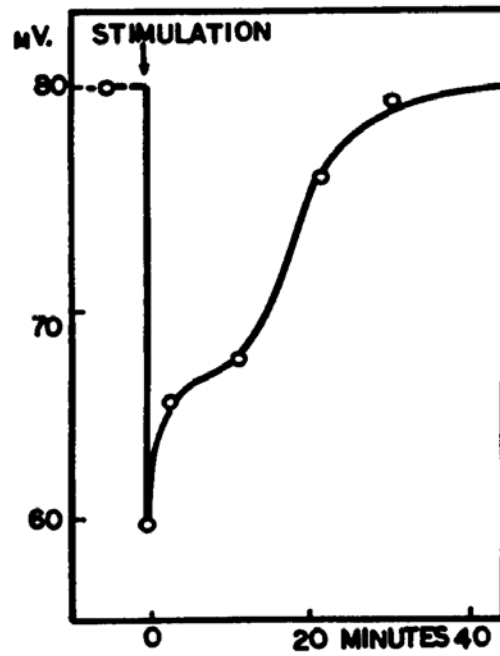


Figure 11.13. The rapid drop and slower recovery of the resting potential of a frog sartorius muscle following a burst of electrical stimulation (tetanization) applied directly to the muscle. (Ling and Gerard 1949a, by permission of Journal of Cellular and Comparative Physiology)

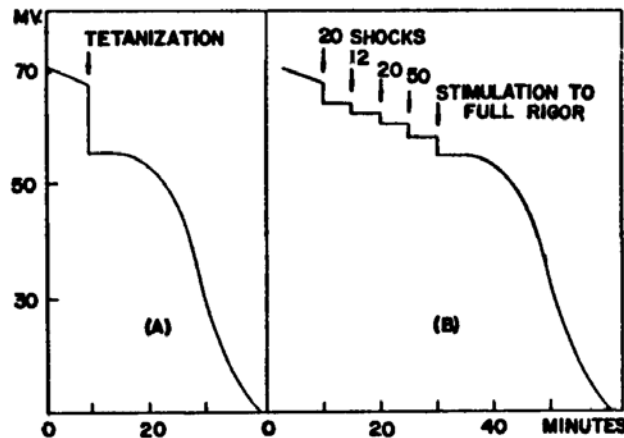


Figure 11.14. Effect of stimulation upon the resting potential of poisoned frog muscles. Muscles kept in Ringer containing 5 mM IAA.

- (A) After a tetanus (left) the resting potential fell immediately to 55 mV at which value it remained for many minutes before it began to fall again.
- (B) If the tetanus was split up into short successive bursts (right) the potential fell in a stepwise fashion with each burst.

(Ling 1952, by permission of Johns Hopkins University Press)

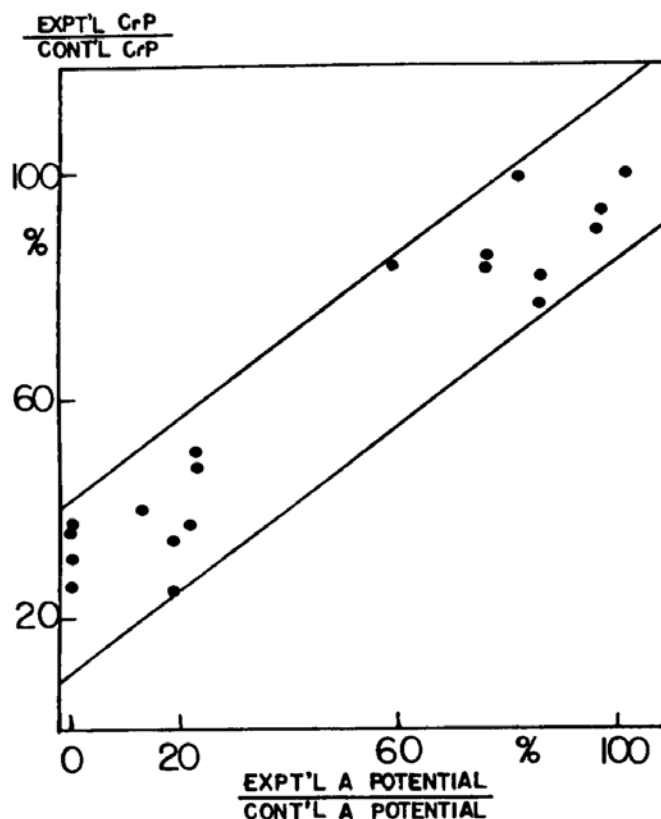


Figure 11.15. Relationship between the concentration of creatine phosphate (CrP) in frog sartorius muscles following exposure to iodoacetate (IAA) for varying lengths of time and the magnitude of its A potential. (*A potential* is that fraction of the resting potential which could be obliterated by electrical tetanization of IAA-poisoned muscle). Both CrP and the A potential are expressed as percentage of their respective initial values. A linear correlation coefficient of +0.94 is found between the two variables. (Ling and Gerard 1949a, by permission of Journal of Cellular and Comparative Physiology)

the A potentials of frog muscle against their respective CrP contents after varying lengths of exposure of the muscles to IAA. Both the A potentials and the CrP contents were given as percentages of their respective normal values before IAA. A linear correlation coefficient of +0.94 was calculated between the two variables, again affirming the theory.

In summary, exposure to pure nitrogen and electrical stimulations of normal or IAA-poisoned muscles lead to a marked fall of the concentration of CrP in the muscle without significantly changing the concentration of ATP. In all three cases, a fall of the resting potential accompanied the fall of CrP concentration. In the case where there was a recovery of CrP concentration, there was an accompanying rise of the resting potential. In IAA-poisoned muscles, the concentration of remaining CrP and the magnitude of the A potential are linearly correlated, with a linear correlation coefficient of +0.94. These comparative studies lend support to the notion that CrP functions as the major congruous anions at the surface and in the cytoplasm of muscle cells and the assumption that there is an equilibrium between the CrP concentration of the cell surface and throughout the whole cell.

When muscles were simultaneously poisoned with pure nitrogen and IAA, the resting potential falls to zero after a period of time which varies with the temperature. At 25°C, the potential lasted only 3 to 4 hours (Figure 11.12A); at 0°C, the resting potential of similarly poisoned muscles lasted much longer [e.g., the resting potential was still 65 mV (from an initial 90 mV) in 10 hours, Ling 1962, 206]. In parallel with the change of the resting potential, the ATP concentration fell from 6 $\mu\text{mole/g}$. fresh muscle to near zero (0.5 $\mu\text{mole/g}$) after only 4 hours at 25°C; at 0°C, the ATP concentration was still at a concentration of 4.6 $\mu\text{mole/g}$. after 10 hours of incubation. So although a methodical study of the quantitative relationship between ATP content and the resting potential is yet to be done, there seems little doubt that ATP is essential for the maintenance of the resting potential just as it is essential for the maintenance of selective K^+ accumulation in the cytoplasm. In both cases, **ATP acts as the premier conservative cardinal adsorbent keeping the proteins involved in such an electronic conformation that their β - and γ -carboxyl groups selectively adsorb K^+ over Na^+ .**

In the next section, I examine the phenomenon of action potential and show how the surface-adsorption theory can readily explain some aspects of action potentials which can be explained by the ionic theory, as well as other aspects of action potentials which *cannot* be readily explained by the ionic theory.

11.5. *Action Potential According to Hodgkin-Huxley and According to the AI Hypothesis*

11.5.1. *The Hodgkin-Huxley Analyses and Interpretation of the Action Potential*

11.5.1.1. *Outline of Theory*

In 1952, Hodgkin and Huxley (and Katz) presented their detailed studies and analyses of the kinetic events underlying action potential in squid axons (Hodgkin and Huxley 1952a, b, c, d; Hodgkin et al. 1952). In these studies, they used an electronic feedback device called the "voltage clamp," which can hold a uniform voltage-difference across the cell surface of the entire length of an axon, for a chosen length of time and at a desired level and polarity (Cole 1949; Marmont 1949).

Hodgkin and Huxley discovered that, in response to the advancing front of an action potential, a local depolarization (or fall of the resting potential) occurs. This early phase of the action potential follows a sudden increase of membrane permeability to Na^+ ; an inward surge of this positively-charged ion creates the "spike" of the action potential. The inward movement of Na^+ soon subsides and is superseded by an outward positive current which is due to an outward movement of K^+ .

In the Hodgkin-Huxley theory of action potential, the driving force for the net movement of a particular ion into or out of the cell is the difference between the membrane potential (ψ) and the equilibrium potential of that ion across the

cell membrane. For Na^+ , the equilibrium potential is called *Na potential* (E_{Na}); its relation to the intra- and extracellular Na^+ concentration is described in the following equation:

$$E_{\text{Na}} = \frac{RT}{F} \ln \frac{[\text{Na}^+]_{\text{ex}}}{[\text{Na}^+]_{\text{in}}}. \quad (52)$$

A strong argument which Hodgkin and Huxley put forth in favor of the Na-potential concept was the demonstration of a small but distinctly outward positive current (at the same time when the usual large surge of inward positive current occurs) when an axon was bathed in a Na^+ -free medium instead of the normal Na^+ -rich sea water. This finding confirms the expectation, based on equation 52, that net movement of Na^+ turns outward during activation when $[\text{Na}^+]_{\text{in}}$ is artificially made higher than $[\text{Na}^+]_{\text{ex}}$.

According to the currently popular view, the activation of the inward Na^+ current and the outward K^+ current is due to the sequential opening of discrete and specific membrane pores called “ Na^+ channels” and “ K^+ channels” respectively. Both “channels” are closed in resting cells.

11.5.1.2. Critique of the Ionic Theory of Action Potential

Some basic concepts of the “ionic theory” of action potential are critically analyzed next.

(1) *The Existence of a Standing “Na Potential”*

In the Hodgkin-Huxley model of action potential as described above, the key driving force behind the initial inward surge of Na^+ during an action potential is the “Na potential.” In magnitude the Na potential is described by equation 52. In normal excitable cells in their normal environment, $[\text{Na}^+]_{\text{ex}} \gg [\text{Na}^+]_{\text{in}}$. There is therefore a strong potential for the external Na^+ to rush into the cell, much as water in a high place has a strong potential to rush to a lower place. According to the Hodgkin-Huxley theory, external Na^+ does not rush into a resting cell because the “gates” of the special pathways for Na^+ in the cell membrane, the “Na channels,” are closed in the resting cell. It is only in response to rapid electrical depolarization that the gates of the Na channels are suddenly thrown open, and the Na^+ ions in the external medium rush into the cell, creating the spike of the action potential.

A concept like this would be more easily understandable if the resting cell membrane were totally impermeable to Na^+ , as was once widely believed. However, tracer studies in the late thirties and early forties have proven unequivocally that the cell membrane is permeable to Na^+ (and K^+) in excited as well as resting cells (Section 1.3; Ling 1984, 53). The established permeability of the resting cell membrane to both Na^+ and K^+ raises the question: “What prevents the Na potential from being dissipated in resting cells?”

Consider that the number of positive charges needed to change the voltage of a one-microfarad condenser by 120 mV is 0.12×10^{-6} coulomb, equivalent to 1.2×10^{-12} moles/cm² (Katz 1966; Hodgkin 1971). According to Katz (1966), the inward flux rate of Na^+ of resting frog muscle is 3.5×10^{-12} moles/cm² sec. At this influx rate, it would take only $(1.2 \times 10^{-12}) / (3.5 \times 10^{-12})$, or 0.34 sec-

onds, to completely discharge the resting potential when the cell membrane is *at rest* and the “Na channels,” according to proponents of the discrete channel concept, are entirely in the *closed state*.

In fact, the Na^+ influx rate given by Katz and used in the above calculation is one of the lowest in the literature. Harris, for example, gives a value 3.5 times higher (1.22×10^{-7} cm/sec) (Harris 1950). With Harris’s figure, it would take only 0.1 second (100 msec) to discharge the resting potential.

Of course, in the ionic theory, the inward flux of Na^+ of resting cells is exactly matched by an equal outward flux of Na^+ due to pumping. Yet, in experimental testing, 5 hours after the total suppression of respiration and glycolysis by the combined action of anoxia, cyanide, Na iodoacetate, and cooling to 0°C , the resting potential of cells remained entirely normal at 88 mV (Ling 1962, 207). Under these conditions, the only energy source remaining would be the ATP, ADP, and creatine phosphate (CrP) in the cells, as described in Section 2.2. We now know that ATP, ADP, and CrP do not really contain utilizable energy in their “high-energy-phosphate bonds” at all. Therefore, ***the hypothesis that there is a “Na potential” in resting nerve and muscle cells across a cell membrane quite permeable to Na^+ is no longer easily defensible.***

In contrast, overwhelming evidence discussed in Chapters 5 and 8 shows that the low level of Na^+ and other large and complex molecules and hydrated ions is due to the low equilibrium-distribution coefficient or *q*-value of Na^+ in cell water. That is, Na^+ is at a state of equilibrium in the water of resting cells and in the external medium. When at equilibrium, intracellular and extracellular ions are, like pools of water, kept at the same level, at equal potential. Therefore, there is no Na^+ potential in the resting cells. ***Without a standing Na potential, the postulated opening of a supposedly closed “Na channel” cannot create an inward Na current.*** Yet an inward Na^+ current does exist during an action potential. Therefore, a different mechanism from that described is in order. The AI hypothesis provides such a mechanism, which will be described in Section 11.5.2.2.

(2) Delayed K^+ Current

In the Hodgkin-Huxley model, membrane depolarization opens the gate of a postulated specific “ K^+ channel,” allowing the escape of the high concentration of free K^+ trapped inside the cells by the closed “ K^+ channel.” However, ***since the resting cell membrane is also quite permeable to this ion, why K^+ does not leak out en masse from the resting cell is unexplained.***

(3) Discrete and Highly Ion-specific “ K^+ Channels” and “ Na^+ Channels” as Rigid Pores Containing Fixed Carboxyl Groups

Half a century after the disproof of Traube’s original atomic-sieve concept, and nearly that long after the disproof of the Boyle-Conway version of the atomic-sieve concept (Sections 1.2.2. and 1.3), some cell physiologists have, unaccountably, seen fit to resurrect the concept of sievelike “channels.” Katz (1966, 63) postulated a membrane channel “little wider than the K ion itself . . .” Hille advocated a $3 \times 5 \text{ \AA}$ “Na channel” (Hille 1975a), Armstrong a “ K^+ channel” 3 \AA in diameter (Armstrong 1975).

Section 9.2.1.4. shows how a combination of preconceived (wrong) ideas and

unjustifiable assumptions generated error concerning the proportion of surface area occupied by aqueous channels of the cell membrane—a misconception on which the concept of narrow, rigid K^+ and Na^+ channels is built.

Figure 11.16 reproduces a diagram of the “selectivity filter,” the Na^+ and K^+ channels according to Hille (1975a). Note that besides the rigid, sievelike structure in both the “ Na^+ channel” and the “ K^+ channel,” a negatively charged carboxyl groups is present. The carboxyl group of the so-called K^+ channel with a pK_a of 4.4 shown in Figure 11.17 corresponds to what I had earlier described as a low c -value carboxyl group (Ling 1960, 162). The carboxyl groups of the so-called Na^+ channel with a pK_a of 5.2 correspond to what I had earlier described

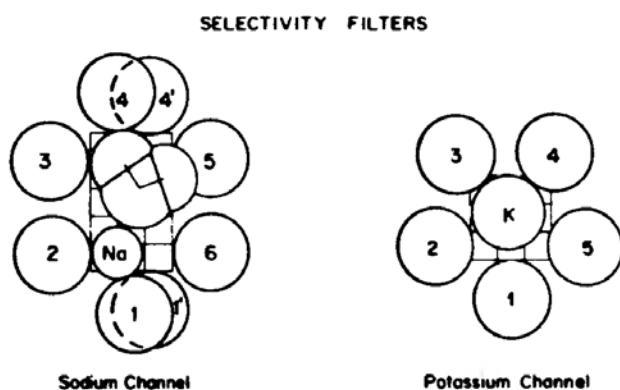


Figure 11.16. Hypothetical structure of selectivity filters of “Na and K channels” with an angstrom grid and permeant ions inside. There is also an H_2O molecule in the Na channel. All numbered atoms are oxygen atoms. In the Na channel 01 and 01' are a negatively charged $-COO^-$ group. (Hille 1975a, by permission of Marcel Dekker, Inc.)

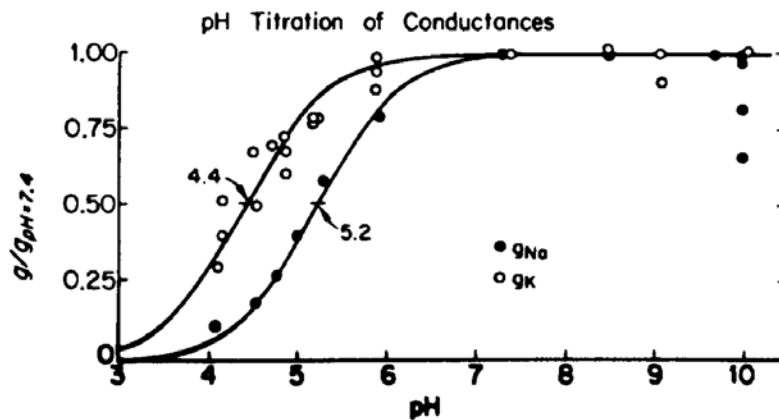


Figure 11.17. Blocking of “Na and K channels” at pH is lowered. Ionic conductance is measured at a potential of +30 to +75 mV and normalized to the value of $pH = 7.4$. Effects appear within seconds and are nearly fully reversible. Curves are theoretical titration curves of simple acids with $pK_a = 4.4$ and 5.2 . (Hille 1975a, by permission of Marcel Dekker, New York)

as a high c -value carboxyl groups (Ling 1960, 163). These are basic concepts I presented many years before Hille.¹¹

To confirm the theory that the initial inward Na^+ current producing the “overshoot” is the consequence of the opening of “channels” specific to Na^+ , a critical assumption is that the opened “ Na^+ channel” is specific and impermeable to K^+ . Were it otherwise, the inward rush of Na^+ in the opened “ Na channel”—following the free- K^+ tenet of the membrane-pump theory—would be counterbalanced by a simultaneous outward rush of K^+ through the same “channel,” each electrically cancelling the other out. In that case, there could be no “overshoot.”

Actually, a method is available to determine if the opened “ Na channel” is permeable to K^+ or not. It is based on the method that Hodgkin and Huxley introduced (described in Section 11.5.1.1) to support their concept that the orientation of the Na^+ -concentration gradients determines the direction of the Na^+ current. When the Na^+ concentration is higher in the external medium than in the cell, the Na^+ current is directed *inward*—as during a normal action potential, occurring in a normal cell within a normal environment. However, when the Na^+ concentration inside the cell is higher than in the external medium, the Na^+ current is directed *outward*—as in a normal squid axon bathed in a Na -free Ringer solution (Section 11.5.1.1, also Hodgkin and Huxley 1952a, 451).

To determine if the open “ Na channel” is truly inaccessible to K^+ traffic as required in the Hodgkin-Huxley theory, one removes all Na^+ from the media bathing both the inside and outside of an axoplasm-free squid axon, e.g., by bathing the axon in an external medium containing no Na^+ , while perfusing the axon internally with a Na^+ -free solution of K^+ salt. *Failure to demonstrate an outward “hump” during activation would indicate that the opened Na^+ channel is indeed impermeable to K^+ as postulated by the theory.*

*Just such an experiment was carried out by Chandler and Meves in 1965. **Contrary to theoretical prediction, they did observe just such an outward hump** (Chandler and Meves 1965, 796). Therefore, the reason that K^+ does not actually move outward, counterbalancing the inrush of Na^+ during activation, must involve a different mechanism from the postulated impermeability of the so-called “ Na channel” to K^+ . Such a mechanism was offered, and will be presented in Section 11.5.2.2.*

11.5.2. Action Potential According to the AI Hypothesis and Experimental Findings in Harmony with the Theory

11.5.2.1. A Sketch of the Theory

At the outset, I must emphasize that the AI hypothesis of action potential is still in its very early infancy. Therefore only a broad outline of the most central problems can be presented.

A central theme of the AI hypothesis is that similar protein-ion-water systems can serve diverse physiological functions. Through near-neighbor inductive interaction, these systems can function as coherent units. As such, they can also

be made to switch between alternative autocoooperative states by the adsorption or desorption of cardinal adsorbents. The diversity of physiological functions often results from differing **locations** in the cell, rather than from the **nature** of the systems (only).

As an example, ouabain, an EDC, causes an essentially similar c -value rise of both the β - and γ -carboxyl groups in the cytoplasm of frog muscle and at the surface of frog eggs. Yet, in the cytoplasm, this c -value rise of the β - and γ -carboxyl groups creates a displacement of bulk-phase K^+ by Na^+ (Section 8.3.2). At the cell surface, a similar c -value rise of the β - and γ -carboxyl groups creates a shift of selectivity in ionic permeability (Table 9.3); a deceleration of Na^+ -efflux rate [Section 9.2.2.3.2(1)]; as well as a partial depolarization of the resting potential (Section 11.4.2.1.).

According to the AI hypothesis, the action potential is the manifestation of a specific case of controlled autocoooperative transition which occurs at the surface of nerve, muscle and other excitable cell and is distinguished by a large c -value change of the surface β - and γ -carboxyl groups and a concomitant depolarization of the cell surface water. The transition from the resting state to the active state is, as a rule, triggered by the electrical depolarization generated at the advancing front of a propagating action potential, as demonstrated by Hodgkin and Huxley (1952 a,b,c,d). While it seems logical that one or more component of the protein-ion-water assembly at the cell surface is acted upon by the activating electric field and that, to be effectively acted upon by the electric field, this target component(s) bears electrical charges, precisely what this component is remains elusive at this moment.

Ca^{++} has often been considered an agent that plays a role in the shift between the resting and active state (Frankenheuser and Hodgkin, 1957). A collection of adsorbed K^+ on neighboring sites, when electrically detached as a group, may launch a propagated indirect F-effect and activation. The activation process could involve dephosphorylation of ATP. Only further investigation can provide us with a definitive answer.

Although we do not know what (if any) cardinal adsorbent controls activation, we can predict that it (or its equivalent) exercises a strong influence over the c -value of cell surface β - and γ -carboxyl groups, as well as the electronic state of the $NHCO$ groups of the cell surface proteins which keep cell-surface water in its intensely polarized state.

The postulated large c -value change of the surface β - and γ -carboxyl groups-controlling the specificity of selective ion permeability, and the depolarization of cell surface water will be the subjects of the immediately following discussion.

(1) *Large c -value changes of surface carboxyl groups:*

The ouabain-induced changes of the cytoplasmic as well as the *resting* cell surface β - and γ -carboxyl groups closely resemble each other both in the direction of the c -value change and in the magnitude of the c -value changes (Section 9.2.2.3). These changes and that occurring at the surface during an action potential are also similar to one another in the *direction* of the c -value changes (i.e., there is a rise), but differ markedly in the *magnitude* of the c -value increase. As shown in Section 8.3.2 (3), the ouabain-induced change of the $K_{Na \rightarrow K}^{00}$ of the bulk

phase cytoplasmic β - and γ -carboxyl groups fell from 100 to 21.7, corresponding to a c -value rise from -4.20 to -3.25 Å. In contrast, during an action potential, $K_{Na \rightarrow K}^{00}$ of the cell surface β - and γ -carboxyl groups falls from 100 to below one. Thus while ouabain only reduces the relative degree (without altering the order) of the preference of K^+ over Na^+ , activation actually inverts their preference order, changing it from preferring K^+ over Na^+ to preferring Na^+ over K^+ .

Theoretical curves in Figure 6.9 show that such a drastic change of $K_{Na \rightarrow K}^{00}$ indicates a much larger increase in the c -value of the β - and γ -carboxyl groups of the active cell surface than those produced by ouabain on the resting cell at its surface and within its cytoplasm, as further discussed below.

(2) *Water depolarization:*

According to the SA theory of action potential, an alteration in the physical state of cell-surface water occurs during an action potential (Ling 1981a, 1982, 1985), even though no similar large response of the water in bulk phase cytoplasm is visible in response to ouabain treatment (see Section 8.3.3. and below). In this aspect, the change underlying an action potential reminds one of the effect of ATP depletion, which also brings about a change in the c -value of the β - and γ -carboxyl groups concomitant with water depolarization (Section 8.4.3.). Thus it appears that only large c -value increases of the β - and γ -carboxyl groups are accompanied by large increases of the c -value-analog of the backbone carbonyl groups (see Section 7.3.3). A large increase of the c -value analog of the carbonyl groups in turn causes α -helix formation and liberation of polarized water. (For other possible causes of the lack of visible sign of water depolarization accompanying lesser c -value change of the β - and γ -carboxyl groups induced by ouabain, see Section 8.3.3.).

Having sketched the bare essentials of the mechanisms of action potential according to the AI hypothesis, I now proceed to a more detailed discussion of the two main events of an action potential in terms of the AI hypothesis: initial Na current and delayed K current.

11.5.2.2. *The Mechanism of the Initial Na^+ Current*

In the AI hypothesis, there is no standing “Na potential” in resting cells (Section 11.5.1.2(1)); only during an action potential, is a Na potential momentarily created. Creation of the Na potential goes step by step with (1) a change of the c -value of the cell surface β - and γ -carboxyl groups from a (resting) low c -value at which K^+ is preferred, to a much higher (reversible) c -value at which Na^+ is overwhelmingly preferred over K^+ , and (2) a (reversible) depolarization and desorption of the cell surface water (see Figure 11.18). Meanwhile, the negative electrostatic repulsion due to the negative charges of the β - and γ -carboxyl groups prevents a rush into the cell of anions like Cl^- (which would have counteracted and thus neutralized the electrical effect of inward Na^+ surge).

A resting potential is created as a partial manifestation of an equilibrium. In this equilibrium state, the tendency for the adsorbed counterions of K^+ at the cell surface to escape to the surrounding medium as a result of thermal bombardment is counterbalanced by electrostatic attraction for the positively charged K^+ ions due to the negatively charged fixed anions and the inside negative resting potential (i.e., the inside of the cell is electrically negative to the outside). Thus

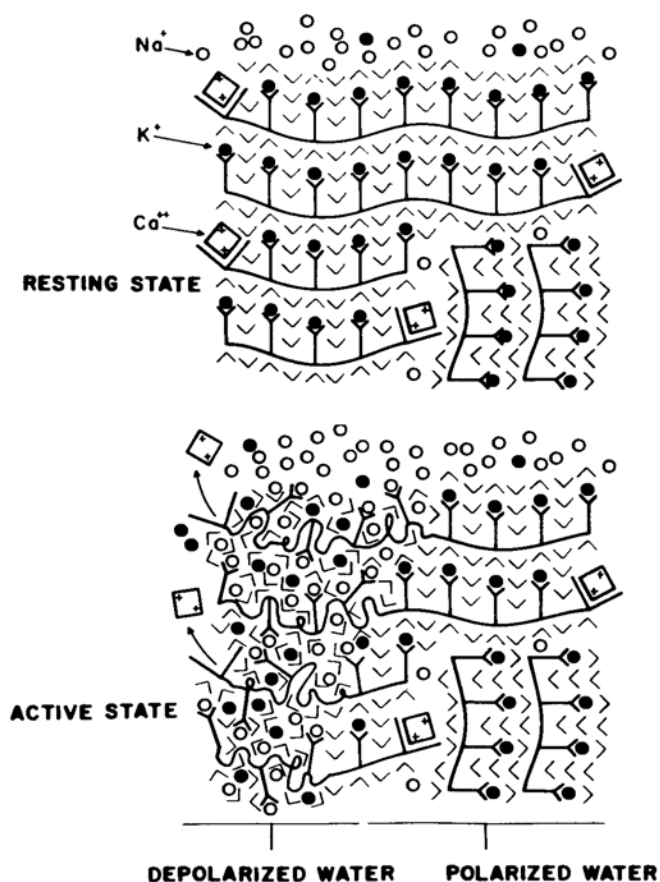


Figure 11.18. Diagram of a resting region of the cell surface (top) and a partially activated region (left side of bottom figure). (\bullet) = K^+ , (\circ) = Na^+ , V = water molecules. Left side of diagram represents cells or cell regions where underlying protein chains run parallel to cell surface; right side represents protein chains running perpendicular to cell surface. (Ling 1982, by permission of Physiological Chemistry and Physics)

at any time a more or less constant number of vacant fixed anions persists near the cell surface. This is the case when the external K^+ concentration is relatively low, as it is, for example, in a normal Ringer solution (i.e., 2.5 mM). However, when the external K^+ concentration is artificially increased to, say, 100 mM, the equilibrium is disturbed and a new one promptly established. As a result, the vacant anionic sites at the cell surface become occupied by K^+ and the resting potential approaches zero. It is true that the Na^+ ion is always present in normal Ringer solution at a high concentration (100 mM); yet even at this concentration Na^+ cannot depolarize the normal resting potential as 100 mM K^+ can, because of the unfavorable adsorption energy of Na^+ for the surface carboxyl groups. That is, in equation 44, \bar{K}_{Na} is so low that $\bar{K}_{\text{Na}} [\text{Na}^+]_{\text{ex}}$ is still too low to affect ψ even at a $[\text{Na}^+]_{\text{ex}}$ of 100 mM.

With cell activation, the c -value of the β - and γ -carboxyl groups rises, in an all-or-none manner, to a much higher value. In consequence, the relative preference of the β - and γ -carboxyl groups for Na^+ (i.e. \bar{K}_{Na}) rises sharply. An external Na^+ concentration of 100 mM, unable to depolarize the resting cell, now suddenly acquires the ability to depolarize the active cell surface. This response

is qualitatively quite similar to the depolarization created by exposure to the EDC ouabain (Figure 11.8) or, in the case of bulk-phase ion accumulation, in response to the withdrawal of an EWC, Ca^{++} (Figure 8.8). In a resting cell, multilayer polarization of the cell water prevents a net influx of Na^+ into the cell because the q -value for Na^+ is low in the polarized water of resting cells. Similarly, in a resting cell, it is adsorption on cytoplasmic β - and γ -carboxyl groups that prevents net efflux of K^+ . **With a transient change of the physical state of the cell surface water to approach that of normal liquid water, a Na potential is momentarily created at the cell surface, and with it a driving force for the external Na^+ to enter the cell.** Like the standing Na potential of Hodgkin and Huxley, the transient Na potential is equal to $RT/F \ln \left[[\text{Na}^+]_{\text{ex}} / [\text{Na}^+]_{\text{in}}^{\text{free}} \right]$, where $[\text{Na}^+]_{\text{in}}^{\text{free}}$ is the *free* intracellular Na^+ concentration. We might then ask how this newly created potential translates into an inward Na^+ current. Let us return to the theory of ion permeation described in Section 9.2.2.1.

As shown in the diagram of Figure 9.11, the electrostatic field exerted by fixed ions on their near vicinity repels, deflects, or captures would-be entering and exiting ions, and mediates their influx or efflux via the adsorption-desorption route. At the surface of resting muscle cells, for example, the low ϵ -value β - and γ -carboxyl groups favor occupancy by K^+ over Na^+ , repelling and limiting Na^+ entry to the energetically less favorable (saltatory) route through intensely polarized cell surface water domains, away from the fixed ions (Figure 9.11). During activation, the ϵ -value transiently shifts to a much higher value, such that Na^+ is preferred over K^+ . As a result, Na^+ permeation is now preferred over K^+ by the (transiently) high ϵ -value β - and γ -carboxyl groups. Water depolarization, which gives rise to the transient Na potential, also enhances the rate of Na^+ permeation by increasing both the equilibrium distribution coefficient of Na^+ in the water (q) and its diffusion coefficient (D) therein (see Section 9.2.1.1).

In summary, the coordinated large ϵ -value increase of the surface β - and γ -carboxyl groups and the ϵ -value-analog increase of the backbone CO groups produce: (i) a local depolarization of the cell surface water, which leads to (ii) the creation of a transient Na^+ potential, and (iii) selectively allows the inward movement of Na^+ , generating the inward Na^+ current. Resting potential is simultaneously annulled, and a Na^+ -concentration-dependent polarity reversal of the potential is created, i.e., the overshoot.

11.5.2.3. *The Mechanism of the Delayed K^+ Current*

The physical bases for the delayed outward K^+ current in the AI hypothesis also differ markedly from that in the Hodgkin-Huxley model [Section 11.5.1.2(2)]. In the AI hypothesis, domains of the cell membrane occupied by low ϵ -value β - and γ -carboxyl groups and polarized water selectively mediate K^+ entry into resting muscles. The same β - and γ -carboxyl groups also mediate the outward flow of K^+ during the later part of the action potential. **The delayed K^+ current is thus not due to the further opening of more K^+ specific channels. Rather, it is the result of the release of cell K^+ from its normal adsorbed state in the resting cell** (Chapter 4). During a normal action potential, the gain of Na^+ and the loss of K^+ are roughly equal in quantity (3 to 4×10^{-12} moles/cm²

of Na^+ gained and K^+ lost). The K^+ lost may be primarily due to displacement by the intruding Na^+ ions on the β - and γ -carboxyl groups transiently favoring Na^+ . On the other hand, under a voltage clamp condition when an external electromotive force (EMF) is applied across the cell surface, the continued loss of K^+ , especially in the absence of external Na^+ , may be due partly to the direct effect of the externally applied EMF in mobilizing the normally adsorbed K^+ .

11.5.2.4. A General Equation for Resting and Action Potential

I have so far presented essentially two equations for cellular potentials, equations 44 along with its improved versions 45 and 50. Now I introduce a third equation in which the role of cell-surface water is taken into account in the creation of action potential:

$$\psi = \text{constant}_1 + \frac{RT}{F} \ln \frac{1}{2[\text{K}^+]_{\text{ex}} \bar{K}_K} \left[1 + \frac{\xi - 1}{\sqrt{(\xi - 1)^2 + 4\xi \exp(\gamma/RT)}} \right] - \frac{RT}{F} \ln \frac{\gamma_{\text{in}}^{\text{Na}} [\text{Na}^+]_{\text{in}}^{\text{free}} + \gamma_{\text{in}}^{\text{K}} [\text{K}^+]_{\text{in}}^{\text{free}}}{\gamma_{\text{ex}}^{\text{Na}} [\text{Na}^+]_{\text{ex}} + \gamma_{\text{ex}}^{\text{K}} [\text{K}^+]_{\text{ex}}}, \quad (53)$$

where the constant₁ has the same meaning as shown in equation 48; $\gamma_{\text{in}}^{\text{Na}}$, $\gamma_{\text{in}}^{\text{K}}$ and $\gamma_{\text{ex}}^{\text{Na}}$, $\gamma_{\text{ex}}^{\text{K}}$ are the activity coefficients of Na^+ and K^+ in the cell-surface-layer water and external solution, respectively. When the cell is at rest, the third term of the right member of equation 53, a diffusion potential term, vanishes—because under this condition $\gamma_{\text{in}}^{\text{Na}} / \gamma_{\text{ex}}^{\text{Na}} = [\text{Na}^+]_{\text{ex}} / [\text{Na}^+]_{\text{in}}^{\text{free}}$ and $\gamma_{\text{in}}^{\text{K}} / \gamma_{\text{ex}}^{\text{K}} = [\text{K}^+]_{\text{ex}} / [\text{K}^+]_{\text{in}}^{\text{free}}$ and thus equation 53 reverts back to equation 50. Now,

$$q_{\text{Na}} = \gamma_{\text{ex}}^{\text{Na}} / \gamma_{\text{in}}^{\text{Na}}; q_{\text{K}} = \gamma_{\text{ex}}^{\text{K}} / \gamma_{\text{in}}^{\text{K}}, \quad (54)$$

where q_{Na} and q_{K} are the equilibrium distribution coefficients of Na^+ and K^+ in the surface cell water. Substituting equation 54 into equation 53, and taking into account the fact that in a normal tissue fluid or Ringer solution ($\gamma_{\text{ex}}^{\text{Na}} [\text{Na}^+]_{\text{ex}} + \gamma_{\text{ex}}^{\text{K}} [\text{K}^+]_{\text{ex}}$) is a constant and $\gamma_{\text{ex}}^{\text{Na}}$ is approximately equal to $\gamma_{\text{ex}}^{\text{K}}$, one can simplify the substituted equation 53 into the following form, noting that constant₁ and constant₂ are not equal:

$$\psi = \text{constant}_2 + \frac{RT}{F} \ln \frac{1}{2[\text{K}^+]_{\text{ex}} \bar{K}_K} \left[1 + \frac{\xi - 1}{\sqrt{(\xi - 1)^2 + 4\xi \exp(\gamma/RT)}} \right] - \frac{RT}{F} \ln \left[\frac{[\text{Na}^+]_{\text{in}}^{\text{free}}}{q_{\text{Na}}} + \frac{[\text{K}^+]_{\text{in}}^{\text{free}}}{q_{\text{K}}} \right]. \quad (55)$$

In summary, during excitation, $K_{\text{Na} \rightarrow \text{K}}^{00}$ (and hence ξ) falls due to the c -value increase of the surface anionic sites; q_{Na} (and q_{K}) concomitantly increase, and a Na^+ potential is thereby transiently created. The intrush of Na^+ brings about not only a cancellation of the resting potential, but an overshoot as well. The influx of Na^+ displaces K^+ from adsorption sites at and near the cell surface, causing an increase of free K^+ (i.e., $[\text{K}^+]_{\text{in}}^{\text{free}}$), and hence the delayed outward K^+ current.

It is clear that, due to autocoooperativity, both $K_{\text{Na} \rightarrow \text{K}}^{00}$ and q_{Na} (and q_{K}) shift abruptly between two discrete states (Ling 1960). The value of ψ in the active

state should be approximated by the value of the peak height of the action potential. The time course of transition between the two autocoperative states is S-shaped, with a steep slope, and demonstratable from a stochastic extension of the one-dimensional Ising model, as has been successfully demonstrated (Huang 1979; Negendank and Karreman 1979; and Huang and Negendank 1980).

11.5.2.5. *Experimental Findings in Harmony with the SA Theory of Action Potential*

The foundation of a scientific *edifice* should be solidly established before one can efficiently tackle *higher level* constructions. While I have provided a general theoretical framework for action potential, I have so far done little experimental work myself to test the thesis introduced. But from the literature one can gather important data that lend support to my hypothesis. (The significance of these experimental findings to this new theoretical framework demonstrates that sound experimental work, even if guided by a theory which itself needs fundamental revision, is often not wasted.)

(1) *The Isolation of a "Na Channel Protein"*

The isolation of a single chain 250,000 dalton "Na channel protein" (Barchi 1984) and its structural elucidation (Noda et al. 1984) are in harmony with the following part of the theory of cellular electrical potential according to the AI hypothesis.

- a. The primary physiologically active structure of the cell membrane is proteinaceous, as I first suggested in 1952 (Ling 1952).
- b. The presence of domains of β - and γ -carboxyl groups in the "Na channel protein" is in harmony with the idea that the key component of the cell membrane determining the ion preference is the anionic β - and γ -carboxyl groups of a membrane protein, first introduced by Ling (1957, 1960).
- c. That the functional activity of this single-chain "Na channel protein" responds to binding of tetrodotoxin and other cardinal adsorbents is in harmony with the kind of allosteric control proposed in the AI hypothesis (see Figures 7.6, 7.8 and 8.14).

(2) *The Similar pK_a Values of the So-called "K⁺ Channels" in the "Open" State and the Surface β - and γ -carboxyl Groups Mediating Normal K⁺ Traffic*

In 1965, Ling and Ochsenfeld measured the effect of different pHs on the rate of entry of labeled K⁺, leading to the conclusion that the pK_a of the β - and γ -carboxyl groups mediating K⁺ entry into resting muscle cells is 4.75 (Figure 9.13). In later publications, Hille showed that the pK_a of the carboxyl groups mediating K⁺ efflux during activation is 4.4 (Figure 11.17). The basic similarity of the two pK_a values (4.75 vs. 4.4) for resting and active cell membranes suggests that in fact the same β - and γ -carboxyl groups mediating K⁺ traffic at rest also mediate outward K⁺ movement during the action potential; and that, unlike the β - and γ -carboxyl groups mediating Na⁺ ion inrush during the initial phase of the action potential, the c -values (and hence pK_a) of the β - and γ -carboxyl groups involved in the delayed outward K⁺ ion movement remain unchanged.

(3) *The Mutability of the Ion Specificity of the "Na⁺ Channels"*

In the current textbook version of action potential, the "Na⁺ channels" and "K⁺ channels" are physically separate and discrete entities. In the AI model, what mediates Na⁺ entry during an action potential is a transient state of the same β - and γ -carboxyl groups that normally mediate (preferential) K⁺ permeation in resting cells. A key issue that distinguishes these two different models is whether the mechanism underlying the selectivity in ion permeability is *mutable* or *immutable*. **Recent years have seen new evidence demonstrating that the ion-specificity and -preference of the so-called "Na⁺ channel" are indeed mutable.**

Khodorov (1978), for example, showed that upon exposure to the South American frog poison betrachotoxin, the "Na⁺ channel" in frog nerve Ranvier nodes changes from preferring Na⁺ over Tl⁺ to preferring Tl⁺ over Na⁺ (Figure 11.19). Khodorov's finding was confirmed by Huang et al. (1979), who found very similar results with neuroblastoma cells. These findings suggest that the β - and γ -carboxyl groups mediating Na⁺ entry are basically similar to the β - and γ -carboxyl group sites giving rise to resting potential, and that both of their *c*-values respond to electron-withdrawing or -donating effects of cardinal adsorbents on appropriate receptor sites. Thus, neither is immutable, as in the postulated discrete "Na channel," discrete "K⁺ channel" concept.

(4) *Large c-value Rise of the β - and γ -carboxyl Group During Activation*

As pointed out earlier, in Section 11.4.1., two types of evidence support the view that during activation, there is a large *c*-value rise of the surface β - and γ -carboxyl groups:

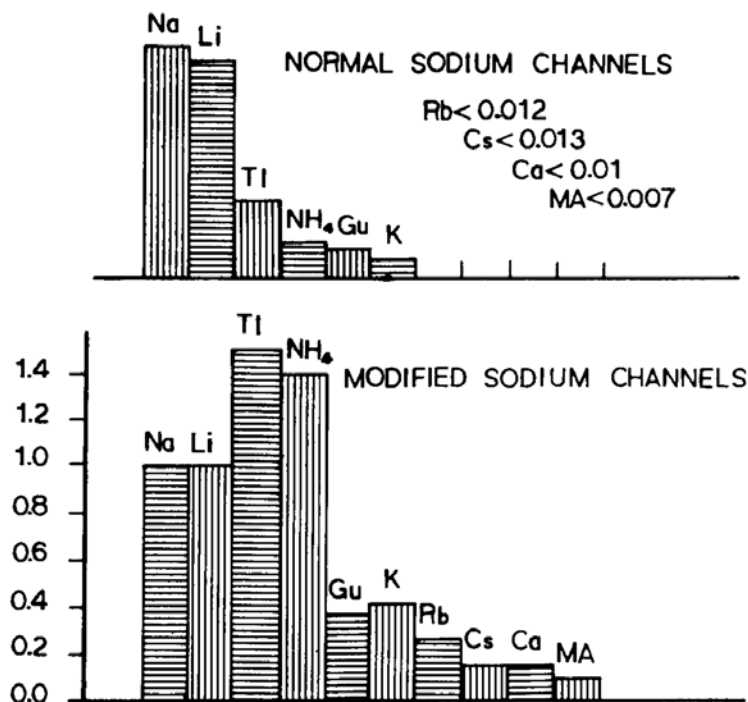


Figure 11.19. Permeability ratios of various ions (as indicated) to that of Na⁺ in normal and betrachotoxin-modified "sodium channels" (mean values). (Khodorov 1978, by permission of Raven Press)

- (a) The pK_a of the cell surface β - and γ -carboxyl groups of resting cells has a relatively low value (i.e., 4.4 to 4.7) (see Ling 1982, 90–91). The anionic sites essential for the inward Na^+ current have a higher pK value. Thus, the pK_a value for the anionic site mediating Na^+ entry for squid axons was given as 5.2 by Hille (1968, 1975) and as 6.5 by Stillman et al. (1971) (see also Figure 11.17).
- (b) The rank order of selectivity of resting surface β - and γ -carboxyl groups is $Rb^+ > Cs^+ > K^+ > Na^+$ for frog muscle (Ling and Ochsenfeld 1965), roughly corresponding to a c -value of -4.20 \AA , according to the theoretical data of Figure 6.9. The rank order of ion selectivity of active surface β - and γ -carboxyl groups essential for the Na^+ current is $Li^+ > Na^+ > K^+ > Rb^+ > Cs^+$ (Chandler and Meves 1965), with permeability ratios relative to Na^+ of 1.1 (Li^+) : 1.0 (Na^+) : 0.083 (K^+) : 0.025 (Rb^+) : 0.016 (Cs^+). This rank order roughly corresponds to a c -value of -2.65 \AA from the theoretical curves of Figure 6.9, where the theoretical absorption constants relative to Na^+ are 1.1 (Li^+) : 1.0 (Na^+) : 0.1 (K^+) : 0.045 (Rb^+) : 0.010 (Cs^+), following the same rank order. (See Section 9.2.2.3. and Ling and Fu 1988, for a discussion on how and why the rank order of the permeability of these ions may match that of their adsorption constants.) ***The two sets of ratios indicate that during activation the c -value rises from a low value (ca. -4.20 \AA) to a much higher one (ca. -2.65 \AA) than that brought about in response to $3.26 \times 10^{-7} \text{ M}$ ouabain (ca. -3.25 \AA , see Figure 6.9), in general agreement with theory.*** In the next section, we shall examine an independent experimental observation that lends support to the concept of depolarization of cell surface water as the underlying cause of the generation of Na potential, and hence of the main event of the action potential, or “spike”.

(5) Membrane Water Depolarization During Activation

Villegas et al (1965) showed that in activated squid axons, not only was there a net gain of Na^+ during an action potential, but there was also a concomitant net gain of erythritol, mannitol, and sucrose (Table 11.2). The increase of permeability to these nonelectrolytes requires Na^+ in the external medium. ***These findings provide evidence that an action potential indeed involves a transient, local depolarization of the cell surface water.***

Since sucrose has a molecular diameter of 8.8 \AA (Renkin 1954), its increased permeability during activation once more refutes the concept of a rigid “ Na channel” with a narrow “bottle neck” (only $3 \times 5 \text{ \AA}$ wide (Hille 1975a) (see Section 11.5.1.2(3)). While the data of Villegas et al. could not be anticipated on the basis of the rigid channel concepts, the data agree perfectly well with the concept of action potential according to the AI hypothesis: it is the intensity of water polarization, rather than the width of rigid pores, that restricts the traffic of larger solutes like hydrated Na^+ , mannitol, and sucrose through the resting cell membranes. With activation, a concomitant increase in the c -value of the β - and γ -carboxyl groups occurs which goes step by step with a depolarization of the intensely polarized water in wide membrane domains dominated by the β - and γ -carboxyl groups. This model readily explains the transient increase of the

Table 11.2 Penetration of [^{14}C]-Erythritol, -Mannitol, and -Sucrose into Resting and Stimulated Squid Axons (Villegas *et al.* (1965), by permission of *Journal of General Physiology*.)

Molecule	Permeability in 10^{-2} cm/sec ^a			
	Resting axon (axon a)	Stimulated at 25/sec (axon b)	Net increase 25 stimulations/sec (paired data) (b - a)	Calculated permeability during activity ^b
Erythritol	3.6 ± 0.4	6.1 ± 1.0	2.5 ± 0.8	110
Mannitol	2.3 ± 0.4	4.0 ± 0.5	1.7 ± 0.3	75
Sucrose	0.9 ± 0.1	1.8 ± 0.3	0.9 ± 0.3	40

^aThe values are mean \pm SE of ten nerve fiber pairs.

^bCalculated permeability during activity obtained by considering that the permeability change per impulse lasts 1 msec.

permeability of sucrose (normally very low, due to the intense water polarization) which goes *pari passu* with the switching of the β - and γ -carboxyl groups to a higher ϵ -value and their occupancy by the intruding Na^+ .

11.6 Summary

This chapter began with the introduction of Bernstein's (1902) membrane theory of cellular electrical potential, and his recognition of the key role of the K^+ ion in the generation of the cellular resting potential. Transient membrane permeability change was seen to be the foundation of action potential.

Following Hodgkin and Katz's important discovery of the transient permeability increase of living cells to Na^+ and the key role of this ion in the creation of action potential, the ionic theory, cast in the form of the Hodgkin-Katz (HK) equation, was introduced. The ionic theory is founded on the belief that the low Na^+ (and other solute) concentration(s) in resting cells is maintained by postulated Na (and other) membrane pumps; and (like Bernstein's membrane theory) on the belief that intracellular K^+ is in a free state. Extensive worldwide testing of the HK equation, however, led to only partial verification. The indifference of resting potential to extracellular chloride concentration led to a (questionable) "modification" of the HK theory; discrepancy between cell K^+ concentration and the theoretically expected value of ψ led to the introduction of another Na pump, an "electrogenic" one.

The recognition of the contradictions in the Na-pump hypothesis, of the pressing need to postulate an adsorbed state of K^+ in the cells, and of the insight offered by the study of glass electrode potential by Horovitz led to the introduction of the SA theory of cellular electrical potential in the mid-fifties. In the course of the 30 years following, three equations (44, 48 and 55) were introduced

to describe cellular electrical potential based on the SA theory. The simplest version (equation 44) is quite similar to Nicolsky's equation for glass-electrode potential. In form, equation 44 may be seen as formally identical to that part of the HK equation which has been experimentally verified, the difference being the meaning of the coefficients for the ionic concentration terms. Edelman's studies of guinea pig heart muscle clearly decide the difference in favor of the SA theory: the coefficients are surface adsorption constants and not permeability constants. With this key clarification, the predicted relationship between ψ and all variables according to equation 44 has been experimentally verified.

The SA theory is in full accord not only with the evidence just mentioned, but also with those experimental findings that refute the ionic theory: the limited energy the cell commands, the adsorbed state of the bulk of cell K^+ , the lack of a causal relationship between the total intracellular K^+ and ψ and between external Cl^- concentrations and ψ . The quantitative relationship seen between (a wide range of) extracellular K^+ concentrations and ψ , not predictable by the HK equation (or any of its modifications), is also quantitatively explained by the second equation of cellular electrical potential (equation 48), which includes nearest-neighbor interaction between cell surface β - and γ -carboxyl groups.

It is equation 48 that provides a quantitative basis for understanding the complex interaction between the concentration of external K^+ and Na^+ , and those of controlling agents, including the electron-donating cardinal adsorbent (EDC) ouabain, and electron-withdrawing cardinal adsorbent (EWC) adrenaline, as well as different temperatures.

The dependence of the resting potential of frog muscle upon the varied levels of creatine phosphate (CrP) content of the muscle in response to bursts of electrical stimulation in the presence or absence of the metabolic inhibitor (IAA) suggests (i) that there is an equilibrium between the level of CrP at the cell surface and throughout the cytoplasm and (ii) that CrP at both locations serves as ATP's "helper" in the role of congruous anion for the selective accumulation of free ions, and against the formation of salt linkages.

The role of CrP as congruous anion in maintaining the resting potential is in harmony with similar roles as congruous anion of CrP (and its counterpart in invertebrate tissues, arginine phosphate or ArP) in the selective accumulation of K^+ in frog muscle cytoplasm and in the adsorption of Na^+ and/or K^+ on the cell surface of squid axon, which determines the nature and rates of Na^+ efflux. The parallel functions of CrP (and ArP) in the maintenance of the resting potential, in the maintenance of K^+ accumulation, and in the maintenance of normal Na^+ efflux combine to illustrate how what may appear as totally different physiological manifestations in fact reflect the operation of the same basic mechanism in similar protein-ion-water systems in different parts of the cell's anatomy.

In the realm of action potential, the Hodgkin-Huxley-Katz analyses and explanations are, without question, major landmarks in the history of cell physiology. The concept of the opening of " Na^+ channels" and " K^+ channels" only during activation would have been much more defensible before the recognition of the permeability of *resting* cells to both ions. With what we know today, it is difficult to understand how a standing " Na potential" can remain undischarged,

before the opening of the postulated Na channel during an action potential, and why K^+ must await the opening of the postulated K channel to leak out. According to the SA theory of action potential, the Na potential is created *only* during activation because the Na^+ potential is not a standing one but created transiently during an action potential; K^+ leaks out during the delayed K^+ current because *only* then is it displaced from retaining intracellular adsorption sites and thus ready to diffuse outward.

In the SA theory, action potential—the magnitude and polarity of which is described by the third equation, equation 55—involves autocoperative change of the cell surface proteins, with a transient change of the surface β - and γ -carboxyl groups from a low c -value (at which K^+ is greatly preferred over Na^+) to a high c -value (at which Na^+ is preferred over K^+), along with concurrent transient depolarization of the cell-membrane water, which offers a general increase of membrane permeability to normally excluded solutes. The postulated high c -value of the cell surface β - and γ -carboxyl groups during activation, verified both from pK_a value measurements and from the inverted rank order of ion specificity, and the discovery that during an action potential there is a Na^+ -dependent increase of permeability to nonelectrolytes as large as sucrose, confirms the SA theory also.

Finally, it must be pointed out that one of the strongest pieces of evidence against the membrane theory of Bernstein, the ionic theory of Hodgkin, Huxley, and Katz, and later modifications, is that they are all built on the assumption that cellular electric potentials are fundamentally membrane potentials. Yet extensive efforts over more than half a century to demonstrate such a membrane potential across model membranes have all failed. Instead, investigations of four types of model systems (glass membrane, collodion membrane, oil membrane, and phospholipid membranes) carried out over half a century have revealed that the potential difference observed in all cases is the algebraic sum of two surface adsorption potentials, due to fixed ions of one polarity or another present on one or both surfaces of the membrane—in full harmony with the surface adsorption theory.

NOTES

1. It turns out that the permeability increase during an action potential may actually have two components: one general and one specific. For details, see Section 11.5.2.

2. Later I discovered that a similar equation had been proposed by Nicolsky, 22 years before, for glass-electrode potential (Nicolsky 1937).

3. Two other types of phase-boundary potentials have been proposed. Beutner (1913, 1914) regarded the observed electrical-potential differences across an organic (membrane) phase as due to an unequal distribution of the anions and cations on each side of the interface. Baur, on the other hand, believed that interfacial potentials arise from selective adsorption of a monolayer of organic ions at the oil-water interface (Baur 1913, 1926; Baur and Kronmann 1917). Both Beutner and Baur implicitly accepted the lipoidal membrane theory, and both attributed the potential difference measured between the inside phase and outside phase of the cell as the algebraic sum of two such interface potentials. This is one difference that sets the phase-boundary theories of Beutner and Baur apart from the SA theory, according to which the resting potential is generated *only at* the outside surface of the cell. A second important difference between the SA theory and the phase-

boundary theories of Beutner and of Baur concerns close-contact adsorption of counterions (e.g., K^+ and Na^+) on fixed ions (e.g., β - and γ -carboxyl groups). As mentioned in Section 4.1, this close-contact adsorption is the foundation of ionic specificity in the AI hypothesis, of which the SA theory is an integral part. Without close-contact association, there is no way for the fixed ions to distinguish counterions like K^+ and Na^+ , which differ from each other *only* in short-range attributes; nor can ion specificity changes associated with electron density or c -value changes of anionic groups be detected (see Section 6.2.4). No such close-contact association was suggested in either Beutner's theory or Baur's (see Figures 2-2 and 2-3 in Davies and Rideal, 1963).

4. The derivation of equation 45 is shown below: Of the K^+ adsorbed on the cell surface sites, only the fraction with enough kinetic energy to overcome both the adsorption-energy barrier and the resting potential barrier is in equilibrium with free K^+ in the external medium. Representing the concentration of adsorbed K^+ on the cell surface as $[K^+]_{ad}$ and the free energy of adsorption of K^+ on the surface sites as $\Delta\tilde{F}_K$, we have

$$[K^+]_{ad} \cdot \exp(-F\psi/RT + \Delta\tilde{F}_K/RT) = [K^+]_{ex}, \quad (A)$$

where F and R are the Faraday and gas constant respectively and T is the absolute temperature. The concentration of adsorbed K^+ in the presence of the competing cation, Na^+ is described by a Langmuir isotherm:

$$[K^+]_{ad} = \frac{[f^-]\tilde{K}_K[K^+]_{ex}}{1 + \tilde{K}_K[K^+]_{ex} + \tilde{K}_{Na}[Na^+]_{ex}}, \quad (B)$$

where $[f^-]$ is the concentration of anionic adsorption sites on the cell surface. \tilde{K}_K (which equals $\exp(\Delta\tilde{F}_K/RT)$) and \tilde{K}_{Na} represent surface adsorption constants of K^+ and Na^+ respectively, and are in units of $(M)^{-1}$. Substituting (B) into (A) and \tilde{K}_K for $\exp(\Delta\tilde{F}_K/RT)$, we have

$$\psi = \frac{RT}{F} \ln [f^-] - \frac{RT}{F} \ln \left[1 + \tilde{K}_K[K^+]_{ex} + \tilde{K}_{Na}[Na^+]_{ex} \right]. \quad (C)$$

5. Sato et al. demonstrated a linear relationship between $\ln [K^+]_{in}$ and ψ in K^+ -depleted frog muscle (Sato et al. 1967). In the AI hypothesis, the protein- K^+ -water systems found in all parts of the living cells behave in essence similarly. However, only the β - and γ -carboxyl groups and their preferentially adsorbed K^+ at the cell surface are related to ψ . Surface adsorption of K^+ reaches equilibrium much faster than bulk phase K^+ , following a change of $[K^+]_{ex}$. If enough time is allowed and equilibrium is then reached between K^+ adsorption at the cell surface and that in the cytoplasm, a *coincidental* relation will be observed between total cell K^+ concentration and ψ , as Sato et al. observed. In this case $[K^+]_{in}$ and $[K^+]_{ad}$ at the cell surface are apparently equal or similar. However, when equilibrium has not been reached between surface K^+ adsorption and cytoplasmic K^+ adsorption, a discrepancy between ψ observed and calculated from the bulk phase K^+ concentration would be expected. This is the case when K^+ -depleted, Na^+ -loaded muscle is returned to a Ringer solution containing a normal concentration of K^+ and ψ is measured rapidly afterwards. As mentioned above, this repeatedly observed discrepancy played a major role in the postulation of the electrogenic pump [see Section 11.2.3.2].

6. This indifference of ψ to external Mg^{++} concentration offers yet another piece of evidence which contradicts the ionic theory. The muscle cell membrane is highly permeable to Mg^{++} (see Gilbert 1960; Scheid et al. 1968; Sparrow 1969; Ling et al. 1983), and Mg^{++} should therefore have a depolarizing effect on ψ , according to the ionic theory—contrary to fact.

7. To determine the ratio of the adsorption constants for two species of monovalent cations (e.g., H^+ and K^+) on the surface anionic sites generating the surface adsorption potential (ψ), we need to find the concentrations of each of these two ions which can cause

the surface adsorption potential to reach the same value (preferably in the straight part of the plot of ψ vs. log of ion concentration). Since only one ion is studied at a time, we obtain from equation 46:

$$\psi = \text{constant}_1 - \frac{RT}{F} \ln \{1 + K_H[H^+]_{\text{ex}}\}, \quad (\text{A})$$

and

$$\psi = \text{constant}_1 - \frac{RT}{F} \ln \{1 + K_K[K^+]_{\text{ex}}\}, \quad (\text{B})$$

where $[H^+]_{\text{ex}}$ and $[K^+]_{\text{ex}}$ are, respectively, the external H^+ and K^+ concentration able to bring the surface adsorption potential, ψ , to the same value.

From equation A and B, we derive

$$K_H/K_K = [K^+]_{\text{ex}}/[H^+]_{\text{ex}}. \quad (\text{C})$$

Equation C shows that the ratio of the concentrations of the two ions that produce the same ψ is the reciprocal of the ratio of their respective surface adsorption constants.

8. With the aid of equation A of endnote 7 of this chapter and the data of Figure 11.6, we can calculate the equilibrium adsorption constant, K_H of H^+ on the fixed carboxyl groups at the collodion electrode surface. The K_H obtained is 10^7 , corresponding to a pK_a of 7.0; this value is nearly three orders of magnitude higher than the pK_a of 4.0 for protein carboxyl groups referred to earlier. Why?

The pK_a of the carboxyl group of acetic acid is 4.76. This value is determined in a solution of *free* acetic acid. The main reason for the difference of this pK_a from the pK_a of the carboxyl groups on the surface of the collodion electrode is the effect of charge fixation on the enhancement of counterion association discussed in Section 4.1. In full agreement, the pK_a of another type of *fixed* carboxyl group on methacrylic-acid exchange resins (with 2% cross-linking agent, DVB) is even higher (*above 9*) (Gregor et al. 1955). The data of Figure 11.6 also permit the calculation of the adsorption constant of K^+ (and of other alkali-metal ions) on carboxyl groups on the surface of the collodion electrodes. K_K obtained is 4.0×10^4 , once more demonstrating the strong influence of charge fixation upon the dissociation of counterions. (In contrast, K^+ does not associate with carboxyl groups of acetate ions at all in free solutions).

The question may be raised next: "if charge fixation enhances the pK_a of carboxyl groups so strongly, why do the fixed carboxyl groups on proteins both *in vitro* and *in vivo* retain a pK_a of close to 4?"

The pK_a of 4 (or values not too far from 4) reflects a combinations of factors, some increasing the pK_a , others decreasing it:

(1) Factor that increases the pK_a : charge fixation enhances the association of H^+ but to a lesser degree in what is called a *semifixed charge system*, exemplified by proteins in solution; charge fixation enhances H^+ association much more strongly at the surface and interior of living cells as well as the surface of collodion-coated electrodes and within ion exchange resins—referred to as *bona-fide fixed charge systems* (Ling 1962, xxxvi).

(2) Factors that decrease the pK_a :

i) Attachment of the carboxyl groups to the (strongly electron-withdrawing) polypeptide chain (see Section 6.2.2.).

ii) Ignored competing cations: To explain, I return to equation 21 in Section 8.1.3, describing the adsorption of labeled K^+ in the presence of nonlabeled K^+ . If the experimenter forgot that the incubating solution contained nonlabeled K^+ , then the association constant he or she obtained (K_{K^*}) would not be the true K_{K^*} , but in fact K_{K^*} divided by the term $(1 + K_K[K^+]_{\text{ex}})$. K_K is the adsorption constant of nonlabeled K^+ and $[K^+]_{\text{ex}}$ is the external concentration of the ignored K^+ . If more than one item is ignored, then the adsorption constant obtained is artificially reduced by $(1 + \sum_{i=1}^n K_i[p_i]_{\text{ex}})$, where K_i and p_i refer to the i th cation of a total of n ignored cations.

Although this sort of imagined forgetfulness may not happen very often, improper application of the theory of complete ionic dissociation (Section 4.1) and the prejudice against the salt-linkage concept (endnote 2 of Chapter 4) have established a broadly accepted practice of ignoring free monovalent ions which may be present in the environment, and fixed cations (e.g., ϵ -amino groups of the same or other proteins) which also compete for the protein carboxyl groups and are, with rare exceptions, always present.

iii) influence of a major conservative cardinal adsorbent like ATP, which is an EWC and hence reduces the c -value and therefore the pK_a of the carboxyl groups.

In summary, although a pK_a of 4 or thereabout remains a valid, distinctive criterion for the identification of protein carboxyl groups, the value itself is a very complex expression of diverse factors and as a whole quite different from the pK_a of acetic acid, though bearing a more or less similar numerical value.

9. The various factors mentioned under footnote 8 which contribute to the different measured pK_a s of the carboxyl groups on the surface of the collodion-coated glass electrode and on living cells tend to affect the affinity of the carboxyl groups for K^+ and for H^+ in the same way. For this reason, the affinity ratio of H^+/K^+ remains valid despite the difference in the measured pK_a of the carboxyl groups in each of these cases.

10. It is well known that, theoretically, a one dimensional chain of cooperatively linked sites does not undergo temperature transition (Ising 1925). However, the real world protein-water-ion assembly which a theoretical, one-dimensional model tries to simulate is actually three dimensional and fully capable of temperature transition, as the data show.

11. That the cell surface membrane β - and γ -carboxyl groups can offer a basic mechanism for selective ionic permeability was a concept first introduced by me in 1953 (Ling 1953). That membrane β - and γ -carboxyl groups with low and high c -value (or pK_a) provide a basis for preferential K^+ permeability and Na^+ permeability was also first published by me, briefly in 1957 and in detail later (Ling 1957, 1960, 1962). Yet Hille has made no reference whatsoever to my earlier work on the subject, nor has he responded substantively to my repeated requests to set the record straight.

THE COMPLETION OF A SCIENTIFIC REVOLUTION AND EVENTS BEYOND

12.1. *Definitions of “Scientific Revolution”*

In the midst of the eighteenth century, Antoine Lavoisier (1734–1794) completed what he called a *scientific revolution*. Joseph Priestly (1733–1804) described Lavoisier’s “chemical revolution” in these words: “There have been few, if any, revolutions in science so great, so sudden and so general . . . of what is now named the new system of chemistry. . . .” (see Cohen 1985).

In 1962 science historian Thomas Kuhn argued that science became what it is today not by a smooth and gradual accumulation of new knowledge, but by upheavals, or “scientific revolutions,” interspersed among periods of smooth progress (Kuhn 1962). Another quarter of a century passed before the majority of science historians accepted Kuhn’s theses (for review, see Cohen 1985).

Kuhn refers to a scientific revolution as a phenomenon that “necessitates the community’s rejection of a time-honored scientific theory in favor of another incompatible with it” (Kuhn 1962). I. Bernard Cohen specifically defined a scientific revolution as the act of the scientific community’s acceptance of a new theory (Cohen 1985). To Lavoisier, his work constituted a scientific revolution regardless of acceptance. To science historians, however, Lavoisier’s revolution became a scientific revolution only *after* its acceptance by the scientific community. To take another case, Gregor Mendel’s work at the time of his death would constitute a scientific revolution according to the definition of Lavoisier, Priestly and other scientists; Gregor Mendel’s work did not constitute a scientific revolution—while his work lay buried and unaccepted after his death—according to the definition of Kuhn, Cohen and other science historians. Clearly, the scientific revolution in cell physiology discussed throughout this volume refers to a scientist’s scientific revolution.

12.2. *A Unique Feature of the Scientific Method as Applied to Cell Physiology*

According to the *scientific method* that human beings have relied on in recent centuries to discover the rules that govern the universe, understanding of a hitherto unexplained phenomenon follows from the verification of the logical deductions or predictions of a hypothesis. But then what is a hypothesis?

To a physicist who has nothing else to lean on, his own imagination or insight sets the limit of his construction of a hypothesis. A hypothesis is an assumption, a guess, a simple postulate. A cell physiologist's hypothesis, on the other hand, must stay within the boundaries of the laws of physics. However, as mentioned in the Introduction, the laws of physics may not be firmly established yet, and when they are, these laws by themselves are as a rule too remote to explain the vastly more complex realm of living phenomena. For this reason, the cell physiologist must construct a hypothesis by extending and elaborating on known physical laws. The hypotheses of a cell physiologist are in fact logical deductions from physicists' laws, and comprise what may be called deduced postulates. How can one be sure that these deduced postulates have universal validity? By making use of the *scientific method*. Deductions must be put to the test by cogent experimental studies of *inanimate models* that involve essential characteristics of living cells but are simple enough to yield straightforward answers. Only after the deduced postulates of a cell physiologist's hypothesis have been verified in the study of simple inanimate models are we justified in applying these postulates to explain the behaviors and properties of living cells.

In summary, to understand the mechanisms of a complex living phenomenon, a biologist must begin with a hypothesis that is, first, a logical deduction from the existing laws of physics and, secondly, verifiable on a relevant inanimate model system. A failure to recognize one or both of these steps would lead back to eighteenth-century *vitalism*, according to which life phenomena fall outside of the realm of physical laws governing the inanimate world, and are mystical in nature.

12.3. *Outlines of Old and New Theory*

If we wish to compare the two theories of cell physiology with which we have been dealing, we will need a brief outline of each theory. Each outline begins with the postulates of the theory, explaining why the cell exists and telling us why it is what it is (chemically), and continues with the postulates explaining each of the four major subjects of basic cell physiology: (1) solute distribution, (2) solute permeability, (3) cell volume and shape, and (4) cellular resting potential, in that order.

12.3.1. *The Membrane-Pump Theory*

According to the membrane-pump theory, the cell owes its continued existence and unique chemical composition to a microscopically thin covering: the *plasma*

membrane. Permeant solutes are kept in the cell water at concentrations different from those anticipated from the rules of passive distribution by the continual activity of specific *pumps*. These pumps are located in the cell membrane and operate at the expense of energy stored in *high-energy-phosphate bonds* of ATP and other organic phosphates. In this theory, the survival of living cells requires **continual** energy expenditure. The bulk of intracellular water and the major intracellular ion, K^+ , exist in the free state, much as they are found in a dilute aqueous solution of KCl.

A *sine qua non* of the membrane-pump theory would be a self-consistent view of the chemical make-up of the cell membrane and the mode of permeation of different solutes through the cell membrane. Yet no broadly accepted, self-consistent view on these subjects can be found. A currently highly visible group of researchers seems to favor the view that the cell membrane represents a continuous phospholipid bilayer with a small number of specific rigid pores or channels (e.g., Na^+ channels, K^+ channels) which remain closed in resting cells but open transiently during activity (see Section 11.5.1.2(3)).

In volume changes, cells, according to the membrane-pump theory, behave like *osmometers*. Sustained cell shrinkage in concentrated solutions of permeant Na^+ and Cl^- is due to the *effective impermeability* of the cell membrane to Na^+ , in consequence of the continued operation of the postulated Na pump (Section 10.1).

In this theory, the outside surface as well as the inside surface of the cell membrane adjoin dilute aqueous solutions. The cellular resting potential is a *membrane potential*. Both the intracellular and extracellular concentrations of permeant ions and their relative permeability rates through the cell membrane (with or without the assistance of electrogenic pumps) determine the magnitude and polarity of the resting potential.

12.3.2. *The Association-Induction (AI) Hypothesis*

According to the AI hypothesis, the cell exists largely as a result of the cohesive interaction among its three major components: protein, ions, and water. Proteins, especially those that are in the form of an extended “fibrous” network, provide a more or less permanent “scaffold” on which other proteins, ions, and water are anchored. The plasma membrane is important to the cell’s existence, but only in the way that, say, the skin of a cucumber or a tomato is important to the cucumber’s or tomato’s existence, rather than in the way the membrane of a balloon is important to a balloon’s.

The physical states of ions and other solutes in the cell, as a rule, fall into two general categories: ions and other solutes are adsorbed on cellular macromolecules (primarily proteins) or freely dissolved in cell water. Virtually all cell water exists in the state of polarized multilayers. This **dynamic** structure is the consequence of the interaction of the bulk of cell water with the exposed $NHCO$ groups of some cell proteins which exist in the *fully-extended conformation*. Generally speaking, solubility in the polarized multilayered water follows the *size rule*: decreasing solubility with increasing size of molecules and hydrated ions.

The high level of K^+ in the resting cell is due to the adsorption of virtually all K^+ in the cell on the β - and γ -carboxyl groups of the aspartic and glutamic residues of cell proteins. The low level of (hydrated) Na^+ in the resting cell is partly due to its weaker adsorption energy (and hence inability to compete successfully against K^+ for the great majority of β - and γ -carboxyl groups), and in part to the low solubility of hydrated Na^+ in the cell water, due to its large size and an incompatibility of the surface structure of the hydrated ion with the dynamic cell water structure.

The protein-ion-water system of a living cell exists in a high (negative) energy, low-entropy *living state*—which requires the occupancy of key controlling protein sites by, and interaction with, the ultimate metabolic product, ATP (and its “helpers”, the congruous anions and the protein “X”). In serving this key role as a cardinal adsorbent, ATP remains as it is without undergoing hydrolysis. The cell exists in a (metastable) equilibrium state, requiring no continual energy expenditure.

Though often richer in lipids, the cell membrane shares the same kind of physico-chemical make-up as the cytoplasm (i.e., it is a closely associated protein-ion-water system maintained at a high (negative) energy, low entropy state). Water in the cell membrane is, as a rule, more intensely polarized than cytoplasmic water. Polarized water, as a rule, makes up a substantial portion of the cell surface in domains which are often dominated by fixed anionic β - and γ -carboxyl groups or fixed cations. Solute permeation is via either the polarized water (saltatory route) or by a process of association with, then libration around, followed by dissociation from, the cell surface fixed ions of opposite electric sign (adsorption-desorption route).

The cell volume and its regulation reflect a balance between (i) the tendency of the cell to gain more water in the form of additional polarized multilayers; (ii) the tendency of the cell to lose cell water, due to the lower equilibrium intracellular concentration (lower than the extracellular) of osmotically active solutes, and (iii) the restraining forces against swelling exerted by salt linkages formed between fixed anions (e.g., β - and γ -carboxyl groups) and fixed cations (e.g., ϵ -amino groups) on the same and on neighboring protein chains.

Only the outside surface of the cell membranes faces a dilute aqueous solution; the inside surface of the cell membrane is continuous with the cytoplasm in the sense that both the cell membrane and the cytoplasm represent fixed-charge systems comprising closely associated, cooperatively linked proteins, ions, and water. The cellular resting potential is a *surface-adsorption potential*. Its magnitude depends on the nature, density, and polarity of fixed ions at the cell surface (e.g., anionic β - and γ -carboxyl groups) and on the nature and concentrations in the external medium of free ions bearing the opposite electric charge as that of the fixed ion. The cellular resting potential does not depend on the concentration of the bulk of intracellular K^+ and other ions.

12.4. *Results of Testing of Theoretical Postulates on Inanimate Models*

The reader who has followed the story of this volume to this point may have noted that all aspects of the association-induction hypothesis are derived from

a single set of deduced postulates: the manifestation of closely associated, cooperatively linked protein-ion-water systems maintained at a high (negative) energy, low entropy living state.

The original Boyle-Conway version of the *membrane theory* was also derived from a single postulate, i.e., the atomic sieve. Repeated efforts to verify this atomic-sieve concept in inanimate model systems, however, all ended in failure (see Section 1.3.). Since the disproof of the Boyle-Conway version of the original membrane theory, its replacement, the membrane-pump theory, has not progressed far beyond being an ad hoc, patched-together version of the original membrane theory. Proponents of the membrane-pump theory have not attempted to present a coherent, comprehensive explanation of *all* basic aspects of cell physiology, some of which the proponents of the original membrane theory, like Boyle and Conway, had tried but failed to explain (Section 1.3). The addition of the pump concept, exemplified by the Na pump, is yet another postulate that has not been successfully verified in inanimate model systems, despite great efforts made (see Section 2.4.4.1.).

Similar difficulties have been encountered in attempting to confirm in inanimate models the theoretical postulates based on the membrane-pump theory concerning membrane permeability and electric potentials (Sections 9.1.3., 9.2.1.2., 9.2.1.4, 11.3.2.1). Most conspicuous is the repeated failure to find an inanimate model membrane which exhibits a true *membrane potential* in which different *rates of permeation* of ions through a membrane model determine the magnitude of the electrical potential difference across it. As mentioned in Section 11.3.2.1., in every case studied, the electrical-potential difference measured across the model membrane turned out to be either a single surface-adsorption potential at one surface alone or an algebraic sum of two surface potentials, one on each side of the membrane model. While they contradict the membrane (pump) theory, these findings are in full accord with the surface-adsorption-potential theory of the cellular resting potential, an integral part of the association-induction hypothesis.

Perhaps even more revealing is the recurring return of the membrane-pump theory to the atomic-sieve idea. As discussed earlier, the atomic sieve was first introduced by Moritz Traube, in the middle of the last century, to explain semi-permeable behaviors of copper-ferrocyanide membranes. It was disproved in the early part of this century (Section 1.2.2.), reintroduced and disproved again in the thirties in connection with the downfall of the Boyle-Conway special version of the atomic-sieve theory (Section 1.3), and once more reintroduced as a key concept used in the construction of the Na⁺-channel, K⁺-channel models now popular (Section 11.5.1.2(3)).

With the exception of the copper-ferrocyanide membrane osmometer demonstrating van't Hoff's law of osmosis, few, if any, of the major postulates of the membrane-pump theory have been put to rigorous testing or, if so, survived it. In sharp contrast, the AI hypothesis has easily passed tests on inanimate models on each basic issue. For details, the reader may refer to Sections 4.2 and 5.2.5.1 on model studies for solute distribution; Sections 9.2.1.1. and 9.2.2.1. on solute permeability; Section 10.2.1 on cell volume regulation; and Section 11.3.2.1 on cellular electrical potentials.

12.5. *The Fulfillment of All the Required Criteria for the Completion of a Scientific Revolution*

The starting point for a scientific revolution is the existence of a time-honored scientific theory which underlies the explanations of a spectrum of related natural phenomena. A revolution begins with the introduction of a contending new theory which deals either with the same or with a broader set of natural phenomena. The new theory is often built upon diametrically opposite basic postulates from those on which the old theory was built. I believe that a successful revolution depends upon meeting a set of five criteria (for background information, see Kuhn 1962, 152).

Criterion 1: The accomplishment of one (or more) crucial set(s) of experiments disproving the old theory, which has (or have) successfully stood the test of (a prolonged period of) time.

Criterion 2: The demonstration that all of the key evidence once considered to unequivocally support the old theory is incorrect or equivocal.

Criterion 3: The disproof of the fundamental postulates of the old theory and the verification of the postulates of the new theory.

Criterion 4: The demonstration that the new theory can predict and explain significant experimental findings that can be explained by the old theory, *as well as* other significant experimental findings which the old theory *cannot* explain.

Criterion 5: Establishing that the new theory, cast in the rigorous form of equations, can quantitatively explain the experimental findings that can also be quantitatively explained by the old theory, *as well as* those that *cannot* be quantitatively explained by the old theory.

In the following section, the five criteria cited above are used to determine if the revolution thus far discussed can be judged complete. Since I am here summarizing earlier discussion, the reader is referred to prior sections of this book as we proceed.

CRITERION 1: Crucial Experimental Disproofs of the Membrane-Pump Theory

A. Crucial Experimental Disproofs of the Membrane-Pump Hypothesis

1. Excessive energy need of the Na pump at the plasma membrane

Under controlled conditions, the Na pump alone would require, at a minimum, 15 to 30 times the total energy available in the cell in order to maintain the steady low level of the Na⁺ ions found in living cells (Section 2.2.). This calculation is based on the assumption that ATP, ADP, and creatine phosphate all contain a large quantity of utilizable energy, an assumption long proven incorrect (Section 2.2.3). Therefore, the true energy discrepancy vastly exceeds even the "15 to 30 times the energy available" figure quoted (Section 2.2.3.).

Three remedial postulations introduced in order to lower the energy requirements of the postulated Na pump were repeatedly put to test and, in time, all disproven (Section 2.2.4.).

2. *The Na pump is only one of the many pumps required at the plasma membrane*

Countless types of ions and solute molecules found in the cells' natural environment, as well as ions and other solutes already synthesized and yet to be synthesized would require pumps (Section 2.2.5).

3. *More pumps required at the membranes of subcellular particles*

Pumps are also required at the membranes of subcellular particles, which, due to their much larger surface area, require even more energy than similar pumps at the plasma membrane (Section 2.2.6.).

The crucial experimental disproof described above (Criterion 1A1) was first published in full in 1962. The main conclusions, as well as the experimental findings that led to the conclusions, have remained unchallenged ever since. ***Criterion 1 for a successful revolution has thus been fulfilled.***

B. *Additional Experimental Disproofs of the Membrane-Pump Theory*

1. *Cytoplasm-free membrane sac does not pump Na⁺ against concentration gradients*

With both ends tied, filled with sea water and ATP, cytoplasm-free squid-axon-membrane sacs offered an ideal preparation for testing the pump theory. Intense efforts have been made to demonstrate active Na⁺ (and K⁺) transport against concentration gradients (Section 2.3.); these have failed. Years have gone by since the announcement of the failed attempts more than a quarter of a century ago (repeatedly cited in many publications); no publication has appeared disputing the validity of the announced failure. ***Criterion 1 has been fulfilled a second time.***

2. *Cells without a functional cell membrane and (postulated) pumps accumulate K⁺ and exclude Na⁺ as do normal cells*

A set of crucial experiments establishing, with the aid of the EMOC technique, that selective accumulation of K⁺ and exclusion of Na⁺ do not require a functional cell membrane and (postulated) pumps, was published in 1978 (Section 4.4.2.1.) and has remained unchallenged ever since. ***Thus Criterion 1 has been fulfilled a third time.***

CRITERION 2: Conclusions from Evidence Once Widely Held as Supporting the Membrane-Pump Theory Reversed or Made Equivocal

A. *Reversal of Evidence for Free Cell K⁺ from K⁺-Mobility Measurements*

High mobility of K⁺ measured in squid axons (and in frog muscle cell segments) was once widely believed to have proven the free state of K⁺ in living cells (Section 2.4.1.). Later work showed that continued normal electrical activity

used in monitoring the health of the squid axon studied did not insure the health of the cell's cytoplasm. Measuring mobility of K^+ in frog muscle cells, Ling and Ochsenfeld reproduced the high K^+ -mobility earlier reported only in cytoplasm inadvertently injured or deliberately killed. In healthy cytoplasm, K^+ -mobility is only one-eighth of that in an isotonic salt solution. These data contradict the membrane-pump theory, but are in harmony with the AI hypothesis (Section 2.4.1.).

B. *Reversal of Evidence for Free K^+ from K^+ -Activity Measurements with Intracellular Microelectrodes*

Intracellular K^+ -sensitive microelectrodes were introduced to measure K^+ activity in very large cells. The early observations were that the K^+ activity in the cells was very close to that of an isotonic solution of KCl, in support of the membrane-pump theory. Subsequent extensive studies of large varieties of cell types revealed an overview quite different from the earlier one. The measured K^+ -activity varied widely from 26% to 120% of the average concentration of K^+ measured by chemical analysis. These data contradict the membrane theory, according to which the K^+ activity should uniformly equal that of a free solution containing the same K^+ concentration. On the other hand, the data are readily explained in terms of the AI hypothesis (Section 2.4.2.).

C. *Reversal of Alleged Proof for Free Water in Living Cells from the Equal Partition of Urea and Ethylene Glycol Between Cell Water and the External Medium*

The demonstration by Hill and others of equal partition of urea and ethylene glycol between cells and their environments was once widely believed to have provided the crucial evidence for the existence of (only) normal free liquid water in living cells (Section 1.4.). In extensive model studies, Ling and coworkers showed that Hill's finding offers no evidence for normal liquid cell water. In accordance with the *size rule* (and other relevant rules), model polarized water which (partially) excludes Na^+ , sugars, etc., does not exclude urea or ethylene glycol (Section 5.2.5.1(3) and (4)).

D. *Alleged Proof of Na Pump Made Equivocal*

Labeled Na^+ in a globule of gelatin injected into amphibian eggs existed at levels lower than in the external medium, after the Na^+ in the gelatin globule had reached diffusion equilibrium with Na^+ in the external medium (Horowitz and Paine, 1979). This sustained low level of Na^+ was believed to have proven continual outward pumping of Na^+ at the plasma membrane of the egg. However, the authors of this work ignored implications of other aspects of their own experimental observations. Thus, K^+ trapped in the gelatin globule exchanged very slowly and must in the meanwhile have functioned as an effectively *impermeant* cation. As such, the trapped K^+ reduced the steady level of other *permeant* cations like Na^+ , as demanded by the mechanism of Donnan equilibrium (Section 2.4.3).

E. *Evidence of Solute Pumping in Hollow Membrane Vesicles Reversed or Made Equivocal*

1. *Natural Membrane Vesicles*

(a) *Red Blood Cell Ghosts*

Active transport of K^+ and Na^+ has been demonstrated in red blood cells that have lost a considerable portion of cytoplasmic proteins following hypotonic lysis. Later studies revealed that the reuptake of K^+ and extrusion of Na^+ of these ghosts quantitatively depend on the concentration of the cytoplasmic proteins (primarily hemoglobin) remaining in the ghosts. In "white ghosts" with intact cell membranes and K,Na -activated ATPase, but with virtually no hemoglobin or other cytoplasmic proteins, no active transport takes place (Section 2.4.4.2.(1)). This finding echoes similar failure to demonstrate active transport of Na^+ in healthy, axoplasm-free, squid-axon-membrane sacs, mentioned under Criterion 1B.

(b) *Other Natural Vesicles*

Studies of solute uptake in bacterial vesicles, sarcoplasmic-reticulum vesicles, and other vesicles have also been widely regarded as having provided support for the membrane-pump theory. However, a closer look reveals that these conclusions were equivocal because the solid contents of these vesicles are not those of empty vesicles, but equal or exceed those of intact cells (Section 2.4.4.2.(2) and (3)).

2. *Artificial Membrane Vesicles*

Claims have been made and widely cited that pure phospholipid-membrane vesicles, containing isolated K, Na -activated ATPase, actively transport Na^+ . Careful examination of the data lead to a different conclusion: it is the different rates of *leakage* of labeled Na^+ from the vesicles during their passage through the Sephadex column (a step introduced to separate the fragile labeled Na^+ -loaded vesicles from the labeled Na^+ in the radioactive Na^+ -loading solution) that gave the false impression of active transport (Section 2.4.4.1.).

Summarizing Criterion 2, one concludes that all the major pieces of evidence once widely believed to verify the membrane-pump theory have been shown to be either incorrect or equivocal. ***Thus Criterion 2 for a successful scientific revolution has also been duly satisfied.***

CRITERION 3: Disproofs of Key Postulates of the Membrane-Pump Theory and Verification of the Key Postulates of the Association-Induction Hypothesis

A. *Disproof of Key Postulates of the Membrane-Pump Theory*

1. *Disproofs of the Free- K^+ Postulate of the Membrane-Pump Theory*

Extensive evidence now exists against the free- K^+ concept and will be discussed under B.1. below.

2. *Disproof of the Free-Water Postulate of the Membrane-Pump Theory*

Extensive evidence now also exists against the free H₂O concept and will be discussed under B.2. below.

3. *Disproof of the Membrane-Pump Concept as the Basis for the Selective K⁺ and Na⁺ Distribution in Unifacial¹ Living Cells*

See paragraph A.1. under Criterion 1 above.

B. *Verification of Key Postulates of the Association-Induction Hypothesis*

1. *Verification of the Adsorbed State of Cell K⁺*

(a) *Verification of Deduced Postulate in Inanimate Model Systems*

(1) The postulate of enhanced counterion association with charge fixation:

Confirmation of this postulate was achieved in the demonstration of enhanced association with countercations following the joining together of isobutyric acid into polyacrylic acid and in the enhanced counterion association observed in non-cross-linked and cross-linked polystyrene sulfonate (Section 4.1).

(2) The postulate of stoichiometric binding of alkali-metal ions on β - and γ -carboxyl groups of proteins:

Confirmation was achieved in hemoglobin after the elimination of competing fixed cations (Section 4.2).

(b) *Verification of the Localized Adsorption of K⁺ and Other Alkali-Metal Ions on β - and γ -Carboxyl Groups of Proteins at the A Bands of Frog Muscle Cells*

(1) *Confirmation of the Predicted Localized Distribution*

Since about half of the β - and γ -carboxyl groups of voluntary-muscle proteins are carried by myosin, and since myosin is found only in the A bands, the AI hypothesis predicts that the majority of the muscle K⁺ and other ions that can reversibly and stoichiometrically replace K⁺ (e.g., Cs⁺, Tl⁺, Rb⁺) will be found in the A bands. Confirmation of this key postulate has been extensive and essentially unanimous. There has been:

i. autoradiographic demonstration of localized distribution of radioactive Cs⁺ and Tl⁺ in A bands in air-dried and in frozen-hydrated muscle fibers (Section 4.4.1.);

ii. transmission-electron-microscopic demonstration of localization of electron-dense Cs⁺ and Tl⁺ at the A bands in frozen dried as well as frozen hydrated muscle cell preparations (Section 4.4.1.);

iii. dispersive x-ray microprobe analysis revealing high density of K⁺ at the A bands (Section 4.4.1.)

(2) *Confirmation of the Adsorption of K⁺ and Other Alkali-Metal Ions on β - and γ -Carboxyl Groups at the A Bands*

i. Pinpointing the K⁺-adsorbing sites at the A bands: The same sequential order of selective accumulation (e.g., Tl⁺ > Cs⁺ > Na⁺) seen in normal cells is preserved in muscle cells without a functional membrane and therefore without the postulated pumps (Section 4.4.2.1.). Differences among

Ti^+ , Cs^+ , and Na^+ are only in short-range attributes; these differences can be recognized only in consequence of close-contact adsorption. Since this close-contact adsorption does not occur at the cell membrane, it must occur primarily in the cytoplasm at the A bands.

ii. The identification of the close-contact-adsorption sites at the A bands as β - and γ -carboxyl groups: acid titration yielded a $\text{p}K_a$ of the alkali-metal ions binding acidic groups characteristic of β - and γ -carboxyl groups (Section 4.4.3.1); confirmation of predicted pH-dependent reduction of alkali-metal accumulation in 2-mm muscle segments by specific carboxyl reagent, EDC (Section 4.4.3.2).

2. Verification of the Existence of the Bulk of Cell Water in the Adsorbed State of Polarized Multilayers

According to the polarized-multilayer theory of cell water, two juxtaposed surfaces each containing a checkerboard of positive and negative sites at proper distances apart (NP-NP system), or a matrix of linear chains containing alternately positive and negative sites also at proper distances apart (NP-NP-NP system) cause multilayer polarization of water. In polarized multilayers, the permanent and induced dipole moment of each water molecule interacts with similar dipoles of not just the water molecules nearer or farther away radially from the fixed-charge sites, but also with dipoles of water molecules surrounding it laterally. Each water molecule, thus "clamped down", is subject to motional restriction, in particular rotational-motional restriction. Polymer chains containing only *N* or *P* sites interspersed between vacant (*O*) sites at proper distances apart constitute what are referred to as *NO-NO-NO* systems and *PO-PO-PO* systems respectively. Like an *NP-NP-NP* system, these variants exercise similar effects on the motional freedom of the water they polarize in multilayers. Rotational-motional restriction of the bulk-phase water in model systems and in living cells is therefore a most fundamental derived postulate (or prediction) of the polarized-multilayer theory of cell water.

Another important derived postulate is size-dependent solvency reduction for solutes in polarized water (the *size rule*) (Section 5.2.3). Other major derived postulates concern increased osmotic activity, enhanced vapor sorption, and freezing-point depression. The confirmations of these derived postulates in inanimate model systems and in living cells are presented together.

- (a) Verification of the Primary Postulate of Reduced Rotational and Other Motional Freedom of Water in Model *NP-NP-NP* Systems (or Modifications) and in Living Cells
 - (1) *Quasi-Elastic Neutron Scattering (QENS)*

The scattering of slow neutrons permits measurement of the rotational (and translational) diffusion coefficient of bulk-phase water, thereby offering the means of testing the predicted lowering of these diffusion coefficients in living cells and in model systems by the polarized multilayer theory of cell water. The work of Trantham et al. (1984) on brine shrimp cysts and of Heidorn et al. (1986) on frog muscle, as well as the work of Rorschach (1984) on model polymer solution of polyethylene oxide (PEO) (an *NO-NO-NO* system), confirmed this

prediction [Section 5.2.5.2(3)]. QENS confirmation of motional restriction offers the most important evidence for this postulate, because QENS measures the motional freedom of the average, and hence the majority, of water molecules in the system.

(2) *Nuclear Magnetic Resonance (NMR)*

In a PEO solution, free of both paramagnetic and diamagnetic “impurities,” NMR can also measure rotational-motional freedom of bulk-phase water. The NMR correlation time (τ_r) observed indicates a modest reduction of rotational freedom (e.g., the τ_r of polarized water is 3 to 19 times longer than the τ_r of normal liquid water). In living cells, τ_r is also reduced although the reduction is obscured by the presence of paramagnetic ions and proteins [Section 5.2.5.2(1)].

(3) *Ultra-High Frequency Dielectric Studies*

Dielectric studies at ultra-high frequency (up to 75 GHz) demonstrate complete lack of free normal liquid water in brine shrimp cyst cells. The bulk of water in this and other types of living cells studied, as well as in solutions of model polymers including PEO, PVME, and PEG, revealed lower characteristic frequency and longer Debye correlation time, τ_D , in agreement with both QENS and NMR findings [Section 5.2.5.2(2)].

(b) *Verification of the Requirements of NP-NP-NP Systems (or Equivalents) for Water Solvency Reduction*

A matrix of proteins existing in the fully-extended conformation constitutes an NP-NP-NP system, and polarizes water in multilayers on the exposed polypeptide NHCO groups. Water so polarized has reduced solubility for Na^+ , sugars, free amino acids and other large solutes according to the *size rule*, and exhibits other physical properties seen in living cells. Native proteins, with most NHCO groups locked in α -helical or other inter- or intramacromolecular H bonds, have been shown to have much less or no effect on water solvency, in agreement with AI hypothesis.

Oxygen-containing polymers [e.g., polyethylene oxide (PEO) and polyvinylpyrrolidone (PVP)] satisfy the theoretical requirements of a NO-NO-NO system. Like fully-extended protein chains, they also polarize, orient, and immobilize bulk-phase water (Sect. 5.2).

(c) *Verification of Other Postulated Properties of Water Existing in the State of Polarized Multilayers*

(1) High osmotic activity: The osmotic activity of polarized water far exceeds that expected from the molar concentration of the fully-extended proteins. This excessive osmotic activity agrees with theory, which requires the interaction of water with fully-extended cell proteins to account for most of the cells' osmotic activity (since the major cell ion, K^+ , is adsorbed and thus osmotically inactive) (Section 5.2.5.4).

(2) Lowered freezing point and reduced rate of freezing: Water in solutions of native proteins at concentrations as high as 50% exhibits no freezing-point depression. In contrast, water existing in the state of polarized multilayers has a lower freezing temperature (and reduced rate of freezing); the degree of lowering follows the protein (e.g., gelatin) or polymer (e.g., PEO) concentration (Section 5.2.5.5). At very high concentrations (e.g., 60%), the water

might not be freezable at liquid-nitrogen temperature. Data agree with the observed unusual freezing pattern seen in living cells.

(3) High vapor sorption: Water in model systems containing fully-extended proteins or polymers, and water in living cells, follows Bradley's multilayer adsorption isotherm. At physiological vapor pressure, polymers and extended proteins as well as living cells take up a comparably greater amount of water, while solutions of native proteins take up much less (Section 5.2.5.3).

(4) The pattern of nonelectrolyte distribution: Linear distribution and the *size rule* are followed by both model polarized water and living cells [Section 5.2.5.1(3)].

CRITERION 4: The Association-Induction Hypothesis Can Explain All Major Experimental Findings That Can Be Explained By The Membrane-Pump Theory, As Well As Other Findings Which The Old Theory Cannot Explain

The experimental findings that both the membrane-pump theory and the AI hypothesis can explain are not to be recited here, because there are no known major phenomenon that can be explained only by the membrane-pump theory. In the following discussion, I review three sets of observations concerning each subject that can be explained by the AI hypothesis, but not by the membrane-pump theory.

A. *Solute Distribution*

1. The AI hypothesis can readily explain the unequal distribution (between cell water and its environment) of *any* water-soluble compound in existence or yet to be synthesized, regardless of their total number (Section 8.1). The membrane-pump theory cannot explain the unequal distribution of *any* water-soluble compound, because the limited energy and limited space in the cell membranes cannot accommodate an endless number of pumps (Section 2.2.5).

2. The AI hypothesis can explain why nonelectrolyte distribution in living cells follows the *size rule*—higher *q*-value for small solutes and lower *q*-value for larger solutes [Section 5.2.5.1(4)]. The membrane-pump theory cannot explain the dependence of *q*-value on molecular weights of the solutes.

3. The AI hypothesis can readily explain the rectilinear distribution of many solutes found in concentrations lower than those of the bathing medium (Section 5.2.3). The membrane-pump theory cannot (see endnote [1] of Chapter 8, also Ling, 1988a).

B. *Permeability*

1. The AI hypothesis can easily explain the bulk-phase-limited diffusion of water into and from frog ovarian eggs and giant barnacle muscle fibers (Section 9.2.1.3.). The membrane-pump theory cannot.

2. The AI hypothesis can readily explain the permeability of living cells to very large molecules and hydrated ions (Sections 9.1.2; 9.2.1.3; 11.5.2.5.(5)), while the model of lipid bilayer cell membranes with rigid pores of small dimensions to fit K^+ and Na^+ (and then only at activity) cannot (Section 11.5.1.2(3)).

3. The membrane-pump theory cannot explain why, after extraction of 95% of the lipids from the inner membrane of liver mitochondria, the trilaminar structure of the cell membrane remains largely unchanged (Section 9.1.3.). The AI hypothesis can explain this phenomena easily, because according to the AI hypothesis, lipids in this type of membrane exist only in pockets and do not form a continuous layer, as required and postulated in the conventional lipid-bilayer model.

C. *Cell Volume and Shape*

1. Cell volume is the sum of the volume of the cell's dry matter (primarily proteins) and the volume of cell water. The invariance of cell volume (or water content) per unit dry weight of each cell type cannot be explained by the membrane-pump theory, because in this theory there is no direct interaction between cell proteins and bulk cell water. But the invariance of cell volume per unit dry weight of each cell type is fully in harmony with the AI hypothesis. According to this theory, cell water exists in the cell in consequence of interaction primarily with certain fully-extended proteins, which make up a constant proportion of the cell's total protein content (Section 5.2.5.3.).

2. The membrane-pump theory cannot explain why the swelling and shrinkage of frog muscle does not follow the prediction of van't Hoff's law. Attempts to interpret the departure as due to the presence of osmotically inactive water, dead cells or the membrane-pump mechanism have all been shown to be invalid (Section 10.1). On the other hand, the entire range of water content and hence cell volume, in the presence of varying water activity, is in accord with the polarized multilayer theory of cell water (Section 5.2.5.3).

3. The membrane-pump theory cannot explain why, in isotonic solutions of various salts, only salts of certain cations and anions (e.g., K^+ and Cl^-) cause extensive sustained swelling, while much less swelling occurs in isotonic solutions of other salts (K^+ , SO_4^-), and shrinkage in still others (Mg^{++} , SO_4^-)—even though K^+ , Cl^- , SO_4^- , and Mg^{++} are all permeant (Ling 1962, 333; Ling et al. 1979). Nor can the membrane-pump theory tell why these swelling and shrinkage responses persist when the (long) muscle cells are cut into 2-mm- and 4-mm-long segments with both ends open (and no membrane regeneration). The AI hypothesis explains these phenomena with ease: KCl is more effective than K_2SO_4 and still more effective than $MgSO_4$ in dissociating and hence removing the restraining salt linkages against uptake of additional layers of polarized water (Section 10.2.2).

D. *Cellular Electrical Potential*

1. The membrane-pump theory cannot explain why the resting potential (ψ) of muscle and nerve is indifferent to the concentration of external (highly permeant) Cl^- and Mg^{++} , without resorting to the questionable practice of partial deletion of a rigorously derived equation [Section 11.2.3.1]. The indifference of ψ to external Cl^- and Mg^{++} concentration is easily explained by the AI hypothesis: in muscle and nerve cells, the cell surfaces carry only (isolated rather

than paired or chelating) monovalent fixed anions, and only monovalent free ions of the opposite electric charge affect ψ , while free ions of the same charge (e.g., Cl^-) or divalent cations do not (Sections 11.3.2.2(2); 11.3.2.3).

2. The membrane-pump theory cannot explain the existence of a resting potential in the face of the now-proven adsorbed state of the bulk of intracellular K^+ . The AI hypothesis concerning resting potential is in full harmony with the adsorbed state of the bulk of intracellular K^+ [Sections 11.2.4(2); 11.3.2.2(3)] because ψ , being a surface-adsorption potential, is indifferent to intracellular ion concentrations.

3. The membrane-pump theory cannot explain why it is the relative *adsorption constants*, rather than their *permeability constants* of external monovalent ions, that determine this relative depolarizing action on ψ . The AI hypothesis is in full accord with these observations (Section 11.3.2.3).

CRITERION 5: The Quantitative Equations Derived on the Basis of the Association-Induction Hypothesis can Explain Major Phenomena Described by Quantitative Equations Based on the Membrane-Pump Theory, as well as Other Major Observations that Cannot be Described by the Quantitative Equations Based on the Membrane-Pump Theory

A. Solute Distribution

1. Membrane-Pump Theory

The only equations proposed for the steady levels of solutes in living cells is for cases where the intracellular solute concentration exceeds the extracellular concentration (e.g., equation A in endnote 1 of Chapter 8). No equation, for example, has been proposed for the distribution of cell Na^+ which exists at lower concentration than in the external medium, despite immense efforts spent in research on this subject (see Ling 1988a).

2. The AI Hypothesis

A general equation for the equilibrium solute distribution in living cells, as well as model systems, was proposed by Ling in 1965 and is presented in Section 8.1 as equation 16.

$$[p_i]_{\text{in}} = \underbrace{\alpha q_i [p_i]_{\text{ex}}}_{\text{free}} + \sum_{l=1}^N \frac{[f]_l}{2} \underbrace{\left(1 + \frac{\xi_l - 1}{\sqrt{(\xi_l - 1)^2 + 4\xi_l \exp \gamma_l / RT}} \right)}_{\text{adsorbed}}. \quad (16)$$

This equation and its various simplified versions shown as equations 15, 17, and 18 (the Troshin equation) can quantitatively describe (to the best of my knowledge) all equilibrium distribution of solutes in living cells so far studied (see Chapter 8 and Ling 1984, Chapter 11), including the equilibrium distribution of Na^+ in living cells.

B. *Permeability*

1. *Membrane-Pump Theory*

Equations for the rate of permeation into living cells have been introduced based on the assumption that combination of the permeant solute with a carrier is required before the solute's dissociation from the carrier and entry into the cells. An example is the equation presented by Epstein and Hagen (1951) for the entry of labeled Rb^+ into barley roots (see Section 9.2.2.1., also Ling 1984, 98). Since the carrier concept has been disproven, equations based on this concept are no longer on solid ground. The data that fit this type of equation, of course, also fit equations based on the AI hypothesis which are on sound foundations.

2. *The AI Hypothesis*

Solute permeation rates into living cells and various model systems have been successfully described by a general equation for membrane-limited permeation (see equation 26 in Section 9.2.2.2).

$$v_i = A_i [p_i]_{\text{ex}} + \sum_{l=1}^N \frac{v_i^{\text{max}(l)}}{2} \left(1 + \frac{\xi_l - 1}{\sqrt{(\xi_l - 1)^2 + 4\xi_l \exp(\gamma_l/RT)}} \right). \quad (26)$$

Equation 26, and its simplified versions (equations 24, 27) as well as more elaborate versions (equation 5 in Ling and Ochsenfeld 1965), are able to explain (as far as I know) all types of permeation rates that cannot be explained by the membrane-pump model (as well as those that can be), including the following: why external K^+ facilitates Rb^+ entry, while external Rb^+ only inhibits K^+ entry into frog muscle cells; why there is autocoooperativity in the rate of solute entry (Ling 1986b). Other equations introduced (equations 10 and 14 in Ling et al. 1967) can describe simple and more complex bulk-phase-limited diffusion of water into living cells (and variations), which cannot be predicted by the membrane-pump model and its equations.

C. *Cell-Volume Regulation*

In terms of the membrane-pump theory, the van't Hoff equation describing the apparently perfect osmometer-like behavior of living cells turns out to be valid only in describing the volume changes of tonoplast-enclosed, and dilute-aqueous-solution filled central vacuoles of old plant cells, but not the plasma-membrane-enclosed cytoplasm of plant or animal cells.

Equation 33 demonstrates that the volume of a cell is in essence that of its water content plus a constant. Cell-volume regulation is therefore the regulation of cell-water content. The general equation for cell water (a), expressed in grams of cell water per 100 grams of cell solids is, according to the AI hypothesis:

$$\log \left[1 + \frac{(1-q)n_2}{n_1} \right] = K_1 K_3^a + K_1. \quad (34)$$

This equation is capable of explaining the different cell volumes maintained in solution containing different concentrations of the *permeant* as well as *impermeant* nonelectrolytes in the external medium, depending on the molecular weights of the nonelectrolytes (Section 10.2.1.2).

D. Cellular Resting Potentials

The Hodgkin-Katz-Goldman equation for cellular resting potential was derived on the basis of the membrane-pump theory. As shown below, only the boxed-in part has been experimentally verified. The remainder has been falsified or is in doubt:

$$\boxed{\psi = \frac{RT}{F} \ln \left[\frac{P_K [K^+]_{in} + P_{Na} [Na^+]_{in} + P_{Cl} [Cl^-]_{ex}}{P_K [K^+]_{ex} + P_{Na} [Na^+]_{ex} + P_{Cl} [Cl^-]_{in}} \right]} \quad (40)$$

The boxed-in part is *in form* the same as the *complete* equation concerning resting potential first presented in the subsidiary surface-adsorption theory of the AI hypothesis:

$$\psi = \text{Constant} - \frac{RT}{F} \ln \left[\bar{K}_K [K^+]_{ex} + \bar{K}_{Na} [Na^+]_{ex} \right]. \quad (44)$$

One difference between the boxed-in verified part of equation 40 and equation 44 lies in the significance of the sets of coefficients. They are *permeability constants* in equation 40 and *adsorption constants* in equation 44. The results of experimental studies by Edelmann favored equation 44 (Section 11.3.2.3).

A more general equation for the surface-adsorption theory was later presented and is shown in Section 11.4.1 as equation 48.

$$\psi = \text{Constant} + \frac{RT}{F} \ln \frac{1}{[K^+]_{ex}} \left[1 + \frac{\xi^s - 1}{\sqrt{(\xi^s - 1)^2 + 4\xi^s \exp(\gamma^s/RT)}} \right]. \quad (48)$$

To the best of my knowledge, all quantitative relationships between the resting potential and temperature, and between the resting potential and varying external K^+ concentrations, both in the presence and absence of various drugs and cardinal adsorbents, have been successfully described by this equation and its variants (Section 11.4.2).

The foregoing comparison between the five criteria necessary for a scientific revolution and the current status of the membrane-pump theory and of the association-induction hypothesis lead to a clear-cut conclusion: a revolution is now complete.

12.6. Outstanding Features of a Valid New Theory

A survey of history shows that, in each scientific revolution, a new theory has, as a rule: (1) broadened coverage beyond the old theory; (2) reduced complex and unrelated observations to coherent phenomena governed by simple rules;

and (3) predicted new phenomena unknown before. The broadening of coverage, the reduction of unmanageable information into simple rules, and the ability to predict new phenomena in turn provide the foundation for new practical applications. In the following sections, I examine the first three characteristics as they apply to the present new theory. The last feature, the prospect of new practical applications, will be the subject of the final section of this volume.

12.6.1. *Expanding Coverage*

That the revolution discussed in this volume has established a theory of the living cell far broader in scope than the membrane-pump theory it replaces requires no further elaboration. As it is without solid and consistent support from inanimate models, the membrane-pump theory is by and large descriptive and ad hoc. Mechanisms mentioned in the membrane-pump theory, like “channel opening,” “channel closing,” etc., are largely rephrasing of observations. The vast reach of the AI hypothesis concerning electronic and molecular mechanisms in physiological control by drugs, ATP, and other cardinal adsorbents, which makes up a good portion of this volume, is at once the substance and example of the much broader scope of coverage of the AI hypothesis.

12.6.2. *Simplicity in Governing Rules*

The simplifications achieved by the AI hypothesis for our understanding of the four most basic cell physiological manifestations—solute distribution, permeability, volume (and shape), and electrical potential—are well reflected, first, in the simplicity of the four sets of equations (equations 16, 26, 34, 48) and their variants that quantitatively describe most, if not all, manifestations of each of these physiological phenomena. Secondly, they are reflected in that each of the four sets of equations is itself the combination of two of the three basic quantitative relationships, each describing the relationship between two of the three major components of the living cell (proteins, water, solutes). These include: the relationship between solutes and cell water (equation 6); the relationship between solutes and cell proteins (and other macromolecules) and between cell proteins and cell proteins (and other macromolecules) (equation 7); and the relationship between cell water and cell proteins (and other macromolecules) (equation 4).

12.6.3. *Predicting New Relationships*

With the discovery of simple rules that govern what used to be massive amounts of fragmented knowledge, and with emphasis on mechanisms that are direct extensions of modern physics, the AI hypothesis has the ability to predict new phenomena. Indeed, this ability is unquestionably at once the hallmark and the most important attribute of all valid new theories. In the course of more than twenty-five years, the predictions of the AI hypothesis made, tested, and

confirmed have been many, I cite eleven examples here for the purpose of illustration.

(1) The concept of enhanced counterion association with charge fixation was first introduced in 1952 and elaborated in 1960 and 1962 (Ling 1952; 1960; 1962). This concept had an unusual history in that it had already been experimentally confirmed by Kern (1948) several years before the theory was proposed, although Kern's experimental work was not known to me until the late seventies. The theory of enhanced counterion association was later further confirmed by Ling and Zhang (Ling and Zhang 1983) (Section 4.1).

(2) The concept that the β - and γ -carboxyl groups of proteins in general have the inherent capability to selectively adsorb alkali-metal ions, but are prevented from doing so in native proteins due to salt-linkage formation was first suggested in 1952 (Ling 1952). It was confirmed in 1984 (Ling and Zhang 1984) (Section 4.2).

(3) The concept that the β - and γ -carboxyl groups of cytoplasmic proteins adsorb and cause the selective accumulation of K^+ in living cells was first introduced in 1951 and 1952 (Ling 1951; 1952). This prediction was *fully* confirmed only recently (see Section 4.4).

(4) The concept that protein in general exhibits *cooperativity* in the binding of ions and other solutes was introduced in 1962 (Ling 1962, 143) and further elaborated in 1964 (Ling 1964). Up to 1965, cooperativity in the accumulation of K^+ and Na^+ in living cells had never been observed. The development in 1969 of the technique of long-term preservation of isolated frog tissues made it possible, for the first time, to study equilibrium ionic distribution under experimental conditions in new ionic media (Ling and Bohr 1969). With this method, autocoooperativity in K^+ and Na^+ accumulation in frog muscle was first confirmed by Ling in 1966 (Ling 1966) (Section 8.2) and has since been widely confirmed in many other tissues as well (Ling 1984, 345–362).

(5) The concept that the β - and γ -carboxyl groups of cell surface proteins provide a selective mechanism for ion permeation into living cells was first introduced briefly in 1952 and 1953 (Section 9.2.2.1), more extensively in 1960 and 1962 (Ling 1960; 1962). It was first experimentally confirmed in 1953 (Ling, 1953) and then in 1965 (Ling and Ochsenfeld 1965) (Section 9.2.2.1, see also Figure 9.12).

(6) The theoretical prediction that the cell surface β - and γ -carboxyl groups and their specific adsorption for alkali-metal ions give rise to resting (and action) potential was first briefly presented in 1955 and 1959 and in more detail in 1960 and 1962—thereby linking the ion-adsorption preference of the surface β - and γ -carboxyl groups to the magnitude of the resting potential. This prediction was confirmed quantitatively by Edelmann in 1973 (see Section 11.3.2.3).

(7) The quantitative theory of the action potential, in which the cell surface β - and γ -carboxyl groups mediating the inward surge of Na^+ should have a high *c*-value and show rank order of ion selectivity favoring Na^+ over K^+ , was briefly presented in 1957 and in more detail in 1960 and 1962 (Ling 1960; 1962). This prediction was confirmed by Chandler and Meves in 1965 and by Hille in 1968 [Sections 11.5.1.2; 11.5.2.5(4)].

(8) The polarized-multilayer theory of cell water was first introduced in 1965 (Ling 1965), then described in greater detail in 1972 (Ling 1972). In this theory, the bulk of cell water is subject to rotational-motional restriction. The concept was confirmed in 1984 by Trantham et al. (1984), using quasi-elastic neutron scattering, and in 1986 by Heidorn et al. (1986)—also by NMR and ultra-high frequency dielectric studies (see Section 5.2.5.2).

(9) The polarized-multilayer theory predicted that the repeating NHCO groups of fully-extended polypeptide chains effectively polarize water in multilayers (Ling 1972), and that water so polarized has reduced solvency for Na^+ , sugars, and free amino acids found as a rule in low concentration in living cells. A corollary of this theory is that native proteins with most of their polypeptide NHCO groups locked in α -helical and other inter- or intramacromolecular H bonds have much less ability to polarize water in multilayers and reduce solvency for Na^+ , etc. The confirmation of this prediction was briefly announced in 1978 (Ling et al. 1978) and presented in detail in 1980 (Ling et al. 1980, 1980a) (Section 5.2.5.1).

(10) The polarized multilayer theory predicts that the q -value of a solute in polarized multilayers decreases with the increasing size of the solute (the *size rule*). This prediction has been repeatedly confirmed (Ling et al. 1973; 1980; 1984, 272) and especially in very recent work (Ling and Hu 1988; Ling, Niu, and Ochsenfeld to be published) (Section 5.2.5.1).

(11) The AI hypothesis of cell volume predicts the dependence of cell volume (in a concentrated non-electrolyte solution of the same concentration) on the molecular weight of the non-electrolytes. This prediction has also been confirmed (Ling 1987) (Section 10.2.1.2).

In reviewing the confirmation of these and other theoretical predictions of the AI hypothesis illustrated above, one sees how the evolvement of the AI hypothesis has followed a standard pattern. Thus the general sequential nature of theory introduction followed by experimental confirmation has chronicled the fact that diverse aspects of the AI hypothesis have separately gone through the steps of classic *scientific method*. As a result, many major concepts introduced in the AI hypothesis have in fact gone a long way towards becoming understanding and new knowledge.

The fact that many aspects of AI theory have also been fully confirmed by inanimate model studies underscores their general validity, thereby reaffirming the belief first clearly propounded by Ludwig, du Bois-Reymond, von Helmholtz, and Brücke: living phenomena in general obey the same set of laws that govern the behaviors of the inanimate universe.

Considering the experimental verification of the predictions of the new theory and the failure of the old theory to produce verifiable predictions or to confirm them experimentally, one is brought to acknowledge an unspoken rule in the use of the *scientific method* (i.e., observation, hypothesis (which yields testable predictions), experimental confirmation of predictions, establishment of hypothesis as new knowledge): a scientific revolution is in fact the path, indeed the only path, of continued scientific progress after a favorable theory has failed the test of the method.

12.7. *The Future*

Predicting the future is an extremely difficult task. Witness the following example. On August 14, 1747, Benjamin Franklin wrote to his friend Peter Collinson about his famed study of electricity and its significance in these words: “If there is no other Use discover’d of Electricity, this, however, is something considerable, that it may help to make a vain Man humble . . .” (Fleming 1972). If an intellect as omnivorous and as imaginative as Franklin’s could not envisage any practical use of electricity other than making “a vain Man humble”, a mere 240 years before the emergence of a new world run on electricity, one might say that it is futile to speculate on the future possible uses of any basic knowledge.

As useful as electricity is today to mankind, one may argue that its benefits might not be entirely unqualified. Thus thoughtless and unrestrained use of electricity may deplete unrenowable resources as well as useful employment on which the happiness and dignity of many may depend.

What is clearer is that alleviating human suffering and protecting the survival of mankind against death-dealing bacteria and viruses, known and yet unknown, are good without qualification. The Chinese believe,

救人一命勝造七級浮屠

“Saving a life is superior to building a seven-storeyed pagoda in praise of God.”

I would also like to cite the words of Herman von Helmholtz, who as a physicist introduced the law of conservation of energy at the age of 26 and as a physician-physiologist wrote a hundred years ago the following: “Perhaps only he can appreciate the immense importance and the frightful practical scope of the problem of medical theory, who has watched the fading eyes of approaching death, and witnessed the distracted grief of affliction, and who has asked himself the solemn question, has all been done which could be done to ward off the dread event? Have all the resources and all the means which science has accumulated become exhausted?” (von Helmholtz 1881, 202).

Such drugs as penicillin and polio vaccine will save countless lives each year as long as humanity lasts. Yet the future discovery of the fundamental laws that determine drug effects, and the unlocking of the mystery of rational drug therapy, may produce countless effective drugs which are even more useful than penicillin and polio vaccines. Such discoveries are still for the future, but the AI hypothesis has already opened the door, if only very slightly. It is on this note of hope that I close this volume.

NOTES

1. For definition of *unifacial* and *bifacial* cells, see last paragraph of Section 2.2.5.

REFERENCES

- Abetsedarskaya L. A. Miftakhutdinova, F. G., and Fedotov, V. D. 1968 *Biofizika* 13:630
[Russian], *Biophysics* [English trans.] 13:750.
- Adrian, R. H. 1956 *J. Physiol.* 133:631.
- Aickin, C. 1986 *Ann. Rev. Physiol.* 48:349.
- Aizono, Y., Roberts J. E. Sonenberg, M., and Swislocki, N. I. 1974 *Arch. Biochem. Biophys.* 163:634.
- Akaike, N. 1975 *J. Physiol.* 245:499.
- Andreoli, T. E. and Troutman, S. 1971 *J. Gen. Physiol.* 57:464.
- Andreoli, T. E., Bangham, J. A. and Tosteson, D. C. 1967 *J. Gen. Physiol.* 50:1729.
- Andreoli, T. E., Tiffenberg, M., and Tosteson, D. C. 1967a *J. Gen. Physiol.* 50:2527.
- Andreoli, T. E., Denni, V. W. and Weigl, A. M. 1969 *J. Gen. Physiol.* 53:133.
- Anfinsen, C. B. 1962 *Brookhaven Symp. Biol.* 15:184.
———. 1967 *Harvey Lect.* 61:95.
- Anner, B. M. 1983 *FEBS* 158:7.
- Arrhenius, S. 1887 *Z. Physik. Chem.* 1:631.
- Armstrong, C. M. 1975 in: *Membranes: A Series of Advances*, Vol. III (G. Eisenman, ed.)
Academic Press, New York, p. 325.
- Avery, O. T., McLeod, C. M., and McCarty, M. 1944 *J. Expt. Med.* 79:137.
- Baker, P. E., Hodgkin, A. L., and Shaw, T. I. 1961 *Nature* 190:885.
- Baker, P. F., Foster, R. F., Gilbert, D. S. and Shaw, T. I. 1971 *J. Physiol.* (London) 219:487.
- Barchi, R. L. 1984 *Trends in Biochem. Sci.* 9:358.
- Bartell, F. E. 1911 *J. Phys. Chem.* 15:659.
- Baur, E. 1913 *Z. Elektrochem.* 19:590.
———. 1926 *Z. Elektrochem.* 32:547.
- Baur, E. and Kronmann, S. 1917 *Z. Phys. Chem.* 92:81.
- Bayliss, W. M. 1927 *Principles of General Physiology*, Longmans, Green, and Co. Ltd. London, 4th ed.
- Beatley, E. H., and Klotz, I. M. 1951 *Biol. Bull.* 101:215.
- Bendall, J. R. 1969 "Muscles, Molecules and Movement; An Essay in the Contraction of Muscle", Amer. Elsevier Publ. Co., New York.
- Benesch, R. and Benesch, R. E. 1969 *Nature* 221:618.
- Benesch, R., Benesch, R. E., and Rogers, W. I. 1954 in: *Glutathione* (S. Colowrick, ed.)
Academic Press, New York, p. 31.
- Benson, S. W. and Ellis, D. A. 1948 *J. Am. Chem. Soc.* 70:3563.
———. 1950 *J. Am. Chem. Soc.* 72:2095.
- Benson, S. W., Ellis, D. A., and Zwanzig, R. W. 1950 *J. Am. Chem. Soc.* 72:2102.
- Berendson, H. J. C., 1962, *J. Chem. Phys.* 36:3297.
- Berendson, H. J. C. and Edzes, H. T. 1973 *Ann. N.Y. Acad. Sci.* 204:459.
- Bernstein, J. 1902 *Pflügers Arch. Ges. Physiol.* 92:521.
———. 1912 *Elektrobiologie*, F. Vieweg und Sohn, Braunschweig.
- Berthelot, M. and Jungfleisch, H. 1872 *Ann. Chim. Phys.* 26:396.
- Bertina, R. M., Schrier, P. I. and Slater, E. C. 1973 *Bioch. Biophys. Acta* 305:503.
- Beutner, R. 1913 *Z. Elektrochem* 19:319, 467.
———. 1914 *Z. Phys. Chem.* 87:385.
- Bigelow, S. L., and Bartell, F. E. 1909 *J. Amer. Chem. Soc.* 31:1194.
- Blanchard, K. C. 1940 *Cold Springs Harbor Symp. Quant. Biol.* 8:1.
- Bloembergen, N., Purcell, E. M., and Pound, R. V. 1948 *Phys. Rev.* 73:679.

- Bochkareva, E. S., Lissen, N. M., and Girshovich, A. S. 1988 *Nature* 336:254.
- Bohr, C., Hasselbach, K., and Krogh, A. 1904 *Skand. Arch. Physiol.* 16:402.
- Boyd, I. A., and Forrester, T. 1968 *J. Physiol. (London)* 199:115.
- Boyer, P. D., Cross, R. L., Chude, O., Dahms, A. S., and Kanazawa, T. 1972 in: *Biochemistry and Biophysics of Mitochondrial Membranes* (G. F. Azzone, E. Carafoli, A. L. Lehninger, E. Qualierello, and N. Siliprandi, eds.), Academic Press, New York, p. 343.
- Boyle, P. J., and Conway, E. J. 1941 *J. Physiol.* 100:1.
- Bradley, S. 1936 *J. Chem. Soc* 1936:1467.
- Branch, G. E. K., and Calvin, M. 1941 *The Theory of Organic Chemistry, An Advanced Course*, Prentice-Hall, Englewood Cliffs, New Jersey.
- Bratton, C. B., Hopkins, A. L., and Weinberg, J. W. 1965 *Science* 147:738.
- Bregman, J. I. 1953 *Ann. N.Y. Acad. Sci.* 57:125.
- Brinley, F. J., and Mullins, L. J. 1968 *J. Gen. Physiol.* 52:181.
- Bronowski, J. 1973 *The Ascent of Man*, Little, Brown and Company, Boston.
- Brooks, S. C. 1940 *Cold Springs Harbor Symp. Quant. Biol.* 8:171.
- Brunauer, S., Emmett, P. H. and Teller, E. 1938 *J. Amer. Chem. Soc* 60:309.
- Brunori, M., Antonini, E., Wyman, J., Zito, R., Taylor, J. F., and Rossi-Fanelli, A. 1964 *J. Biol. Chem.*
- Buck, B., and Goodford, P. J. 1966 *J. Physiol.* 183:551.
- Bull, H. 1944 *J. Amer. Chem. Soc.* 66:1499.
- Bunch, W., and Edwards, C. 1969 *J. Physiol.* 202:683.
- Bunch, W. H. and Kallsen, G. 1969 *Science* 164:1178.
- Burawoy, A. 1959 in: *Hydrogen Bonding*, (D. Hadži and H. W. Thompson, eds.), Pergamon Press, New York.
- Burk, N. F. 1943 *J. Phys. Chem.* 47:104.
- Caillé, J. P., and Hinke, J. A. M. 1974 *Can. J. Physiol. Pharmacol.* 52:814.
- . 1960 *J. Physiol. (London)* 152:545.
- Caldwell, P. C., Hodgkin, A. L., Keynes, R. D. and Shaw, T. I. 1960 *J. Physiol. (London)* 152:561.
- Cameron, I. L. 1988 *Physiol. Chem. Phys. & Med. NMR* 20:221.
- Cameron, I. L., Hardman, W. E., Hunter, K. E., Haskin, C., Smith, N. K. R., and Fullerton, G. D. 1990 in "The State of Potassium in the Cell" compiled by W. Negendank and L. Edelmann, Scanning Microscopy International, P. O. Box 66507, AMF O'Hare (Chicago), Il 60666.
- Cardon, J. W., and Boyer, P. D. 1978 *Europ. J. Biochem.* 92:443.
- Careri, G., Fasella, P., and Gratton, E. 1975 *CRC Crit. Rev. Biochem.* 3:141.
- Carr, C. W. 1956 *Arch. Biochem. Biophys.* 62:476.
- Chambers, R., and Hale, H. P. 1932 *Proc. Roy. Soc. London Ser. B* 110:336.
- Chambers, R., and Höfler, K. 1931 *Protoplasm* 12:338.
- Chandler, W. K., and Meves, H. 1965 *J. Physiol.* 180:788.
- Chang, D. C., Hazlewood, C. F., Nichols, B. L., and Forschach, H. E. 1972 *Nature* 235:170.
- Chang, D. C., Rorschach, H. E., Nichols, B. L., and Hazlewood, C. F. 1973 *Ann. N.Y. Acad. Sci.* 204:434.
- Chang, T. and Penefsky, H. S. 1973 *J. Biol. Chem.* 248:2746.
- Changeux, J. P. 1981 *Harvey Lectures* 75:85.
- Chanutin, A. and Curnish, R. R. 1967 *Arch. Biochem. Biophys.* 121:96.
- Chanutin, A. and Hermann, E. 1969 *Arch. Biochem. Biophys.* 131:180.
- Chapman, N. B. and Shorter, J. 1972 *Advances in Linear Free Energy Relationships*, Plenum Publishing Corp., New York.
- Chaudry, I. H. 1982 *Yale J. Biol. Med.* 55:1.
- Chaudry, I. H. and Baue, A. E. 1980 *Biochem. Biophys. Acta* 628:336.
- Chaudry, I. H. and Gould, M. K. 1970 *Biochem. Biophys. Acta* 196:320.
- Chiang, M. C. 1987 *The Rule of Homologous Linearity of Organic Compounds*, Science Press, Beijing, Peoples Republic of China.
- Chiang, M. C., and Tai, T. C. 1963 *Sci. Sin.* 12:785.

- . 1985 *Physiol. Chem. Phys. and Med. NMR* 17:271.
- Christian, J. H. B. and Waltho, J. A. 1962 *Biochem. Biophys. Acta* 65:506.
- Chou, P. Y., and Fasman, G. D. 1974 *Biochem.* 13:211.
- . 1978 *Adv. Enzymol.* 47:45.
- Christensen, H. N. 1955 in: *Amino Acid Metabolism* (W. D. McElroy, and B. Glass, eds.), Johns Hopkins University Press, Baltimore, MD, p. 63.
- Clark, M. R., and Shoheit, S. B. 1976 *Blood* 47:121.
- . 1980–1981 *Tex. Rep. Biol. Med.* 40:417.
- Clegg, J. S., Szwarnowski, S., McClean, V. E. R., Sheppard, R. J., and Grant, E. H. 1982 *Biochem. Biophys. Acta* 721:458.
- Clegg, J. S., McClean, V. E. R., Szwarnowski, S., and Sheppard, R. J. 1984 *Phys. Med. Biol.* 29:1409.
- Cleveland, G. C., Chang, D. C., Hazlewood, C. F., and Rorschach, H. E. 1976 *Biophys. J.* 16:1403.
- Cohen, I. B. 1985 *Revolution in Science*, Harvard University Press, Cambridge.
- Cohen, G. N., and Monod, J. 1957 *Bacteriol. Rev.* 21:169.
- Cohn, W. E., and Cohn, E. T. 1939 *Proc. Soc. Exp. Biol. Med.* 41:445.
- Colacicco, G. 1965 *Nature* 207:936.
- Cole, K. S. 1932 *J. Cell. Comp. Physiol.* 1:1.
- . 1949 *Arch. Sci. Physiol.* 3:253.
- Cole, K. S., and Curtis, H. J. 1938–1939 *J. Gen. Physiol.* 22:671.
- Collander, R. 1959 in *Plant Physiology*, Vol. 2 (F. C. Steward, ed.) Academic Press, New York, p. 3.
- Collander, R. and Bärlund, H. 1933 *Acta Bot. Fenn.* 11:1.
- Conway, E. J. and Cruess-Callaghan, G. 1937 *Biochem J.* 31:828.
- Conway, E. J., Kernan, R. P., and Zadunaisky, J. A. 1961 *J. Physiol.* 155:263.
- Cooke, R. and Kuntz, I. D. 1974 *Ann. Rev. Biophys. Bioengineer.* 3:95.
- Cope, F. W. 1967 *J. Gen. Physiol.* 50:1353.
- . 1969 *Biophys. J.* 9:303.
- Coraboeuf, E., and Weidemann, S. 1954 *Helv. Physiol. Acta* 12:32.
- Coulson, C. A. 1959 in *Hydrogen Bonding* (D. Hadži and H. W. Thompson, eds.), Pergamon Press, New York, pp. 339–360.
- Cowgill, R. W. 1963 *Biochem. Biophys. Acta* 100:36.
- Curtis, H. J., and Cole, K. S. 1942 *J. Cell. Comp. Physiol.* 19:135.
- Czarnetzky, E. J., and Schmidt, C. L. A. 1931 *J. Biol. Chem.* 92:453.
- Damadian, R., 1971, *Science* 171:1151.
- Damadian, R., Goldsmith, M., and Minkoff, L. 1977 *Physiol. Chem. Phys.* 9:97.
- Davies, J. T., and Rideal, E. K. 1963 *Interfacial Phenomena*, 2nd ed., Academic Press, New York.
- Davson, H. and Danielli, J. F. 1943 *The Permeability of Natural Membranes* (2nd ed.), Cambridge University Press, London.
- Dawkins, A. W. J., Gabriel, C., Sheppard, R. J., and Grant, E. H. 1981 *Phys. Med. Biol.* 26:1.
- Dawson, D. M. 1966 *Biochem. Biophys. Acta* 113:246.
- Dean, R. 1941 *Biol. Symp.* 3:331.
- de Boer, J. H. and Zwicker, C. 1929 *Z. Physik. Chem.* B3:407.
- Debye, P., and Hückel, W. 1923 *Phys. Z.* 24:185.
- Deutsch, D. 1981 *Am. Lab.* 13:54.
- deVries, H. 1884 *Jahrb. wiss. Bot.* 14:427.
- Dewar, M. J. S. 1949 *The Electronic Theory of Organic Chemistry*, Oxford University Press, London.
- Dewey, M. M., and Barr, L. 1970 *Curr. Tops. In Memb. and Transport* 1:1.
- Dick, D. A. T. 1984 *Nature* 311:682.
- Dirkin, M. N., and Mook, H. W. 1931 *J. Physiol. (London)* 73:349.
- Dodge, J. T., Mitchell, C., and Hanahan, D. J. 1963 *Arch. Bioch. Biophys.* 100:119.

- Donnan, F. G. 1924 *Chem. Rev.* 1:73.
- Donnan, F. G. and Allmand, A. J. 1914 *J. Chem. Soc.* 105:1941.
- Dorsey, N. F. 1940 *Properties of Ordinary Water Substance*, A. C. S. Monograph 81, American Chemical Society, New York.
- Doty, P., and Katz, S. 1951 cited by Doty, P. and Edsall, J. T. in: *Adv. Protein Chem.* 6:35.
- Draper, M. H., and Weidmann, S. 1951 *J. Physiol.* 115:74.
- du Bois-Reymond, E. 1843 *Ann. Physik. Chem.* 58:1.
- . 1848, 1849 “*Untersuchungen über Thierische Elektrizität*” Vol. 1 and Vol. 2, Reimer, Berlin.
- Dujardin, F. 1835 “Sur les prétendus estomacs des animalcules infusoires et sur une substance appelée sarcode”, part 2 of “Recherche sur les organismes inférieur”, *Annales de sciences naturelles: partie zoologique*, 2d Ser., 4.
- . 1838 *Annales de sciences naturelles, partie zoologique*, 2d Sér. 10:240.
- Dünwald, H. and Wagner, C. 1934 *Z. Physik. Chem.* B24:53.
- Edelhoch, H., Brand, L., and Wilchek, M. 1967 *Biochem.* 6:547.
- Edelmann, L. 1973 *Ann. NY Acad. Sci.* 204:534.
- . 1977 *Physiol. Chem. Phys.* 9:313.
- . 1978 *Microsc. Acta Suppl.* 2:166.
- . 1980 *Physiol. Chem. Phys.* 12:509.
- . 1980a *Histochem.* 67:233.
- . 1980–1981 *Intern. Cell Biology*, ed. H. G. Schweiger, Springer-Verlag, Berlin, NY, p. 941.
- . 1983, *Physiol. Chem. Phys. and Med. NMR* 15:337.
- . 1984 *Scanning Electron Microscopy II*:875.
- . 1984a *Physiol. Chem. Phys. & Med. NMR* 16:499.
- . 1986 in: *Science of Biological Specimen Preparation* (M. Müller, R. P. Becker, A. Boyde, and J. J. Wolosewick, eds.) SEM Inc., AMF O'Hare, Chicago, Ill., p. 33.
- . 1986a *Scanning Electron Microsc.* SEM Inc., Chicago, Ill. IV: 1337.
- . 1988 *Scanning Microscopy* 2:1.
- . 1989 *Scanning Microscopy* 3:1219.
- . 1991 “Adsorption Staining of Freeze-substituted and Low Temperature Biological Material with Cesium” *Scanning Microscopy* 5:xxx
- Edsall, J. T. 1953 in “The Proteins” ed. Neurath, H. and Bailey, K. Vol. 1, Part B. 563, Academic Press, N.Y.
- . 1958 in: “Conference on Hemoglobin 2–3 May, 1957”, *Nat. Acad. Sci. Nat. Res. Conc.*, Washington D.C., p. 1.
- Edsall, J. T. and Wyman, J. 1958 *Biophysical Chemistry*, Vol. 1, Academic Press, New York.
- Eggleston, J. C., Saryan, L. A., and Hollis, D. P. 1978 *Cancer Res.* 35:1326.
- Eggleston, G. and Eggleston, P. 1933 *Quant. J. Expt. Physiol.* 23:391.
- Ehrenpreis, S. 1967 *Ann NY Acad Sci (Discussion)* 144:754.
- Ehrensvar, G., and Sillen, L. G. 1938 *Nature* 141:788.
- Eigen, M., and Hammes, G. G. 1963 *Adv. Enzymol.* 25:1.
- Eisenberg, D., and Kauzmann, W. 1969 *The Structure and Properties of Water*, Oxford Univ. Press, New York.
- Eisenman, G. 1961 in “Membrane Transport and Metabolism” eds. Kleinzeller, A. and Kotyk, A. Academic Press, N.Y. p. 163.
- Eisenman, G. (ed.) 1967 “Glass Electrodes for Hydrogen and Other Cations; Principles and Practices” Marcel Dekker Inc., N.Y.
- Engel, M. B., Catchpole, H. R. and Joseph, N. R. 1960 *Science* 132:669.
- Engelmann, T. W. 1873 *Pflügers Arch. Ges. Physiol.* 7:155.
- Elgsaeter, A., Stokke, B. T., Mikkelsen, A., and Bromton, D. 1986 *Science* 234:1217.
- Englander, S. W., and Rolfe, A. 1973 *J. Biol. Chem.* 248:4852.
- Epstein, E., and Hagen, C. E. 1952 *Plant Physiol.* 27:457.
- Ernst, E. 1958 “Die Muskeltätigkeit. Versuch einer Biophysik des querstreiften Muskels” *Hungarian Acad. Sci., Budapest*, p. 355.

- . 1963 *Biophysics of the Striated Muscle*, 2nd ed., Hungarian Academy of Science, Budapest.
- Ernst, E., and Scheffer, L. 1928 *Pflügers Arch. Ges. Physiol.* 220:655.
- Ernster, L., and Kuylenstierna B. 1970 in: *Membranes of Mitochondria and Chloroplasts* (E. Racker, ed.) Van Nostrand Reinhold, New York, p. 191.
- Everett, C. T., Redwood, W. R., and Haydon, D. A. 1969 *J. Theor. Biol.* 22:20.
- Falk, G., and Gerard, R. W. 1954 *J. Cell Comp. Physiol.* 43:393.
- Fenn, W. O., and Cobb, D. M. 1934 *J. Gen. Physiol.* 17:629.
- Ferry, J. D. 1948 *Adv. Proc. Chem.* 4:1.
- Feynman, R. P. 1939 *Phys. Rev.* 56:340.
- Finch, E. D., Harmon, J. F., and Muller, B. H. 1971 *Arch. Biochem. Biophys.* 147:299.
- Findlay, A. 1919 *Osmotic Pressure*, 2nd ed., Longmans, Green, London.
- Finkelstein, A. V., and Ptitsyn, O. B. 1971 *J. Mol. Biol.* 62:613.
- Fischer, E. 1894 *Ber. dtsh. chem. Ges.* 27:2985.
- Fischer, M. H. 1921 *Oedema and Nephritis: A Critical Experimental and Clinical Study of the Physiology and Pathology of Water Absorption by the Living Organism*, 3rd ed., Wiley, New York.
- Fischer, M. H. and Moore, G. 1907 *Am. J. Physiol.* 20:330.
- Fischer, M. H. and Suer, W. J. 1938 *Arch. Pathol.* 26:51.
- Fleischer, S., Fleischer, B., and Stoeckenius, W. 1967 *J. Cell. Biol.* 32:193.
- Fleming, T. 1972 *The Founding Fathers: Benjamin Franklin, A Biography in His Own Words*, Harper and Row.
- Forslind, E. 1952 *Proc. Swed. Cement Concrete Res. Inst.* No. 16.
- Foster, J. F. and Serman, M. D. 1956 *J. Amer. Chem. Soc.* 78:3656.
- Fowler, R. and Guggenheim, E. A. 1960 *Statistical Thermodynamics*, Cambridge University, Cambridge.
- Frankenhauser, B. and Hodgkin, A. L. 1957 *J. Physiol.* 137:218.
- Frankenheim, M. L. 1835 "Die Lehre von der Cohäsion", Breslau. p. 158.
- Frazer, J. C. W. 1927 *The Direct Measurement of Osmotic Pressure*, Columbia University Press, New York.
- Freedman, J. C. 1976 *Biochem. Biophys. Acta* 455:989.
- Fukunaga, Y. and Sakiyama, F. 1982 *J. Biochem. (Tokyo)* 92:155.
- Fukunaga, Y., Katsuragi, Y., Izumi, T. and Sakiyama, F. 1982 *J. Biochem. (Tokyo)* 92:129.
- Gabriel, C., Sheppard, R. J., and Grant, E. H. 1983 *Phys. Med. Biol.* 28:43.
- Gale, E. F. 1947 *J. Gen. Microbiol.* 1:53.
- Garnier, J., Osguthorpe, D. J., and Robson, B. 1978 *J. Mol. Biol.* 120:97.
- Gary-Bobo, C. M., and Lindenberg, A. B. 1969 *J. Coll. Interf. Sci.* 29:702.
- Gehler, J. S. T. 1825 "Phys. Wörterbuch", Leipzig, 1:40.
- George, P., and Rutman, R. J. 1960 *Prog. Biophys. Biophys. Chem.* 10:1.
- Gilbert, D. L. 1960 *J. Gen. Physiol.* 43:1103.
- Ginzburg, M., Sachs, L. and Ginzburg, B. J. 1971 *J. Membr. Biol.* 5:78.
- Glader, B. E., and Nathan, D. G. 1978 *Blood* 51:983.
- Glasstone, S. 1946 *Textbook of Physical Chemistry*, 2nd ed., Van Nostrand, New York.
- . 1947 "Thermodynamics for Chemists", van Nostrand Co., Inc., N.Y.
- Glynn, I. M. 1977 *Trends in Biochem. Sci.* (TIBS) 2:N225.
- Glynn, I. M. and Karlsh, S. J. D. 1975 *Ann. Rev. Physiol.* 37:13.
- Glynn, I. M. and Lew, V. L. 1970 *J. Physiol.* 207:393.
- Goldin, S. M. and Tong, S. W. 1974 *J. Biol. Chem.* 249:5907.
- Goldman, D. E. 1943 *J. Gen. Physiol.* 27:37.
- Goody, R. S., Hofmann, W., and Mannherz, H. G. 1977 *Europ. J. Biochem.* 78:317.
- Gorman, A. L. F., and Marmor, M. F. 1970 *J. Physiol.* 210:897.
- Gorodissky, H. 1928 *Z. Physiol. Chem.* 175:261.
- Gorter, E. and Grendel, F. 1925 *J. Exp. Med.* 41:439.
- Gortner, R. A. 1938 *Outline of Biochemistry*, 2nd ed. John Wiley and Sons, Inc., New York.
- Gortner, R. A. and Gortner, W. A. 1934 *J. Gen. Physiol.* 17:327.

- Graham, T. 1833 *Phil. Mag.* 2:175, 269, 351.
———. 1861 *Philos. Trans. R. Soc. London* 151:183.
- Greco, F. A. 1982 *Amer. Lab.* 15:80.
- Gregor, H. P. 1951 *J. Am. Chem. Soc.* 73:642.
- Gregor, H. P., Hamilton, M. J., Becher J. and Berstein, F. 1955 *J. Phys. Chem.* 59:874.
- Guggenheim, E. A. 1950 "Thermodynamics, An Advanced Treatment for Chemists and Physicists, Interscience Publ. Inc., N.Y.
- Gulati, J. 1973 *Ann. N.Y. Acad. Sci.* 204:337.
- Gulati, J., Ochsenfeld, M. M., and Ling, G. N. 1971 *Biophys. J.* 11:973.
- Gurd, F. R. N. and Rothgeb, T. M. 1979 *Adv. Prot. Chem.* 33:73.
- Gustavson, K. H. 1956 *The Chemistry and Reactivity of Collagens*, Academic Press, Inc., New York.
- Hagiwara, S., Chichibu, S., and Naka, K. I. 1964 *J. Gen. Physiol.* 48:163.
- Hahn, L., Hevesy, G., and Rebbe, O. H. 1939 *Nature* 143:1021.
- Hales, S. T., 1732, *Haemastatics. Statistical Essays*, Vol. 2, cited by Overton, 1902.
- Hall, T. S. 1969 *Ideas of Life and Matter*, Vol. 1 and 2, University of Chicago Press, Chicago.
- Hallet, J. 1965 *Fed. Proc. Symp.* 24:S34.
- Hamburger, H. J. 1904 *Osmotische Druck und Ionenlehre in den medicinischen Wissenschaften*, Band I u. III, Bergman, Wiesbaden.
- Hammett, L. P. 1940 *Physical Organic Chemistry*, McGraw Hill, New York.
- Hansson-Mild, H., James, T. L., and Gillen, K. T. 1972 *J. Cell Physiol.* 80:155.
- Hargens, A. R., Bowie, L. J., Lent, D., Carreathers, S., Peters, R. M., Hammel, H. T., and Scholander, P. F. 1980 *Proc. Nat. Acad. Sci.* 77:4310.
- Harkins, W. D. 1945 *Science* 102:292.
- Harris, E. J. 1950 *Trans. Faraday Soc.* 46:872.
- Harris, E. J. and Burn, G. P. 1949 *Trans. Farad. Soc.* 45:508.
- Harris, F. E. and Rice, S. A. 1954 *J. Chem. Phys.* 24:1258.
- Harris, J. W. 1950 *Proc. Soc. Exp. Biol. Med.* 75:197.
- Harvey, E. N. 1931 *Biol. Bull.* 60:67.
- Harvey, E. and Collander, R. 1932 *J. Frankl. Inst.* 1:214.
- Harvey, E. N. and Danielli, J. F. 1939 *Usp. Souvrem. Biol.* 10:471.
- Haugaard, G. 1941 *J. Phys. Chem.* 45:148.
- Hazlewood, C. F. 1979 in: *Cell Associated Water* (W. Drost-Hansen and J. Clegg, eds.) Academic Press, New York. p. 165.
- Hazlewood, C. F., and Kellermayer, M. 1990 in "The State of Potassium in the Cell", compiled by W. Negendank and Edelmann, L., Scanning Microscopy International, P. O. Box 66507, AMF O'Hare (Chicago), Ill. 60666.
- Hazlewood, C. F. and Nichol, B. L. 1969 *Johns Hopkins Medical J.* 125:119.
- Hazlewood, C. F., Nichols, B. L., and Chamberlain, N. F. 1969 *Nature* 222:747.
- Hazlewood, C. F., Singer, D. B., and Beall, P. 1979 *Physiol. Chem. Phys.* 11:181.
- Hearse, D. J., Stewart, D. A., and Brainbridge, M. V. 1976 *Circulation* 54:193.
- Heidorn, D. B. 1985 "A Quasielastic Neutron Scattering Study of Water Diffusion in Frog Muscle", Ph.D. Thesis, Rice University, Houston.
- Heidorn, D. B., Roschach, H. E., Hazlewood, C. F., Ling, G. N., and Nicklow, R. M. 1986 *Biophys. J.* 49:92A.
- Heppel, L. A. 1939 *Amer. J. Physiol.* 127:385.
- Heppel, L. 1940 *Amer. J. Physiol.* 128:449.
- Herskovits, T. T., Gadegbeku, B. and Jaillet, H. 1970 *J. Biol. Chem.* 245:2588.
- Higgins, T. J. C., Allsop, D., Bailey, P. J., and D'Souza, E. D. A. 1981 *J. Mol. Cell. Cardiol.* 13:599.
- Hilden, S. and Hokin, L. E. 1976 *Biochem. Biophys. Res. Comm.* 69:521.
- Hilden, S., Rhee, H. M., and Hokin, L. E. 1974 *J. Biol. Chem.* 249:7432.
- Hill, A. V. 1910 *J. Physiol. (London)* 40:iv.
———. 1930 *Proc. Roy. Soc. (London) Ser. B* 106:477.
- Hill, A. V. and Kupalov, P. S. 1930 *Proc. Roy. Soc. (London) Ser. B* 106:445.

- Hill, T. L. 1946, *J. Chem. Phys.* 14:263.
- Hille, B. 1968 *J. Gen. Physiol.* 51:221.
- . 1975 *Fed. Proc.* 34:1318.
- . 1975a in *Membranes: a Series of Advances*, Vol. 3, p. 255.
- Hinke, J. A. M. 1959 *Nature* 184:1257.
- . 1961 *J. Physiol. (London)* 156:314.
- Hirata, H., Altendorf, K., and Harold, F. M. 1974 *J. Biol. Chem.* 249:2939.
- Höber, R. 1929 *Pflügers Arch. ges. Physiol.* 216:540.
- Hodge, A. J., and Schmidt, F. O. 1960 *Proc. Nat. Acad. Sci. USA* 46:186.
- Hodgkin, A. L. 1951 *Biol. Rev.* 26:339.
- . 1958 *Proc. Roy. Soc. (London) Ser. B* 148:1.
- . 1971 *The Conduction of the Nervous Impulse*, Liverpool University Press, Liverpool.
- Hodgkin, A. L. and Horowicz, P. 1959 *J. Physiol.* 148:127.
- Hodgkin, A. L. and Huxley, A. F. 1952a *J. Physiol. (London)* 116:449.
- . 1952b *J. Physiol. (London)* 116:473.
- . 1952c *J. Physiol. (London)* 116:497.
- . 1952d *J. Physiol. (London)* 117:500.
- Hodgkin, A. L. and Katz, B. 1949 *J. Physiol. (London)* 108:37.
- . 1949a *J. Physiol. (London)* 109:240.
- Hodgkin, A. L. and Keynes, R. D. 1953 *J. Physiol. (London)* 119:513.
- . 1955 *J. Physiol. (London)* 128:61.
- . 1955a *J. Physiol. (London)* 128:28.
- Hodgkin, A. L., Huxley, A. F. and Katz, B. 1952 *J. Physiol. (London)* 116:424.
- Hodgman, C. D., Weast, R. C., and Selby, S. M. 1961 *Handbook of Chemistry and Physics*, The Chemical Rubber Publishing Company, Cleveland.
- Hoffman, J. F. and Kregenow, F. N. 1966 *Ann. NY Acad. Sci.* 137:566.
- Höfler, K. 1918 *Deutschr. d. K. Akad. d. Wissenschaften in Wien, Math-Naturw. Kl* 95:99.
- Holleman, L. W. J., Bungenberg de Jong, H. G., and Modderman, R. S. T. 1934 *Kolloid Beih.* 39:334.
- Hopfer, U., Lehninger, A. L., and Lenarz, W. J. 1970 *J. Biol. Med.* 2:41.
- Horovitz, K. 1923 *Z. Phys.* 15:369.
- Horowicz, P., and Gerber, C. J. 1965 *J. Gen. Physiol.* 48:515.
- Horowitz, S. B., and Paine, P. L. 1979 *Biophys. J.* 25:45.
- Horowitz, S. B., Paine, P. L., Tluczek, L., and Reynhout, J. K. 1979 *Biophys. J.* 25:33.
- House, C. R. 1974 *Water Transport in Cells and Tissues*, Williams and Wilkins, Co., Baltimore.
- Huang, H. W. 1979 *J. Chem. Phys.* 70:2390.
- Huang, H. W. and Negendank, W. 1980 *J. Chem. Phys.* 73:4136.
- Huang, L. M., Catterall, W. A., and Ehrenstein, G. 1979 *J. Gen. Physiol.* 73:839.
- Hughes, W. L. 1954 in "The Proteins" (Neurath, H. and Bailey, K. eds.) Vol. 2, Part B. 663, Academic Press, N.Y.
- Hughes, T. R., and Klotz, I. M. 1956 in: *Methods of Biochemical Analyses*, Vol. III, (D. Glick, ed.), Interscience Publ. Inc., New York, p. 265–299.
- Hutchings, B. L., 1969, *Biochim. Biophys. Acta* 174:734.
- Hunt, J. A. and Ingram, V. M. 1959 *Nature* 184:640.
- Hunter, F. R. and Parpart, A. K. 1938 *J. Cell. Comp. Physiol.* 12:309.
- Hurt, E. C. 1987 *TIBS* 12:370.
- Huxley, A. F. and Niedergerke, R. 1958 *J. Physiol. (London)* 144:403.
- Huxley, T. H. 1853 *Review I, The British and Foreign Medico-Chronological Review* 12:285.
- Imae, T., Fasman, G. D., Hinkle, P. M., and Tashjian, A. H. 1975 *Bioch. Biophys. Res. Comm.* 62:923.
- Inch, W. R., McCredie, J. A., Knispel, R. R., Thompson, R. T., and Pintar, M. M. 1974, *J. Natl. Cancer Res.* 52:353.
- Infante, A. A. and Davies, R. C. 1962 *Biochem. Biophys. Res. Commun.* 9:410.
- Ingold, C. K. 1953 *Structure and Mechanism in Organic Chemistry*, Cornell University Press, Ithaca.

- Ising, E. 1925 *Z. Phys.* 31:253.
- Jacobsen, B. 1955 *Svensk. Kem. Tidskr.* 67:1.
- Jacobson, C. F., and Linderstrøm-Lang, K. U. 1949 *Nature* 164:411.
- Jain, M. K. 1972 *The Bimolecular Lipid Membrane: A System*, van Nostrand Rheinhold, New York.
- James, H. M., and Coolidge, A. S. 1933 *J. Chem. Phys.* 1:825.
- Jensen, W. N., Bromberg, P. A., and Barefield, K. 1969 *Clin. Res.* 17:464.
- Jones, A. W. 1965 Ph.D. Thesis Appendix, University of Pennsylvania, Philadelphia.
- Jones, I. D. and Gortner, R. A. 1932 *J. Phys. Chem.* 36:387.
- Jordan-Lloyd, D. and Shore, A. 1938 *The Chemistry of Proteins*, 2nd ed., J. A. Churchill, London.
- Joseph, N. R., Engel, M. B., and Catchpole, H. R. 1961 *Nature* 191:1175.
- Kaatze, U. 1975 *Adv. Molecular Relaxation Processes* 7:71.
- Kaatze, U., Göttmann, O., Rodbielski, R., Pottel, R., and U. Terveer 1978 *J. Phys. Chem.* 82:112.
- Kaback, H. R. 1976 *J. Cell Physiol.* 89:575.
- Kanazawa, T., Yamada, S. and Tonomura, Y. 1970 *J. Biochem.* 68:593.
- Kao, C. Y. 1956 *Biol. Bull.* 111:292.
- Karasaki, S. 1963 *J. Ultrastructure Res.* 9:225.
- Karreman, G. 1980 *Cooperative Phenomenon in Biology*, Pergamon Press, New York.
- Katz, B. 1966 *Nerve, Muscle, and Synapse*, McGraw-Hill, New York.
- Katz, J. R. 1919 *Kolloidchem. Beih.* 9:1.
- Katz, S. 1950 Ph.D. Thesis, Harvard University, Boston.
- Katz, Y. and Diamond, J. M. 1974 *J. Membr. Biol.* 17:87.
- Kayser, H., 1881 *Ann. Phys.* 14:451.
- Kellermayer, M. 1980–1981 *Intern. Cell Biol.* p. 915 ed. Schweiger, H. G., Springer Verlag, Berlin.
- Kellermayer, M., Ladany, A., Jobst, K., Szucs, G., Trombitas, K., and Hazlewood, C. F. 1986 *Proc. Nat. Acad. Sci.* 83:1011.
- Kerly, M. and Ronzoni, E. 1933 *J. Biol. Chem.* 103:161.
- Kern, W. 1948 *Makromol. Chem.* 2:279.
- Kernan, R. P. 1970 in: *Membranes and Ion Transport*, Vol. 1 (E. E. Bittar, ed.), Wiley-Interscience, New York, p. 395.
- Keynes, R. D. 1954 *Proc. Roy. Soc., London, Ser. B.* 142:359.
- Keynes, R. D. and Maisel, G. W. 1954 *Proc. R. Soc. London Ser. B.* 142:383.
- Khodorov, B. I. 1978 in: *Membrane Transport Processes*, Vol. 2 (D. T. Tosteson, A. Yu Ovchinnikov, and R. Latorre, eds.) Raven Press, New York, p. 153.
- Kipnis, D. M. and Cori, C. F. 1957 *J. Biol. Chem.* 224:681.
- Kleinfeld, S. 1985 "A Machine Called Indomitable", Times Books, A Division of Random House, N.Y.
- Klinger, R. G., Zahn, D. P., Brox, D. H., and Frundes, H. E. 1971 *Europ. J. Biochem.* 18:171.
- Klotz, I. M. 1958 *Science* 128:815.
- . 1973 *Ann. N.Y. Acad. Sci.* 226:18.
- Knowles, A. F., and Racker, E. 1975 *J. Biol. Chem.* 250:1949.
- Koechlin, B. A. 1955 *J. Biophys. Biochem. Cytol* 1:511.
- Koketsu, K. 1971 *Adv. Biophys.* 2:77.
- Koketsu, K. and Kimura, Y. 1960 *J. Cell Comp. Physiol.* 55:239.
- Kolotilova, A. I. and Engel'gardt, V. A. 1937 *Biokhimiya* 2:387.
- Konev, S. V. 1967 *Fluorescence and Phosphorescence of Proteins and Nucleic Acids*, Plenum Publishing Corporation, New York.
- Kossiakoff, A., and Harker, D. 1938 *J. Amer. Chem. Soc.* 60:2047.
- Kuhn, T. 1962 *The Structure of Scientific Revolution*, University of Chicago Press, Chicago.
- Kunkel, 1889 *Pflügers Arch. ges Physiol.* 36:353.
- Kuntz, I. D. and Zipp, A. 1977 *New England J. Med.* 297:262.

- Kuntz, I. D. and Kauzmann, W. 1974 *Adv. Prot. Chem.* 28:239.
- Küntzel, A., 1944, in: *Handbuch der Gerbereichemie*, Vol. 1, Part 1, Springer, Vienna, p. 519.
- Küntzel, A. and Schwank, M. 1940 *Collegium* 12:489.
- Kushmerick, M. J., and Podolsky, R. J. 1969 *Science* 166:1297.
- Langmuir, I. 1916 *J. Amer. Chem. Soc.* 38:2221.
- . 1918 *J. Amer. Chem. Soc.* 40:1361.
- Lardy, H. A. and Lin, C. H. C. 1969 in "*Inhibitors—Tools in Cell Research*" (Büchers, Th. and Sies, H., eds.) p. 279, Springer Verlag, Berlin.
- Lark-Horovitz, K. 1931 *Nature* 127:440.
- Lauffer, M. A. 1975 *Entropy-Driven Processes in Biology*, Springer-Verlag, New York.
- Leaf, A. 1956 *Biochem. J.* 62:241.
- LeChatelier, H. 1885 *Compt. Rend.* 100: 441.
- Lee, C. O. and Armstrong, W. McD. 1972 *Science*, 175:1261.
- Lehninger, A. L. 1964 *The Mitochondrion*, Benjamin, Menlo Park, California.
- . 1975 *Biochemistry: The Molecular Basis of Cell Structure and Function*, 2nd ed. Worth Publishers, Inc., N.Y.
- Lev, A. A. 1964 *Nature* 201:1132.
- Levi, H., and Ussing, H. H. 1948 *Acta physiol. Scand.* 16:232.
- Levine, R., and Goldstein, M. S. 1955 *Rec. Prog. Horm. Res.* 11:343.
- Lewis, G. N. 1923 *Valence and Structure of Atoms and Molecules*, Chemical Catalogue, New York.
- Lewis, M. S., and Saroff, H. A. 1957 *J. Amer. Chem. Soc.* 79:2112.
- Lillie, R. S. 1923 *Protoplasmic Action and Nervous Action*, 1st ed., University of Chicago Press, Chicago.
- Linderstrøm-Lang, K. U. and Schellman, J. A. 1959 in "The Enzymes" ed. Boyer, P. D., Lardy, H. and Myrback, Acad. Press, New York, 2nd ed., Vol. 1.
- Ling, G. N. 1951 *Amer. J. Physiol.* 167:806.
- . 1952 in: *Phosphorous Metabolism* (Vol. II) (W. D. McElroy and B. Glass, eds.) The John Hopkins University Press, Baltimore, p. 748.
- . 1953 *Proc. 19th Internat. Physiol. Congr.*, Montreal, Canada, p. 566.
- . 1954 *Amer. J. Physiol.* 170:656.
- . 1955 *Fed. Proc.* 14:93.
- . 1955a *Amer. J. Phys. Med.* 34:89.
- . 1957 *Fed. Proc.* 16:81.
- . 1959 *Fed. Proc.* 18:371.
- . 1960 *J. Gen. Physiol.* 43:149.
- . 1962 *A Physical Theory of the Living State: The Association-Induction Hypothesis*, Blaisdell, Waltham, Mass.
- . 1964 *J. Biopolymers* 1:91.
- . 1964a *Texas Reports on Biol. and Med.* 22:244.
- . 1965 *Ann. N.Y. Acad. Sci.* 125:401.
- . 1965a *Fed. Proc.* 24:S-103.
- . 1965b *Persp. Biol. and Med.* 9:87.
- . 1966 *Fed. Proc. Symp.* 25:958.
- . 1966a *Ann. N.Y. Acad. Sci.* 137:837.
- . 1967 in: *Glass Electrodes for Hydrogen and Other Cations* (G. Eisenman, ed.) Marcel Dekker, Inc., NY, p. 284–292.
- . 1969 *Intl. Rev. of Cytol.* 26:1.
- . 1969a *Nature* 221:386.
- . 1970 *Int. J. Neurosci.* 1:129.
- . 1970a *Proc. Nat. Acad. Sci.* 67:296.
- . 1972 in: *Water and Aqueous Solutions, Structure, Thermodynamics, and Transport Processes* (A. Horne, ed.) Wiley-Interscience, New York, p. 663–699.
- . 1973 *Physiol. Chem. Phys.* 5:295.

- . 1973a *Biophys. J.* 13:807.
- . 1977 *Physiol. Chem. Phys.* 9:319.
- . 1977a *Physiol. Chem. Phys.* 9:217.
- . 1977b *Science* 198:1281.
- . 1977c *Mol. Cell. Biochem.* 15:159.
- . 1978 *J. Physiol.* 280:105.
- . 1978a *Bioelectrochem. and Bioenerg.* 5:411.
- . 1978b *Physiol. Chem. Phys.* 10:353.
- . 1979 in: *The Aqueous Cytoplasm* (A. D. Keith, ed.) Marcel Dekker, Inc., New York, p. 23.
- . 1979a in: *Cell-Associated Water* (W. Drost-Hanson and J. Clegg, eds.) Academic Press, Inc., New York, p. 261.
- . 1979b *Physiol. Chem. Phys.* 11:59.
- . 1979c *TIBS* 4: N134.
- . 1980 *Physiol. Chem. Phys.* 12:215.
- . 1980a in: *Cooperative Phenomena in Biology* (G. Karreman, ed.) Pergamon Press, New York, p. 39.
- . 1981 *Physiol. Chem. Phys.* 13:29.
- . 1981a in: *Die Zelle: Struktur und Funktion*, 3rd ed., (H. Metzner, ed.) Wissenschaftlich Verlagsgesellschaft mbH, Stuttgart, Germany, p. 356.
- . 1982 *Physiol. Chem. Phys.* 14:47.
- . 1983 *Physiol. Chem. Phys. and Med. NMR* 15:155.
- . 1983a *Physiol. Chem. Phys. and Med. NMR* 15:505.
- . 1983b *Physiol. Chem. Phys. and Med. NMR* 15:511.
- . 1984 *In Search of the Physical Basis of Life*, Plenum Publishing Corp., New York.
- . 1984a *Physiol. Chem. Phys. and Med. NMR* 16:293.
- . 1985 in: *Modern Bioelectrochemistry* (F. Gutmann and H. Keyzer, eds.) Plenum Press, New York, p. 45.
- . 1986 *Physiol. Chem. Phys. and Med. NMR* 18:131.
- . 1986a *Physiol. Chem. Phys. and Med. NMR* 18:3.
- . 1986b *Physiol. Chem. Phys. and Med. NMR* 18:125.
- . 1987 *Physiol. Chem. Phys. & Med. NMR* 19:159.
- . 1987b *Physiol. Chem. Phys. & Med. NMR* 19:199.
- . 1988 *Scanning Microscopy* 2:871.
- . 1988a *Physiol. Chem. Phys. & Med. NMR* 20:281.
- . 1989 *Physiol. Chem. Phys. & Med. NMR* 21:13.
- . 1989a *Physiol. Chem. Phys. & Med. NMR* 21:15.
- . 1990 *Scanning Microscopy* 4:737.
- . 1990a *Scanning Microscopy* 4:723.
- . 1991 *Scanning Microscopy* 5 Supplement:xxx.
- Ling, G. N., and Balter, M. 1975 *Physiol. Chem. Phys.* 7:529.
- Ling, G. N. and Bohr, G. 1969 *Physiol. Chem. Phys.* 1:591.
- . 1970 *Biophys. J.* 10:519.
- . 1971 *Physiol. Chem. Phys.* 3:573.
- . 1971a *Physiol. Chem. Phys.* 3:431.
- Ling, G. N. and Cope, F. W. 1969 *Science* 163:1335.
- Ling, G. N. and Ferguson, E. 1970 *Physiol. Chem. Phys.* 2:516.
- Ling, G. N. and Fu, Y. 1988 *Physiol. Chem. Phys. & Med. NMR* 20:61.
- Ling, G. N. and Gerard, R. W. 1949 *J. Cell. Comp. Physiol.* 34:383.
- . 1949a *J. Cell. Comp. Physiol.* 34:413.
- . 1950 *Nature* 165:113.
- Ling, G. N. and Hu, W. 1987 *Physiol. Chem. Phys. & Med. NMR* 19:251.
- . 1988 *Physiol. Chem. Phys. & Med. NMR* 20:293.
- Ling, G. N. and Kwon, Y. 1983 *Physiol. Chem. Phys. and Med. NMR* 15:239.
- Ling, G. N. and Murphy, R. C. 1983 *Physiol. Chem. Phys. and Med. NMR* 15:137.

- Ling, G. N. and Negendank, W. 1970 *Physiol. Chem. Phys.* 2:15.
———. 1980 *Persps. in Biol. and Med.* 23:215.
- Ling, G. N., and Ochsenfeld, M. M. 1965 *Biophys. J.* 5:777.
———. 1966 *J. Gen. Physiol.* 49:819.
———. 1973 *Science* 181:78.
———. 1973a *Ann. N.Y. Acad. Sci.* 204:325.
———. 1977 *Physiol. Chem. Phys.* 9:427.
———. 1983 *Physiol. Chem. Phys. and Med. NMR* 15:127.
———. 1986 *Physiol. Chem. Phys. and Med. NMR* 18:109.
———. 1987 *Physiol. Chem. Phys.* 19:177.
———. 1989 *Physiol. Chem. Phys. & Med. NMR* 21:19.
———. 1991 *Physiol. Chem. Phys. & Med. NMR* 23:133.
———. 1991a *Physiol. Chem. Phys. & Med. NMR* 24:xxx.
- Ling, G. N. and Palmer, L. 1972 *Physiol. Chem. Phys.* 4:517.
- Ling, G. N. and Peterson, K. 1977 *Bull. of Math. Biol.* 39:721.
- Ling, G. N. and Tucker, M. 1980 *J. Nat. Canc. Inst.* 64:1199.
———. 1983 *Physiol. Chem. Phys. and Med. NMR* 15:311.
- Ling, G. N. and Walton, C. L. 1975 *Physiol. Chem. Phys.* 7:215.
———. 1975a *Physiol. Chem. Phys.* 7:501.
———. 1976 *Science* 191:293.
- Ling, G. N. and Will, S. 1969 *Physiol. Chem. Phys.* 1:263.
- Ling, G. N. and Woodbury, J. W. 1949 *J. Cell Comp. Physiol.* 34:407.
- Ling, G. N., and Zhang, Z. L. 1983 *Physiol. Chem. Phys. and Med. NMR* 15:251.
———. 1983a *Physiol. Chem. Phys. and Med. NMR* 15:391.
———. 1984 *Physiol. Chem. Phys. and Med. NMR* 16:221.
- Ling, G. N., Ochsenfeld, M. M., and Karreman, G. 1967 *J. Gen. Physiol.* 50:1807.
- Ling, G. N., Neville, M. C., Shannon, P., and Will, S. 1969 *Physiol. Chem. Phys.* 1:42.
- Ling, G. N., Neville, M. C., Will, S., and Shannon, P. 1969a *Physiol. Chem. Phys.* 1:85.
- Ling, G. N., Will, S. and Shannon, P. 1969b *Physiol. Chem. Phys.* 1:355.
- Ling, G. N., Miller, C., and Ochsenfeld, M. M. 1973 *Ann. N.Y. Acad. Sci.* 204:6.
- Ling, G. N., Ochsenfeld, M. M., Walton, C. L., and Bersinger, T. J. 1978 *Physiol. Chem. Phys.* 10:87.
- Ling, G. N., Walton, C., and Ling, M. R. 1979 *J. Cell. Physiol.* 101:261.
- Ling, G. N., Walton, C., and Bersinger, T. J. 1980 *Physiol. Chem. Phys.* 12:111.
- Ling, G. N., Ochsenfeld, M. M., Walton, C., and Bersinger, T. J. 1980a *Physiol. Chem. Phys.* 12:3.
- Ling, G. N., Walton, C. L. and Ochsenfeld, M. M. 1981 *J. Cell. Physiol.* 106:385.
- Ling, G. N., Walton, C. L., and Ochsenfeld, M. M. 1983 *Physiol. Chem. Phys. and Med. NMR* 15:379.
- Ling, G. N., Zodda, D., and Sellers, M. 1984 *Physiol. Chem. Phys. and Med. NMR* 16:381.
- Ling, G. N., Baxter, J. D., and Leitman, M. I. 1984a *Physiol. Chem. Phys. & Med. NMR* 16:405.
- Ling, G. N., Kolebic, T. and Damadian, R. 1990 *Physiol. Chem. Phys. and Med. NMR* 22:1
- Ling, G. N., Niu, Z. L., and Ochsenfeld, M. M. 1991 *Physiol. Chem. Phys. and Med. NMR* 23:xxx
- Lipman, F. 1941 *Adv. Enzymol.* 1:99.
- Loeb, S., and Sourirajan, S. 1960 *University of California, Los Angeles, Dept. Engineering Report No. 60.*
- Lohmann, K. 1935 *Biochem. Z.* 282:120.
- Lowey, S. and Luck, S. M. 1969 *Biochem.* 8:3195.
- Lucké, B. and McCutcheon, M. 1932 *Physiol. Rev.* 12:68.
- Ludwig, C. 1849 *Z. Ration. Med. von Henle* 8:1.
- Lundsgaard, E. 1930 *Biochem. Z.* 227:51.
- Lux, S. E., John, K. M., and Karnovsky, M. J. 1976 *J. Clin. Invest.* 58:955.
- Luyet, B. and Rapatz, G. 1956 *Biodynamica* 8:1.

- MacDonald, J. S. 1900 *Proc. Royal Soc. (London)* 67:310.
- MacDonald, R. C., and Bangham, A. D. 1972 *J. Memb. Biol.* 7:29.
- MacDonald, R. E., and Lanyi, J. K. 1975 *Biochem.* 14:2882.
- MacKnight, A. D. C., and Leaf, A. 1977 *Physiol. Rev.* 57:510.
- MacLeod, J. 1932 *Quart. J. Exp. Physiol.* 22:275.
- MacLeod, J., and Ponder, E. 1936 *J. Physiol.* 86:147.
- McBain, J. W. 1932 *The Sorption of Gases and Vapors by Solids*, George Rutledge and Sons, London.
- McKinley, D., and Meissner, G. 1977 *Febs Lett.* 82:47.
- McLaren, A. D., Jensen, W. A., and Jacobson, L. 1960 *Plant Physiol.* 35:549.
- McMahon, B. C., Hartung, E. J., and Walbran, W. J. 1940 *Trans. Farad. Soc.* 36:515.
- Maloff, B. L., Scordillis, S. P., Reynolds, C., and Tedeshi, H. 1978 *J. Cell Biol.* 78:199.
- Manning, G. S. 1969 *J. Chem. Phys.* 51:924.
- . 1978 *Quart. Rev. Biophys.* 2:179.
- Manwell, C. 1958 *Science* 127:593.
- Marchesi, V. T., and Palade, G. E. 1967 *J. Cell Biol.* 35:385.
- Marmont, G. 1949 *J. Cell. Comp. Physiol.* 34:351.
- Marsh, D. J., De Bruin, S. H., and Gratzer, W. B. 1977 *Biochemistry* 16:1738.
- Masuda, H., and de Meis, D. L. 1973 *Biochem.* 12:4581.
- Meyerhof, O. and Schultz, W. 1931 *Biochem. Z.* 236:54.
- Michaelis, L., 1926 *Naturwissenschaften* 15:33.
- Michaelis, L., and Fujita, A. 1925 *Biochem. Z.* 161:47.
- Michaelis, L., and Perlzweig, W. A. 1927 *J. Gen. Physiol.* 10:575.
- Miller, C., and Ling, G. N. 1970 *Physiol. Chem. Phys.* 2:495.
- Mills, R. 1973 *J. Phys. Chem.* 77:685.
- Minkoff, L., and Damadian, R. 1973 *Biophys. J.* 13:167.
- Miyamoto, V. K. 1966 "DC Electrical Properties of Lipid Bilayer Membranes" Ph.D. Thesis, The Johns Hopkins University, Baltimore.
- Miyamoto, V. K. and Thompson, T. E. 1967 *J. Colloid Interf. Sci.* 25:16.
- Mizushima, S. 1954 *Structure of Molecules and Internal Rotation*, Academic Press, New York.
- Mond, R., and Amson, K. 1928 *Pflügers Arch. Ges. Physiol.* 220:69.
- Mond, R., and Netter, H. 1930 *Pflügers Arch. Ges. Physiol.* 224:702.
- Monod, J. and Jacob, F. 1961 *Cold Spring Harbor Symp. Quant. Biol.* 26:389.
- Monoï, H. 1976 *Biophys. J.* 16:1349.
- Moore, B., and Roaf, H. E. 1908 *Biochem. J.* 3:55.
- Moran, T. 1926 *Proc. R. Soc. London Ser. A* 112:30.
- Morowitz, H. J., and Terry, T. M. 1969 *Biochim. Biophys. Acta* 183:276.
- Müller, P. 1975 *Ann. N.Y. Acad. Sci.* 264:97.
- Müller, P., Rudin, D. O., Tien, H. T., and Wescott, W. C. 1962 *Nature* 194:979.
- Mullins, L. J. 1942 *Fed. Proc.* 1:61.
- Mullins, L. J., and Brinley, F. J. 1969 *J. Gen. Physiol.* 53:704.
- Mullins, L. J., and Noda, K. 1963 *J. Gen. Physiol.* 47:117.
- Murayama, M. 1964 *Nature* 202:258.
- Nakao, M., Nakao, T., Yamazoe, S. and Yoshikawa, H. 1961 *J. Biochem. (Tokyo)* 49:487.
- Nasse, O. 1869 *Pflügers Arch. Ges. Physiol.* 2:97.
- Negendank, W. and Karreman, G. 1979 *J. Cell Physiol.* 98:107.
- Negendank, W. and Shaller, C. 1979 *J. Cell. Physiol.* 98:539.
- Nernst, W. 1889 *Z. Phys. Chem.* 4:129.
- . 1891 *Z. Physik. Chem.* 8:110.
- . 1892 *Z. Phys. Chem.* 9:137.
- Netter, H. 1928 *Pflügers Arch. Ges. Physiol.* 220:107.
- Neuschloss, S. M. 1926 *Pflügers Arch. Ges. Physiol.* 213:19, 40, 47.
- Newton, R., and Gortner, W. A. 1922 *Bot. Gaz.* 74:442.
- Nicolosky, B. P. 1937 *Acta Physicochim U.R.S.S.* 7:597.
- Noda, M., Shimizu, S., Tanake, T., et al., and Numa, S. 1984 *Nature* 312:121.

- Norman, D., Menozzi, P., Reid, D., Lester, G., and Hechter, O. 1959 *J. Gen. Physiol.* 42:1277.
- Odeblad, E., Bhar, B. N., and Lindstrom, G., 1956, *Arch. Biochem. Biophys.* 63:221.
- Ohki, S. 1972 *Biochim. Biophys. Acta* 282:55.
- Ohtsuki, I., Maruyama, K., and Ehashi, S. 1986 *Adv. Prot. Chem* 38:1.
- Oikawa, T., Spyropoulos, C. S., Tasaki, I., and Teorell, T. 1961 *Acta Physiol. Scand.* 52:195.
- Okamoto, K., and Quastel, J. H. 1970 *Biochem. J.* 120:25.
- Ostwald, W. 1890 *Z. Phys. Chem.* 6:71.
- Overton, E. 1895 *Vierteljahrssch. Naturforsch. Ges. Zurich* 40:159.
- . 1899 *Vierteljahrssch. Naturforsch. Ges. Zurich* 44:88.
- . 1902 *Pflügers Arch. Ges. Physiol.* 92:115, 346.
- . 1904 *Pflügers Arch. Ges. Physiol.* 105:176.
- Palmer, L. G., Century, T. J., and Civan, M. M. 1978 *J. Memb. Biol.* 40:25.
- Parsons, D. F., Williams, G. R., Thompson, W., Wilson, D. and Chance, B. 1967 in: *Proc. Symp. Mitochondrial Structure and Function* (J. M. Tager, S. Papa, E. Quagliariello, and E. C. Slater, eds.) Bioch. Biophys. Acta Library.
- Passow, H. 1965 in: *Proceedings of the 23rd Internat. Congr. of Physiol. Sci., Tokyo (Congress Series No. 87) Amsterdam Excerpta Medica*, p. 555.
- Passow, H. and Schnell, K. 1969 *Experientia* 25:460.
- Pauling, L., 1945 *J. Amer. Chem. Soc.* 67:555.
- . 1960 "The Nature of the Chemical Bond" 3rd ed., Cornell University Press, Ithaca, N.Y.
- Peachey, L. D., 1965 *J. Cell Biol.* 25:209.
- Perutz, M. 1969 *Proc. R. Soc. London Series B* 173:113.
- . 1970 *Nature* 228:726.
- . 1979 *Ann. Rev. Biochem.* 48:327.
- Perutz, M. F., and Mitchison, J. M. 1950 *Nature* 166:677.
- Perutz, M. F., Muirhead, H., Cox, J. M., Goaman, L. C. G., Mathews, F. S., McGandy, E. L., and Webb, L. E. 1968 *Nature* 219:29.
- Pfeffer, W. F. 1877 *Osmotische Untersuchungen: Studien zur Zell-Mechanik*, Englemann, Leipzig.
- Piez, K. A., Weiss, E., and Lewis, M. S. 1960 *J. Biol. Chem.* 235:1987.
- Pigman, W. 1957 *The Carbohydrates. Chemistry, Biochemistry, Physiology*, Academic Press, New York.
- Piper, H. M., Schwartz, P., Hütter, J. F., and Spieckermann, P. G. 1984 *J. Mol. Cell Cardiol.* 16:995.
- Plowe, J. Q. 1931 *Protoplasm* 12:196.
- Podolsky, R. J., and Kitzinger, C. 1955 *Fed. Proc.* 14:115.
- Podolsky, R. J., and Morales, M. F. 1956 *J. Biol. Chem.* 218:945.
- Ponder, E. 1936 *Physiol. Rev.* 16:19.
- . 1940 *Cold Springs Harbor Symp. Quant. Biol.* 8:133.
- . 1948 *Hemolysis and Related Phenomena*, Grune and Stratton, New York.
- Post, R. L. and Jolly, P. C. 1975 *Biochim. Biophys. Acta* 25:118.
- Pratt, J. R. and Marshall, K. J. 1974 *J. Pharm. Pharmacol.* 26:427.
- Procter, H. R. and Wilson, J. A. 1916 *J. Chem. Soc.* 109:307.
- Prulière, G. and Douzou, P. 1989 "Sol-gel processing of actin to obtain homogeneous glasses at low temperature" *Biophys. Chem.* 34:311.
- Prulière, G., Nguyen, Richter, K. and Dubochet, J. 1990 "Vitrification of low concentration of G-actin/ α -actinin solutions" *Biophys. Chem.* xx:xxx.
- Putnam, F. W. 1953 in: *The Proteins*, ed. H. Neurath, and K. Bailey, Vol. 1, Part B., Academic Press, N.Y., pp. 846–847.
- Racker, E. 1970 *Essays in Biochemistry* 6:1.
- Redwood, W. R. and Haydon, D. A. 1969 *J. Theoret. Biol.* 22:1.
- Reiser, A. 1959 in: *Hydrogen Bonding* (D. Hadži and H. W. Thompson, eds.), Pergamon Press, New York, p. 446.

- Reisin, I. L. and Gulati, J. 1973 *Ann. N.Y. Acad. Sci.* 204:358.
- Reisin, I. L. and Ling, G. N. 1973 *Physiol. Chem. Phys.* 5:183.
- Renkin, E. M. 1954 *J. Gen. Physiol.* 38:225.
- Riggs, A. 1961 *J. Biol. Chem.* 236:1948.
- Roberts, I. Z. and Wolffe, E. L. 1951 *Arch. Biochem. Biophys.* 33:165.
- Robertson, J. D. 1960 *Prog. Biophys. Biophys. Chem.* 10:343.
- Robinson, J. R. 1950 *Proc. Roy. Soc. B.* 137:378.
- . 1956 *J. Physiol. (London)* 134:216.
- Robinson, W. 1931 *J. Biol. Chem.* 92:699.
- Rogus, E., and Zierler, K. L. 1970 *Fed. Proc.* 29:455.
- Roos, A. and Boron, W. F. 1981 *Physiol. Rev.* 61:296.
- Rorschach, H. E. 1984 in: *Water and Ions in Biological Systems*, (V. Vasilescu, ed.) Plenum Press, New York.
- Rossi-Fanelli, A., Antonini, E., and Caputo, A. 1964 *Adv. Protein Chem.* 19:73.
- Rothman, J. and Kornberg, R. D. 1986 *Nature* 322:209.
- Rubinshtein, D. L. 1939 "Is There a Semipermeable Cell Membrane?", Sb: *The Problem of Permeability (Problema pronitsayemosii)*, Tr. Conf. Mosk. ohshch. fiziol., Moscow, p. 7, 72, 112, 201.
- Rubner, M. 1922 *Abh. Preuss. Akad. Wiss., Phys.-Math. Klasse* pp. 3–70.
- Rushbrook, G. S. 1949 "Introduction to Statistical Mechanics" Oxford at the Clarendon Press, Oxford, England.
- Ryser, H. J. P. 1968 *Science* 159:390.
- Sacks, J. 1939 *Amer. J. Physiol.* 126:388.
- Saladino, A. J., Bentley, P. J. and Trump, B. F. 1969 *Amer. J. Pathol.* 54:421.
- Sartiano, G. P., and Hayes, R. L. 1977 *J. Lab. Clin. Med.* 89:30.
- Sato, M., Akaike, N., and Nishi, R. 1967 *Kumamoto Med. J.* 20:39.
- Scatchard, G. 1949 *Ann. N.Y. Acad. Sci.* 51:660.
- Schatzmann, H. J. 1953 *Helv. Physiol. Pharmacol. Acta* 11:346.
- Scheid, P., Straub, R. W., and Hermenau, W. 1968 *Pflügers Arch. Ges. Physiol.* 301:124.
- Scheraga, H. A. 1974 *Curr. Topics Biochem.* 1973:1.
- Schliwa, M. 1986 "The Cytoskeleton: An Introductory Survey" Springer Verlag, New York.
- Schultz, R. D., and Asunmaa, S. K. 1969 *Recent Prog. Surface Sci.* 3:291.
- Schultz, R. D., Asunmaa, S. K., Guter, G. A., and Littman, F. E. 1969 *Characterization of Ordered Water in Hydrophilic Membrane Pores*, Paper 10,247 (March) McDonnell Douglas Corp., Newport Beach, Calif.
- Schultze, M. 1861 *Müller's Arch. für Anatomie und Physiologie und für wissenschaftliche Medicin*, Berlin, p. 1.
- Schwann, T. 1839 *Mikroskopische Untersuchungen über die Ubereinstimmung in der Struktur und der Wachstum der Thiere und Pflanzen*, Berlin.
- Schwarz, G., and Seeling, J. 1968 *Biopolymers* 6:1623.
- Seitz, P. K., Hazlewood, C. F., and Clegg, J. S. 1980 *The Brine Shrimp, Atermia*, Vol. 2,545 (G. Persoone, P. Surgeloos, O. Roels, and E. Jaspers, eds.) Universa Press, Wetteren, Belgium.
- Shanes, A. M., and Bianchi, C. P. 1959 *J. Gen. Physiol.* 42:1123.
- Shaw, F. H. and Simon, S. E. 1955 *Aust. J. Exp. Biol. Med. Sci.* 3:153.
- Shaw, F. H., Simon, S. E., and Johnstone, B. M. 1956 *J. Gen. Physiol.* 40:1.
- Shull, C. A. 1913 *Bot. Gaz* 56:169.
- . 1924 *Ecology* 5:230.
- Singer, C. 1962 *A History of Biology to About the Year 1900*, 3rd ed. Abelard-Schuman, London and New York.
- Singer, S. J., and Nicolson, G. L. 1972 *Science* 175:720.
- Sjöstrand, F. S. 1963 *J. Ultrastruc. Res.* 9:340.
- Sjöström, M. and Thornell, L. E. 1975 *J. Microsc.* 103:101.
- Skou, J. C. 1957 *Biochim. Biophys. Acta* 23:394.
- Smith, R. P., Rhee, T., Magee, J. L., and Eyring, H. 1951 *J. Amer. Chem. Soc.* 73: 2263.

- Sollner, K., Abrams, I., and Carr, C. W. 1941 *J. Gen. Physiol.* 24:467.
———. 1941a *J. Gen. Physiol.* 25:7.
- Somlyo, A. V., Shuman, H., and Somlyo, A. P. 1977 *J. Cell Biol.* 74:828.
- Somlyo, A. V., Gonzales-Serratos, H., Shuman, H., McClellan, G., and Somlyo, A. P. 1981 *J. Cell Biol.* 90:577.
- Spanswick, R. M. 1968 *Nature* 218:357.
- Sparrow, M. P. 1969 *J. Physiol (London)* 205:19.
- Speakman, J. B., and Hirst, M. C. 1931 *Nature* 127:665.
- Stanley, P. E. and Williams, S. G. 1969 *Anal. Biochem.* 29:381.
- Stecher, P. G. 1968 *The Merck Index*, 8th ed. Merck and Company, Rahway, N.J.
- Steinbach, B. 1940 *J. Biol. Chem.* 133:695.
- Steinbach, H. B. 1940a *Cold Springs Harbor Symp. Quant. Biol.* 8:242.
- Steinhardt, J., and Zaiser, E. M. 1951 *J. Biol. Chem.* 190:197.
———. 1955 *Adv. Prot. Chem.* 10:151.
- Steinhardt, J. Fugitt, C. H. and Harris, M. 1941 *J. Research Nat. Bur. Standards* 26:293.
- Steinmann, A., and Gränicher, H. 1957 *Helv. Phys. Acta* 30:553.
- Stiasny, E., and Scotti, H. 1930 *Ber. deut. chem. Ges.* 63:2977.
- Stillman, I. M., Gilbert, D. L., and Robbins, M. 1970 *Biochim. Biophys. Acta* 203:338.
- Stillman, I. M., Gilbert, C. L., and Lipidsy, R. J. 1971 *Biophys. J.* 11:55a.
- Stone, F. W. and Stratta, J. J. 1967 *Encyclopedia of Polymer Science and Technology*, vol. 6, 103.
- Strugger, S. 1932 *Ber. dtsch. bot. Ges.* 50:24.
- Szent-Györgyi, A. 1957 *Bioenergetics*, Academic Press, New York.
- Taft, R. W. 1953 *J. Amer. Chem. Soc.* 75:4231.
———. 1960 *J. Phys. Chem.* 64:1805.
- Taft, R. W., and Lewis, I. C. 1958 *J. Amer. Chem. Soc.* 80:2436.
- Talaat, S. M., Masston, W. H., and Schilling, J. A. 1964 *Surgery* 55:813.
- Tanaka, S., and Scheraga, H. A. 1976 *Macromol.* 9:168.
- Tanford, C. 1968 *Adv. Protein Chem.* 23:121.
- Taniguchi, K., and Post, R. L. 1975 *J. Biol. Chem.* 250:3010.
- Tasaki, I., and Takenaka, T. 1963 *Proc. Nat. Acad. Sci. USA* 50:619.
———. 1964 *Proc. Nat. Acad. Sci. USA* 52:804.
- Tasaki, I., Luxoro, M., and Ruarte, A. 1965 *Science* 150:899.
- Taylor, J. F., Antonini, E., Wyman, J., and Brunori, M. 1963 *Fed. Proc.* 22:596.
- Terner, C. Eggleston, L. V. and Krebs, H. A. 1950 *Biochem. J.* 47:139.
- Thoenes, F. 1925 *Biochem. Z.* 157:174.
- Thomas, R. C. 1972 *Physiol. Rev.* 52:563.
- Tigyi, J., Kallay, N., Tigyi-Sebes, A., and Trombitas, K. 1981 in: *International Cell Biology, 1980-1981* (H. G. Schweiger, ed.), Springer, Berlin, p. 925.
- Tilney, L. G. and Detmar, P. 1975 *J. Cell Biol.* 66:508.
- Tinker, F. 1916 *Proc. R. Soc. London* 92A:357.
- Tobias, J. M. 1950 *J. Cell Comp. Physiol.* 36:1.
- Tosteson, D. C. and Hoffman, J. F. 1960 *J. Gen. Physiol.* 44:169.
- Tournon, J. and El-Bayoumi, M. A. 1971 *J. Amer. Chem. Soc.* 93:6396.
- Trantham, E. C., Rorschach, H. E., Clegg, J. C., Hazlewood, C. F., Nicklow, R. M., and Wakabayashi, N. 1984 *Biophys. J.* 45:927.
- Traube, M. 1867 *Arch. Anat. Physiol. u. Wiss. Med.* p. 87-128, p. 129-165.
- Trombitás, C., and Tigyi-Sebes, A. 1979 *Acta Physiol. Acad. Sci. Hung.* 14:271.
- Troshin, A. S. 1951a *Byull. Eksp. Biol. Med.* 31:180.
———. 1951b *Byull. Eksp. Biol. Med.* 31:285.
———. 1951c *Byull. Eksp. Biol. Med.* 32:162.
———. 1951d *Byull. Eksp. Biol. Med.* 33:228.
———. 1951e *Biokhimiya* 16:164.
———. 1956 *Problema Kletochnoi pronitsaemosti* (The Problem of Cell Permeability), Moskva-Leningrad.

- . 1958 *Das Problem der Zellpermeabilität*, Gustav Fischer Verlag, Jena.
- . 1966 *Problems of Cell Permeability* (M. G. Hell, transl) (W. F. Widdas, ed.), Pergamon Press, London.
- Tsuboi, M. 1951 *J. Chem. Soc. Japan* 72:146.
- . 1952 *Bull. Chem. Soc. Japan* 25:60.
- Ullman, R. 1970 *Biopolymers* 9:471.
- Ullrich, H. 1939 *Arch. exp. Zellforsch.* 22:496.
- Ussing, H. 1949 *Physiol. Rev.* 29:127.
- Van Slyke, D. D., Wu, H., and McLean, F. C., 1923, *J. Biol. Chem.* 56:765.
- van't Hoff, J. H. 1885 *Kon. Svenska Vetenskaps-Akad. Handl.* 21:42.
- Veis, A. 1964 *The Macromolecular Chemistry of Gelatin*, Academic Press, New York.
- Villegas, R., Blei, M., and Villegas, G. M. 1965 *J. Gen. Physiol.* 48:35.
- von Helmholtz, H. 1881 *Popular Lectures*.
- von Korösy, K. 1914–1915 *Z. Physiol. Chem.* 93:154.
- von Mural, A. 1934 *Arch. ges. Physiol.* 234:653.
- von Zglinicki, T. 1988 *Gen. Physiol. Biophys.* 7:495.
- Wada, A., Tanaka, T., and Kihara, H. 1972 *Biopolymers* 11:587.
- Walter, J. A., and Hope, A. B. 1971 *Aust. J. Biol. Soc.* 57:729.
- Wang, J. H., Robinson, C. V., and Edelman, I. S. 1953 *J. Amer. Chem. Soc.* 75:466.
- White, J. F., 1976 *Am. J. Physiol.* 231:1214.
- Wilkinson, J. H., and Robinson, J. M. 1974 *Nature* 249:662.
- Wilson, T. H. 1954 *Science* 120:104.
- Wiseman, G. 1964 *Absorption from the Intestine*, Academic Press, New York.
- Wood, R. E., Wirth, F. P., and Morgan, H. E. 1968 *Biochim. Biophys. Acta* 163:171.
- Wu, H. 1931 *Chinese J. Physiol.* 5:321.
- Yamamoto, M., Ishizawa, M., and Endo, H. 1971 *J. Mol. Biol.* 58:103.
- Yao, Q. Z., Tian, M., and Tsou, C. L. 1984 *Biochem.* 23:2740.
- Zierler, K. L. 1958 *Ann. N.Y. Acad. Sci.* 75:223.
- . 1972 *Scand. J. Clin. Lab. Invest.* 29:343.

INDEX

References are to page numbers, figure numbers (f), table numbers (t), endnote numbers (n) and equation numbers (eq). The designation 115f refers to the (only) figure on page 115; in contrast, 191f8.16 refers to Figure 8.16 on page 191, on which two figures appear. Page number of an entry where its definition is given, is in **bold face**. Under the entry "equation," this index also provides page numbers for all equations presented. The symbol "lg" following a figure citation represents legend of the figure. The symbol "ins" following a figure number refers to inset in the figure. Greek alphabets are listed according to their English spelling: α , alpha; β , beta; γ , gamma; ξ , xi; ρ , rho; σ , sigma; τ , tau; ψ , psi.

- a. *See a-value*
- a-value*, **256**
 - relation to q or q -value, 257, 257eq34, 35
- A band. *See K⁺*
- acid dissociation constant. *See pK_a*
- across-the-board electron-density change.
 - See electron density*
- actin as protein-X, 203n5
- actin in red-cell ghosts, 272n3, 4
- action potential, 273, 274, 281
 - Bernstein theory of, 274
 - Hodgkin-Huxley theory of, 299
 - Surface-adsorption theory of, 303
 - delayed K⁺ current in, 307, 309
 - initial Na⁺ current in, 305
 - large c -value rise in, 304, 310
 - water depolarization in, 305, 311, 312t
- activation energy for water-, nonelectrolyte-diffusion
 - in cellulose acetate membrane, 215
 - in frog skin, 215
- actomyosin gel. *See adsorption*
- adenoid activity, 9. *See also pump*
- adenosine diphosphate. *See ADP*
- adenosine triphosphate. *See ATP*
- ADP (adenosine diphosphate)
 - adsorption constant on myosin, 187
 - adsorption of, on fluorescence, 181, 182f
 - adsorption on myosin, 187
 - as EDC, 187, 243
 - injection of, on "K⁺ sensitivity," 242
- adrenaline, 292, 292f
- adsorption, 35
 - constants, K_i , K_j , 161
 - definition and history, **37n5**
 - energy of ions vs. c -values, 126–27, 128f
 - importance of, in AI hypothesis, 35
 - localized, 34, 37n5
 - mediating inductive effect, 181–82
 - near-neighbor interaction for coherence in, 135
 - of anions, relative strength of (in lyotropic series), 116, 117f.
 - of Cs⁺, Rb⁺ etc.
 - low-pH suppression of, in EM sections, 65
 - low-pH suppression of, in muscle segments, 61, 62f
 - on EM sections, 57–61, 58f, 60f
 - of ions on acid of diff. c -value, 126
 - enhancement due to charge fixation, 40, 40t
 - homogeneity of, in cells, 169, 171
 - of Rb⁺ on isolated actomyosin, 165, 164f8.2B
 - one-adsorbent-one site, 35
 - one-one stoichiometry between (adsorbed) anion/cation, 35
 - with different $-\gamma/2$, 138f
- adsorption-desorption route of ion permeation (Route 2), 230, 231f, 234f, 307, 322
 - fraction of K⁺ entry into frog muscle via, 234, 234f
 - fraction of Na⁺ entry into frog muscle via, 234, 234f
 - into ion-exchange-resin, 233, 232f9.12B
 - into sheep's wool, 233
- agar-gel filament
 - as model for bulk-phase-limited diffusion, 220
 - water efflux from, influx into, 221f
- AIDS (acquired immunity deficiency), xxi
- all-or-none change. *See autocoooperative transition*
- allosteric control, 149, 152
- α , water content, 161

- α -actinin as protein-X, 203n5
 α -helical potential, **118**, **119t**
 amino-acid residues in proteins
 electron-donating strength of, 118–19
 anoxia
 effect on cell-enzyme retention,
 191f8.16
 effect on cell volume, 267f10.10
 effect on K^+ , ATP, CrP, P, in muscle,
 194f
 effect on resting potential, 295, 296f
 antsemipermeability
 of lipid membranes, 215
 arginine phosphate. *See* ArP
 ArP (arginine phosphate)
 injected into poisoned axon, 239,
 240f9.16B, 241f9.17B
 influence on " K^+ sensitivity," 242
 structural formula of, 242
 Artemia-cyst cells. *See* brine-shrimp-cyst
 cells
 association-induction hypothesis (AI hy-
 pothesis, AIH), xxi, 321
 atomic sieve, 3, 10, 323
 atomic sieve theory
 of Boyle-Conway, 10
 of Mond-Amson, 4, 206–7
 of "Na channel" "K channel," 301–3
 of Traube, 3, 206
 ATP (adenosine triphosphate)
 adsorbed in cells, 188
 adsorption constant on myosin, 180
 adsorption on myosin, 180
 as conservative cardinal adsorbent,
 171–72
 as counterpart of magnet in nail-model,
 32
 as EWC, 180–81
 as living-state-conserving cardinal ad-
 sorbent, 179
 conc. of, in muscle during anoxia, 194,
 194f
 conc. of, in poisoned muscle, 13
 vs. K^+ , Na^+ , sucrose conc., 193f
 conc. profile in EMOC preparation,
 198f
 control of
 cell permeability, 238–44, 240f9.16A,
 241f9.17A
 cell shape, 268–70, 269f, 270f
 cell volume, 265–68, 266eq38,
 267f10.11, 268f
 resting potential, 294–99
 selective ionic accumulation, 188,
 189f, 192f, 193f, 194f
 size-dependent solute exclusion in
 cells, 190, 192f, 193f
 soluble proteins in cells, 188–90,
 191f8.16
 effect on fluorescence of aurovertin-
 complex, 181–82, 182f
 effect of depletion of, on
 enzyme release from cells, 188–91,
 191f8.16
 Na^+ efflux rate of frog muscle, squid
 axon, 238–42
 energy in synthesis of, for work perfor-
 mance, 155, 179–80
 free energy of adsorption on myosin,
 180
 heat of hydrolysis, obsolete and correct
 value, 15, 179
 "helpers." *See* ATP "helpers"
 in maintaining the living state, 178, 197
 quantitative relation to K^+ conc. in
 cells, 188
 quantitative relation to soluble proteins
 in cells, 188, 190, 191f8.16
 required for K^+ accumulation in eryth-
 rocytes, 39
 role in work performance, 178
 synthesis, not from ion-gradient dissi-
 pation, 16
 time course of depletion of, 192f
 antiparallel to Na^+ gain, 190–92,
 192f
 antiparallel to sucrose gain, 192, 192f
 in parallel with K^+ loss, 192f
 ATP "helpers," 182–86
 congruous anions as, 183, 184f
 protein-X as, 184, 184f
 aurovertin, 181
 fluorescence of F_1 -ATPase complex
 with, 182f
 autocooperative adsorption
 definition, **138**
 of K^+ - Na^+ in cells, 169, 173, 169f,
 170f, 174f8.10, 174f8.11
 autocooperative transition, 159
 controlled, 144
 by cardinal adsorbent, 145
 by ouabain, 173, 291
 spontaneous, 143
 backbone carbonyl groups
 adsorb K^+ in Halobacteria, 67n9
 high electron density of, favors α -heli-
 cal conf., 120
 low electron density of, favors fully ex-
 tended conf., 120

- backbone NHCO groups
 as seat of bulk-phase-water adsorption, 73
- bacterial vesicles
 not hollow, 27
- Bernstein, J., 273
- Berthelot-Nernst Partition Law, 77, 110n3
- β -, γ -carboxyl groups, 34f3.3, 39, 149, 151, 262, 266, 269, 281–82, 304, 322
- autocooperative interaction among, 141
- confirmed as K^+ -adsorbing groups in muscle
 from acid titration study, 62f
 from carboxyl-specific-reagent effect, 63t
- c*-value affected by ouabain, 172–77, 174f8.10, 174f8.11, 175t, 177f
- high H^+/K^+ selectivity ratio of, 248n6
- liberated from salt-linkages by NaOH
 K^+ , Na^+ adsorption on, 41, 42
- rank order of selectivity: $Na > Li > K > Rb, Cs$, 44
- strong near-neighbor-interaction among, 141, 142f
- selective ionic adsorption on, determines resting potential, 286, 286f, 287–88, 287f, 288f
- uranium binding on, 48
- bifacial cells, 10, 19
- Bohr effect, 153
- interpretation based on AI hypothesis, 154–55
- Boltzmann, L., xxiv, 36
- bound water, 6, 105. *See also* Schwellungswasser, imbibition water
- bovine serum albumin, 150
- Boyle and Conway, 4
- atomic sieve theory of, 4
- Bradley multilayer adsorption isotherm, 38n5, 70, 80, 100, 257
- obedience to, of water in frog muscle cells, 99
- obedience to, of water in gelatin gel, 100
- “breathing” of proteins, 146
- brine-shrimp-cyst cells (*Artemia* cyst cells), 96
- QENS studies of water in, 98f
- UHFD studies of water in, 96
- bulk-phase-limited diffusion, 218, 219f9.6BD
- of water in agar gel filament, 221f9.7BD
- of water in frog ovarian egg, 222f9.8
- of water in giant barnacle muscle, 222f9.9, 223f
- c*. *See c*-value
- c*-value
 change in response to ouabain, 176, 177f
- definition, **126, 127f**
- of cell-surface β - and γ -carboxyl groups, 282, 311
- c'*-value, definition, **147**
- c*-value analogue, definition, **147, 147f**
- c'*-value analogue, definition, **147, 147f**
- Ca^{++} as conservative cardinal adsorbent, 171, 172f
- cancer, ix, 94
- longer T_1, T_2 of water protons in
 from less-intensely polarized water, 94
- from lower paramagnetic-ion (Mn, Fe) content, 94
- carbodiimide, 62. 63t *See* EDC (second entry of two)
- carboxyhemoglobin, 150, 150f
- acid binding on, 150f
- carboxyl groups. *See also* β - and γ -carboxyl groups
- cause electric potential of collodion membranes, 283–84
- cardinal adsorbent, 32, 142, 143, 153, 159, 171–72, 196, 235, 238, 265, 292, 304. *See also* EWC, EDC
- classification, 145
- conservative, 171–72
- ATP as, 171
- Ca^{++} as, 171, 172f
- definition, **144**
- diagrammatic illustration of, 143f7.6B, 147f, 149f
- ouabain as, 172
- controls solute distribution, 172–77
- controls permeability, 235–37
- controls resting potential, 290–92
- cardinal site, **144**
- cell membrane
- as lipid bilayers, 205, 208
- as a dry membrane, 212
- not enough lipid to form continuous cover, 213
- as phospholipid-protein-polarized-water system, 205, 212
- as a wet membrane, 212
- contents of lipids and of proteins, 212

- cell membrane, (*Continued*)
 differences between theoretical models, 212
 non-regeneration of, at cut end of muscle cells, 53f
 unable to accommodate endless pumps, 18
- cell potassium, 39. *See* K^+
- cell shape, 249
 control of, 263
 determined by cytoplasmic proteins, 263–65, 265f
- Cell Theory of Schwann, xxii
- cell volume, 249
 control by ATP, 266, 267f10.11, 268f
 control by Na^+ and Cl^- , 266–68, 267f10.10
 determined by cytoplasmic protein(s), 253, 264, 265f
 new quantitative theory of, 253, 257, 258f10.4
 evidence for 258f10.5, 260t
- cell water, 69
 less than 6% proteins polarizes all, 75, 75f
 polarized multilayer theory of, 73–77
- cellular electrical potentials, 4, 273. *See also* resting potential, action potential
- centrifugation-extractable fluid
 from cut-muscle segments, 254f
 from intact, normal muscle, 254f
 from swollen muscle, 254f
- cellulose-acetate membrane, 213
 1:1 correspondence in permeability of, with frog skin, 214f
 semipermeability of, 214f, 215
- cesium ion. *See* Cs^+
- CG electrode. *See* collodion-coated electrode
- characteristic frequency, 96. *See also* dielectric relaxation time
- charge fixation
 enhances counterion association, 39, 40t
- charge site, polarity and geometry of
 on stability of multilayer water structure, 74f
- chloride ion. *See* Cl^-
- Cl^- (chloride ion)
 as congruous anion in RBC, 183
 barred from entering cell during activity, 305
 in cell swelling, 262
 in lyotropic series, 116, 117f
 membrane permeability to, 4, 210–11
 coacervate state, not needed in solute exclusion, 85
 coherence among multitude, 135
 of swimming fish, 135, 136f
 role of near-neighbor interaction, 135
- collagen, phenol binding on, 140, 141f, 153
- collodion membrane, 220, 283
 microsac, water efflux from, 220, 221f
- collodion-coated-glass electrode (CG electrode), 284, 284f, 287f
 as model of cell potential, 283
 indifferent to external Mg^{++} , 288f
- colloid, 3
 new definition of, 85
 old definition of, 3
- colloid chemistry, 6–7
- colloidal condition of matter, 3
- conformation state of proteins, 152
- congruous anions, 183, 184f
 chloride as, 183
 concentration of, relation to K^+ concentration, 193
 creatine phosphate as, 183, 193, 295–97
 definition, 183
 influence on Na^+ -efflux-rate change of poisoned cells
 of stable isethionate in squid axon, 243–44
 of unstable CrP in frog muscle, 243–44
 inorganic phosphate as, 195, 248n7
 isethionate as, 183, 243
 L-glutamate as, 183
 phosphates (various) as, 183, 203n4
- conservative cardinal adsorbent, 171–72
 ATP as, 171
 Ca^{++} as, 171, 172f
- controlled autocoooperative transition, 143f7.6B, 144, 147
 attribute of directionality, 144
 attribute of here-to-there, 144
 attribute of one-on-many, 144
 attribute of timing, 144
 by adrenaline, of resting potential 292
 by ATP (and “helpers”)
 illustration of, 184f
 of cell permeability, 238–44
 of cell shape, 268
 of cell volume, 265
 of model, 155

- of resting potential, 294–99
 - of solute distribution in cells, 188–98
- by Ca^{++} , of K^+/Na^+ distribution, 171–72
- by H^+ , in model, 149
- by HCl in model, 150
- by IHP in model, 152
- by insulin on D-glucose uptake, 163
- by ouabain
 - of ion permeability, 235–37
 - of resting potential, 291 (also 279)
 - of solute distribution, 172–78
- model of, focus on backbone sites, 147, 147f
 - Model 1, interaction with EDC, 148
 - Model 2, interaction with EWC, 148
- model of, focus on functional groups
 - on short side chains, 148–49, 149f
- role of indirect F-process in, 148
- cooperative adsorption
 - of Na^+ on hemoglobin at high pH, 142f
 - of oxygen on hemoglobin, 152
 - of phenol on collagen, 141, 141f
 - theory of, 136
- cooperative interaction
 - among backbone NHCO groups, 140
 - among β - and γ -carboxyl groups, 141
- cooperative phenomena, 138
- cooperative states
 - transition between and control, 142
- copper-ferrocyanide gel
 - as model of plasma membrane, 3, 215, 249, 323
 - sucrose exclusion from water in, 215
- counterion association
 - enhancement from charge fixation, 39, 40, 40t
- creatine phosphate (phosphocreatine, CrP). *See* CrP
- Crevice hypothesis
 - disproof, 137
 - explaining S-shaped oxygen binding curve, 137
- CrP (creatine phosphate, phosphocreatine)
 - as congruous anion in muscle, 183
 - concentration of,
 - change during anoxia, 194, 194f
 - correlation with “A” potential, 298f
 - fall in poisoned muscle, 13
 - in frog muscle, 204n6
 - relation to ATP concentration, 204n7
 - in maintaining resting potential, 294–99
 - structural formula of, 183
- cryoprotectants
 - as nonelectrolytes with abnormally high q -value, 91f5.9B
- Cs^+ (cesium ion). *See also* Tl^+
 - distribution in presence of K^+ , 168
 - localization in A bands
 - in autoradiography, air-dried muscle, 46, 46f
 - in autoradiography, frozen-hydrated muscle, 48, 49f
 - in TEM, freeze-dried muscle section, 47, 47f
- cut muscle segments. *See also* EMOC
 - centrifugation-extractable water in, 254f
 - identify K^+/Na^+ -adsorbing groups in, 61, 62f, 63t
 - illustration of 2mm-4mm, 262f
 - no membrane regeneration at cut end of, 51, 53f
 - volume change of, in salt solutions, 262, 263f
 - water contents in, 254f
- Damadian, R. V.
 - as discoverer of longer T_1 , T_2 in cancer cells, 94
 - as inventor of MRI, xxvnl,
- Darwin, C., xxii, xxiv
- death as entropy-driven process, 182
- deBoer-Zwicker multilayer-adsorption isotherm, xii, 38n5
- Debye dielectric relaxation time. *See* dielectric relaxation time
- Debye and Hückel
 - dilute solution theory of, 39
- D-effect, 133n4
- denaturation
 - by NaOH, 41eq3
 - by urea, GuHCl, SDS, n-propanol, 85, 86f5.6, 86f5.7, 88t
 - by urea, illustration of, 86f5.6
 - early definition, **37n4**
- diagram of part of living cell, 33, 34f
- dialysis. *See also* equilibrium dialysis
 - invented by Graham, 7n2
- “dialyzed squid axon”
 - demonstrated no active Na^+ transport, 20
- dielectric dispersion, 96
- dielectric relaxation time (τ_D), 96

- dielectric relaxation time, (*Continued*)
 of water in living cells and extrovert models, 96
 relation to characteristic frequency, 96
 relation to (NMR) rotational correlation time, 96
- diffusion coefficient of K^+
 in squid axon, 21
 in frog muscle, 21
- diffusion coefficient of water
 rotational, 97
 translational, 97, 224t
- dilute solution theory, xxiv
 membrane theory as, xxiii
- 2,3-diphosphoglycerate. *See* 2,3-DPG
- direct F-effect, 116. *See also* F-effect
- dispersive X-ray microanalysis
 of localized K^+ distribution in muscle, 51f
 of localized K^+ , Rb^+ , Cs^+ , Tl^+ in muscle, 52f
- dissociation constant. *See* pK_a
 of glycine peptides, 117, 117t
 shows inductive effect via polypeptide chain, 117, 132f6.11A
- distance between protein chains vs. protein conc., 75f
- Distribution Law of Berthelot and Nernst, 77, 110n3
- Donnan equilibrium, 17, 29n6
 impermeant ion lowers conc. of ion of like charge in same phase, 22, 30n1
- Donnan ratio (r)
 observed differ from predicted 17, 17t
- 2, 3-DPG (2, 3-diphosphoglycerate). *See also* IHP, ATP
 as cardinal adsorbent for oxygen binding, 152
- drug, xi, xxi, 339
- du Bois-Reymond, E.,
 early investigator of action potential, xi, 273, 338
 for physicochemical approach to living phenomena, xxiii
- Dujardin, F., as discoverer of sarcode (protoplasm), 2
- dynamic structure. *See also* dynamic systems
 of water, protoplasm, 33, 73, 321
- dynamic systems, proteins as, 146
- electron-donating-cardinal adsorbent. *See* EDC
- EDC (electron-donating cardinal adsorbent), 148, 159
 definition, 145
 in controlled cooperative transition, 147–48, 147f Model 1
- EDC (1-ethyl-3-(3-dimethylaminopropyl)carbodiimide), 62, 63t
- effectively-membrane-pumpless-open-ended-cell preparation. *See* EMOC preparation
- effector, 118
- efflux profile, 220
- EIC (electron indifferent cardinal adsorbent)
 definition, 145
- electrical polarization (induction). *See also* F-effect
 in $-\gamma/2$, 159
- electrogenic pump
 definition, 277–78
 evidence against, 280
- electron density of backbone carbonyl groups.
 across-the-board rise or fall in response to EDC, EWC resp., 147, 147f
 high value of, favors α -helix conf., 120
 low value of, favors fully-extended conf., 120
- electron density of functional groups on short side chains
 across-the-board rise or fall in response to EDC, EWC resp., 148, 149f
- electron-indifferent-cardinal adsorbent. *See* EIC
- electron-donating effect, 113
- electron-donating power
 of side chains vs. -helical potential, 119, 119t, 120f
- electronegativity
 definition, 133n1
 in inductive effect, 112
- electron microscopic sections. *See* EM sections
- electron-withdrawing-cardinal adsorbent. *See* EWC
- electron withdrawing effect, 113
- electrostatic bond (ionic bond)
 mediating inductive effect, 115
- EM sections of frog muscle
 freeze-dried-embedded (unfixed, unstained), 47f4.6B to F
 freeze-dried/-substituted, Cs^+ -stained in vitro, 58f

- at cut end of muscle, 199f8.23(3)
 away from cut end of muscle, 199f8.23(4)
 Cs⁺-loaded in vivo, 47f4.6B
 Cs⁺-loaded in vivo, after leaching, 47f4.6E
 normal, K⁺-“loaded,” 47f4.6F
 Tl⁺-loaded, after exposure to moist air, 47f4.6D
 Tl⁺-loaded in vivo, 47f4.6C
 frozen-hydrated
 normal K⁺-“loaded” muscle, 50f4.8b
 Tl⁺-loaded muscle in vivo, 50f4.8a
 glutaraldehyde-fixed, uranium-stained, 47f4.6A
 at cut end of muscle, 199f8.23(1)
 away from cut end, 199f8.23(2)
 1, 5, 120 min. after cut, 53f
 granular Tl⁺ precipitate in, 47f4.6D
 emergentist, 36n3
 EMOC preparation (effectively-membrane-pump-less-open-ended-cell preparation), 51
 diagrammatic illustration of, 54f
 in determining K⁺ mobility in cytoplasm, 21
 in disproving membrane-pump theory, 54
 in disproving ouabain as Na-pump inhibitor, 172, 173f
 in supporting ouabain as cardinal adsorbent, 172
 labelled K⁺/labelled Na⁺-distribution in, 55f
 Tl⁺, Cs⁺ and Na⁺ distribution in, 57f
 total K⁺, labelled K⁺/Na⁺ distribution in, 56f
 E_{Na} (sodium potential), 300, 300eq52, 307
 energy/entropy of living and dead states, 33f
 energy source for work performance, 187
 enthalpy of ATP hydrolysis, lower than believed, 15
 entropy
 definition **35n2**
 gain during deoxygenation, 153
 explanation based on AI hypothesis, 155
 enzyme, retention in, release from cells, effect of anoxia on, 191f8.16
 effect of externally-added ATP, ADP on, 191f8.17
 relation to ATP conc., 191f8.16
 equation 1, Nernst eq., 4, 274
 equation 2, Donnan equilibrium, 17
 equation 3, unmasking of carboxyl groups, 41
 equation 4, Bradley isotherm, 70
 equation 5, Bradley isotherm, log-log form, 70
 equation 6, Berthelot-Nernst eq., 77
 equation 7, Yang-Ling isotherm, 137
 equation 8, ξ , 137
 equation 9, Langmuir isotherm, simplified, 138
 equation 10, Yang-Ling isotherm, ratio form, 138
 equation 11, Hill eq., 139
 equation 12, tangent of log-log plot of Yang-Ling isotherm, 139
 equation 13, $-\gamma/2$ vs. $|\Delta F_{T \rightarrow}^{00}|$, 140
 equation 14, for free and cooperatively adsorbed solute, 161
 equation 15, for free and noncooperatively adsorbed solute, 161
 equation 16, general equation for solute distribution, 161
 equation 17, free-solute distribution, 162
 equation 18, Troshin eq., 163
 equation 19, Langmuir isotherm, 166
 equation 20, reciprocal form of Langmuir isotherm, 166
 equation 21, Langmuir isotherm with competing species, 167
 equation 22, reciprocal Langmuir isotherm with competition, 167
 equation 23, ion exchange at surface anionic sites, 230
 equation 24, rate of K⁺ entry with competing Rb⁺, 231
 equation 25, reciprocal form of K⁺ entry with competing Rb⁺, 231
 equation 26, general eq. for ion permeation, 235
 equation 27, simplified general eq. for ion entry, 235
 equation 28, rate of permeation vs. adsorption constants, 237
 equation 29, π vs. C , 249
 equation 30, π vs. T , 250
 equation 31, van't Hoff eq., 250
 equation 32, V vs. C , 250
 equation 33, cell volume, its components, 256
 equation 34, a vs. q , 257
 equation 35, log-log plot of a vs. q , 257
 equation 36, KCl, swelling in, 262

- equation 37, NaCl, weak swelling in, 262
 equation 38, NaCl swelling with ATP depletion, 266
 equation 39, HKG eq., 275
 equation 40, verified portion of HKG eq., 277
 equation 41, modified HKG eq., 277
 equation 42, second modified HKG eq., 277
 equation 43, third modified HKG eq., 278
 equation 44, SA theory eq., 281
 equation 45, SA eq., 2nd form, 281
 equation 46, SA theory eq., general, 3rd form, 281
 equation 47, constant, 281
 equation 48, SA theory with cooperativity, 289
 equation 49, ξ , 289
 equation 50, explicit eq. of SA theory with cooperativity, 290
 equation 51, explicit eq. of simplified SA theory, 290
 equation 52, Na potential eq., 300
 equation 53, general eq. of resting and action potential, 308
 equation 54, q vs. γ 's, 308
 equation 55, 2nd general eq. of resting and action potential, 308
 equilibrium dialysis, 81
 used in model studies 86f5.7, 90f, 91f5.9A, 88t
 equilibrium water sorption
 extremely slow at near-saturation vapor-pressure, 110n6
 erythrocyte (RBC), *See* red blood cells
 ethylene glycol, equal partition of. *See also* Partition Law
 between cell and external water, 6–7, 91f5.9B
 between model and bathing solution, 91f5.9A
 exchange diffusion of Ussing, 16
 extroverts, 107
 definition 107
 enhance osmotic activity, 80, 101–2
 lower freezing point, freezing rate, 102–6
 reduce solvency for large solutes, 81–92
 restrict rotational (translational) freedom, 92–98
 strongly adsorb water at near-saturation, 97–101, 100f
- EWC (electron-withdrawing-cardinal adsorbent)
 adrenaline as, on resting potential, 292
 definition, 145, 160
 H⁺ as, in urea/water binding, 149
- $\Delta F_{j \rightarrow i}^{00}$, (intrinsic free energy change for j -to- i adsorption exchange)
 for displacement of K⁺ by labelled Cs⁺, 171
 for displacement of K⁺ by labelled K⁺, 171
- $|\Delta F_{j \rightarrow i}^{00}|$ (absolute value of F_{ij})
 relation to $-\gamma/2$, 140, 170
- FDNB (fluorodinitrobenzene), 195
 effect on cell K⁺, CrP, ATP, 196f
 inhibits creatine kinase, 195
 shows CrP as deputy primary CA, 196
- F-effect, 133n4
 direct F-effect, 116, 130, 133n4
 “unit distance” of operation, 130
 indirect F-effect, 142,
- ferrihemoglobin, 150
 titration of, 151
- fixed cations
 in erythrocyte membranes, 218
 neutralization of, liberates fixed anions, 42f4.2, 43f
- fluorescence, 123–25, 181–82
 falls with more attached peptide bonds, 124t
 falls with protonation of distant α -amino group, 125f
 of aurovertin-F₁ ATPase complex, 182f
 of tyrosine and tryptophane, inductive effect on, 123–25
 yield, 123
 inductive effect on 124–25
- Franklin, Benjamin, 339
- free energy
 of dimerization, 113, 115f
 of hydrolysis of ATP, CrP, 15
- free volume reduction, enhancing counterion association, 40
- free-water tenet in membrane theory, 29n7
- freezing-point depression, 6, 7, 102, 104, 105f5.15B
- frog skin
 as example of bifacial cells, 10
 permeability of water, nonelectrolytes, 214, 214f
- fully-extended-conformation of protein, 121

- converting native protein into, by urea, GuHCl, 85
 - definition, 33
 - different from “extended conformation,” 33
 - in gelatin, 81
 - in oxygen-containing polymers, 84
- functional groups on short side chains
 - across-the-board electron-density gain from EDC, 148, 149f
 - across-the-board electron-density loss from EWC, 148, 149f
 - list of, 116
 - physiologically active, 116
- functional groups on long side chains, 116
- $\gamma_{\text{ex}}^{\text{Na}}, \gamma_{\text{in}}^{\text{K}}$ (activity coefficient of K^+ , Na^+ in external medium or cell resp.) 308
 - $\gamma/2$ (nearest-neighbor interaction energy), 137, 138f, 141, 151, 161, 170, 289, 291, 292, 293
 - relation to $|\Delta F_{\text{f} \rightarrow \text{u}}^{\text{oo}}|$, 140, 170
 - relation to Hill coefficient, n , 139
 - $\gamma'/2$, same as $-\gamma/2$ but refers to adsorption on surface sites, 289
- gang of sites, 144, 187
- gel state. *See also* jello
 - not essential for solute exclusion, 85
- gelatin
 - as model of protoplasm, 3
 - at least 54% of NHCO groups fully-extended, 81
 - colloid, named after, 3
 - exclusion of Na_2SO_4 from, 81
 - high osmolarity of solution of, 101f
 - historic quest for understanding of, resolved, 81
 - polypeptide chain fully-extended, 81
 - unusual amino acid composition, 81
 - water in gelatin gel polarized, 81
 - irregular ice formed in, 104f
 - nonfreezing of 65% gel of, 102
 - sorption of water by, at near-saturation, 100, 100f
- genetic code, xxii
- germ plasm and genetics, xxii
- glass electrode, 282. *See also* CG electrode, PCG electrode.
- glass-membrane electric potential
 - as model of resting potential, 282
- D-glucose
 - equilibrium level in muscle, 18f, 163, 163f
 - “primer” in insulin-induced uptake of, 171
- L-glucose, equilibrium level in muscle, 18f
- L-glutamate, as congruous anion, 183, 185t
- glycolysis inhibition. *See* iodoacetate
- Graham, T., 3, 218
 - as founder of colloid chemistry, 3
 - as inventor of dialysis, 7n2
- Great Wall of China, 135
- guanidine HCl, 85, 86f5.7, 88t
- H^+ (hydrogen ion)
 - as EWC, controls urea/ H_2O binding, 149
 - in carboxyhemoglobin titration, 150f
- hydrogen ion, *See* H^+
- H-bond
 - mediating inductive effect, 115
 - strength of, target of inductive effect, 115f
 - strength in dimerization vs σ_{Hammett} , 115f
- Hamilton, Sir William, as author of Law of Parsimony, 30n10
- helix-random-coil transition
 - high speed of, 146
- Helmholtz, von, H., *See* von Helmholtz
- “helper” (ATP “helpers”) 182–83, 322, *See also* congruous anion, protein-X
- hemoglobin
 - alkali-denatured, 41, 87
 - conformation change in, 154f
 - global changes during oxygenation-deoxygenation, 153, 155
 - in ghosts, linearly related to K^+ regained, 44, 45f
 - in ghosts, linearly related to Na^+ extruded, 44, 45f
 - in sickle-cell anemia, 263
 - native, 87
 - native, not adsorbing K^+/Na^+ in vitro, 41
 - oxygen binding on, 136
- hexagonal ice, 104, 104f5.14a
- high-energy-phosphate bond, ($\sim\text{P}$), 179
 - evidence against concept of, 15, 15t
- high-(negative)-energy, 35, 35n1
- high-(negative)-energy—low-entropy (living) state, 31
- Hill, A. V., 6, 139
 - conclusion of, reversed, 87
 - impact on colloidal approach to cell physiology, 6–7

- Hill coefficient (n)
 identified as $\exp(-\gamma/2RT)$, 139
- Hill's (empirical) eq. as tangent to Yang-Ling isotherm, 139
- HKG equation (Hodgkin-Katz-Goldman equation)
- Hodgkin-Katz-Goldman equation (HKG eq.), 275
 challenge to modification of, 277
 incomplete verification, 276–277
 modifications, 277
 results of experimental testing, 276
- Hofmeister series (lyotropic series)
 of invariant relation among anions, explained, 116, 117f
- hollow membrane vesicles, not hollow, 25–28
- hybrid red cells, 265f. *See also* sickle-cell anemia
 proving cytoplasmic proteins determine cell shape, 264, 265f
- hydrogen ion. *See* H^+
- IAA. *See* iodoacetate
- ice crystal
 irregular, in living cells, gelatin, PVP, 102, 104f5.14b
 shape of, in 35% serum albumin and 50% gelatin, 104f
- ice formation in single muscle fibers, 103f
- ice-spike formation in muscle cells, 102–3
- I-effect (inductive effect), 133n4
- IHP (inositol hexaphosphate)
 as cardinal adsorbent, 152f, 153, 173
 controls oxygen binding on hemoglobin, 152, 152f
- imbibition water, xxiii, 6, 252. *See* Schwellungswasser
- inanimate models, xxiv, 274, 320
 failure to find, for membrane-pump theory, 211, 322–23
 failure to find, for postulated ionophores, 211
 for AIH of cell electrical potentials, 282–85
 for AIH of cell volume, 256f
 for AIH of solute distribution, 41, 42f4.2, 90f5.8A, 91f5.9A, 108t
 for AIH of solute permeation, 214f, 232f9.12B
- indirect F-effect, definition, 142. *See also* F-effect
- indirect F-process
 definition, 142
 in controlled autocoperative transition, 147, 148
 “indirect method” for demonstrating relation between ATP/CrP and resting potential, description of, 295
 induced dipole of water molecule, 69
 induction (electrical polarization), 111, 112
 as equivalent of “turning” in lock-key analogy, 145
 induction constants, 113, 114f, 115f. *See also* inductive indices
 of Hammett, 115f
 of Taft, 114f
 inductive component in $-\gamma/2$, 139
 inductive effect
 evidence for transmission through 3 peptides-linkages, 117, 118, 120, 120f, 125f, 132f
 explains heme-heme interaction in terms of, 137, 154–55
 illustration of distant transmission of, 132f
 in determining bulk-phase-water adsorption, 121
 in determining protein structure, 118, 119t
 on tyrosyl and tryptophanyl fluorescence, 123, 125f
 target of, 118
 transmission over distance in small molecules, 112
 inductive indices of Chiang and Tai, 113
 induction theory, 112, 113
 for short-range interaction of protein structure, 118
 of Chiang and Tai, 113
 of G. N. Lewis, 112–13
 influx-profile-analysis method, 218
 applied to water influx into barnacle muscle, 223f
 applied to water influx into frog egg, 222f9.8, 223
- injury
 effect on in vitro Cs^+ staining of EM sections, 197–98, 199f
 effect on K^+ accumulation, 198f
 effect on K^+ diffusion rate in cytoplasm, 21
 effect on Na^+ exclusion, 198f
 swelling from, vs. ATP conc., 266, 266eq38, 267f10.11, 268f
 swelling from, vs. NaCl conc., 266, 266eq.38, 267f10.10
- inositol hexaphosphate. *See* IHP

- insulin
 as cardinal adsorbent for D-glucose adsorption, 171
 effect on D-glucose distribution, 163, 163f
 no detectable effect on q of D-glucose, explanation, 177–78. *See also* water-polarizing protein
- intensely-polarized water
 in activated cellulose acetate membrane, 213
 in living cell membrane, 213
- interfacial tension
 at oil/water interface, 209
 at phospholipid/water interface, 209
- intermediate-range-interaction in protein structure, 118
- intestinal epithelium
 as example of bifacial cells, 10
 specificity in sugar transport across, 19
- intracellular pH, 41, 111
- intracellular “reference phase” studies
 did not establish Na pump in unifacial cells, 22
 vs. Law of Parsimony, 22, 30n10
- intrinsic-equilibrium-constant. *See* K_j^{00} ,
- intrinsic-free-energy of adsorption-exchange ($\Delta F_{j \rightarrow i}^{00}$)
 relation to $-\gamma/2$, 140eq13
- introverts. *See also* extroverts. native proteins
 definition, **107**
 less water sorption at high vapor pressure, 99, 100f
 low osmotic activity in solutions of, 80
 minimal effect on freezing point, rate, 105, 105f5.15a
 weak effect on water polarization, solvency, 81–92, 108t
- in-vitro adsorption of K^+ , Cs^+ on EM sections, 57, 58f
- iodoacetate (IAA)
 as inhibitor of glycolysis, 10, 12f, 189f, 192f, 296f11.12A, 297f11.14, 298f
- ion adsorption
 different rank order of selective, of $K^+ > Na^+ > Li^+$ in sulfonic, phosphonic and carboxylic exchange resins, 129t
 four configurations of linear model of, 126
 rank order of selective
 on cytoplasmic β -/ γ -carboxyl groups, 176
 on surface β -/ γ -carboxyl groups, 237, 237t, 286f, 311
 theory of, on oxyacid at different c -values, 125–30, 128f, 129f
 selective, in sulfonic resin with varying DVB, 130f
 selective, on β - and γ -carboxyl groups, 125, 287f
- ion efflux, rate of
 K^+ , slow and explanation, 238
 Na^+ , fast and explanation, 238
- ion-exchange-resin. *See also* ion adsorption
 NMR of Na^+ in, 203n3
- Ionic theory, 275
 critique of standing Na potential, 300–301
 critique on concept of rigid K^+ and Na^+ channels, 301
 critique on explanation of delayed K^+ current, 301
 evidence for and against, 276–77, 279–80
- ionophores, 210, 216
 failure to find natural, 211
 failure to increase K^+ permeability of frog egg, 217, 217f
 of frog muscle, 217, 217f
 of inner membrane of liver mitochondria, 218
 of squid axon, 217
 partial success of, increasing RBC K^+ permeability, 217, 217f
 use in sizing lipid-bilayer-barrier in membrane, 216, 216f
- isethionate
 as congruous anion in squid axon, 183
 role in slow Na^+ -efflux of poisoned squid axon, 243–44
- Ising model, one-dimensional, 137
 no temperature transition in, 317n10
- jello, 81
 cause of standing-up quality, 110n4
- Jordan-Lloyd’s theory of protein hydration, 72
- K_i , K_j (adsorption constants) 161
 definition, **161**
- \bar{K}_K , \bar{K}_{Na} (adsorption constants on surface carboxyl groups), 281, 286, eqs. 44–46, 50–51, 53–55
- $K_{j \rightarrow i}^{00}$ (intrinsic equilibrium constant for j -to- i adsorption exchange), 137
 definition, **137**, **161**
 relation to K_i , K_j , 161, 171

- $K_{Na \rightarrow K}^{00}$ (intrinsic equilibrium constant for Na^+ -to- K^+ adsorption exchange)
effect of ouabain on, 173
- K^+ (potassium ion), 39. *See also* protein-water- K^+ system
accumulation in cells, 4
activity of, in cell,
diversity, contradicting membrane theory, 21
measurement with K^+ -electrode, 21
adsorption
homogeneity of, in cell, 167f, 169, 171
on β - and γ -carboxyl groups, 45–65
concentration in muscle,
indifference to Mg^{++} , contradicts membrane-theory, 166
in EMOC of muscle cells, 50, 54
in Halobacteria, 67n9
in presence of competing ions, 167–69, 167f, 168f
obedience to eq. 22, 167f, 168f
relation to ATP conc., 189f, 193f
localization in A band, 46, 58
mobility of,
in muscle, healthy, injured and killed, 21
in squid axon, 21
permeation
into egg, muscle and RBC cells, 217, 217f
surface-limited, 230
preference over Na^+ at low c -value, 127, 128f, 129f
specific electrode for, 21. *See also* Na^+ -specific electrode
inability of sizing resting cytoplasmic K^+ activity, 21
living cells behaving like, 276
- K^+ and Na^+
absence of transport in hollow red cell ghosts, 27f
adsorbed state of, 175
adsorption in cell, early model, 126
as monitors for life-death of living cells, 1,
conc. profile vs. ATP profile in EMOC, 198f
distribution as focus for presenting AI hypothesis, 33
in poisoned muscle, 11t
membrane permeability to, 4
 K^+ over Na^+ preference
at lower c -value, 127, 128f, 129f
- “ K^+ sensitivity” in Na^+ efflux from squid axon, 239
effect of injected ArP on, 241f9.17B
effect of injected ATP on, 241f9.17A
- KCl, isot. solution of, cell swelling in, 260, 262eq.36
- lactate dehydrogenase, release with ATP depletion, 191f8.16B
- LAMMA (laser microprobe mass analysis)
shows in vitro selective K^+/Cs^+ adsorption in EM sections, 59, 60, 60f
- Langmuir adsorption isotherm, 37n5, 137–38, 201n1, 230
as key component in equations of cell potential, 44, (see 315n4 eqB)
cell volume, Ling-Peterson, 1977
solute distribution, eq 18 (Troshin eq)
solute permeation, eq 24
saturability and competition in, 201n1
- laser-microprobe-microanalysis. *See* LAMMA
- Lavoisier, A. xxiv, 319
- Law of Macroscopic Electroneutrality, 40, 66n1
- Law of Parsimony, 30n10
- Le Chatelier principle, 15, 29n4
- Lewis, G. N., 112–13
- life and death of a living cell, 1
diagnosis of, 1
- life as flame, 36n3
- life as organization, 36n3
relation to concept of living state, 37n3
- linear distribution of solutes, 77, 87
in frog muscle cell water, 90f5.8B
in solution of NaOH-denatured hemoglobin, 90f5.8A
in solution of native hemoglobin, 87
in solution of PEO, 92
slope of, equals q -value of solute, 77
- linear-distribution rule
definition, 77
incompatible with pump theory, 201n1
relation to Partition Law, 77
- Lipid-protein-polarized-water-membrane model
coherence and control in, 212
versatility in, 212
- lipoidal membrane theory
origin of, 206
modifications of, 206
reintroduction of, 208
- liver mitochondria inner membrane

- K^+ permeability of, indifferent to valinomycin, 218
 trilaminar structure indifferent to lipid removal, 211
 living cell, early theories of, 2
 Living state, 31, 144
 as high-(negative)-energy—low-entropy state
 definition of, **31–32**
 concept, relation to historical views
 of life as “état de chose,” 36n3
 of life as organization, 36n3
 maintenance of,
 by ATP and “helpers,” 182–86, 197, 203n5
 demonstration of, in EMOC studies, 198f
 in frozen-dried, embedded EM sections, 198
 lock-and-key analogy
 in specificity of small-molecule-protein interaction, 145
 induction as “turning” of key in, 145, 158n1
 long-range interaction in protein structure, 118
 Ludwig, C. xxiii, 338
 as champion of physico-chemical interpretation of Life, xxiii
 “Carl Ludwig’s problem” xxiii
 lyotropic series, (Hofmeister series) 116, 117f
- Magnesium ion. *See* Mg^{++}
 Mg^{++}
 adsorption of, on aurovertin- F_1 ATPase fluorescence, 182, 182f
 distribution in muscle
 indifference to K^+ , 165
 vs. Troshin eq., 165, 165f
 indifference of cell K^+ level to, 165f
 indifference of collodion electrode to, 288f11.7A
 indifference of resting potential to, 288f11.7B
 permeability of living cell to, 5, 315n6
 magnet-nails-iron-filing model, 32, 32f, 111, 178
 magnetic resonance imaging. *See* MRI
 malic dehydrogenase, release with ATP depletion, 191f8.16A
 maximum-available-energy of poisoned muscle vs. minimum-needed-energy for postulated Na pump, 12–14, 14t
 Maxwellian demon, 9, 28n1
 vs. First, Second Law of Thermodynamics, 28n1
 membrane lipids, removal of, did not destroy trilaminar structure
 of liver mitochondria inner membrane, 211
 of microbial membrane, 211
 membrane permeability to many large molecules, 208
 “membrane physiology,” mostly misnomer, 205
 membrane potential
 definition, **273**
 inanimate models for, not found, 276, 282–85, 323
 resting potential as, 4
 role of ion permeability, in theory of, 273
 theory of resting and action potential as, 273
 membrane-pump hypothesis, xxi, xxii, 320, 323
 disproof of, 28
 history of, 9
 (pure) membrane sac of axoplasm-free-squid-axon
 failure to demonstrate K^+/Na^+ pumping in, 20
 (undiscovered) metabolic activity of living cells
 nonexistent or insignificant, 10–11
 metabolic inhibition, effect of
 on cell ATP level, 189f, 192f, 194f, 196f
 on cell CrP level, 194f, 196f
 on cell enzyme release, 191f8.16
 on cell K^+ level, 10, 11t, 189f, 192f, 194f, 196f
 on cell Na^+ level, 192f
 on cell P, level, 194f
 on cell shape, 269, 269f, 270, 270f
 on cell volume, 267f10.10, 268f
 on Na^+ -efflux rate, 12f, 240f, 241f
 on resting potential, 295–98, 296f, 298f. *See also* 297f11.14
 mixed-lipid-fixed charge-dominated-polarized-water membrane (Type II membrane), 216, 216f
 mobility. *See* diffusion coefficient of K^+ . *See also* K^+
 molecular weight of nonelectrolytes

- molecular weight, (*Continued*)
 vs. cell-volume in solution of, 261f
 vs. q in muscle water, 91f5.9B
 vs. q in solution of NaOH-hemoglobin, 91f5.9A
 vs. permeability through frog skin, cellulose-acetate, 214f
- monactin. *See also* ionophores
 on K^+ permeability of living cells, 217, 217f
- mosaic-membrane-model, 206
- mouse-controlled-seasaw-model, 145, 146f
- MRI (magnetic resonance imaging), xi, xxiii1, xxv
 role of AI hypothesis in creation of, xiii1
- multilayer polarization of water
 accompanying charge fixation, 69
 as cause of invariant water contents of cell types, 97–98
 heat of adsorption of, on titanium dioxide, 71, 71t
 obedience to Bradley-isotherm
 of gelatin, 80, 100
 of frog muscle, 99
 physics of, 69
 role of induction in, 70
- myosin
 carboxyl groups on, as major K^+ -adsorbing sites, 62–65
 found only in A bands of muscle, 46
- N sites, definition, **73**
- Na^+ (sodium ion)
 conc. in muscle, vs. ATP level, 193f
 distribution in muscle in presence of K^+ , 163, 164f8.2A
 efflux of, 239
 divergent responses of frog muscle and squid axon to metabolic poison, explanation, 241–42
 low external K^+ conc. on rate of, 239
 rate of, from muscle, unaffected by poison, 12f
 localization in A bands in K^+ -depleted muscle, 48
 membrane permeability to, rules out Type I mechanism of solute distribution, 5
 role of, in action potential, 275
- ^{23}Na NMR
 shows adsorbed Na^+ in K^+ -depleted muscle, 175, 175t
- Na^+ over K^+ preference, 127
 at higher c -value, 127, 128f, 129f
- NaCl (sodium chloride)
 role of, in swelling of ATP-depleted cell, 266
- Na potential (sodium potential), 300, 301
 definition, **300**
 “standing,” in ionic theory, 300
 transient, in AI hypothesis, 307
- Na-pump hypothesis
 disproof of
 from EMOC studies, 54
 from excessive energy need of, 10–19
 from failed-attempts to find inanimate models, 20, 22–28
 reasons for being a poor theory, 9
 remedial postulations in attempts to save
 exchange diffusion, 16
 non-energy-consuming pump, 16
 sequestration of Na^+ in SR, 16
- Na^+ -sensitive-electrode-like behavior of living cells, 276
- Na^+ -specific electrode in measuring Na^+ adsorption 42f4.2
- nail-iron-filing model. *See* magnet-nails-iron-filing model
- native protein, 39, 104. *See also* introverts
 conversion to fully-extended conformation, 85
 definition, 37n4
 presence of, does not or weakly affect water properties, 108t
 cause shrinkage, 108t
 depress freezing point, 105f
 generate osmotic activity, 101, 101f
 reduce solvency, 80, 82t5.2A, 86f5.7, 88t, 91f5.9Aa
 retard freezing rate, 105f5.15a
 sorb water, 100f
- near-neighbor interaction.
 key to coherence among multitudes, 135
- nearest-neighbor-interaction-energy ($-\gamma/2$). *See also* autocoooperative adsorption
 definition **137**
 determines nature of adsorption
 when negative, heterocoooperative, 138
 when positive, autocoooperative, 138
 when zero, noncooperative (Langmuir), 137
 major inductive component in, 139
 relation to intrinsic-free-energy of adsorption, 140

- nearest neighbor transmissivity factor (τ),
definition **140**
- nebulin, 67n3
- Nernst equation (equation 1), 4, 274
- NHCO groups of protein backbones
as adsorption sites in autocoperative
transition, 148
- NMR (nuclear magnetic resonance), 93
method for detecting rotational restric-
tion of water, 93
- NMR-invisible Na^+ , 175
as evidence for Na^+ adsorption, 175,
203n3
- NMR relaxation times (T_1 , T_2), 93, 110n5
of water protons in living cells, 93–94
of solutions containing tissue ashes, 95t
- nonactin, 217, 217f. *See also* ionophores
- nonelectrolyte distribution
in frog muscle, 90f5.8B, 91f5.9B, 162
in NaOH-denatured hemoglobin solu-
tion, 90f5.8A, 91f5.9A
- nonelectrolyte permeability, 206, 207f,
208, 213, 214f
- non-energy-consuming-Na pump, 16
as Maxwellian demon, 28n1
other evidence against, 16
- non-freezing water, 6
- NO-NO system, definition, **73**
- NO-NO-NO system, definition, **75**
- non-solvent water, 6
Hill's disproof of, 6
- "non-solvent" water, "minimum,"
definition, **85–87**
in SDS, n-propanol denatured protein
solutions, 86f5.7
in solution of native proteins, 86f5.7
in urea and GuHCl denatured protein
solutions, 86f5.7
- NP system, definition **73**
- NP-NP system, definition **73**
uniform polarization of water in, 76f
- NP-NP-NP system, 225
definition, **74**
of CONH sites on fully extended pro-
tein chains, 75
uniform polarization of water in, 76f
- nuclear magnetic resonance. *See* NMR
- null-point method, 99, 110n6
for water sorption study near satura-
tion, 100, 100f, 110n6
- oil potential, 282
- one-on-many
capability, 144
- control of functional groups on short
side chains, 148
relationship, 150
- osmotic activity, 101
lesser enhancement due to introvert
models, 80, 101
of gelatin, PEO, native hemoglobin so-
lutions, 101f
strong enhancement due to extrovert
models, 80, 101
- osmotic pressure, definition **249**
- ouabain
as cardinal-adsorbent controlling cell
 K^+/Na^+ 172, 173f, 174f8.10f8.11
as EDC, from rank-order change of 5
alkali ions, 176, 177f
as secondary cardinal adsorbent, 177
as specific Na pump-inhibitor, disproof
of, 172, 173f
controls K^+/Na^+ transition, 176
effect on Cs^+ permeation with compet-
ing ions, 236, 236f
effect on K^+ of frog muscle, 173
effect on resting potential, 291
effect on Na^+ -efflux rate, 239
no apparent effect on q -value of cells,
177–78
- overshoot, 275
- Overton, E., 211
as founder of lipoidal membrane
theory, 9
on Quellungswasser in cells, 252, 272n1
suggested "adenoid" activity for electro-
lytes, 9
- oxygen
adsorption on hemoglobin vs AI hy-
pothesis, 139f
sigmoid adsorption curve, 137
uptake by RBCs, 169, 169f8.6ins
- oxygenation-deoxygenation of hemoglo-
bin
global changes in, 153
involving changes in c -value, entropy,
salt linkages, SH reactivity, solubil-
ity, 153
resembles oxidation-reduction of, 154
- P_K , P_{Na} , P_{Cl} , permeability constants,
275eq39, 2772eqs.40, 41
- P-x (unidentified protein, protein-X)
as an ATP "helper," 184, 184f
- P-sites, definition, **73**
- paradox and possible resolution
increasing experimental supports for
opposed theories, 72

- paradox and possible resolution,
(*Continued*)
one primary structure, more than one
secondary structures, 120
- paramagnetic ions (Mn, Fe)
lower content in cancer cells, 94
effect on longer T_1 , T_2 of water in
cancer, 94
- Partition Law. *See* Distribution Law
- passive outward diffusion of Na^+
minimal, in membrane theory and why,
11
- paucimolecular membrane model, 206
- Pauling's theory of protein hydration,
72
- PCG electrode. *See* polylysine-treated-col-
lodion-coated-glass electrode
- peptide linkage
high polarizability of, 116–17
in inductive effect transmission, 116–
17
transmissivity factor, 116
- “perfect osmometer” behavior
definition **250**
demonstration in plant cells, 251t
not seen in plasma-membrane enclosed
cytoplasm, 251, 252
tonoplast enclosed vacuole as seat of,
251
- permanent dipole moment of water, 69
- PEG (poly(ethylene glycol)). *See also* extro-
verts
in preserving cut muscle segments, 61,
62f, 63t
- PEO (poly(ethylene oxide)). *See also* extro-
verts
effect on motional restriction of water
from
NMR studies, 94
QENS studies, 96–97, 98f
UHFD studies, 96
effect on properties of water, including
(Debye) dielectric relaxation time, 96
freezing-point, freezing-rate 104
NMR relaxation times, 94
osmotic activity, 101f
rotational (and translational) diffu-
sion coefficients, 96–97, 98f5.10A
solvency for Na sulfate/citrate 82t,
84f5.5A
vapor sorption at near saturation,
100f
structural formula of, 84
permeability to ions.
control of, 235
high, in resting living-cell membranes,
210
lipoidal membrane theory cannot ex-
plain, 211
selectivity in, from transient adsorption,
230–31
virtually nil through phospholipid bi-
layers, 210
- permeability to K^+ , 217. *See also* permea-
tion of ions
surface-limited, 230
with and without ionophores,
of frog egg, frog muscle, human
RBC, 217f
- permeability to nonelectrolytes
of cellulose-acetate membrane, 214,
214f
of frog skin, 214, 214f
of *Nitella*
rate-limiting step possibly at tono-
plast, 247nl
vs. oil solubility, 207f
- permeability to water, 213
accord between data from living cells
and phospholipid bilayer models
on, not real, 226, 228
bulk-phase-limited,
in frog egg, 222f9.8
in giant barnacle muscle, 222f9.9,
223f
theory and model studies, 218–25
of living cells, 209, 210t
of phospholipid bilayers, extremely low,
229
serious error in data from living cells,
226–28
- permeation of ions
adsorption-desorption route of, (Route
2), 231f
cooperative interaction in 235
control by cardinal adsorbent, 235
control by ouabain, 235–36
 Cs^+ into frog eggs, 235–36
effect of ouabain on, 236f, 237t
 Cs^+ into ion-exchange-resin sheet,
232f9.12B
 K^+ into frog muscle, 232, 232f9.12A,
234t
 Rb^+ into barley roots, 232
saltatory route (Route 1), 231f
percentage of K^+ entry via, 234, 234f
percentage of Na^+ entry via, 234f
- Pfeffer, W., 3, 249

- pH dependency
 of Cs^+ adsorption in vitro on EM muscle section, 65
 of electric potential of PCG electrode, 284f
 of K^+ efflux during activity, 302f11.17
 of K^+ permeation into frog muscle, 233, 233f
 of Na^+ influx in activity, 302f11.17
 of Na^+ uptake of muscle segments, 62f
 of resting potential, 288–89
 of Rb^+ adsorption on isolated actomyosin, 64, 164f8.2B
- phase-boundary potential
 of Baur, 314n3
 of Beutner, 314n3
- phenol binding on collagen, autocoperative, 141, 141f
- phosphates adsorbed
 residual charges for K^+ adsorption, evidence against, 203n4
- phosphocreatine. *See* creatine phosphate
- phospholipid-membrane model of cell potential, 284
- pK_a (acid dissociation constant)
 in identifying β - and γ -carboxyl groups as K^+ -adsorbing, 61
 of analogous carboxylic acids, 118–19
 representing electron-donating/withdrawing strength of side chains, 119, 119t, 120f
- Planck, M. xxiv
- plasmolysis, 250f
- PM theory (polarized-multilayer theory of cell water, models), 73
- polarizability
 of anionic oxyacid group in theory, 128f, 129f
 influence on H^+ preference over K^+ , 133n8
 of carboxyl groups, high
 high H^+/K^+ preference from, 287, 287f
 of sulfonic groups, low
 low H^+/K^+ preference from, 130f
 of water molecules, 69
- polarized-multilayer theory of cell water (PM theory), 73
 models for, 73
- polarized water
 diagrams, of membrane surface area occupied by, 216f
 illustration of rotational motional restriction of, 79f
 in cell membranes, 216
- poly(ethylene oxide). *See* PEO
- polylysine-treated-collodion-coated glass electrode (PCG electrode), 284
 pH dependency of sensitivity to cations or anions, 284f
- poly(vinylmethylether). *See* PVME
- polyvinylpyrrolidone. *See* PVP
- PO-PO system, definition, 73
- pores in membranes
 as large domains filled with intensely-polarized water, 215
 critical size of, in sieve theory
 of Collander-Bärlund, 206
 of Conway-Boyle, 4
 of Mond-Amson, 4
 of rigid K^+ channel, Na^+ channel, 301, 302f11.16
 of Traube 3
- potassium ion. *See* K^+
- Priestley, J., 319
- primer. *See* D-glucose
- protein-X (P-x, unidentified protein), 184, 184f, 203–4n5
 as ATP “helper,” 184
 evidence for existence, 184–86
 possible identification with α -actinin, 203n5
 possible identification with actin (profilamentous, G^*), 186
 possibly related to reticuloce-lysate protein, 186
 possibly related to 20S heat-shock protein, 186
 possibly related to “unfolding protein,” 186
- protein-water- K^+ system, 31
- proteins. *See also* protein-X, water-polarizing protein
 as dynamic systems, 146
 cytoplasmic,
 determines cell shape, 264–65, 265f
 determines cell swelling/shrinkage, 253–55
 determines cell volume, 253, 264, 265f
 determines (invariant) cell-water content, 97–101
 effect on NMR relaxation times of water, 94
 second (and additional) conformation, reason for, 120, 153
 secondary structure as consequence of primary structure, 118

- proteins, (*Continued*)
 soluble, in cells
 effect of external ATP and ADP on release of, from injured cells, 190. 191f8.17
 relation to ATP concentration, 188–90, 191f8.16
- protoplasm, 2–3
- Protoplasmic doctrine of Max Schultze, 2
- protoplasmic theory, 6
- PVME (poly(vinylmethylether)), 84. *See also* extroverts
- effect on
 dielectric relaxation times, 96
 freezing point/rate, 105, 105f5.15b
 NMR relaxation time, 94
 solvency of water for Na citrate, 84, 84f5.5B
 structural formula of, 84
 vapor sorption at near-saturation vapor pressure, 100f
- ψ , resting (& action) potential, eqs.1, 39, 46, 48, 50, 51, 53, 55
- PVP (polyvinylpyrrolidone). *See* extroverts
- effect on
 dielectric relaxation time, 96
 lowering freezing-point/rate, 104
 NMR relaxation time, 94
 shape of ice crystals, 104
 solvency for Na₂SO₄, 82t5.2C, F
 structural formula of, 84
 vapor sorption at near-saturation vapor pressure, 100f
- pump
 concept for solute distribution in unifacial cells, disproof, 10–20
 many needed at plasma membrane, 17
 many needed at subcellular-particle membranes, 19
- pump-leak hypothesis, 252
- pure-lipid-membrane, (Type I) 216f
- pure-, or effectively-pure-fixed-charge-polarized-water membrane (Type III), 216f
- q_i (q -value for i th solute), 161. *See also* q -value
- q -value
 definition 77
 from slopes of linear distribution curves, 87, 90f
 indifferent to insulin, ouabain; explanation, 177–78
 relation to molecular weight of nonelectrolytes
 in frog muscle cell water, 91f5.9B
 in solution of NaOH denatured hemoglobin, 91f5.9Ab
 in solutions of native hemoglobin, 91f5.9Aa
 solutes of low, causes cell shrinkage, 255
- QENS (quasielastic neutron scattering), 96–97
 in studies of motional restriction of water, 96–97
 of water, KCl-, PEO-solution, Artemia cyst cells, muscle, 98f
- Queen Victoria's transistor radio, xxii
- Quellungswasser, 252, 272n1. *See also* Schwellungswasser
- quenching of fluorescence, 123. *See* fluorescence
- r , Donnan ratio, 17
- rational drug therapy, 339
- RBC. *See* red blood cells
- receptor sites, as cardinal sites, 144
- rectilinear solute distribution. *See also* Distribution Law
 observed, refutes pump theory, 162, 201n1
- red blood cells (RBC, erythrocytes), *See also* red cell ghosts
 effect of ionophores on K⁺ permeability of, 217, 217f
 oxygen uptake of, 169, 169f8.6ins
 shape, effect of ATP depletion on, 269, 269f
- red-cell ghosts
 solid ghosts(only) accumulate K⁺ and extrude Na⁺, 25–27
- regular sites, 144, 187. *See also* 143f
- resting potential, 273
 as equilibrium phenomenon in Bernstein theory and AI hypothesis, 275. 280
 as membrane potential in membrane theory, 4
 as steady-state phenomenon in ionic theory, 275
 β - and γ -carboxyl groups generating, 287–88, 287f, 288f
 control of, theory of, 289–90
 adrenaline as EWC, 292f
 cooling-induced thermal transition, 293f, 293t, 294f
 dual-mechanism theory, supports, 278f, 279f
 ouabain as EDC, 290, 291f

- effect of anoxia on, 295, 296f
 general equations, surface-adsorption theory, 281, 289, 308
 indifference to Mg^{++} concentration, 287, 288f
 limiting passive Na^+ -efflux, 11
 of molluscan neurones
 as affected by external K^+ , Na^+ , cooling, 278f, 294f
 of Na^+ -loaded rat muscle
 as affected by external K^+ , Na^+ , ouabain, 279f, 291f
 selective ion permeability or adsorption, 286
 under control of CrP and ATP, 294–99
 reversible unfolding of proteins, 146
 revolution. *See* scientific revolution
 completion in cell physiology, xxi, xxiii, 319
 ρ -value
 definition, 77
 for Na citrate, in solution of native proteins, gelatin, etc., 81–85, 82t
 for sucrose, in solutions of native, denatured proteins, 88t
 rotational correlation time (τ_r)
 definition, 93
 measures rotational restriction of water, 93–95
 of PEO, PVME, PVP-dominated water, 94
 relation to dielectric relaxation time, 96
 rotational diffusion coefficient of water
 diagram of restricted, (also of excluded solutes), 79f
 in brine-shrimp-cyst cells, 97, 98f5.10B
 in frog muscle, 97, 98f5.10C
 rotational restriction of
 bulk-phase water in living cells, 92
 bulk-phase water in solutions containing extroverts and solutes, 78, 79f, 80
 butterfly in spider web, size-dependent, 79f
 introverts, 80
 $R \rightarrow T$ transition of hemoglobin, 153
 SA theory. *See* surface adsorption theory of cell potentials
 salt linkage
 dissociation in HCl, 151
 formation of, during deoxygenation, 153–55
 formation prevents K^+ , Na^+ adsorption, 41
 formed at high c-values of carboxyl groups, 127–28
 in maintaining cell volume of healthy cells, 259
 in strong swelling effect of isotonic KCl, 260
 in weak swelling effect of isotonic NaCl, 260
 prejudice against concept of, history of, 66n2
 salt-linkage hypothesis for nonadsorption of ions in native proteins, 41
 saltatory route (Route I) 231f, 234, 238, 322
 percentage of K^+ entry via, 234f
 percentage of Na^+ entry via, 234f
 sarcoid, 2. *See* protoplasm
 sarcoplasmic reticulum vesicles (SR)
 sequestration of Na^+ in, to save Na-pump hypothesis, 16
 surface area of, 19
 vesicles, not hollow, 27
 Scatchard plot, 141, 142f
 cooperativity in adsorption from, 141
 in vitro Na^+ adsorption on hemoglobin at high pH, 142f
 strong interaction among carboxyl groups seen in, 142f
 Schultze, M., as proponent of Protoplasmic Doctrine, 2
 Schwann, T., as founder of Cell Theory, xxii, 9
 Schwellungswasser, xxiii, 6. *See also* Quellungswasser
 Scientific Method, 320
 Scientific revolution,
 historians' 319
 scientists' 319
 SDS (sodium dodecyl sulfate), 85, 107. *See* introverts
 does not convert native proteins to fully extended conf., 85
 sea-saw-chain model, 145, 146f
 secondary cardinal adsorbent, 177
 seed of Xanthium globatum
 absorbs water from saturated LiCl solution, 69
 semipermeability, 206
 history of, 206
 of diverse membrane models studied, 213
 SH-groups reactivity
 enhanced by urea
 in simple thiols, 122f, 123t
 in proteins, 122

- SH-groups reactivity, (*Continued*)
 decrease of, in deoxygenation of hemoglobin, 155
 influenced by inductive effect, 121
 short-range interaction of protein structure
 of prime importance in protein folding, 118
 short side chains. *See* functional groups on short side chains
 sickle-cell anemia
 faulty gene in, 264
 hemoglobin S in, 264
 tactoid formation in N_2 , 264
 membrane defect as cause of, 264
 red-cell hybrids vs. seat of sickling, 264, 265f
 "sickling" in N_2
 water loss with, 263
 osmotic fall with, 263
 σ , σ_{Hammett} , induction constant, Hammett's induction constant resp.
 Singer-Nicolson lipid-bilayer membrane model, 208, 209f
 size-dependency in
 polarized multilayer (PM) theory of, 92
 solute exclusion from models and living cells, confirming PM hypothesis, 92
 solute exclusion from polarized water, 79f
 solute exclusion from water containing extrovert models, not introvert models, 80
 water and nonelectrolytes permeation through layer of intensely polarized water, 213
 size rule, 77–78
 confirmation of
 in models, 90f5.8A, 91f5.9Aa
 in muscle, 90f5.8B, 91f5.9B
 exception to, 78
 in permeation through intensely polarized water, 215
 in q -values of nonelectrolyte
 in extrovert models, 91f5.9A
 in frog muscle, 91f5.9B
 in solute exclusion, 78
 "sodium channels," 301, 302f11.16, f11.17, 310, 310f
 "sodium channel protein," 309
 sodium dodecyl sulfate. *See* SDS
 does not convert native proteins to extroverts, 85
 sodium-pump hypothesis. *See* Na-pump hypothesis
 reasons for being a poor theory, 9
 solvency for Na_2SO_4
 in solutions of native protein, gelatin, oxygen-containing polymers and methylcellulose, 82t
 solubility of hemoglobin reduced in deoxygenation, 153, 155
 soluble proteins in cells
 relation to ATP concentration, 188–90, 191f8.16
 solute distribution
 as central theme of AI hypothesis, 159
 enthalpy term for,
 surface component, 78
 volume component, 78
 entropy term for, 78
 mechanism of, in polarized multilayers of water, 77
 primarily as adsorbed species, 166
 role of rotational restriction in, 79f
 size-dependency, 80
 solute distribution, Type I, II, III mechanism of, 1–2, 159
 soma, x
 relation to cell physiology proper, xxii
 spontaneous autocoooperative transition, 143, 143f7.6A. *See also* controlled autocoooperative transition
 squid axon
 axoplasm-free membrane-sac does not pump K^+/Na^+ , 20
 "dialyzed," does not pump K^+/Na^+ , 20
 K^+ permeability indifferent to valinomycin, 217
 SR. *See* sarcoplasmic reticulum
 statistical mechanics, xxiv. 35n2, 136
 stereochemical model of heme-heme interaction, 154
 sucrose, equilibrium concentration of
 in copper ferrocyanide gel, 215
 in frog muscle, 90f5.8B, 91f5.9B
 in liposomes, 225
 in native/denatured protein solution, 86f, 88t, 90f5.8A, 91f5.9A
 in relation to ATP, 192f, 193f
 sulfhydryl-group reactivity. *See* SH-group reactivity
 supercooling of normal liquid water, 7
 surface-adsorption potential (SA potential), 280

- theory of resting potential as, 280
 equation for, 280–81, 289–90, 308
 quantitative confirmation, 285, 291f, 292f, 294f
 unanimous confirmation from model studies, 282–85
- surface-adsorption theory of cellular electrical potentials, 280. *See also* surface adsorption potential
- surface-(or membrane)-limited diffusion, 218, 219f
- swelling of healthy cells
 in hypotonic solutions, 254f
 in isotonic KCl solutions, 262
- swelling of injured or poisoned cells
 role of ATP depletion in, 267f10.11, 268f
 role of NaCl, 266, 267f10.10
 role of salt-linkage dissociation in, 266
- swelling/shrinkage of cut-muscle segments
 in isot. solutions of diverse anions and cations, 262–63, 263f
- swelling/shrinkage of intact muscle cells
 in solutions of permeant solutes, 257–61
 only laterally, 263
- synthetic-phospholipid vesicles with pump
 reported active transport of Na^+ in, serious fault in, 22–25
 schematic of procedures used, 23f
- T_1 , T_2 . *See* NMR relaxation time
- τ , (nearest neighbor transmissivity factor)
 140, 171
 value estimated for K^+/Na^+ in muscle, 170
- taenia coli, description, 172
 K^+ distribution in, control by Ca^{++} , 172, 172f
 temperature transition in, 293, 293f11.10, t11.1
- TEM (transmission electron microscopy). *See* EM section
- temperature transition
 in K^+/Na^+ distribution, taenia coli, 293, 293f,t
 in resting potential, 294, 294f
 Ising model, not predicted in, 317n10
- titin, 67n3
- Tl^+ (thallous ion)
 TEM of muscle sections loaded with, 47, 47f
- tonoplast (vacuolar membrane), 250
- transistor radio of Queen Victoria, xxii
- transmissivity factor
 nearest neighbor (τ), 140, 171
 through CH_2 groups, 113
- Traube, M., 3, 206, 249
- trigger groups, 150, 150f
- trilaminar membranes not destroyed by lipid removal, 211
- Troshin equation (equation 18), 163, 203n2
 describing D-glucose distribution in muscle, 163f
- tryptophane fluorescence of, 123, 124t
- “turning” of key in lock-and-key analogy, 145
- Type I, II, III mechanism for asymmetrical solute distribution, 1–2, 159
- tyrosine fluorescence of, 123, 124t.
- UHFD (ultra-high-frequency-dielectric studies), 95
 of water in brine-shrimp-cyst cells, 96
 of water in solution of PEO, PVP, PVME, 96
- ultra-high-frequency-dielectric study. *See* UHFD
- unifacial cell, definition, 10, 19
- unidentified protein (P-x). *See* protein-X
- uniformity in K^+ adsorption in cells, 169, 171
- universality rule, 192
- unmasking of β - and γ -carboxyl groups, due to high pH, 42f
 for K^+ , Na^+ adsorption, 42f
- urea, 87
 binding on protein backbone, 149
 denaturation, 86f5.6
 enhancement of SH reactivity, 122
 of simple thiols, 123t
 equal distribution of,
 between cell/ext water, 6, 91f5.9B
 between model and bathing solution, 87
 historical role of discovery of, 6–7
 overall electron-donating effect, 122
- valinomycin, 216, 216f. *See also* ionophores
- van't Hoff, 4
 Law of Osmosis from, 250
- virus, death-dealing, 339
- vital dyes as monitor of life and death of living cells, 1

- vitalism, xxiii, 320
 von Helmholtz, H., xxiii, 338, 339
- water
 absorption from saturated LiCl, by seeds, 69
 adsorption on proteins, 72, 100f, 149
 adsorption on protein backbone, 149
 as polarized multilayers, 34f
 content on NMR relaxation, 94
 in NMR studies of oxygen-containing polymers, 94
 liberation of adsorbed, 128, 149
 osmotically inactive, 252
 permeability to, 213, 218–23, 225–30
 physicochemical properties of, in cells/models, summary 108t
 restricted rotation of, 79f, 80, 92–97
 sorption at physiological vapor pressure,
 in living cells, and extrovert models, 100f
 underlies invariant water content of each cell type, 69, 100, 253
- water content of living cells
 invariance in each cell type, proposed cause of, 100
- water-polarizing protein(s) in cells
 maintaining a steady polarized state of cell water, 177–78
 possible identification with actin, 186, 203n5
- Williams of Occam's razor, 30n10
- X-ray analysis (see despersive X-ray microanalysis)
 ξ , definition, **137**
 ξ' , definition, **289**
- Yang-Ling cooperative adsorption isotherm, 38n5, 136–38, 140
 as major component in equations of cellular electrical potentials, eq.48, eq.50, eq.53, eq.55
 cell volume (Ling, Peterson, 1977)
 cell permeability, eq. 26, eq.27
 solute distribution, eq. 14, eq.16
 relation to Hill's empirical eq. (eq.11), 139
 relation to Langmuir adsorption isotherm, 137–38, 138f
- zipper-like unmasking, of protein carboxyl groups, 150